INVESTIGATION INTO THE MECHANISMS OF FORMATION AND PREVENTION OF BARIUM SULPHATE OILFIELD SCALE

by

SCOTT STEWART SHAW

Submitted for the Degree of Doctor of Philosophy in

PETROLEUM ENGINEERING

Institute of Petroleum Engineering
Heriot-Watt University, Edinburgh
EH14 4AS

May 2012

ABSTRACT

The performance of barium sulphate oilfield scale inhibitors (SIs) is affected by a number of factors, including temperature, pH and brine composition. This thesis focuses mainly on the effect of varying brine composition – in particular, Ca^{2+} and Mg^{2+} divalent cations on SI inhibition efficiency (IE) and minimum inhibitor concentration (MIC) levels. The molar ratio of Ca^{2+}/Mg^{2+} in field formation waters is known to vary widely and is typically between 1 and 10. Since Ca^{2+} tends to improve the performance of phosphonate scale inhibitors and Mg^{2+} "poisons" them, then the effect of Ca^{2+}/Mg^{2+} ratio is of great practical importance in SI applications. This occurs since Ca^{2+} has the ability to be incorporated into the growing barium sulphate lattice whereas Mg^{2+} cannot. The effect of divalent ions on polymeric SIs is rather less and different SIs respond in different ways, as reported in detail here.

In this work, the possible mechanisms of scale inhibition are discussed with regard to different generic SI types, e.g. sulphonated polymers, phosphonates, etc. A range of 9 phosphonate and 9 polymeric SIs are tested. The SIs tested are categorised into Type 1 and Type 2 scale inhibitors, with regard to their sensitivity to Ca^{2+} and Mg^{2+} cations. Furthermore, they are all sub-categorised into further sub-types – Type A and Type B – depending on their compatibility at higher levels of calcium, $[Ca^{2+}]$ = ~1000–2000ppm. At the end of this work, all SIs are given categorisation codes, e.g. Type 1A, Type 2B etc., depending on this classification. In series of additional experiments, the effect of varying pH on IE/MIC is examined; the degree of SI depletion from solution is monitored during static IE experiments (these are referred to as SI consumption experiments); and ESEM images and EDAX analyses of scale deposits are obtained. The relation between IE and SI chemical molecular structure is also explained.

Of the SIs tested, only three are classed as Type 1 because MIC is primarily affected by $BaSO_4$ Saturation Ratio, not molar ratio Ca^{2+}/Mg^{2+}. Conversely, the MIC of all other SIs tested is primarily affected by molar ratio Ca^{2+}/Mg^{2+}; these are classed as Type 2. There are notable differences between the SI consumption profiles ([SI] remaining vs. time) of Type 1 and Type 2 SIs. Generally Type 1 SIs are not consumed significantly and maintain good IE and a high % of SI in solution over long periods, e.g. 96 hours; whereas Type 2 species are consumed rapidly, sometimes to ~ 0% in solution and IE also declines rapidly. There are two exceptions to this general observation – HEDP and HPAA. Non-ICP analytical methods for SI assay, including C18/Hyamine and Pinacyanol techniques can be applied for the assay of non-ICP detectable SIs such as MAT during static IE/consumption experiments. The IE of all SIs depends on their chemical structure. Chemical structures of SI-metal complexes presented in this thesis illustrate that SI molecules containing multiple amino methylene phosphonate functional groups have the greatest tendency to be Type 1 (e.g. OMTHP, DETPMP, and PMPA). This relies upon the inclusion of nitrogen atoms within the main carbon chain of SI molecules.

ACKNOWLEDGEMENTS

I would like to start by thanking my supervisors, Professor Ken Sorbie and Professor Eric Mackay for offering me the opportunity to come to Heriot-Watt University to study for this doctorate. Ken's guidance, patience, support and encouragement made this work possible.

I would like to express my sincere thanks to FAST for funding my PhD. My gratitude also goes out to FAST 3 and FAST 4 JIP sponsors (Baker Hughes, BG Group, BP, BWA Water Additives, Champion Technologies, Chevron, Clariant Oil Services, Conoco-Phillips, Equion, Halliburton, MI Swaco, MWV, Nalco, Petrobras, Petronas, PTT, REP, Rhodia, Saudi Aramco, Shell, Statoil, Talisman Energy, ThermPhos and Total) for their input, financial support and the provision of test phosphonate and polymeric scale inhibitor samples for my research.

Many thanks go to Lorraine Boak for her guidance in the laboratory, especially with the ICP spectrometer, and Dr. Jim Buckman for his help in obtaining ESEM images and EDAX analysis data from barium sulphate scale deposits.

Special thanks also go to my parents William and Robina who encouraged and supported me throughout my studies.

TABLE OF CONTENTS

LIST OF FIGURES

LIST OF TABLES

NOMENCLATURE

ABBREVIATION	MEANING
AFM	Atomic Force Microscopy
AMPS	2-acrylamido-2-methylpropane sulphonic acid (monomer)
Ca–PPCA	Calcium–PPCA compound
Ca–SI	Calcium–SI compound
CHS	C18 / Hyamine / spectrophotometry (or spectrophotometric)
CTP-A and CTP-B	Ter-polymers containing carboxylate, sulphonate and cationic quaternary ammonium functional groups
DETPMP	Diethylenetriamine pentakis (methylene phosphonic acid) – penta-phosphonate
DTPA	Diethyl Triamine Penta Acetic Acid
EABMPA	Ethanolaminebis (methylene phosphonic acid) – di-phosphonate
EDTA	Ethylene Diamine Tetra Acetic Acid
EDTMPA	Ethylene diamine tetra (methylene phosphonic acid) – tetra-phosphonate
ESEM	Environmental Scanning Electron Microscopy
FAST	Flow Assurance and Scale Team
ΔG_f	Gibbs Free Energy of Formation / kJ/mol
ΔH_f	Enthalpy of Formation / kJ/mol
HDPE	High Density Polyethylene
HEDP	1-Hydroxyethylidene-1,1-di-phosphonic acid – di-phosphonate
Hexa-P	A hexa-phosphonate SI (generic description)
HMTPMP	Bishexamethylenetriamine pentakis (methylene phosphonic acid) – penta-phosphonate
HMDP	Hexamethylenediamine tetrakis (methylene phosphonic acid) – tetra-phosphonate
HPAA	2-Hydroxyphosphonoacetic acid – mono-phosphonate and mono-carboxylate
HWU	Heriot-Watt University
ICP	Inductively coupled plasma atomic emission spectroscopy

ICP-MS	Inductively coupled plasma mass spectrometry
IPE	Institute of Petroleum Engineering
ID	Inner Diameter
IE	Inhibition Efficiency (of barium sulphate in this work, (%))
K	Kelvin
K_a	Acid dissociation constant
K_{Ba}	SI-metal binding constant to Ba^{2+} at a specific T and pH
K_{Ca}	SI-metal binding constant to Ca^{2+} at a specific T and pH
K_{Mg}	SI-metal binding constant to Mg^{2+} at a specific T and pH
K_{Sr}	SI-metal binding constant to Sr^{2+} at a specific T and pH
M^+	Monovalent cation such as Na^+, K^+, etc.
M^{2+}	Divalent cation such as Mg^{2+}, Ca^{2+}, Sr^{2+}, Ba^{2+}, Zn^{2+}, Cu^{2+}, etc.
$[M^+]$	Monovalent cation concentration (ppm), $M^+ = Na^+$, K^+, etc.
$[M^{2+}]$	Divalent cation concentration (ppm), $M^{2+} = Ca^{2+}$, Mg^{2+}, etc.
MAT	Maleic acid ter-polymer
MIC	Minimum Inhibitor Concentration (ppm active)
mM/L	Millimoles per Litre
μm	Micrometres
MW	Molecular weight (grams per Mole)
MSBC	Mild Scaling Base Case
MSFC	Mild Scaling Fixed Case
nm	Nanometres
NSSW	North Sea Sea Water
NTP	Nitrilotris (methylene phosphonic acid) – tri-phosphonate
OMTHP	Octamethylenetetraamine hexakis (methylene phosphonic acid) – hexa-phosphonate
PAA	Polyacrylic acid
pK_a	$-Log_{10} K_a$
pH	$-Log_{10}[H^+]$ ($[H^+]$ in moles/L)
PMA	Polymaleic acid
PMPA	Phosphinomethylated polyamine (a poly-phosphonate)
PPCA	Phosphino polycarboxylic acid

PFC	P-functionalised co-polymer
PPT	Precipitate
PS	Pinacyanol / spectrophotometry (or spectrophotometric)
ΔS_f	Entropy of Formation / kJ/mol
pm	Picometres
PVS	Polyvinylsulphonate
rpm	Revolutions per minute
SEM	Scanning Electron Microscopy
SI	Scale Inhibitor
[SI]	Scale inhibitor concentration (ppm active)
SPPCA	Sulphonated phosphino polycarboxylic acid
SR	Saturation ratio (of barite in this work)
SW	Sea Water
SXRD	Synchrotron X-Ray Diffraction
T	Temperature (^oC or K – units will be stated)
TBR	Tube Blocking Rig
VS-Co	Vinylsulphonate acrylic acid co-polymer
X_m or X_{molar}	Total number of moles of calcium + magnesium (Ca^{2+}+Mg^{2+})

LIST OF PUBLICATIONS

S.S.Shaw, K.S.Sorbie and L.S.Boak: "The Effects of Barium Sulphate Saturation Ratio, Calcium and Magnesium on the Inhibition Efficiency: I: Phosphonate Scale Inhibitors", Paper SPE 130373, presented at the SPE International Conference on Oilfield Scale, Aberdeen, UK, 26−27 May 2010.
(Accepted for Journal publication – SPE Production and Operations).

S.S.Shaw, K.S.Sorbie and L.S.Boak: "The Effects of Barium Sulphate Saturation Ratio, Calcium and Magnesium on the Inhibition Efficiency: II: Polymeric Scale Inhibitors", Paper SPE 130374, presented at the SPE International Conference on Oilfield Scale, Aberdeen, UK, 26−27 May 2010.
(Accepted for Journal publication – SPE Production and Operations).

S.S.Shaw and K.S.Sorbie: "The Effect of pH on Static Barium Sulphate Inhibition Efficiency and Minimum Inhibitor Concentration of Generic Scale Inhibitors", Paper SPE 155094, presented at the SPE International Conference on Oilfield Scale, Aberdeen, UK, 30−31 May 2012.

S.S.Shaw, T.D.Welton and K.S.Sorbie: "The Relation between Barite Inhibition by Phosphonate Scale Inhibitors and the Structures of Phosphonate-Metal Complexes", Paper SPE 155114, presented at the SPE International Conference on Oilfield Scale, Aberdeen, UK, 30−31 May 2012.

Chapter 1: Introduction and Field Significance

Chapter 1 Summary: This Chapter introduces the barium sulphate scale problem and discusses the relevance of static laboratory barium sulphate inhibition efficiency (IE) testing work to prevent mineral scale formation in oil production systems. Previous IE work and new findings of this PhD are summarised, the aims and objectives of the thesis are listed and a brief outline of the thesis is given.

1.1 Background to Barium Sulphate Oilfield Scale

Barium sulphate or "barite" mineral scale ($BaSO_4$) forms in oilfield production systems when two incompatible brines mix: for example North Sea Sea Water (NSSW) (sulphate rich) and Forties formation water (contains Ba^{2+}, Sr^{2+} and Ca^{2+} scaling ions) (Jordan et al., 2008, Graham et al., 1997a, 2003; Simpson et al., 2005; Sorbie et al., 2000; Todd and Yuan, 1990, 1992; Yuan et al., 1997b). The barite co-precipitates with celestite ($SrSO_4$) and deposits can build up either on the inner walls of oilfield pipelines (resulting in reduced inner diameter, ID) and also within production valves, pumps, separators, etc. (Nenniger et al., 1990; Frenier and Ziauddin, 2010; Yuan and Todd, 1991). These deposits often also contain a small percentage of calcium sulphate, due to the presence of Ca^{2+} cations. Formation waters may also contain a significant concentration of radioactive isotopes (uranium and thorium decay products) which also precipitate as sulphate salts and may render the scale sufficiently radioactive to be a potential health problem (Putnis et al., 1995). Precipitation of insoluble salts may also occur as a result of pH or temperature changes in the NSSW brine prior to mixing with FW (Read and Ringen, 1982). These mineral scale deposits result in a decrease in production, regardless of where exactly the deposit forms (Collins, 2005). Deposits formed within pipes result in reduced flow or even eventual complete blockage of the pipeline, in the absence of intervention using chemical scale inhibitors (SIs) which help inhibit scale (barium sulphate, calcium carbonate, etc.) precipitation and deposition (Feasey et al., 2004; Graham et al., 2001a, 2002c; Webb et al; 1998; Wylde et al., 2002). In high pressure, high temperature (HP/HT) wells, the SI selected must be compatible with the brine and thermally stable under the field conditions (Dyer et al., 1999; Graham et al., 1997b, 2001a). Generally, all barium sulphate SIs *easily* prevent strontium and calcium sulphate

precipitation since both of these deposits are much softer and more soluble than barium sulphate (Nancollas, 1985) and are thus much more easily inhibited. In oilfield applications, barium sulphate is the hardest scale to prevent and/or remove (Nancollas, 1985; Quiroga et al., 2004). Since it is very costly to replace expensive production equipment which has been blocked or damaged by mineral scale, it is generally considered to be a better option to try to prevent the occurrence of the problem in the first place by using chemical SIs (Kokal et al., 1996; Mowery, 1985). Generally, this is more economic than allowing the scale to form and having to subsequently remove it, either mechanically or chemically. The use of sulphate reduction technology is also well documented (Al-Riyami et al., 2008; Boak et al., 2005; Chen et al., 2007; Collins et al., 2004; Davis and McElhiney, 2002; Jordan et al., 2008; McElhiney et al., 2006; Scott, 1993; Vu et al., 2000). This thesis discusses the performance of an extensive range of phosphonate and polymeric SIs in static barium sulphate IE experiments, under various test conditions, and the mechanisms of scale inhibition. Other workers have also studied the mechanisms of barite formation and inhibition and a variety of other problematic oilfield scales including calcite, gypsum, iron carbonate and sulphides (Greenberg and Tomson, 1992; He et al., 1994; Kan et al., 2005; Okocha et al., 2008; Sorbie and Laing, 2004; Tomson et al., 2002, 2003, 2004).

1.2 Introduction to Static Barium Sulphate Inhibition Efficiency

The static barium sulphate inhibition efficiency (IE) (%) is a measure of how effective a SI is at preventing barite formation under a specific set of experimental test conditions, i.e. T, pH, etc., and at a particular time after mixing the two incompatible brines, e.g. usually 2 hours or 22 hours (Boak et al., 1999; Sorbie et al., 2000; Yuan et al., 1997a, 1997b; Yuan, 2001). Hence, 2 and 22 hour IE (%) is often referred to. These sampling times are chosen largely chosen for convenience. In unseeded static IE tests, nucleation occurs ~½hr to ~3hrs after mixing NSSW/FW brines. Therefore, an early-time sampling time of 2 hours is reasonable for practical reasons (FAST EPM, 2006). The 22hr sampling time examines the crystal growth inhibition ability of SIs. This exact sampling time is less crucial than the 2 hour sampling time because the reaction rate has slowed significantly by 22 hours. In some studies, sampling has been carried out after 22 hours and prior to 2 hours (see Chapters 9 to 11). Sometimes IE continues to decline after 22 hours, depending on the [SI] and test conditions.

When a SI has an IE ≥ 90% at both 2 and 22 hours, this is referred to as the "Minimum Inhibitor Concentration" or MIC. For any scale inhibitor (SI) to be suitable for use in the oilfield, it is a commonly used working criterion in the laboratory that MIC is achieved when IE ≥ 90% at *both* 2 hour and 22 hour residence times. However, sometimes in a particular application variants on this definition of MIC are used e.g. it may be adequate in some application to define MIC as when IE ≥ 90% at 2 hours only. The MIC of a given SI may be determined in either static IE tests or in dynamic tube blocking tests. For static (jar) tests, IE is mathematically a percentage (%) given by the following expression:

$$I.E. = 100\left(\frac{C(t) - C_b(t)}{C_o - C_b(t)}\right) \qquad \text{(Eq. 1.1)}$$

where C(t) = test sample Ba^{2+} concentration at time, t (ppm); C_O = control sample Ba^{2+} concentration at time, t = 0 (ppm); and $C_b(t)$ = Ba^{2+} concentration in the blank solution (containing no SI) at time, t (ppm).

Accordingly, solutions containing higher [SI] are most likely to have the highest IE although this is *not always* what is observed, due to other chemical reactions which can occur, involving the SI. In particular, static IE experiments presented in this thesis are carried out varying pH, [Ba^{2+}], [Ca^{2+}] and [Mg^{2+}]. The important role of divalent cations Ca^{2+} and Mg^{2+} upon the functionality of the SIs is investigated in some detail and the significance of the *molar ratio* Ca^{2+}/Mg^{2+} on the inhibition efficiency of a wide range of SIs is investigated. A schematic diagram of the static barium sulphate IE procedure is shown in Figure 1.1. SI may also be assayed in addition to [Ba^{2+}] – these types of experiment are presented in Chapters 9 to 11.

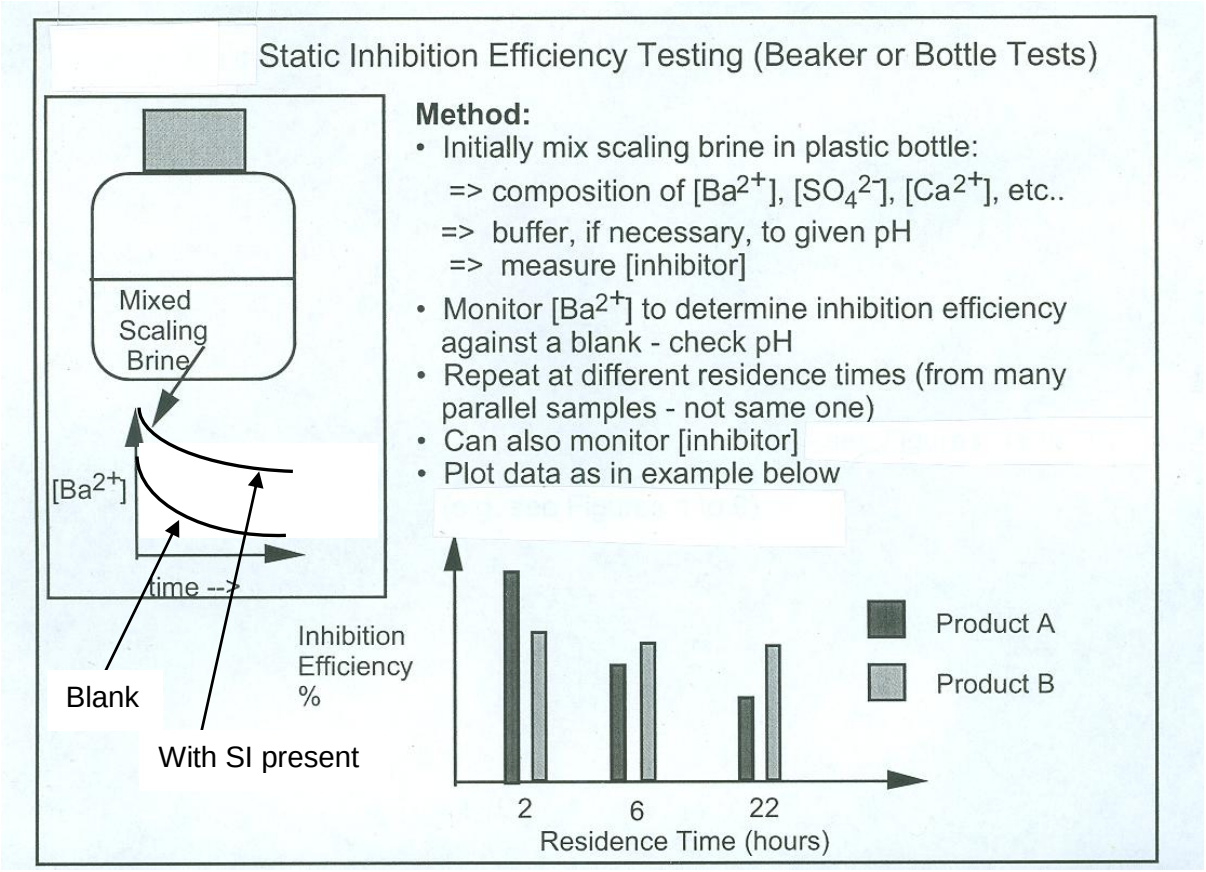

Figure 1.1 – Schematic procedure for static barium sulphate IE tests (Sorbie et al., 2000).

The IE of any scale inhibitor depends upon a number of conditions, such as: temperature (T), pressure (P), brine mix pH and brine composition (both NSSW and FW) and on the final mixing ratio NSSW/FW. In this context, it is the scaling brine composition (including pH) and scale species supersaturation, Sp, or saturation ratio (SR) of the final resultant brine mixture that are the most important factors. The brine pH affects the extent of dissociation of the SI molecules, and thus, directly affects their ability to complex with divalent cations, including Ba^{2+}, Sr^{2+}, Ca^{2+} and Mg^{2+}. All of these divalent cations can form sulphate scale, except Mg^{2+}. pH effects are investigated in this work in Chapter 7. As a general point, if any of these variables (SR, pH, NSSW/FW mixing ratio etc.) are to be investigated in the laboratory, all the other conditions should be kept constant to enable a reliable and clearly interpretable test to be carried out.

The two main classes of SI are polymeric species (e.g. PPCA, PVS, VS-Co, etc.) and phosphonates (e.g. DETPMP, HMTPMP, EDTMPA, HEDP, HPAA etc.). Polymeric SIs

usually function mainly through a nucleation inhibition mechanism and perform best over short residence times (Boak et al., 1999; Sorbie et al., 2000; Sorbie and Laing, 2004) – the most notable exception to this being PMPA (a poly-phosphonate), which performs well over extended residence times (22hr+). Phosphonates (including PMPA), on the other hand, function mainly through a crystal growth retardation mechanism and perform better over longer residence times (Boak et al., 1999; Graham et al., 1997a, 2003). In some instances, phosphonate SIs are not the best choice for use in severe barite scaling systems, for example, in low pH systems (Cushner et al., 1988; Singleton et al., 2000). Polymeric SIs such as PVS and VS-Co are better suited for low pH applications because generic phosphonate SIs such as DETPMP would be associated and therefore not able to inhibit barite scale formation. However, polymeric SIs such as PVS and VS-Co do not exhibit good retention properties (Singleton et al., 2000). The synthesis of an SI such as the poly-phosphonate PMPA was undertaken to try and capture the associated benefits of both polymeric (e.g. low pH applications) and generic phosphonate SIs (good retention) (Jackson et al., 1996; Przybylinski et al., 1999; Singleton et al., 2000). In addition to PMPA, some polymeric "di-phosphonate end-capped" polymers have been synthesised using a vinylidene di-phosphonic acid monomer (Davis et al., 2003; Fleming et al., 2004). Such di-phosphonate end-capped polymers have improved adsorption properties compared to their non-phosphonated analogues due to the inclusion of the phosphonate functional groups in these molecules. The main disadvantage of phosphonation of SIs is that in doing so, there is a concomitant decrease in their "environmental friendliness" (Jordan et al., 2010, 2011; Taj et al., 2006).

No scale inhibitor functions exclusively through just one type of mechanism (nucleation inhibition or crystal growth retardation) – both mechanisms are always involved but to different extents (Boak et al., 1999; Graham et al., 1997a, 2003; Sorbie et al., 2000). Brine pH is particularly important with regard to phosphonate type SIs – because it affects the extent of dissociation of these molecules (i.e. speciation) – see Chapter 7. The extent of dissociation, in turn, affects how efficient the SI will be in preventing barium sulphate scale.

In oilfield produced waters, the mineral scaling problem is a "moving target" since the Sea Water/formation water (NSSW/FW) mixing ratio is constantly changing. Therefore, for barium sulphate for example, the barite saturation ratio (SR), the yield of barite precipitate and molar ratio of Ca^{2+}/Mg^{2+} in the produced waters are all evolving over time. This thesis

describes the effects of saturation ratio (SR), brine molar ratio Ca^{2+}/Mg^{2+} and pH on the barium sulphate IE of 9 phosphonate SIs and 9 polymeric SIs, viz: OMTHP (a hexa-phosphonate), DETPMP (a penta-phosphonate), HMTPMP (a penta-phosphonate), HMDP (a tetra-phosphonate), EDTMPA (a tetra-phosphonate), NTP (a tri-phosphonate), HEDP (a di-phosphonate), EABMPA (a di-phosphonate), HPAA (a mono-phosphonate and mono-carboxylate), PMPA (a poly-phosphonate), PPCA, SPPCA, MAT (a green SI), PVS, VS-Co, a generic P-functionalised co-polymer (PFC) and cationic ter-polymers A and B (CTP-A and CTP-B). In this thesis, the term "green SI" applies to SIs which only contain carbon, oxygen, and hydrogen atoms (no phosphorus and no sulphur atoms), see Chapter 4. Some green SIs may also contain nitrogen.

1.3 Barium Sulphate Saturation Ratio (SR) and Precipitated Amounts

Phosphonate SIs can be very sensitive to brine $[Ca^{2+}]$ and $[Mg^{2+}]$ (Shaw et al., 2010a) and this is described and explained in detail in this thesis. Since the brine mixing ratio of NSSW/FW determines both the molar ratio of Ca^{2+}/Mg^{2+} in the produced brine and the barium sulphate saturation ratio (see Figure 1.2) – it has a significant effect upon IE when phosphonate SIs are being deployed (Shaw et al., 2010a). The equation for SR is given below:

$$SR = \frac{[Ba^{2+}]_o[SO_4^{2-}]_o}{K_{sp}} \qquad \text{(Eq. 1.2)}$$

where $[Ba^{2+}]_o$ = initial barium ion concentration (mol/L); $[SO_4^{2-}]$ = initial sulphate ion concentration (mol/L); and K_{sp} = barium sulphate solubility product, at temperature T, specific pH and ionic strength level.

The mixing ratio NSSW/FW determines the $[Ba^{2+}]$ in the mix and therefore the SR and the level of precipitated $BaSO_4(s)$, see Figure 1.3. Precipitate which forms is actually a co-precipitate of barium and strontium sulphate – this occurs in the field and in IE test bottles. There is also a small percentage of calcium inclusion. If the test sample is a blank, a Ba/Sr co-precipitate will form. If SI is present, some strontium sulphate can still form – but the quantity of Sr^{2+} precipitated is much less than in an equivalent blank bottle because strontium sulphate is much more easily preventable than barium sulphate, by means of chemical scale inhibitors. All static IE experiments described in this thesis are carried out at 95°C, at a

produced water pH = 5.5 (this is normally achieved by using a sodium acetate / acetic acid pH buffer solution) to broadly match conditions in the oilfield, *except* in Chapter 7, where the effect of *varying* pH on IE at 95^{o}C is investigated.

In some selected IE experiments, Sr^{2+} was assayed in addition to Ba^{2+} at each sampling time, to determine the strontium sulphate and barium sulphate inhibition efficiencies. All strontium sulphate inhibition efficiencies at 2 and 22 hours were found to be in the range of ~75-100%, testing phosphonate SIs, e.g. NTP, confirming this scale is easily inhibited. It is actually more difficult to inhibit barite in strontium-free brine. This is because the absence of strontium chloride in the brine results in an increase in barite SR because ionic strength is inadvertently reduced. Indeed, this was checked using MultiScale. For a 50/50 NSSW/FW Base Case brine mix, SR barite (with strontium chloride present) = 322.46 (see Figure 1.2). If strontium chloride is absent, SR barite = 324.82. The barite scale which forms in the absence of Sr^{2+} is also much harder because a mixed Ba/$SrSO_4$ scale can no longer form, thus allowing a much more thermodynamically stable crystal lattice of barite to crystallise. If, however, the ionic strength is maintained, i.e. if all Sr^{2+} removed is replaced by Na^{+}, there is very little change in the barite SR. If Sr^{2+} is replaced by Na^{+}, the barite SR lowers slightly to 321.44. So, at a fixed ionic strength level, it is slightly better to have Na^{+} present rather than Sr^{2+} - this decreases the barite SR by ~1 unit. This may be because at fixed ionic strength, the formation of a mixed Ba/Sr/Ca scale is slightly more energetically favourable than the formation of barite scale with only limited Ca^{2+} inclusion. Taking into account the previous points, the possibility of $SrSO_4$ co-precipitating with $BaSO_4$ is very unlikely to have any effect upon measured MIC levels for barite inhibition. If all Sr^{2+} is replaced with Na^{+} to maintain ionic strength, MICs should remain at about the same level.

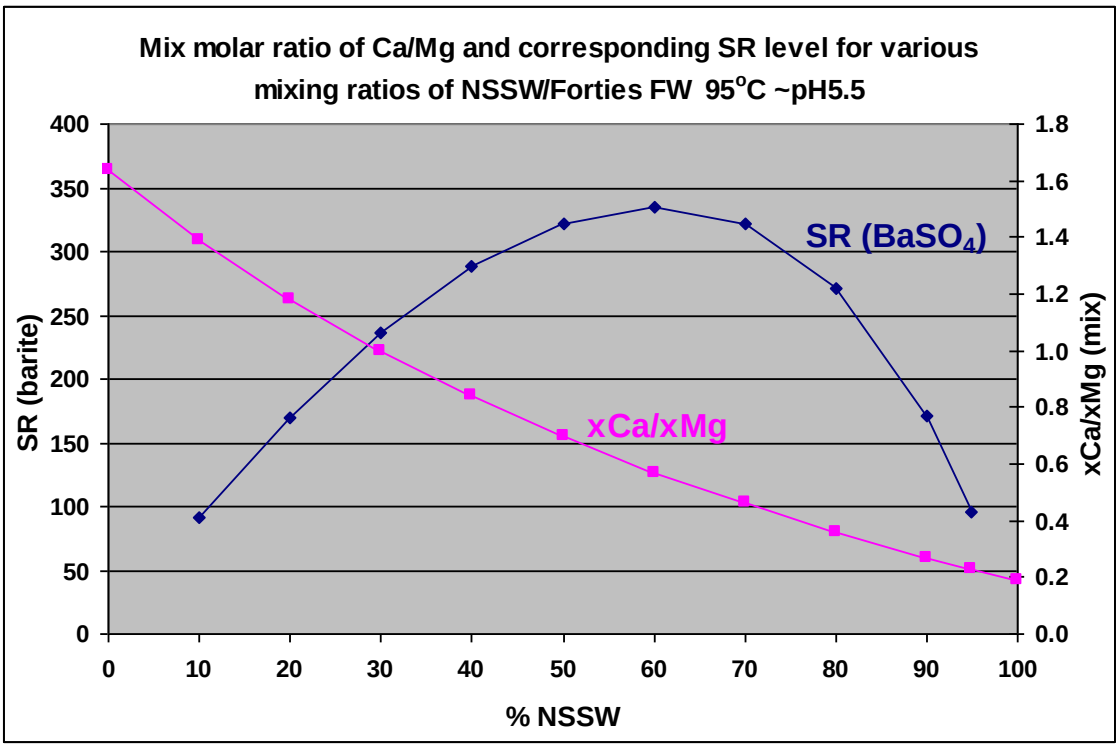

Figure 1.2 – Barium sulphate saturation ratio as a function of mixing ratio NSSW/FW and also the resultant mix molar ratio Ca^{2+}/Mg^{2+}. Conditions: T = 95°C, pH = 5.5.

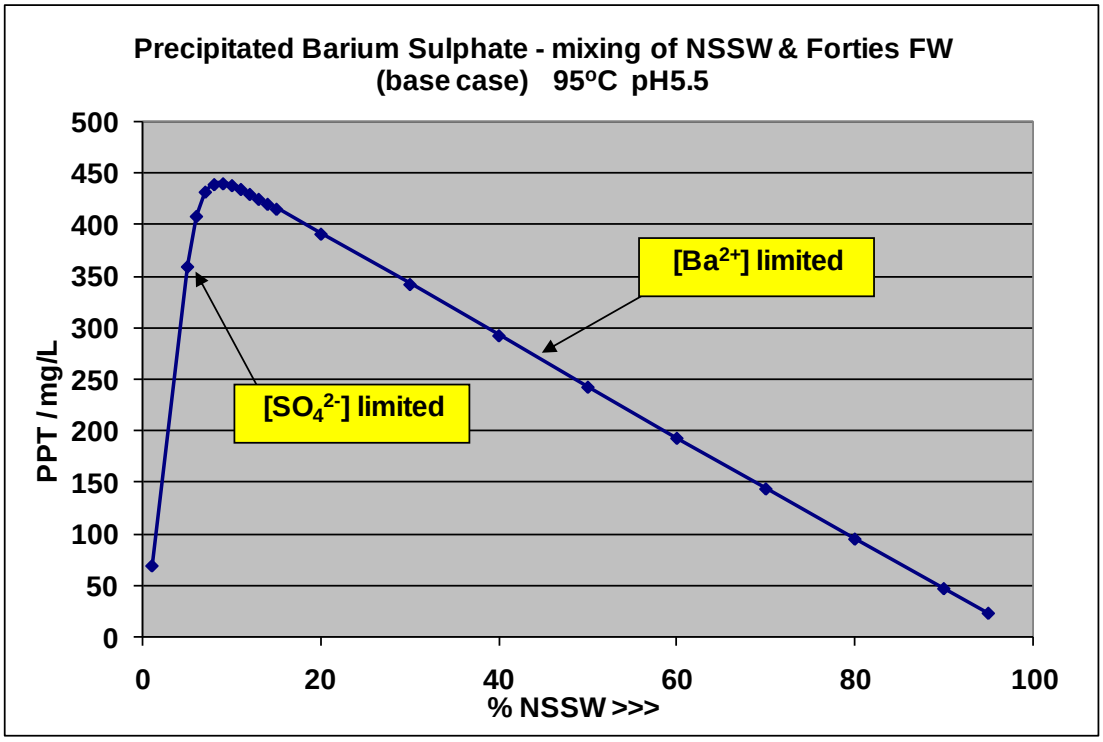

Figure 1.3 – Maximum yield of barite formed (mg/L) as a function of mixing ratio NSSW/FW. Conditions: 95°C, pH5.5.

1.4 Scale Inhibitor Binding to Ca^{2+} and Mg^{2+}

Different SIs have different affinities for Ca^{2+} and Mg^{2+}, i.e. some may bond more strongly to Mg^{2+} (e.g. DETPMP) (Sorbie and Laing, 2004) or they may bond more strongly to Ca^{2+}. SI molecules are essentially weak polyacids of the form, H_nA and they must be dissociated in order to complex metal ions (e.g. Ca^{2+} and Ba^{2+}) successfully. Different SIs have different affinities for metal ions, M^{2+} and this is quantified by the magnitude of the ligand-metal binding constant (or stability constant) (Boak et al., 1999; Graham et al., 1997a, 2003; Duan et al., 1999; Sanchez-Moreno et al., 2004; Popov et al., 2001; Sawada et al., 1986, 1988, 1991, 1993a, 1993b, 2000). Such differences in the SI−M binding constants (e.g. where M = Ca^{2+} or Mg^{2+}) will be reflected in the SI IE capability. Those that bond very strongly to Mg^{2+} but not very well to Ca^{2+} ($K_{Mg} > K_{Ca}$) at around pH 5.5 are likely to perform worse in barium sulphate scale prevention than those having a stronger affinity to Ca^{2+} than Mg^{2+} ($K_{Ca} > K_{Mg}$). For DETPMP, there is not much difference in the affinity to Ca^{2+} and Mg^{2+} ($K_{Ca} \approx K_{Mg}$); compare $K_{Ca} \approx 5.0 \times 10^{10}$ with $K_{Mg} \approx 6.3 \times 10^{10}$ (Sorbie and Laing, 2004) which are almost the same in magnitude, but the binding to Mg^{2+} is slightly stronger. This means Ca^{2+} is less likely to displace the Mg^{2+} complexed SI, unless it is present in large excess. The pH and temperature conditions are not specified for these binding constants, but they are still informative and suitable for modelling purposes. In previous work, it has been proposed that this "removed Mg^{2+}–bound SI" essentially prevents the bound SI from inhibiting barite scale; hence the SI is effectively "poisoned" by the Mg^{2+} (Boak et al., 1999; Graham et al., 1997a, 2003; Shaw et al., 2010a; Sorbie and Laing, 2004).

The small ionic radius of Mg^{2+} coupled with its oxophilicity (high affinity for oxygen ligands such as phosphonate) results in unusually strong Mg^{2+}–ligand binding constants (Weston, 2009). It is for this reason, in biochemistry, for example, in the human body, most phosphonate compounds exist bound to Mg^{2+}. In biological systems, the second most common ligand bonded to Mg^{2+}, after water, is carboxylate anions (Weston, 2009). With their negative charge, carboxylate functional groups are significantly better ligands than water, for a hexa-co-ordinated Mg^{2+} cation (Weston, 2009) (water molecules are neutral ligands bonded to Mg^{2+} by means of an oxygen atom lone-pair of electrons). The order of decreasing magnitude of the binding constants for the 9 phosphonate SIs to either Ca^{2+} or Mg^{2+} will depend upon their specific binding constant values (to Ca^{2+} and Mg^{2+}, i.e. K_{Ca} and K_{Mg}).

Polymers may bind to calcium (Ca^{2+}) and magnesium (Mg^{2+}) ions by means of dissociated carboxylic acid functional groups ($-COO^-$) or by means of dissociated phosphonic acid functional groups ($-PO_3^{2-}$). Sulphonate functional groups ($-SO_3^-$) do not bind very strongly to divalent cations since these are highly dissociated at pH5.5 (the standard IE test pH) (Sorbie and Laing, 2004). The pK_a values for sulphonic acids are generally very low (they are strongly acidic) – the actual value is dependent upon the chemical environment in which the sulphonate group is located, i.e. the presence of other functional groups adjacent can have an influence, etc. (Sorbie and Laing, 2004). The presence of sulphonate groups can cause SI to work effectively at lower temperatures (e.g. 5^oC using PVS) and also low pH levels – due to the highly acidic nature of these functional groups. An extremely low pH level is required before sulphonated species become associated (protonated) (Sorbie and Laing, 2004).

1.5 Field Significance of this Study

Practically, brine Ca^{2+} and Mg^{2+} are very important since their concentrations vary significantly in field formation waters, as illustrated in Figure 1.4. This figure shows the levels of Ca^{2+} and Mg^{2+} in ~300 field formation waters from fields around the world (FAST database). Figure 1.5 shows that the molar ratio of Ca^{2+}/Mg^{2+} in ~84% of the formation waters falls within the range 1 to 10. Most of the experimental work presented in this thesis involves experiments where the produced water molar ratio Ca^{2+}/Mg^{2+} falls within this same range of values – hence the experimental results are directly applicable to field conditions.

Experiments involving the monitoring of SI in solution (Chapters 9 to 11) are beneficial, as they give an insight into what is actually happening to the SI over time indicating whether it remains in solution, or is consumed (i.e. removed from solution), into the forming scale. Again, this is directly applicable to the field since it will also occur in the oilfield when these SIs are being deployed. Figure 1.6 illustrates how the barium saturation ratio (SR) and produced water molar ratio Ca^{2+}/Mg^{2+} change as a function of mixing ratio NSSW/FW. The resultant mix molar ratio Ca^{2+}/Mg^{2+} depends upon which FW is mixed with the NSSW. In the work described in this thesis, Forties FW is used exclusively, which normally contains a molar ratio of Ca^{2+}/Mg^{2+} = 1.64, and a $[Ba^{2+}]$ = 269ppm, *except* in Chapter 8 where Forties FW containing 100ppm Ba^{2+} is used to investigate *mild scaling* conditions. The molar ratio of Ca^{2+}/Mg^{2+} in the Forties FW is only varied in experiments varying Ca^{2+}/Mg^{2+} in the produced water at a specific NSSW/FW mixing ratio, and in Fixed Case IE tests. The NSSW contains a molar ratio of Ca^{2+}/Mg^{2+} = 0.19, however, in Fixed Case IE tests, NSSW containing no Ca^{2+} and no Mg^{2+} is used. See Chapter 3 for all brine compositions. The barium sulphate saturation ratio (SR) largely depends upon the $[Ba^{2+}]$ in the produced water, and is only very marginally altered by changes in $[Ca^{2+}]$ and $[Mg^{2+}]$ (due to salinity / TDS / ionic strength changes) – see Figure 1.2.

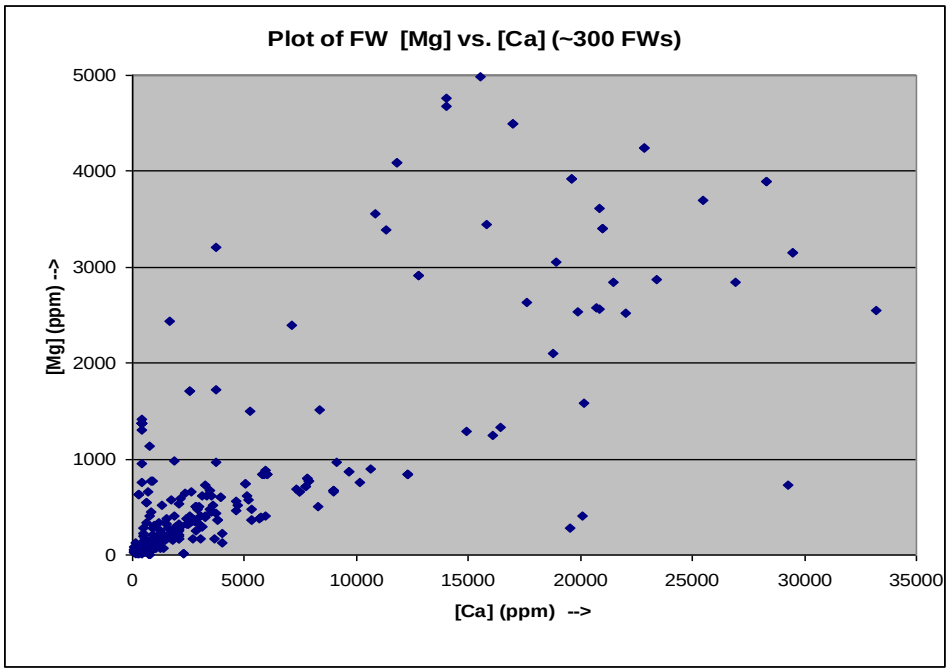

Figure 1.4 – Levels of Ca^{2+} and Mg^{2+} in ~300 field formation waters (FAST database, IPE, HWU).

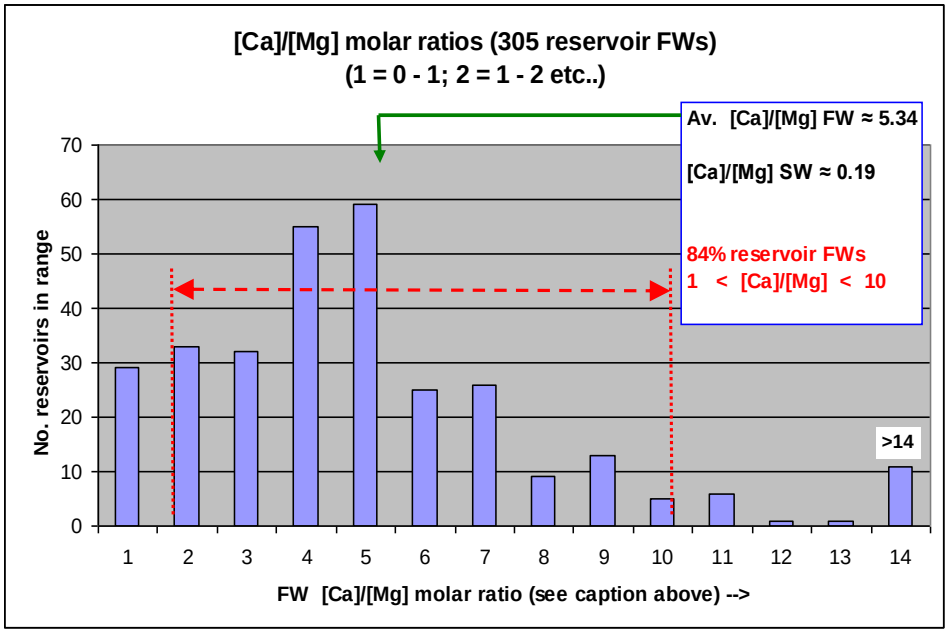

Figure 1.5 – Molar Ratio Ca^{2+}/Mg^{2+} in ~300 field formation waters (FAST database, IPE, HWU).

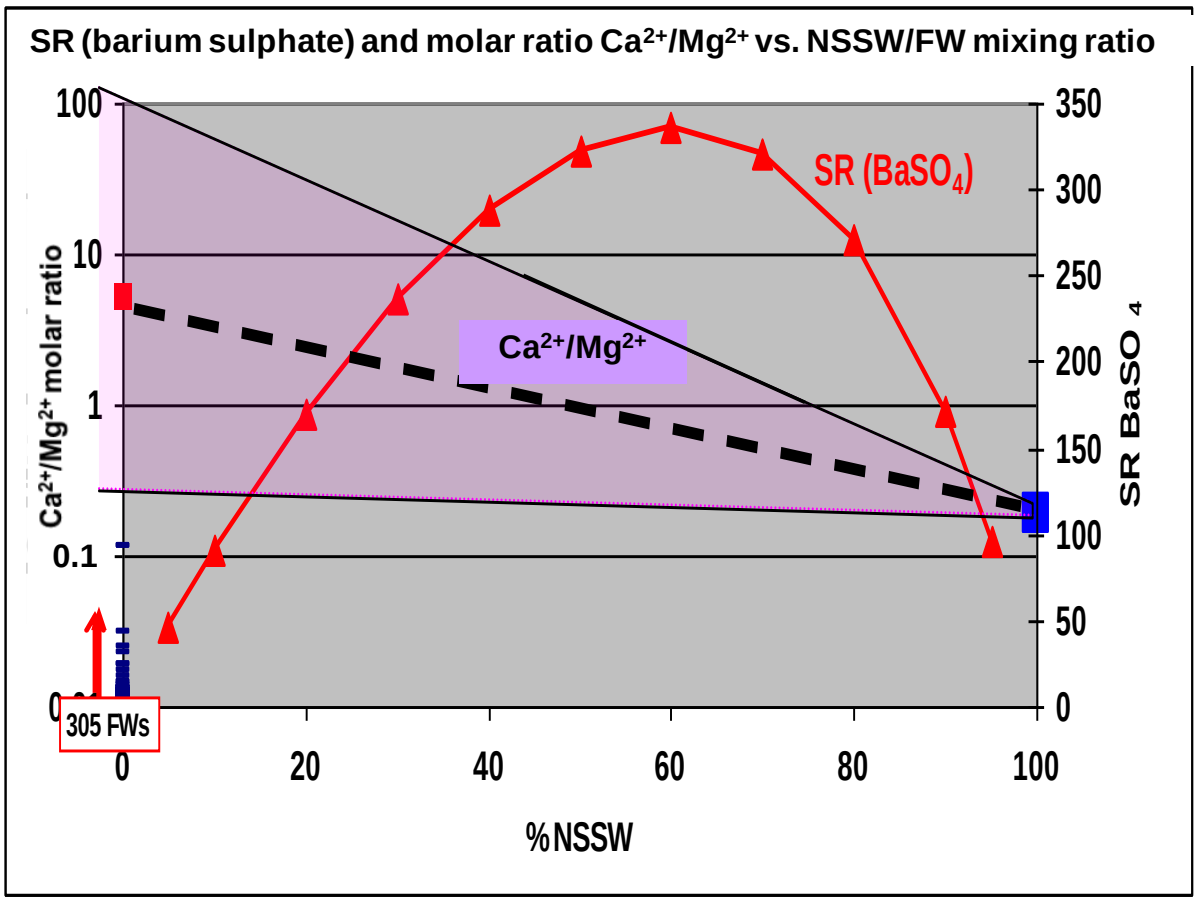

Figure 1.6 – Barium sulphate saturation ratio and produced water molar ratio Ca^{2+}/Mg^{2+} as a function of mixing ratio NSSW/FW.

1.6 Summary of Previous Static Barium Sulphate IE Work and New Findings from this PhD

Prior to this work being undertaken, only the basic generic effects of Ca^{2+} and Mg^{2+} were known, viz. Ca^{2+} improves the performance of phosphonate SIs (e.g. DETPMP and Hexa-P) whereas Mg^{2+} "poisons" (Boak et al., 1999; Sorbie et al., 2000; Graham et al., 1997a, 2003; Sorbie and Laing, 2004). Secondly, only a very narrow range of phosphonate SIs were tested in this earlier static IE work. Indeed, only DETPMP and Hexa-P were tested (Boak et al., 1999; Sorbie et al., 2000; Graham et al., 1997a, 2003; Yuan et al., 1998). Some previous studies have investigated the impairment of SI function by commonly used organic anions such as $EDTA^{4-}$, citrate and gluconate (Barthorpe, 1993; Yuan et al., 1998). These anions may be used as scale dissolvers or as additives in a SI formulation, thus operating simultaneously with SI in field brines (Barthorpe, 1993; Yuan et al., 1998). As a result of the

work described in this thesis, the range of phosphonate SIs examined in barium sulphate IE tests has now been increased to 9. In the experiments described in this thesis, in Chapter 5, eight phosphonate SI products are tested over a *wide range* of NSSW/FW mixing ratios (i.e. barite SR and molar ratio Ca^{2+}/Mg^{2+} varying) whereas previously, only one mixing ratio was routinely tested, usually the highest SR mixing ratio, or near to this, e.g. 60/40 or 50/50 Base Case NSSW/FW, meaning Ca^{2+}/Mg^{2+} was *not* varied in these tests (Boak et al., 1999; Sorbie et al., 2000; Graham et al., 1997a, 2003), and so the full significance of Ca^{2+}/Mg^{2+} effects on MIC were unknown. In previous work it was generally accepted that a 60/40 NSSW/FW Base Case static IE test always represented the "worst case" scenario – but the findings of this thesis illustrate that this is usually *not* true. From the IE results presented in this thesis, it is now known that only testing one brine mixing ratio (as done in previous work) is unsatisfactory because it neglects the possible effects of Ca^{2+} and Mg^{2+} on IE, which can be severe. The work undertaken in this thesis has shown that the "worst case" is more often Base Case 80/20 NSSW/FW (Type 2 SIs), rather than 60/40 NSSW/FW (Type 1 SIs) – see Chapter 5. The best example of this is EDTMPA (Type 2) which had a 22 hour 80/20 NSSW/FW Base Case MIC = ~400ppm. The work presented in this thesis has shown that the majority of SIs (phosphonates and polymers) are very sensitive to Ca^{2+} and Mg^{2+} (Type 2 products). This property can be a benefit or detrimental, depending on the circumstances and field conditions, etc.

From earlier work, it was known generic SIs, e.g. PPCA and PVS are also improved by Ca^{2+} but not as much as phosphonates (Boak et al., 1999; Sorbie et al., 2000; Graham et al., 1997a, 2003; Sorbie and Laing, 2004). This statement is still true, but in the new work described in this thesis, a range of 9 different polymers are tested in the same way as 8 different phosphonates, in that they are tested over a wide range of NSSW/FW mixing ratios, fully investigating the effects of SR and Ca^{2+}/Mg^{2+} on MIC. This was not done in previous work testing polymers (Boak et al., 1999; Sorbie et al., 2000; Graham et al., 1997a, 2003; Sorbie and Laing, 2004; Yuan et al., 1997a, 1998; Yuan, 2001, 2002). Prior to this PhD, it was also known SIs operated by two mechanisms (Boak et al., 1999; Gill, 1996; Graham et al., 1997a; 2003; Sorbie et al., 2000; Sorbie and Laing, 2004; Yuan et al., 1998): These mechanisms are nucleation inhibition and crystal growth retardation. All SIs operate by both mechanisms but to varying degrees. These two statements are still true, however the work presented in this thesis also illustrates that SI chemical structure plays a very important role with regard to

barium sulphate IE – particularly the inclusion of amino methylene phosphonate functional groups – this increases the molecules metal chelation ability (see Chapter 12). Chapter 12 also conjectures reasons for differences between the IE performance of chemically similar SIs, for example DETPMP and HMTPMP. In previous IE work, no comparisons were made between the IE of chemically similar species such as these two pentaphosphonates (Boak et al., 1999; Gill, 1996; Graham et al., 1997a; 2003; Sorbie et al., 2000; Sorbie and Laing, 2004; Yuan et al., 1998). HMTPMP was not tested in previous barite IE work at all. From earlier work, it was known polymers perform better (lower MIC) in dynamic tests (TBR) whereas phosphonates perform better in static tests – this relates to inhibition mechanisms (Sorbie et al., 2000). This statement is still true – TBR tests examine early residence time IE, therefore polymers give better results, even although in field conditions, they may not be the best choice (Sorbie et al., 2000).

A large proportion of the static IE results presented in this thesis involve the assay of SI in solution at various residence times (in addition to Ba^{2+}), these experiments are referred to as SI consumption experiments. Hundreds of these tests have been carried out during this PhD, testing a total of 15 different SIs (of the SIs described in this thesis, only EABMPA, CTP-A and CTP-B are excluded from these tests). In earlier work, only DETPMP, Hexa-P and PPCA were tested in this way (Graham et al., 1997a; 2003; Sorbie et al., 2000). In this thesis, PVS, VS-Co, MAT, PFC and PPCA are tested in consumption experiments and SI assayed by a non-ICP analytical method such as Hyamine or Pinacyanol (see Chapter 11). Non-ICP methods were not used to assay SI in these tests in previous work (Graham et al., 1997a; 2003; Sorbie et al., 2000). In previous work, PVS, VS-Co and MAT were not tested at all in consumption experiments because they are non-ICP detectable. PVS and VS-Co could be detected by ICP by means of [S]; however this cannot be done in these IE tests due to the sample matrix containing sulphate anions and PVS quenching solution.

Prior to this thesis, there was no classification system for SIs (i.e. Type 1 or Type 2 and Type A or Type B), based on their performance in static IE experiments (Boak et al., 1999; Graham et al., 1997a; 2003; Sorbie et al., 2000; Sorbie and Laing, 2004). The systematic classification of barite SIs is an entirely new and useful concept which can be applied to *any* scale inhibitor, even if the chemical nature of the SI is unknown, e.g. PFC. A total of 18 chemically different products are tested in the work described in this thesis – 9 phosphonate

SIs and 9 polymeric SIs. A study as detailed and extensive as the work described in this thesis has never been undertaken before, investigating the effects of barite SR, Ca^{2+}/Mg^{2+} and pH on static barium sulphate IE. There is also very little literature proposing mechanistic explanations for differences in barium sulphate IE between different SI products – particularly phosphonate SIs. Several papers propose structures for metal-phosphonate complexes (Sawada et al., 1986, 1988, 1991, 1993a, 1993b, 2000; Martell 1971a, 1971b; Ockerbloom and Martell 1957), but this is *not* related to static barium sulphate IE performance. Only metal chelation is discussed in the quoted literature. The metal complexation chemistry of PPCA (a polymeric SI) is discussed by Xiao et al. (2001). In Chapter 12 of this thesis, the relationship between phosphonate SI structure and static IE is conjectured. Again, this concept is entirely new. It has never been attempted by any other workers.

1.7 Aim of this Thesis

The aim of this thesis is to improve understanding of:

(i) barium sulphate inhibition by phosphonate and polymeric SIs,

(ii) the role of Ca^{2+} and Mg^{2+} in the inhibition process and their effect upon MIC,

(iii) the effect and importance of pH with regard to the function of various SIs and effect upon MIC,

(iv) the fate of SI during static IE experiments (in addition to measuring IE),

(v) the role of chemical structure of the various SIs (phosphonates and polymers) on their IE and the effect of Ca^{2+} and Mg^{2+} on this IE behaviour.

All 18 SIs (except EABMPA) have been tested in static barium sulphate IE "MIC vs. NSSW/FW mixing ratio" tests where the MIC is determined for various saturation ratios and consequently, brine molar ratios Ca^{2+}/Mg^{2+} (Base Case tests). These experiments are then repeated at fixed molar ratio Ca^{2+}/Mg^{2+}, and the MICs determined again (Fixed Case tests). All SIs (except EABMPA, CTP-A and CTP-B) have been assayed during static IE experiments to determine the fate of SI (in addition to IE at each sampling time) – these are referred to as SI consumption experiments (Chapters 9 and 10). In such experiments, usually SI can be assayed by means of ICP spectroscopy if they contain phosphorus, however,

products which are phosphorus-free must be assayed by a different analytical method. Non-phosphorus containing SIs MAT, PVS and VS-Co are assayed by the Hyamine and Pinacyanol analytical methods – this is discussed in Chapter 11. In Chapter 7, selected products are tested for IE at different pH levels: 4.5, 5.5, 6.5 and 7.5. The chemical analysis of SI products (% phosphorus, % sulphur), etc. is presented in Chapter 4. The relation between static barium sulphate IE and SI chemical structure is discussed in Chapter 12.

1.8 Structure of the Thesis

Chapter 2 (Literature Review) discusses how scale inhibitors work and the known generic effects of divalent ions Ca^{2+} and Mg^{2+} , temperature and pH on generic SI species (PVS, PPCA, DETPMP). Uninhibited (SI-free) scale formation mechanisms (homogeneous and heterogeneous nucleation and crystal growth), the effect of M^{2+} on calcium carbonate scaling and surface deposition studies are also reviewed.

Chapter 3 (Experimental Details) gives the brine compositions and reagent compositions used for all experiments described in this thesis. The laboratory synthetic brine preparation procedure is described. The scale inhibitor structures are listed (phosphonates and polymers). 3-dimensional models of all the phosphonate SIs are also presented.

Chapter 4 (Chemical Analysis of Scale Inhibitor Products) presents experimental results on the chemical analysis of SI products for % phosphorus, % sulphur, sodium, potassium, calcium and magnesium content. The pH of the various SI stock solutions is also measured. The implications of these test results with regard to the assay of these SIs during IE experiments is discussed and some comments are made on their environmental "friendliness".

Chapter 5 (MIC vs. Mixing Ratio NSSW/FW Experiments – Phosphonate SIs) presents an extensive series of experimental results, testing all 9 phosphonate SIs (except EABMPA) in MIC vs. % NSSW tests. In these tests, the 2 and 22 hour MIC is measured for each SI under "Base Case" and "Fixed Case" experimental conditions, as described in Section 1.7. In these experiments, the influence of the molar ratio Ca^{2+}/Mg^{2+} on MIC is examined in detail for each of the species tested.

Chapter 6 (MIC vs. Mixing Ratio NSSW/FW Experiments – Polymeric SIs) presents an extensive series of experimental results, testing all the polymeric SIs in MIC vs. % NSSW tests, in the same way as for the phosphonates in Chapter 5. In addition, compatibility experiments are carried out testing PPCA and additional IE tests varying the molar ratio Ca^{2+}/Mg^{2+} in the brine mix are presented for PPCA, SPPCA, MAT, CTP-A and CTP-B.

Chapter 7 (Inhibition Efficiency Experiments – Varying pH) presents a selection of IE experiments carried out at pH 4.5, 5.5, 6.5 and 7.5 under Base Case and Fixed Case conditions. All other test conditions are kept constant at T=95^{o}C, mixing ratio = 80/20 NSSW/FW. The aim of these experiments is to investigate the effect of pH on SI IE and MIC. The SIs DETPMP, HMTPMP, EDTMPA and PPCA are tested.

Chapter 8 (Mild Scaling Conditions – IE Experiments) presents IE results similar to Chapter 5, testing DETPMP, HMTPMP and PPCA, except here, the $[Ba^{2+}]$ in the Forties FW is lower, $[Ba^{2+}]$ = 100ppm. This is a mild scaling system. Once again MIC is measured for selected mixing ratios NSSW/FW, under Base Case and Fixed Case conditions.

Chapter 9 (SI Consumption Experiments – Phosphonates) presents a selection of IE experiments involving multiple sampling times (~10), over extended residence times, where the [SI] is assayed at each sampling time (in addition to $[Ba^{2+}]$) – testing phosphonate SIs OMTHP, DETPMP, HMTPMP, HMDP, EDTMPA, NTP, HEDP and HPAA. SI is assayed by ICP spectroscopy by means of [P]. In some cases, Environmental Scanning Electron Microscopy (ESEM) images and Energy Dispersive X-Ray Analysis (EDAX) analyses of the scale deposits which had formed in each test bottle (blanks and SI-containing), are also obtained.

Chapter 10 (SI Consumption Experiments – Polymers) presents a selection of IE experiments involving multiple sampling times (~10), over extended residence times, where the [SI] is assayed at each sampling time (in addition to $[Ba^{2+}]$) – testing polymeric SIs PPCA, SPPCA, PFC and PMPA. SI is assayed by ICP spectroscopy – all polymers tested here are phosphorus-containing.

Chapter 11 (SI Consumption Experiments – Polymers – Analysis of SI by Non-ICP Analytical Methods) presents a selection of IE experiments involving multiple sampling times (~10), over extended residence times, where the [SI] is assayed at each sampling time (in addition to [Ba^{2+}]) – testing specific polymeric SIs. Phosphorus-containing polymers PPCA and PFC are assayed by ICP spectroscopy (by means of [P]) *and* by the C18/Hyamine/spectrophotometric (CHS) analytical technique (for PPCA) or Pinacyanol/spectrophotometric (PS) analytical technique (for PFC). ICP SI assay results are compared with results obtained by CHS and PS. Non-P-tagged, "green" polymer MAT is assayed exclusively by the CHS method, and sulphonated species PVS and VS-Co are assayed exclusively by the PS method. The PS analytical method is suitable for the assay of sulphonated polymers whereas the CHS method is suitable for the assay of non-sulphonated polymers only.

Chapter 12 (Explaining Scale Inhibition: Chemical Structures and Mechanisms) presents an extensive range of possible SI-metal complex structures for all 18 phosphonate and polymeric SIs (except PFC) tested in static barium sulphate IE tests and discusses the various experimental factors, such as pH, which affect the formation of such structures. The mechanistic relation between observed static IE and these conjectured complex structures is discussed in detail. Conclusions are given regarding which SI chemical structural properties give rise to the best IE, etc.

Final conclusions and recommendations for future work are presented in **Chapter 13.**

Chapter 2: Literature Review

Chapter 2 Summary: This Chapter presents a survey of published work on barium sulphate inhibition efficiency (IE) mechanisms and divalent ion (Ca^{2+}/Mg^{2+}) effects upon IE, relevant to the experimental work presented herein. Topics reviewed include mechanisms of barium sulphate scale formation (in the absence of SI), SI dissociation and speciation, including binding to Ca^{2+} and Mg^{2+}, temperature and pH effects upon barium sulphate SI functionality. Laboratory methods for determining SI binding constants to M^{2+} ions are discussed. Nucleation inhibition and crystal growth retardation inhibition mechanisms are discussed and the advantages and disadvantages of deploying phosphonate and polymeric type SIs in the field are considered. The general properties of phosphonate and polymeric SIs are discussed along with the mechanisms by which they operate. The effect of SI on crystal morphology is also discussed. The effect of Mg^{2+} on calcium carbonate inhibition is reviewed and surface deposition studies are discussed.

2.1 Mechanisms of Scale Formation

2.1.1 Introduction

Precipitation of barium sulphate occurs in produced waters due to the barium and sulphate ions being supersaturated in solution (Bedrikovetsky et al., 2004; Fan et al., 2011; Gill, 1996). This means there are higher concentrations of barium and sulphate ions present in solution compared to the concentrations which would normally be present at equilibrium. There are three steps in the precipitation process: (i) achievement of supersaturation; (ii) nucleation; and (iii) growth of the nuclei to form particles (Gill, 1996). In the case of barium and sulphate ions, at equilibrium, only a trace of barium ions are left in solution in a blank test sample. This is due to the fact that the solubility of barium sulphate is extremely low, and the thermodynamic driving force for barium sulphate formation is so high. At equilibrium, barium is almost completely depleted from solution in a closed system, e.g. in a static IE test. There are slight variations in the barium sulphate solubility at different temperatures – solubility increases at higher temperatures (Nancollas, 1985). On the other hand, calcium carbonate becomes less soluble at higher temperatures (Nancollas, 1985). The

kinetics of barium sulphate formation is extremely slow. This is because there is a high tendency for barium sulphate to form *metastable* supersaturated solutions (Nancollas, 1985). If metastable supersaturated solutions exist, this delays precipitation. The supersaturation level is affected by changes in temperature (Laing et al., 2003; Sorbie and Laing, 2004; Yuan, 2002), pressure and pH, all of which may change during oil production. Saturation ratio and supersaturation are synonymous terms. For a supersaturated brine system there are a number of mechanisms involved in scale formation, these are: homogeneous nucleation, heterogeneous nucleation and subsequent crystal growth. These mechanisms occur in both uninhibited (SI free) and SI-containing systems. Each of these mechanistic steps are described in detail below.

2.1.2 Homogenous Nucleation

In a homogenous nucleation process, the formation of the solid phase is throughout the liquid phase without any foreign solid phase being present (Chen et al., 2005a). For initial homogeneous nucleation, there are two enthalpy terms that control this process (Naono, 1967; Nancollas, 1985). These relate to the favourable free energy pertaining to the release of supersaturation and an opposing (unfavourable) free energy which relates to the creation of a surface and the resultant free energy terms are illustrated in Figure 2.1. In supersaturated systems, agglomeration of scaling ions to a critical size leads ultimately to precipitation as the supersaturation is released. However, in mildly supersaturated solutions, the unfavourable free energy due to the creation of a surface can lead to the dissolution of agglomerated particles and in this manner supersaturated systems can remain *metastable* for long periods of time. For example, in a blank static IE test bottle, barite does not fully precipitate instantaneously, the reaction takes several hours before equilibrium is reached (or before the supersaturation is fully released). In a static IE test blank bottle, at 2 hours there is usually still a significant quantity of barium cations in solution – the exact concentration depends upon the NSSW/FW mixing ratio being tested. For higher %NSSW mixing ratios, there is likely to be less [Ba^{2+}] in solution because the initial [Ba^{2+}] is less. Invariably, at 22 hours, there is only a trace of Ba^{2+} left in solution (<< 1ppm), since by which time, the supersaturation of the system has been fully released.

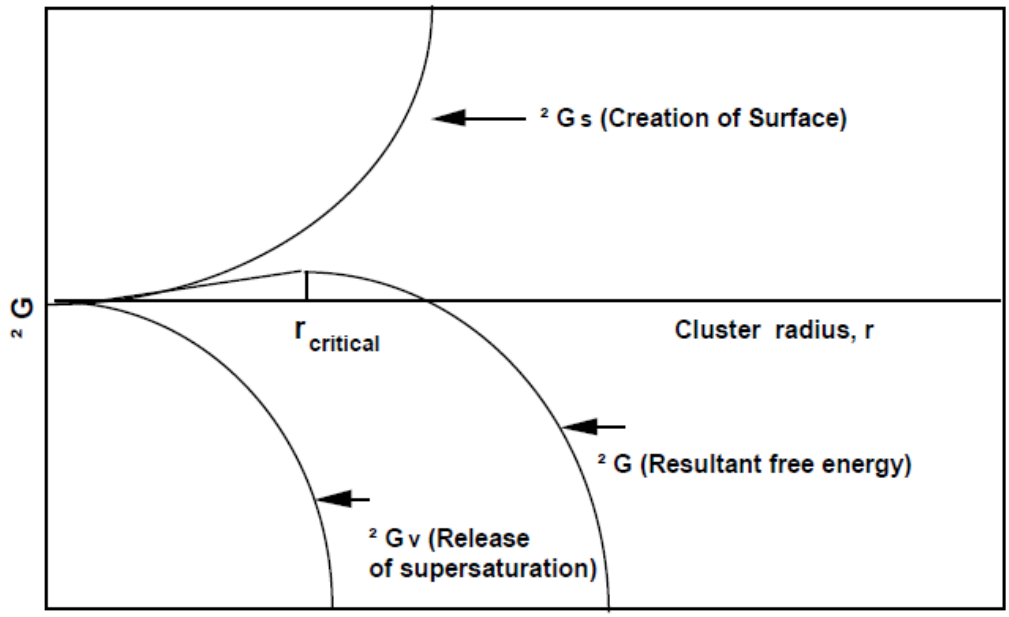

Figure 2.1 – Free energy of nucleation as a function of cluster radius (Nancollas, 1985, p.150, fig.1).

2.1.3 Heterogeneous Nucleation

In field production scenarios it is recognised that precipitation is more likely to occur on surfaces which are already present in the system (Nancollas, 1985). Such surfaces may be existing scale deposits, metal surfaces offering available sites for adsorption of lattice ions (production equipment, pipelines etc.) or the rock formation itself. Heterogeneous nucleation on such surfaces is more favourable than homogeneous nucleation since the free energy barrier (due to the creation of a surface) has been significantly reduced (Nancollas, 1985). This is illustrated schematically in Figure 2.2 which shows that heterogeneous nucleation will generally require a lower supersaturation than that required for homogenous nucleation to occur (Nancollas, 1985).

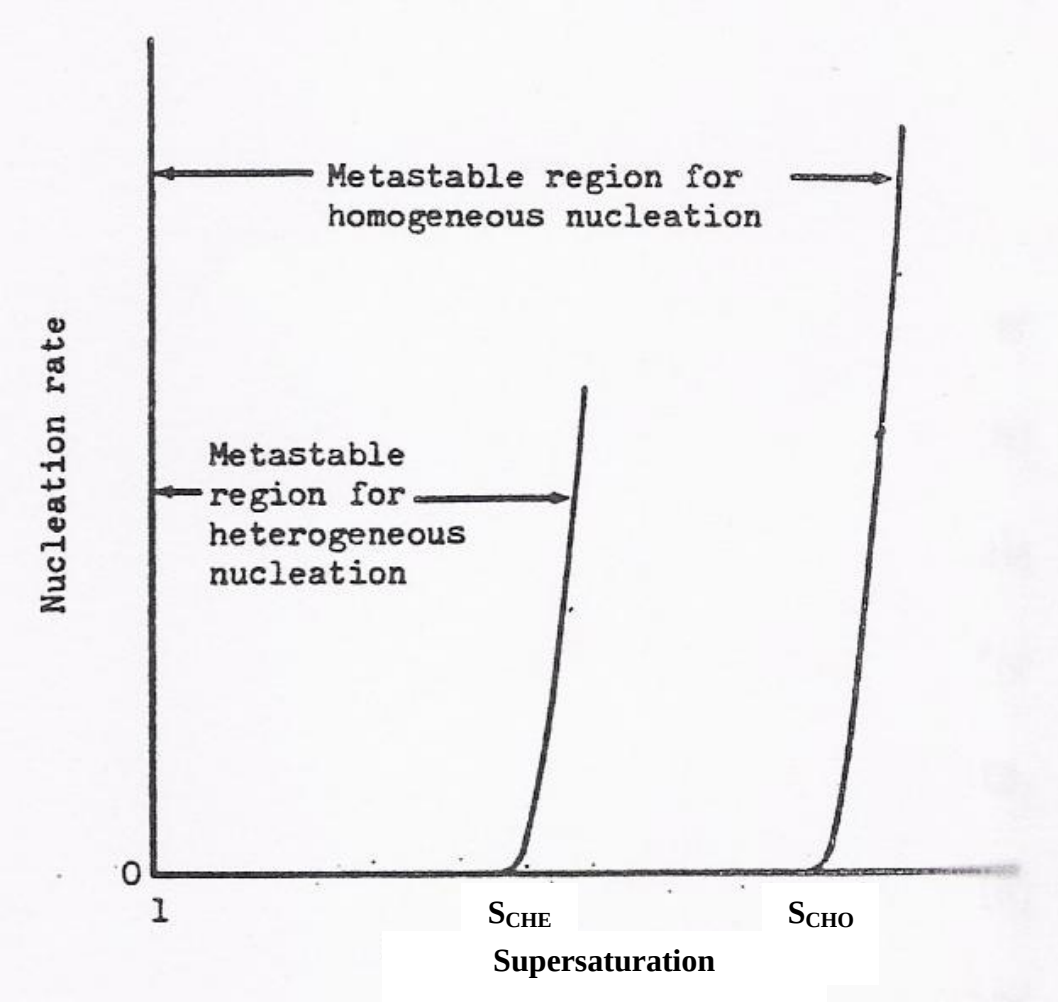

Figure 2.2 – Nucleation rate plotted against supersaturation (Nancollas, 1985, p.150, fig.2).

The nucleation rate is extremely sensitive to supersaturation, as shown in Figure 2.2. The supersaturation level at which the rate of heterogeneous nucleation increases rapidly is known as the critical supersaturation for homogenous nucleation (S_{CHO}) and the supersaturation level at which the rate of heterogeneous nucleation increases rapidly is known as the critical supersaturation for heterogeneous nucleation (S_{CHE}). S_{CHO} and S_{CHE} are shown schematically in Figure 2.2 ($S_{CHE} << S_{CHO}$). Heterogeneous nucleation can be explained as the formation of new solid phase particles catalysed by the presence of a foreign solid phase, for example, a metal surface (Chen et al., 2005a). However, this may not be the best explanation, since the solid surface offering available sites for adsorption of lattice ions can also be existing mineral scale deposits (Nancollas, 1985). Existing mineral scale may not be considered a "foreign surface" because it is chemically the same as the ions in solution (only in a different phase,

i.e. solid). The presence of suitable adsorption sites, e.g. metal surfaces, encourages precipitation, and reduces the likelihood of metastability (Nancollas, 1985). This is shown schematically in Figure 2.3. In Figure 2.3, "E" represents potential energy, e.g. supersaturation, and "X" represents time. In this generic figure, state (1) could represent a *homogenous* barium sulphate supersaturated system (high supersaturation); state (2) could represent the creation of a nucleation surface (adsorption site, e.g. metal surface). This step requires *some* energy; and state (3) could represent a *heterogeneous* barium sulphate supersaturated system (which is of lower energy).

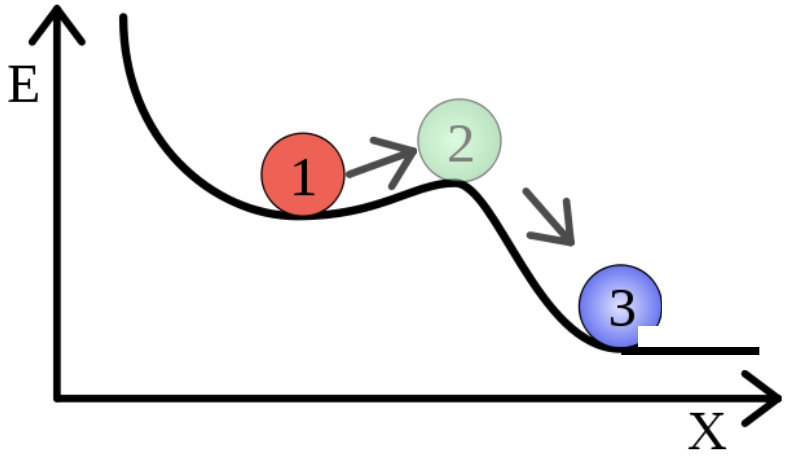

Figure 2.3 − A metastable system with a weakly stable state (1), an unstable transition state (2) and a strongly stable state (3). [1]

In laboratory static IE tests, the mechanism of barite precipitation is likely to be primarily homogenous nucleation; however, the attainment of "homogenous" nucleation conditions is very difficult to achieve even when extreme precautions are taken to exclude impurities and foreign particles from solutions (Nancollas and Reddy, 1974). In static barium sulphate IE tests, the only available surfaces for heterogeneous nucleation are (i) plastic interior surface of the test bottles (HDPE), or (ii) existing scale deposits (containing $Ba/Sr/SO_4$). Foreign substances and dust particles can readily act as sites for the formation of the precipitating phase (Nancollas and Reddy, 1974), thereby permitting heterogeneous nucleation. For this reason, all brines used in static barium sulphate IE tests are filtered through 0.45µm membrane filter paper prior to use in tests (see Section 3.3). This is standard laboratory procedure (FAST EPM, IPE, HWU, 2006).

2.1.4 Crystal Growth

After nucleation has occurred either by means of homogeneous nucleation or heterogeneous nucleation, crystal growth will occur until the supersaturation of the system is completely released (Nancollas and Liu, 1975). The surface of crystalline solids such as barium sulphate is heterogeneous with new growth occurring preferentially on certain crystal faces, and then only at certain surface active sites (Liu and Griffiths, 1979). Active sites can be kinks or steps on the crystal surface (Nancollas, 1985) as illustrated schematically in Figure 2.4. Such active growth sites allow further growth because collision of solution ions at these sites leaves the colliding ions effectively in contact with several surface ions enabling strong bonds to be formed. Scaling ions which land on flat areas of surface have the propensity to bounce back into solution (due to weaker/fewer contact points) or move around the surface until they are effectively trapped by multiple binding at the active growth sites (Nancollas and Reddy, 1974).

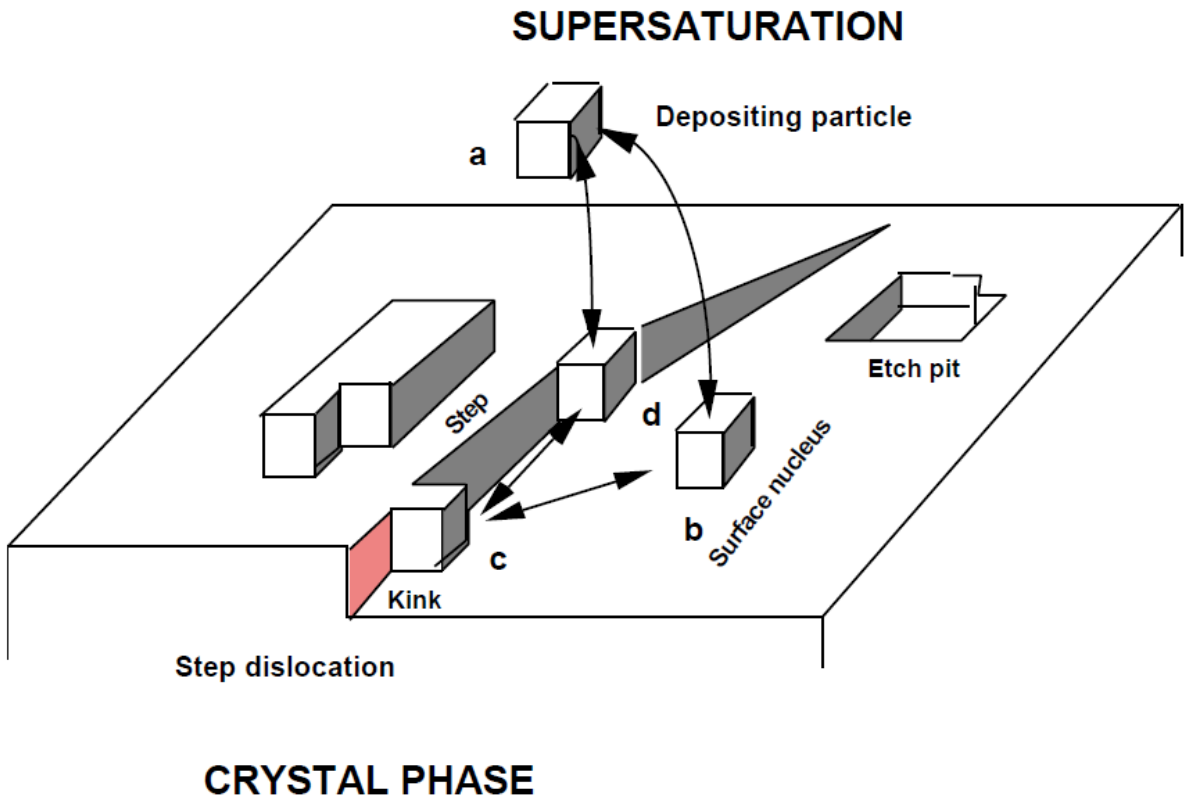

Figure 2.4 – Representation of a crystal surface complete with defects (Nancollas, 1985, p.152, fig.3).

2.2 SI Speciation and Binding to Ca^{2+} and Mg^{2+}

Work from the FAST group at Heriot-Watt U. has indicated that phosphonate SI bonded to Mg^{2+} is rendered ineffective and only Ca^{2+} bonded SI is freely available for barium sulphate scale inhibition (Boak et al., 1999; Graham et al., 1997a, 2003; Sorbie et al., 2000; Sorbie and Laing, 2004). Other workers have reported similar findings on the effect of Ca^{2+} on phosphonate SIs, whereby Ca^{2+} enhances the static IE (Sweeney and Cooper, 1993). Ca^{2+} also improves the adsorption properties of phosphonate SIs onto many substrates such as consolidated and crushed sandstone, by providing a "bridge" between anionic (i.e. dissociated) scale inhibitors and the substrate (Sorbie et al., 1993). This property is important for SI "squeeze treatments" to improve SI retention (Bunney et al., 1997; Jordan et al., 1994, 1996; Montgomerie et al., 2009). Similar effects of Ca^{2+} and Mg^{2+} upon the IE of polymeric SIs have been reported (Boak et al., 1999; Graham et al., 1997a, 2003; Sorbie and Laing, 2004). However, in the case of PPCA, it has been reported that IE decreases in brine containing high levels of Ca^{2+}, e.g. ~2000ppm+ [Ca^{2+}] (Graham et al., 2003; Shaw et al., 2010b). The ability of a phosphonate SI to complex successfully with metal ions, M^{2+}, depends on the speciation of the SI which depends strongly on pH (see Section 2.3.2). Other less abundant cations (in oilfield brines), for example, Fe^{2+} are also know to influence the IE of phosphonate and polymeric SIs (Stoppelenburg and Yuan, 2000; Smith et al., 2008), however this subject is not discussed in this thesis because it is of less importance in practical applications. The main cations of interest are Ca^{2+} and Mg^{2+} which are both present in high concentrations in oilfield brines. Brine compositions are given in Chapter 3.

The reason for the Mg "poisoning" of the SI is thought to be due to the fact that SI−Mg^{2+} complex is *not* incorporated into the growing barite scale lattice whereas Ca^{2+} bonded SI *and* "free" non-SI bonded Ca^{2+} *does* have this ability (Sorbie and Laing, 2004). It has been reported that in an uninhibited solution (containing no SI), ~6% of the Ba^{2+} can be substituted by Ca^{2+} (Sorbie and Laing, 2004). Figure 2.5 shows the calcium inclusion (molar ratio Ca/Ba) into barite in an uninhibited solution at three temperatures: 5, 50 and 95^{o}C with varying initial [Ca^{2+}] in the brine (Sorbie and Laing, 2004). Clearly, there is greater calcium inclusion when the initial brine [Ca^{2+}] is higher and this is consistent with what is found in this work in the EDAX analyses of scale deposits (Chapter 9). Furthermore, the presence of SI generally increases the % Ca inclusion up to ~12% (Sorbie and Laing, 2004). Figure 2.5 also shows Ca^{2+} inclusion increases at lower temperatures. In order to inhibit barium

sulphate crystal growth, SI must incorporate into the growing scale and this is why Mg^{2+} is detrimental whereas Ca^{2+} is beneficial to the function of phosphonate SIs (Sorbie and Laing, 2004). This mechanistic view is illustrated schematically in Figure 2.6.

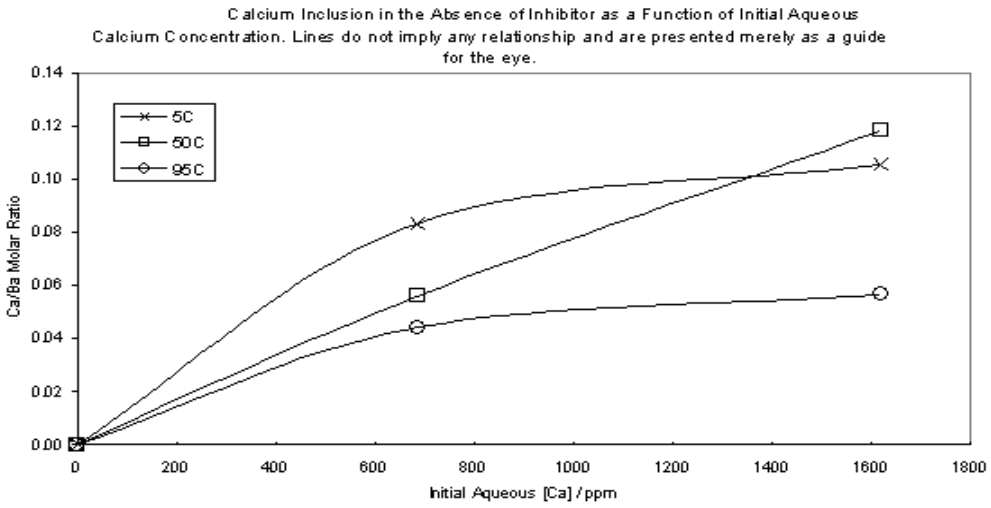

Figure 2.5 – Calcium inclusion, Ca/Ba molar ratio vs. initial [Ca^{2+}] (Sorbie and Laing, 2004).

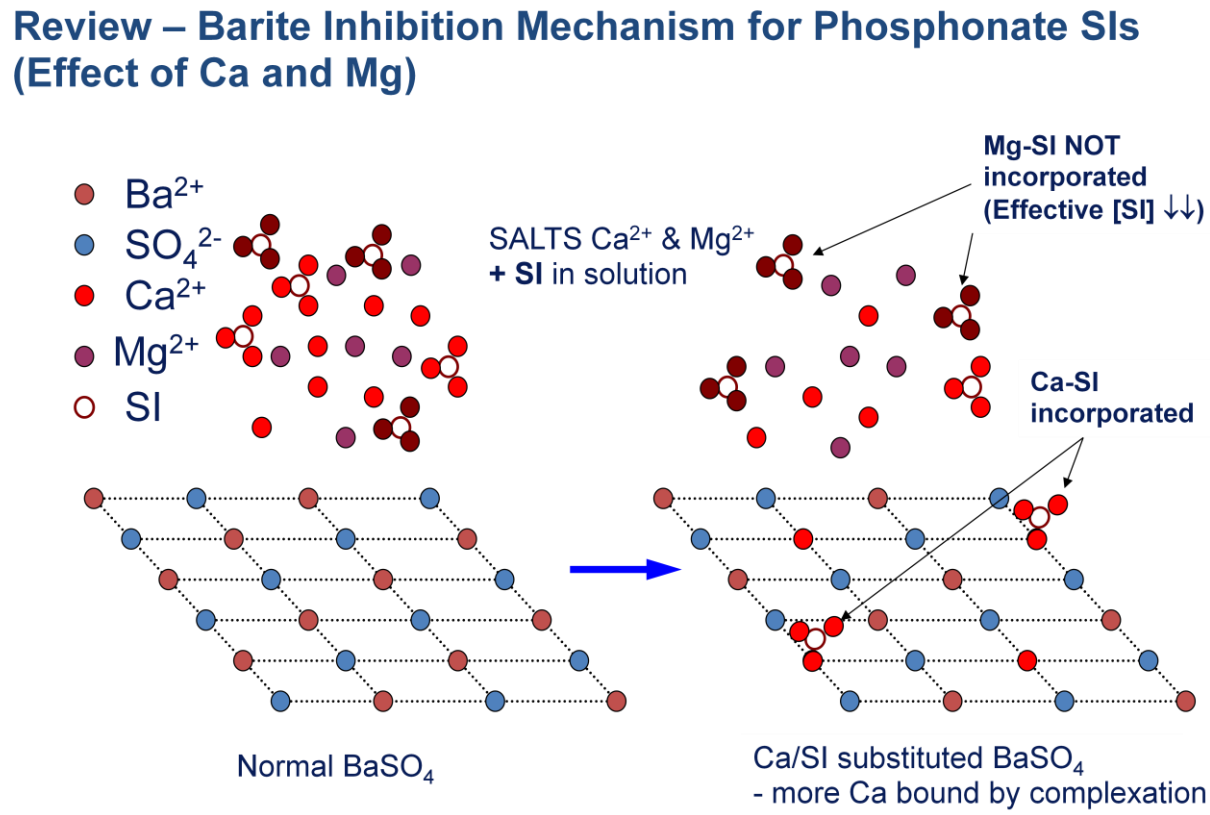

Figure 2.6 – Schematic diagram illustrating phosphonate SI Ca-SI inclusion into the barite lattice and Mg-SI "poisoning" (Sorbie and Laing, 2004).

Neither Mg^{2+} nor SI bound Mg^{2+} can be incorporated into the growing barite lattice due to the small size of the Mg^{2+} cation, in comparison to divalent cations which can, i.e. Ca^{2+} and Sr^{2+}. In order to explain this fully, the physical size of these cations must be compared with the size of sulphate anions. A compound is most likely to be insoluble, i.e. precipitate, if the anions and cations are similarly sized because this maximises the forces of attraction between the oppositely charged ions. Whether a compound is soluble or insoluble in water depends on the magnitude of two enthalpy terms: (i) forces of attraction between ions of the solid and water molecules (enthalpy of hydration), and (ii) forces of attraction between the oppositely charged ions in the solid (enthalpy of formation). If (ii) > (i), the compound will be insoluble [2]. Barium sulphate is an extremely stable compound because the barium and sulphate ions are similarly sized, thus maximising the forces of attraction between anions and cations. Table 2.1 presents the ionic radii of divalent cations Mg^{2+}, Ca^{2+}, Sr^{2+} and Ba^{2+} [3]. Sr^{2+} has an ionic radius ~16pm < Ba^{2+}, Ca^{2+} has an ionic radius ~37pm < Ba^{2+}, and Mg^{2+} has an ionic

radius ~65pm < Ba^{2+}. $MgSO_4$ is very soluble due to the fact that Mg^{2+} and SO_4^{2-} ions cannot pack together in a thermodynamically favourable arrangement. On the contrary, Ba^{2+} and Sr^{2+} and Ca^{2+} can pack together efficiently with SO_4^{2-}. This packing efficiency *increases* on going down Group II, hence the reason why the solubility of the M^{2+} sulphates decreases. This also explains why barite is the *hardest* scale – because Ba^{2+} and SO_4^{2-} can pack together the most efficiently. If SI is bound to any of these Group II divalent cations, the SI becomes incorporated into growing barite scale in conjunction with the M^{2+} cation only if the size of the M^{2+} cation is similar to Ba^{2+}. This explains why only SI bound to Ca^{2+}, Sr^{2+} or Ba^{2+} can inhibit further crystal growth. Since there is always $[Ca^{2+}] >>> [Sr^{2+}]$ and $[Ba^{2+}]$ in laboratory and field conditions – this is why it is predominantly Ca^{2+} which is involved in this inhibition mechanism. Higher levels of Sr^{2+} in laboratory brines may also improve barite IE in a similar way to Ca^{2+}, but this is just conjecture. Although this test could be done in the laboratory, it would have less field relevance because the levels of Sr^{2+} in field brines are obviously << Ca^{2+}. If, for example, in a laboratory test, Ca^{2+} is replaced by Sr^{2+} in synthetic brines, similar effects on barite IE may be observed, whereby higher $[Sr^{2+}]$ levels improve barite IE. This could be investigated by future researchers. Note that strontium sulphate is easily inhibited by barite SIs, and is also more soluble than barite.

Element	**Ionic Radius, M^{2+} (picometres)**
Magnesium	78
Calcium	106
Strontium	127
Barium	143

Table 2.1 – Ionic Radii of Mg^{2+}, Ca^{2+}, Sr^{2+} and Ba^{2+} (picometres) [3].

Table 2.2 presents the enthalpy of formation values (kJ/mol) for Mg, Ca, Sr and Ba sulphates at 298K and 1 atm. (Majzlan et al., 2002; [4]). ΔH_f for $MgSO_4$ (~ −1280 kJ/mol) [4] is ~150 to ~190 kJ/mol < ΔH_f for Ca, Sr and Ba sulphates (−1434 to −1473 kJ/mol). This indicates that the $MgSO_4$ crystal lattice is less stable than Ca, Sr and Ba sulphates and $MgSO_4$ is the easiest compound to solubilise. The more large and negative the ΔH_f term is, the more likely the Gibbs free energy change (ΔG) for the reaction will be negative. The more negative the ΔG term is, the more favourable the chemical reaction will be. ΔG is defined by Equation 2.1 at a fixed T (K). If ΔG is not negative, the reaction will not occur at the T in question. All

precipitation reactions from solution involve a decrease in entropy (S); therefore the term ΔS is always going to be negative. If TΔS in Equation 2.1 is negative, this will make ΔG more positive. In the cases discussed here, $-\Delta H_f > -T\Delta S_f$ only for barium and strontium sulphates at 298K, thus these precipitation reactions are spontaneous at room temperature.

Sulphate	**ΔH_f / kJ/mol** *	**Reference(s)**
Magnesium	−1278	[4]
Calcium	−1434 / −1435	Majzlan et al., 2002 / [4]
Strontium	−1452	Majzlan et al., 2002
Barium	−1465 / −1473	Majzlan et al., 2002 / [4]

*Rounded off to nearest whole number.

Table 2.2 – Enthalpy of Formation (ΔH_f) of Mg, Ca, Sr and Ba sulphates at 298K, 1 atm. (Majzlan et al., 2002 / [4]).

$$\Delta G = \Delta H - T\Delta S \qquad \text{(Eq. 2.1)}$$

Where: T = temperature (K); ΔG = Gibbs free energy change (kJ/mol); ΔH = Enthalpy change (kJ/mol); and ΔS = Entropy change (kJ/mol).

For DETPMP, the binding constants to Mg^{2+} (K_{Mg}), Ca^{2+} (K_{Ca}) and Ba^{2+} (K_{Ba}) are known to be 6.3 x 10^{10}, 5.0 x 10^{10} and 1.58 x 10^{8} respectively (Sorbie and Laing, 2004). The pH and temperature conditions are not specified for these binding constants, but they are still informative and suitable for modelling purposes. The binding constants K_{Mg}, K_{Ca} and K_{Ba} are defined by Equations 2.2 to 2.7, where x_i denotes the equilibrium activity of species i, where i = Ca.A, Mg.A, Ba.A, Ca, Mg, Ba or A. It follows that, when SI is present in brine containing Ca^{2+} and Mg^{2+}, virtually all SI will exist complexed with one of these divalent cations, based on the magnitude of these binding constants, i.e. there will be almost no uncomplexed, "free" SI (denoted A). The binding constants for other phosphonate SI species to Ca^{2+} and Mg^{2+} are not known, but laboratory methods for determining these constants experimentally may be possible. All SI-metal binding constants are *pH and temperature dependant*, including those quoted for DETPMP above.

$$Ca + A \underset{}{\overset{K_{Ca}}{\rightleftharpoons}} Ca.A \qquad \text{(Eq. 2.2)}$$

$$Mg + A \overset{K_{Mg}}{\rightleftarrows} Mg.A \qquad \text{(Eq. 2.3)}$$

$$Ba + A \overset{K_{Ba}}{\rightleftarrows} Ba.A \qquad \text{(Eq. 2.4)}$$

$$K_{Ca} = \frac{x_{Ca.A}}{x_{Ca} x_A} \qquad \text{(Eq. 2.5)}$$

$$K_{Mg} = \frac{x_{Mg.A}}{x_{Mg} x_A} \qquad \text{(Eq. 2.6)}$$

$$K_{Ba} = \frac{x_{Ba.A}}{x_{Ba} x_A} \qquad \text{(Eq. 2.7)}$$

A wide range of experimental methods have been applied to the determination of ligand-metal binding constants to ions such as Ca^{2+} and Mg^{2+}. These methods include potentiometry, spectrophotometry, NMR and acid-base titrations. (Billo, 2001). The majority of ligands, including dissociated phosphonate SIs are weak bases. Phosphonate SIs can be protonated, i.e. associated by acidification and then titrated with base. The formation of SI–M^{2+} complex clearly involves competition between the metal cations and protons for the anionic ligand base. The progress of this reaction can be monitored by measuring continuously the pH of an acidified phosphonic acid / metal ion solution. Each rise in pH corresponds to the formation of a metal complex with the progressively dissociating ligand because the protons have been displaced by M^{2+}. As in any acid-base titration, the protons removed from the SI react with base to produce water molecules. Most commonly, a solution containing metal ion, ligand (e.g. phosphonate SI solution), and acid is titrated with base (e.g. NaOH) (Billo, 2001).

2.3 Temperature and pH Effects on Generic SI Functionalities (PVS, PPCA, DETPMP)

2.3.1 Temperature

It is known that sulphonated polymers and co-polymers such as PVS and VS-Co perform better at lower temperatures, e.g. 5^{o}C, whereas the converse is true of phosphonates (Cushner et al., 1988; Laing et al., 2003; Sorbie and Laing, 2004; Yuan et al., 1997b; Yuan, 2001, 2002). The barium sulphate SR is higher at lower temperatures (Sorbie and Laing, 2004; Yuan, 2001) and this therefore explains the trend observed for phosphonate SIs, since MIC would be expected to rise at lower temperatures. For sulphonated polymeric species, the

improved IE at lower temperatures can be explained in terms of reaction kinetics. At 5°C, barium sulphate SR is high (SR being ~10x greater than at 95°C) but the rate of formation is sufficiently slow to allow the PVS or VS-Co to successfully inhibit the process by means of nucleation inhibition. PPCA also performs better than DETPMP at lower temperatures because it too has greater nucleation inhibition properties compared to DETPMP and other phosphonate SIs (Sorbie et al., 2000; Sorbie and Laing, 2004). Figure 2.7 and Figure 2.8 exemplify these points, where DETPMP, PPCA and PVS are tested at 5, 50 and 95°C under mild scaling conditions (Brent FW, Ba^{2+} = 20ppm) and severe scaling conditions (Forties FW, Ba^{2+} = 252ppm) (Sorbie and Laing, 2004). It is clear from Figure 2.7 and Figure 2.8 that PVS and indeed PPCA, perform better at the lower temperatures of 5 and 50°C, whereas DETPMP performs best at 95°C. At 5°C, PVS is clearly the best performer, under mild *and* severe scaling conditions.

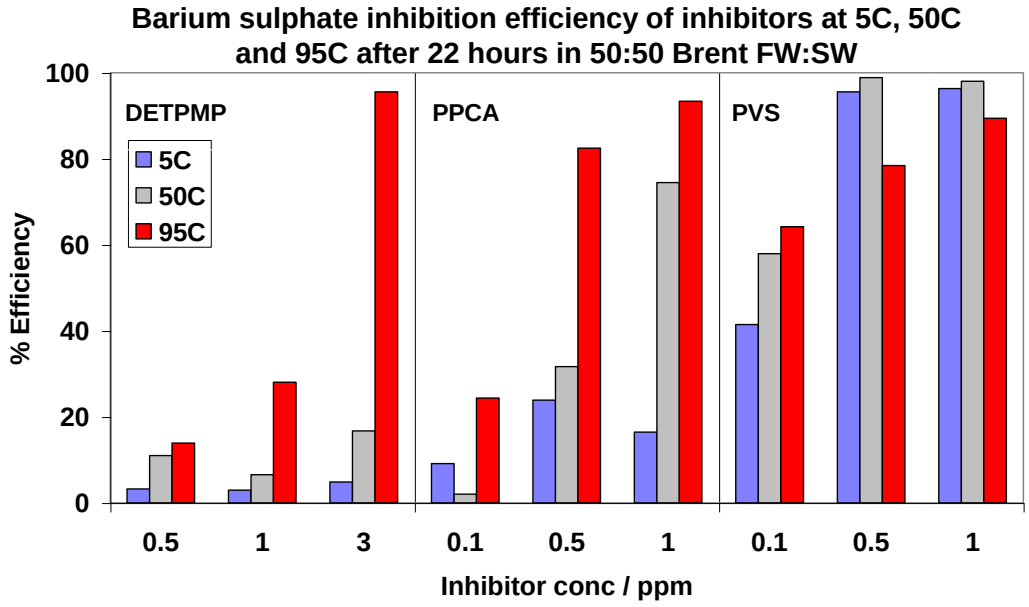

Figure 2.7 – Barium sulphate 22 hour IE of DETPMP, PPCA and PVS at 5, 50 and 95°C after mixing Brent FW/SW (mild scaling), 50/50, pH5.5. (Sorbie and Laing, 2004)

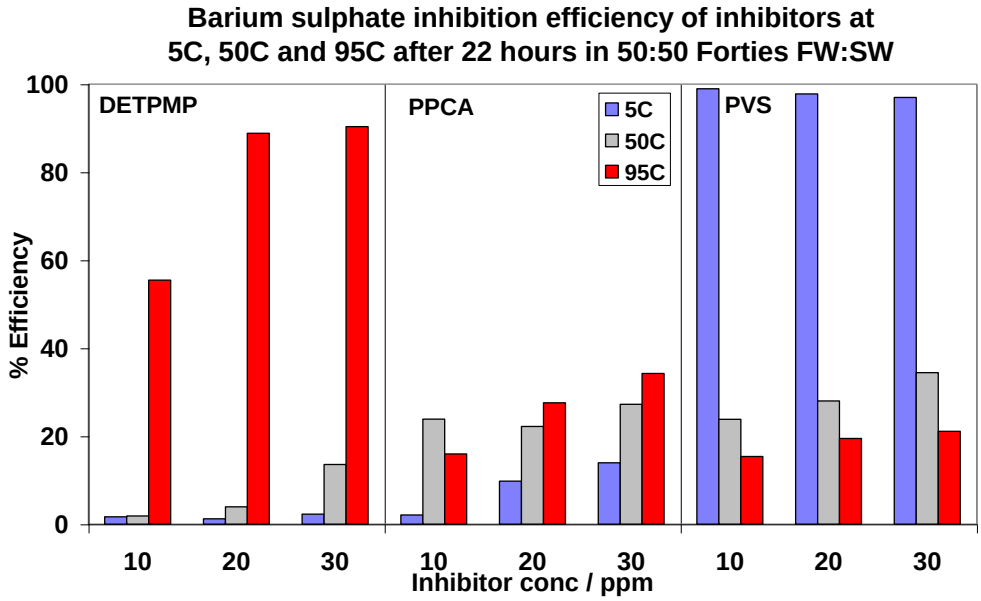

Figure 2.8 – Barium sulphate 22 hour IE of DETPMP, PPCA and PVS at 5, 50 and 95°C after mixing Forties FW/SW (severe scaling), 50/50, pH5.5. (Sorbie and Laing, 2004)

2.3.2 pH

Variations in brine pH are known to affect the IE of non-sulphonated (e.g. DETPMP and PPCA) species much *more* compared to their sulphonated analogues (e.g. PVS) (Cushner et al., 1988; Ramsey and Cenegy, 1985; Singleton et al., 2000). This is attributed to the fact that variations in pH affect the speciation of phosphonic acid and carboxylic acid functional groups, whereas it has much less effect on the speciation of sulphonic acid functional groups which are highly dissociated at all test pH levels – an extremely low pH is required to fully associate sulphonate functional groups. Thus, within the pH range SIs are generally tested (pH ~4 to ~8.5); variations in pH have little or no effect upon the IE of PVS. Polymers which are only part sulphonated, such as VS-Co and SPPCA are affected to some degree by varying pH, due to the presence of carboxylate functional groups which are more susceptible. Figure 2.9 demonstrates these points, where DETPMP, PPCA and PVS are tested at pH2 and pH5, both at 95°C (Sorbie and Laing, 2004). Clearly, the DETPMP and PPCA do not function at all at pH2 since only a very low level of IE is achieved at 0.5 hours and 1 hour. Conversely, the IE of PVS is enhanced at the lower pH level, with ~50% IE being achieved at 24 hours. A higher $[H^+]$ must benefit the PVS although this is most likely an ionic strength effect. At lower pH levels such as pH2, phosphonate and polycarboxylate SIs lose their ability to

complex with M^{2+} ions and thus their ability to inhibit barium sulphate because they become more associated (Cushner et al., 1988; Ramsey and Cenegy, 1985; Sorbie and Laing, 2004). This area of research is examined in further detail in Chapter 7 of this thesis where the effect of varying pH on the IE and MIC level of four SIs tested in this work is investigated.

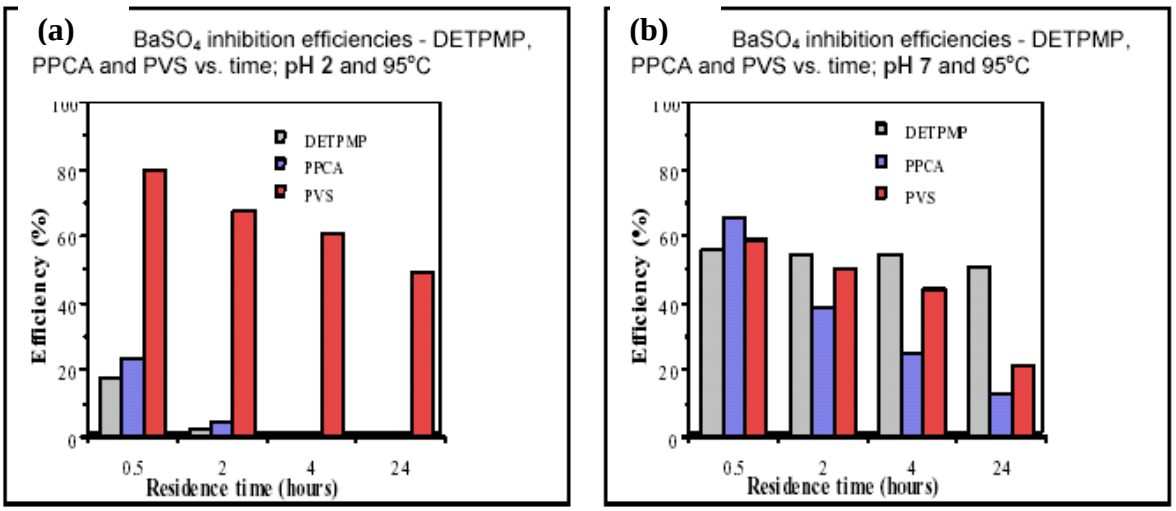

Figure 2.9 – Barium sulphate IE of DETPMP, PPCA and PVS at 0.5, 2, 4 and 24 hours after mixing NSSW/FW at pH 2 (a) and pH 7 (b) (Sorbie and Laing, 2004)

2.4 Dynamic Barium Sulphate Inhibition Efficiency Tests - TBR

Although not included in this thesis, the dynamic "tube blocking" performance test (TBR), commonly used for scale inhibitor selection in oilfield environments, partly examines the ability of scale inhibitors to prevent adherence and growth within micro-bore coils (Bazin et al., 2005; Graham et al., 2002a; Graham and McMahon, 2002; Yuan et al., 1997a, 1997b; Yuan, 2001). These experiments involve monitoring the differential pressure (ΔP) across a thin steel tube over time where two non-scaling components (e.g. NSSW and FW) of a scaling brine are mixed at the inlet of this tube. This is a dynamic or flowing test. ΔP is monitored until the tube starts to block. This test is done without SI present to determine a "blank" scaling time, and then repeated with SI present in one of the brines. The TBR procedure is illustrated schematically in Figure 2.10 (Sorbie et al., 2000).

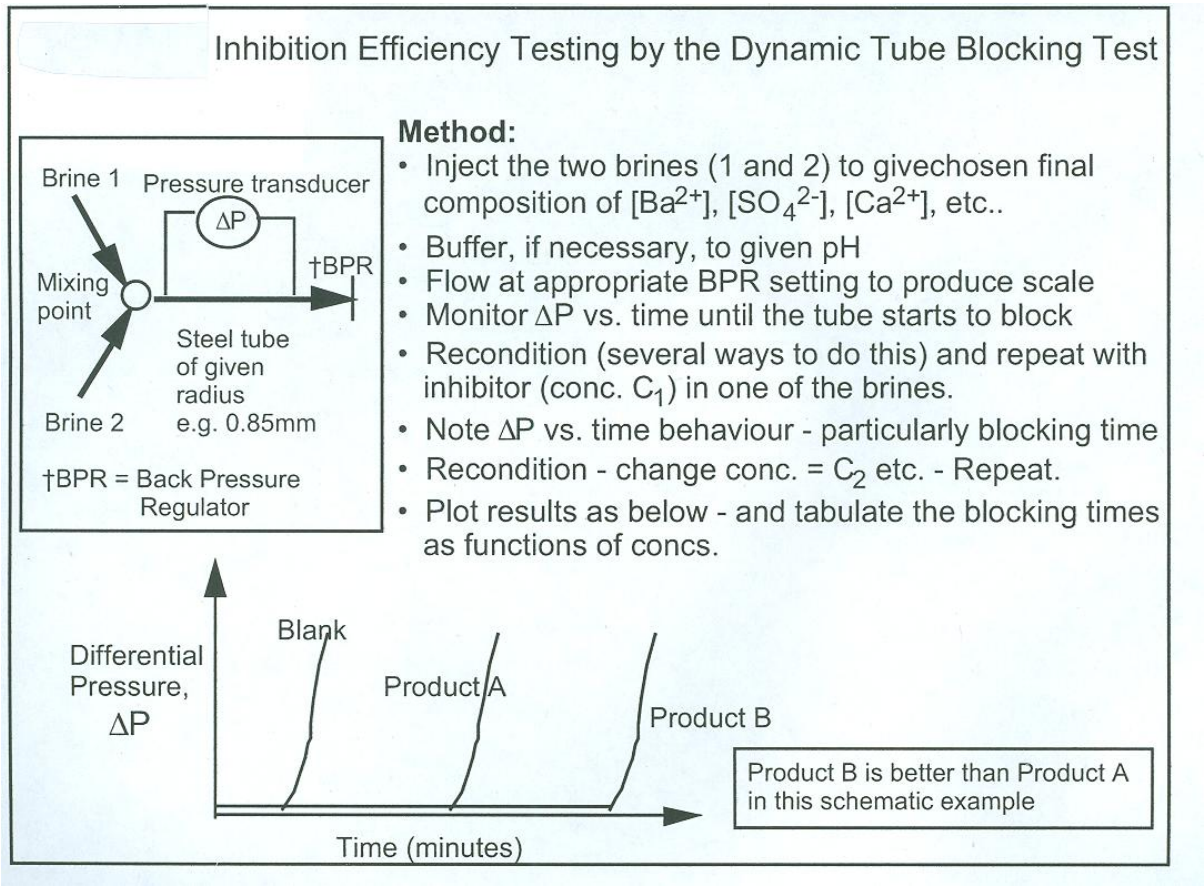

Figure 2.10 − Schematic procedure for dynamic (TBR) barium sulphate IE tests (Sorbie et al., 2000).

In TBR tests, the "better" a SI is, the longer it will take for the tube to start to block, e.g. Product B in Figure 2.10. In this type of test, polymers often perform better than phosphonate SIs because polymers operate mechanistically mainly by nucleation inhibition. The TBR test evaluates short-term IE performance, for example < 10 seconds after mixing brines (Graham and McMahon, 2002). TBR tests often give rise to different selection and ranking of scale inhibitor products than that obtained through conventional static barium sulphate IE tests (Graham and McMahon, 2002; Yuan et al., 1997a). Such discrepancies have been explained in terms of: (i) short residence time (generally < 10 seconds) compared with static IE tests (2 – 24 hours), (ii) dispersant / anti-agglomerant properties of certain inhibitor species, (iii) differences between nucleation and crystal growth inhibition effects, in addition to (iv) the impact of scale adhesion on the walls of the micro-bore tubing (Graham and McMahon, 2002; Yuan et al., 1997a). Moreover recent studies have shown that partial

inhibition of bulk precipitation by scale inhibitor chemicals in static IE tests can result in increased levels of adhesion and growth on metal surfaces (Graham and McMahon, 2002). Even static and dynamic IE performance results (e.g. MICs) obtained from different laboratories following similar laboratory procedures can be significantly different (Graham et al., 2002a). Historically TBR tests were developed for choosing calcium carbonate and calcium sulphate SIs for boiler and pipe applications where residence times are short (Sorbie et al., 2000). Residence times in oilfield applications are much longer (minutes to many hours) (Sorbie et al., 2000). TBR tests were not considered in this work because the scope of study was so wide already. Many of the factors examined in this thesis could not have been fully examined in dynamic IE tests. If some TBR tests had been carried out, perhaps some of the polymers would have outperformed phosphonate SIs. From TBR MICs, is possible to calculate the performance quotient, if the equivalent bulk (static) MIC is known. See Equation 2.8 in Section 2.5 which discusses nucleation inhibition and crystal growth inhibition mechanisms.

2.5 Nucleation Inhibition and Crystal Growth Retardation IE Mechanisms

There are two main mechanisms by which SIs inhibit scale formation: nucleation inhibition and crystal growth retardation (Sorbie et al., 2000). Nucleation inhibition is defined as the disruption of the thermodynamic stability of the growing nucleons. The inhibition mechanism involves endothermic adsorption of SIs causing dissolution of the barium sulphate embryos (Graham et al., 2003). Crystal growth retardation is defined as the interference or blocking of scale crystal growth processes. The inhibition mechanism then involves *irreversible* adsorption of SI at active growth sites on the barium sulphate crystals, resulting in their blockage (Graham et al., 2003). Clearly, this adsorbed SI will be depleted from solution. In Chapters 9 to 11, experimental work is presented where the [SI] in solution is assayed at various stages of static IE experiments, in addition to [Ba^{2+}] , thus monitoring the profile of the inhibitor consumption into the growing barite lattice.

Broadly, all SIs operate by means of nucleation inhibition and crystal growth retardation but to varying degrees (Sorbie and Laing, 2004; Graham et al., 1997a, 2003; Boak et al., 1999). It is also known that polymeric SIs work mainly by nucleation inhibition because they work less well in achieving good crystal growth inhibition and perform well (i.e. low MIC) in

dynamic tube blocking experiments (Sorbie et al., 2000). This is particularly true of PVS, which is probably the polymer which has *least* crystal growth inhibition properties (Sorbie et al., 2000; Sorbie and Laing, 2004). The weak metal binding of the highly dissociated state of PVS means that it plays less of a role in the crystal growth mechanism. As discussed in Section 2.2, in order to inhibit barium sulphate crystal growth, SI (phosphonate or polymeric) must be able to *incorporate* into the growing scale lattice in combination with Ca^{2+} or adsorb onto the crystal surface. It is known that sulphonate groups do not bind to Ca^{2+} or Mg^{2+} cations because these functional groups are highly dissociative, i.e. they have very low K_a values (Graham et al., 2003), as discussed in Section 2.3.2. The mean pK_a value for PVS = ~3 (Sorbie and Laing, 2004) whereas for DETPMP = ~4.5 (Sorbie and Laing, 2004). Thus, sulphonated homo-polymers and co-polymers such as PVS, SPPCA and VS-Co have the greatest nucleation inhibition properties and less crystal growth properties.

Highly phosphonated SIs (e.g. DETPMP) have the greatest crystal growth inhibition ability – this includes most phosphonate SIs and PMPA (a poly-phosphonate). Similarly, PPCA (phosphino polycarboxylic acid) and non-polymeric, mono-phosphonated, mono-carboxylated species such as HPAA (hydroxyphosphonoacetic acid) also have crystal growth inhibition qualities, although probably not as good as highly phosphonated species. For this reason, sometimes selected phosphonated and/or carboxylated SIs are used synergistically to improve their crystal growth inhibition properties. HPAA and HEDP have been used synergistically in order to achieve both corrosion and scale inhibition qualities in cooling system applications (Marín-Cruz et al., 2006). Carboxylated species, particularly polycarboxylates such as PPCA and MAT are generally regarded as having crystal growth properties in-between those of sulphonated polymers and conventional phosphonate SIs. These differences can be explained by the differences in the binding constants for sulphonate, carboxylate and phosphonate functional groups to Ca^{2+} cations. At any selected pH and temperature, Ca^{2+} and Mg^{2+} bond strongest to phosphonate groups (large binding constants, like those quoted for DETPMP above), followed by carboxylate (moderate binding constants), followed by sulphonate (extremely weaker binding constants). It follows that co-polymers such as VS-Co will operate by means of both nucleation inhibition and crystal growth inhibition in very broadly similar amounts. Phosphonates and sulphonated polymers may also be used synergistically in blends, to yield better IE (since both mechanisms of scale inhibition can operate effectively, simultaneously).

SIs which operate mainly by nucleation inhibition tend to be polymers and these products have the lowest MICs when tested dynamically in a tube blocking IE experiment. Dynamic tube blocking evaluates SI *early-time* scale inhibition performance which is indicative of nucleation inhibition potential (Sorbie et al., 2000). On the contrary, crystal growth inhibition potential is established by means of SI *long-term* IE performance, such as ~2 to 22 hours after mixing NSSW/FW, usually in a *static* IE test. These static IE tests are the main focus of this thesis. A quantity has been defined, denoted the *performance quotient* for a selected SI and set of conditions – see Equation 2.8. The performance quotient is the ratio of static MIC to tube-blocking MIC for a fixed set of test conditions. The performance quotient values for PVS, PPCA and DETPMP are 7.5, 3.6 and 1.2 respectively (Sorbie and Laing, 2004). Clearly, the *higher* the performance quotient value is (i.e. the ratio MIC_{ST}/MIC_{TB}), the more the SI in question will operate by means of nucleation inhibition. Conversely, the *lower* the performance quotient value is, the more the SI in question will operate by means of the crystal growth inhibition mechanism. These values of PQ for PVS, PPCA and DETPMP reflect the inhibition mechanisms by which they operate – this is also reflected in the static IE experimental results, testing these three products, presented in this thesis. PVS and other polymers performed much more poorly at the 22 hour sampling time, in comparison to most conventional phosphonate SIs. PVS provides the best example of this behaviour – in Chapter 6; a 22 hour MIC for PVS cannot be reached.

$$PQ = \frac{MIC_{ST}}{MIC_{TB}} \qquad \text{(Eq. 2.8)}$$

2.6 Phosphonates vs. Polymers

In terms of barium sulphate IE, phosphonate SIs are considered better SIs compared to their polymeric analogues, whereas in terms of environmental "friendliness" of the products, the converse is true, i.e. polymers are favoured (Jordan et al., 2010, 2011; Taj et al., 2006; Inches et al., 2006). This is because it is the presence of phosphonate functionality (usually as an amino phosphonate) which yields the best IE and SI retention (Jackson et al., 1996; Singleton et al., 2000). The downside to this is that the higher the phosphorus content in SIs, the more environmentally unacceptable they become (Jordan et al., 2010, 2011; Todd et al., 2010; Wilson et al., 2010). Some polymeric SIs have been phosphonate "end-capped" (Davis et al., 2003; Fleming et al., 2004), this improves their IE but decreases their biodegradability. PMPA is an example of a poly-phosphonate SI which has significantly better IE and retention properties compared to other non-phosphonated polymeric SIs (Przybylinski et al; Singleton et al., 2000). However PMPA has an extremely high phosphorus content, at a level comparable with conventional phosphonate SIs (see Chapter 4), and indeed, it is currently thought that PMPA may *not* in fact be a polymer at all. This knowledge was gained through communication with the PMPA manufacturer.

The recent move away from phosphonates, towards the development and deployment of polymeric SIs (particularly "green" chemistries) is occurring essentially because of environmental concerns (Todd et al., 2010; Wilson et al., 2010). Recent government legislation has banned the use of phosphonate SIs in certain parts of the world, such as Norway, where phosphonates, including PMPA are not permitted (Jordan et al., 2010, 2011). The main problem associated with green polymers, which contain no phosphorus and no sulphur, is that their IE is much poorer, particularly over long periods of time. However, sulphonated polymers such as PVS and VS-Co do have advantages over phosphonates, in that they are particularly suitable for use in low pH systems, for example, pH < 4 (Graham et al., 2003), where phosphonate SIs would not function because the molecules would be largely associated at this low pH, unable to inhibit barium sulphate.

When designing and synthesising a new SI, one of the main aims of chemical manufacturers is to produce a product which will achieve good IE coupled with reasonable environmental properties, and thus attract interest from service companies in a competitive marketplace (Todd et al., 2010). Other important factors are also considered such as supply chain cost and

other physicochemical properties, e.g. adsorption, compatibility and thermal stability. It is for this reason that many P-tagged polymers have been synthesised, such as PPCA, SPPCA, P-functionalised polymers and co-polymers, etc. These products typically contain low levels of phosphorus, and are sometimes considered "yellow" products, rather than fully "green". Firstly, their IE properties are generally better than fully "green" products such as maleic acid ter-polymer (MAT), and they are not as environmentally hazardous as phosphonates (Todd et al., 2010). Secondly, by P-tagging polymeric SIs, this enables such products to be assayed by ICP spectroscopy by means of [P] in various laboratory experiments (Boak and Sorbie, 2010). Problems can arise, for example, if all the detected phosphorus (by ICP spectroscopy) is not part of the active SI, but instead part of other SI formulation constituents or SI degradation products – this area of work is discussed in more detail in Chapter 11. Other laboratory analytical techniques are available for the assay of non-ICP detectable, green SIs and non-P-tagged polymers, such as the C18 / Hyamine technique and the Pinacyanol technique. Hyamine and Pinacyanol are both chemical reagents which react with specific functional groups present on polymer molecules (Boak and Sorbie, 2010). Hyamine reacts with polycarboxylated products whereas Pinacyanol reacts with sulphonated species. Both the Hyamine and Pinacyanol analytical methods involve the spectrophotometric analysis of test samples at 500nm and 485nm respectively, as discussed in some detail in Chapter 11. The C18 / Hyamine analytical method may also be used for the analysis of P-containing, polycarboxylated SIs, e.g. PPCA, and so can sometimes be compared analytically with ICP spectroscopy in certain analysis work (Boak and Sorbie, 2010).

2.7 Scale Crystal Morphologies

A chemical model of barite is shown in Figure 2.11 [5]. In this model, the silver spheres represent barium cations (with charge +2), the tan spheres represent sulphur, and the red spheres represent oxygen. Each sulphate (SO_4) unit in the crystal structure has an overall charge of −2. Barite is a mineral consisting of barium sulphate ($BaSO_4$), known for its range of colours and varied crystal forms. Some images of barite crystals are shown in Figure 2.12 to Figure 2.16 [6-9]. In dry sandy areas, barite can take an interesting form when it crystallises, for instance, when a shallow salt basin evaporates. In these cases, not only can the barite crystals form in a rosette shape, but they can also incorporate some of the surrounding sand into the crystal structure, forming a "desert rose", as shown in Figure 2.12.

"Desert rose" barite is found in only a few places around the globe [6]. Oklahoma (USA) is one of those places, and since the local red soil colours have coloured its desert roses a ruddy hue, desert rose barite was named the official state rock of Oklahoma [6]. In mixed deposits, other minerals such as calcite and fluorite can cause crystals to be brightly coloured, such as in Figure 2.15 and Figure 2.16 [9]. In Figure 2.15, the golden colour is due to the presence of calcite, and in Figure 2.16, the purple colour is due to the presence of fluorite.

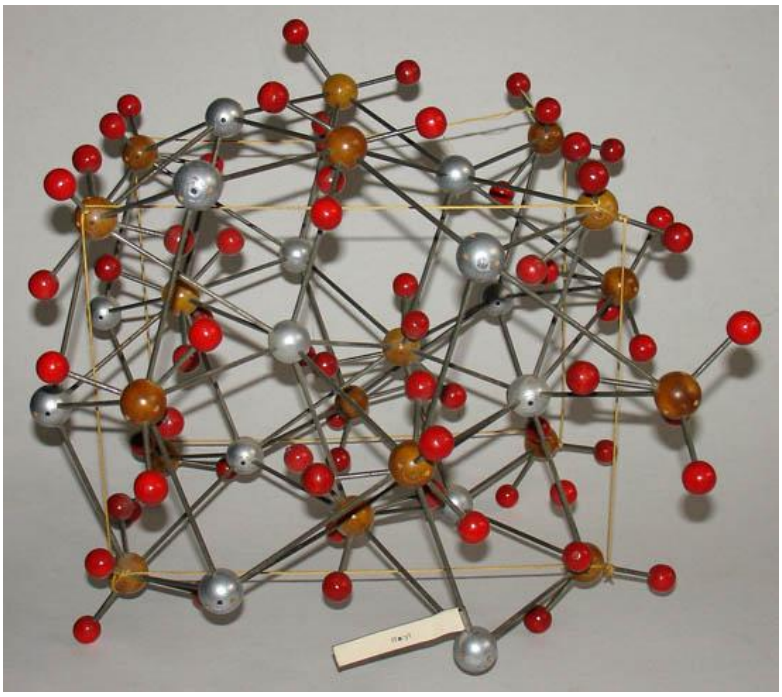

Figure 2.11 – Barite chemical model [5].

Figure 2.12 – "Desert Rose" barite from Oklahoma, USA [6].

Figure 2.13 – Barite from Rosebery Mine, Rosebery, Tasmania, Australia [7].

Figure 2.14 − Radiating crystal structure in the interior of a barite nodule, near Indiahoma, Comanche County, USA [8].

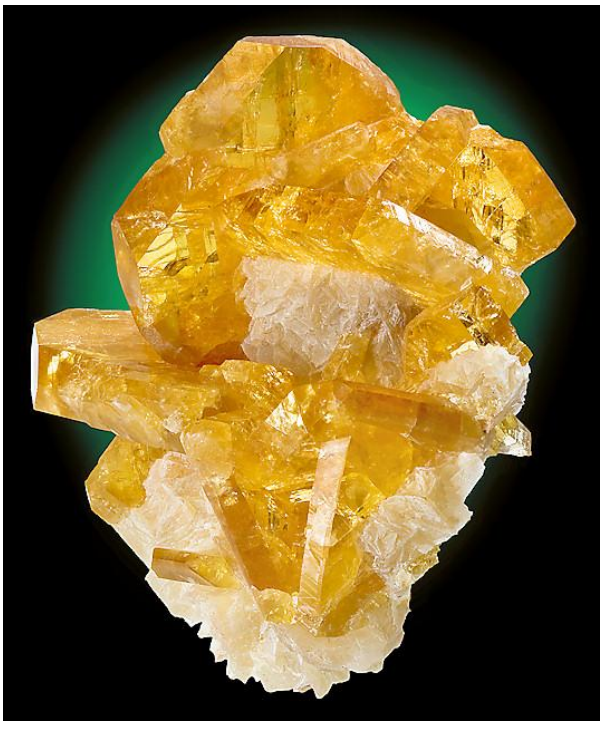

Figure 2.15 – "Golden barite" (mixed barite and calcite) from Meikle Mine, Elko County, Nevada, USA [9].

Figure 2.16 – Fluorite barite (mixed fluorite and barite) from Berbes Mine, Berbes, Asturias, Spain [9].

The presence of SI causes normal barium sulphate crystal growth to be inhibited and distorted or modified (Nancollas and Liu, 1975). The morphology of the resultant scale crystals depends to some degree on the nature of the SI. The relationship between *SI structure* and *crystal structure* is discussed in the paper by Gill and Varsanik (1986) where molecular modelling is used to illustrate this connection. The paper discusses the possibility of designing new SIs based on spatial inter-atomic matching between crystal growth centres and the active groups on SI molecules such as phosphonate, carboxylate and sulphonate; this is often referred to as the "lattice matching" approach to designing scale inhibitors. Possible relationships between SI and crystal morphology are discussed in detail in Chapter 9 of this thesis, where ESEM images and EDAX analyses of an extensive range of scale deposits formed in static IE experiments are obtained, in the presence of phosphonate SIs OMTHP, DETPMP, HMTPMP and HMDP. Blank (uninhibited) scale deposits are also retained and ESEM/EDAX compared with the SI-containing deposits. EDAX provides composition data, giving an insight into the degree of Ca^{2+} inclusion into the barite lattice and other compositional data, e.g. %Ba, %Sr.

2.8 Calcium Carbonate Scale − Effect of Divalent Cations

Various studies have investigated the mechanisms of calcium carbonate inhibition (Eroini et al., 2011; Martinod et al., 2011; Nancollas et al., 2004; Re and Gill, 1996). In addition to divalent cations having an effect on barite formation, it has been widely reported that ions such as Mg^{2+}, Ba^{2+}, Sr^{2+}, Mn^{2+} and SO_4^{2-} present in FW and NSSW brines have the ability to inhibit the growth of calcite scale (Akin and Lagerwerff, 1965; Mucci and Morse, 1983; Dromgoole and Walter, 1990; Gutjahr et al., 1996; Chen et al., 2005b, 2006). Dawe, 2000 and Zhang et al., 2001 illustrated that the calcite growth rate could be well described by considering inhibition exclusively by Mg^{2+}. Nucleation and crystal growth rates of $CaCO_3$ may be affected strongly be Mg^{2+} present in FW and NSSW brines (Reddy and Nancollas, 1976). Figure 2.17 shows the effect of Mg^{2+} on surface deposition. The mass of calcite deposit decreases as $[Mg^{2+}]$ in solution increases (Chen et al., 2005b, 2006). In bulk tests, there is also less calcite precipitation as the $[Mg^{2+}]$ in the bulk solution increases – see Figure 2.18 (Chen et al., 2005b, 2006).

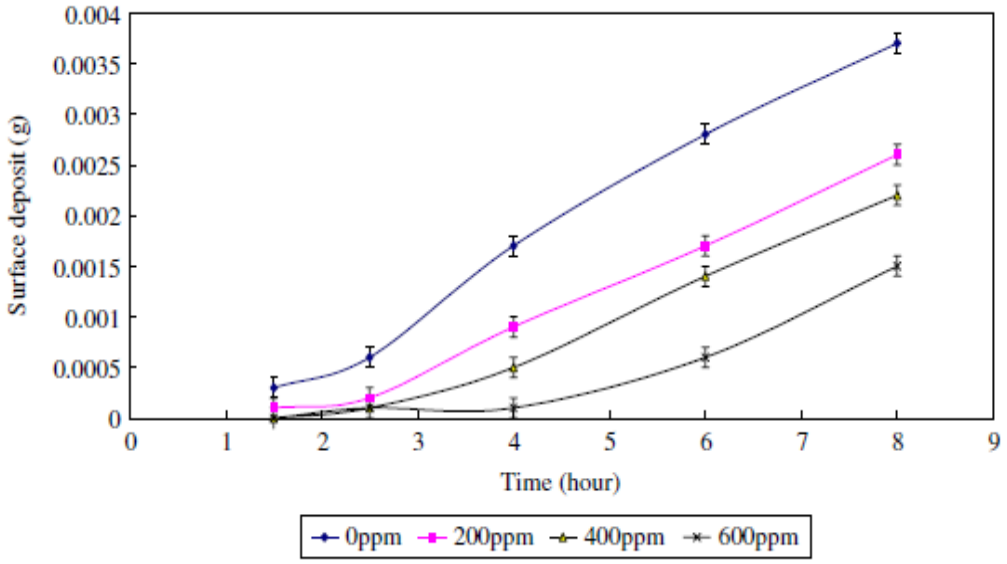

Figure 2.17 – Effect of Mg^{2+} on surface deposition under 1500 rpm at 20°C (Chen et al., 2006).

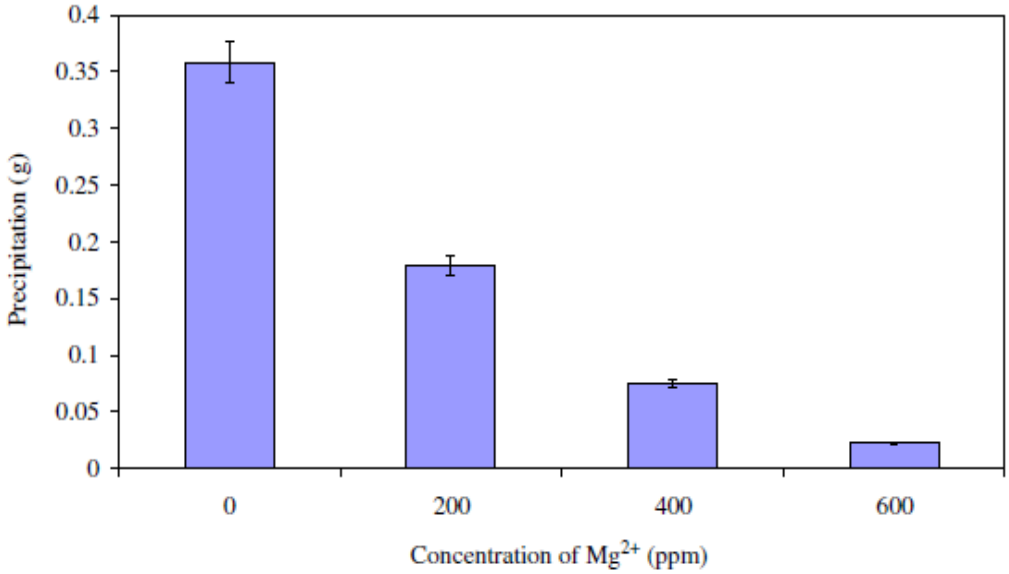

Figure 2.18 – Effect of Mg^{2+} on precipitation formed in bulk solution at 8 hours under 1500 RDE at 20°C (Chen et al., 2006).

Some SEM studies have also been carried out by Chen et al., 2005b, 2006. Figure 2.19 shows some SEM images of calcium carbonate scale deposited on a metal surface in brine containing various [Mg^{2+}], after 8 hours. The number of calcium carbonate crystals deposited on the surface decreases as the [Mg^{2+}] in the solution increases. In the blank solution (0ppm Mg^{2+}), mainly vaterite scale crystals form (a polymorph of calcium carbonate), only a small quantity of calcite is observed. As [Mg^{2+}] increases in the bulk solution, the ratio of the amount of vaterite to calcite crystals decreases.

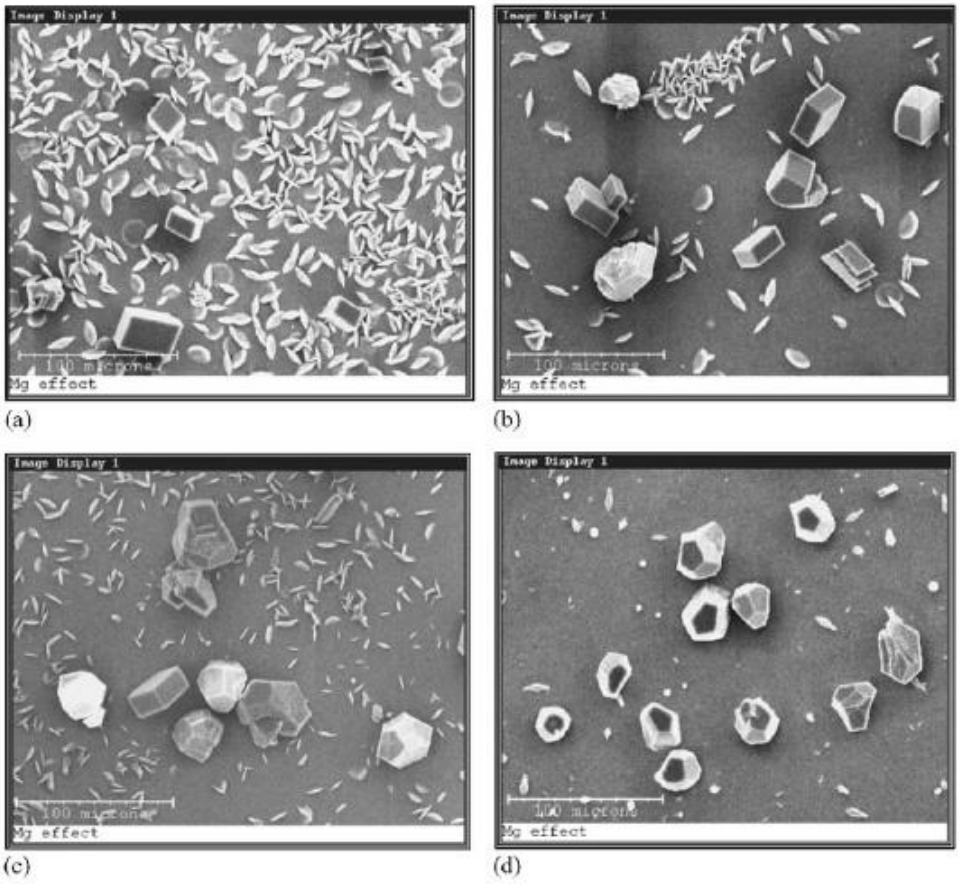

Figure 2.19 – Microscopy of scale formed in brine containing various levels of Mg^{2+}, at 8 hours and 20°C: (a) 0ppm Mg^{2+}; (b) 200ppm Mg^{2+}; (c) 400ppm Mg^{2+}; and (d) 600ppm Mg^{2+}(Chen et al., 2006).

Chen et al., 2005b, 2006 also investigated the inhibition efficiency of Mg^{2+} on calcium carbonate precipitation and deposition. A typical test result is shown in Figure 2.20. Mg^{2+} affects both the extent of precipitation and deposition of calcium carbonate.

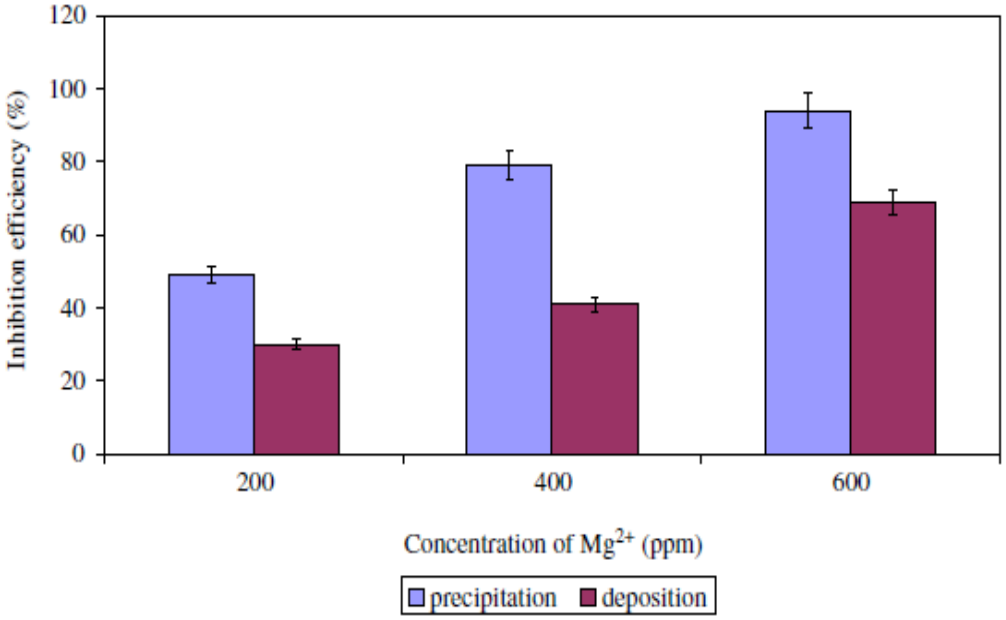

Figure 2.20 – Inhibition Efficiency of Mg^{2+} on bulk precipitation and surface deposition after 8 hours at 1500 rpm at 20°C (Chen et al., 2005b, 2006).

Clearly Mg^{2+} inhibits calcium carbonate scale formed on metal surfaces and in the bulk solution. Mg^{2+} has a greater inhibiting effect on bulk precipitation than surface deposition. This indicates that different inhibition mechanisms are likely involved in these two different processes. The effects of Mg^{2+} are also apparent in the SEM images presented.

2.9 Barium Sulphate – Surface Studies

From an oilfield scale prevention perspective, interest recently has focused on understanding the relationship between heterogeneous nucleation and growth on pipeline surfaces (adhesion) rather than homogeneous nucleation and growth from bulk solution (as in static IE tests) (Graham and McMahon, 2002). The trend towards understanding heterogeneous nucleation and growth has gained interest because scale adhesion is recognised as a much more serious issue than homogeneous "bulk" precipitation (Graham and McMahon, 2002; Nancollas and Liu, 1975; Weintritt and Cowan, 1967). Numerous scientific experiments have been performed investigating barite deposition onto various surfaces (Cheong et al., 2008; Graham et al., 2001b, 2004; Labille et al., 2002; Mavredaki et al., 2010, 2011; Morizot

and Neville, 2000; Neville et al., 1999, 2002; Wylde et al., 2001). In this section, a brief review of this area of work will be discussed. Surface studies frequently involve the use of Atomic Force Microscopy (AFM) to view barite deposits on various surfaces either in the absence (blank) or presence of scale inhibitors such as PPCA and DETPMP (Mavredaki et al., 2010). Synchrotron X-Ray Diffraction (SXRD) can also be used to assess barium sulphate formation on surfaces (Mavredaki et al., 2008, 2011). Some AFM images are presented in Figure 2.21 and Figure 2.22. The barite crystal morphology and size is often dependent on the brine composition. This was investigated in the paper by Mavredaki et al., 2011. The barite crystals shown in Figure 2.21 were deposited from the brines given in Table 2.3. The size of the crystals formed is related to the brine compositions. For instance, the large crystals shown in Figure 2.21(c) were formed from brine containing 3,982ppm Ba^{2+} (see Table 2.3). Figure 2.22 illustrates that the crystal morphology is changed when SI is present, and this in turn, depends on the nature of the SI. The crystals formed in the presence of PPCA (Figure 2.22(b) and (c)) are morphologically different from those formed in the presence of DETPMP (Figure 2.22(d) and (e)). Figure 2.22(a) shows uninhibited barite crystals. In Chapter 9 of this thesis, a similar study of barite deposits formed from bulk solution is undertaken, with analysis done by ESEM/EDAX. ESEM images obtained of scale deposits formed in the absence and presence of SIs has shown findings similar to the AFM images presented here. The presence of SI changed the crystal morphology and this in turn, depends on the nature of the SI. All ESEM images presented in Chapter 9 are of blank scale deposits, or scale deposits containing phosphonate SIs. However, a small number of deposits (from static IE tests) containing PPCA were also analysed by ESEM/EDAX, and the crystal morphology was found to be different compared to when phosphonate SIs were present.

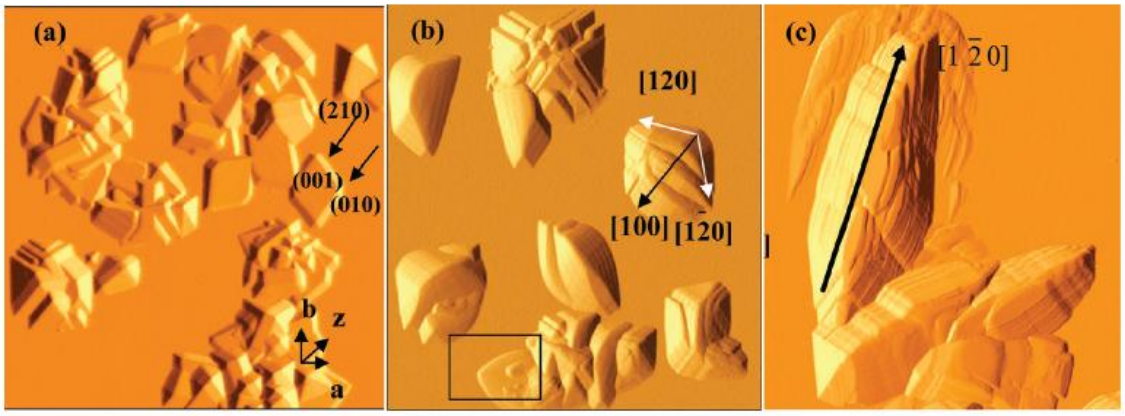

Figure 2.21 − AFM images of $BaSO_4$ morphologies deposited from 3 different brine mix compositions (see Table 2.3). All images are 20µm X 20µm (Mavredaki et al., 2010).

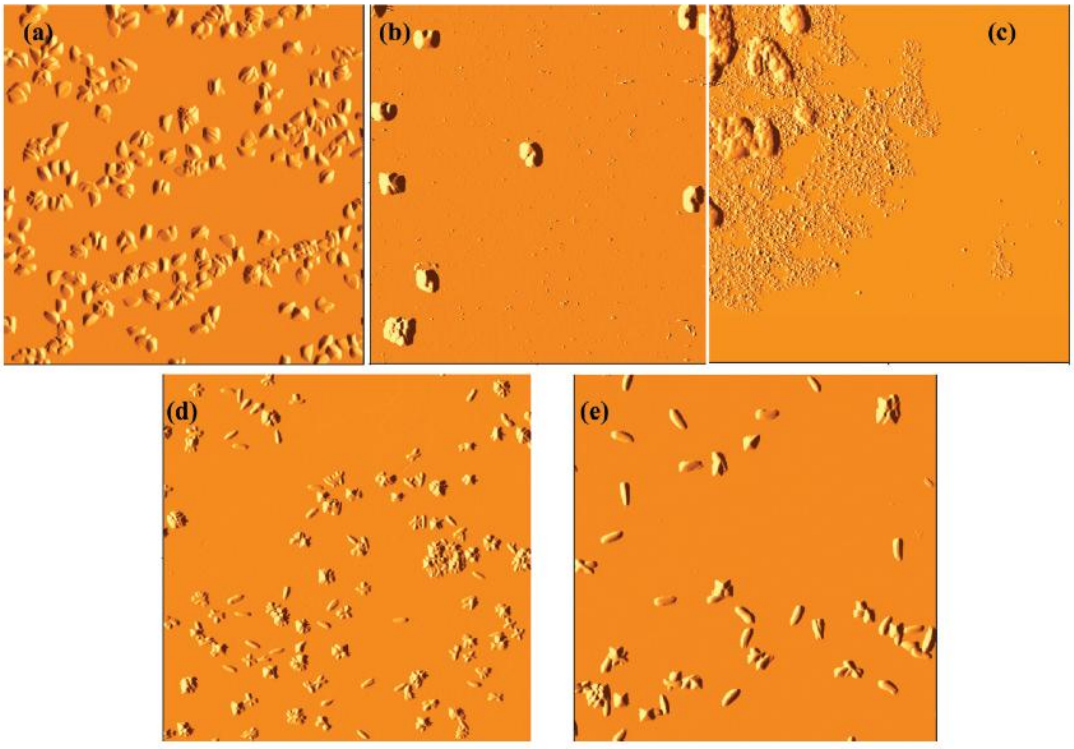

Figure 2.22 − AFM images (100µm X 100µm) of deposited barite after treatment with (a) no inhibitor, (b) 4 ppm PPCA, (c) 10 ppm PPCA, (d) 4 ppm DETPMP and (e) 10 ppm DETPMP (Mavredaki et al., 2010).

	mixture A		mixture B		mixture C	
type of ions	formation water	synthetic seawater	formation water	synthetic seawater	formation water	synthetic seawater
K^+	400 ppm	350 ppm	1906 ppm	380 ppm	1906 ppm	380 ppm
Ca^{2+}	200 ppm	700 ppm	2033 ppm	405 ppm	2033 ppm	405 ppm
Mg^{2+}	700 ppm	200 ppm	547 ppm	1215 ppm	547 ppm	1215 ppm
Ba^{2+}	100 ppm	0 ppm	80 ppm	0 ppm	3982 ppm	0 ppm
Sr^{2+}	200 ppm	350 ppm	417 ppm	0 ppm	417 ppm	0 ppm
SO_4^{2-}	0 ppm	101 ppm	0 ppm	2780 ppm	0 ppm	2780 ppm
Na^+	13570 ppm	17940 ppm	26535 ppm	10900 ppm	26535 ppm	10900 ppm

Table 2.3 − Brine compositions (mixtures A, B and C) used in the AFM experiments (Mavredaki et al., 2010).

Chapter 3: Experimental Details

Chapter 3 Summary: This Chapter describes all aspects of laboratory experimental procedures relevant to the experimental results presented in this thesis. This Chapter describes brine preparation, brine compositions for *all* experiments undertaken, static IE procedures, SI/Ca^{2+} precipitation experiment procedure, chemical reagents and wet chemical analytical procedures for [SI] using C18 Hyamine and Pinacyanol.

3.1 Brine Preparation

All brines are prepared by dissolving the appropriate inorganic salts in distilled water (DW). All salts are weighed out individually and added to a 10L plastic bucket. The bucket is then filled about ¾ full with DW. An overhead electric mixer is then placed into the plastic bucket, and the mixture stirred for about an hour until complete dissolution of the salts is achieved. Usually a 20L batch of any particular brine composition is prepared at any one time, thus, the quantity of each salt weighed out is appropriate for 20L of DW. After all the salts are dissolved completely in the 7-8L of DW in the plastic bucket, a 5L volumetric flask is filled 4 times and made up to the meniscus. Each of the 5L portions is added to a 20L plastic brine storage container. Additional distilled water must be added to the volumetric flask in order to fill it 4 times, in addition to the 7-8L of salt-containing DW initially prepared. After 20L of distilled water, including the dissolved salts is added to the 20L container – this is then stirred for 2-3 hours to ensure homogeneity. Once the 20L of brine in the storage container has been stirred for the required time interval, only then is the concentration of each ion in the brine at the required concentration (per 20L DW). Prior to use in static inhibition efficiency experiments, this prepared brine is filtered through 0.45μm membrane filter paper. Filtering removes any physical impurities from the brine which could be problematic in the experiments, e.g. the presence of solid particles could induce scale formation prematurely (this would be heterogeneous nucleation).

3.2 Brine Compositions

The vast majority of IE experiments are carried out under either "Base Case" or "Fixed Case" test conditions. In the Base Case tests, normal composition North Sea Sea Water (NSSW) and Forties formation water (FW) brines are used, compositions are given in Table 3.1 and Table 3.2 respectively. The [Ca^{2+}] and [Mg^{2+}] in the produced water depends upon the mixing ratio of NSSW/FW being evaluated in the normal Base Case conditions. In all Fixed Case tests, NSSW containing no Ca^{2+} and no Mg^{2+} is used – the composition is given in Table 3.3. In all Fixed Case tests, the FW contains appropriate quantities of Ca^{2+} and Mg^{2+} such that the final brine mix always contains 2000ppm Ca^{2+} and 739ppm Mg^{2+}, regardless of the initial NSSW/FW mixing ratio. Table 3.4 and Table 3.5 give the FW compositions used in the Fixed Case IE tests. Bicarbonate (HCO_3^-) anions are excluded from brines used in static IE tests because this would cause problems. High pressure vessels would be required to prevent evolution of CO_2 (Sorbie et al., 2000). If CO_2 is evolved, this could possibly cause a rise in pH, which would directly affect IE results, particularly if pH sensitive phosphonate SIs are being tested. Secondly, the presence of some bicarbonate anions would have a minimal effect upon the barite SR; therefore it is acceptable for static IE tests to be conducted in the absence of bicarbonate anions. Thirdly, if calcium carbonate is forming simultaneously to barite and celestite, it could affect barite IE results, although the effect is likely to be very mild.

In some experiments, the molar ratio Ca^{2+}/Mg^{2+} in the produced water is varied to investigate the effect upon IE – the brines used for these experiments are slightly more complex in that a variety of different FW compositions are required, each FW containing a different concentration of Ca^{2+} and Mg^{2+}. Table 3.6 to Table 3.9 give the FW brine Ca^{2+}, Mg^{2+} and Cl^- for experiments presented in Chapters 6, 9 and 10 where PPCA, MAT, SPPCA, PFC, PMPA, CTP-A, CTP-B, DETPMP and HMTPMP are tested in brines varying the mix molar ratio Ca^{2+}/Mg^{2+}. In these cases, the other FW ion concentrations (Na^+, K^+, Ba^{2+} and Sr^{2+}) are given in Table 3.4. In these experiments, the FW is always mixed with Fixed Case "blank" NSSW which contains 0ppm Ca^{2+} and 0ppm Mg^{2+} (see Table 3.3).

In the experiment where PFC is tested with Ca^{2+}/Mg^{2+} = 0.19, 0.57 and 1.64, in the Ca^{2+}/Mg^{2+} = 0.57 test, Base Case brines are used (Table 3.1and Table 3.2); this is the molar ratio Ca^{2+}/Mg^{2+} in the brine mix which occurs naturally when these two brines are mixed.

When additional molar ratios Ca^{2+}/Mg^{2+} = 0.19 and 1.64 are tested, the total number of moles of Ca^{2+} and Mg^{2+} in the brine mix stayed the same as in the Ca^{2+}/Mg^{2+} = 0.57 mix, but Fixed Case NSSW is used, which contained 0ppm Ca^{2+} and 0ppm Mg^{2+} (Table 3.3), and mixed with the FWs given in Table 3.9. The produced water total number of moles of (Ca^{2+}+Mg^{2+}), X_m is fixed = 72.3 millimoles/L, only the molar ratio Ca^{2+}/Mg^{2+} varies between these experiments, therefore total dissolved solids (ppm) varied but ionic strength (moles/L) remained constant. This can be illustrated by calculation (using the chloride ion concentration):

In the Base Case 60/40 NSSW/FW Ca^{2+}/Mg^{2+} = 0.57 test (X_m = 72.3mM/L):
$[Cl^-]$ (mix) = {(0.6*19773)+(0.4*55279)} = (11863.8+22111.6) = ~ 33975ppm

In the 60/40 NSSW/FW Ca^{2+}/Mg^{2+} = 0.19 and 1.64 tests (X_m = 72.3mM/L):
$[Cl^-]$ (mix) = {(0.6*15026)+(0.4*62402)} = (9015.6+24960.8) = ~ 33976ppm

Therefore, both the ionic strength and produced water $[Cl^-]$ are constant in the PFC experiments varying Ca^{2+}/Mg^{2+} = 0.19, 0.57 and 1.64 (Section 6.6.2). This statement also applies to the experiments presented in Chapter 10, Sections 10.1 and 10.2 with Ca^{2+}/Mg^{2+} = 0.19 and 1.64.

A series of *mild scaling* IE tests are also carried out – in these cases, the NSSW used is the same as shown Table 3.1 and Table 3.3. However, the FW contains 100ppm Ba^{2+} rather than 269ppm Ba^{2+}. The *mild scaling* Base Case and Fixed Case FW compositions are given in Table 3.10, Table 3.11 and Table 3.12.

Two static compatibility experiments involving PPCA are carried out. For these experiments, sulphate-free NSSW (Fixed Case composition) is used in one case – see Table 3.13, and FW containing no Ba^{2+} and no Sr^{2+} is used in both cases (Fixed Case 80/20 NSSW/FW composition) – see Table 3.14.

Ion	Conc. / ppm	Formula
Na^+	10890	NaCl
Ca^{2+}	428	$CaCl_2.6H_2O$
Mg^{2+}	1368	$MgCl_2.6H_2O$
K^+	460	KCl
Ba^{2+}	0	$BaCl_2.2H_2O$
Sr^{2+}	0	$SrCl_2.6H_2O$
SO_4^{2-}	2960	Na_2SO_4
Cl^-	19773	–

Table 3.1 – North Sea Sea Water (NSSW) composition – used in Base Case experiments (severe and mild scaling).

Ion	Conc. / ppm	Formula
Na^+	31275	NaCl
Ca^{2+}	2000	$CaCl_2.6H_2O$
Mg^{2+}	739	$MgCl_2.6H_2O$
K^+	654	KCl
Ba^{2+}	269	$BaCl_2.2H_2O$
Sr^{2+}	771	$SrCl_2.6H_2O$
SO_4^{2-}	0	Na_2SO_4
Cl^-	55279	–

Table 3.2 – Forties FW composition – used in Base Case experiments (severe scaling only).

Ion	Conc. / ppm	Formula
Na^+	10890	NaCl
Ca^{2+}	0	$CaCl_2.6H_2O$
Mg^{2+}	0	$MgCl_2.6H_2O$
K^+	460	KCl
Ba^{2+}	0	$BaCl_2.2H_2O$
Sr^{2+}	0	$SrCl_2.6H_2O$
SO_4^{2-}	2960	Na_2SO_4
Cl^-	15026	–

Table 3.3 – North Sea Sea Water (NSSW) composition – used in Fixed Case experiments (severe and mild scaling).

Ion	Conc. / ppm	Formula
Na^+	31275	NaCl
Ca^{2+}	See Tables 3.5-3.9	$CaCl_2.6H_2O$
Mg^{2+}	See Tables 3.5-3.9	$MgCl_2.6H_2O$
K^+	654	KCl
Ba^{2+}	269	$BaCl_2.2H_2O$
Sr^{2+}	771	$SrCl_2.6H_2O$
SO_4^{2-}	0	Na_2SO_4
Cl^-	See Tables 3.5-3.9	–

Table 3.4 – Forties FW composition – used in Fixed Case experiments (except Ca^{2+}, Mg^{2+} and Cl^-) (severe scaling tests only).

Mixing Ratio NSSW/FW	**FW [Mg^{2+}] / ppm**	**FW [Ca^{2+}] / ppm**	**FW [Cl^-] / ppm**
10/90	821	2,222	55,911
20/80	924	2,500	56,702
30/70	1,056	2,857	57,719
40/60	1,232	3,333	59,075
50/50	1,478	4,000	60,972
60/40	1,848	5,000	63,819
70/30	2,463	6,667	68,563
80/20	3,695	10,000	78,053
90/10	7,390	20,000	106,520

Table 3.5 – Formation Water Ca^{2+}, Mg^{2+} and Cl^- content – applying to all Fixed Case IE experiments (severe scaling only). N.B. FW composition for 40/60 NSSW/FW is given for information only – this mixing ratio was not tested in any experiment.

Molar Ratio Ca^{2+}/Mg^{2+}	**[Ca^{2+}] / ppm**	**[Mg^{2+}] / ppm**	**[Cl^-] / ppm Δ**
1	2004	1216	~56675
2	2672	810	~56675
4	3206	486	~56675

Δ Since in this experiment, the total molar concentration (moles per litre) of ([Mg^{2+}] + [Ca^{2+}]) = 0.05 (in produced water and FW), the molar chloride ion concentration and total dissolved solids concentration in the FW and final mix of brines remains almost constant and thus also the level of supersaturation.

Table 3.6 – Formation water Ca, Mg and Cl – experiment testing DETPMP, varying Ca/Mg, Section 9.3.1 (Chapter 9).

Ion ↓ Ca/Mg (FW & MIX) →	**0**	**0.05**	**0.1**	**0.15**	**0.25**	**0.35**	**0.5**	**0.75**	**1**	**1.25**	**1.5**	**1.64**	**5**	**10**	∞
Ca^{2+} / ppm	0	765	1465	2100	3220	4170	5365	6895	8045	8940	9655	10000	13410	14630	16090
Mg^{2+} / ppm	9760	9295	8875	8485	7810	7230	6505	5575	4880	4340	3905	3695	1625	885	0
Cl^- / ppm	~78053	~78053	~78053	~78053	~78053	~78053	~78053	~78053	~78053	~78053	~78053	~78053	~78053	~78053	~78053

Table 3.7 – Formation water Ca, Mg and Cl – experiments testing PPCA, MAT and SPPCA, varying Ca/Mg, Sections 6.2.3 (PPCA), 6.3.2 (MAT) and 6.4.2 (SPPCA) (Chapter 6).

Molar Ratio Ca^{2+}/Mg^{2+}	**[Ca^{2+}] FW / ppm**	**[Mg^{2+}] FW / ppm**	**FW [Cl^-] / ppm**
0	0	4880	~63818 (constant)
0.1	733	4438	~63818 (constant)
0.25	1610	3905	~63818 (constant)
1	4023	2440	~63818 (constant)
5	6705	813	~63818 (constant)
∞	8045	0	~63818 (constant)

Table 3.8 – Formation water Ca, Mg and Cl – experiment testing CTP-A and CTP-B, varying Ca/Mg, Section 6.9.2.

Ion	**Ca^{2+}/Mg^{2+} = 0.19 expt. / ppm**	**Ca^{2+}/Mg^{2+} = 0.57 expt. / ppm**	**Ca^{2+}/Mg^{2+} = 1.64 expt. / ppm**
Ca^{2+}	1158	2000	4500
Mg^{2+}	3693	739	1665
Cl^-	~62402 *	~55279 *	~62402 *

*The [Cl^-] and ionic strength of the *produced water* in the 3 experiments testing PFC is *constant*. This is because in the Base Case experiment (Ca^{2+}/Mg^{2+} = 0.57), the above FW is mixed with Base Case NSSW (Table 3.1), which contains 428ppm Ca^{2+} and 1368ppm Mg^{2+} ([Cl^-] = 19773ppm), whereas in the experiments where Ca^{2+}/Mg^{2+} = 0.19 and 1.64, the above FWs are mixed with Fixed Case NSSW (Table 3.3) which contains 0ppm Ca^{2+} and 0ppm Mg^{2+} ([Cl^-] = 15026ppm).

Table 3.9 – Formation water Ca, Mg and Cl – experiments testing polymers in Sections 10.2 and 10.3 (Chapter 10) and PFC in Section 6.6.2 (Chapter 6).

Ion	Conc. / ppm	Formula
Na^{2+}	31275	NaCl
Ca^{2+}	2000	$CaCl_2.6H_2O$
Mg^{2+}	739	$MgCl_2.6H_2O$
K^+	654	KCl
Ba^{2+}	100	$BaCl_2.2H_2O$
Sr^{2+}	771	$SrCl_2.6H_2O$
SO_4^{2-}	0	Na_2SO_4
Cl^-	55191	–

Table 3.10 – Forties FW composition – used in mild scaling Base Case (MSBC) experiments.

Ion	Conc. / ppm	Formula
Na^{2+}	31275	NaCl
Ca^{2+}	See Table 3.12	$CaCl_2.6H_2O$
Mg^{2+}	See Table 3.12	$MgCl_2.6H_2O$
K^+	654	KCl
Ba^{2+}	100	$BaCl_2.2H_2O$
Sr^{2+}	771	$SrCl_2.6H_2O$
SO_4^{2-}	0	Na_2SO_4
Cl^-	See Table 3.12	–

Table 3.11 – Forties FW composition – used in mild scaling Fixed Case (MSFC) experiments.

Mixing Ratio NSSW/FW	FW [Mg^{2+}] / ppm	FW [Ca^{2+}] / ppm	FW [Cl^-] / ppm
30/70	1,056	2,857	57,631
60/40	1,848	5,000	63,732
80/20	3,695	10,000	77,965

Table 3.12 – Formation Water Ca^{2+}, Mg^{2+} and Cl^- content – applying to all mild scaling Fixed Case (MSFC) IE experiments. N.B. [Mg^{2+}] and [Ca^{2+}] are the same as in Table 3.5, however, [Cl^-] is lower due to the lower [Ba^{2+}] in the mild scaling FW.

Ion	Conc. / ppm	Formula
Na^+	11598 *	NaCl
Ca^{2+}	0	$CaCl_2.6H_2O$
Mg^{2+}	0	$MgCl_2.6H_2O$
K^+	460	KCl
Ba^{2+}	0	$BaCl_2.2H_2O$
Sr^{2+}	0	$SrCl_2.6H_2O$
SO_4^{2-}	0	Na_2SO_4
Cl^-	18303 *	–

*extra NaCl added to maintain ionic strength of the produced water to same level in both static compatibility experiments.

Table 3.13 – Sulphate-free NSSW (no Ca^{2+}, no Mg^{2+}) composition – used in one of the compatibility experiments testing PPCA.

Ion	Conc. / ppm	Formula
Na^+	31275	NaCl
Ca^{2+}	10000	$CaCl_2.6H_2O$
Mg^{2+}	3695	$MgCl_2.6H_2O$
K^+	654	KCl
Ba^{2+}	0	$BaCl_2.2H_2O$
Sr^{2+}	0	$SrCl_2.6H_2O$
SO_4^{2-}	0	Na_2SO_4
Cl^-	77290	–

Table 3.14 – Barium and strontium free FW – used in both compatibility experiments testing PPCA.

3.3 Static Inhibition Efficiency Test Procedure

3.3.1 Buffered Tests

The static barium sulphate IE test procedure is as follows:

In these tests each individual test condition is conducted in duplicate to allow anomalous results to be immediately recognised. Tests would be repeated if the difference in the recorded efficiencies was > 5 – 10%.

1. Prepare the two brines (NSSW and Forties FW) by dissolving the appropriate salts in distilled water (as described in Section 3.1).

2. Vacuum filter brines separately through 0.45μm membrane filter paper.

3. Dissolve the inhibitor in DW to create a stock solution of 10,000ppm active SI.

4. The inhibitor solution is then further diluted in NSSW (SI/NSSW solutions) to give the required concentration for the particular test. Each inhibitor concentration is tested in duplicate.
   Note: the concentration of inhibitor in NSSW (SI/NSSW) must be higher than that required for the test by a factor which accounts for the dilution when mixed with the formation water.

5. Measure out appropriate volumes of Forties FW, NSSW and NSSW/SI solutions into separate HDPE bottles. For example, for an 80:20 mix, measure out 160ml NSSW and SI/NSSW solutions and 40ml of FW for each test.

6. Add 2ml of buffer solution (see Section 3.4 for buffer solution compositions) to whichever brine (NSSW or FW) represents the largest volume, taking extreme care not to introduce impurities and cap all bottles securely. Shake the bottles to ensure full mixing of buffer with solution. The buffer dosage (after the mixing stage) is: 2ml buffer / 200 ml final brine mixture.

Note: The actual pH obtained must be checked prior to testing: For example, for an 80:20% NSSW:FW mix, add 2ml of buffer to 160ml NSSW. Record the individual pH values of 160ml NSSW + 2ml buffer and of unbuffered FW (40ml). Add the FW to the NSSW and record the pH, checking it is of appropriate value, ~pH4.5 or ~pH5.5 (as appropriate).

7. Place the bottles containing the NSSW and SI/NSSW into a water bath and the bottles containing the FW into an oven, both set to the required temperature ($95^{o}C$), for tests of an 80:20 NSSW:FW mixing ratio. Leave for ~60 minutes to reach test temperature.

8. After 60 minutes, mix the two brines together. For an 80:20 mixing ratio, add the FW to the NSSW and SI/NSSW solutions and shake quickly, ensuring maximum mixing is achieved. Start a stop clock (t = 0).

9. The tests are then sampled at the required time, t = 2 and 22 hours (these are standard sampling times, early-time and long-term), as described in Section 3.5. If it is an SI consumption experiment involving multiple sampling times and extended residence times, then e.g. t = ½, 1, 2, 3, 4, 5, 6, 22, 48, 72 and 96 – these sampling times can be altered / omitted to suit the particular experiment.

The static compatibility experiments described in Section 6.2.1 (testing PPCA) are done following the same procedure as described above, at pH5.5, except specific ions are omitted from the brines used, i.e. Ba^{2+}, Sr^{2+} and SO_4^{2-}.

3.3.2 Non-Buffered (pH adjusted) Tests

For IE tests by the pH adjustment method, the procedure changes slightly, viz:

1. Prepare the two brines (NSSW and Forties FW) by dissolving the appropriate salts in distilled water.

2. Vacuum filter brines separately through 0.45μm membrane filter paper.

3. pH adjust to pH4.5, pH5.5, pH6.5 or pH7.5 (as appropriate) using 0.1M NaOH and/or 10% HCl, enough Forties formation water to complete the experiment. Do NOT pH adjust the NSSW.

4. Dissolve the inhibitors in DW to create stock solutions of 10,000ppm active SI.

5. The inhibitor solutions are then further diluted in NSSW (SI/NSSW solutions) to give the required concentration for the particular test. Each inhibitor concentration is tested in duplicate.
   Note: the concentration of inhibitor in NSSW (SI/NSSW) must be higher than that required for the test by a factor which accounts for the dilution when mixed with the formation water.

6. Measure out appropriate volumes of pH adjusted Forties FW, non-pH adjusted NSSW and non-pH adjusted NSSW/SI solutions into separate HDPE bottles. For example, for an 80:20 mix, measure out 160ml NSSW and SI/NSSW solutions and 40ml of FW for each test.

7. Using 0.1N NaOH and/or 10% HCl, pH adjust to pH4.5, pH5.5, pH6.5 or pH7.5 (as appropriate), all the NSSW bottles – this needs to be done for each test bottle individually, i.e. blanks and SI-containing bottles.

8. Having now pH adjusted all the test bottles, place the bottles containing the NSSW and SI/NSSW into a water bath and the bottles containing the FW into an oven, both set to the required temperature (95^{o}C), for tests of an 80:20 NSSW:FW mixing ratio. Leave for ~60 minutes to reach test temperature.

9. After 60 minutes, mix the two brines together. For an 80:20 mixing ratio, add the FW to the NSSW and SI/NSSW solutions and shake quickly, ensuring maximum mixing is achieved. Start a stop clock (t = 0).

10. The tests are then sampled at the required time, t = 2 and 22 hours (these are standard sampling times, early-time and long-term), as described in Section 3.5. If it is an SI consumption experiment involving multiple sampling times and extended residence times, then e.g. t = ½, 1, 2, 3, 4, 5, 6, 22, 48, 72 and 96 – these sampling times can be altered / omitted to suit the particular experiment.

3.4 Buffer Solutions

All static IE tests are carried out at pH5.5 (using sodium acetate / acetic acid buffer), *except* where the effect of varying pH on IE is investigated (Chapter 7). Where pH is varied, tests are carried out at pH4.5, 5.5, 6.5 and 7.5. To achieve pH 4.5 or pH 5.5, a sodium acetate / acetic acid buffer can be used – see Table 3.15 for composition details. These buffer solutions are added to test bottles at a concentration of 1ml/100ml brine. Brine pH (using the buffer solutions) is checked to be adequate prior to experiments. It is not possible to use a sodium acetate / acetic acid buffer system to achieve pH6.5 or pH7.5 because these pH levels are outwith the buffering region for this buffer – see Table 3.16 [10]. The use of phosphate buffers to achieve pH6.5 or pH7.5 could affect the IE, and so are best avoided in this work. Selected IE tests at pH4.5 and pH5.5 are repeated in the absence of buffer (i.e. by pH adjustment). In buffer-free IE tests, to achieve pH4.5, pH5.5, pH6.5 or pH7.5, NSSW test bottles are individually pH *adjusted* using 0.1M NaOH and/or 10%HCl, prior to the mixing stage of the experiment (i.e. the pH adjustment is done after the NSSW/SI dilutions have been completed). Bulk FW is pH adjusted to pH4.5, pH5.5, pH6.5 or pH7.5 (as appropriate) prior to measuring into test bottles because no SI is added to the FW prior to the mixing stage of the experiment. Furthermore, the final pH of selected test bottles is also measured and

recorded after static IE experiments are completed, to ensure the correct pH level has been maintained throughout the entire IE experiment, regardless of whether buffer is present or not (full details are presented in Chapter 7).

pH	Sodium Acetate Trihydrate grams/100ml DW	Acetic Acid grams/100ml DW
4.5	13.6	4.0
5.5	13.6	0.4

Table 3.15 – Preparation details for pH4.5 and pH5.5 acetic acid / sodium acetate buffer solutions – to prepare 100ml.

Components	pH range
HCl, Sodium citrate	1 − 5
Citric acid, Sodium citrate	2.5 − 5.6
Acetic acid, Sodium acetate	3.7 − 5.6
K_2HPO_4, KH_2PO_4	5.8 − 8
Na_2HPO_4, NaH_2PO_4	6 − 7.5
CHES (*N*-Cyclohexyl-2-aminoethanesulphonic acid)	8.6 − 10
Borax, Sodium hydroxide	9.2 − 11

Table 3.16 − A selection of buffer systems and the pH range over which they can be used [10].

3.5 Quenching Solution, Sampling and Analysis

3.5.1 Standard procedure

The sampling procedure is carried out as follows:

The stabilising/dilution solution contains 1,000ppm "as supplied" commercial polyvinyl sulphonate scale inhibitor* (PVS) and 3,000ppm potassium (as KCl) in distilled water, adjusted to pH 8 – 8.5 by dropwise addition of 0.1N NaOH and/or 10% HCl. The KCl/PVS solution is continually stirred using a magnetic stirring plate and magnetic stirring bar during pH adjustment, to ensure continuous solution pH homogeneity. The solution of 1,000 ppm "as supplied" PVS has been shown to effectively stabilise (or quench) samples and thus prevent further precipitation. The potassium is included in this solution to act as an ionisation suppressant for the atomic absorption determination of barium. This is only included in current work for emergencies, since the standard analytical approach currently used within FAST laboratories for barium, is inductively coupled plasma (ICP) spectroscopy. 9ml or

5ml* of this potassium/PVS quenching solution is added to a test-tube at room temperature using an Eppendorf automatic pipette. After the required time interval, 1ml or 5ml* of the particular test supernatant waters is removed using an Eppendorf automatic pipette and immediately added to the 9ml or 5ml* of potassium chloride/PVS quenching solution. The samples are then analysed by ICP spectroscopy for the particular ions of interest, e.g. barium.
Note: A polycarboxylate scale inhibitor was initially used in the quenching solution. However, more recent tests using very high salinity formation brines resulted in precipitation of a polycarboxylate/divalent cation complex following sampling.

*The volume of sample taken from test bottles (either 1ml or 5ml) depends upon the NSSW/FW mixing ratio being evaluated in the IE test. For mixing ratios up to 70% NSSW, 1ml sample is sampled into 9ml KCl/PVS. For higher % NSSW mixing ratios 80/20, 90/10 and 95/5, 5ml is sampled into 5ml KCl/PVS – this is to ensure the [Ba^{2+}] is sufficiently high enough (post sampling) to be assayed by ICP spectroscopy successfully. In cases where [SI] is assayed by means of [P] by ICP spectroscopy (e.g. Chapters 9, 10 and 11), the 5ml sample into 5ml quenching solution sampling procedure was selected – this time to ensure the [SI] is sufficiently high enough (post sampling) to be detected by ICP spectroscopy – this is of particular importance when assaying for low [P]-containing P-tagged polymers such as PPCA. All ICP calibration standards (both barium and SI) are prepared in the appropriate diluent solution to ensure in every case, ICP calibration standards prepared are matrix-matched with the test-samples. In the case of 1ml sampling into 9ml KCl/PVS, the diluent solution is KCl/PVS quenching solution. In the case of 5ml sampling into 5ml KCl/PVS, the diluent solution contains appropriate concentrations of brine ions (excluding sulphate and barium) and KCl/PVS (which is present in the IE quenching solution). The concentration of the brine ions in the diluent solution depends on which NSSW/FW mixing ratio is being tested in the IE experiment (either 80/20, 90/10 or 95/5 NSSW/FW). For example, for mixing ratio 80/20 NSSW/FW, the diluent solution contains (by volume) 50% KCl/PVS, 40% NSSW (sulphate-free) and 20% FW (Fixed Case FW, suitable for 80/20 tests, excluding Ba^{2+} − see Table 3.4 and Table 3.5).

The required efficiencies for $BaSO_4$ inhibition are then calculated using the following equation:

$$\%Efficiency(t) = \frac{(M_B - M_I)x100}{M_B} = \frac{(C_O - C_B) - (C_O - C_I)x100}{(C_O - C_B)} = \frac{(C_I - C_B)x100}{(C_O - C_B)} \quad \text{(Eq. 3.1)}$$

Where;

M_B = Mass of barium (or other cations) precipitated in supersaturated blank solution.

M_I = Mass of barium (or other cations) precipitated in test solution.

C_O = Concentration of barium (or other cations) originally in solution (i.e. t=0).

C_I = Concentration of barium (or other cations) at sampling.

C_B = Concentration of barium (or other cations) in the blank solution (no inhibitor) at the same conditions and sampling time as C_I above.

(t) = Sampling time.

Note: C_O is determined by adding the test NSSW and Forties FW to the KCl/PVS quenching solution in the appropriate ratio, as used for the quenched test solutions. C_O samples are added to the ICP analysis of test samples at regular intervals to allow for instrumental errors to be accounted for.

3.5.2 Procedure Modification for Pinacyanol Assayed Test-Samples

Where there is a need to assay test-samples for sulphonated SI, as in 3 of the experiments presented in Chapter 11, a DETPMP-containing quenching solution is used rather than a PVS-containing one. The procedure is exactly the same as described in Section 3.5.1, except that DETPMP replaces PVS. In the one instance where PFC (a sulphonated SI) is assayed by ICP spectroscopy and by Pinacyanol / spectrophotometry, two sets of test-tubes were prepared for the IE sampling. One set of test-tubes contained 5ml of PVS-containing quenching solution. These samples were for the ICP analysis for [PFC] by means of [P], and so this quenching solution had to be DETPMP-free. The other set of test-tubes contained 5ml of DETPMP-containing quenching solution. These samples were for the Pinacyanol / spectrophotometric determination of [PFC], and so this quenching solution had to be PVS-free. Any PVS present would also react with the Pinacyanol reagent, creating false, enhanced results for [PFC].

3.5.3 Procedure Modification for Hyamine Assayed Test-Samples

In experiments where test-samples are analysed for [SI] by means of the C18 / Hyamine / spectrophotometric technique, in addition to taking a sample for ICP analysis (sampled into a test-tube), a 25ml sample is taken from each test-bottle and added this to 25ml of PVS-containing quenching solution (into a 100ml plastic bottle). A larger volume of sample is required for the C18 / Hyamine analysis. Furthermore, since this procedure clearly involves removing a large volume of liquid from each test bottle – in the static IE test, separate test bottles are heated (in duplicate) for each sampling time, i.e. 2 bottles for the ½ hour test, 2 bottles for the 1 hour test, etc. Only 2 blank bottles require to be heated, since only one sample is taken from these 2 SI-free bottles for SI analysis (at the final sampling time).

3.6 C18 / Hyamine / Spectrophotometric (CHS) Analytical Technique

3.6.1 Overview

This method is based on the turbidimetric determination of the precipitation obtained by the interaction of anionic polyelectrolytes, such as COO^- ions from COOH groups, with a quaternary ammonium salt such as Hyamine 1622. Baker Performance Chemicals supplied a working method to the former FAST, the OSRG, in 1994. This was examined for a range of polyacrylate based inhibitors in synthetic sea water. Since the method is susceptible to interferences from dissolved ions, in particular chloride ions, a separation stage involving adsorption onto C18 cartridges is necessary. Thus, the analytical procedure is much more solution robust than those for phosphonate based inhibitors. The process by which these cartridges perform is discussed below.

Sep-Pak C18 cartridges (design and purpose): This is a single use disposable cartridge containing an octadecylsilane ($Si(CH_3)_2C_{18}H_{37}$) bonded phase packing material., When using the cartridges with aqueous solutions, it is necessary to pre-wet the cartridge with a water miscible solvent such as methanol, then flush with water before use (see Figure 3.1). The C18 cartridge adsorbs neutral/hydrogen bonding species strongly, but does not adsorb charged species. Thus, in order to adsorb, the inhibitor must be in an un-charged state. To achieve this, the pH of the PPCA or MAT inhibitor solution is reduced to pH 1.5–2. The pK_a value for a carboxylic acid grouping is ~4.5. Thus, at this low pH of 1.5–2, the inhibitor is effectively in the un-dissociated (uncharged) acid form. On passing through the C18

cartridge under such conditions, the inhibitor is adsorbed and effectively separated from the interfering salts, which are charged and therefore do not adsorb. The inhibitor can then be eluted from the cartridge free from the interfering salts prior to colorimetric analysis.

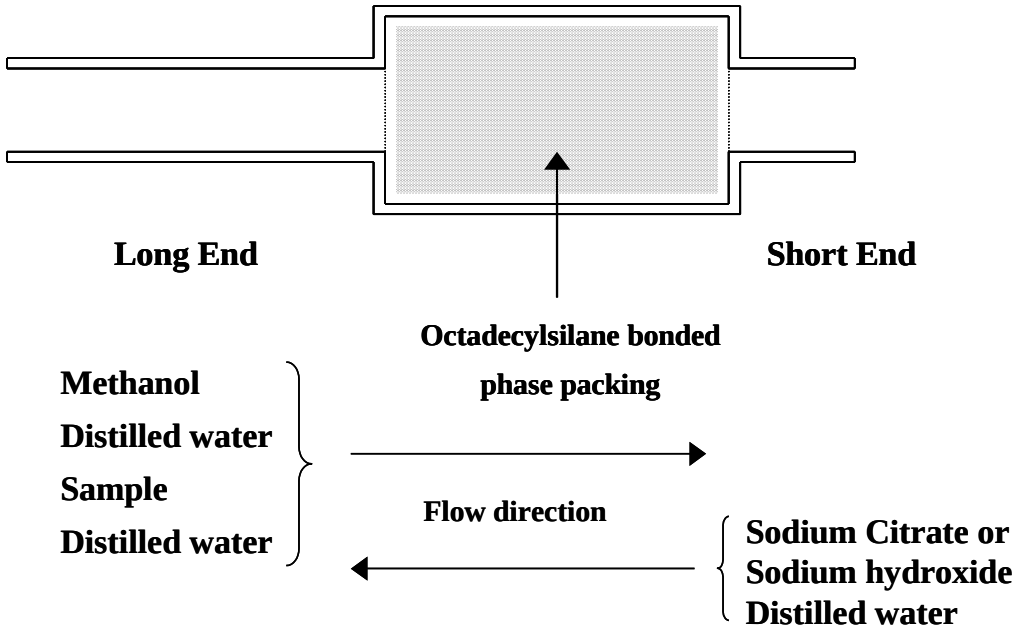

Figure 3.1 – Sep-Pak C-18 cartridge description

The polyacrylate/polymalate based species PPCA and MAT can be eluted with a variety of eluents including sodium hydroxide and citrate buffers. The choice of eluent is determined by the analytical method of choice so as to give minimal interference upon colour development/detection. For example, for Hyamine detection, a citrate buffer is the eluent of choice.

3.6.2 Equipment Required

UV/Visible Scanning Spectrophotometer (500nm)
Razel Syringe Pumps (supplied by Semat Technical (UK) Limited)
50ml volumetric flasks
Hyamine 1622 (supplied by VWR)
Sodium Tri-Citrate (supplied by VWR)
Sep Pak C18 cartridges (supplied by Waters)
5, 10 and 60ml plastipak syringes (supplied by VWR)

Optical cells (2 cm path length)
10% Hydrochloric Acid, Analar grade (conc. supplied by VWR)

3.6.3 Procedure

1. Dilute a 1,000ppm active SI/DW stock solution down to make 50ml standards at concentrations of 0 – 10ppm active in the appropriate brine i.e. NSSW, FW, diluent solution.

2. Adjust 50ml of each standard solution to pH 1.5 – 2.0 by drop-wise addition of hydrochloric acid 10% v/v.

3. Attach a 5ml syringe of methanol to the long end of a Sep-Pak C18 cartridge. Pass the methanol through the cartridge drop-wise and discard the expelled solution.

4. Using a syringe, pass 10ml of distilled water slowly through the cartridge and discard the expelled solution.

5. Using a 60 ml syringe and the Razel syringe pumps, pass inhibitor solution through the cartridge. Collect the fluid in a cup.

6. Wash the cartridge from the same end with 10ml of distilled water from a syringe, again utilising the Razel syringe pumps. The combined collected fluids from Steps 5 and 6 for each of the standard solutions can now be discarded, as the inhibitor should be adsorbed onto the cartridge.

7. Invert the cartridge and attach to the short end, a 10ml syringe containing 10ml of a 5% solution of sodium citrate (desorbing agent) in distilled water.

8. Elute the inhibitor slowly from the C18 cartridge using the 10ml of sodium citrate solution on the syringe pumps and collect each eluent in a 50ml volumetric flask.

9. Using the same 10ml syringe, pass 10ml of distilled water through the C18 cartridge, again collecting the eluent in the 50ml volumetric flask.

10. Pipette 10 ml of a 5,000ppm (as supplied) aqueous solution of Hyamine 1622 into the flask and dilute to the mark (50ml) with distilled water. A 1 minute time interval is suggested for addition of Hyamine to each flask to allow for analysis time on the UV/visible spectrophotometer.

11. Shake the volumetric flask quickly to ensure that the solutions are mixed and leave to stand for 40 minutes.

12. After 40 minutes, measure the absorbance of each of the standard solutions at 500nm using a UV/visible spectrophotometer. Use the tungsten lamp. Note – 500nm is in the "visible" light region of the electromagnetic spectrum.

13. Construct a calibration graph from the recorded standard solution absorbance values. It is normally a 3rd order curve.

14. Perform repeat analyses at known concentrations, to determine the repeatability of the method using the previously constructed calibration graph.

15. Repeat the procedure for samples and determine the concentration of chemical in the solution using their recorded absorbance values and the previously constructed calibration graph.

3.6.4 Reagent Chemical Structure

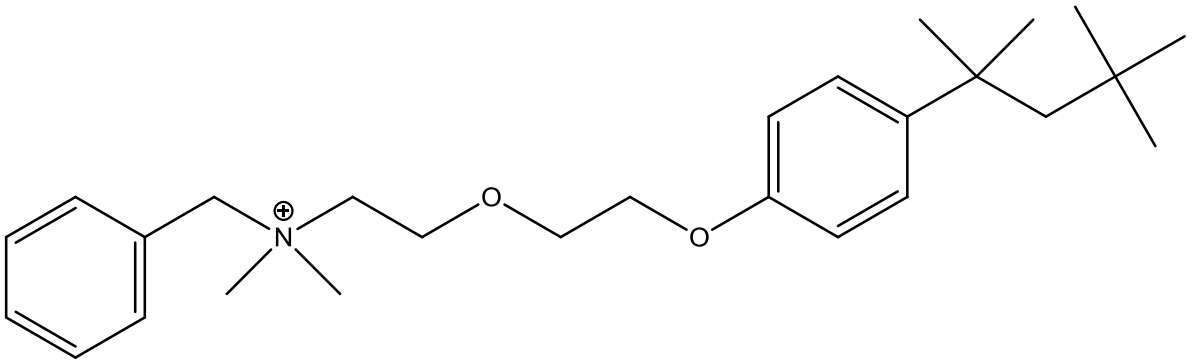

Figure 3.2 – Chemical structure of the chemical reagent Hyamine 1622 (a quaternary ammonium cation).

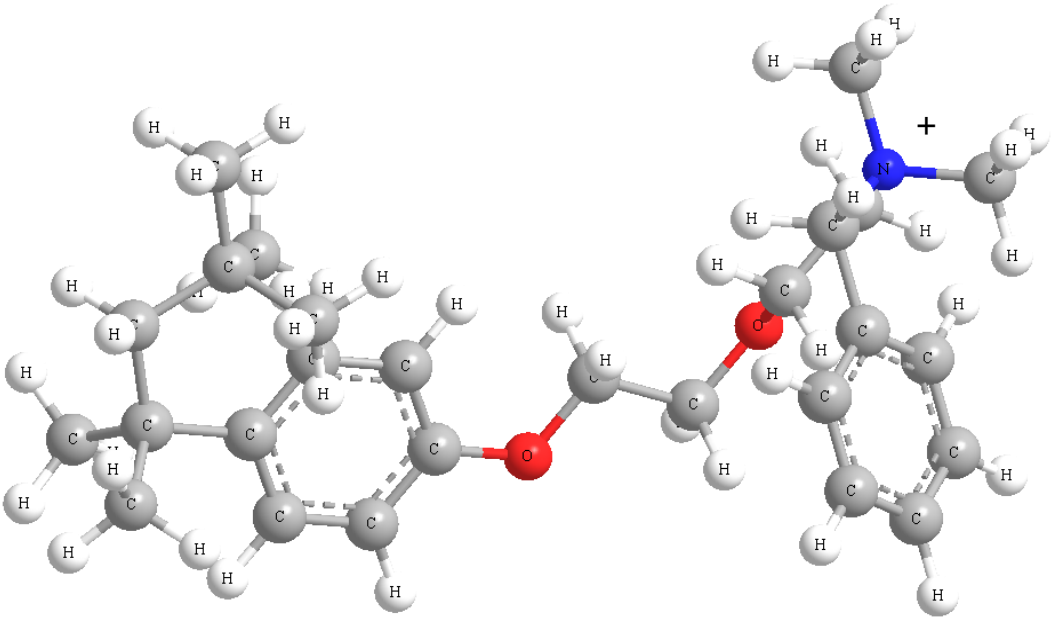

Figure 3.3 – ChemDraw molecular model of the chemical reagent Hyamine 1622 (a quaternary ammonium cation).

3.7 Pinacyanol / Spectrophotometric (PS) Analytical Technique

3.7.1 Overview

For sulphonated scale inhibitors such as PFC, PVS, VS-Co, SPPCA, etc., analysis by the Hyamine 1622 method is very poor, since separation of the inhibitors using C18 cartridges is not possible due to the ionic nature of the sulphonic acid group. Without separation from brine electrolytes, the Hyamine 1622 method gives very poor analysis due to interferences, particularly from chloride ions. In order to assay the various polyvinyl sulphonate inhibitors and co-polymers containing vinyl sulphonate groupings, several unpublished analytical procedures were obtained from Marathon and Baker Performance Chemicals. A method very similar to that reported by McTeir et al. (1993) was examined in more detail and shown to be acceptable in synthetic Sea Water. Due to the presence of interfering brine electrolytes, the method is inherently less accurate than the methods reported for phosphonate and PPCA inhibitors. However, due to the very short time required for this analytical technique, repeat analysis allows for the statistical accuracy to be greatly improved. It is recommended that at least three separate assays are conducted for each sample. Furthermore, this analytical technique gives a curve, which requires many points for calibration.

3.7.2 Procedure

1. Dilute a SI/DW stock solution down to make 20ml standards at concentrations: 0, 1, 2, 5, 8, 10, 15, 20 and 30ppm (active) in the appropriate matrix i.e. NSSW, FW, etc., with which to determine a calibration curve.

2. Add 1ml of the standard inhibitor solutions to 20ml of freshly prepared pinacyanol dye solution.

3. After exactly 2 minutes (after addition of 1ml test sample to 20ml dye solution, measure the absorbance of each sample at 485nm in a 2cm cell, using the UV/visible scanning spectrophotometer. Use a stop clock to measure the 2 minute time interval. 485nm is within the visible range of light. **Note:** Ensure the 2 cm cell is cleaned and rinsed thoroughly between test samples, thus ensuring no residual dye is present in the cell which could skew absorbance readings.

4. Subtract the 0ppm (blank) absorption signal from that of the standards and plot a normalised calibration curve.*

5. Perform repeats at known concentrations, e.g. 2 and 10ppm to determine the repeatability of the method using the previously constructed calibration graph. Analyse blank (0ppm) samples before and after a run of analysis (to allow for drifts).

6. Repeat the process for samples and determine the concentration of the chemical in the solution using their recorded absorbance values and the previously constructed calibration graph.

* Due to the instability of the dye solution once prepared, the calibration samples should be analysed immediately prior to analysis of repeat samples or actual test samples, using the same freshly prepared dye solution.

3.7.3 Reagent Chemical Structure

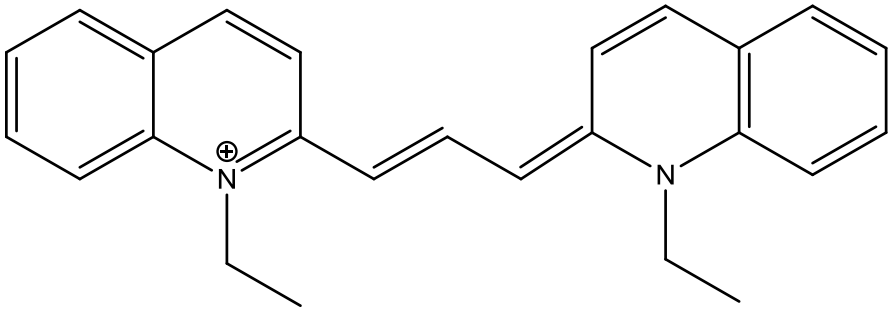

Figure 3.4 – Chemical structure of the Pinacyanol quaternary ammonium cation.

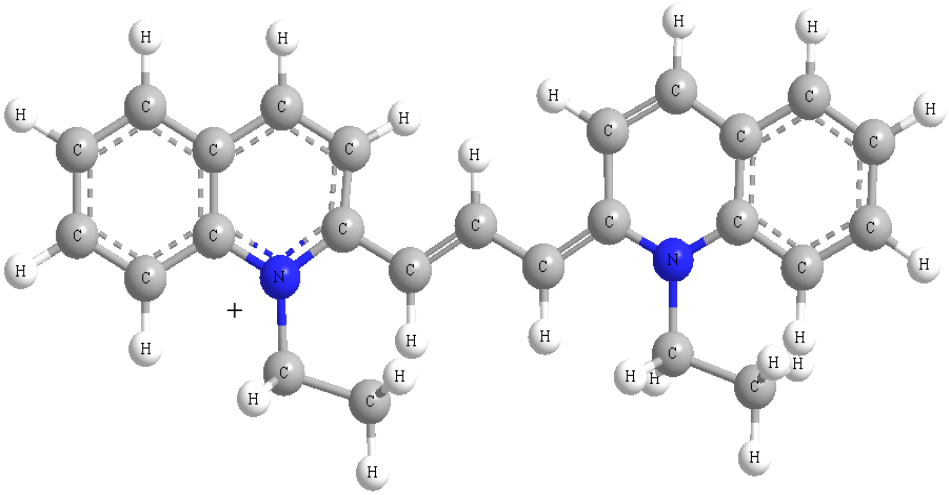

Figure 3.5 – ChemDraw molecular model of the Pinacyanol quaternary ammonium cation.

3.8 Procedure for Ca^{2+}/DETPMP/OMTHP static precipitation experiments (in DW).

These experiments are referred to in Chapter 12. These static precipitation experiments are very different from the static compatibility tests described in Chapter 6 (testing PPCA) because the test is *not* carried out in brine, but instead in DW. The principal aim of these experiments is to investigate the complexation of SI with Ca^{2+} (which can precipitate with SI). Only the SI in question, Ca^{2+} cations, and Cl^- are present in the test bottles. In particular, these experiments can be used to determine the molar ratio of precipitated M^{2+}/SI, i.e. to determine how many divalent cations are precipitated per molecule of SI. These tests are conducted at a fixed pH because pH affects the speciation of SI molecules and thus, the possible complexes which can form, and the stoichiometry of the precipitated compound. The pH is fixed by pH adjustment because the presence of buffer could affect SI function and precipitation. This test is carried out at a selection of temperatures (precipitation varies with temperature), to see if the molar ratio of M^{2+}/SI varies with temperature or remains constant. This experiment is mainly applicable to phosphonate SIs. So far, OMTHP (hexa-phosphonate) and DETPMP (penta-phosphonate) have been tested with Ca^{2+}. Solutions are prepared containing known quantities of SI and known quantities of Ca^{2+}. The solute calcium chloride hexa-hydrate is used to prepare the solutions. The [SI] can be fixed and a selection of [Ca^{2+}]s tested, or alternatively, a fixed [Ca^{2+}] can be chosen, and the [SI] varied.

The static precipitation experimental procedure is as follows:

1. Dissolve the SI in DW to create a stock solution of 10,000ppm active SI (for preparation of ICP calibration standards).
2. Dissolve the DETPMP inhibitor in DW to create a stock solution of 100,000ppm active SI (for SI dilutions).
3. If the experiment is at a fixed [SI], varying [Ca^{2+}], pH adjust 2500ml of DW to ~pH2 using 37% HCl (effectively preparing an HCl solution) to be used for preparation of each calcium chloride/SI solution (Step 4).

   If the experiment is at a fixed [Ca^{2+}], varying [SI], prepare a bulk Ca^{2+} solution (of appropriate concentration) in DW (e.g. 5L), and acidify to ~pH2 using 37% HCl just prior to making up to the 5L mark with DW. This acidified bulk Ca^{2+} solution is then used to prepare each calcium chloride/SI solution (Step 4).

4. If the experiment is at a fixed [SI], varying [Ca^{2+}], then prepare each calcium chloride/SI solution by firstly dissolving the appropriate quantity of calcium chloride hexahydrate ($CaCl.6H_2O$) in ~300ml of the pH2 HCl solution prepared in Step 3 and then adding the required volume of 100,000ppm active SI stock solution prior to making up to the mark in a 500ml volumetric flask. This solution is used to prepare 2 duplicate test bottles (2 x 200ml). Add 37% HCl prior to making up to the mark (if required), to prevent SI/Ca precipitation.

If the experiment is at a fixed [Ca^{2+}], varying [SI], simply prepare each test solution in a 500ml volumetric flask using the bulk Ca^{2+} acidified solution prepared in Step 3, by adding appropriate volumes of 100,000ppm active SI stock solution prior to making up to the mark. This solution is used to prepare 2 duplicate test bottles (2 x 200ml). Again, add 37% HCl prior to making up to the mark (if required), to prevent SI/Ca precipitation.

5. Measure 200ml of each solution into duplicate HDPE test bottles using a 250ml measuring cylinder. Retain the leftover 100ml of each solution for preparation of control samples (see Step 11).

6. pH adjust all the test bottles to pH5.5 using 0.1N NaOH / 12.5N NaOH / 37%HCl / 10% HCl.

7. After 24 hours, remove 1ml of supernatant liquid from each test bottle and add to 9ml of DW in a test-tube.

8. Place the same test bottles into a waterbath, set to 50^{o}C. Repeat step 7.

9. Repeat step 8 at 75^{o}C, and then at 95^{o}C. Therefore 4 sets of test-tubes are required (one set for 20^{o}C, one set for 50^{o}C, one set for 75^{o}C and one set for 95^{o}C).

10. After all tests have been completed, and test bottles allowed to cool to room temperature, measure and record the final pH of each test bottle, to check if a pH of ~5.5 has been maintained throughout the experiment.

11. Prepare control samples (using the leftover solutions from Step 5).

12. Prepare all necessary ICP calibration standards (SI and Ca^{2+}) in the correct background matrix, i.e. DW.

13. ICP spectroscopic analysis for [Ca^{2+}] and [SI].

3.9 Scale Inhibitors

3.9.1 Phosphonates

OMTHP (hexa-phosphonate)

Octa Methylene Tetraamine Hexa (Methylene Phosphonic Acid) – OMTHP

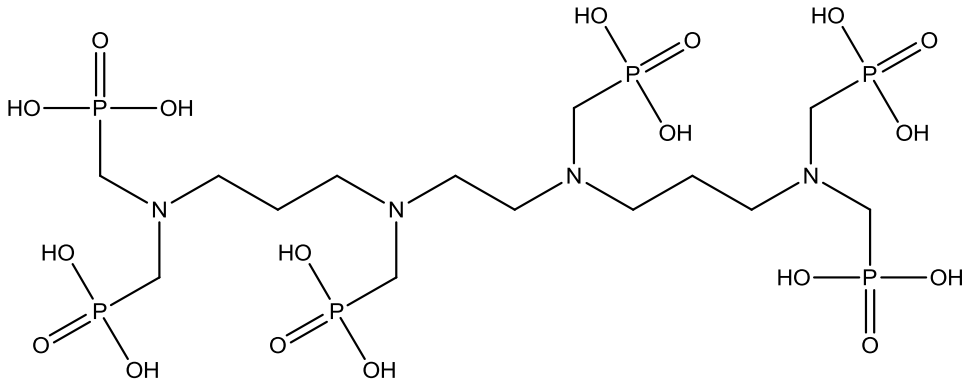

Figure 3.6 – Chemical molecular structure of OMTHP (hexa-phosphonate).

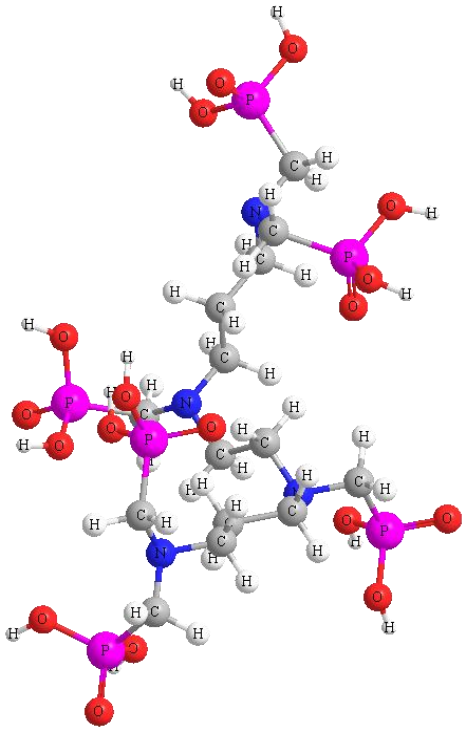

Figure 3.7 – ChemDraw molecular model of OMTHP (hexa-phosphonate).

DETPMP (penta-phosphonate)

DiEthylene Triamine Penta (Methylene Phosphonic Acid) – DETPMP

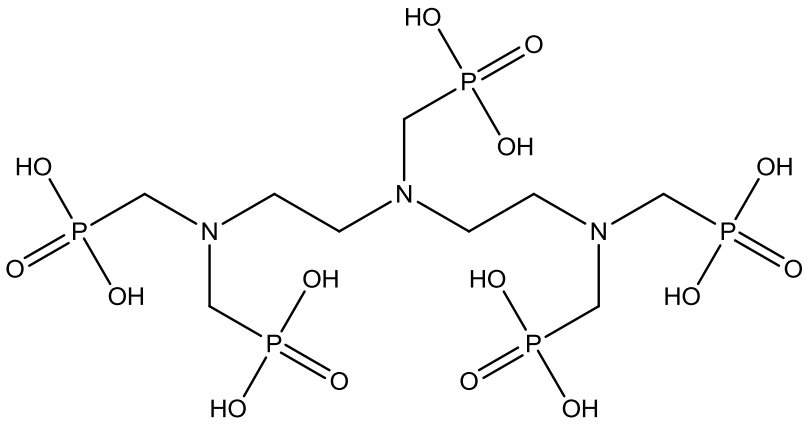

Figure 3.8 – Chemical molecular structure of DETPMP (penta-phosphonate).

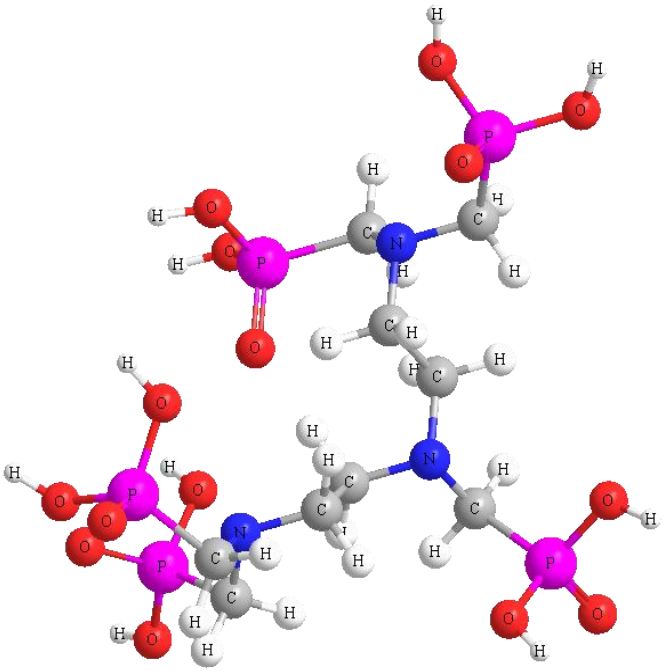

Figure 3.9 – ChemDraw molecular model of DETPMP (penta-phosphonate).

HMTPMP (penta-phosphonate)

Bis(HexaMethylene) Triamine Pentabis (Methylene Phosphonic Acid) – HMTPMP

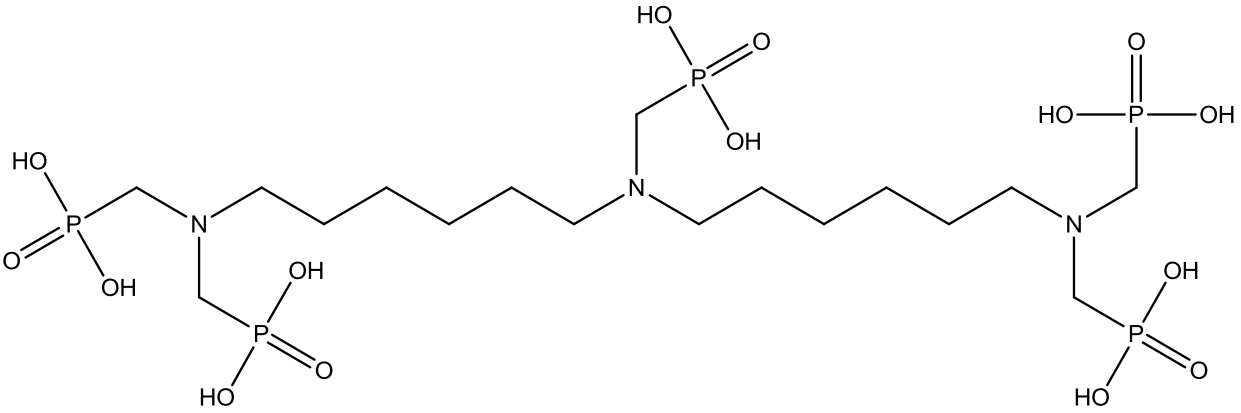

Figure 3.10 – Chemical molecular structure of HMTPMP (penta-phosphonate).

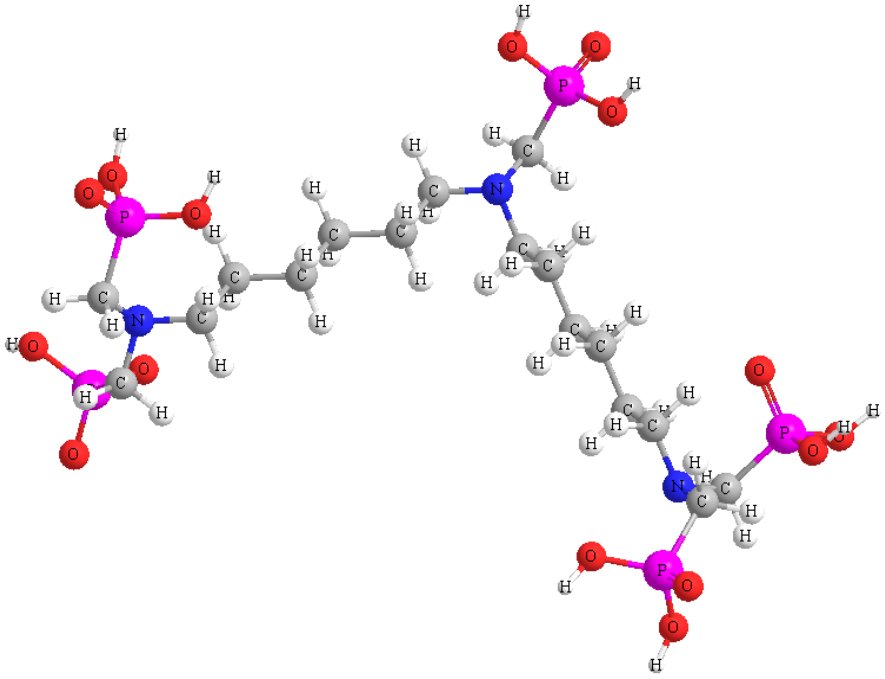

Figure 3.11 – ChemDraw molecular model of HMTPMP (penta-phosphonate).

HMDP (tetra-phosphonate)

HexaMethylene Diamine Tetra (Methylene Phosphonic Acid) – HMDP

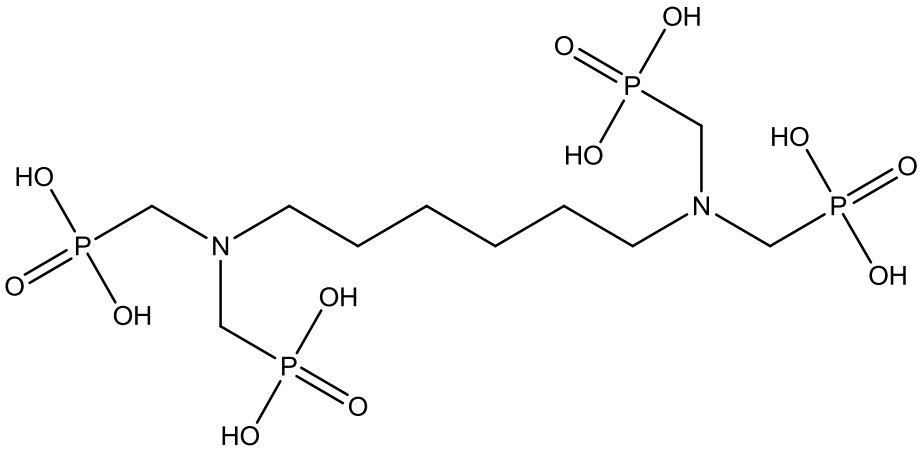

Figure 3.12 – Chemical molecular structure of HMDP (tetra-phosphonate).

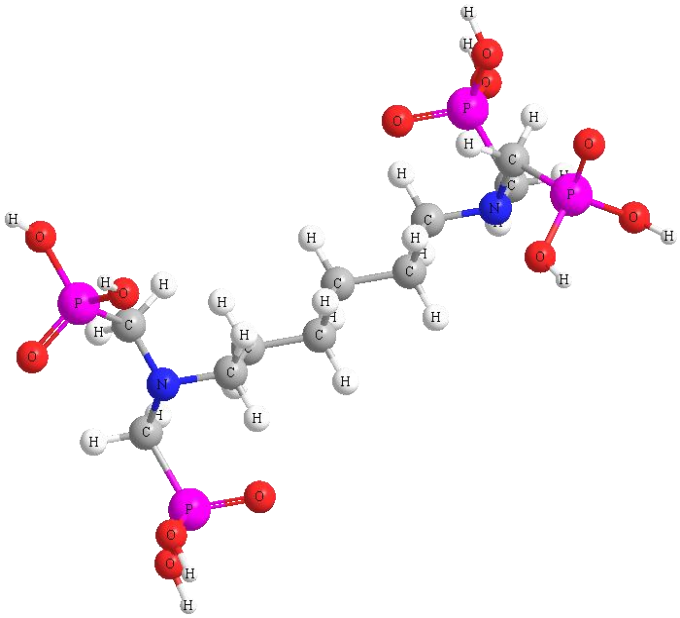

Figure 3.13 – ChemDraw molecular model of HMDP (tetra-phosphonate).

EDTMPA (tetra-phosphonate)

Ethylene Diamine Tetra (Methylene Phosphonic Acid)

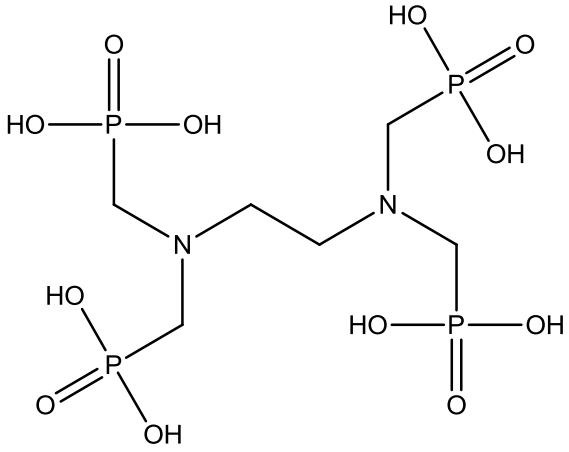

Figure 3.14 – Chemical molecular structure of EDTMPA (tetra-phosphonate).

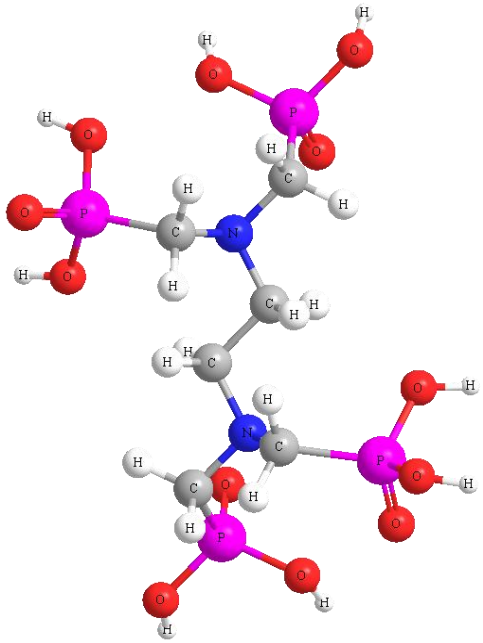

Figure 3.15 – ChemDraw molecular model of EDTMPA (tetra-phosphonate).

NTP (tri-phosphonate)

NitriloTris (Methylene Phosphonic Acid) – NTP

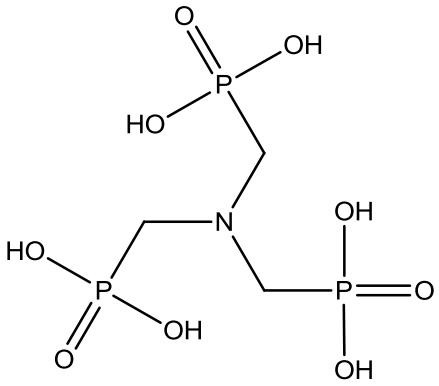

Figure 3.16 – Chemical molecular structure of NTP (tri-phosphonate).

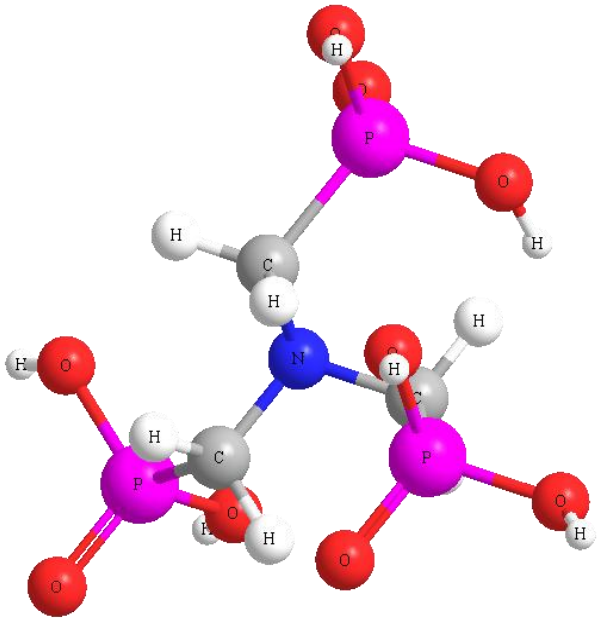

Figure 3.17 – ChemDraw molecular model of NTP (tri-phosphonate).

EABMPA (di-phosphonate)

EthanolAmineBis (Methylene Phosphonic Acid)

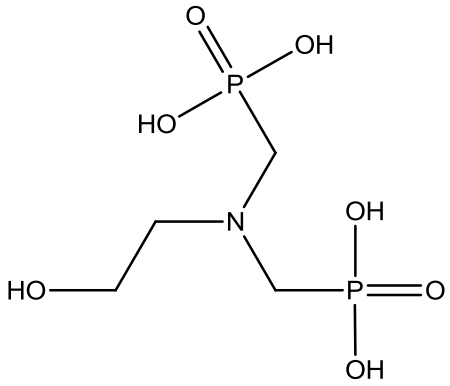

Figure 3.18 – Chemical molecular structure of EABMPA (di-phosphonate).

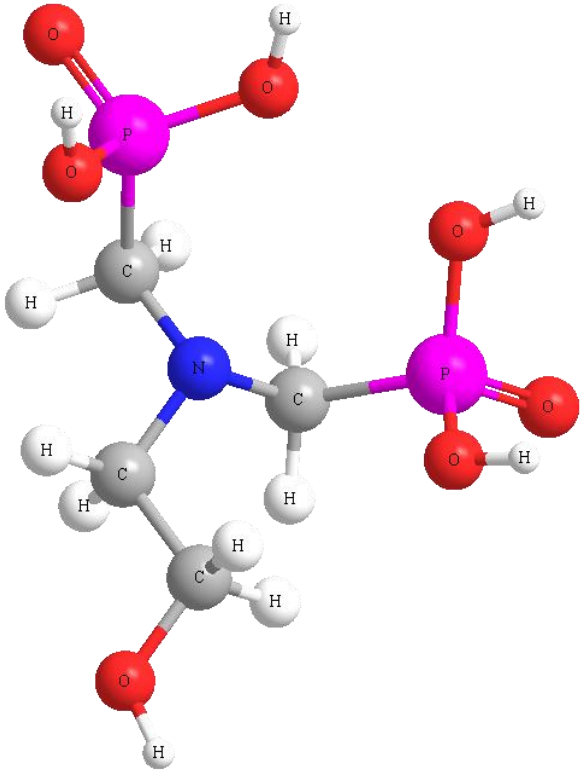

Figure 3.19 – ChemDraw molecular model of EABMPA (di-phosphonate).

HEDP (di-phosphonate)

1-HydroxyEthylidene-1,1-Di-Phosphonic Acid

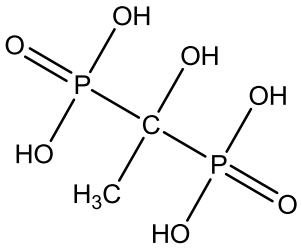

Figure 3.20 – Chemical molecular structure of HEDP (di-phosphonate).

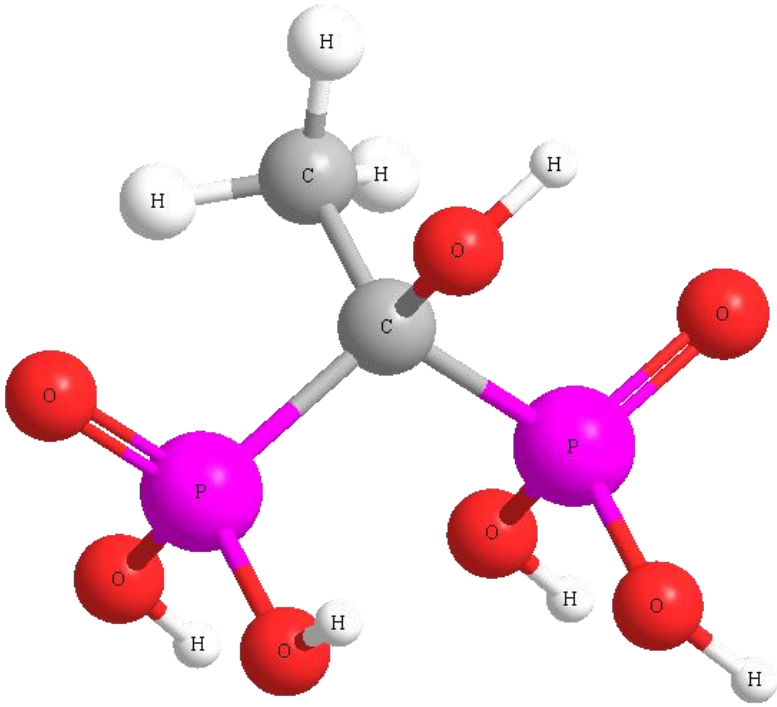

Figure 3.21 – ChemDraw molecular model of HEDP (di-phosphonate).

HPAA (mono-phosphonate & mono-carboxylate)

2-HydroxyPhosphonoAcetic Acid

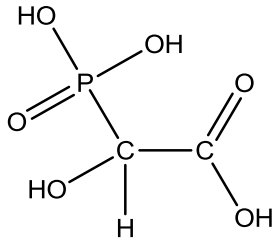

Figure 3.22 – Chemical molecular structure of HPAA (mono-phosphonate, mono-carboxylate).

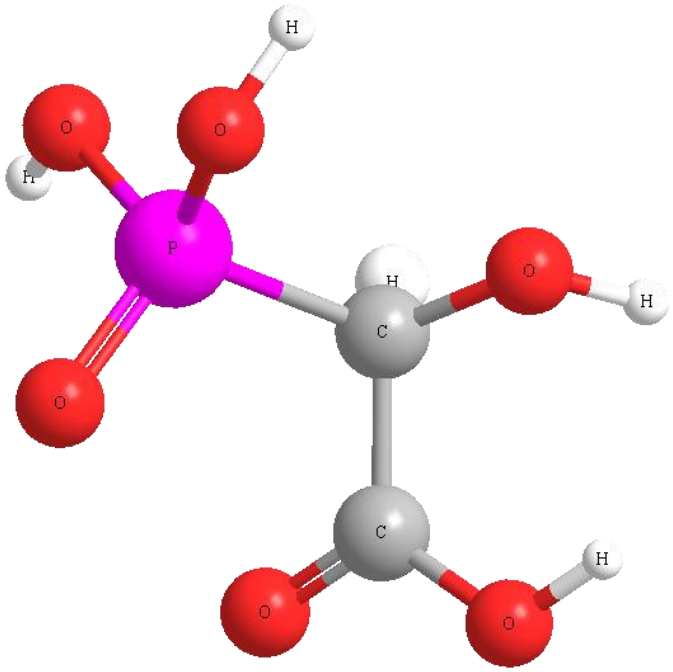

Figure 3.23 – ChemDraw molecular model of HPAA (mono-phosphonate, mono-carboxylate).

3.9.2 Polymers

PPCA – Phosphino PolyCarboxylic acid

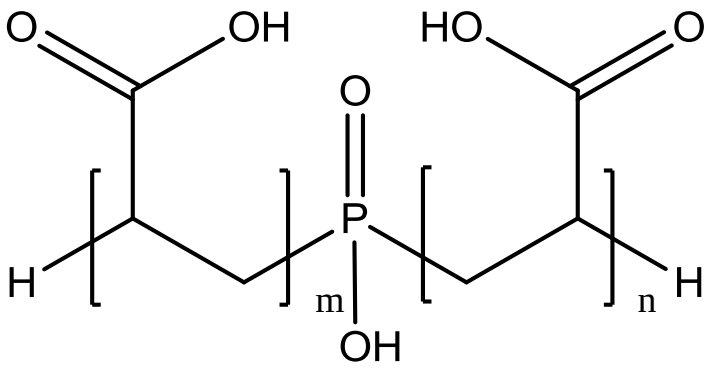

Figure 3.24 – Chemical molecular structure of PPCA.

MAT – Maleic Acid Ter-Polymer (a "green" SI)

Monomers: Maleic acid (MA) / Vinyl Acetate (VA) / Ethyl Acrylate (EA).

This is a "green" scale inhibitor.

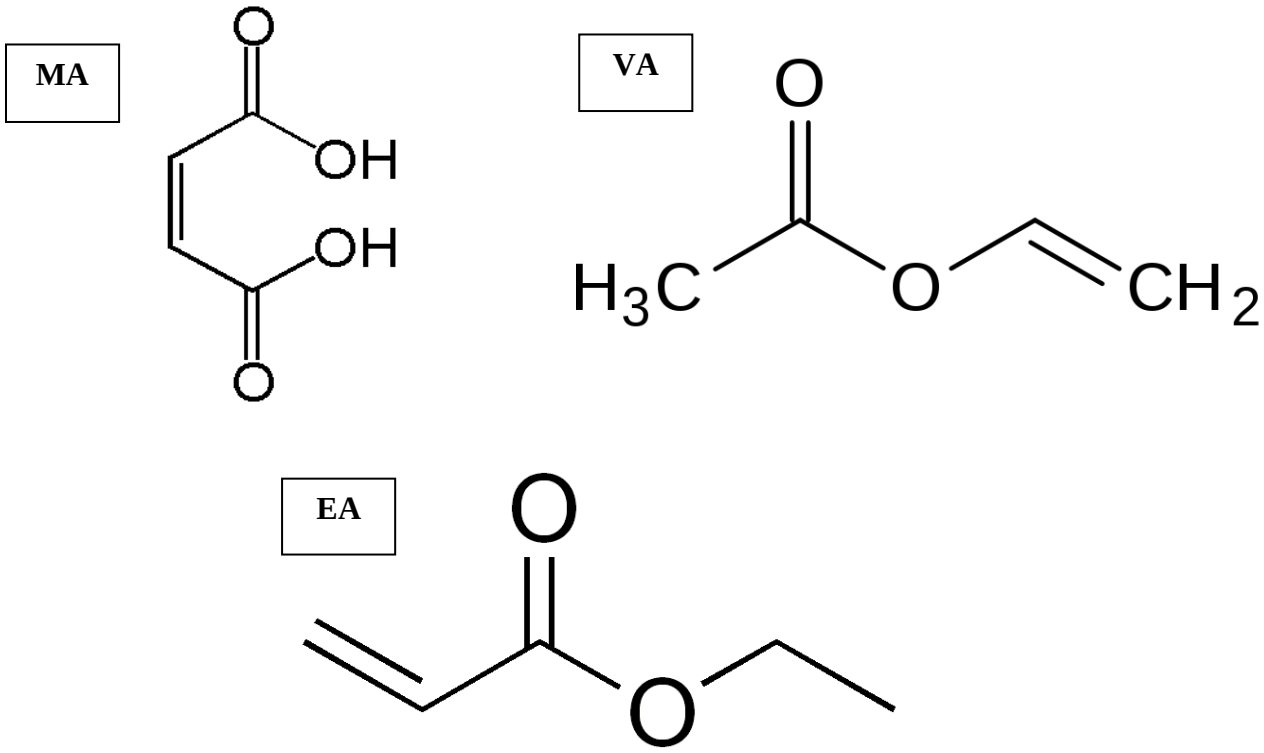

Figure 3.25 – MAT monomer structures: Maleic Acid (MA), Vinyl Acetate (VA), and Ethyl Acrylate (EA).

SPPCA – Sulphonated Phosphino PolyCarboxylic Acid

Monomers: Acrylic Acid and AMPS (2-acrylamido-2-methylpropane sulphonic acid).

Structure: Same as Figure 3.24 but sulphonated – some of the carboxylate functional groups will be replaced by AMPS side chains. This replacement may be ~50%, but depends upon the synthesis.

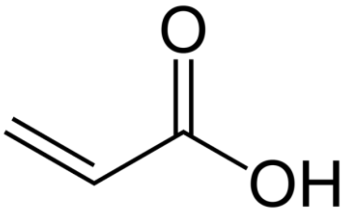

Acrylic Acid

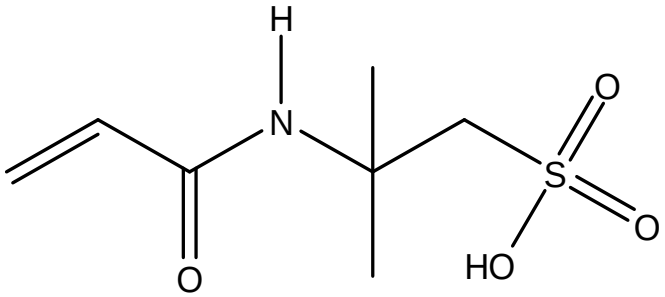

AMPS (2-acrylamido-2-methylpropane sulphonic acid)

Figure 3.26 – SPPCA monomer structures: Acrylic Acid and AMPS.

PVS (PolyVinylSulphonate)

Monomer: Vinyl Sulphonate.

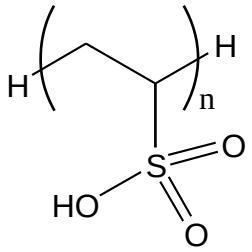

Polyvinyl sulphonate - PVS

Figure 3.27 – Chemical molecular structure of PVS.

VS-Co (VinylSulphonate Acrylic Acid Co-Polymer)

Monomers: Acrylic Acid and Vinyl Sulphonate.

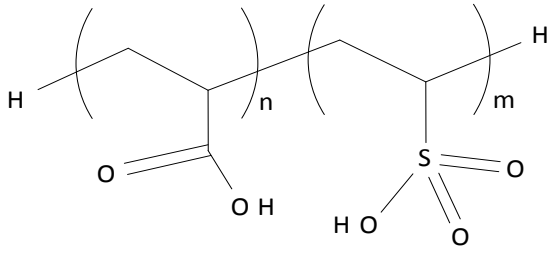

Figure 3.28 – Chemical molecular structure of VS-Co.

PMPA (PhosphinoMethylated PolyAmine – a Poly-Phosphonate)

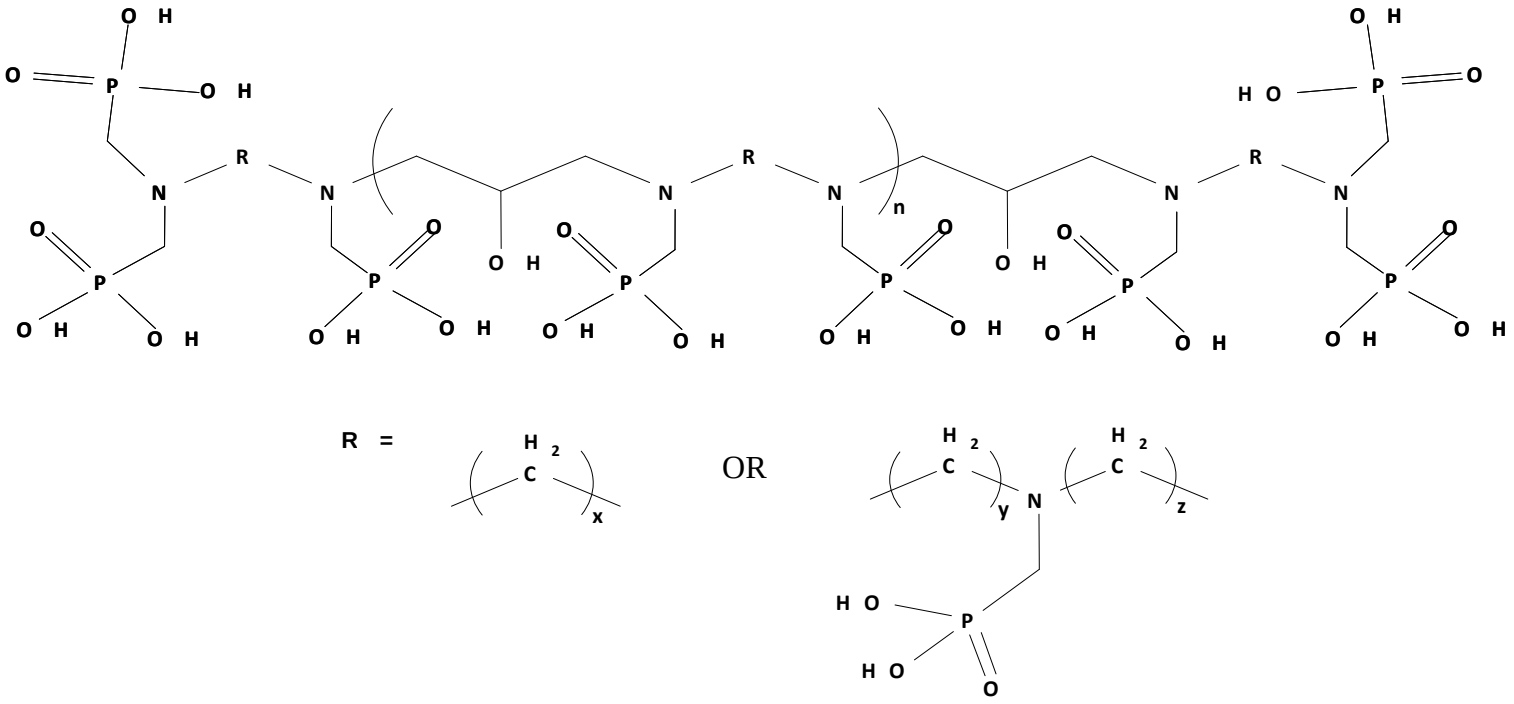

Figure 3.29 – Chemical molecular structure of PMPA.

P-Functionalised Co-Polymer (PFC)

This is a sulphonated polycarboxylated polymer containing phosphorus. The exact molecular structure was not disclosed to FAST. Hence in this thesis, it is given the generic name: "P-Functionalised Co-Polymer", and is named as such throughout (abbreviated PFC). This Product was supplied by a FAST sponsor company (see Acknowledgements page) to FAST for laboratory static barium sulphate IE testing/evaluation.

Cationic Ter-Polymers A and B (CTP-A and CTP-B)

Monomers: Sodium Allyl Sulphonate, Maleic Acid and an Allyl Quaternary Ammonium compound (to obtain positively charged functional groups).

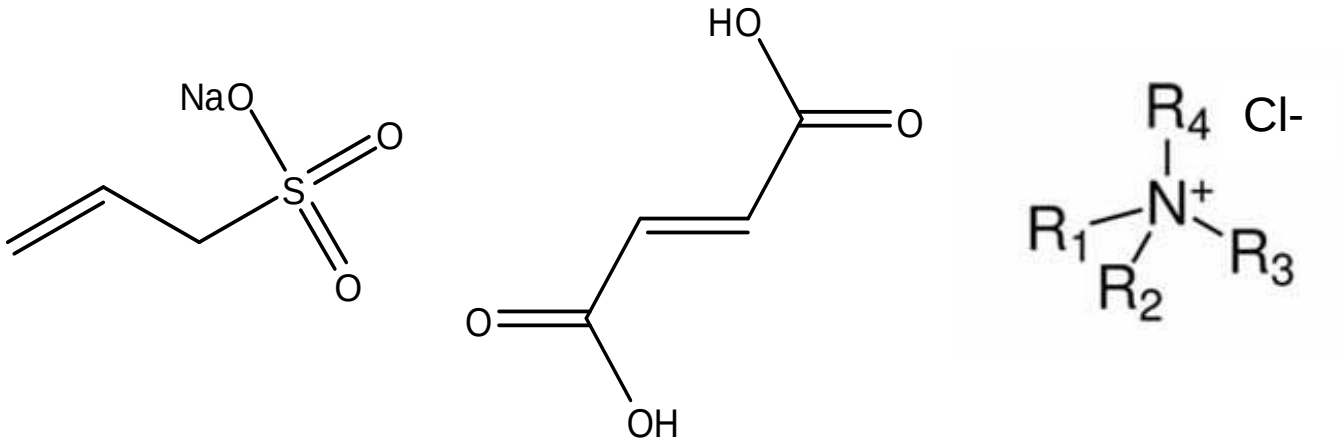

Figure 3.30 – CTP-A and CTP-B monomer structures: Sodium Allyl Sulphonate, Maleic Acid and Allyl Quaternary Ammonium Chloride (generic).

Notes: One of the "R" groups in the quaternary ammonium cation must contain a C=C bond to facilitate addition polymerisation – hence the reason why this monomer is described as an "allyl" quaternary ammonium compound. "Allyl" signifies the presence of a double-bond (un-saturation). The functional groups R_1, R_2, R_3 and R_4 may differ between CTP-A and CTP-B. The % of each monomer used in their synthesis may also vary.

Chapter 4: Chemical Analysis of Scale Inhibitor Products

Chapter 4 Summary: This Chapter describes the chemical analysis of the majority of the scale inhibitors (SIs) tested in this work. Each SI is analysed for % phosphorus and pH. In some cases the SI formulation is also assayed for Na^+, K^+, Ca^{2+} and Mg^{2+}. Furthermore, the polymeric SIs are also analysed for % sulphur. In some static IE experiments, SI is assayed at various times in the test in addition to [Ba^{2+}] (see Chapters 9 to 11); therefore analytical data such as SI phosphorus content is of significant importance.

4.1 Introduction

Scale inhibitors (SIs) which contain no phosphorus and no sulphur are commonly described as "green" species (Taj et al., 2006). Some products only contain a small quantity of phosphorus; these species are sometimes described as "yellow" products. Phosphorus "tagged" polymers such as PPCA fall into this "yellow" category. Products containing large quantities of phosphorus are usually the most environmentally hazardous, and are sometimes described as "red" or "black" products, as in the papers by Jordan et al., (2010, 2011). All conventional phosphonate SIs are classed as "red" species. This analytical work was carried out to gain a better understanding of the chemical nature of the various SI products, making further IE experiments involving the assay of these species by means of ICP spectroscopy (by means of [P]) or using other analytical techniques easier to approach and plan.

4.2 Phosphonates

4.2.1 Phosphorus

Table 4.1 gives the molecular weight (MW), g/mole phosphorus, theoretical and experimental % phosphorus values for the range of 9 phosphonate SIs tested in this work. The experimental % phosphorus values were determined by ICP spectroscopic analysis. This data is presented graphically in Figure 4.1. Excellent agreement is seen between the theoretical and experimental assay of P in these SIs.

PRODUCT	Associated phosphonic acid RMM / g/mole	g/mol P	Wt. %P Calculated (in associated acid form) NO Na or K	% P in scale inhibitor (from ICP)
OMTHP	738.40	185.82	25.2	26.1
DETPMP	573.25	154.85	27.0	28.1
HMTPMP	685.49	154.85	22.6	22.7
HMDP	492.28	123.88	25.2	27.8
EDTMPA	436.12	123.88	28.4	28.4
NTP	299.07	92.91	31.1	31.3
HEDP	206.03	61.94	30.1	30.6
EABMPA	249.12	61.94	24.9	25.3
HPAA	156.03	30.97	19.9	19.1

Table 4.1 – Molecular weight of the Phosphonate SIs tested in this work, their g/mole phosphorus, theoretical % phosphorus and experimental % phosphorus (by ICP spectroscopy).

The order of increasing % P is thus (taking calculated values), as follows:
HPAA < HMTPMP < EABMPA < OMTHP = HMDP < DETPMP < EDTMPA < HEDP < NTP

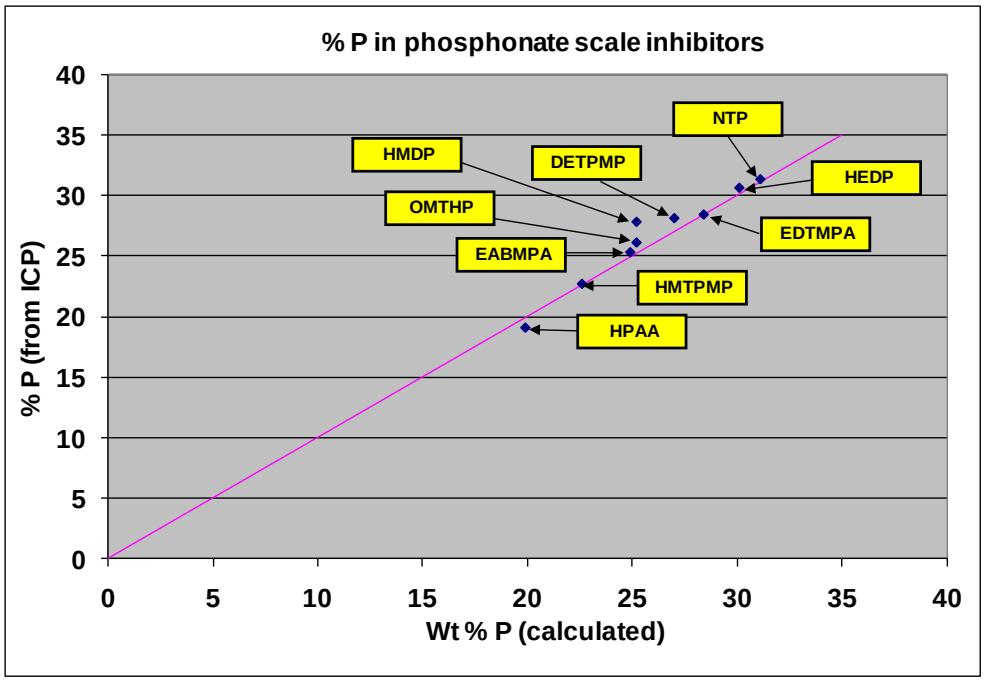

Figure 4.1 – Plot of experimental % P (by ICP spectroscopy) vs. theoretical % P (calculated) for the 9 phosphonate products tested in this work.

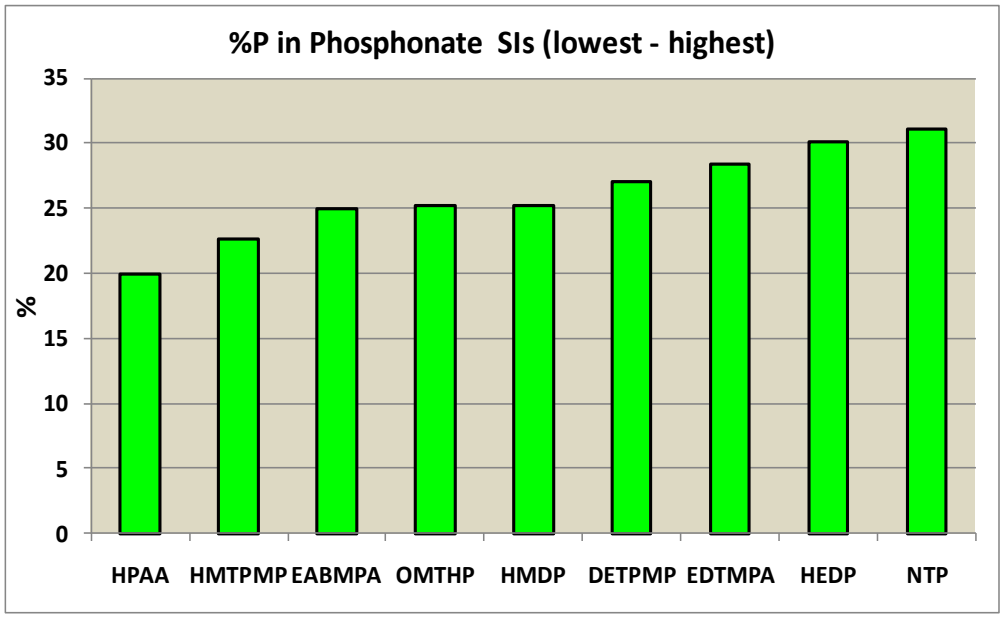

Figure 4.2 – Theoretical (calculated) weight % phosphorus (lowest – highest) in the 9 phosphonate SIs studied in this work.

4.2.2 Na^+, K^+, Ca^{2+} and Mg^{2+}

Phosphonate products OMTHP, DETPMP, HMTPMP, HMDP, NTP and EABMPA were analysed for [Na^+], [K^+], [Ca^{2+}] and [Mg^{2+}]. In each case, a 10,000ppm active DW solution was analysed by ICP spectroscopy. Figure 4.3 presents the results for [Na^+] and [K^+]. Only trace amounts of [Ca^{2+}] and [Mg^{2+}] were detected in the samples (these results are not shown).

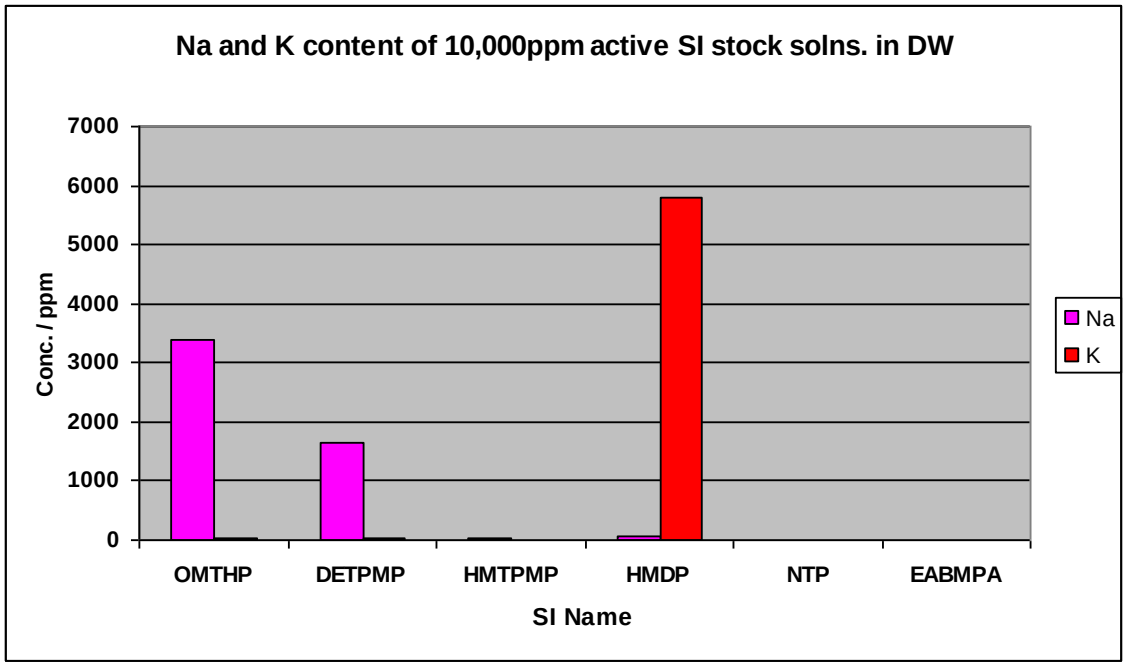

Figure 4.3 – [Na^+] and [K^+] (ppm) in 10,000ppm active OMTHP, DETPMP, HMTPMP, HMDP, NTP and EABMPA SI/DW solutions.

4.2.3 pH

All 9 phosphonate products were tested for pH. Again, a 10,000ppm active SI/DW solution was tested. Of these 9 products, all are acidic, except OMTHP and HMDP which both had near-neutral pH values. Table 4.2 and Figure 4.4 present the pH test results for the phosphonates. The near-neutral formulations may exist as phosphonate salts whereas those which are acidic are phosphonic acids. From Figure 4.3, it can be deduced that the OMTHP formulation exists as a sodium phosphonate solution whereas the HMDP formulation exists as a potassium phosphonate formulation. The DETPMP formulation is a partially-neutralised phosphonic acid solution – hence the presence of some sodium ions.

Scale Inhibitor *	**pH of 10,000ppm active stock solution (in DW), measured at 20^{o}C**	**Nature of Formulation (i.e. salt or acidic)**
HMDP (4P)	6.69	Salt Solution
OMTHP (6P)	6.39	Salt Solution
DETPMP (5P)	2.09	Partially neutralised Salt Solution (Acidic Salt Solution)
HEDP (2P)	1.62	Acid Solution
EABMPA (2P)	1.57	Acid Solution
EDTMPA (4P)	1.44	Acid Solution
NTP (3P)	1.44	Acid Solution
HMTPMP (5P)	1.42	Acid Solution
HPAA (1P, 1C)	1.36	Acid Solution

* The number and letter in brackets after the SI abbreviation denotes how many phosphonate and/or carboxylate functional groups are present per SI molecule, e.g. 1P, 1C denotes 1 phosphonate group and 1 carboxylate group.

Table 4.2 – Phosphonate scale inhibitors, pH of their 10,000ppm active stock solutions (in DW, measured at 20^{o}C) and nature of the formulation (acid/salt). Listed in order of decreasing pH.

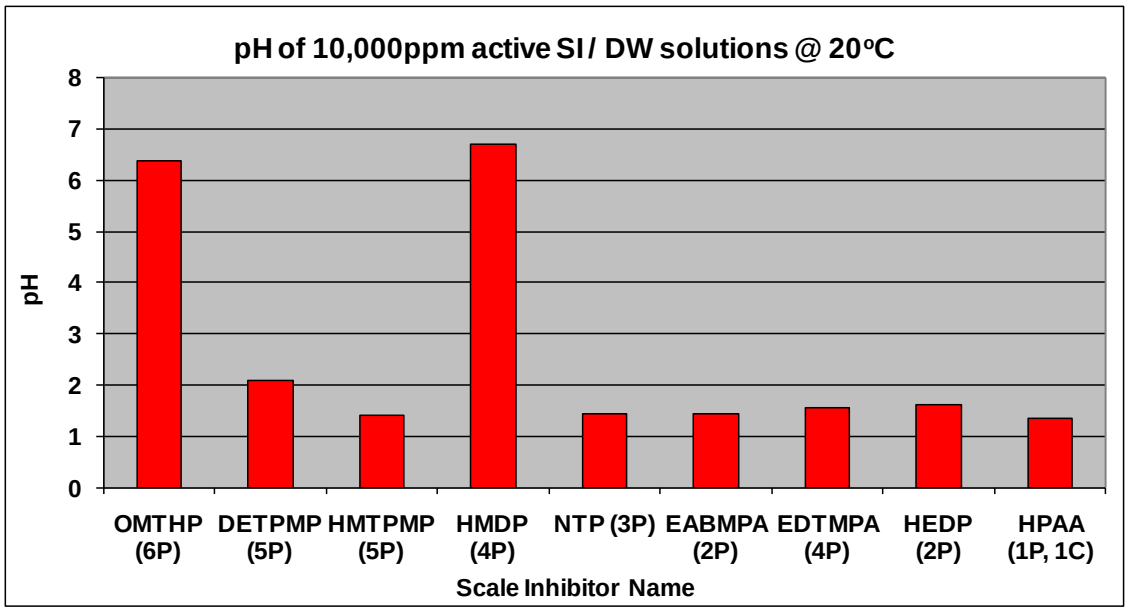

Figure 4.4 – pH of 10,000ppm active phosphonate SI/DW stock solutions – measured using a pH meter at 20°C.

4.3 Polymers

4.3.1 % Phosphorus and % Sulphur

All polymer products (except the cationic ter-polymers) were analysed by ICP spectroscopy for phosphorus and sulphur content. Two formulations of the PMPA, one at pH3 and one at pH5 – were both analysed. At the time of this experiment, the cationic ter-polymers had not been received by FAST; hence these products are omitted here. Two analytical spectral lines (wavelengths) were used for the phosphorus analyses, λ = 177.440nm and 214.914nm – results of both analyses are shown in Figure 4.5 for all the products tested. DETPMP (penta-phosphonate) was re-analysed alongside the polymers – to ensure the reliability of the analysis.

Figure 4.6 gives the % phosphorus and the % sulphur in each of the products. The % P or S is calculated by Equation 4.1. Figure 4.7 presents the results in a different way, showing the % P and % S for each product, as a proportion of the total mass of product (100%).

Both cationic ter-polymers are analysed by ICP spectroscopy in a later experiment, to determine the extent of sulphonation of these products (% sulphur).

% P or S = (X/Y)*100 (Eq. 4.1)

where X = ppm P or S (from ICP analysis)

Y = Concentration of test solution analysed (ppm active)

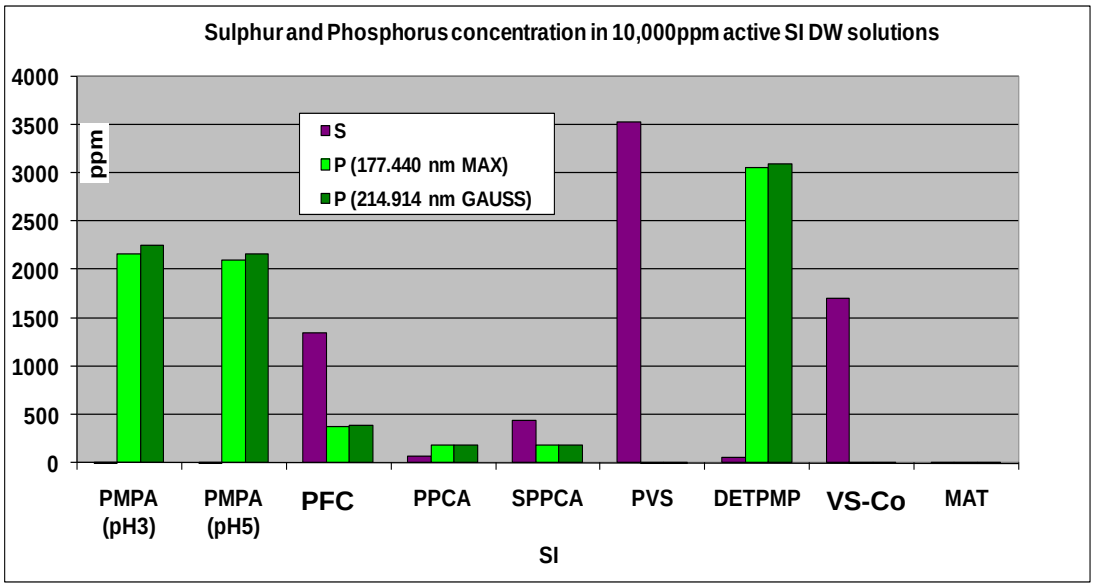

Figure 4.5 – Sulphur and phosphorus concentration (ppm) in 10,000ppm active SI DW solutions, determined by ICP spectroscopic analysis.

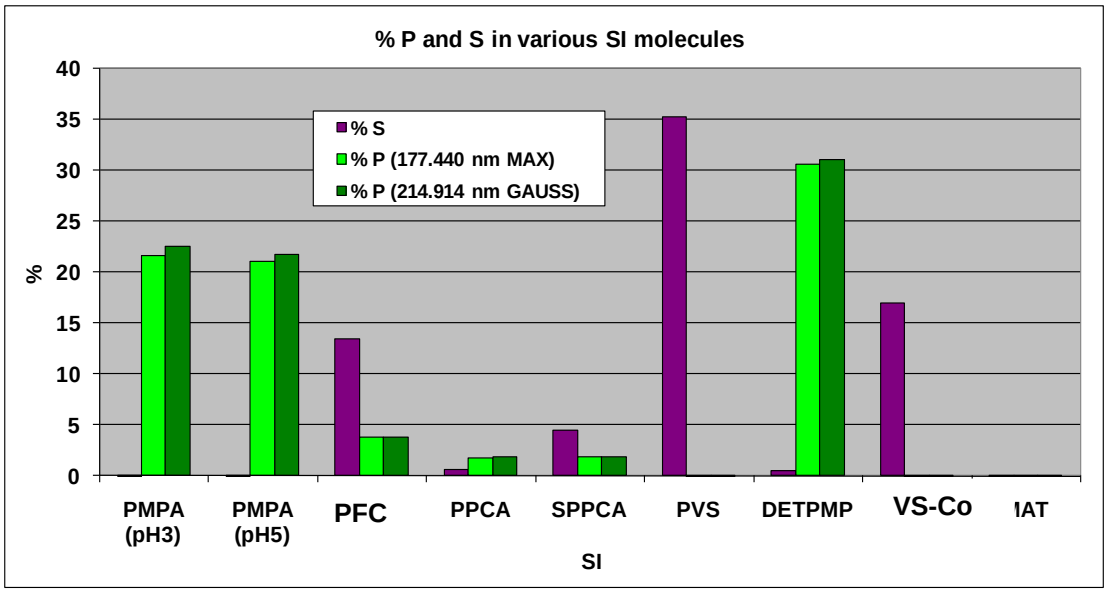

Figure 4.6 – % sulphur and % phosphorus in various SI molecules, determined by ICP spectroscopic analysis.

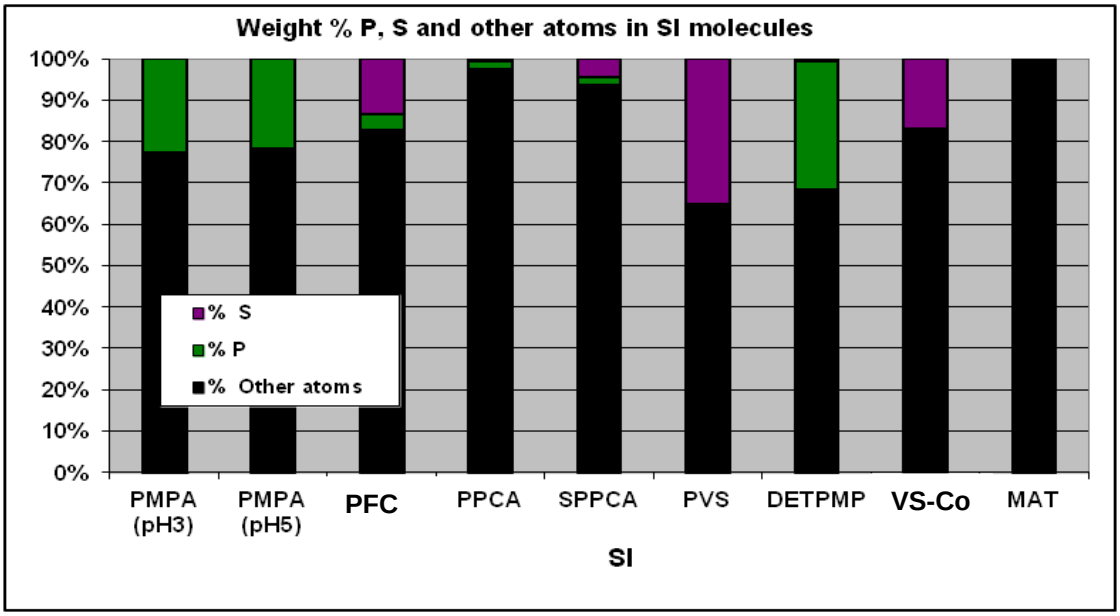

Figure 4.7 – Weight % P, S and other atoms in SI molecules. Other atoms = carbon, oxygen, hydrogen, and in some cases (i.e. PMPA, SPPCA, DETPMP), also nitrogen.

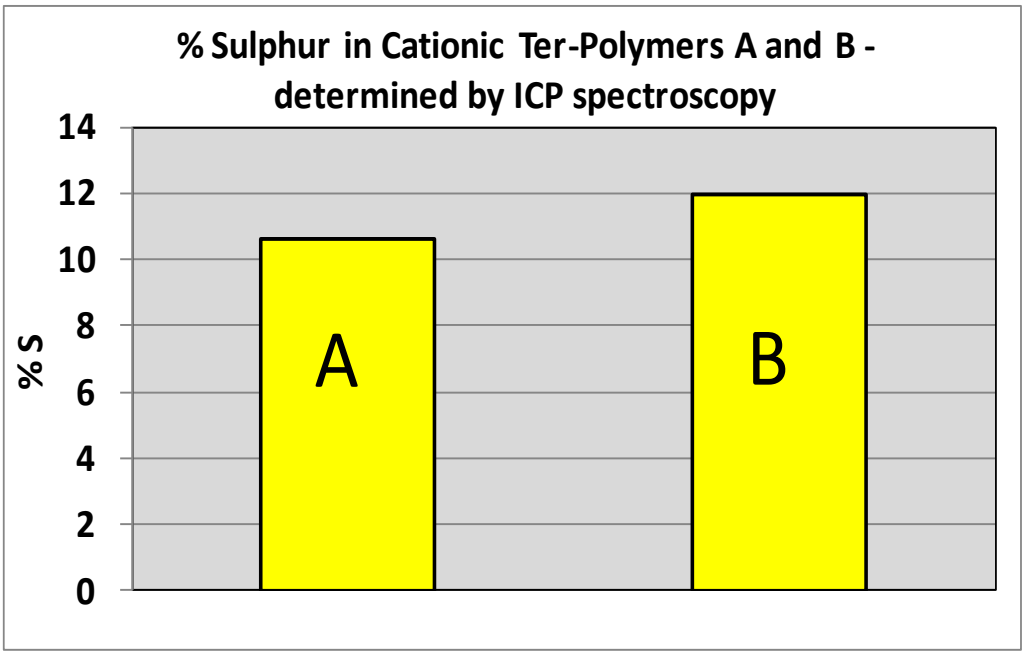

Figure 4.8 – Approximate % sulphur in cationic ter-polymers A and B – measured by ICP spectroscopy. Both cationic ter-polymers A and B contain sulphonated monomers.

From Figure 4.5, Figure 4.6 and Figure 4.7, of the polymers, the PMPA contains the largest proportion of phosphorus (~20%). PMPA is therefore classed as a "red" product. The PFC, PPCA and SPPCA each contain a small amount of phosphorus. All are P-tagged polymers. As expected, the PVS contains the largest % sulphur – this is a homopolymer of vinyl sulphonate. The VS-Co contains roughly half the quantity of sulphur as PVS – this observation suggesting that the VS-Co has been synthesised from a 50/50 % mix of vinyl sulphonate and acrylic acid monomers. Both PFC and SPPCA are sulphonated species, these too contain some sulphur, the latter containing the lesser amount.

From Figure 4.8, it is clear that CTP-B (~12% S) contains slightly more sulphur than CTP-A (~10.5% S). Taking into account the % sulphur data in Figure 4.6 and Figure 4.8, clearly, CTP-A and CTP-B contain more sulphur than SPPCA, but not as much as in PFC, VS-Co and PVS.

4.3.2 Na^+, K^+, Ca^{2+} and Mg^{2+}

As is the case with the phosphonates, a high level of sodium or potassium in the SI 10,000ppm active DW solution suggests the product exists as a salt solution. In the case of polymeric SIs, the polymer would exist in anionic form – charge balancing the sodium or potassium cations. Figure 4.9 presents the sodium and potassium analysis results for the polymers. Figure 4.10 presents the calcium and magnesium analysis results – no significant quantities of either of these elements are detected in any of the polymeric stock solutions. Once again, DETPMP has been included in both Figures.

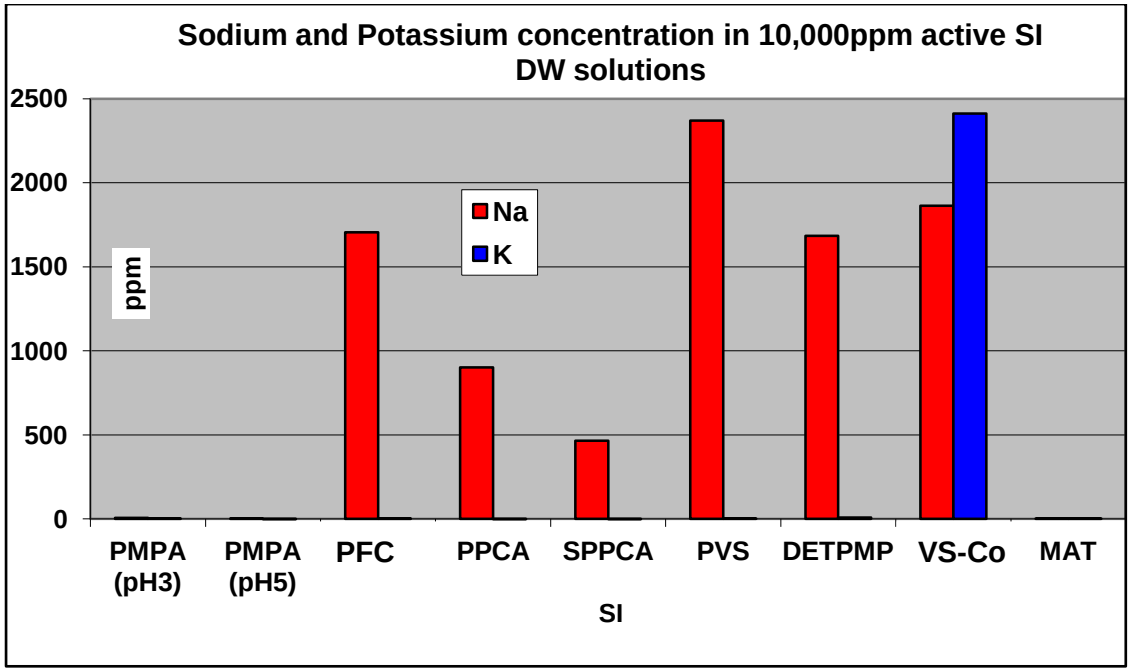

Figure 4.9 – Sodium and potassium concentration (ppm) in 10,000ppm active SI DW solutions.

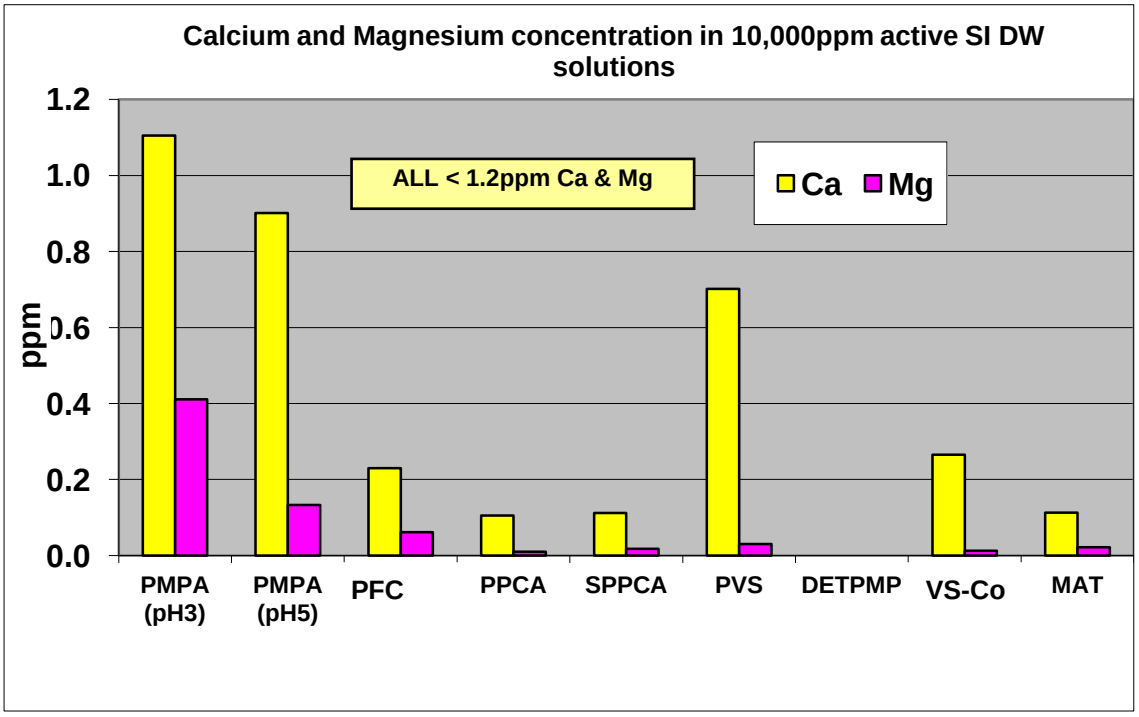

Figure 4.10 – Calcium and magnesium concentration (ppm) in 10,000ppm active SI DW solutions (note the very low scale: maximum here of ~1.2ppm).

4.3.3 pH

Table 4.3 and Figure 4.11 present pH test results, testing the polymers (except CTP-A and CTP-B). Once again, DETPMP is included here for reference.

Scale Inhibitor	**pH at 20°C**
PMPA (pH3)	3.41
PMPA (pH5)	5.39
PFC	6.90
PPCA	4.73
SPPCA	3.20
PVS	7.56
DETPMP	2.15
VS-Co	7.50
MAT	2.03

Table 4.3 – pH of various 10,000ppm active SI solutions (in DW), measured at room temperature (20°C).

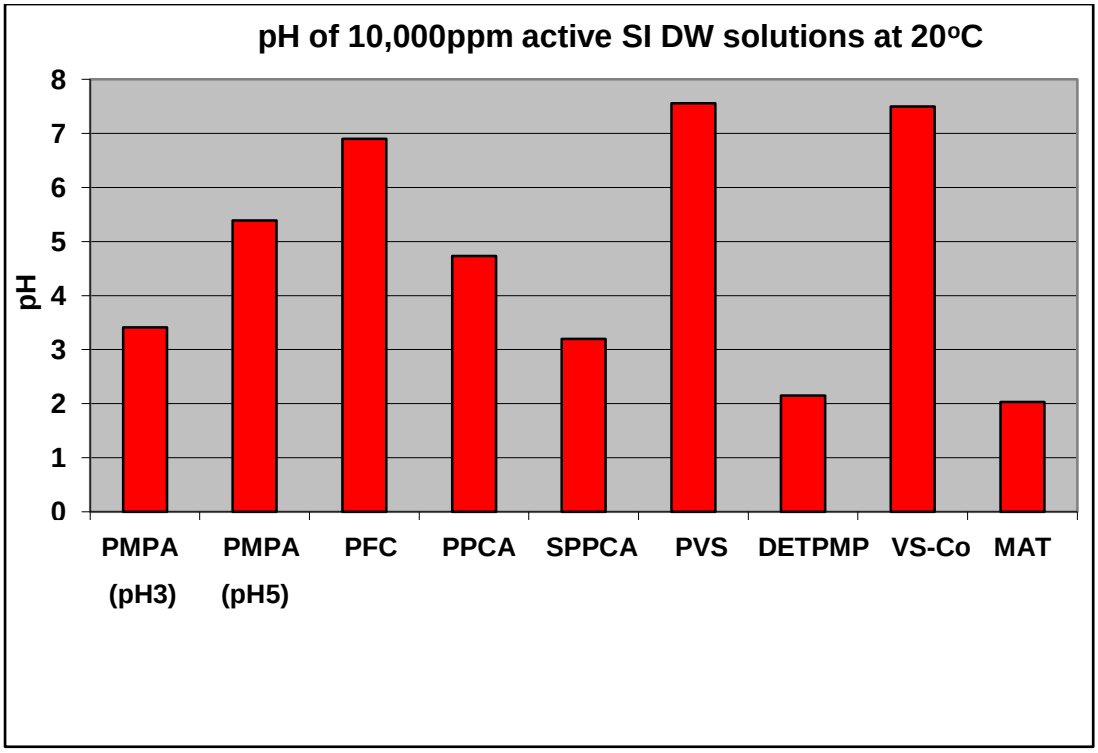

Figure 4.11 – pH of various 10,000ppm active SI solutions (in DW), measured at room temperature (20°C).

From the data presented in Figure 4.9 and Figure 4.11, it is clear that PFC, PVS and VS-Co may exist as polymer salt solutions. The polymer would exist as the anionic part of the salt. PVS and PFC may exist as sodium salts, whereas the VS-Co may exist as a mixed sodium / potassium salt – since large concentrations of both sodium and potassium were detected in the 10,000ppm active stock solution. The PMPA and MAT formulations are both clearly polymeric acids, and do not exist as salts. The PMPA formulation would be simply pH adjusted by the manufacturer to pH 3 or pH 5 – since no sodium or potassium is present. The PPCA and SPPCA may exist as partially neutralised acid solutions – since some sodium was detected in these stock solutions, with pH levels 3−5.

4.4 Summary and Conclusions

The experimentally determined % P in each of the phosphonate SIs correlated extremely well with the calculated / theoretical values. Thus, it is confirmed that the chemical nature of each SI is as presented in Section 3.9.1 of this thesis. It is important to note that the % P is a measure of the weight % P *per molecule, or per mole* of SI. For instance, tri-phosphonate NTP contains 3 phosphorus atoms per molecule, contains a large % P = 31.1% – because the NTP molecule is small. A hexa-phosphonate OMTHP molecule contains double the number of phosphorus atoms per molecule (6), but has a lower % P = 25.2% – because the OMTHP molecule is much larger than the NTP molecule, i.e. there are many more *non-phosphorus* elements present in the structure such as carbon, oxygen, hydrogen and nitrogen, resulting in a lower weight % P. The HEDP (di-phosphonate) molecule is also small, comparable with NTP. The HEDP has a % P = 30.1%, which is about 1% less than in NTP. Thus, the *order of increasing % P ≠ order of increasing number of phosphorus atoms per molecule.* Instead, the % P depends largely upon two factors:

(i) number of phosphorus atoms per molecule; and much more importantly;

(ii) molecular weight (MW) of the molecule – in particular, the molecular weight of the *sum of all the non-phosphorus atoms present.*

Small molecules such as NTP and HEDP are the most likely to have a large weight % P. The phosphonate SI with the lowest % P is HPAA – but in this case, despite the molecule being fairly small, factor (i) above is the most likely cause of the lower % P, i.e. because it is a mono-phosphonate. By contrast, the second lowest % P value is for penta-phosphonate SI HMTPMP – but in this case, factor (ii) above is the cause – the molecule is very elongated – the main chain contains 12 carbon atoms and 3 nitrogen atoms, thereby making the molecule heavier. Another point to note is that OMTHP (hexa-phosphonate) and HMDP (tetra-phosphonate) have the same weight % P, even although one has 6 phosphorus atoms per molecule and the other has 4 phosphorus atoms per molecule – this underlines the points outlined above.

Of the polymers analysed, the largest % P was detected in poly-phosphonate SI, PMPA (~22%); it was noted earlier that there is some suspicion that this is not in fact a polymer. Other phosphorus-containing SIs: PFC, PPCA and SPPCA contain a significantly smaller quantity of phosphorus (all <5%). As expected, the largest % S was detected in PVS – this is a sulphonated homopolymer, so this is very plausible. No sulphur or phosphorus was detected in MAT, as expected. MAT is non-sulphonated and non-phosphonated. The MAT molecules contain only carbon, oxygen and hydrogen atoms – making analysis for this SI by standard ICP spectroscopy impossible. For SIs such as MAT, ICP-MS could be used as an analytical method. The element of choice in SI molecules most commonly used for ICP analysis is phosphorus. Sulphur could be detected, but this is problematic because sulphur is very often present in the background solvent since:

(i) Sulphate anions are present in produced waters; and

(ii) A PVS quenching solution is used routinely (see Section 3.5) – the sulphur contained in the PVS would be detected in addition to any present in other SI – the signal would be much stronger than it should be (i.e. enhanced), giving an erroneous [S].

A small quantity of phosphorus is sometimes added to an SI structure on purpose (during SI syntheses) to make chemical analysis for such SIs easier (e.g. P-tagged polymers: PFC, PPCA and SPPCA). The main problem of having too high a phosphorus content in SIs is environmental concerns. "Green" SIs such as MAT are less hazardous to the environment. MAT is synthesised from maleic acid, vinyl acetate and ethyl acrylate monomers – all these compounds exist naturally in the biological environment – one is an organic acid, the two others are esters. High phosphorus-containing phosphonates and PMPA would be classified by OSPARCOM or PARCOM (Taj et al., 2006) as "Red" or "Black" SIs, because they are much more toxic to the environment (and also their biodegradation products) when they enter the eco-system. Other, more time-consuming analytical methods, such as wet chemical analysis (involving spectrophotometric analysis) (Boak and Sorbie, 2010), must be used in order to analyse for SIs containing no phosphorus, e.g. MAT. Table 4.4 lists all the SIs tested in this work, their % P, % S, and classification as red, yellow or green, based on the OSPARCOM / PARCOM classification criteria (Taj et al., 2006).

SI Name	Approximate % Phosphorus	Approximate % Sulphur	Likely OSPARCOM / PARCOM Environmental Classification (i.e. Red, Yellow or Green)
OMTHP	26	0	Red
DETPMP	28	0	Red
HMTPMP	23	0	Red
HMDP	28	0	Red
EDTMPA	28	0	Red
NTP	31	0	Red
EABMPA	25	0	Red
HEDP	30	0	Red
HPAA	20	0	Red
PMPA	22	0	Red
PPCA	2	1	Yellow
SPPCA	2	5	Yellow
PVS	0	35	Yellow
VS-Co	0	17	Yellow
PFC	4	14	Yellow
CTP-A	0	11	Yellow
CTP-B	0	12	Yellow
MAT	0	0	Green

Table 4.4 – OSPARCOM / PARCOM classification of the SIs tested in this work as red, yellow or green, plus their % P and % S (rounded to the nearest whole number).

The pH data and analysis of SI stock solutions for sodium and potassium makes it possible to establish whether a SI formulation exists as an acid solution or a salt solution. Those containing high levels of sodium and/or potassium usually have a near-neutral pH whereas those containing little or no sodium and/or potassium have acidic pH levels. All of the phosphonate SI formulations are acidic, except OMTHP and HMDP which exist as sodium and potassium salts, respectively. The HPAA had the lowest pH value of 1.36 – this molecule also contains a carboxylic acid functional group, this could explain why this formulation is slightly more acidic than the other phosphonic acid formulations. Phosphonate SIs are moderately dissociated weak acids. "Phosphonate" is simply the name given to

dissociated, anionic SI, e.g. $R{-}PO_3^{2-}$. If this anion were protonated, i.e. $R{-}PO_3H_2$, it becomes a phosphonic acid. Some phosphonate SI formulations exist as sodium or potassium salt solutions whereas others are aqueous acid solutions. This is because it is only phosphonate anions that are the active species giving rise to scale inhibition properties. Phosphonic acids become active when they are deployed in an environment at, for example, pH 5.5. At pH 5.5, the molecules become moderately dissociated, and thus, active. Similar observations were found in the analysis of polymers. The VS-Co formulation was unique, in that it may exist as a mixed sodium / potassium salt. However, in the case of polymers, the presence of sodium and/or potassium could also be due to the presence of sodium or potassium sulphate in the SI formulation. These compounds are commonly used as activators in the synthesis of polymeric SIs. Therefore the sodium and potassium analysis results for polymeric SIs need to be interpreted with caution. No significant quantities of calcium or magnesium were detected in *any* SI/DW stock solution.

The purpose of this Chapter was to give as full a chemical characterisation as possible of the various phosphonate and polymeric scale inhibitors used in this work. Later observation may then be referred back to these compositional findings.

Chapter 5: MIC vs. Mixing Ratio NSSW/FW Experiments – Phosphonate SIs

Chapter 5 Summary: This Chapter describes an extensive series of experiments measuring the static barium sulphate inhibition efficiency (IE) of a range of 8 *phosphonate* SIs. Their sensitivity to divalent cations Ca^{2+} and Mg^{2+} is investigated and how both this factor and the barite saturation ratio (SR) affect their MIC level. All the phosphonate species are tested in MIC vs. mixing ratio experiments where the 2 and 22 hour MIC is determined in various brine mix compositions. EABMPA (a di-phosphonate) is excluded from this work since its barite IE was much too poor.

5.1 Introduction

Conventional phosphonate type scale inhibitors (SIs) are commonly applied for barium sulphate and calcium carbonate scale prevention in oilfields (Graham et al., 2002c; Ralston, 1969). Barium sulphate forms when the injection water (NSSW – usually sulphate rich) is injected into barium containing formation water (FW). It is well known that the inhibition efficiency (IE) of barite scale inhibitors is affected by the barium sulphate saturation ratio (SR) of the brine mix and, in addition, the presence of divalent cations, Ca^{2+} and Mg^{2+} (Boak et al., 1999; Shaw et al., 2010a). What is less well known is that the precise balance between these factors (SR and Ca^{2+}/Mg^{2+} ratio) can vary significantly for different phosphonate species (Shaw et al., 2010a). This Chapter presents novel IE experimental results for the 8 phosphonate scale inhibitors, OMTHP, DETPMP, HMTPMP, HMDP, EDTMPA, NTP, HEDP and HPAA. Minimum Inhibitor Concentration (MIC) levels for each SI are established by testing them over a wide range of brine NSSW/FW mixing ratios which changes (i) barite saturation ratio and precipitated mass; (ii) molar ratio of Ca^{2+}/Mg^{2+}; and (iii) the ionic strength of the brine mix. EABMPA was *not* included in this work, since its barium sulphate IE was so poor; it was not possible to test this product in this series of experiments.

In a static scale inhibition efficiency test for barium sulphate, Inhibition Efficiency (IE, as %) is defined by Equation 5.1, at a given time, t, after mixing the scaling brines.

$$I.E. = 100\left(\frac{C(t) - C_b(t)}{C_o - C_b(t)}\right) \qquad \text{(Eq. 5.1)}$$

where C(t) = test sample Ba^{2+} concentration at time, t (ppm); C_O = control sample Ba^{2+} concentration at time, t = 0 (ppm); and $C_b(t)$ = Ba^{2+} concentration in the blank solution (containing no SI) at time, t (ppm).

Barium sulphate saturation ratio (SR) is a dimensionless quantity, which is defined as follows:

$$SR = \frac{[Ba^{2+}]_o[SO_4{}^{2-}]_o}{K_{sp}} \qquad \text{(Eq. 5.2)}$$

where $[Ba^{2+}]_o$ = initial barium ion concentration (mol/L); $[SO_4^{2-}]$ = initial sulphate ion concentration (mol/L); and K_{sp} = barium sulphate solubility product, at temperature T, specific pH and ionic strength level. Note that SR depends on a number of experimental conditions, including the NSSW:FW mixing ratio, temperature (T), pH, and ionic strength. Since T=95^{o}C and pH=5.5 in all IE experiments described in this chapter, only the brine mixing ratio and ionic strength variables affect SR in the tests described here. The variation of SR with brine mixing ratio and ionic strength (i.e. Base Case vs. Fixed Case) is illustrated in Figure 5.1.

In this Chapter, it will be illustrated that phosphonate SIs can be categorised into two types based on their MIC vs. %NSSW behaviour: Type 1 (e.g. DETPMP and OMTHP) are affected principally by SR and are rather less sensitive to Ca^{2+}/Mg^{2+} ratio although they do show some sensitivity to the latter factor. Type 2 (e.g. HMTPMP and HMDP) which are much more severely affected by brine Ca^{2+}/Mg^{2+} ratio as well as SR. To demonstrate these effects conclusively, a series of IE experiments are presented with varying $[Ca^{2+}]$ and $[Mg^{2+}]$ (which normally occurs in the field as the NSSW/FW ratio changes over time) and then a similar series of experiments are repeated at a fixed Ca^{2+}/Mg^{2+} molar ratio. The MIC level measured for both Types 1 and 2 phosphonate SI always correlates well with the barite saturation ratio at fixed Ca^{2+}/Mg^{2+} molar ratio (Fixed Case). In addition, the MICs of both types of SI are much lower in the Fixed Case experiments (higher Ca^{2+}/Mg^{2+} molar ratio), compared to the Base Case due to the beneficial effect of higher $[Ca^{2+}]$. The effects observed are important

for field application of phosphonate SIs since they show how the various species are sensitive to the changing scaling problems as the % NSSW increases, in terms of SR and Ca^{2+}/Mg^{2+} molar ratio. These results also give some important insights into the mechanism of how different phosphonates actually work at inhibiting barite scale.

5.2 Experimental Methods

The 8 phosphonate SIs listed above were tested under (a) Base Case conditions – which refers to the mixing of normal composition NSSW and Forties FW, and (b) Fixed Case conditions – where NSSW (containing no Ca^{2+} or Mg^{2+}) is mixed with Forties FW containing appropriate quantities of Ca^{2+} and Mg^{2+} such that the produced water [Ca^{2+}] is held fixed at 2000ppm, and [Mg^{2+}] is fixed at 739ppm. This gives a constant produced brine molar ratio, Ca^{2+}/Mg^{2+} = 1.64 (the value appropriate for the FW). Clearly, in the Fixed Case experiments, the concentration of Ca^{2+} and Mg^{2+} in the FW will depend upon the mixing ratio NSSW:FW being evaluated. Brine compositions used for the various Base Case and Fixed Case IE experiments are given in Chapter 3, Tables 3.1 (Base Case NSSW), 3.2 (Base Case FW), 3.3 (Fixed Case NSSW), 3.4 (Fixed Case FW) and 3.5 (Fixed Case FW Ca^{2+}, Mg^{2+} and Cl^-). The 9th phosphonate SI, EABMPA was tested using brine mixing ratio 50/50, under Base Case and Fixed Case conditions. Very limited barite IE was achieved at 2 hours (up to ~20% IE, Base Case) and no IE (i.e. 0%) was achieved at 22 hours under both Base Case and Fixed Case conditions. This phosphonate SI is actually recommended for calcium carbonate inhibition, not barite inhibition. No EABMPA IE results are presented in this Chapter.

Figure 5.1 shows the predicted SR and the produced water molar ratio Ca^{2+}/Mg^{2+} as a function of the % seawater (NSSW) for Base Case experimental conditions, at 95^{o}C and pH 5.5. The SR applying to Fixed Case conditions is also shown on the chart. The SR is almost identical for both Base Case and Fixed Case conditions and hence the Ca^{2+}/Mg^{2+} molar ratio has very little direct effect on SR. Figure 1.3 (in the Introduction chapter) shows how the corresponding mass of precipitated barite changes as the mixing ratio NSSW:Forties FW is altered. The maximum yield of barite is formed around 10:90 NSSW:Forties FW despite the SR being relatively low for this mixing ratio. Thus, it is relatively easy to inhibit this larger mass of barite forming at lower SR (i.e. at 10:90 NSSW:FW), but much more difficult to inhibit a smaller mass forming at higher SR (e.g. at 60:40 NSSW:FW).

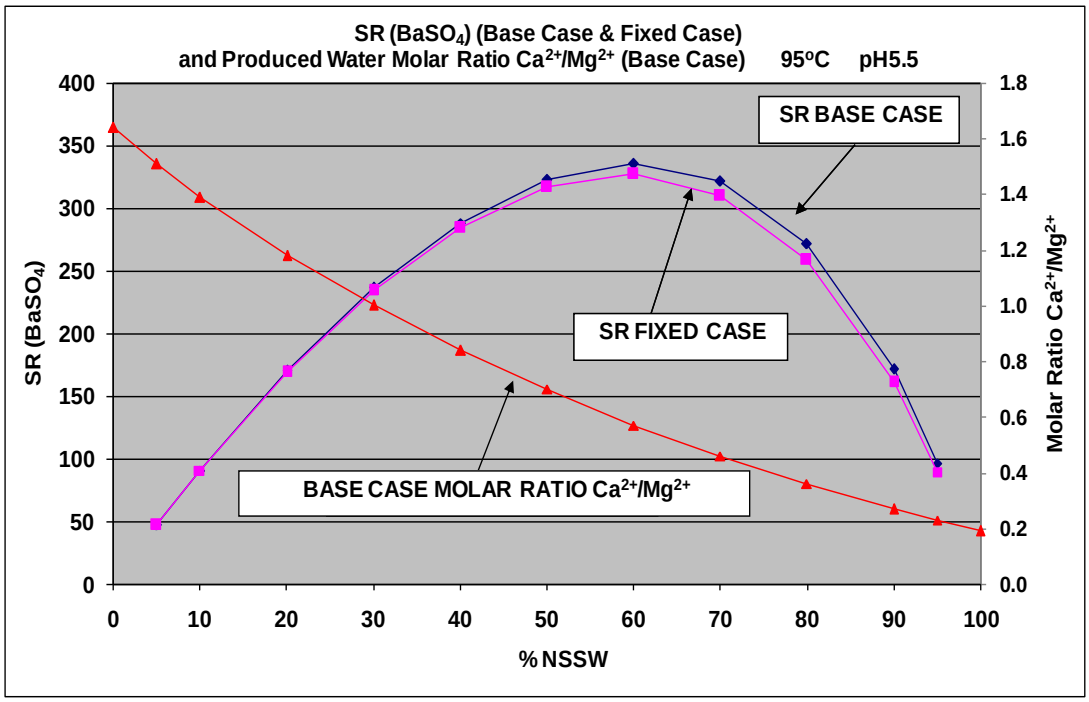

Figure 5.1 – Barite saturation ratio (SR) vs. %NSSW (applying to Base Case and Fixed Case experimental conditions) and also the resultant brine mix molar ratio Ca^{2+}/Mg^{2+} (applying to Base Case experimental conditions). Conditions: 95°C, pH5.5.

5.3 MIC vs. Mixing Ratio NSSW/FW: OMTHP, DETPMP, HMTPMP and HMDP – Base Case

Base Case static MIC values at 2 and 22 hours were measured for all the phosphonate SIs described in this thesis (except EABMPA) over a wide range of NSSW:FW compositions from 10:90 to 95:5. Testing DETPMP and HMTPMP, all mixing ratios between 10:90 and 95:5 were tested, whereas for the others, only selected mixing ratios were tested. For the normal (i.e. Base Case) IE experiments, then this varies both the barite saturation ratio (SR) and the Ca^{2+}/Mg^{2+} molar ratio in the produced water, as discussed in Section 5.2. An MIC determination at a particular NSSW:FW mixing composition requires that IE is determined for a range of SI concentrations. This usually involves two experimental IE passes with the first roughly bounding the MIC and the second one locating it more accurately, typically ~8 – 10 [SI]s are tested to find the MIC values at 2 hours and 22 hours for a given brine mixing ratio, SI and set of conditions. These MIC results are actually shown as comparisons of pairs of SIs where the Base Case MIC at a range of NSSW:FW mixes for DETPMP and HMTPMP

is compared in Figure 5.2 at 2 hours and Figure 5.3 at 22 hours; similarly, OMTHP and HMDP Base Case MICs are compared in Figure 5.4 at 2 hours and Figure 5.5 at 22 hours. MIC results in Figure 5.2 and Figure 5.3 (DETPMP and HMTPMP) have been measured at 10 intermediate compositions whereas the data in Figure 5.4 and Figure 5.5 (OMTHP and HMDP) have been measured at 6 compositions. These two sets of comparisons show very similar behaviour as discussed below.

The MIC results for the two penta-phosphonates DETPMP and HMTPMP are firstly compared in Figure 5.2 (2 hours) and Figure 5.3 (22 hours). Referring to Figure 5.1, the maximum saturation ratio (SR) of barite is at ~60% NSSW composition in the mix. At both 2 and 22 hours, it can be observed from Figure 5.2 and Figure 5.3 that the MIC vs. brine composition of the DETPMP correlates very well with SR showing a clear maximum in MIC at the 60% NSSW value. However, this is not the case for the HMTPMP results, although the MIC values do show some correlation with SR. For the HMTPMP, much higher MIC values are measured at compositions above the maximum SR and this is especially marked for the 22 hour results in Figure 5.3. For example, from Figure 5.3 the HMTPMP MIC value at 80:20 NSSW:FW is ~90ppm, compared with an MIC at the maximum SR value (NSSW:FW 60:40) of ~50ppm. It is quite clear that in addition to SR, another factor is operating which significantly affects the MIC of the HMTPMP. It has already suggested that this factor is the Ca^{2+}/Mg^{2+} molar ratio in the brine mix − which decreases in the normal (i.e. Base Case) NSSW:FW mix (as % NSSW increases) and this conjecture is developed and tested below.

A similar comparison between the MIC results for the hexa-phosphonate OMTHP and the tetra-phosphonate HMDP is presented in Figure 5.4 (2 hours) and Figure 5.5 (22 hours). It is evident from these figures that the MIC values of the hexa-phosphonate are much lower than those of the tetra-phosphonate. Although the MIC levels for these two species are rather different, it is still clear that the MIC values for the OMTHP closely track the SR values (similar to DETPMP) and the HMDP has much higher MIC values at the higher NSSW compositions (similar to HMTPMP). For example, the MIC for the HMDP at NSSW:FW 80:20 is ~80ppm at 22 hours (Figure 5.5) compared with ~50ppm at the maximum SR level (NSSW:FW 60:40).

The initial results discussed above for OMTHP, DETPMP, HMTPMP and HMDP tested in this study show that, when normal IE experiments are performed at various % NSSW brine mix compositions, then the barite saturation ratio (SR) does significantly influence the MIC values with broadly increased MIC being observed for all four phosphonates as SR increases. However, for two of the species, DETPMP and OMTHP, the SR appears to be the primary control on MIC, whereas for HMTPMP and HMDP the SR has some influence but there is clearly another major factor operating. A very clear way of illustrating this situation and summarising the findings of these Base Case IE experiments (i.e. with Ca^{2+}/Mg^{2+} molar ratio varying) is shown in Figure 5.6(a)–(d) where plots of MIC vs. SR are shown for DETPMP (a), OMTHP (b), HMTPMP (c) and HMDP (d). The SR at each % NSSW is taken from MultiScale scale prediction software calculations and this quantity is double valued since the same SR appears for lower and higher % NSSW values, as illustrated in Figure 5.1. In Figure 5.6, a clear distinction in the MIC vs. SR correlation is observed where the MIC for DETPMP and OMTHP (Figure 5.6(a) and (b)) clearly correlates very closely with SR. On the contrary, the MIC values for HMTPMP and HMDP (Figure 5.6(c) and (d)) correlate very poorly with SR. This type of figure is rather unfamiliar in oilfield scale studies but it is a very informative way of plotting these IE results in a manner that clarifies the relation between MIC and barite SR and it suggests whether other factors are involved (as in Figure 5.6(c) and (d)). Since "normal", i.e. Base Case NSSW:FW brine mixing involves changing both SR and produced water Ca^{2+}/Mg^{2+} molar ratio, then this latter factor was the main suspect causing these elevations in MIC level (as in Figure 5.6(c) and (d)), since Ca^{2+} is known to help phosphonates inhibit barite formation and Mg^{2+} is known to "poison" them (Boak et al., 1999; Graham et al., 1997a, 2003; Sorbie et al., 2000; Sorbie and Laing, 2004). To establish this, the MIC vs. %NSSW tests described above were repeated, but where Ca^{2+}/Mg^{2+} molar ratio was fixed as described in Section 5.4.

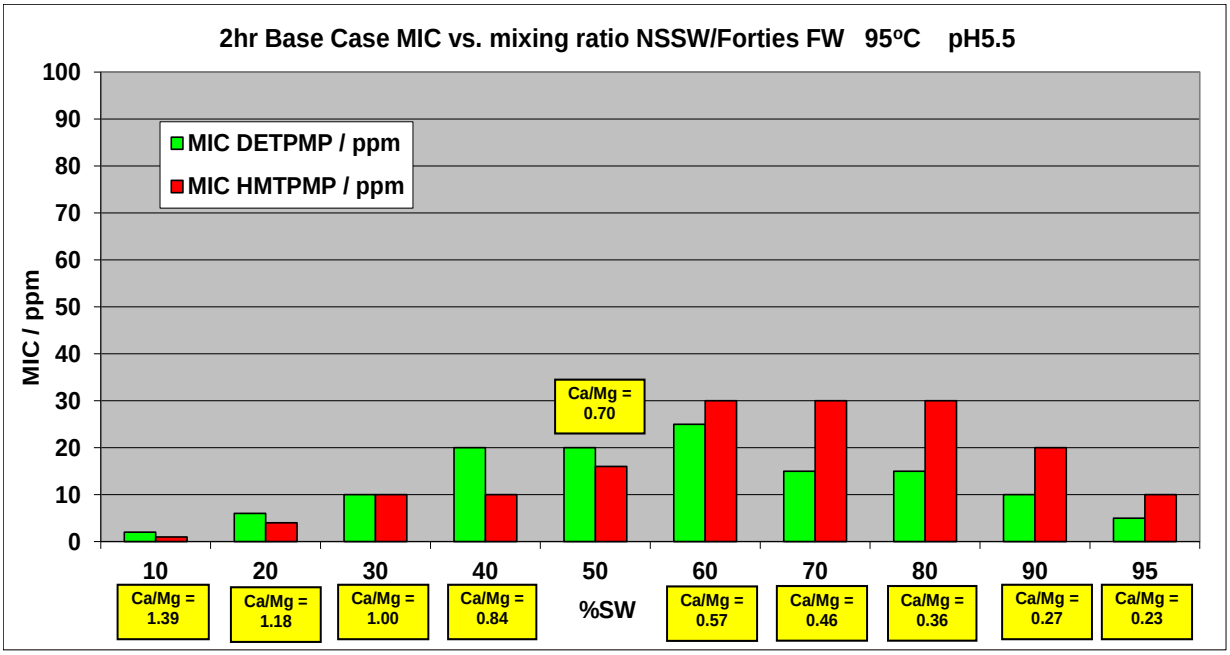

Figure 5.2 – Base Case 2hr MIC values testing SIs DETPMP and HMTPMP vs. %NSSW. 95°C, pH5.5.

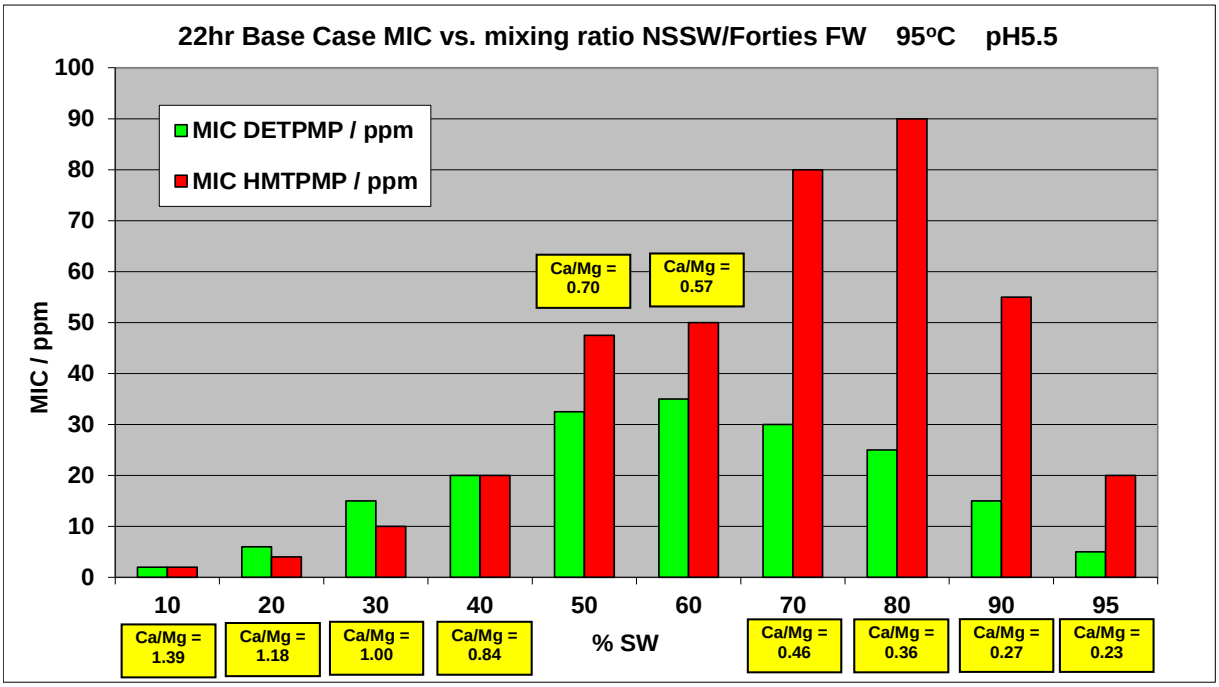

Figure 5.3 – Base Case 22hr MIC values testing SIs DETPMP and HMTPMP vs. %NSSW. 95°C, pH5.5.

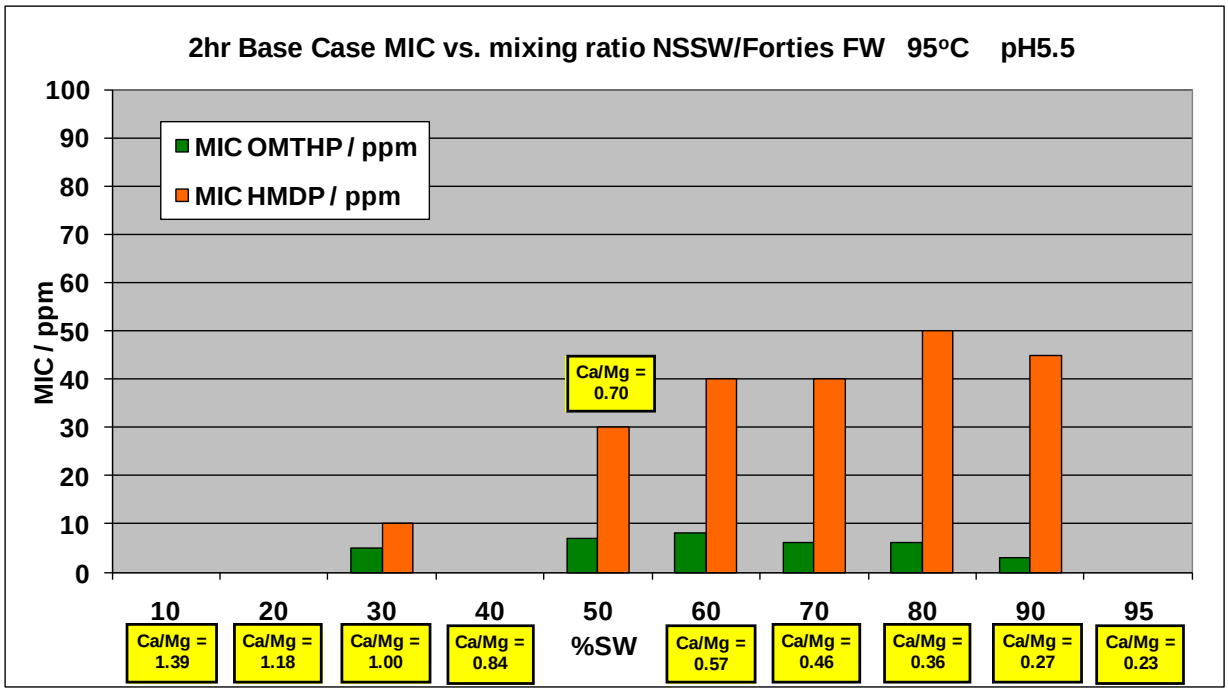

Figure 5.4 – Base Case 2hr MIC values testing SIs OMTHP and HMDP vs. %NSSW. 95°C, pH5.5.

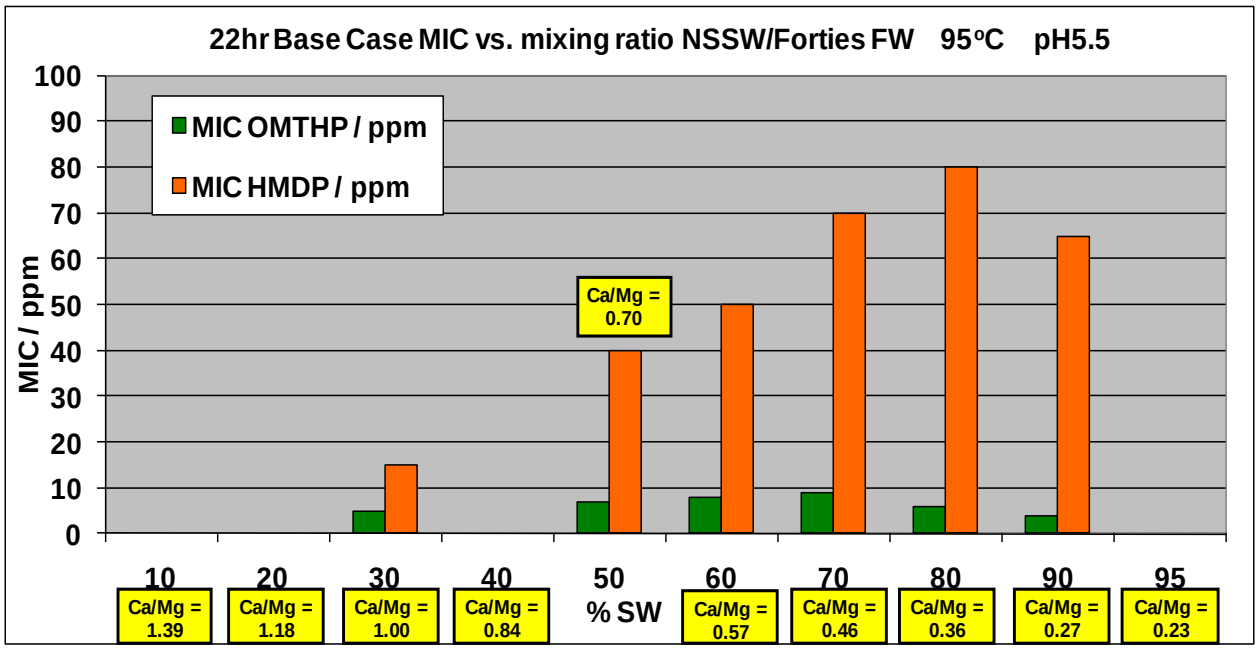

Figure 5.5 – Base Case 22hr MIC values testing SIs OMTHP and HMDP vs. %NSSW. 95°C, pH5.5.

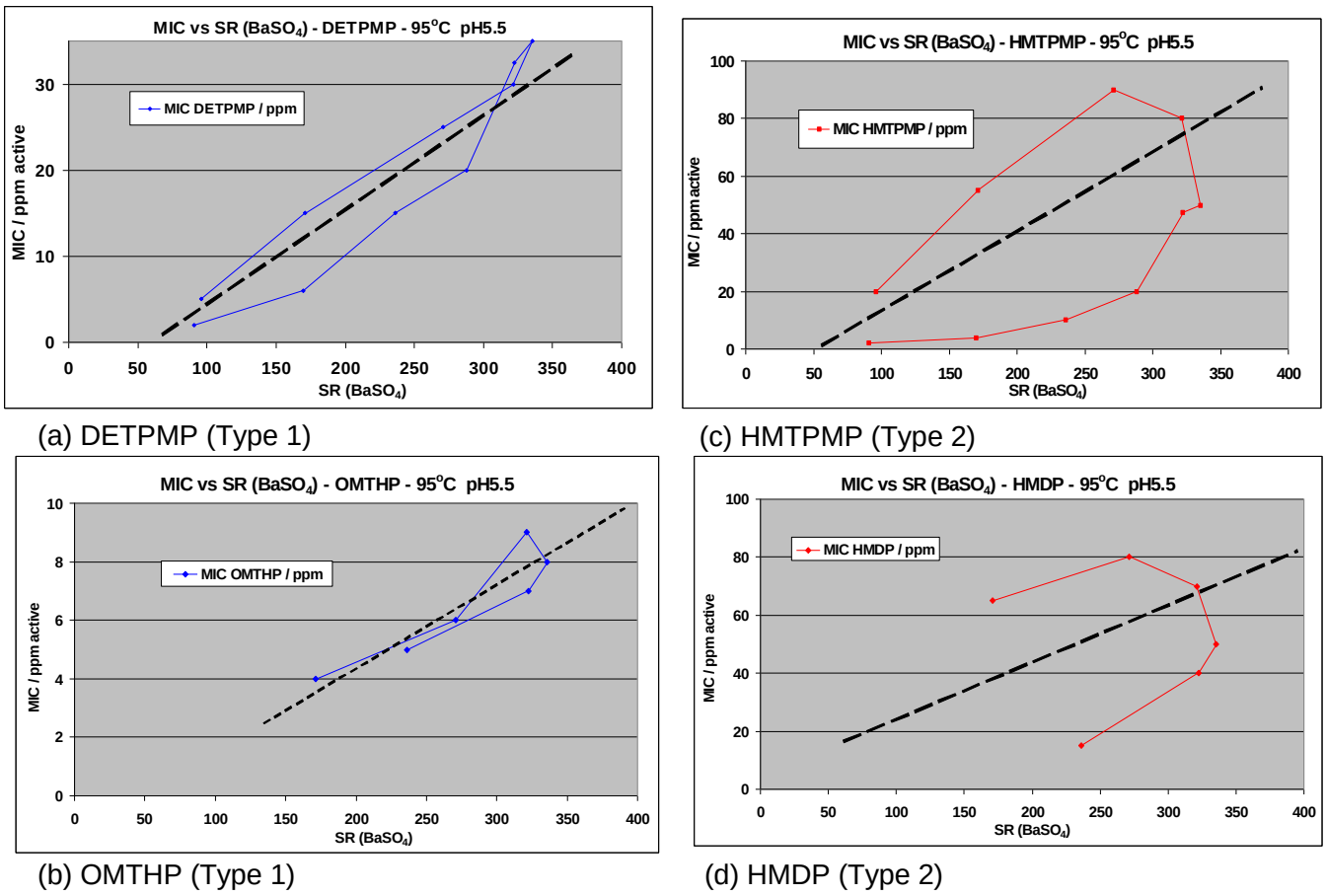

Figure 5.6(a)−(d) – Plots of Base Case 22 hour MIC vs. barium sulphate SR for (a) DETPMP, (b) OMTHP, (c) HMTPMP and (d) HMDP showing that the 22 hour MIC values for the former two SIs correlate much more closely with barite SR than do the latter, suggesting that another factor is strongly affecting the MIC of HMTPMP and HMDP. 95°C, pH5.5.

5.4 MIC vs. Mixing Ratio NSSW/FW: OMTHP, DETPMP, HMTPMP and HMDP – Fixed Case

Two different types of MIC vs. %NSSW behaviour were observed in the above "normal" (i.e. Base Case) brine mixing experiments, viz. that the MIC of some phosphonates (DETPMP and OMTHP) appear to correlate very well with just SR, while others (HMTPMP and HMDP) are affected very significantly by other factors (possibly Ca^{2+}/Mg^{2+} molar ratio).

This led us to design a new series of MIC vs. %NSSW experiments where the brine compositions were modified such that, whatever the NSSW:FW mix composition was, the Ca^{2+}/Mg^{2+} molar ratio was held constant. All of the conditions of these constant Ca^{2+}/Mg^{2+} molar ratio experiments were as selected previously for the Base Case experiments, viz. the mix pH = 5.5, T = 95°C, sampling times = 2 and 22 hours. However, the Ca^{2+} and Mg^{2+} ion compositions in all brine mixes was held constant at $[Ca^{2+}]$ = 2000ppm and $[Mg^{2+}]$ = 739ppm, corresponding to a molar ratio of Ca^{2+}/Mg^{2+} = 1.64, as in the pure 100% FW. Thus, the remaining "variables" in the brine mix were the concentration of other ionic species; these being (i) divalent species $[Ba^{2+}]$, $[Sr^{2+}]$ and $[SO_4^{2-}]$, which are the principal ions affecting barite SR and (ii) monovalent species $[Na^+]$, $[K^+]$ and $[Cl^-]$. In the fixed molar ratio Ca^{2+}/Mg^{2+} experiments (Fixed Case), the brine mix ionic strength over the higher % NSSW mixing ratios is greater than in the Base Case experiments and this is known to have some effect on the actual barium sulphate saturation ratio. However, the SR levels illustrated in Figure 5.1 (applying to Base Case and Fixed Case conditions) show that this effect is secondary. Ionic strength, ***I***, is defined by:

$$Ionic\ Strength, I = \frac{1}{2}\sum_i c_i z_i^2 \qquad \text{(Eq.5.3)}$$

where c_i = molar concentration of ion ***i*** (mol/L); and z_i is its charge. The units for ionic strength, ***I***, are mol/L.

As previously, in these Fixed Case experiments, comparisons of the MIC values measured at a range of NSSW:FW brine mix compositions are made (with fixed Ca^{2+}/Mg^{2+} molar ratio = 1.64) for the pairs of SI – DETPMP / HMTPMP and OMTHP / HMDP. The experimental results of the Fixed Case DETPMP / HMTPMP comparison are shown in Figure 5.7 (2 hours) and Figure 5.8 (22 hours) and the corresponding Fixed Case results are shown for OMTHP / HMDP in Figure 5.9 (2 hours) and Figure 5.10 (22 hours).

Before addressing the results in these figures, it is very instructive to calibrate the changes that have occurred. To do this, consider the iso-saturation ratio (Iso-SR) values of two example compositions, as follows: For NSSW:FW mixing ratio 20:80, barite SR = 170 (Base Case); 169 (Fixed Case) which corresponds very closely to mixing ratio 90:10 where barite SR = 171 (Base Case); 161 (Fixed Case). Thus, if SR is solely controlling the MIC, then

these two compositions should have approximately the same MIC values. The experimental MIC values are tabulated in Table 5.1 for the Base Case (Ca^{2+}/Mg^{2+} molar ratio varying) and Fixed Case (Ca^{2+}/Mg^{2+} molar ratio fixed) at the two compositions NSSW:FW = 20:80 and 90:10 for the DETPMP / HMTPMP comparison. From Table 5.1, note that the MIC values for DETPMP at 20:80 and 90:10 compositions go from ~7ppm and ~15ppm, respectively, for the Base Case (Ca^{2+}/Mg^{2+} molar ratio varying) to corresponding values of ~4ppm and ~2ppm for the Fixed Case (Ca^{2+} /Mg^{2+} molar ratio fixed, = 1.64). The fact that both MIC values reduce under Fixed Case experimental conditions, testing DETPMP is due to the beneficial effect of a higher [Ca^{2+}] on IE. The related MIC values for HMTPMP 20:80 and 90:10 compositions go from ~5ppm and ~55ppm, respectively, for the Base Case (Ca^{2+}/Mg^{2+} molar ratio varying) to corresponding values of ~4ppm and ~7ppm for the Fixed Case (Ca^{2+} /Mg^{2+} molar ratio fixed, = 1.64). Clearly, the much bigger improvement in MIC at the 90:10 composition for HMTPMP must, similarly, be due to the beneficial effect of a much higher [Ca^{2+}] level (585ppm Ca^{2+} in 90:10 normal Base Case mix increases to 2000ppm in the corresponding 90:10 Fixed Case mix) and a lower [Mg^{2+}] level (1305ppm Mg^{2+} in 90:10 normal Base Case mix decreases to 739ppm in the corresponding 90:10 Fixed Case mix). These results show that the HMTPMP is much more sensitive to the brine Ca^{2+}/Mg^{2+} molar ratio than the conventional DETPMP but that both species show qualitatively the same sensitivities (Ca^{2+} assists and Mg^{2+} "poisons", or reduces IE). Note that corresponding results for OMTHP / HMDP are not included in Table 5.1, but very similar trends are observed.

The same analysis can be made from a closer examination of the Fixed Case MIC vs. %NSSW comparisons for DETPMP / HMTPMP in Figure 5.7 (2 hours) and Figure 5.8 (22 hours) and also for OMTHP / HMDP in Figure 5.9 (2 hours) and Figure 5.10 (22 hours). The 2 hour MIC results comparison for DETPMP / HMTPMP in Figure 5.7 shows that the MIC results for both species are now very close and show a maximum at the same brine mix (70:30 NSSW:FW). The greatly skewed behaviour of the HMTPMP Base Case MIC vs. %NSSW observed in Figure 5.3 is not apparent here. This is a strong indication that when the effect of Ca^{2+}/Mg^{2+} molar ratio is controlled for, then the MIC depends principally on the SR of the brine mix. The 22 hour MIC results for DETPMP / HMTPMP in Figure 5.8 show quite similar results, although the actual MIC values for the HMTPMP are rather higher than those for the DETPMP and these longer time results still show a slight skew to higher % NSSW levels. The results for OMTHP / HMDP in Figure 5.9 and Figure 5.10 show similar

behaviour. The MIC levels of the HMDP for the Fixed Case (Ca^{2+}/Mg^{2+} molar ratio fixed) are lower than those for the Base Case (Ca^{2+}/Mg^{2+} molar ratio varying), compare Figure 5.4 and Figure 5.5 with Figure 5.9 and Figure 5.10, and the MIC values are much less skewed to the higher % NSSW side. Again it was found that both DETPMP and OMTHP behave quite similarly and likewise for HMTPMP and HMDP.

A very careful analysis of the entire MIC vs. %NSSW results collected reveals one further observation. As noted above, in both the Base Case (Ca^{2+}/Mg^{2+} molar ratio varying) and Fixed Case (Ca^{2+}/Mg^{2+} molar ratio fixed) results, the actual produced water ionic strength, ***I***, decreases with increasing % NSSW and this is a further variable in experiments. The SR results in Figure 5.1 indicate that ionic strength does not significantly affect the barite saturation ratio, SR, but it may still in itself have an influence on the IE of the various SIs. The produced water ionic strength does actually have a limited effect on IE, and this affects the two "pairs" of phosphonates described in Sections 5.3 and 5.4, in different ways. The IE results indicate that – over the salinity (ionic strength) range involved in experiments here – the DETPMP / OMTHP species work somewhat better at lower ionic strength and the HMTPMP / HMDP species work rather better at higher ionic strength. Table 5.1, which presents the Base Case and Fixed Case MICs for DETPMP and HMTPMP for the iso-saturation ratio (iso-SR) NSSW:FW mixing ratios 20:80 and 90:10 exemplifies the ionic strength effect (since in these Fixed Case tests, Ca^{2+}/Mg^{2+} molar ratio is fixed and barite SR is also about constant – examine Figure 5.1). Referring to the Fixed Case MICs in Table 5.1, testing DETPMP, the 20:80 NSSW:FW MIC is 2ppm higher than for the 90:10 NSSW:FW mixing ratio, whereas testing HMTPMP, the converse is true: 20:80 NSSW:FW MIC is 3ppm lower than for the 90:10 NSSW:FW mixing ratio. It is highly likely this ionic strength effect is causing the slight skewing of the HMTPMP / HMDP MIC results in the Fixed Case (Ca^{2+}/Mg^{2+} molar ratio fixed, = 1.64) at higher % NSSW mixing ratios (i.e. at lower produced water ionic strength levels), since these species work better in higher ionic strength brine (i.e. in higher % **FW** brine mixes), provided the produced water Ca^{2+}/Mg^{2+} molar ratio and barite SR variables are both constant.

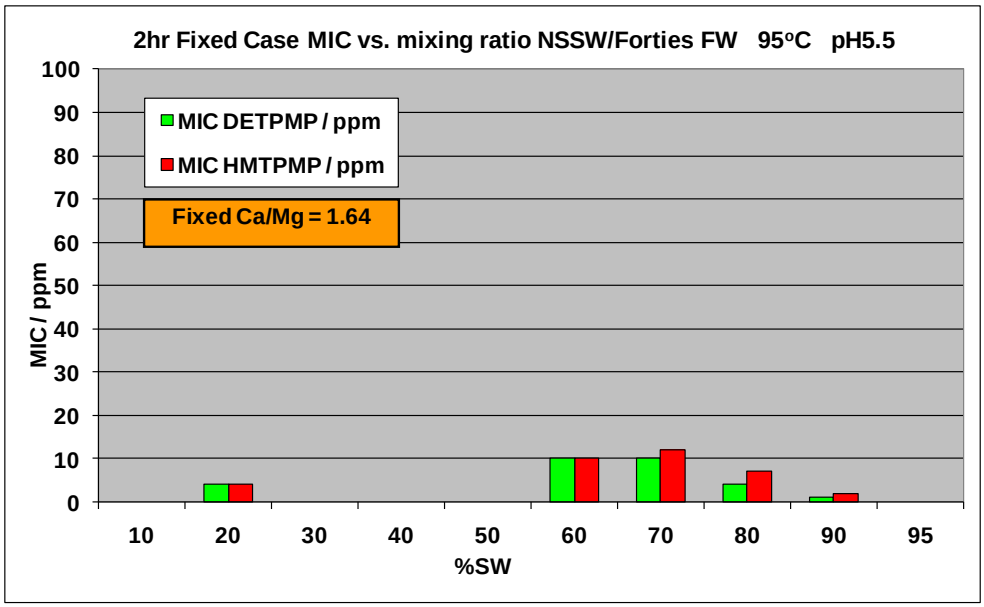

Figure 5.7 – Fixed Case 2hr MIC values testing SIs DETPMP and HMTPMP vs. %NSSW at fixed produced water molar ratio Ca^{2+}/Mg^{2+} = 1.64, with $[Ca^{2+}]$ = 2000ppm and $[Mg^{2+}]$ = 739ppm in the mix. 95°C, pH5.5.

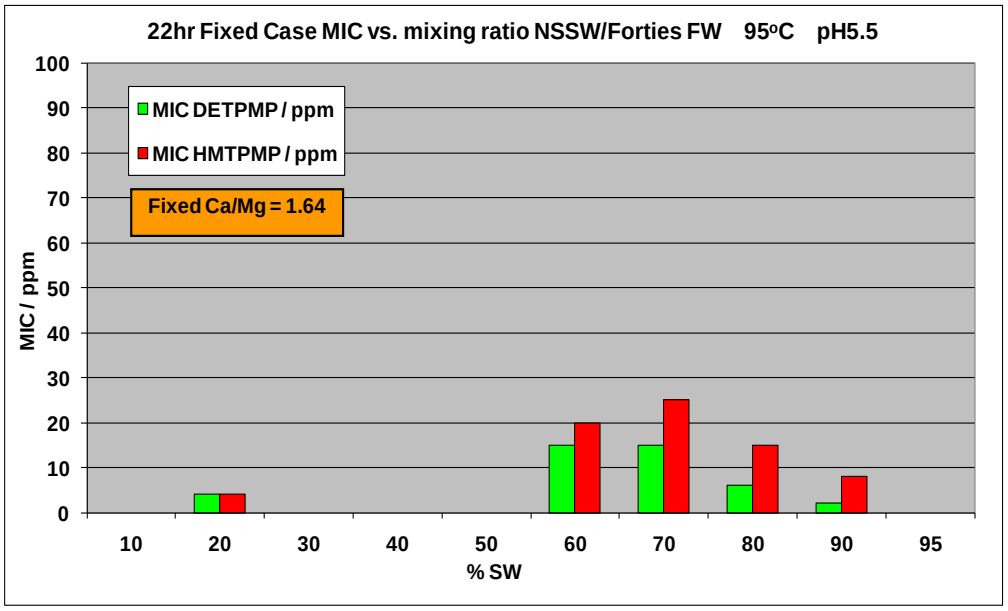

Figure 5.8 – Fixed Case 22hr MIC values testing SIs DETPMP and HMTPMP vs. %NSSW at fixed produced water molar ratio Ca^{2+}/Mg^{2+} = 1.64, with $[Ca^{2+}]$ = 2000ppm and $[Mg^{2+}]$ = 739ppm in the mix. 95°C, pH5.5.

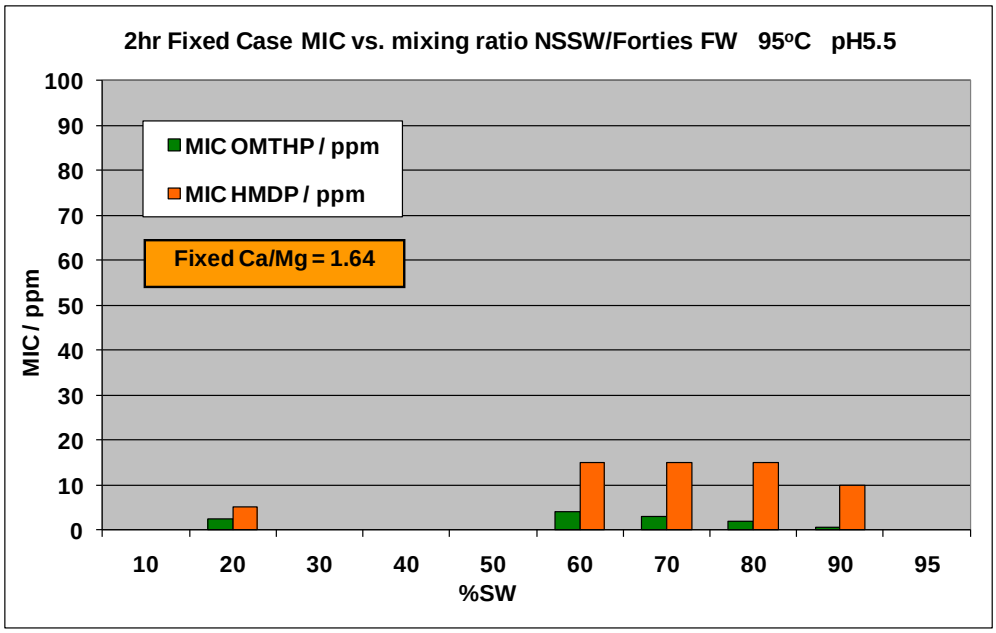

Figure 5.9 – Fixed Case 2hr MIC values testing SIs OMTHP and HMDP vs. %NSSW at fixed produced water molar ratio Ca^{2+}/Mg^{2+} = 1.64, with $[Ca^{2+}]$ = 2000ppm and $[Mg^{2+}]$ = 739ppm in the mix. 95°C, pH5.5.

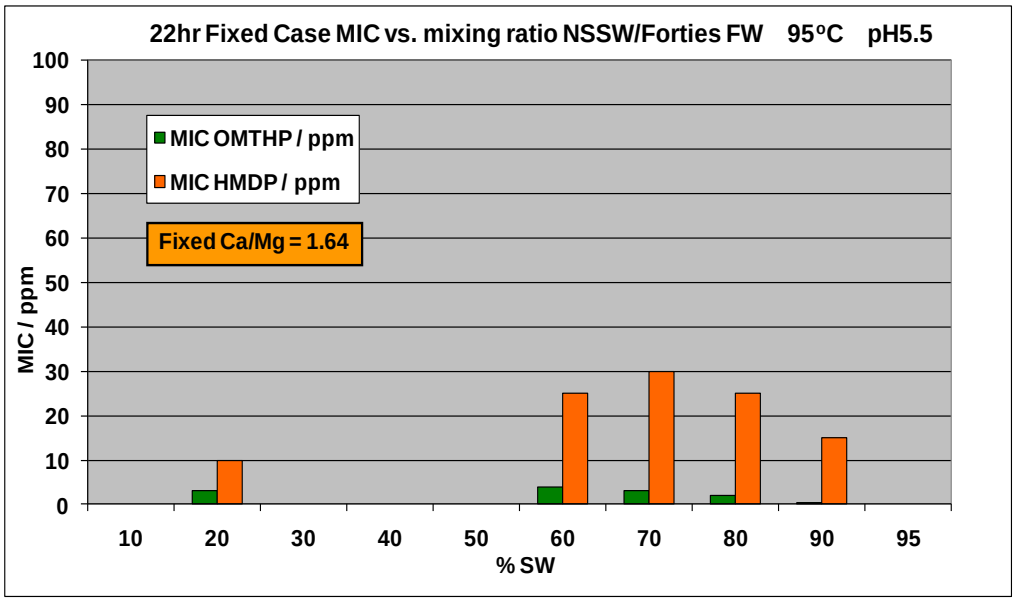

Figure 5.10 – Fixed Case 22hr MIC values testing SIs OMTHP and HMDP vs. %NSSW at fixed produced water molar ratio Ca^{2+}/Mg^{2+} = 1.64, with $[Ca^{2+}]$ = 2000ppm and $[Mg^{2+}]$ = 739ppm in the mix. 95°C, pH5.5.

SI	Base Case (Ca^{2+}/Mg^{2+} Varying) or Fixed Case (Ca^{2+}/Mg^{2+} Fixed)	22hr MIC at NSSW:FW = 20:80 (ppm). SR = 170 (Base Case); 169 (Fixed Case)	22hr MIC at NSSW:FW = 90:10 (ppm). SR = 171 (Base Case); 161 (Fixed Case)
DETPMP	Base Case	~7	~15
HMTPMP	Base Case	~5	~55
DETPMP	Fixed Case	~4	~2
HMTPMP	Fixed Case	~4	~7

Table 5.1 – Comparison of the 22 hour MIC levels for DETPMP and HMTPMP at different % NSSW compositions with approximately equal SR (barite) values for the Base Case (Ca^{2+}/Mg^{2+} molar ratio varying) and Fixed Case (Ca^{2+}/Mg^{2+} molar ratio fixed).

5.5 MIC vs. Mixing Ratio NSSW/FW: EDTMPA

By examining Figure 5.11 and Figure 5.12, it is clear that the Base Case 2 and 22 hour MICs for SI EDTMPA are not correlating with the level of barite saturation ratio (SR) for the mixing ratio in question, in particular, for NSSW % ratios > 60% (see Figure 5.1) – instead another factor is influencing the MIC level. On the contrary, the Fixed Case MICs do correlate with the barite saturation ratio level, thus, the highest 2 and 22 hour MICs are observed testing brine mix 60:40 NSSW:FW. In Base Case experiments, the Ca^{2+}/Mg^{2+} molar ratio in the brine mix varies, whereas in the Fixed Case experiments, the Ca^{2+}/Mg^{2+} molar ratio is fixed at 1.64. Testing EDTMPA, the Base Case 2 hour MIC becomes progressively larger, from < 10ppm for brine mixing ratio 30:70 NSSW:FW, to ~70ppm for brine mixing ratio 90:10 NSSW:FW – see Figure 5.11. This is due to the molar ratio Ca^{2+}/Mg^{2+} in the brine mix becoming progressively lower, with increasing % NSSW, from 1.00 (30:70 NSSW:FW) to 0.27 (90:10 NSSW:FW). In Sections 5.3 and 5.4, it was identified that Ca^{2+} is beneficial and Mg^{2+} is detrimental to the IE of OMTHP, DETPMP, HMTPMP and HMDP. This generic observation continues to apply here.

The highest Base Case 22 hour MIC measured for EDTMPA was ~400ppm, for brine mixing ratios 70:30 and 80:20 NSSW:FW. In contrast, the 60:40 22 hour MIC is only ~50ppm – see Figure 5.12. If only barite saturation ratio is affecting MIC, then the 60:40 NSSW:FW MIC would be expected to be the highest. Clearly this is not the case testing EDTMPA. The highest 22 hour MICs measured for HMTPMP and HMDP were 90ppm and 80ppm respectively, both MICs applying to Base Case brine mixing ratio 80:20 NSSW:FW, 95°C, pH5.5. In the case of EDTMPA, the Ca^{2+}/Mg^{2+} effect is much more marked compared with HMTPMP and HEDP, since the EDTMPA 70:30 and 80:20 NSSW:FW Base Case 22 hour MICs are both as high as ~400ppm {cf. 80ppm (70:30) and 90ppm (80:20) for HMTPMP; 70ppm (70:30) and 80ppm (80:20) for HMDP}. Thus, EDTMPA could be best described as "*ultra-sensitive*" to Ca^{2+} and Mg^{2+} divalent ions.

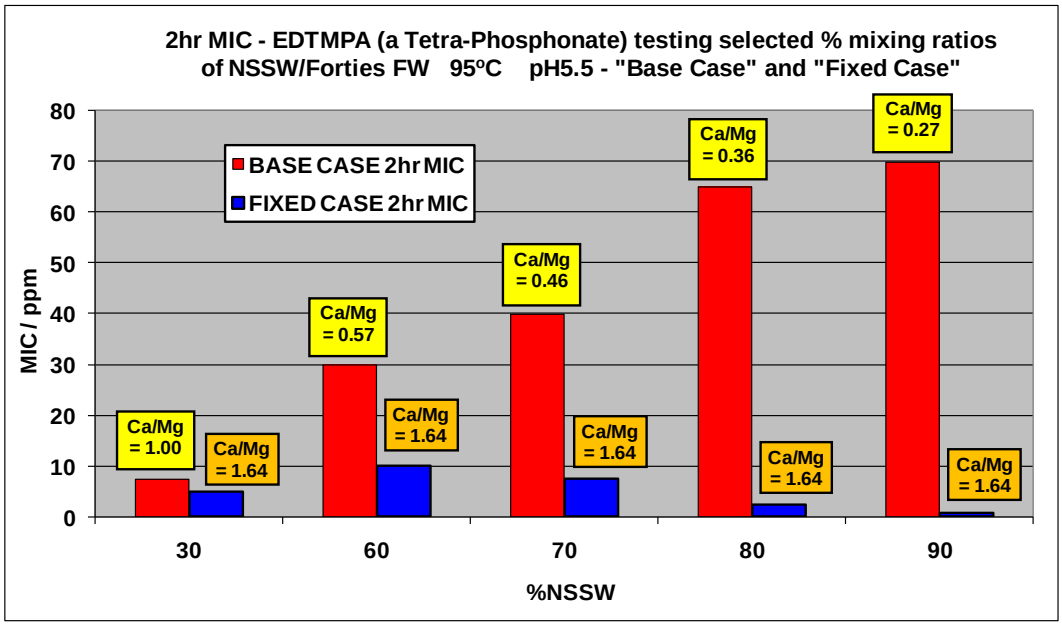

Figure 5.11 – 2 hour MIC vs. %NSSW, SI EDTMPA (tetra-phosphonate), 95°C, pH5.5, Base Case and Fixed Case experimental conditions.

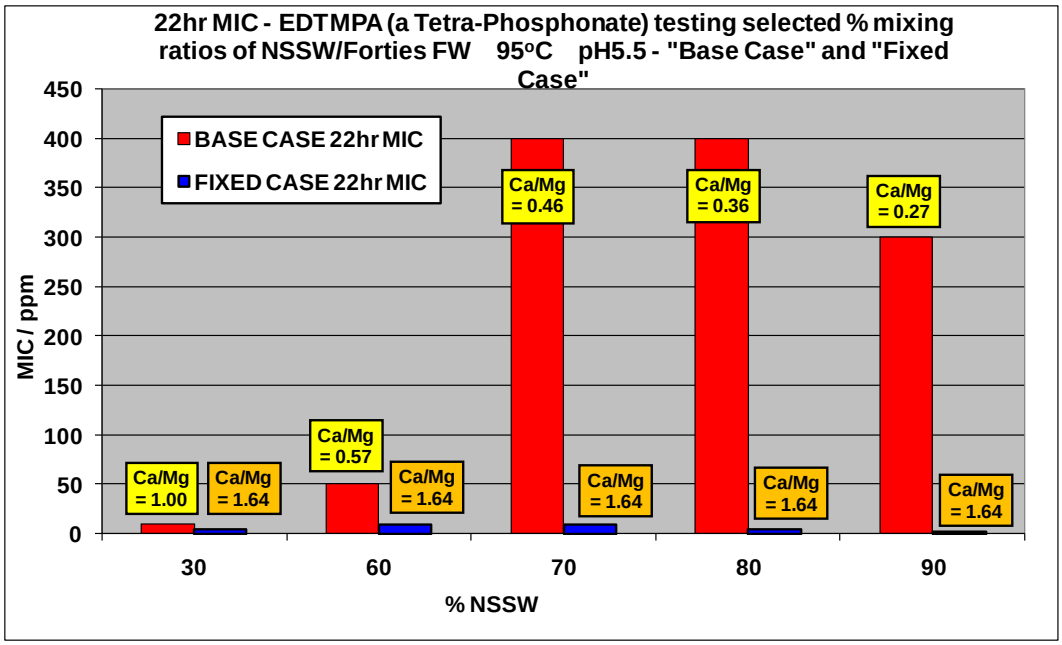

Figure 5.12 – 22 hour MIC vs. %NSSW, SI EDTMPA (tetra-phosphonate), 95°C, pH5.5, Base Case and Fixed Case experimental conditions.

5.6 MIC vs. Mixing Ratio NSSW/FW: NTP

By examining Figure 5.13 and Figure 5.14, it is clear the Base Case NTP MICs are not correlating with the SR profile (Figure 5.1). The 2 and 22 hour Base Case 70:30 MICs should be ≈ 50:50 Base Case MICs – this is clearly not the case. 2 and 22 hour 70:30 Base Case MIC > 2 and 22 hour 50:50 Base Case MIC (Figure 5.13 and Figure 5.14). Similarly, the 2 and 22 hour 80:20 Base Case MICs should be < 2 and 22 hour 70:30 Base Case MICs, taking only SR into account. Instead, 2 and 22 hour 70:30 Base Case MICs ≈ 2 and 22 hour 80:20 Base Case MICs (Figure 5.13 and Figure 5.14). As observed when testing HMTPMP and HMDP, another factor is influencing the NTP Base Case MICs, most notably in the case of mixing ratios > 60% NSSW.

The NTP Fixed Case MIC results are also interesting. Based on SR (Figure 5.1), 2 and 22 hour Fixed Case 50:50 MICs should be ≈ 2 and 22 hour Fixed Case 70:30 MICs. However, 2 and 22 hour Fixed Case 70:30 MICs > 2 and 22 hour Fixed Case 50:50 MICs. At 2 hours, 70:30 Fixed Case MIC = 40ppm and 50:50 Fixed Case MIC = 30ppm (Figure 5.13) – a difference of 10ppm. At 22 hours, 70:30 Fixed Case MIC = 55ppm and 50:50 Fixed Case

MIC = 40ppm (Figure 5.14) – a difference of 15ppm. As outlined previously for OMTHP, DETPMP, HMTPMP and HMDP, these NTP MIC differences are due to salinity / ionic strength changes of the brine mix, since in both these cases (50:50 and 70:30 Fixed Case), Ca^{2+}/Mg^{2+} molar ratio is fixed and SR is about constant (Figure 5.1). The only remaining variable is salinity / ionic strength. Thus, NTP performs better (i.e. lower MICs) in higher salinity brine, the same trend observed testing HMTPMP and HMDP.

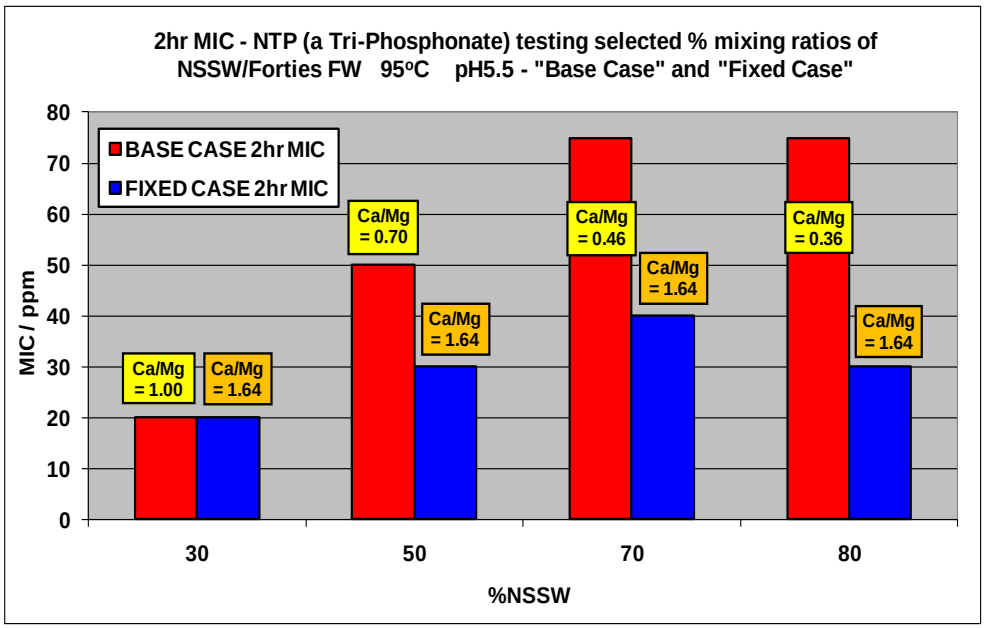

Figure 5.13 – 2 hour MIC vs. %NSSW, SI NTP (tri-phosphonate), 95°C, pH5.5, Base Case and Fixed Case experimental conditions.

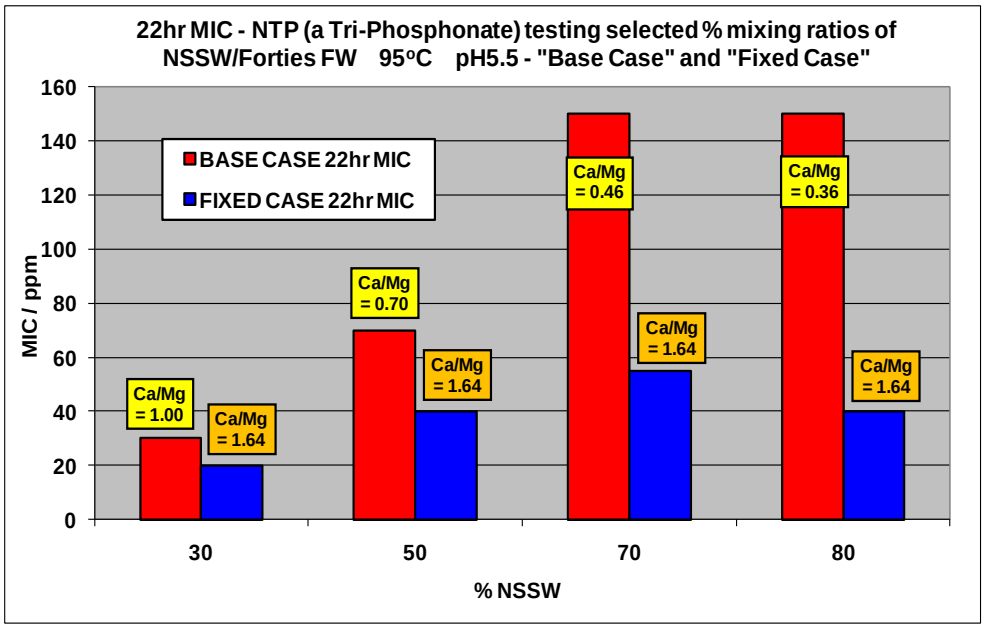

Figure 5.14 – 22 hour MIC vs. %NSSW, SI NTP (tri-phosphonate), 95°C, pH5.5, Base Case and Fixed Case experimental conditions.

5.7 MIC vs. Mixing Ratio NSSW/FW: HEDP

By examining Figure 5.15 and Figure 5.16, it is clear that HEDP always performs better under Fixed Case experimental conditions, at both 2 and 22 hour residence times – i.e. the Fixed Case MIC is always < (or, in one case =) the corresponding Base Case MIC. It is also noticeable that the difference between the Fixed Case and Base Case MICs (for any chosen NSSW:FW mixing ratio) becomes larger as the %NSSW increases, i.e. the smallest difference between Fixed Case and Base Case MICs is observed for mixing ratio 30:70 NSSW:FW – a difference of ~5ppm at 22 hours, and a difference of 0ppm at 2 hours (i.e. at 2 hours, the Base Case and Fixed Case HEDP MICs are equal). By contrast, the 90:10 Base Case MIC is about 4x larger than the 90:10 Fixed Case MIC (again at 2 *and* 22 hours). This effect is most likely due to the fact that the difference between Base Case and Fixed Case molar ratio Ca^{2+}/Mg^{2+} in the produced brine (for any selected mixing ratio NSSW:FW) becomes larger with increasing %NSSW – see Table 5.2. For example, for mixing ratio 30:70 NSSW:FW, the difference between the base and Fixed Case produced brine molar ratio Ca^{2+}/Mg^{2+} = (1.64 – 1.00) = 0.64, whereas for mixing ratio 90:10 NSSW:FW, the difference is more than double, = (1.64 – 0.27) = 1.37. However, the barite saturation ratio applying to brine mixing ratio 90:10 NSSW:FW < 30:70 NSSW:FW – see Figure 5.1 and Table 5.2,

therefore the 90:10 NSSW:FW MIC should be < 30:70 NSSW:FW MIC. This is *not* the case for the Base Case HEDP IE tests – once again due to Ca^{2+}/Mg^{2+} effects on the SI.

By examining Figure 5.15, it is apparent that the Base Case 70:30, 80:20, and 90:10 MICs are about the same – and secondly, all are > the 60:40 NSSW:FW MIC. Taking barite saturation ratio into account (Figure 5.1), the MICs should reduce with increasing %NSSW (after 60:40 NSSW:FW), i.e.: 90:10 NSSW:FW MIC < 80:20 NSSW:FW MIC < 70:30 NSSW:FW MIC < 60:40 NSSW:FW MIC. Since the 70:30, 80:20, and 90:10 NSSW:FW 2 hour MICs are (i) all > 60:40 NSSW:FW MIC; and (ii) fail to decrease with increasing %NSSW, this again suggests another factor is influencing the MIC, most likely Ca^{2+}/Mg^{2+} molar ratio. Similarly, with reference to Figure 5.16, two important points to note are: Base Case 60:40 NSSW:FW MIC ≈ 70:30 NSSW:FW MIC; and Base Case 80:20 NSSW:FW MIC ≈ 90:10 NSSW:FW MIC. Considering barite SR only: Base Case 60:40 NSSW:FW MIC should be > 70:30 NSSW:FW MIC; and Base Case 80:20 NSSW:FW MIC should be > 90:10 NSSW:FW MIC.

When testing SIs in this way, the detrimental / poisoning effect of a low Ca^{2+}/Mg^{2+} molar ratio is always observed typically, testing NSSW:FW brine mixes > 60% NSSW, because in such brine mixes, the $[Mg^{2+}] > [Ca^{2+}]$. For example, in the 90:10 NSSW:FW brine mix, the $[Mg^{2+}]$ = 1305ppm, $[Ca^{2+}]$ = 585ppm; in the 80:20 NSSW:FW brine mix, the $[Mg^{2+}]$ = 1242ppm, $[Ca^{2+}]$ = 742ppm. Mg^{2+} bonded SI is often described as "poisoned" SI or "ineffective SI" (Sorbie and Laing, 2004; Boak et al., 1999). When significant quantities of effective SI become "poisoned" by Mg^{2+}, the consequence is an elevation in the MIC level. The HEDP 2 and 22 hour IE levels were very often similar, or at the same level (%), i.e. good IE is maintained over long residence times, up to 22 hours. For example, the 2 and 22 hour Base Case 80:20 and 90:10 MICs are equal (40ppm) – see Figure 5.15 and Figure 5.16. This kind of behaviour was observed testing OMTHP (hexa-phosphonate) and DETPMP (di-phosphonate). For example, the Base Case 2 and 22 hour DETPMP 40/60 MICs are both = 20ppm – see Figure 5.2 and Figure 5.3. The Base Case 2 and 22 hour OMTHP 30/70 MICs are both = 5ppm – see Figure 5.4 and Figure 5.5.

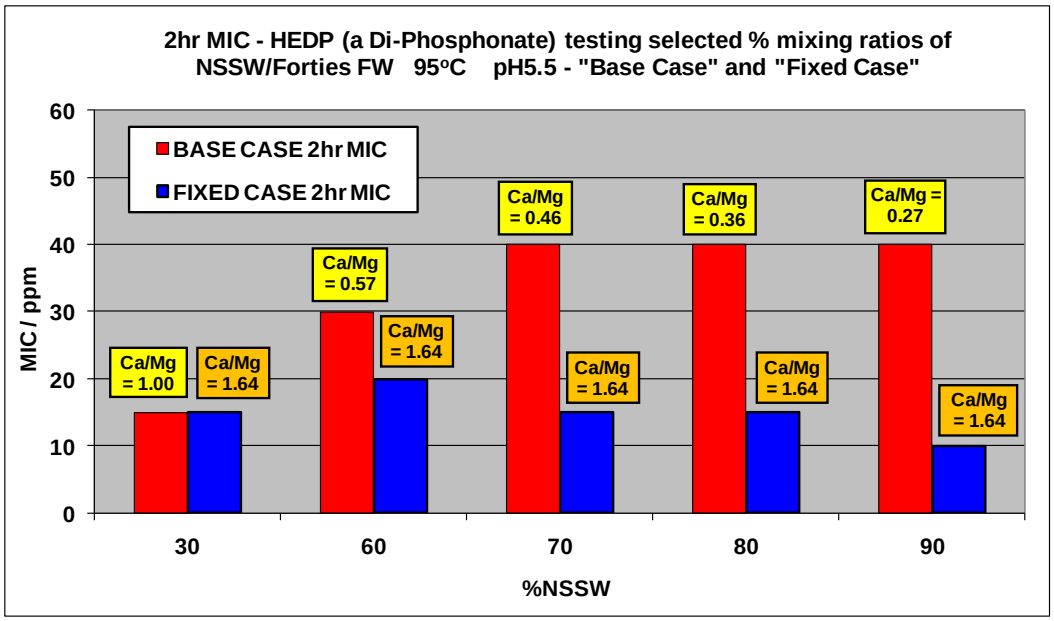

Figure 5.15 – 2 hour MIC vs. %NSSW, SI HEDP (di-phosphonate), 95°C, pH5.5, Base Case and Fixed Case experimental conditions.

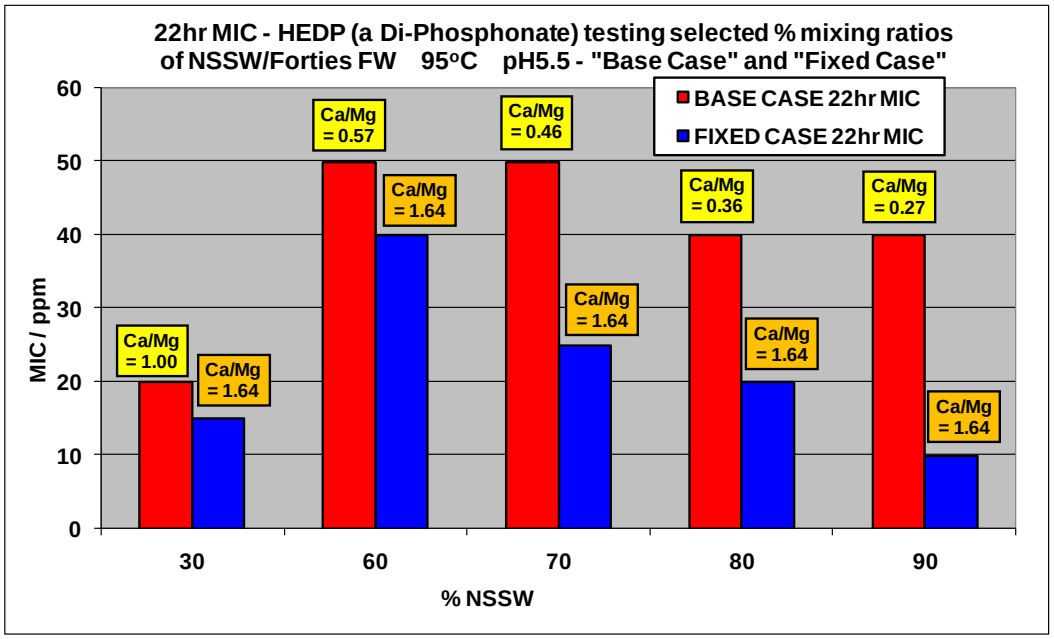

Figure 5.16 – 22 hour MIC vs. %NSSW, SI HEDP (di-phosphonate), 95°C, pH5.5, Base Case and Fixed Case experimental conditions.

Mixing Ratio NSSW/Forties FW	**Base Case SR ($BaSO_4$)**	**Base Case Mix Molar Ratio Ca^{2+}/Mg^{2+}**	**Difference between Base Case and Fixed Case Molar Ratio Ca^{2+}/Mg^{2+} (i.e. $\Delta Ca^{2+}/Mg^{2+}$)**
30/70	236	1.00	0.64
60/40	336	0.57	1.07
70/30	321	0.46	1.18
80/20	271	0.36	1.28
90/10	171	0.27	1.37

Table 5.2 – NSSW/FW mixing ratios selected for testing SI HEDP, SR barite (Base Case), Base Case produced water molar ratio Ca^{2+}/Mg^{2+}, and difference between the produced water molar ratio Ca^{2+}/Mg^{2+} changing from Base Case to Fixed Case test conditions.

5.8 MIC vs. Mixing Ratio NSSW/FW: HPAA

With reference to Figure 5.17 and Figure 5.18, it is clear that:

(i) the highest HPAA 2 hour MIC is measured for NSSW:FW brine mixing ratio 80:20;

(ii) the highest HPAA 22 hour MIC is measured for NSSW:FW brine mixing ratios 70:30 and 80:20;

(iii) for all mixing profiles NSSW:FW, the Fixed Case MIC is < the Base Case MIC (NB. at both 2 and 22 hours) with the exception of mixing ratio 30:70 NSSW:FW at 2 hours only – where both Fixed Case and Base Case MIC levels are equal; and

(iv) the difference between the Fixed Case and Base Case MIC (for any selected brine mixing ratio NSSW:FW) becomes larger with increasing % NSSW.

Observations (i), (ii) and (iv) suggest another factor is strongly influencing the MIC of HPAA, as observed testing HMTPMP, HMDP, EDTMPA, NTP and HEDP. Like HPAA, all the other phosphonate products performed better under Fixed Case conditions, i.e. Fixed Case

MIC < or = Base Case MIC or Fixed Case IE > Base Case IE for any selected [SI] and set of conditions.

Compared with HEDP, the elevation of MIC levels testing mixing ratios > 60% NSSW is more marked in the case of HPAA. For instance, with reference to Figure 5.17, the Base Case 80:20 NSSW:FW 2 hour MIC is > 70:30 NSSW:FW MIC, whereas, testing HEDP, 80:20 NSSW:FW Base Case MIC ≈ 70:30 NSSW:FW Base Case MIC – see Figure 5.15. Secondly, with reference to Figure 5.18, the HPAA 22 hour 70:30 NSSW:FW Base Case MIC ≈ 22 hour 80:20 NSSW:FW Base Case MIC, whereas for HEDP: 22 hour 80:20 NSSW:FW Base Case MIC < 70:30 NSSW:FW Base Case MIC (see Figure 5.16) – this trend would normally be expected in terms of SR – but as noted previously, for HEDP, the 90:10 NSSW:FW Base Case 22 hour MIC is ≈ 80:20 NSSW:FW Base Case 22 hour MIC – this does *not* correlate with the SR profile (Figure 5.1). Thus, there are still some anomalous features in the HEDP MIC results, suggesting it is not exclusively SR which is influencing MIC.

The MIC results obtained for HPAA are similar to results for HMTPMP (penta-phosphonate) and HMDP (tetra-phosphonate) – see Figure 5.3 and Figure 5.5. The highest measured 22 hour HMTPMP and HMDP Base Case MICs were both for brine mix 80:20 NSSW:FW – 90ppm and 80ppm respectively. The highest measured 2 hour Base Case MIC for HMTPMP was found testing brine mixes 60:40, 70:30 and 80:20 NSSW:FW (all ~30ppm) – see Figure 5.2. The highest HMDP Base Case 2 hour MIC was measured testing brine mix 80:20 NSSW:FW (= ~50ppm) – see Figure 5.4. Similarly, testing HPAA, the highest 2 hour Base Case MIC was detected testing brine mix 80:20 NSSW:FW (Figure 5.17) and the highest 22 hour Base Case MICs were measured testing brine mixes 70:30 and 80:20 NSSW:FW – both these MICs were ~125ppm (Figure 5.18). Like HMTPMP (penta-phosphonate), HMDP (tetra-phosphonate), EDTMPA (tetra-phosphonate), NTP (tri-phosphonate) and HEDP (di-phosphonate); the MIC levels of HPAA (mono-phosphonate, mono-carboxylate) are strongly influenced by another factor, in addition to SR, this being the molar ratio Ca^{2+}/Mg^{2+}.

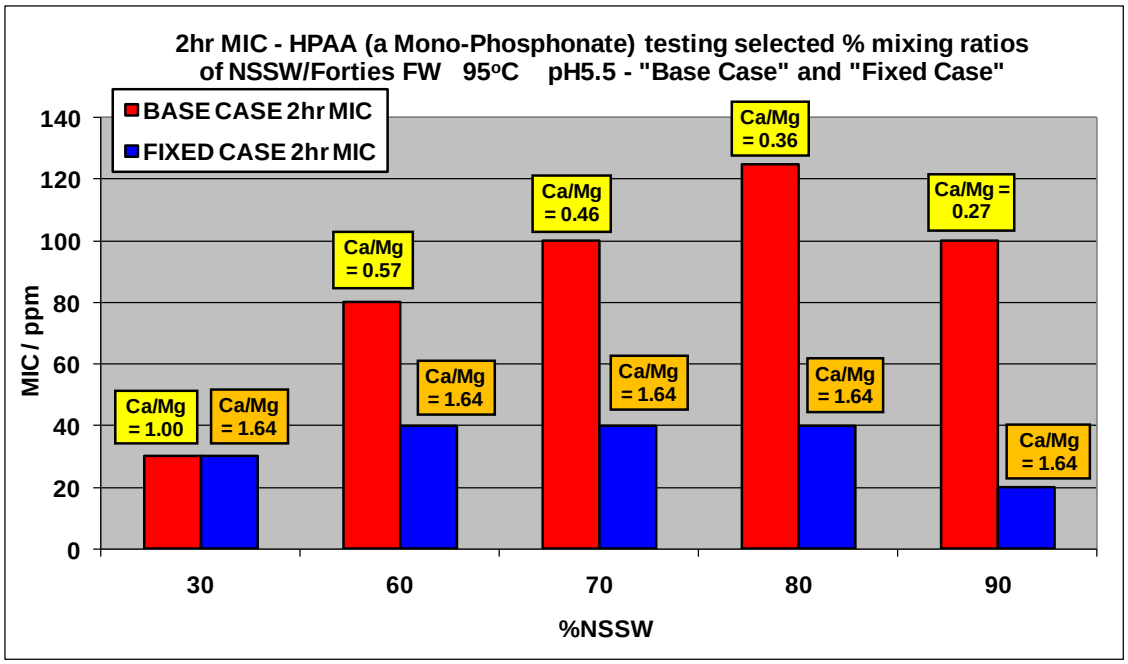

Figure 5.17 – 2 hour MIC vs. %NSSW, SI HPAA (mono-phosphonate, mono-carboxylate), 95°C, pH5.5, Base Case and Fixed Case experimental conditions.

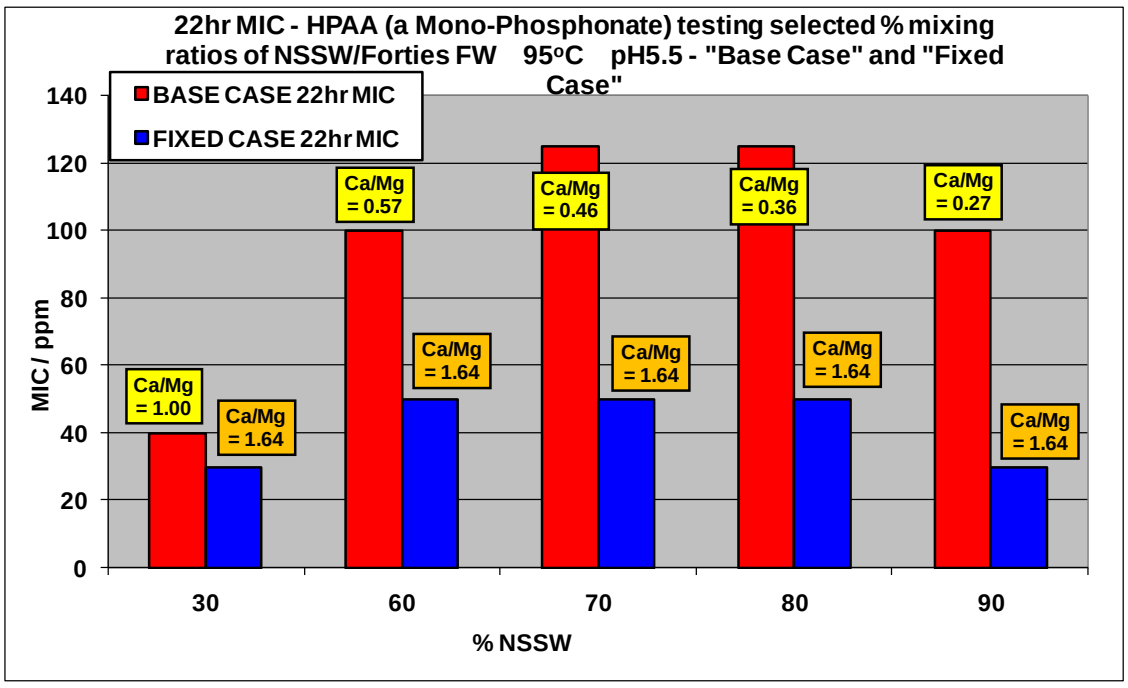

Figure 5.18 – 22 hour MIC vs. %NSSW, SI HPAA (mono-phosphonate, mono-carboxylate), 95°C, pH5.5, Base Case and Fixed Case experimental conditions.

5.9 Ionic Strength Effect upon IE/MIC at fixed SR and fixed Molar Ratio Ca^{2+}/Mg^{2+} – 50/50 NSSW/FW vs. 70/30 NSSW/FW

Previous sections of this chapter have outlined the effect of ionic strength upon the IE of OMTHP, DETPMP, HMTPMP, HMDP and NTP at fixed SR and fixed molar ratio Ca^{2+}/Mg^{2+}. In the case of OMTHP, DETPMP, HMTPMP and HMDP, a comparison of MICs for Fixed Case NSSW/FW mixing ratios 20/80 and 90/10 was made. SR 20/20 Fixed Case = 169, SR 90/10 Fixed Case = 161, therefore SR 20/80 Fixed Case ≈ SR 90/10 Fixed Case. In the case of NTP, a comparison of MICs for Fixed Case NSSW/FW mixing ratios 50/50 and 70/30 was made. SR 50/50 Fixed Case = 316, SR 70/30 Fixed Case = 310, therefore SR 50/50 Fixed Case ≈ SR 70/30 Fixed Case. NTP was tested under Fixed Case conditions using both these mixing ratios in Section 5.6. In order to obtain a full picture of the ionic strength effect upon the IE of all 8 phosphonate SIs tested in MIC vs. %NSSW experiments, an additional 7 IE experiments were carried out testing OMTHP, DETPMP, HMTPMP, HMDP, EDTMPA, HEDP and HPAA with NSSW/FW Fixed Case mixing ratio 50/50 (Fixed Case) – therefore enabling a comparison of 50/50 NSSW/FW (SR=316) with 70/30 NSSW/FW (SR=310). These 7 SIs have already been tested with NSSW/FW Fixed Case mixing ratio 70/30 in Sections 5.4, 5.5, 5.7 and 5.8. Findings for all 8 phosphonate SIs are presented in Figure 5.19 and Figure 5.20 where the 2 and 22 hour 50/50 and 70/30 Fixed Case MICs have been plotted together for each of these SIs.

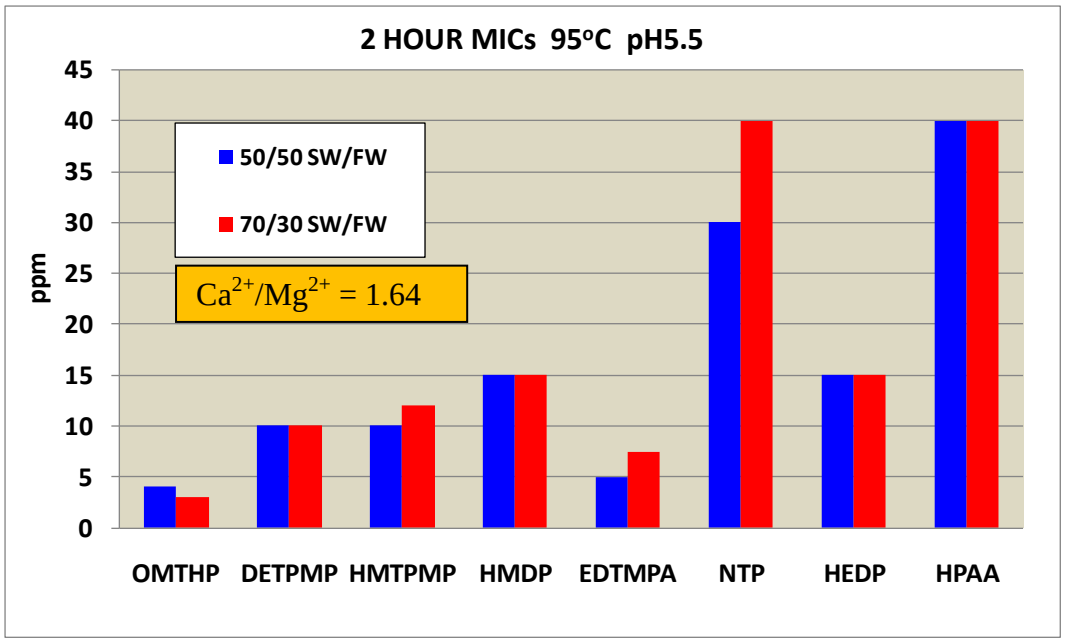

Figure 5.19 – Fixed Case 2 hour MICs for OMTHP, DETPMP, HMTPMP, HMDP, EDTMPA, NTP, HEDP and HPAA. Iso-SR NSSW/FW mixing ratios 50/50 and 70/30. 95°C, pH5.5, Ca^{2+}/Mg^{2+} = 1.64.

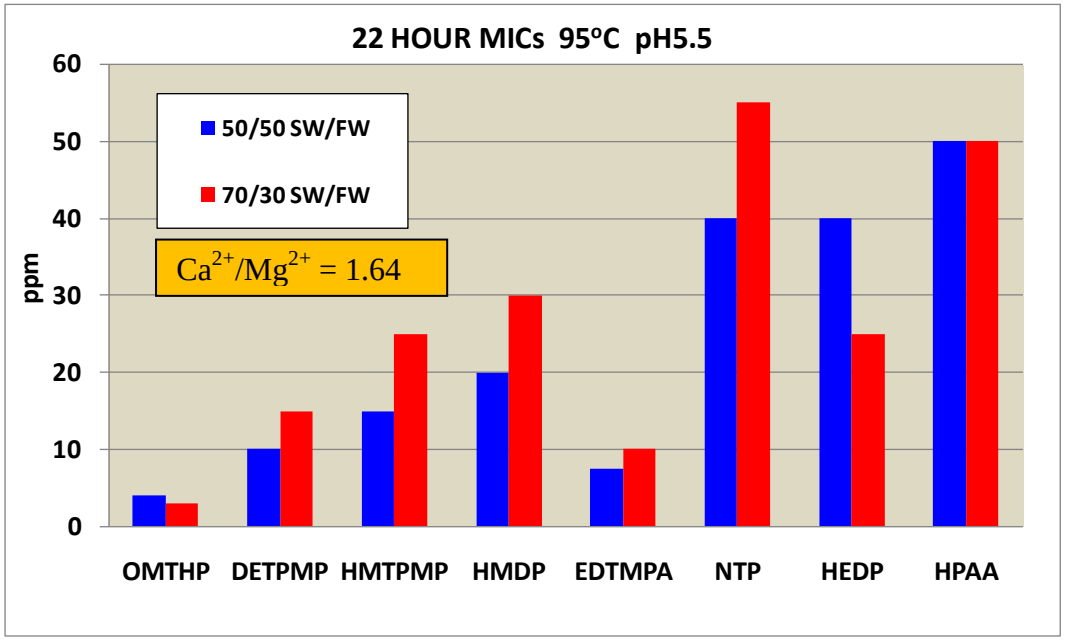

Figure 5.20 – Fixed Case 22 hour MICs for OMTHP, DETPMP, HMTPMP, HMDP, EDTMPA, NTP, HEDP and HPAA. Iso-SR NSSW/FW mixing ratios 50/50 and 70/30. 95°C, pH5.5, Ca^{2+}/Mg^{2+} = 1.64.

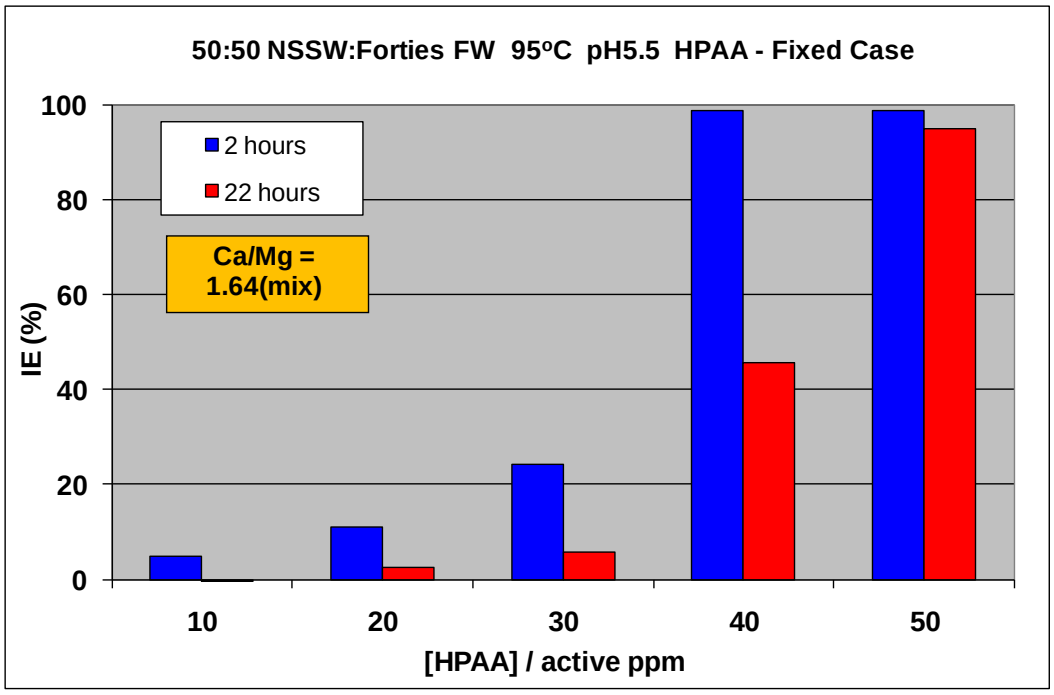

Figure 5.21 – 50/50 NSSW/FW; Fixed Case; Ca^{2+}/Mg^{2+} molar ratio = 1.64; HPAA; 95°C, pH5.5; [SI]s: 10, 20, 30, 40 and 50ppm.

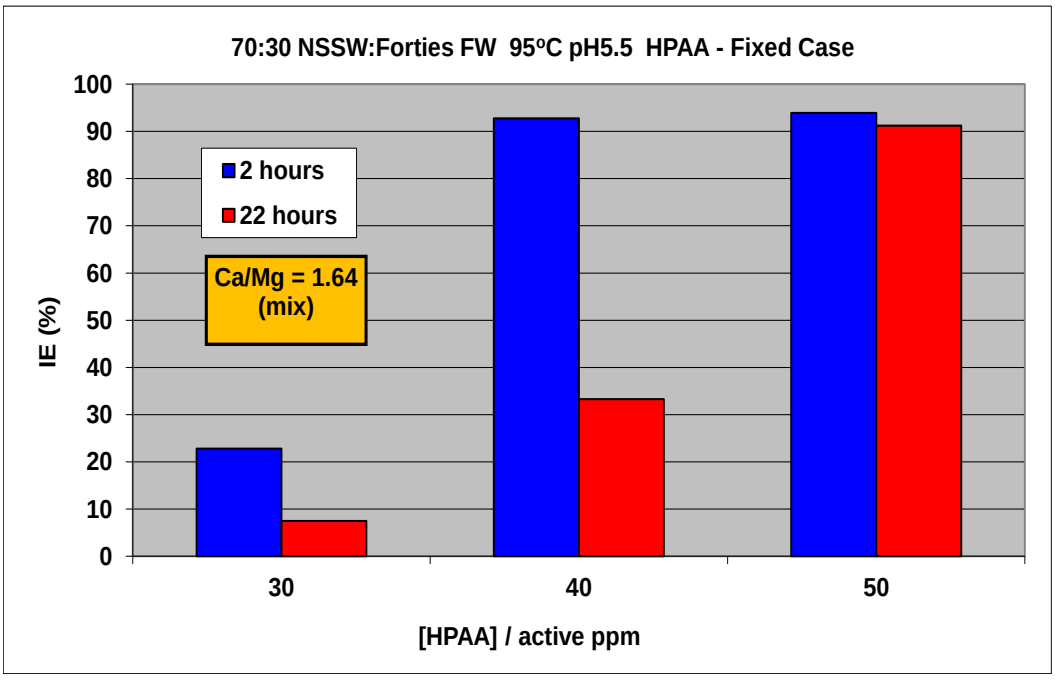

Figure 5.22 – 70/30 NSSW/FW; Fixed Case; Ca^{2+}/Mg^{2+} molar ratio = 1.64; HPAA; 95°C, pH5.5; [SI]s: 30, 40 and 50ppm.

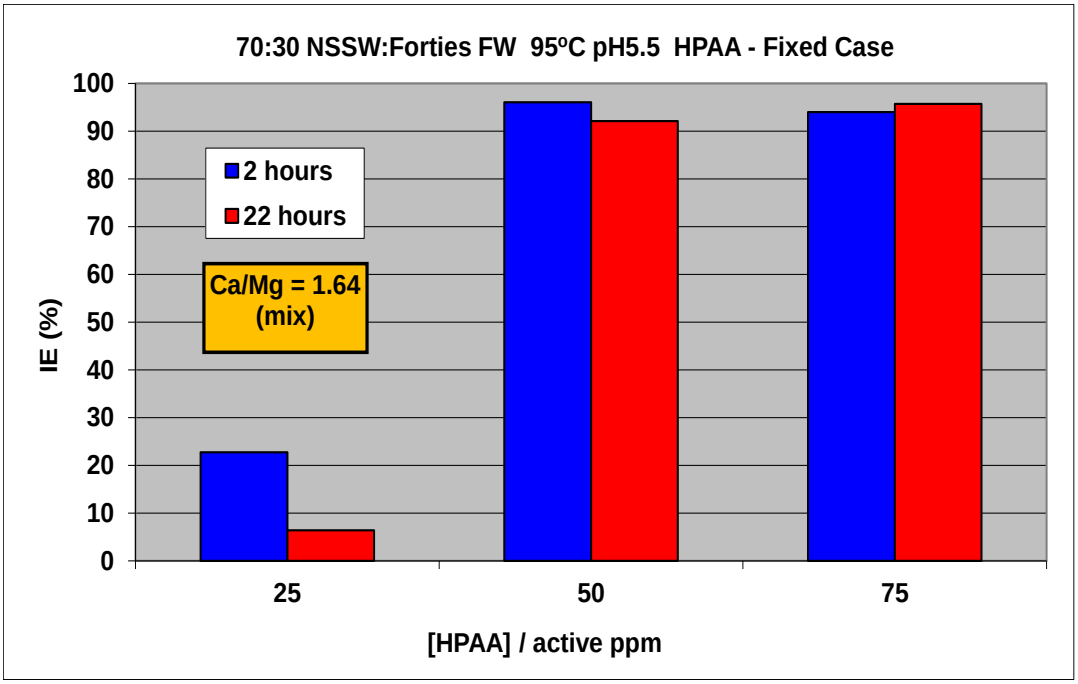

Figure 5.23 – 70/30 NSSW/FW; Fixed Case; Ca^{2+}/Mg^{2+} molar ratio = 1.64; HPAA; 95°C, pH5.5; [SI]s: 25, 50 and 75ppm.

In these experiments testing OMTHP, DETPMP, HMTPMP, HMDP, EDTMPA, NTP, HEDP and HPAA, the molar ratio Ca^{2+}/Mg^{2+} = 1.64 in all cases. The barium sulphate saturation ratio 50/50 Fixed Case ≈ 70/30 Fixed Case – see Figure 5.1. Therefore any differences in IE between the 50/50 Fixed Case and 70/30 Fixed Case IE experiments *must* be due to ionic strength / salinity changes, since all other variables are constant (SR is ~constant). By examining Figure 5.19 and Figure 5.20, it is clear that the DETPMP, HMTPMP, HMDP, EDTMPA and NTP performed better (i.e. higher IE, lower MIC) in the 50/50 NSSW/FW Fixed Case IE test (i.e. the higher salinity mix) at 22 hours. These observations corroborate initial findings testing Type 2 phosphonate SIs HMTPMP and HMDP in Section 5.4 where a comparison of the 20/80 and 90/10 NSSW/FW MICs was made at fixed SR and Ca^{2+}/Mg^{2+}, but it contradicts initial observations for DETPMP. Conversely, only OMTHP and HEDP performed better (i.e. higher IE, lower MIC) in the 70/30 NSSW/FW Fixed Case IE test (i.e. the lower salinity mix). Similarly, this corroborates initial observations testing OMTHP in Section 5.4 where a comparison of the 20/80 and 90/10 NSSW/FW MICs was made at fixed SR and Ca^{2+}/Mg^{2+}.

The 2 *and* 22 hour 50/50 and 70/30 Fixed Case MICs for HPAA are equal, which implies that there is very little effect of varying ionic strength at fixed SR and fixed molar ratio Ca^{2+}/Mg^{2+} upon IE. However, on close examination of the IE charts testing HPAA (see Figure 5.21 – Figure 5.23), it is clear that it too performed better in the 50/50 mix, despite the 2 and 22 hour MICs being broadly equal for 50/50 and 70/30 NSSW/FW. Table 5.3 summarises the ionic strength effect upon IE at constant SR and Ca^{2+}/Mg^{2+} findings for all phosphonate SIs tested in MIC vs. %NSSW experiments – in relation to 50/50 and 70/30 Fixed Case IE tests which were performed testing all 8 species.

The findings of these ionic strength experiments lead to the conclusion that in fact there is ***no relationship*** between Type 1 and Type 2 SIs and the ionic strength effect upon their IE at fixed SR and fixed molar ratio Ca^{2+}/Mg^{2+}, as has been previously reported in paper Shaw et al., 2010a. Instead, a general conclusion can be made: most of the phosphonate SIs perform better in higher ionic strength mixes (e.g. 50/50) at fixed SR and fixed Ca^{2+}/Mg^{2+}, ***regardless of their Type***. Indeed, sometimes there was no difference in 2 and 22 hour MICs (50/50 vs. 70/30), for example, HPAA. The ionic strength effect upon phosphonate SI IE is most certainly a very mild effect which is usually barely noticeable. Only the OMTHP (Type 1) and HEDP (Type 2) performed better in the lower ionic strength mix (70/30 NSSW/FW) at fixed SR and fixed molar ratio Ca^{2+}/Mg^{2+}.

Scale Inhibitor	**Higher IE (OR lower MIC) in 50/50 or 70/30 NSSW/FW Fixed Case experiment at 22 hours?**	**Better IE in higher or lower ionic strength mix at ~constant SR and constant Ca^{2+}/Mg^{2+}?**
OMTHP	70/30	Lower Ionic Strength better
DETPMP	50/50	Higher Ionic Strength better
HMTPMP	50/50	Higher Ionic Strength better
HMDP	50/50	Higher Ionic Strength better
EDTMPA	50/50	Higher Ionic Strength better
NTP	50/50	Higher Ionic Strength better
HEDP	70/30	Lower Ionic Strength better
HPAA	50/50	Higher Ionic Strength better

Table 5.3 – Table of phosphonate SIs, their Type, and stating whether they performed better in 70/30 NSSW/FW or 50/50 NSSW/FW brine mixes when tested at fixed SR and fixed molar ratio Ca^{2+}/Mg^{2+}.

5.10 Summary and Conclusions

In this Chapter, a wide range of static barium sulphate MIC vs. %NSSW experimental results have been presented on 8 commercially available conventional phosphonate barite scale inhibitors, viz. OMTHP (hexa-P), DETPMP (penta-P), HMTPMP (penta-P), HMDP (tetra-P), EDTMPA (tetra-P), NTP (tri-P), HEDP (di-P) and HPAA (mono-P, mono-C). The main type of experiment has been the standard bulk static MIC test, but carried out across a wide range of North Sea Sea Water (NSSW):Formation Water (FW) compositions, from NSSW:FW 10:90 to 95:5. When a "normal" (i.e. Base Case) scan of MIC vs. %NSSW is made, at least three important variables are being changed experimentally, i.e. barite saturation ratio (SR), produced water Ca^{2+}/Mg^{2+} molar ratio and produced water ionic strength, ***I***. These three main variables are known to affect the performance of the different phosphonate scale inhibitors but the extent of the effect that each of these variables may have has not been previously reported. Clearly, the Ca^{2+}/Mg^{2+} molar ratio affects some species only mildly, e.g. OMTHP and DETPMP, whereas other are affected severely, e.g. EDTMPA (ultra-sensitive).

The conventional phosphonate SIs divide into two groups based on their IE behaviour which will be denoted as **Type 1** and **Type 2**. The main characteristics of these behavioural types are as follows:

Type 1 Phosphonates (i.e. OMTHP and DETPMP):

- **(i)** Barite IE is principally affected by barite SR;
- **(ii)** Barite IE affected by brine Ca^{2+}/Mg^{2+} molar ratio is a *secondary* effect (Ca^{2+} assists and Mg^{2+} "poisons" inhibition of barite);
- **(iii)** Ionic strength influence upon IE is a *tertiary* effect which is only noticeable when SR and Ca^{2+}/Mg^{2+} molar ratio variables are fixed. Most phosphonate SIs perform better in higher ionic strength mixes, under such conditions, *regardless* of their Type.
- **(iv)** IE tends *not* to decline very much over time i.e. IE quite similar at 2 and 22 hours.

Type 2 Phosphonates (i.e. HMTPMP, HMDP, EDTMPA, NTP, EABMPA, HEDP and HPAA):

- **(i)** Barite IE is principally affected by brine Ca^{2+}/Mg^{2+} molar ratio (Ca^{2+} assists and Mg^{2+} "poisons" inhibition of barite);
- **(ii)** Barite IE affected by barite SR as a *secondary* effect;
- **(iii)** Ionic strength influence upon IE is a *tertiary* effect which is only noticeable when SR and Ca^{2+}/Mg^{2+} molar ratio variables are fixed. Most phosphonate SIs perform better in higher ionic strength mixes, under such conditions, *regardless* of their Type.
- **(iv)** IE tends to decline *markedly* over time i.e. IE is much lower at 22 hours compared to at 2 hours – although this is much less clear in the case of HEDP and HPAA which both performed well over long residence times (i.e. at 22 hours), under certain conditions, implying these 2 SIs may have *limited* Type 1 character.

Note: EABMPA was classed as Type 2 based solely on characteristic (iv) listed above. 0% IE was achieved at 22 hours, under Base Case and Fixed Case test conditions (50/50 NSSW/FW, 95^{o}C, pH5.5).

A range of supporting SI "consumption" and IE experiments were performed testing all phosphonate SIs described in this chapter, except EABMPA (see Chapter 9) in which it is clearly demonstrated that Type 1 phosphonate SIs are generally not consumed into the barite lattice (i.e. depleted from solution) to the same extent as the Type 2 phosphonate SIs –with the notable exception of HEDP and HPAA which both gave consumption profiles more typical of Type 1 species. In *all* cases, the level of SI in solution was found to correlate very well with the corresponding level of barite IE at any particular sampling time. These observations are consistent with the IE vs. time behaviour of all 8 phosphonate SI species described in this Chapter, particularly HEDP and HPAA which both exhibited limited Type 1 properties, e.g. good long-term (i.e. 22 hour) IE under certain test conditions.

ESEM images of the scale deposits formed in *some* of these IE/SI consumption experiments (taken from test bottles containing no SI, OMTHP, DETPMP, HMTPMP and HMDP) indicated that there are two distinct types of crystal morphology – depending broadly on the

type of conventional phosphonate SI being tested (i.e. Type 1 or Type 2) and this could possibly be used as a fingerprint to establish which type of phosphonate SI was present in the original static barium sulphate inhibition efficiency experiment – see Chapter 9. Scale deposits formed in test bottles containing EDTMPA, NTP, HEDP and HPAA were not analysed by ESEM/EDAX, partly because 3 of these SIs had not been received at the time of this work – therefore this area of work is restricted to OMTHP (Type 1), DETPMP (Type 1), HMTPMP (Type 2) and HEDP (Type 2).

Practically, it may be useful to deploy a Type 2 SI in high [Ca^{2+}] reservoirs, since the IE of these SIs is enhanced much more by Ca^{2+}; e.g. it may be better to use EDTMPA or HMTPMP rather than DETPMP. As a corollary, Type 1 phosphonates are more appropriate for lower calcium production brines (although if the [Ca^{2+}] is too low, even these will be adversely affected). Likewise, in high [Mg^{2+}] reservoirs, it may be best to deploy a Type 1 SI such as OMTHP or DETPMP, since the IE of these species is suppressed much less severely by Mg^{2+} compared to their Type 2 analogues. Alternatively, a blend of DETPMP (Type 1) and HMTPMP (Type 2) may be deployed synergistically, so that the benefits of using both types of SI would be gained. In terms of monitoring squeeze treatments, this work shows that it is very beneficial to monitor both calcium and magnesium ions in the produced brine and even to plot the [Ca^{2+}]/[Mg^{2+}] ratio over time in order to be aware of its value given its important effects on phosphonate SIs, Type 2 in particular.

Chapter 6: MIC vs. Mixing Ratio NSSW/FW Experiments – Polymeric SIs

Chapter 6 Summary: This Chapter describes the static barium sulphate IE of a range of 9 polymeric SIs. Their sensitivity to divalent cations Ca^{2+} and Mg^{2+} is investigated and how this factor and SR affect their MIC level is established. All the test species are tested in MIC vs. mixing ratio experiments where the 2 and 22 hour MIC is determined in various brine mix compositions.

6.1 Introduction

Many applications of polymeric scale inhibitors (SIs) have been reported in the oilfield literature (Burr et al., 1987; Pardue, 1991; Fleming et al., 2004; Hen et al., 1995; Jordan et al., 1995; Rabaioli and Lockhart, 1995; Bezzera et al., 1999; Davis et al., 2003; Montgomerie et al., 2009; Jordan et al., 2010, 2011; Todd et al., 2010; Hasson et al., 2011). More recently, a number of "green" barium sulphate and calcium carbonate scale inhibitors have been proposed (e.g. MAT, PAA, PMA, polyaspartate, etc.) and all of these are polymeric in nature (Chen et al., 2011; Dickinson et al., 2011; Hasson et al., 2011; Inches et al., 2006; Wilson et al., 2010). "Green" SIs, or "yellow" designated species are more environmentally friendly than traditional "red" phosphonate type SIs (Jordan, et al., 2010, 2011). In an effort to protect the marine environment, a number of regulatory systems have been introduced regarding the evaluation and toxicity of oilfield scale inhibitors, for example, REACH (Registration, Evaluation, and Authorisation of Chemicals) (Castanares et al., 2008; Galvan and Smith, 2010; Henson, 2011; Jacoby, 2011), PARCOM, OSPARCOM, HMCS, etc. (Taj et al., 2006). Common oilfield scales include barium, calcium and strontium sulphates and calcium carbonate (Clemmit et al., 1985). Barite is the hardest, most difficult inorganic scale to prevent and to remove. In this Chapter the inhibition of barite using polymeric SIs is investigated. The barite IE of polymeric SIs has been extensively tested in a wide range of brine mix compositions. It is known that the presence of divalent cations (Ca^{2+} and Mg^{2+}) has some effect on the barite IE of polymeric SIs as reported previously (Graham et al., 2003; Boak et al., 1999; Shaw et al., 2010b). However, this influence is *less marked* than the effect

of Ca^{2+} and Mg^{2+} on phosphonate SI species (Graham et al., 2003; Sorbie and Laing, 2004; Shaw et al., 2010a).

In this work, an extensive range of static barium sulphate inhibition efficiency experiments were carried out testing the following polymeric scale inhibitors (SIs): PPCA (phosphino poly carboxylic acid), MAT (a green ter-polymer), SPPCA (a P-containing sulphonated co-polymer), PMPA (phosphino methylated polyamine – described as a poly-phosphonate), PFC (a generic P-functionalised co-polymer), PVS (poly vinyl sulphonate), VS-Co (a sulphonate co-polymer with polyacrylate), CTP-A and CTP-B (cationic ter-polymers A and B, of interest in that they are *cationic*); further details of these polymeric SI structures are given in Chapter 3, Section 3.9.2. For the exact definition of barite IE, see Chapter 3, Equation 3.1. These polymeric IE experiments were performed on a range of mixing ratios of North Sea Sea Water (NSSW) / Forties Formation Water (FW) between 10/90 and 80/20. The SIs were tested under two sets of experimental conditions (i.e. Base Case and Fixed Case) in the same way as the phosphonate SIs (Chapter 5). The Base Case and Fixed Case brine compositions are given in Chapter 3, Tables 3.1 (Base Case NSSW), 3.2 (Base Case FW), 3.3 (Fixed Case NSSW), 3.4 (Fixed Case FW) and 3.5 (Fixed Case FW Ca^{2+}, Mg^{2+} and Cl^{-}).

Additional experiments varying the molar ratio Ca^{2+}/Mg^{2+} in the produced water were carried out testing PPCA, MAT and SPPCA. In these experiments, the [SI] was fixed at a value below its MIC (where the MIC may be its 2 or 22 hour value) and the total molar quantity of divalent ions in the produced water, $X_m = [Mg^{2+}]+[Ca^{2+}]$, was fixed = 80.3 millimoles/L. Ionic strength, $[Cl^{-}]$, temperature and pH variables were also held constant. X_m = 80.3 mM/L is held constant in all Fixed Case IE experiments, therefore this X_m value was chosen for these additional experiments at fixed [SI]. In each case, the [SI] tested is in the pre-2 or 22 hour MIC region such that variations in IE due to changes in $[Ca^{2+}]$ and $[Mg^{2+}]$ are clearly visible. If too high a [SI] level is tested in these experiments, IE may be >90% regardless of the brine $[Ca^{2+}]$ and $[Mg^{2+}]$ and IE sensitivities due to divalent ions Ca^{2+} and Mg^{2+} would be masked. The objective is to be able to see variations in IE; this is usually at the 22 hour sampling time, but occasionally trends are visible at 2 hours – depending on the [SI] selected for the test. An 80/20 NSSW/FW mixing ratio was chosen for these experiments testing PPCA, MAT, and SPPCA. The cationic ter-polymers were tested similarly, except mixing ratio 60/40 NSSW/FW was selected, Base Case experimental conditions, X_m = 72.3 mM/L

fixed – testing molar ratios Ca^{2+}/Mg^{2+} = 0.1, 0.25, 0.5, 1, 5, and ∞, at a fixed [SI] = 15ppm (for both cationic ter-polymers – pre-2hr MIC for both these species). The IE and MIC of PFC was also determined under the same test conditions as for the cationic ter-polymers, but with Ca^{2+}/Mg^{2+} molar ratio = 0.19 and 1.64, see Section 6.6.2.

When polymeric SIs are being deployed, precipitation in high calcium brines can sometimes be an issue (Graham et al., 2003). Precipitation with calcium can be beneficial for SI retention in SI squeeze treatments, but only if the SI re-dissolves and continues to inhibit barite (Jordan et al., 1994, 1996; Malandrino et al., 1995). On the contrary, SI precipitation with Ca^{2+} is detrimental in continuous injection applications. Phosphorus "tagged" polycarboxylate SIs such as PPCA are often used for precipitation squeeze treatments in the North Sea where precipitation may be induced by high [Ca^{2+}], high [SI], temperature or pH effects (Rabaioli and Lockhart, 1995; Bezerra et al., 1999). In this work, two static compatibility experiments were carried out testing PPCA to investigate its tolerance to a high brine [Ca^{2+}], at the same [Ca^{2+}] level selected for all the Fixed Case static inhibition efficiency experiments (i.e. [Ca^{2+}] = 2000ppm). Results demonstrate conclusively that precipitation of a Ca–PPCA compound does indeed occur. A small quantity of calcium sulphate precipitate forms in an uninhibited solution (in the presence of sulphate) when the mix [Ca^{2+}] = 2000ppm, which is included in the barite/celestite mixed scale.

6.2 PPCA

6.2.1 Compatibility Experiments

6.2.1.1 Introduction

A static compatibility experiment was firstly carried out in the absence of barium (Ba^{2+}) and strontium (Sr^{2+}) scaling ions, to establish if any precipitation of SI with brine calcium (Ca^{2+}) occurs in a brine mix with [Ca^{2+}] = 2000ppm. An 80/20 NSSW/FW mixing ratio was selected for this test; the brines used were the same as for the 80/20 NSSW/FW Fixed Case IE tests (see Section 6.2.2), except Ba^{2+} and Sr^{2+} ions were absent. The NSSW and FW brine compositions used for this experiment are given in Tables 3.3 and 3.14 (Chapter 3). Analysis was carried out for SI and Ca^{2+} by ICP spectroscopy. PPCA was assayed by means of [P]. As in the IE experiments, a sample was taken from the test bottles at 2 and 22 hours after the mixing of NSSW/FW. In addition, another sample was taken from each bottle, after the test

bottles were allowed to cool to room temperature – 25 hours after mixing NSSW with FW (i.e. 3 hours cooling – the bottles were removed from the water bath immediately after the 22 hour sampling). The following [SI]s were tested: 50, 100, 600 and 1000ppm. Blank samples (no SI present) were tested to see if any calcium sulphate scale formed. This static compatibility experiment was actually performed after observing poor Fixed Case IE results, testing PPCA.

In this first static compatibility experiment, the possibility of calcium sulphate scale forming was not eliminated – hence this experiment was repeated with a brine mix containing no barium, no strontium *and* no sulphate ions. Removing the sulphate anions from the NSSW completely eliminates the possibility of calcium sulphate formation. Therefore, any measured decreases in brine calcium (Ca^{2+}) must now be due exclusively to precipitation with SI (i.e. PPCA). Again, in this second compatibility experiment, an 80/20 NSSW/FW mixing ratio was selected for the test. Furthermore, additional NaCl was added to the NSSW to compensate for the Na_2SO_4 removed, thus maintaining the ionic strength (I) to the same level in both types of static compatibility test (i.e. sulphate present tests and sulphate absent tests). In this second compatibility test, PPCA was tested at 100ppm and 1000ppm. Again, blank samples (no SI present) were tested. Tables 3.13 and 3.14 in Chapter 3 (Experimental Details) give the NSSW and FW brine compositions used for this second static compatibility test.

6.2.1.2 No Barium (Ba^{2+}) and No Strontium (Sr^{2+}) Static Compatibility Experiment

Figure 6.1 shows the % PPCA removed from solution at various times in the 80/20 NSSW/FW Fixed Case static compatibility experiment, in the absence of Ba^{2+} and Sr^{2+} scaling ions, testing various initial PPCA concentrations as shown. Results in Figure 6.1 indicate that ~ 40% of the PPCA was removed from solution 22 hours after mixing NSSW with FW, when PPCA was tested at 50ppm active**.** This removed SI must be precipitating with the brine Ca^{2+}, since both Ba^{2+} and Sr^{2+} were absent**.** Similarly, when higher PPCA concentrations were tested, SI was again removed from solution. The mass of SI–Ca precipitated increases with [PPCA]. For example, at 22 hours, in the 50ppm PPCA test, ~ (0.38*50) ppm = 19ppm PPCA precipitated, whereas in the 1000ppm PPCA test, ~ (0.12*1000) ppm = 120ppm PPCA precipitated (Figure 6.1). In static barite IE tests, lower

[PPCA]s are more commonly tested, e.g. up to ~100ppm. Thus, some SI–Ca precipitation may be encountered when PPCA is tested in high Ca^{2+} brines. The precipitated SI is ineffective in scale control, as confirmed in static barite IE as shown in Fixed Case test results (see Figure 6.3 and Figure 6.4). Corresponding decreases in $[Ca^{2+}]$ were observed, although this is more difficult to detect, since $[Ca^{2+}]_o$ = 2000ppm. Only a small % of this 2000ppm Ca^{2+} would precipitate with SI, therefore measured decreases in $[Ca^{2+}]$ of around 6% are plausible. 6% of 2000ppm is a decrease of ~120ppm Ca^{2+} – hence it is sometimes problematic to detect very small decreases (120ppm or less) in solution $[Ca^{2+}]$ by ICP spectroscopy, when the $[Ca^{2+}]_o$ = 2000ppm.

Sampling was also carried out 25 hours after mixing NSSW with FW. When the test bottles were allowed to cool on the open bench (over a 3 hour period – from 22 hours to 25 hours), the visible white precipitate in the test bottles disappeared (i.e. re-dissolved). Analysis of the 25 hour samples taken at room temperature (RT) indeed confirmed that some SI and Ca^{2+} is going back into solution because of the increased solubility of the Ca–SI complex at RT (~20^{o}C). Furthermore, calcium sulphate is more soluble at lower temperatures (Clemmit et al., 1985). The precipitate formed in the test bottles will be a mixed deposit of Ca^{2+} ions bound to both SO_4^{2-} and SI^{n-} ions (because SO_4^{2-} ions are present). Calcium sulphate becomes more soluble at lower temperatures (Abu-Khamsin and Ahmad, 2005) – which also explains why some SI was also going back into solution. SI will be released back into solution from the solid calcium sulphate deposit which is progressively re-dissolving on cooling. Decreases in $[Ca^{2+}]$ were also measured in the blank test bottles and this confirms the formation of calcium sulphate scale under these test conditions (in the absence of PPCA). When SI *was* present, the removed Ca^{2+} is most likely removed in combination with both SI^{n-} and SO_4^{2-} ions and this is why this experiment was repeated in the absence of sulphate anions, i.e. to determine how much Ca^{2+} is precipitating with SI alone (i.e. *not* in combination with SO_4^{2-}).

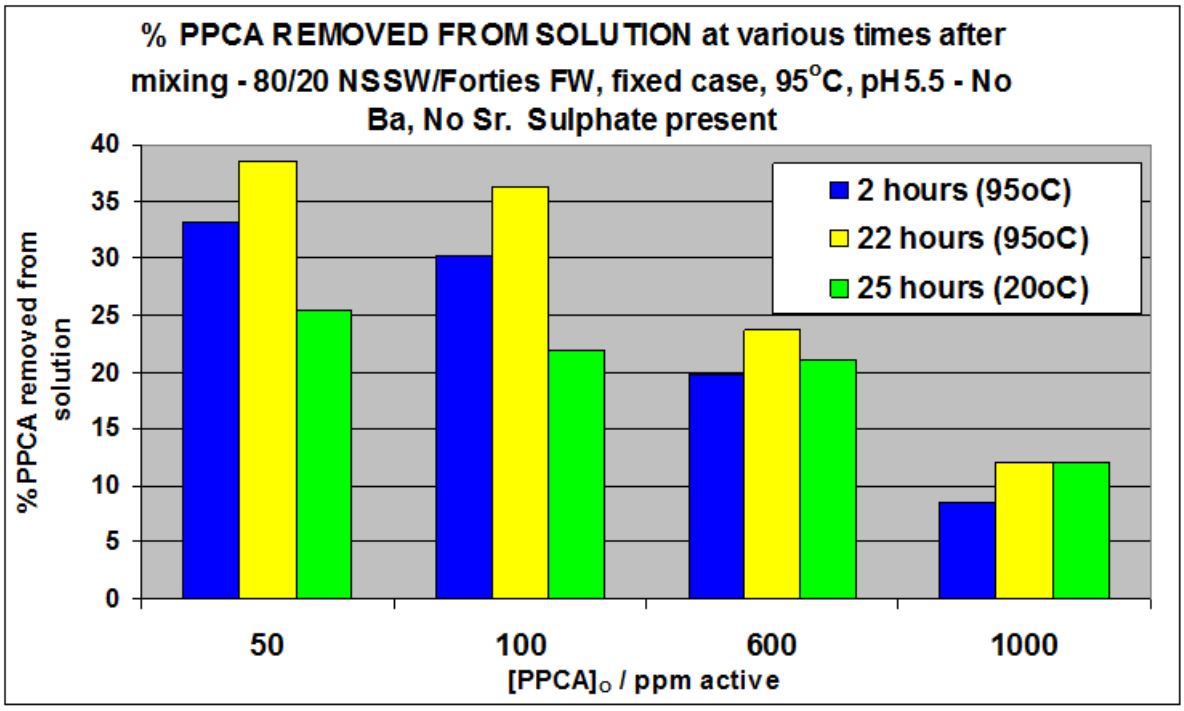

Figure 6.1 − Static compatibility experiment results. % PPCA removed from solution at various times after mixing NSSW and FW. There are four $[PPCA]_o$ values, = 50, 100, 600 and 1000ppm. 80/20 NSSW/FW, Fixed Case conditions, 95°C, pH5.5. No Ba^{2+}, No Sr^{2+}.

6.2.1.3 No Barium (Ba^{2+}), No Strontium (Sr^{2+}) and No Sulphate (SO_4^{2-}) Static Compatibility Experiment

Figure 6.2 shows the % PPCA removed from solution in this second static compatibility experiment – this time in the absence of Ba^{2+}, Sr^{2+} and SO_4^{2-} ions. Once again, these results confirm that PPCA is being removed from solution. At 22 hours after mixing, NSSW (containing no SO_4^{2-}) with FW (containing no Ba^{2+} and no Sr^{2+}), 35–40% of PPCA is removed from solution from an initial 100ppm PPCA. This finding is broadly similar to the static compatibility experimental results in the presence of SO_4^{2-} anions (Figure 6.1). Once again, a lower % SI is removed when the [SI] is higher and SI is going back into solution after cooling to room temperature (~20°C). These results suggest that not only is $CaSO_4$ more soluble at lower temperatures, but a Ca–PPCA compound also appears to be more soluble at lower temperatures.

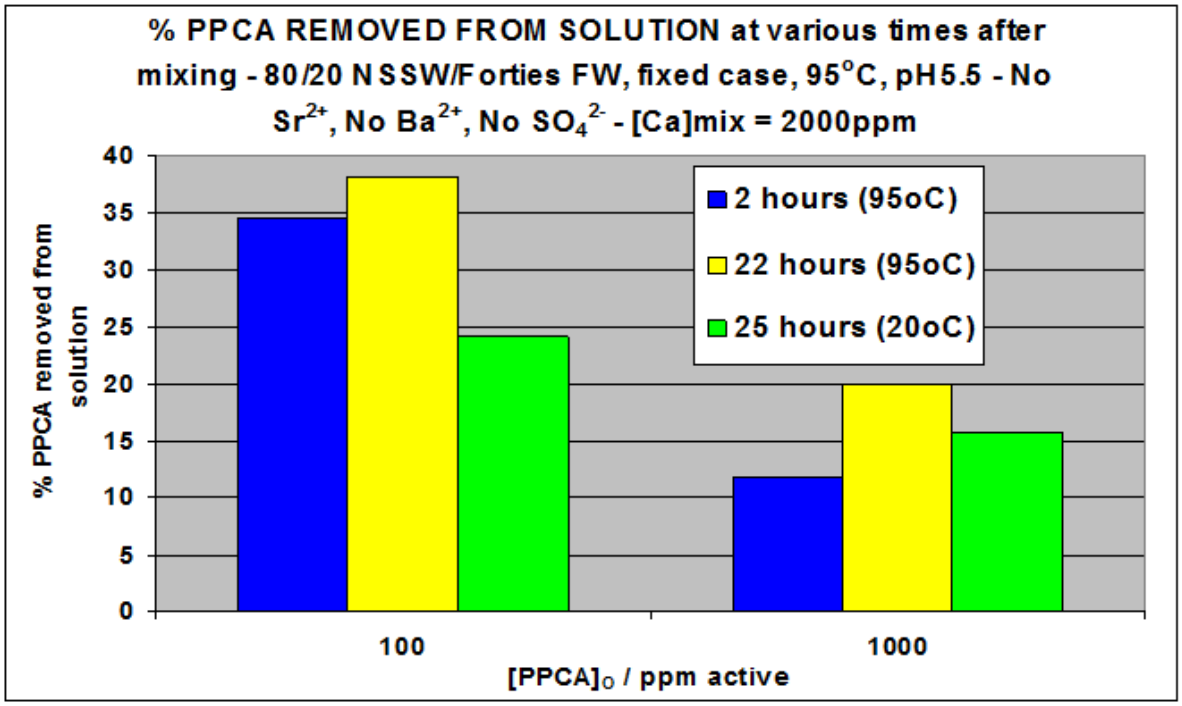

Figure 6.2 − Static compatibility experiment results. % PPCA removed from solution at various times after mixing NSSW and FW. There are two $[PPCA]_o$ values, = 100 and 1000ppm. 80/20 NSSW/FW, Fixed Case conditions, 95°C, pH5.5. No Ba^{2+}, No Sr^{2+}, and No SO_4^{2-}.

6.2.2 MIC vs. Mixing Ratio NSSW/FW

Figure 6.3 and Figure 6.4 present the MIC values for PPCA for the Base Case and Fixed Case experimental conditions at 2 hours and 22 hours, respectively. In Figure 6.3 and Figure 6.4, the MIC values broadly follow the order of decreasing barite saturation ratio (SR) level for the various mixing ratios NSSW/FW (i.e. 60/40 MIC > 80/20 MIC > 30/70 MIC > 10/90 MIC). The PPCA performs worse (for any selected mixing ratio NSSW/FW) in most cases under Fixed Case experimental conditions where the produced water $[Ca^{2+}]$ = 2000ppm and $[Mg^{2+}]$ = 739ppm. The measured Base Case 2 or 22 hour MIC is never greater than the Fixed Case 2 or 22 hour MIC for any mixing ratio NSSW/FW tested. A high barite saturation ratio in conjunction with a high $[Ca^{2+}]$ = 2000ppm causes the MIC for PPCA to increase significantly. Hence the highest 2 and 22 hour MICs are measured for the Fixed Case 60/40 and 80/20 NSSW/FW mixing ratios. In addition, the Base Case produced water $[Ca^{2+}]$ is lower for NSSW/FW mixing ratios 60/40 and 80/20 compared to mixing ratios 10/90 and 30/70 (see Figure 5.1), implying that the difference between the Base Case and Fixed Case

MIC level is likely to be greatest for higher % NSSW mixing ratios such as 60/40 and 80/20 NSSW/FW due to the incompatibility issue with [Ca^{2+}]. This is indeed what was observed at 2 and 22 hours. The static compatibility tests discussed in Section 6.2.1 illustrate quite conclusively that the poor performance of PPCA in the Fixed Case IE tests is due to formation of an SI–Ca precipitate, leaving behind a lower concentration of effective (i.e. active) SI in solution to inhibit barium sulphate scale.

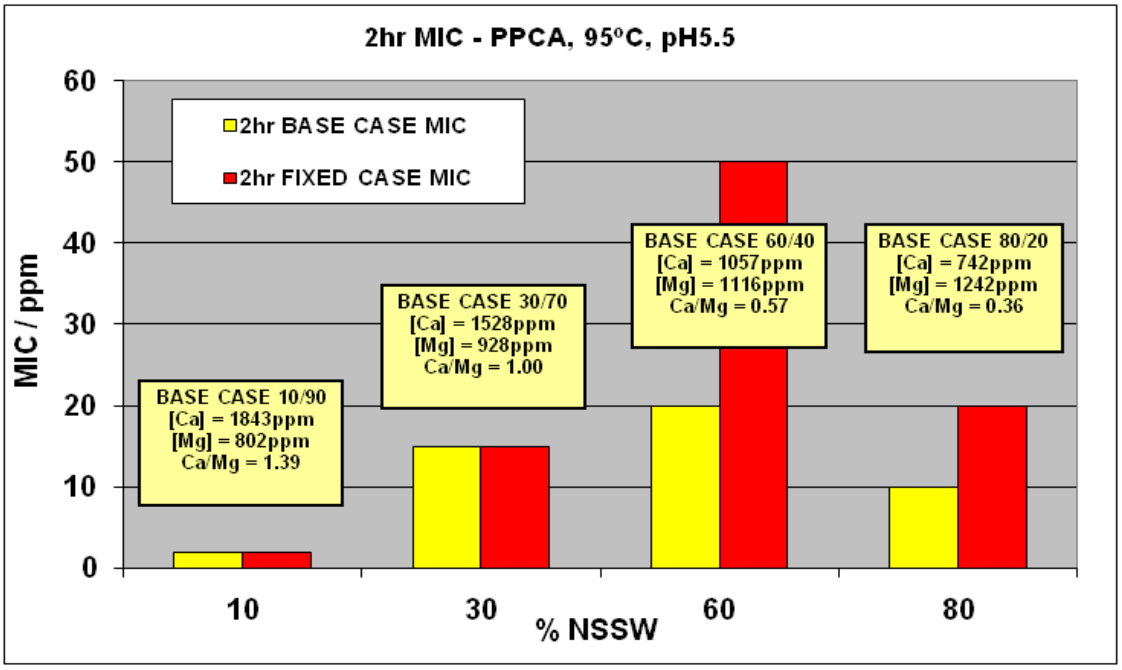

Figure 6.3 − 2 hour MIC vs. % NSSW, testing PPCA - Base Case and Fixed Case experimental conditions, 95°C, pH5.5.

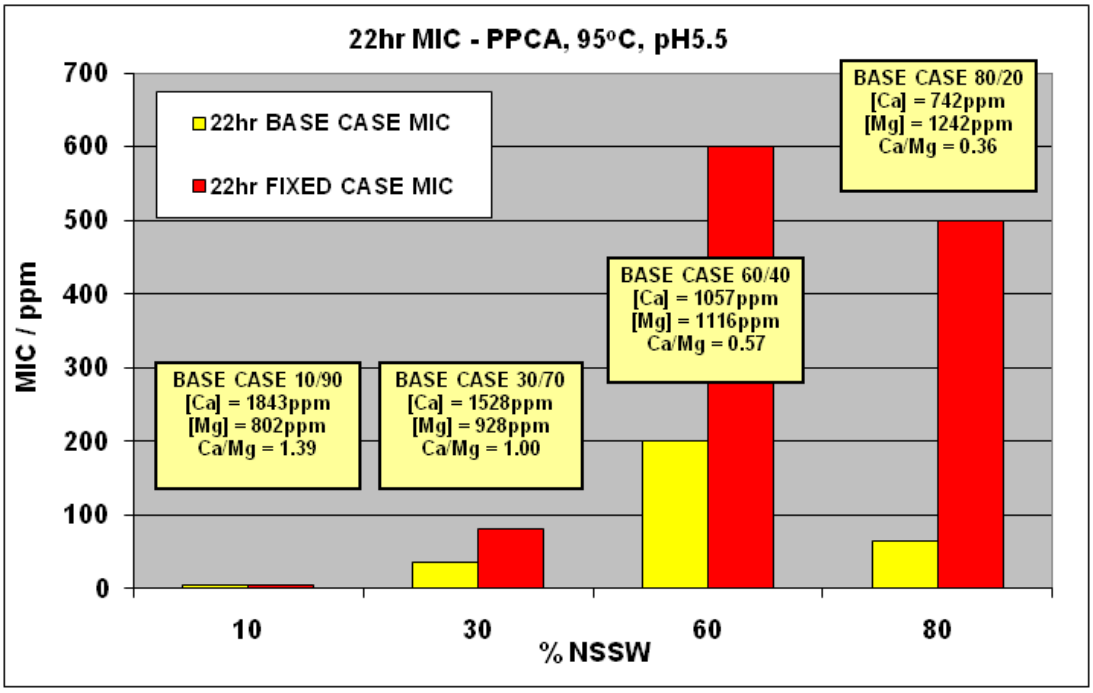

Figure 6.4 − 22 hour MIC vs. % NSSW, testing PPCA - Base Case and Fixed Case experimental conditions, 95°C, pH5.5.

6.2.3 Fixed [SI] – Varying Molar Ratio Ca^{2+}/Mg^{2+}

These experiments were designed to investigate the effect of varying the produced water molar ratio Ca^{2+}/Mg^{2+}, while keeping the total molar quantity of divalent ions and [SI] constant, i.e. $X_m = (Ca^{2+}+Mg^{2+})$ and [SI] constant. The total molar quantity of divalent ions (X_m) in the produced water was kept at the same level as in the Fixed Case IE experiments (Section 6.2.2) = 80.3 mM/L. The [SI] tested was fixed at 32ppm (pre-22hr PPCA MIC). Sampling times = 2 and 22 hours after mixing NSSW and FW. T = 95°C and pH = 5.5. For these experiments, the following brine molar ratios of Ca^{2+}/Mg^{2+} were tested: 0 (i.e. no Ca^{2+}, all 80.3 mM/L is Mg^{2+}), 0.05, 0.1, 0.15, 0.25, 0.35, 0.5, 0.75, 1, 1.25, 1.5, 1.64 (as in the Fixed Case IE experiments), 5, 10 and ∞ (i.e. no Mg^{2+}, all 80.3 mM/L is Ca^{2+}). Table 6.1 gives the produced water composition for each molar ratio Ca^{2+}/Mg^{2+} tested. The NSSW and FW compositions used for this experiment are given in Chapter 3, Tables 3.3 (NSSW), 3.4 (FW) and 3.7 (FW Ca^{2+}, Mg^{2+} and Cl^-). Calcium (Ca^{2+}) is beneficial to the performance of PPCA, but only at low or moderate levels (e.g. ~500–700ppm Ca^{2+} is the optimum concentration range for good barite IE to be achievable). When the calcium concentration becomes too high, SI–Ca precipitation occurs and thus the beneficial effect of calcium on IE is diminished. Testing PPCA at 32ppm with molar ratio Ca^{2+}/Mg^{2+} = 5, Ca–SI precipitation begins to occur at 2 hours (see Figure 6.5). When molar ratio Ca^{2+}/Mg^{2+} = 0.35, Ca–SI precipitation begins to occur at 22 hours, and this becomes progressively worse as the molar ratio Ca^{2+}/Mg^{2+} increases (see Figure 6.5).

The results in Figure 6.5 establish the optimum brine [Ca^{2+}] for IE for a fixed [PPCA] = 32ppm and NSSW/FW mixing ratio 80/20. From previous IE test results, this optimum brine [Ca^{2+}] was expected to be in the range 600–700ppm to achieve the highest IE at 22 hours; in fact, Figure 6.5 shows that the best IE performance is achieved when molar ratio Ca^{2+}/Mg^{2+} = 0.25, i.e. [Ca^{2+}] = 644ppm and [Mg^{2+}] = 1562ppm. The optimum brine [Ca^{2+}] will be dependent upon a number of factors, viz. [Ba^{2+}] (mix), i.e. the barite saturation ratio (SR) (or mixing ratio NSSW/FW), the [SI] tested, temperature, pH, etc. Also, magnesium (Mg^{2+}) is detrimental – since when no calcium is present, and all X_m (= 80.3 mM/L) of divalent ions in the produced water is magnesium (i.e. molar ratio Ca^{2+}/Mg^{2+} = 0 in Figure 6.5), both 2 hour and 22 hour IE are lower, compared to when some calcium displaces magnesium (i.e. molar ratio Ca^{2+}/Mg^{2+} = 0.05). Note the improvement in the 2 hour IE induced by having just

153ppm calcium present*; the 2 hour IE increases from ~70% to ~90% (i.e. 2 hour MIC is achieved).

*On changing from molar ratio Ca^{2+}/Mg^{2+} = 0 → molar ratio Ca^{2+}/Mg^{2+} = 0.05, ~4 millimoles of Mg^{2+} has been displaced, i.e. replaced by ~4 millimoles of Ca^{2+} in the produced water. Given that $X_m = (Ca^{2+}+Mg^{2+})$ = 80.3 millimoles/L, this is equivalent to approximately just 1/20 of the total Mg^{2+} in the system being replaced by Ca^{2+}. 1/20 of 80.3 = ~4. 153ppm Ca^{2+} ≡ ~4 millimoles of Ca^{2+}. Hence, the increase of ~20% 2 hour IE has resulted from an insignificant change in brine chemistry, but in these circumstances, clearly this small change has had a significant effect on IE.

Molar Ratio Ca^{2+}/Mg^{2+}	**Ca^{2+}/Mg^{2+} (as a fraction)**	**Ca^{2+} / millimoles/L ***	**Mg^{2+} / millimoles/L ***	**ppm Ca^{2+}**	**ppm Mg^{2+}**
0	$0/X_{molar}$	0	$=X_{molar}$=80.3	0	1952
0.05	1/20	3.8	76.5	153	1859
0.1	1/10	7.3	73.0	293	1775
0.15	3/20	10.5	69.8	420	1697
0.25	¼	16.1	64.2	644	1562
0.35	7/20	20.8	59.5	834	1446
0.5	½	26.8	53.5	1073	1301
0.75	¾	34.4	45.9	1379	1115
1	1/1	40.1	40.1	1609	976
1.25	5/4	44.6	35.7	1788	868
1.5	3/2	48.2	32.1	1931	781
1.64	≈33/20	49.9	30.4	2000	739
5	5/1	66.9	13.4	2682	325
10	10/1	73.0	7.3	2926	177
∞	$X_{molar}/0$	$=X_{molar}$=80.3	0	3218	0

* Rounded off to 1 decimal place.

Table 6.1 – Produced water compositions for each molar ratio Ca^{2+}/Mg^{2+}, testing SI PPCA.

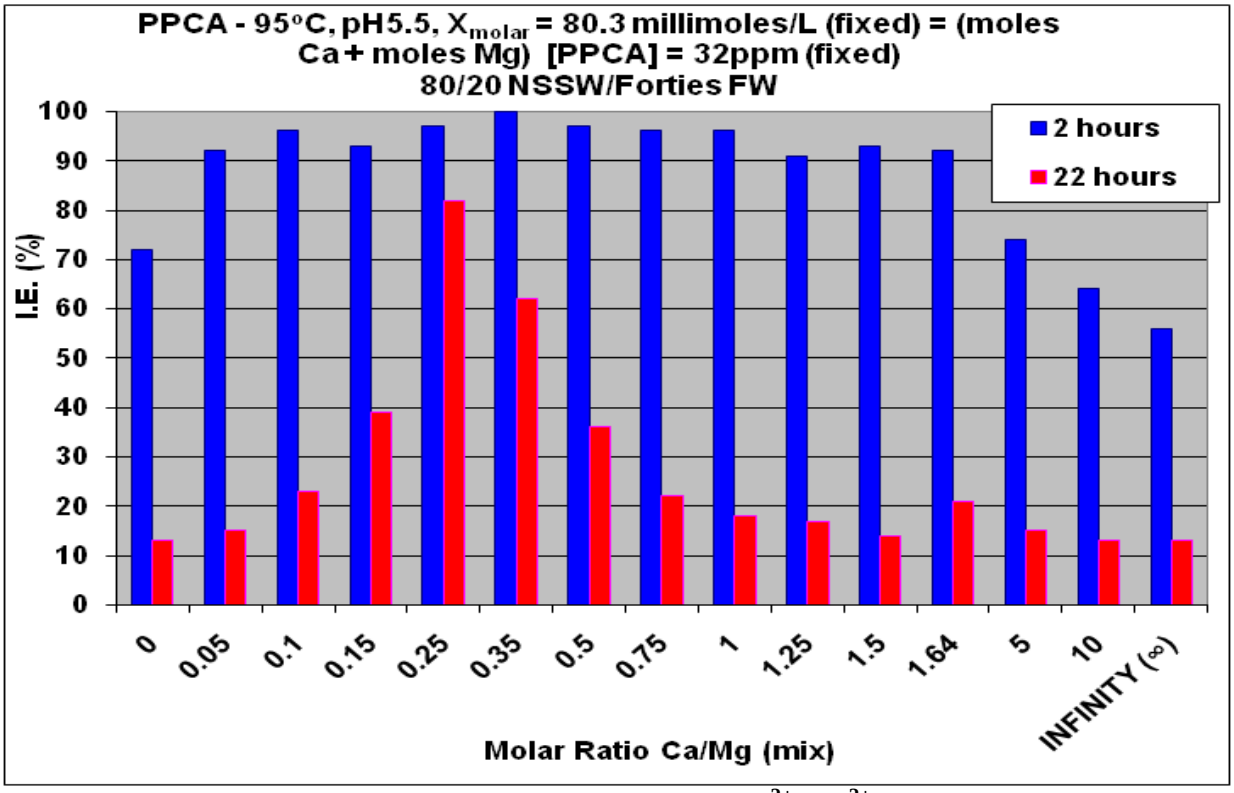

Figure 6.5 – IE testing PPCA – varying molar ratio Ca^{2+}/Mg^{2+} in the produced water. X_m, (moles Ca^{2+} + moles Mg^{2+}) = 80.3 millimoles/L in produced water constantly. 15 molar ratios Ca^{2+}/Mg^{2+} tested: 0, 0.05, 0.1, 0.15, 0.25, 0.35, 0.5, 0.75, 1, 1.25, 1.5, 1.64, 5, 10 and ∞. [PPCA] = 32ppm (i.e. pre-22 hour MIC).

6.3 MAT (a "green" ter-polymer)

6.3.1 MIC vs. Mixing Ratio NSSW/FW

Figure 6.6 and Figure 6.7 present the experimental MIC vs. % NSSW for three brine mix compositions for the green SI, maleic acid ter-polymer (MAT), at 2 hours and 22 hours, respectively, for both the Base Case (Ca^{2+}/Mg^{2+} varying) and the Fixed Case (Ca^{2+}/Mg^{2+} fixed) experimental conditions. For MAT, the 2 and 22 hour Base Case 30/70 NSSW/FW MICs are higher than the 80/20 NSSW/FW MICs, despite the barite saturation ratio level being lower for the 30/70 mixing case (see Figure 5.1). Presumably this is attributable to a detrimental effect of higher produced water [Ca^{2+}] in the 30/70 NSSW/FW case. The 2 hour Base Case and Fixed Case MICs measured for MAT are broadly similar (see Figure 6.6). At the 22 hour residence time, MAT performs markedly worse in the Fixed Case IE tests (Figure 6.7). This is the same trend observed testing PPCA, but the underlying reason for this may be different for the MAT species. MAT was not tested in a static compatibility experiment;

therefore the poorer IE in the Fixed Cases may not be due to precipitation of a SI–Ca compound. If MAT was tested in a static compatibility experiment, the analysis for [SI] would have to involve a wet chemical analytical procedure, i.e. involving the chemical reagent Hyamine and spectrophotometric analysis, since MAT contains no phosphorus and no sulphur – it is therefore a non-ICP detectable species (Boak and Sorbie, 2010). The poor Fixed Case IE could be due to SI incompatibility with high [Ca^{2+}] or there may be a mechanistic reason why – involving SI and Ca^{2+}. The manufacturer of the MAT product reports that it is calcium "tolerant".

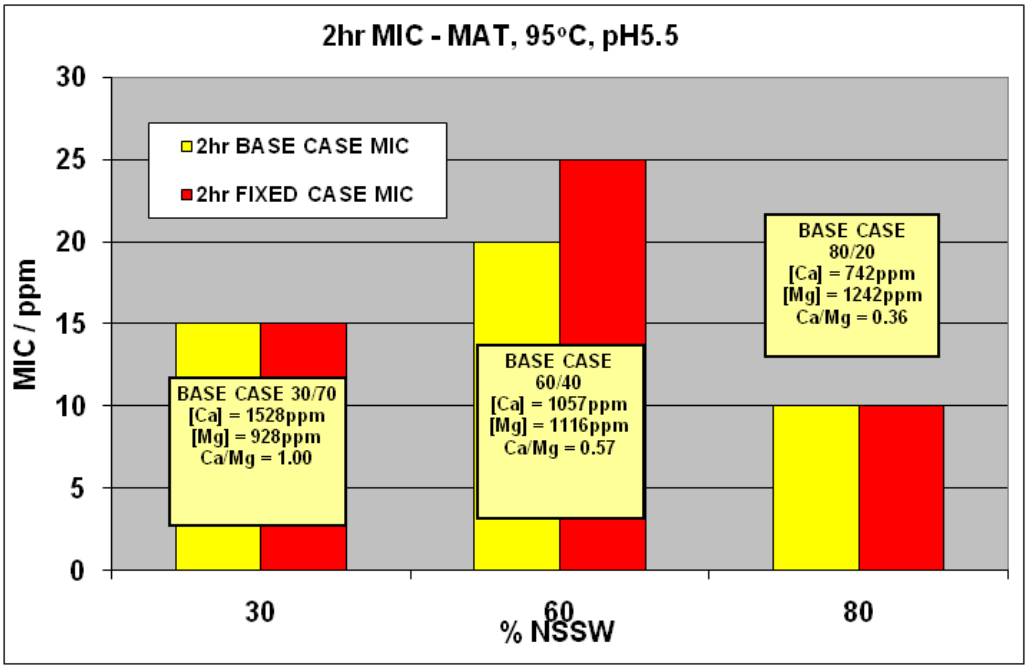

Figure 6.6 − 2 hour MIC vs. % NSSW, testing MAT - Base Case and Fixed Case experimental conditions, 95°C, pH5.5.

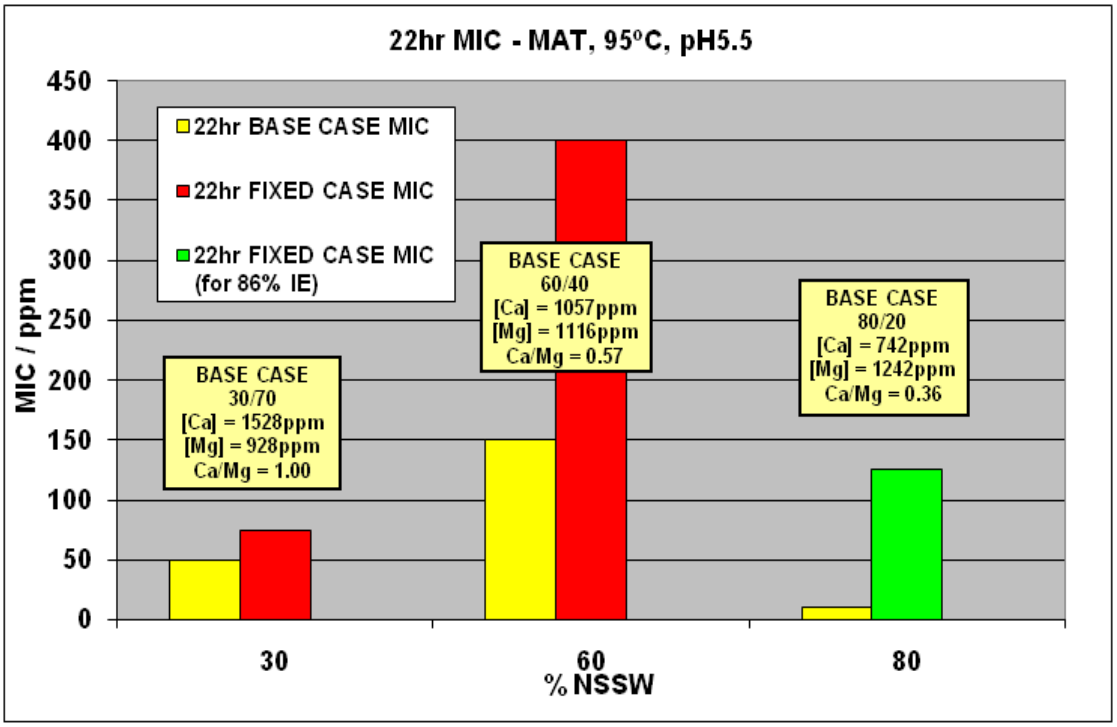

Figure 6.7 − 22 hour MIC vs. % NSSW, testing MAT - Base Case and Fixed Case experimental conditions, 95°C, pH5.5.

6.3.2 Fixed [SI] – Varying Molar Ratio Ca^{2+}/Mg^{2+}

MAT was tested at 5ppm – this is pre-2 hour MIC. The following brine molar ratios of Ca^{2+}/Mg^{2+} were tested: 0 (i.e. no Ca^{2+}, all 80.3 mM/L is Mg^{2+}), 0.25, 0.5, 0.75, 1, 1.25, 1.5, 1.64 (as in the Fixed Case IE experiments), 5, 10 and ∞ (i.e. no Mg^{2+}, all 80.3 mM/L is Ca^{2+}). Table 6.1 includes the produced water compositions for these Ca^{2+}/Mg^{2+} molar ratios tested. The NSSW and FW compositions used for this experiment are given in Chapter 3, Tables 3.3 (NSSW), 3.4 (FW) and 3.7 (FW Ca^{2+}, Mg^{2+} and Cl^-). Figure 6.8 shows the 2 and 22 hour IE of MAT vs. molar ratio Ca^{2+}/Mg^{2+}. [MAT] is held at 5ppm which is less than the 2 hour MIC level for the NSSW/FW mixing ratio = 80/20. All other test conditions were the same as for the experiment testing PPCA (see Section 6.2.3). MAT exhibits similar IE behaviour to the PPCA (see Figure 6.5) but the high [Ca^{2+}] incompatibility is not as marked (see Figure 6.8) which could be because the [SI] tested is lower in the case of MAT (=5ppm), compared to PPCA (=32ppm). As the molar ratio Ca^{2+}/Mg^{2+} increases, IE increases at 2 and 22 hour residence times. However, when molar ratio $Ca^{2+}/Mg^{2+} > 0.75$, the IE levels off at both 2 and 22 hour residence times. When molar ratio $Ca^{2+}/Mg^{2+} > 5$, slow SI–Ca precipitation may be

occurring, causing the 22 hour IE to start to decline. The highest 2 hour (i.e. short-term) IE was achieved for molar ratios Ca^{2+}/Mg^{2+} = 5, 10 and ∞, possibly due to the high [Ca^{2+}] benefiting the SI before precipitation or other mechanistic issues have had time to develop fully (e.g. kinetic effects).

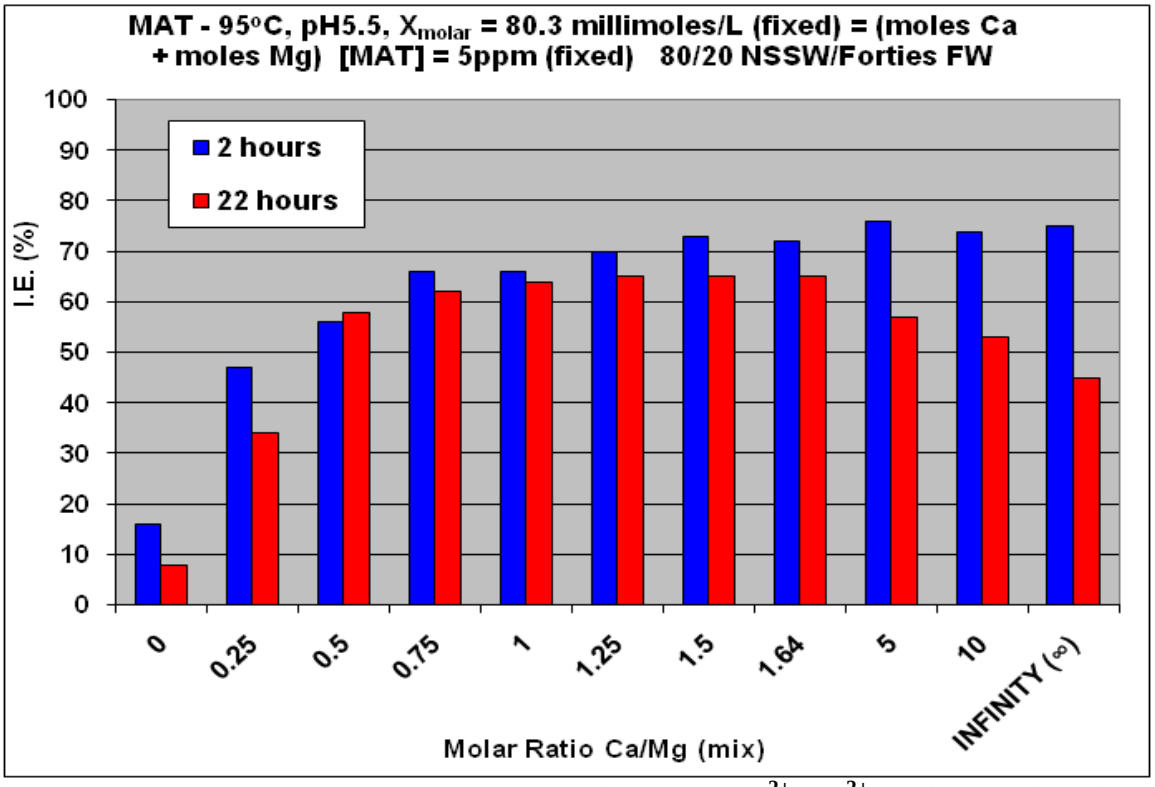

Figure 6.8 – IE testing MAT – varying molar ratio Ca^{2+}/Mg^{2+} in the produced water. X_m (moles Ca^{2+} + moles Mg^{2+}) = 80.3 millimoles/L in produced water constantly. 11 molar ratios Ca^{2+}/Mg^{2+} tested: 0, 0.25, 0.5, 0.75, 1, 1.25, 1.5, 1.64, 5, 10 and ∞. [MAT] = 5ppm (i.e. pre-2 hour MIC).

6.4 SPPCA

6.4.1 MIC vs. Mixing Ratio NSSW/FW

Figure 6.9 and Figure 6.10 present the experimental MIC vs. % NSSW for three brine mix compositions for SPPCA at 2 hours and 22 hours, respectively, for both the Base Case (Ca^{2+}/Mg^{2+} varying) and the Fixed Case (Ca^{2+}/Mg^{2+} fixed) experimental conditions. The highest Fixed Case 2 and 22 hour MIC levels were measured for the 60/40 NSSW/FW mixing ratio, followed by 80/20, then 30/70. This trend correlates with the order of decreasing barite saturation ratio (SR) applying to these mixing ratios NSSW/FW (SR in

Figure 5.1 shows 60/40 > 80/20 > 30/70), and is the result one would expect when the concentration of divalent ions, Ca^{2+} and Mg^{2+} in the produced water are fixed. The higher [Mg^{2+}] in the 80/20 NSSW/FW Base Case produced water may be elevating the 80/20 NSSW/FW 22 hour MIC to > MIC for 60/40 NSSW/FW. Figure 6.10 shows that at 200ppm [SPPCA] only 38% IE is achieved for the mixing ratio 80/20 NSSW/FW (Base Case). These findings suggest a fairly high [Mg^{2+}] concentration (i.e. 1242ppm Mg^{2+} in an 80/20 NSSW/FW Base Case mix) is having a very detrimental effect upon the function of SPPCA, in the same way as observed with conventional phosphonate SIs (Chapter 5). For example, the 22 hour 80/20 Base Case MIC for HMTPMP (a type 2 conventional phosphonate) was = 90ppm – compared to 50ppm for the 60/40 Base Case (highest SR) test (Shaw et al., 2010a). The lowest SPPCA Base Case 22 hour MIC was for 30/70 NSSW/FW, in line with the barite SR level for this mixing ratio.

When SPPCA was tested, the 2 and 22 hour Fixed Case MICs were always < Base Case MICs (see Figure 6.9 and Figure 6.10). This is the same behaviour as observed testing conventional phosphonate SIs (Shaw et al., 2010a) and the opposite trend to that observed testing non-sulphonated polycarboxylate species PPCA and MAT. The only difference between the molecular structures of PPCA and SPPCA is that the SPPCA is sulphonated whereas the PPCA is not. The presence of sulphonate functional groups on the SPPCA molecule prevents precipitation with brine calcium. SPPCA benefits from high levels of calcium, like conventional phosphonate SIs. Magnesium appears to be detrimental to polymeric SIs PPCA, MAT *and* SPPCA, hence the Base Case 22 hour 80/20 NSSW/FW SPPCA MIC is unachievable (i.e. 90% IE or greater at 22 hours cannot be reached under these conditions).

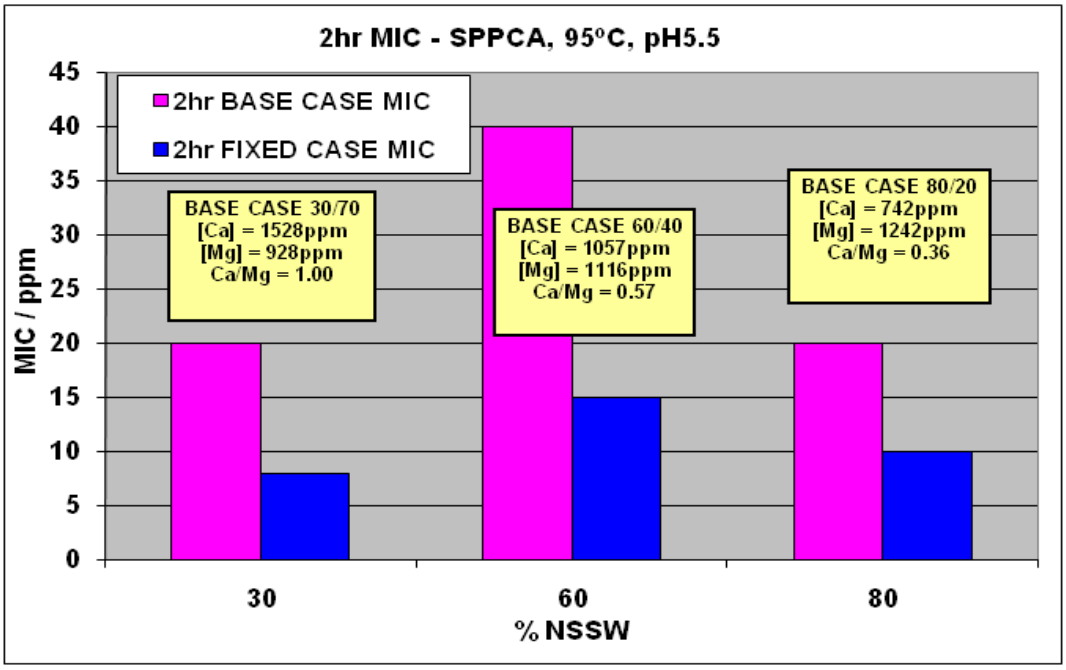

Figure 6.9 – 2 hour MIC vs. % NSSW, testing SPPCA - Base Case and Fixed Case experimental conditions, 95°C, pH5.5.

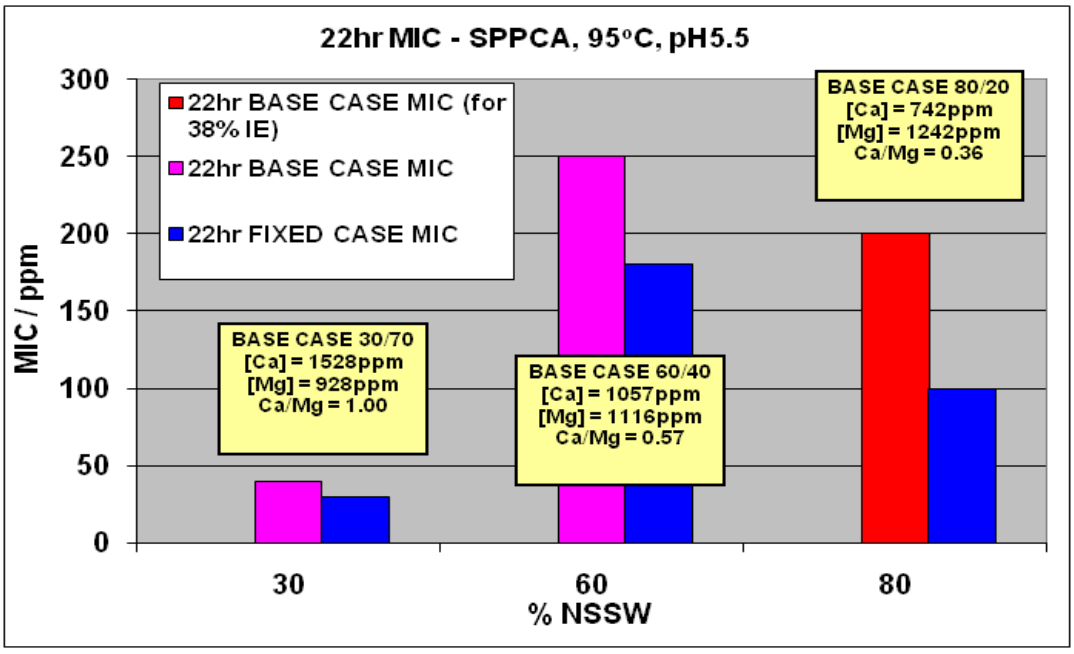

Figure 6.10 – 22 hour MIC vs. % NSSW, testing SPPCA - Base Case and Fixed Case experimental conditions, 95°C, pH5.5.

6.4.2 Fixed [SI] – Varying Molar Ratio Ca^{2+}/Mg^{2+}

SPPCA was tested at 5ppm – this is pre-2 hour MIC. The following brine molar ratios of Ca^{2+}/Mg^{2+} were tested: 0 (i.e. no Ca^{2+}, all 80.3 mM/L is Mg^{2+}), 0.25, 0.5, 0.75, 1, 1.25, 1.5, 1.64 (as in the Fixed Case IE experiments), 5, 10 and ∞ (i.e. no Mg^{2+}, all 80.3 mM/L is Ca^{2+}). Table 6.1 includes the produced water compositions for these Ca^{2+}/Mg^{2+} molar ratios tested. The NSSW and FW compositions used for this experiment are given in Chapter 3, Tables 3.3 (NSSW), 3.4 (FW) and 3.7 (FW Ca^{2+}, Mg^{2+} and Cl^-). Figure 6.11 shows the 2 and 22 hour IE of SPPCA vs. molar ratio Ca^{2+}/Mg^{2+} for [SPPCA] = 5ppm (pre-2 hour MIC) and NSSW/FW mixing ratio = 80/20. Results in Figure 6.11 indicate that, as the produced water molar ratio Ca^{2+}/Mg^{2+} increases, the 2 hour IE increases, indicating that calcium is beneficial to the IE performance of SPPCA. The highest IE at 2 hours is reached when all 80.3 mM/L of X_m is calcium (Mg^{2+} absent, molar ratio $Ca^{2+}/Mg^{2+} = \infty$). The 22 hour IE also increases slightly with increasing produced water molar ratio Ca^{2+}/Mg^{2+}. If a higher [SI] had been tested, larger increases in the 22 hour IE would be expected as the molar ratio Ca^{2+}/Mg^{2+} progressively increases. A pre-2 hour or a pre-22 hour MIC SI concentration (i.e. values of [SI] < MIC) is normally selected for these types of experiment, such that variations in either the 2 or 22 hour IE are likely to be visible, i.e. not masked due to the test [SI] being too high. Testing SPPCA and MAT, a pre-2 hour MIC [SI] of 5ppm was chosen in both cases, whereas for PPCA, a pre-22 hour MIC [SI] of 32ppm was selected. The [SI] chosen for this type of experiment is largely arbitrary – if the test [SI] is constant, then the same trends in IE with varying molar ratio Ca^{2+}/Mg^{2+} should become apparent in either the 2 or 22 hour IE. Clearly, higher brine [Ca^{2+}], such as 2000ppm+ (i.e. molar ratio Ca^{2+}/Mg^{2+} = 1.64+) is very beneficial to the IE performance of SPPCA.

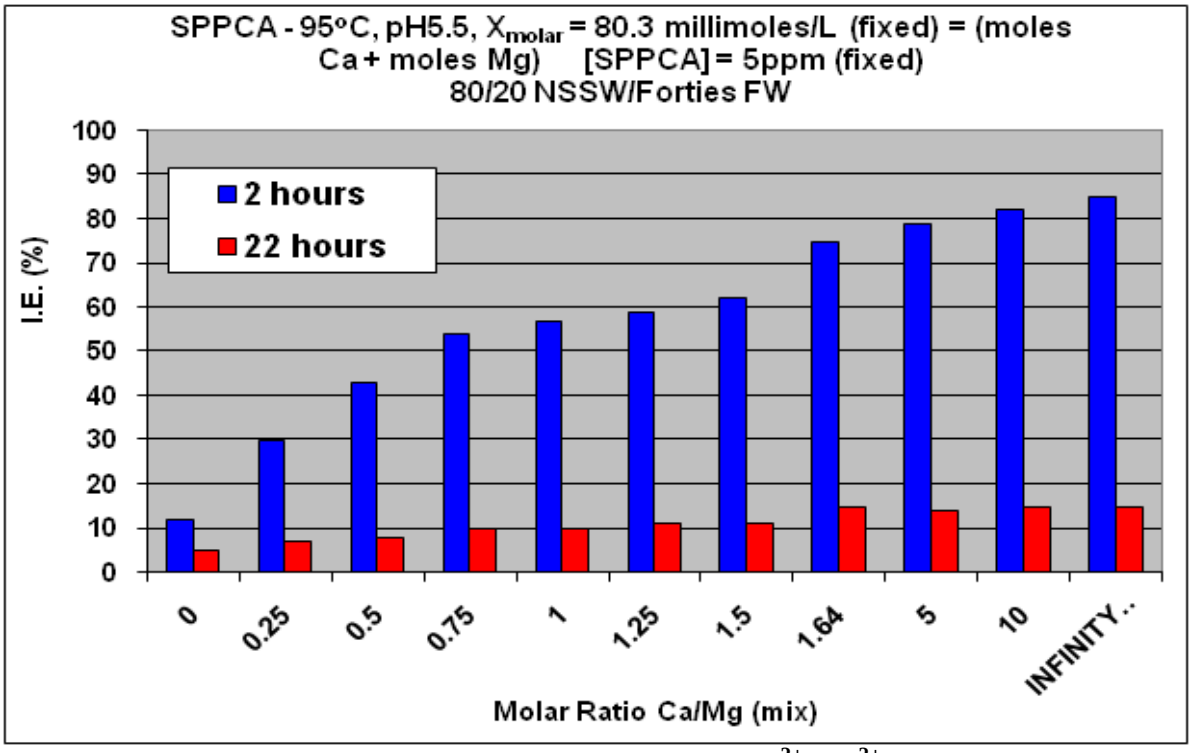

Figure 6.11 – IE testing SPPCA – varying molar ratio Ca^{2+}/Mg^{2+} in the produced water. X_m, (moles Ca^{2+} + moles Mg^{2+}) = 80.3millimoles/L in produced water constantly. 11 molar ratios Ca^{2+}/Mg^{2+} tested: 0, 0.25, 0.5, 0.75, 1, 1.25, 1.5, 1.64, 5, 10 and ∞. [SPPCA] = 5ppm (i.e. pre-2 hour MIC).

6.5 PMPA – MIC vs. Mixing Ratio NSSW/FW

In some instances, for example, at low pH, conventional phosphonate SIs are not the best choice for use in severe barite scaling systems (Cushner et al., 1988; Singleton et al., 2000). Polymeric SIs, such as PVS and VS-Co, may be better suited for low pH applications because phosphonate functional groups present on conventional phosphonate SIs such as DETPMP would be fully associated at this low pH level and therefore such SIs would be less able to inhibit barite scale formation. However, PVS and VS-Co do not possess good retention properties associated with the conventional phosphonate SIs (Jackson et al., 1996; Singleton et al., 2000). The synthesis of a SI such as poly-phosphonate PMPA was undertaken, as a compromise, to try and capture the associated benefits of both polymeric (e.g. low pH applications) and conventional phosphonate SIs (i.e. good retention) (Jackson et al., 1996; Przybylinski et al., 1999; Singleton et al., 2000). In addition to PMPA, some polymeric "di-phosphonate end-capped" polymers have been synthesised using a vinylidene di-phosphonic acid monomer (Davis et al., 2003). Such di-phosphonate end-capped polymers also exhibit

better adsorption / retention properties compared to their non-phosphonated (i.e. non-P-tagged) analogues – obviously due to the inclusion of the phosphonate functional groups in these molecules (Fleming et al., 2004).

Figure 6.12 and Figure 6.13 present the experimental MIC vs. % NSSW for three brine mix compositions for PMPA at 2 hours and 22 hours, respectively, for both the Base Case (Ca^{2+}/Mg^{2+} varying) and the Fixed Case (Ca^{2+}/Mg^{2+} fixed) experimental conditions. In contrast to PPCA and MAT, no incompatibility issues or loss of functionality with high [Ca^{2+}] are apparent for PMPA. The IE behaviour of poly-phosphonate PMPA is remarkably similar to that of the conventional phosphonate SIs (Chapter 5). The PMPA MICs are slightly higher than those measured testing the conventional penta-phosphonate, DETPMP. The IE behaviour of PMPA most closely resembles Type 1 phosphonate behaviour. The 22 hour PMPA 80/20 NSSW/FW Base Case MIC is much lower compared to, for example, type 2 penta-phosphonate HMTPMP (= 90ppm). The detrimental effect of a higher [Mg^{2+}] in the 80/20 NSSW/FW Base Case is less severe when PMPA is being tested. Nevertheless, the 22 hour PMPA 80/20 NSSW/FW Base Case MIC ≈ 22 hour 60/40 NSSW/FW Base Case MIC, therefore Mg^{2+} is confirmed to be detrimental to this species. Testing PMPA, all Fixed Case MICs (2 and 22 hour), for every tested mixing ratio NSSW/FW are < corresponding Base Case experiment, hence Ca^{2+} is very beneficial and this again mirrors classic conventional phosphonate SI behaviour. PMPA behaves more like a conventional phosphonate SI than like a polymeric SI. Indeed, there has been some suggestion recently that PMPA is *not* in fact polymeric at all and this would be very consistent with observations here. This knowledge was gained through communication with the PMPA manufacturer.

If PMPA is inserted into a sequence of conventional phosphonate SIs in terms of increasing MIC level (on going from left to right in the sequence), the sequence would be: OMTHP (6P, Type 1) > DETPMP (5P, Type 1) > PMPA (Poly-P) > HMTPMP (5P, Type 2) > HMDP (4P, Type 2) > NTP (3P, Type 2) > HEDP (2P, Type 2) ≈ HPAA (1P, 1C, Type 2) >>>> EABMPA (2P, Type 2); where ">" implies has a higher IE than (when all are tested at the same [SI] and under the same test conditions). The number and letter in brackets after the phosphonate SI abbreviations denotes how many phosphonate and/or carboxylate functional groups are present per SI molecule, e.g. 1P, 1C denotes 1 phosphonate group and 1

carboxylate group. PMPA performed better than conventional phosphonates: HMTPMP (5P), HMDP (4P), NTP (3P), HEDP (2P), HPAA (1P, 1C) and EABMPA (2P), but not as well as DETPMP (5P) or OMTHP (6P). Note that the PMPA performed better than all the *Type 2* phosphonate SIs tested in Chapter 5.

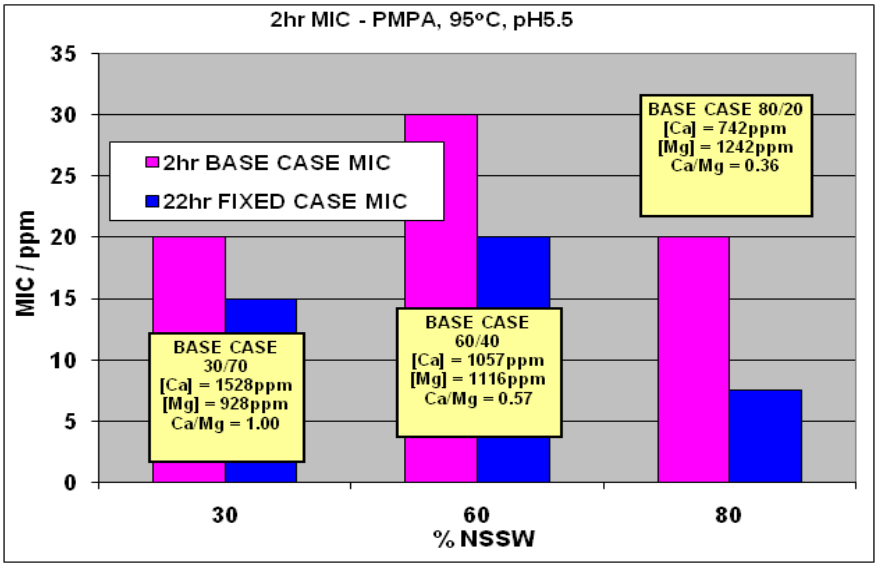

Figure 6.12 – 2 hour MIC vs. % NSSW, testing PMPA – Base Case and Fixed Case experimental conditions, 95°C, pH5.5.

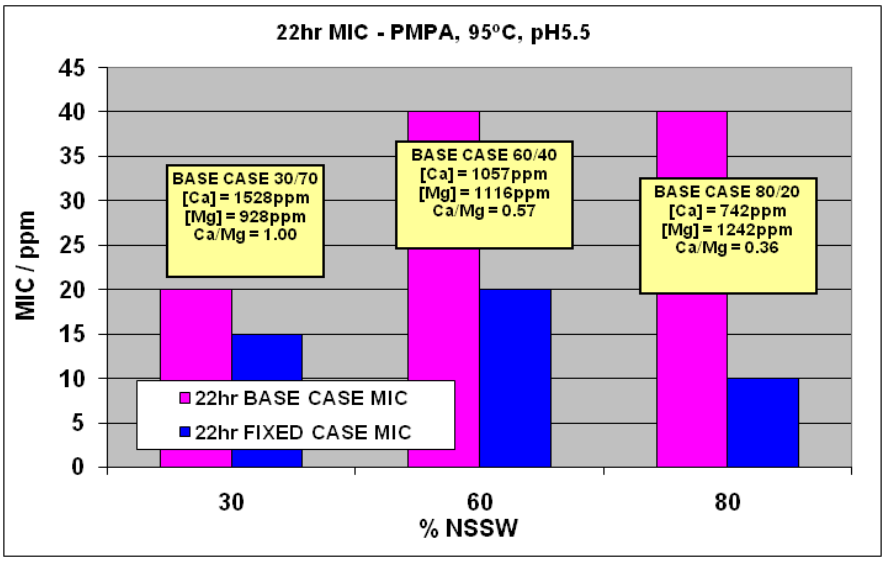

Figure 6.13 – 22 hour MIC vs. % NSSW, testing PMPA – Base Case and Fixed Case experimental conditions, 95°C, pH5.5.

6.6 PFC

6.6.1 MIC vs. Mixing Ratio NSSW/FW

Figures 6.14 and 6.15 present the experimental MIC vs. % NSSW for three brine mix compositions for a generic P-functionalised co-polymer (PFC) at 2 hours and 22 hours, respectively, for both the Base Case (Ca^{2+}/Mg^{2+} varying) and Fixed Case (Ca^{2+}/Mg^{2+} fixed) experimental conditions. P-functionalised co-polymer exhibits the same sensitivity to calcium and magnesium as polymeric polycarboxylated species PPCA and MAT, i.e. 22 hour Base Case MICs < 22 hour Fixed Case MICs. This is the opposite trend to what was observed testing conventional phosphonate SIs (Chapter 5).

The reason why a high [Ca^{2+}] = 2000ppm is detrimental to the IE of PFC could be the same as for PPCA, i.e. precipitation of SI with Ca^{2+}. Although static compatibility experimental results for PFC are not presented in this thesis, two preliminary experiments were conducted, testing PFC in a similar way to PPCA, i.e. testing brines in which Ba^{2+}, Sr^{2+} and SO_4^{2-} ions were absent. Once again, both Ca^{2+} and [SI] were assayed by ICP spectroscopy, at 2 and 22 hour residence times. Results strongly suggested precipitation of a SI–Ca compound *was* occurring – on some occasions, measured decreases in solution [SI] were in the region of 20-25%. This adds weight to the theory that polycarboxylate SIs in particular – may be susceptible to precipitate in high Ca^{2+} brines – PFC is polycarboxylated, however, also has some degree of sulphonation. By contrast, SPPCA, which (like PFC) is also P-tagged, carboxylated and sulphonated, precipitation of Ca–SPPCA does *not* occur and Ca^{2+} is very beneficial to this SI. Clearly, the differences between the IE behaviour of PFC and SPPCA must be related to specific differences in their chemical structures.

Low to moderate levels of calcium appear to be beneficial to PFC – the lowest Base Case 22 hour MIC is for 30/70 NSSW/FW where [Ca^{2+}] in the produced water = 1528ppm (see Figure 6.15) and this is similar behaviour to that observed for PPCA. As noted previously in the testing of other polymeric SIs (e.g. PMPA and SPPCA), at 22 hours: 60/40 Base Case MIC ≈ 80/20 Base Case MIC (Figure 6.15), once again indicating magnesium (Mg^{2+}) is detrimental because the SR level for 80/20 NSSW/FW is < SR for 60/40 NSSW/FW (see Figure 5.1). Mg^{2+} is also detrimental to the functionality of conventional phosphonate SIs, causing an SI "poisoning" effect – Mg^{2+} bonded SI is essentially rendered ineffective. The PFC Fixed Case

22 hour MICs correlate with the barite SR level – the highest MIC is measured for the 60/40 NSSW/FW mixing ratio, followed by 80/20, then 30/70. This is as expected when [Ca^{2+}] and [Mg^{2+}] are fixed – this is the same order of decreasing barite SR for these mixing ratios NSSW/FW, i.e. 60/40 > 80/20 > 30/70, see Figure 5.1.

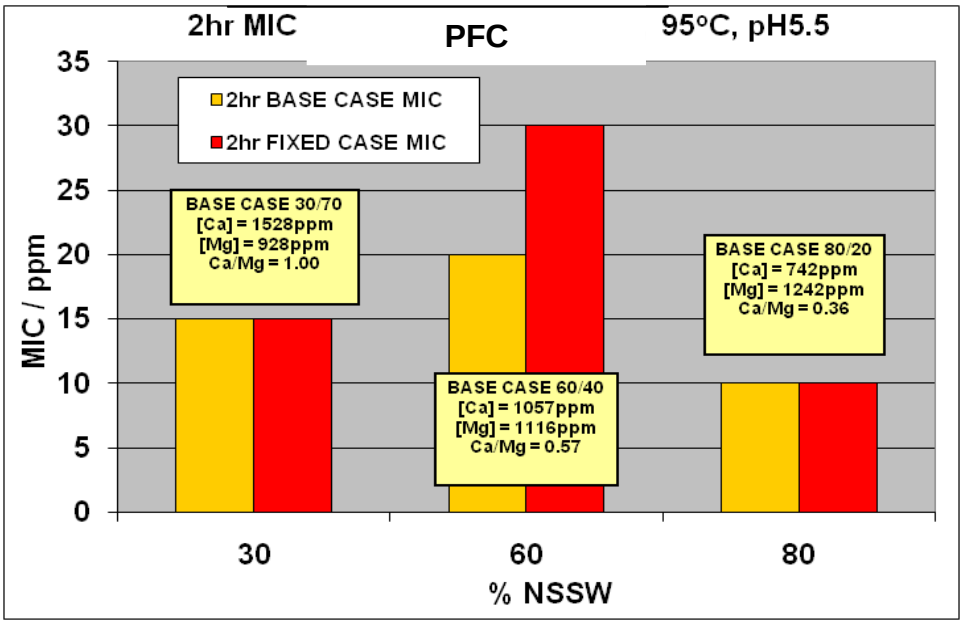

Figure 6.14 – 2 hour MIC vs. % NSSW, testing PFC - Base Case and Fixed Case experimental conditions, 95°C, pH5.5.

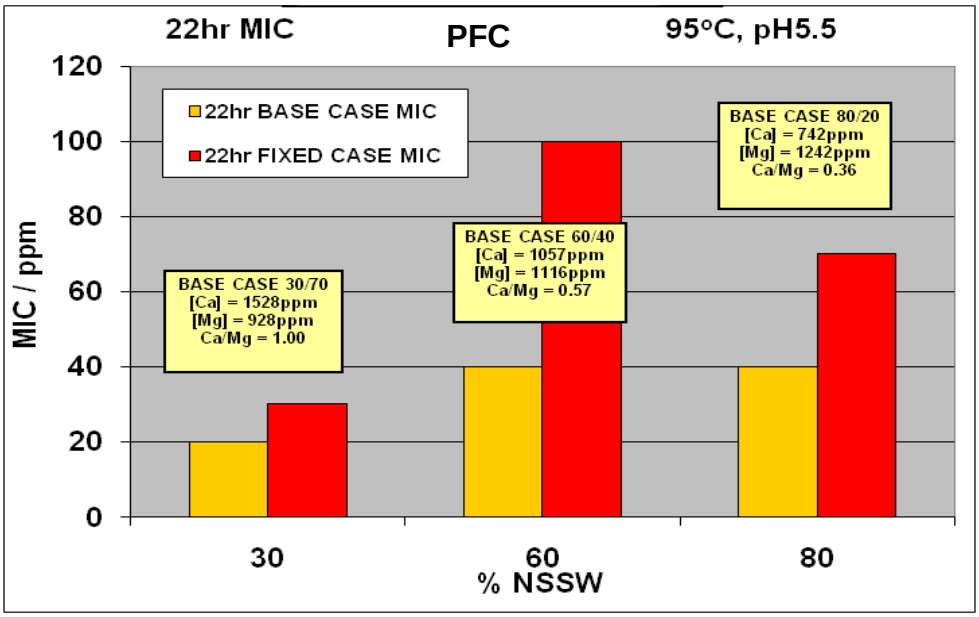

Figure 6.15 – 22 hour MIC vs. % NSSW, testing PFC - Base Case and Fixed Case experimental conditions, 95°C, pH5.5.

6.6.2 Ca^{2+}/Mg^{2+} = 0.19, 0.57 and 1.64

MIC results are included here with molar ratio Ca^{2+}/Mg^{2+} = 0.57, for comparison with Ca^{2+}/Mg^{2+} = 0.19 and 1.64, since molar ratio Ca^{2+}/Mg^{2+} = 0.57 is equivalent to Base Case 60/40 test conditions where X_m = 72.3mM/L. The NSSW and FW compositions used for the Ca^{2+}/Mg^{2+} = 0.19 and 1.64 cases are given in Chapter 3, Tables 3.3 (NSSW), 3.4 (FW) and 3.9 (FW Ca^{2+}, Mg^{2+} and Cl^-). For the Base Case (Ca^{2+}/Mg^{2+} = 0.57), Base Case brines were used (Chapter 3, Tables 3.1 and 3.2).

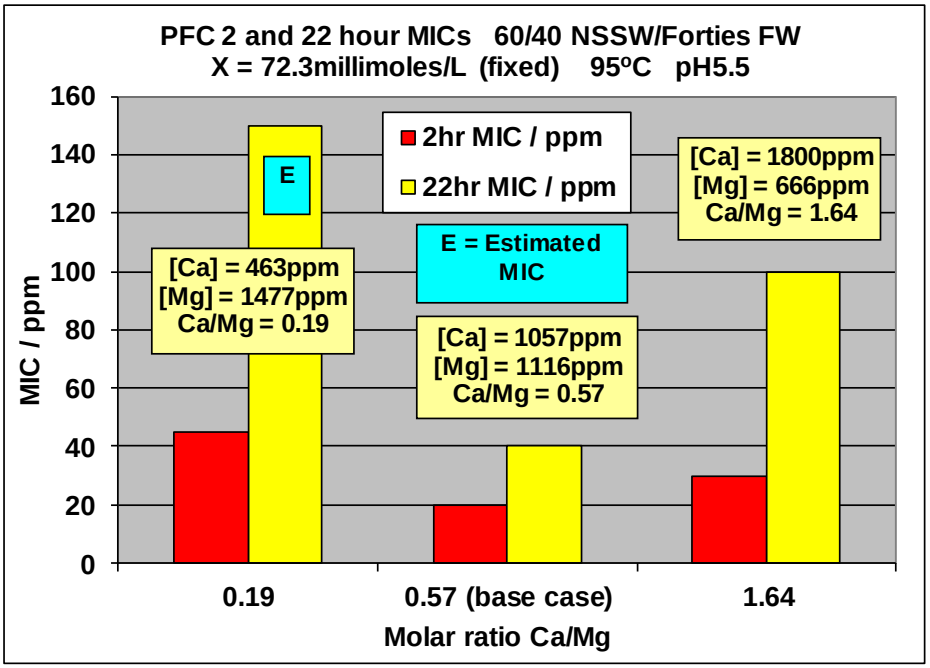

Figure 6.16 – 2 and 22 hour PFC MICs. Ca^{2+}/Mg^{2+} molar ratios 0.19, 0.57 and 1.64. X=72.3 mmol/L, 95°C, pH5.5.

6.7 PVS – MIC vs. Mixing Ratio NSSW/FW

Figure 6.17 presents the experimental MIC vs. % NSSW for two brine mix compositions for PVS at 2 hours, for both the Base Case (Ca^{2+}/Mg^{2+} varying) and the Fixed Case (Ca^{2+}/Mg^{2+} fixed) experimental conditions. Both the 60/40 and 80/20 NSSW/FW Fixed Case MICs are < corresponding Base Case MICs. In the Base Case 80/20 NSSW/FW experiment, 2 hour IE often reached ~85% testing [SI]s 30, 40, 50, and 60ppm, whereas in the Fixed Case 80/20 NSSW/FW experiment, > 90% IE was achieved at 2 hours for 20ppm [SI]. Clearly the higher [Ca^{2+}] in the Fixed Case must be causing the small (~5–10%) increase in 2 hour IE, which is sufficient for the 2 hour MIC to be reached at a much lower [SI]; this has been induced by the higher brine [Ca^{2+}]. Similarly, the 80/20 NSSW/FW 22 hour IE in the Fixed

Case is also ~5-10% greater than in the Base Case for each [SI] tested. Thus, the 2 and 22 hour IE of PVS is affected similarly by changes in $[Ca^{2+}]$ and $[Mg^{2+}]$. In the Base Case 80/20 NSSW/FW produced water, $[Ca^{2+}]$ = 742ppm whereas in the Fixed Case 80/20 NSSW/FW produced water, $[Ca^{2+}]$ = 2000ppm – a change of +1258ppm $[Ca^{2+}]$. In contrast, the change in $[Mg^{2+}]$, changing from Base Case to Fixed Case 80/20 NSSW/FW is −503ppm. The IE of PVS is therefore mildly affected by $[Ca^{2+}]$ and $[Mg^{2+}]$ – observed changes in IE are only in the region of ~5–10% – but as discussed, this may be sufficient to make the difference between a "pass" and a "fail" in a static barite IE test.

Since the 80/20 NSSW/FW 2 hour Base Case MIC is > 60/40 NSSW/FW Base Case MIC, this must be due to the detrimental effect of the lower molar ratio Ca^{2+}/Mg^{2+} = 0.36 in the 80/20 NSSW/FW produced water, compared to higher molar ratio Ca^{2+}/Mg^{2+} = 0.57 in the 60/40 NSSW/FW produced water – because the barite SR 80/20 NSSW/FW < SR 60/40 NSSW/FW (see Figure 5.1). This same type of MIC behaviour has been observed numerous times before, i.e. testing SIs PMPA, SPPCA, PPCA and Type 2 phosphonates HMTPMP, HMDP, EDTMPA etc. Testing PVS, when $[Ca^{2+}]$ and $[Mg^{2+}]$ are fixed, the converse is true, i.e. a lower MIC for the 80/20 NSSW/FW case is measured, compared to the 60/40 NSSW/FW case (Figure 6.17). This is what would normally be expected in terms of barite saturation ratio levels applying to these mixing ratios NSSW/FW (see Figure 5.1). Once again, this same Fixed Case IE behaviour has been observed testing all conventional phosphonate SIs, PMPA and SPPCA.

PVS has been tested extensively in previous work to establish the Base Case 50/50 NSSW/FW 22 hour MIC. [SI]s up to 5,000ppm have been tested which failed to reach 22 hour MIC (Inches et al., 2006), hence this was not investigated further here. The barite saturation ratio level for 50/50 NSSW/FW is only marginally lower than for 60/40 NSSW/FW (see Figure 5.1) and it is still a severe scaling system. PVS performs particularly poorly over long residence times – this is classic polymeric behaviour. It functions mainly as a nucleation inhibitor, i.e. it is very effective over short residence times such as ~2 hours). Furthermore, PVS works particularly better at cooler temperatures (much lower than 95^{o}C), for example 5^{o}C. Previous work testing PVS has confirmed this (Sorbie and Laing, 2004; Sorbie et al., 2000). The principal reason for the better performance at 5^{o}C is because at this

cooler temperature, the *kinetics* of barite formation is much slower, making it easier to inhibit, using SI PVS (Sorbie and Laing, 2004).

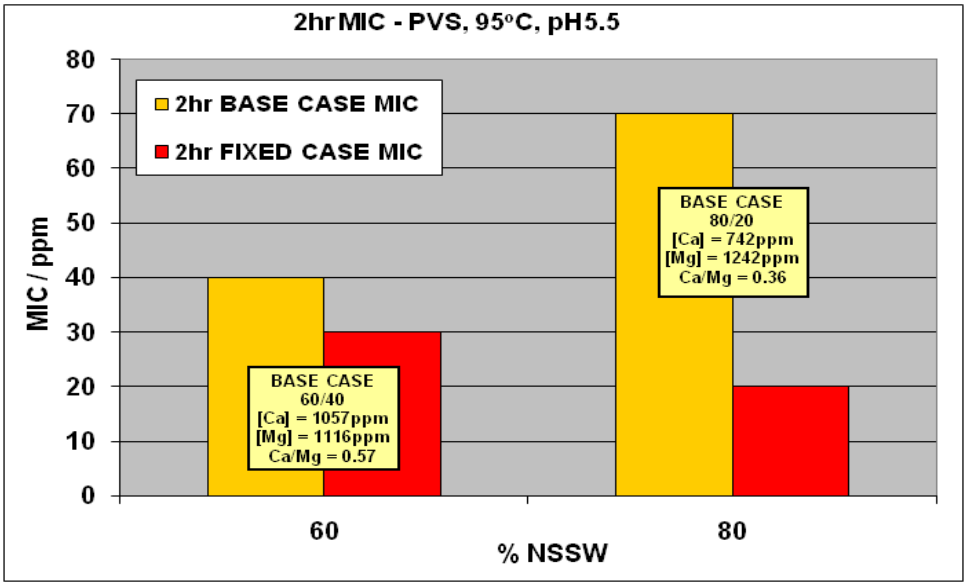

Figure 6.17 – 2 hour MIC vs. % NSSW, testing PVS - Base Case and Fixed Case experimental conditions, 95°C, pH5.5.

6.8 VS-Co – MIC vs. Mixing Ratio NSSW/FW

Figure 6.18 and Figure 6.19 present the experimental MIC vs. % NSSW for two brine mix compositions for the sulphonated acrylic acid co-polymer (VS-Co) at 2 hours and 22 hours, respectively, for both Base Case (Ca^{2+}/Mg^{2+} varying) and Fixed Case (Ca^{2+}/Mg^{2+} fixed) experimental conditions. VS-Co behaves similarly to the PVS in that the 2 and 22 hour 80/20 NSSW/FW Base Case MICs are > 60/40 NSSW/FW Base Case MICs whereas the opposite is true for the corresponding Fixed Cases: i.e. the 80/20 NSSW/FW 2 and 22 hour MICs are < 60/40 NSSW/FW 2 and 22 hour MICs. Yet again, a lower produced water Base Case molar ratio Ca^{2+}/Mg^{2+} = 0.36 appears to be detrimental – hence the higher 80/20 NSSW/FW Base Case 2 and 22 hour MICs, testing VS-Co – despite the saturation ratio level being lower for 80/20 NSSW/FW compared to 60/40 NSSW/FW (see Figure 5.1).

Figure 6.20 shows the effect of a varying molar ratio Ca^{2+}/Mg^{2+} on the IE of both VS-Co and PVS, and this is much more marked for VS-Co than for PVS, i.e. differences between Base Case and Fixed Case IE (%) are in the range of ~20–30%, with the Fixed Case IE being more efficient. In the case of PVS, the differences in IE were in the range of ~5–10%. These

differences between the IE of PVS and VS-Co are due to differences in the chemical nature of these SI molecules. The VS-Co contains both carboxylate and sulphonate functional groups (heteropolymeric, see Figure 3.23), whereas the PVS contains exclusively sulphonate functional groups (homopolymeric, see Figure 3.22). The sulphonate functional groups are known to only interact weakly with brine Ca^{2+} and Mg^{2+} i.e. these groups are highly dissociative and do not bond strongly to divalent cations (i.e. Ba^{2+}, Sr^{2+}, Ca^{2+}, and Mg^{2+}) (Boak et al., 1999; Graham et al., 2003; Sorbie et al., 2000; Sorbie and Laing, 2004). A very low pH (pH ~1) would be required to fully associate (protonate) these sulphonate groups. It is for this reason PVS works predominantly as a nucleation inhibitor – since it must have the ability to complex Ba^{2+} in order to function effectively by crystal growth blocking. Carboxylate functional groups *do* bond to Ca^{2+} and Mg^{2+} significantly more strongly than sulphonate groups, thus VS-Co is influenced much more strongly by Ca^{2+} and Mg^{2+} compared to PVS (Boak et al., 1999; Graham et al., 2003; Sorbie et al., 2000; Sorbie and Laing, 2004).

From other related analytical experimental work (see Chapter 4), it is highly likely the VS-Co is approximately a 50/50 mix of carboxylate and sulphonate monomers, therefore the VS-Co may contain 50% less sulphonate functional groups than the PVS. PPCA, SPPCA, MAT and PFC are also affected more severely than PVS by Ca^{2+} and Mg^{2+} for the same reason i.e. the presence of carboxylate functional groups. VS-Co, PPCA, SPPCA, MAT, and PFC all have some crystal growth blocking qualities due to the presence of the carboxylate functional groups (Boak et al., 1999; Graham et al., 2003; Sorbie et al., 2000; Sorbie and Laing, 2004). The best crystal growth blocking SIs are generally phosphonates, due to the presence of the phosphonate functional groups which bind to Ca^{2+} and Mg^{2+} much more strongly than carboxylate functional groups. The presence of phosphonate functional groups usually yields the best crystal growth inhibition properties in a SI. Ca^{2+} and Mg^{2+} bond strongest to phosphonate groups (large binding constants), followed by carboxylate (moderate binding constants), followed by sulphonate (extremely weaker binding constants).

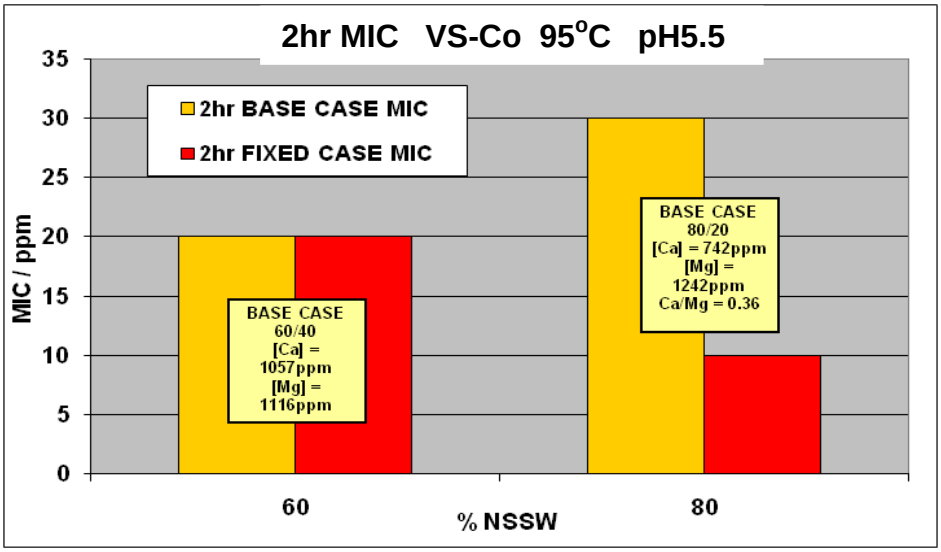

Figure 6.18 – 2 hour MIC vs. % NSSW, testing VS-Co - Base Case and Fixed Case experimental conditions, 95°C, pH5.5.

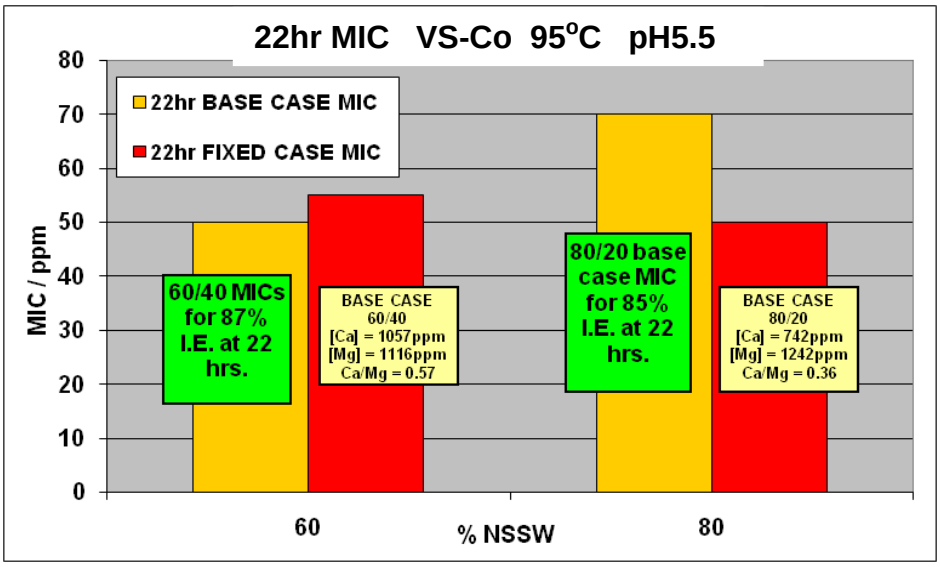

Figure 6.19 – 22 hour MIC vs. % NSSW, testing VS-Co - Base Case and Fixed Case experimental conditions, 95°C, pH5.5.

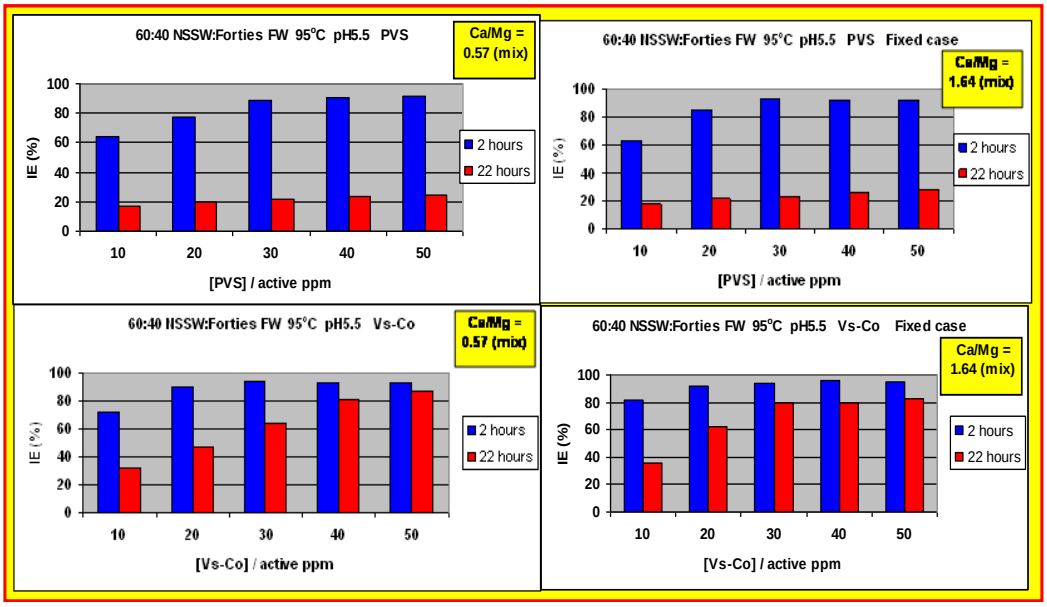

Figure 6.20 – IE vs. [SI], testing PVS and VS-Co, 60/40 NSSW/FW, 95°C, pH5.5, Base Case (produced water molar ratio Ca^{2+}/Mg^{2+} = 0.57) and Fixed Case (produced water molar ratio Ca^{2+}/Mg^{2+} = 1.64), [SI]s: 10, 20, 30, 40 and 50ppm.

6.9 CTP-A and CTP-B

6.9.1 MIC vs. Mixing Ratio NSSW/FW

Two cationic ter-polymers (CTP) were tested which were synthesised from maleic acid, allyl sulphonate, and an allyl cationic quaternary ammonium monomer. The difference between cationic ter-polymers A and B is in the % of each monomer species used in the synthesis, hence the degree of sulphonation and cationic content vary between CTP-A and CTP-B. Secondly, the functional groups (R_1, R_2, R_3 and R_4) attached to the quaternary ammonium monomer nitrogen atom may vary between the two polymers – see Figure 3.30.

Figure 6.21 and Figure 6.22 show, under both Base Case and Fixed Case experimental conditions, 60/40 NSSW/FW, 95°C, pH5.5, at 2 and 22 hour sampling times, CTP-B outperforms CTP-A, i.e. MIC of CTP-B < CTP-A. The 22 hour MICs of both CTPs are very high, ≥150ppm and these SI concentrations are higher than would normally be applied practically in the field. At both 2 and 22 hour residence times, both SIs perform better under Fixed Case conditions. Hence, a high [Ca^{2+}] is beneficial to the IE of both these CTP species.

Like other polymeric species (e.g. PVS, VS-Co, PPCA, etc.), both CTPs performed poorly over long residence times (i.e. at 22 hours).

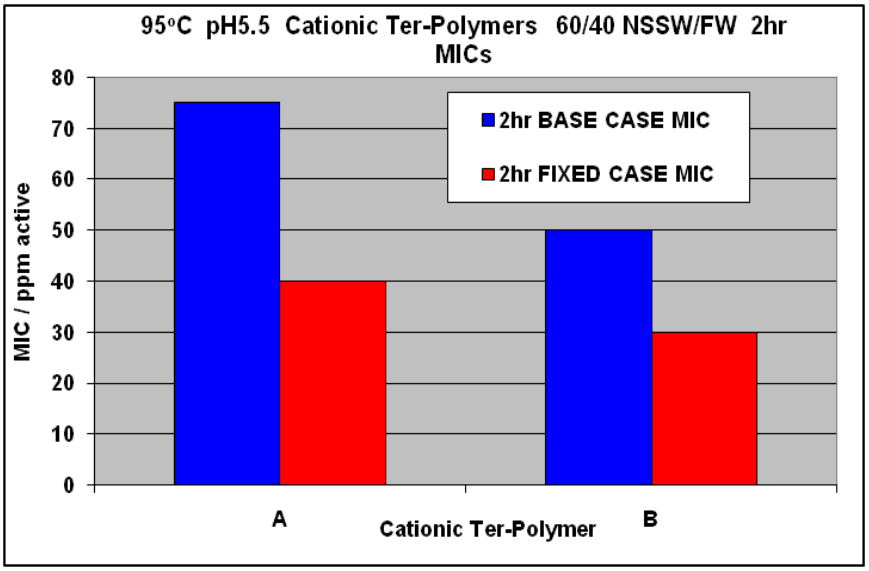

Figure 6.21 – 2 hour MIC data, testing CTP-A and CTP-B - Base Case and Fixed Case 60/40 NSSW/FW experimental conditions (i.e. testing produced water molar ratios Ca^{2+}/Mg^{2+} = 0.57 and 1.64), 95°C, pH5.5, fixed barite SR = ~330 – See Figure 5.1.

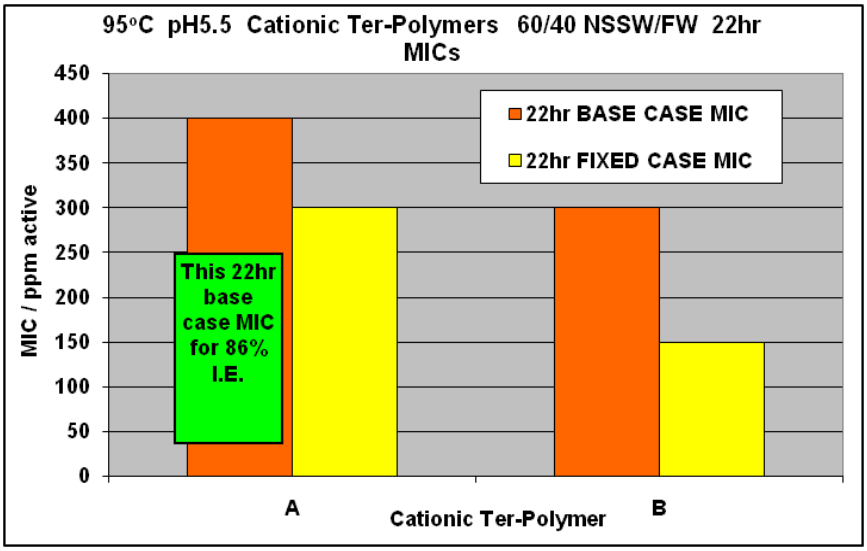

Figure 6.22 – 22 hour MIC data, testing CTP-A and CTP-B - Base Case and Fixed Case 60/40 NSSW/FW experimental conditions (i.e. testing produced water molar ratios Ca^{2+}/Mg^{2+} = 0.57 and 1.64), 95°C, pH5.5, fixed barite SR = ~330 – See Figure 5.1.

6.9.2 Fixed [SI] – Varying Molar Ratio Ca^{2+}/Mg^{2+}

Testing the cationic ter-polymers, mixing ratio NSSW/FW 60/40 was selected, testing produced brine molar ratios Ca^{2+}/Mg^{2+} = 0.1, 0.5, 1, 5, and ∞. As in the experiments testing PPCA, SPPCA and MAT, the total number of moles of (Ca^{2+} + Mg^{2+}) in the brine mix was fixed = 80.3mM/L. Furthermore, the [SI] was constant, = 15ppm in both cases such that the specific effects of Ca^{2+} and Mg^{2+} on these species could be demonstrated. 15ppm is pre-2 hour MIC for both cationic ter-polymers. Since both cationic ter-polymers are tested at the same [SI] – the IE results and Ca^{2+}/Mg^{2+} effects on each species can thus be compared fairly with one another.

Table 6.2 gives the produced water [Ca^{2+}] and [Mg^{2+}] for every molar ratio Ca^{2+}/Mg^{2+} tested in this experiment. The NSSW and FW brine compositions used for this experiment are given in Chapter 3, Tables 3.3 (NSSW), 3.4 (FW) and 3.8 (FW Ca^{2+}, Mg^{2+} and Cl^{-}).

As shown in Figure 6.23, CTP-B outperforms CTP-A under all six experimental conditions (i.e. all six test brine molar ratios Ca^{2+}/Mg^{2+}). As the molar ratio Ca^{2+}/Mg^{2+} increases, the IE of both CTP-A and CTP-B generally improves at 2 and 22 hours. In both cases, the lowest IE is measured in the absence of Ca^{2+} (molar ratio = 0), whereas the highest IE is achieved in the absence of Mg^{2+} (molar ratio = ∞). This experiment confirms Ca^{2+} is beneficial to the barite IE of both these cationic species, whereas Mg^{2+} is detrimental.

Molar Ratio Ca^{2+}/Mg^{2+}	**Molar Ratio Ca^{2+}/Mg^{2+} (as a fraction)**	**Produced Water $[Ca^{2+}]$ / mM/L ***	**Produced Water $[Mg^{2+}]$ / mM/L ***	**Produced Water ppm Ca^{2+}**	**Produced Water ppm Mg^{2+}**
0	$0/X_{molar}$	0	$=X_{molar}=80.3$	0	1952
0.1	1/10	7.3	73.0	293	1775
0.25	¼	16.1	64.2	644	1562
1	1/1	40.1	40.1	1609	976
5	5/1	66.9	13.4	2682	325
∞	$X_{molar}/0$	$=X_{molar}=80.3$	0	3218	0

*The sum of the values in these 2 columns = 80.3 mM/L.

Table 6.2 – Produced water compositions for the experiment at fixed [SI] – testing CTP-A and CTP-B. X_{molar} = (moles Ca^{2+} + moles Mg^{2+}) in the produced water = 80.3 mM/L (constant).

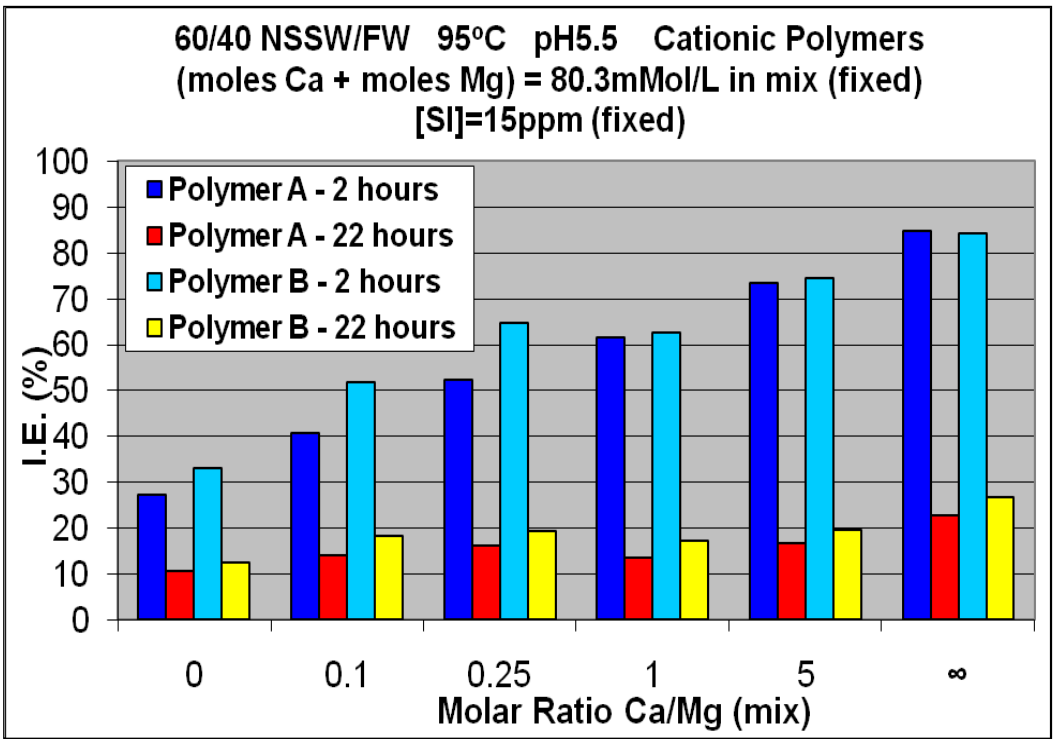

Figure 6.23 – IE testing CTP-A and CTP-B – varying molar ratio Ca^{2+}/Mg^{2+} in the produced water. X_m, (moles Ca^{2+} + moles Mg^{2+}) = 80.3millimoles/L in produced water constantly. 6 molar ratios Ca^{2+}/Mg^{2+} tested: 0, 0.1, 0.25, 1, 5 and ∞. [CTP-A] and [CTP-B] = 15ppm (i.e. pre-2 hour MIC for both SIs).

6.10 Summary and Conclusions

6.10.1 General

This Chapter describes a study of the barite inhibition efficiency (IE) of a series of 9 polymeric scale inhibitors, PPCA, MAT, SPPCA, PMPA, PFC, PVS, VS-Co, CTP-A and CTP-B. In particular, how the IE is affected by saturation ratio (SR) and the Ca^{2+}/Mg^{2+} molar ratio in the brine mix was investigated. This work closely parallels a similar study of phosphonate SIs (Chapter 5). These experiments show that that the MIC of all polymeric species correlates broadly with SR but there is a clear additional effect of brine [Ca^{2+}] and [Mg^{2+}] on the IE of all the polymeric SIs tested. However, this divalent ion effect on IE for polymeric SIs is not as "general" an effect as has been observed in the testing of phosphonate SIs. Instead the Ca^{2+}/Mg^{2+} effect appears to be specific to each polymeric SI. For polymeric SIs, the Ca^{2+}/Mg^{2+} effect on IE depends broadly on two factors, viz. (i) the specific functional groups and atoms that are present (e.g. carboxylate, sulphonate, phosphonate etc. and N, O donor atoms); and (ii) the abundance of these various functional groups and linking atoms. The IE behaviour may also show a dependence on molecular weight but this factor was not studied in this work. Since the entire range of SIs tested (i.e. phosphonates and polymers) are effective against strontium sulphate also – the Ca^{2+}/Mg^{2+} effect upon strontium sulphate IE will most probably be the same as for barium sulphate. Strontium sulphate scale is inhibited by all SIs described in this thesis (much lower celestite SR), except EABMPA (di-phosphonate) which is recommended for the inhibition of calcium carbonate scale in boiler water systems etc., *not* for barite inhibition. Often calcium sulphate scale does not form at all under the test conditions described in this thesis; however it is preventable using these SIs. Most of the polymers studied here are also known to be effective against calcium carbonate formation but this subject was not investigated in this work.

Experiments have indicated that most polymers (except PPCA, MAT and PFC) would be best suited for application in higher [Ca^{2+}] waters, for optimum barite IE to be achieved. This is much the same behaviour exhibited by conventional phosphonate SI species, e.g. DETPMP, HMTPMP, HMDP, NTP, etc. The beneficial effect of Ca^{2+} is largely due to possible Ca^{2+} integration into the barite crystal lattice – in conjunction with polymeric or phosphonate SI – to inhibit the barite crystal growth. Higher [Ca^{2+}] tends to benefit the majority of SIs, unless there is an underlying incompatibility or functionality issue, as observed with PPCA, MAT

and PFC for example. In contrast, Mg^{2+} is detrimental as it cannot be integrated into the barite lattice, but can bond strongly to SI phosphonate or carboxylate functional groups, rendering them ineffective or much *less* effective (Boak et al., 1999; Graham et al., 1997a, 2003; Shaw et al., 2010a and 2010b). These points are quite well demonstrated in Figure 6.16 where PFC was tested in brine mixes with Ca^{2+}/Mg^{2+} = 0.19, 0.57 and 1.64. Clearly, the lowest MICs were measured with Ca^{2+}/Mg^{2+} = 0.57, however MIC increases on decreasing the molar ratio Ca^{2+}/Mg^{2+} to 0.19 (higher Mg^{2+}), but *also* increases on increasing the molar ratio Ca^{2+}/Mg^{2+} to 1.64 (higher Ca^{2+}). Thus, the presence of moderate concentrations of both cations yields the highest (optimum) IE – but a higher concentration of either cation is clearly detrimental to the PFC IE. Since in most cases (except PPCA, MAT and PFC), Mg^{2+} and Ca^{2+} have a similar effect on the effectiveness of polymeric SIs as conventional phosphonates (Chapter 4), it is certainly the case that carboxylate functional groups are "poisoned" by Mg^{2+} in exactly the same way as phosphonate groups, regardless of whether these functional groups are present in small molecules, e.g. HPAA, or polymers, e.g. PPCA, MAT. The severity of the effect is clearly much greater with phosphonate functional groups because the M^{2+}–O–P binding constant is >> M^{2+}–O–C binding constant. This conclusion does not apply to sulphonate functional groups which are highly dissociated even at low pH, and do not bind strongly to divalent cations.

When selecting a SI to deploy in the oilfield, a number of factors must be taken into consideration, such as the field conditions, for example, reservoir temperature, $[Ca^{2+}]$, $[Mg^{2+}]$, pH, etc. Phosphonate SIs, for example do not function at low pH (see Chapter 7) – for such conditions a polymeric SI such as PVS would be the SI of choice. At higher pH levels, for example, ~pH5.5, phosphonate SIs are often the best choice since they have good retention properties, but are less environmentally friendly. Polymers tend to be more environmentally friendly than phosphonates, but they are markedly less effective for longer term (>22hour) inhibition efficiency, as observed in this Chapter. When new SIs are being considered, both SI performance and environmental factors must be taken into consideration and a compromise reached. It is for these reasons that some of the new SI products being synthesised and introduced to the market are P-tagged polymers. This is in order to supply a product with reasonable environmental properties *and* reasonable retention properties.

6.10.2 Systematic Categorisation of all SIs – Based on IE vs. Mixing Ratio Tests

Based on 2 and 22 hour IE data for the polymers described in this Chapter, polymers can be classified as **Type 1** or **Type 2** in the same way as the phosphonate SIs in Chapter 5. All of the polymers studied here have been classified as being Type 2, with the exception of PMPA (which does not have a "regular polymer" structure). The 22 hour IE of PMPA is very good, i.e. often maintained at a high level, similar to that attained at 2 hours – this characteristic is associated with Type 1 phosphonate species (e.g. OMTHP and DETPMP). By comparing Figure 6.12 and Figure 6.13 it is clear that often the 2 and 22 hour PMPA MICs are equal for any set of experimental conditions. The 22 hour IE of all the other polymers was generally markedly poorer in comparison to 2 hours.

Having now tested 9 phosphonate and 9 polymeric SIs in static barium sulphate IE and MIC vs. mixing ratio NSSW/FW experiments, all SIs can now be classified as:

(i) Either **Type 1** or **Type 2** (based on IE and Ca^{2+} / Mg^{2+} sensitivity)

(ii) Either **Type A** or **Type B** (based on compatibility/incompatibility with [Ca^{2+}] = ~1000–2000ppm+)

Type 1 Scale Inhibitors: Definition – Mg^{2+} detrimental to IE, Ca^{2+} beneficial to IE. MIC principally affected by SR under Base Case and Fixed Case conditions. Ca^{2+}/Mg^{2+} effect is secondary. IE maintained over long residence times, e.g. 22 hour+. Type 1 inhibitors with their A and B classifications are as follows:

Phosphonates:

(i) OMTHP (Type A)

(ii) DETPMP (Type A)

Poly-phosphonate:

(iii) PMPA (Type A) [NB. There is doubt that this is in fact polymeric in nature]

Type 2 Scale Inhibitors: Definition – Mg^{2+} detrimental to IE, Ca^{2+} beneficial to IE. MIC principally affected by molar ratio Ca^{2+}/Mg^{2+} under Base Case conditions. MIC/IE affected by SR as a secondary effect under Base Case conditions. IE tends to decline markedly over time, i.e. 22 hour IE is much poorer compared to at 2 hours. Type 2 inhibitors with their A and B classifications are as follows:

Phosphonates:

(i) HMTPMP (Type A)
(ii) HMDP (Type A)
(iii) EDTMPA (Type A)
(iv) NTP (Type A)
(v) EABMPA (Type A)
(vi) HEDP (Type A)
(vii) HPAA (Type A)

Polymers:

(viii) PPCA (Type B)
(ix) SPPCA (Type A)
(x) MAT (Type B)
(xi) PFC (Type B)
(xii) PVS (Type A)
(xiii) VS-Co (Type A)
(xiv) CTP-A (Type A)
(xv) CTP-B (Type A)

Type A Scale Inhibitors: Definition – Mg^{2+} detrimental to IE, Ca^{2+} beneficial to IE. Perform better in brine mixes containing $[Ca^{2+}]$ = 2000ppm (i.e. under Fixed Case test conditions).

Type B Scale Inhibitors: Definition – Mg^{2+} detrimental to IE. Low to moderate levels of Ca^{2+} beneficial to IE. Higher levels of Ca^{2+}, typically ~1000–2000ppm, detrimental to IE due to SI precipitation with Ca^{2+} (e.g. PPCA), *or* due to other Ca^{2+}/SI mechanistic issues. Thus, Type B SIs perform better (i.e. lower MIC, higher IE) under Base Case test conditions.

SIs are denoted "2A", "2B", etc., based on the above two classification systems, e.g. SPPCA would be denoted "2A" because it is a Type 2 and Type A SI.

Table 6.3 gives the appropriate categorisation code for all phosphonate and polymeric SIs tested thus far, in static barium sulphate IE experiments.

SCALE INHIBITOR*	GENERIC SI TYPE	CATEGORISATION CODE
OMTHP (6P)	PHOSPHONATE	1A
DETPMP (5P)	PHOSPHONATE	1A
HMTPMP (5P)	PHOSPHONATE	2A
HMDP (4P)	PHOSPHONATE	2A
EDTMPA (4P)	PHOSPHONATE	2A
NTP (3P)	PHOSPHONATE	2A
EABMPA (2P)	PHOSPHONATE	2A
HEDP (2P)	PHOSPHONATE	2A
HPAA (1P, 1C)	PHOSPHONATE	2A
PPCA	POLYMER	2B
SPPCA	POLYMER	2A
PVS	POLYMER	2A
VS-Co	POLYMER	2A
PMPA	POLY-PHOSPHONATE	1A
MAT	POLYMER	2B
PFC	POLYMER	2B
CTP-A	POLYMER	2A
CTP-B	POLYMER	2A

*The number and letter in brackets after the phosphonate SI abbreviations denotes how many phosphonate and/or carboxylate functional groups are present per SI molecule, e.g. 1P, 1C denotes 1 phosphonate group and 1 carboxylate group.

Table 6.3 – Categorisation of all SIs tested in MIC vs. mixing ratio NSSW/FW tests, as i) either phosphonate, polymer, or poly-phosphonate; ii) Type 1 or Type 2; and iii) either Type A or Type B.

Chapter 7: Inhibition Efficiency (IE) Experiments Varying pH

Chapter 7 Summary: In this Chapter, the effect of varying pH on the inhibition efficiency (IE) and MIC of various SIs is investigated. The normal test pH used in the vast majority of IE measurements in this thesis is pH5.5. However, in this Chapter experiments are conducted at additional pH levels of 4.5, 6.5 and 7.5. The same [SI]s are tested at each pH level such that differences in IE are clearly comparable. A solution pH of 4.5 and 5.5 can be achieved and maintained by using a sodium acetate / acetic acid buffer. All experiments conducted at pH 6.5 and pH7.5 are carried out by buffer-free pH adjustment, because these pH levels are outwith the operating pH range of the sodium acetate / acetic acid buffer. Selected experiments at pH4.5 and pH5.5 are also repeated in a buffer free system.

7.1 Introduction

pH is an important variable as it affects the speciation of weak polyacid molecules, including phosphonic acids (Ramsey and Cenegy, 1985). Figure 7.1 illustrates the speciation of a simple tri-protic acid, citric acid, with increasing pH. Clearly, the pH will determine the fraction (%) of each species present in any solution – the same principle applies to the phosphonate and polymeric SIs tested in this work. Polyprotic weak acid K_a values can be determined by acid-base titration – this subject is discussed in the paper by Litchinsky et al., 1969. If a citric acid solution was titrated with sodium hydroxide, the pH curve obtained would resemble that shown in Figure 7.2. Citric acid has three relatively similar dissociation constants (K_a), thus instead of three (or at least two) separate end points being detected, a long buffer region is observed, followed by only one marked increase in pH (equivalence point). Similar problems are encountered if a phosphonic acid solution, such as DETPMP (effectively the weak acid, $H_{10}A$) is titrated with a sodium hydroxide solution, in which case multiple increases in pH are expected on the pH curve. In the case of DETPMP, the various steps in the titration tend to overlap and be much less clear, making such a titration much more problematic to carry out practically. Most of the acid dissociation constants for the commonly used tetra-phosphonate, EDTMPA and penta-phosphonate, DETPMP are known (Bull. 53-39(E) ME-3, 1988). The speciation chart for EDTMPA is shown in Figure 7.3, and for DETPMP in Figure 7.4 (Bull. 53-39(E) ME-3, 1988). Note for DETPMP, K_{a1} is

estimated; and for EDTMPA, K_{a1} and K_{a2} are estimated. From Figure 7.3 for example, it can be deduced that at the standard static IE test pH = 5.5, EDTMPA will dissociate into ~30% H_5A^{3-}, ~60% H_4A^{4-} and ~10% H_3A^{5-}. At pH5.5, DETPMP will dissociate into a mix of ~40% H_5A^{5-}, ~50% H_6A^{4-}, ~5% H_7A^{3-} and ~5% H_4A^{6-} (Figure 7.4). Clearly, DETPMP has 10 dissociation constant values because each phosphonic acid functional group contains 2 acidic protons, whereas EDTMPA has 8 dissociation constants (contains 4 phosphonic acid groups, each has 2 acidic protons). The correlation of SI structure and barium sulphate inhibition in low pH environments is discussed in the paper by Breen et al., 1990.

Table 7.1 gives the possible dissociation species for all the phosphonate SIs evaluated in this thesis. It is known that phosphonate SIs must be in a moderately dissociated state in order to form stable complexes with cations Ba^{2+}, Sr^{2+}, Ca^{2+} and Mg^{2+}. Generally, the more dissociated a SI molecule is, the greater its metal-complexing ability, and the larger the binding constant, K_b (to M^{2+}). Phosphonate SIs would therefore be expected to perform better at higher pH levels > pH5.5 because they should become more highly dissociated; and worse at pH levels < pH5.5 because they should become less dissociated (i.e. more associated or more protonated). The more highly dissociated a SI is, the greater its barium sulphate IE should become (at a fixed [SI]), i.e. IE is a function of pH if all other test variables are kept constant (i.e. temperature, mixing ratio NSSW/FW, [SI] etc.).

In previous Chapters, all the static IE experiments undertaken testing both phosphonate and polymeric SIs were carried out at pH 5.5, as in the standard experimental procedure. This is because pH 5.5 is taken as a "typical" pH level at which these SIs would be subjected to in field conditions, and thus, the most suitable pH level at which to test them in the laboratory. Reservoir pH levels can range from as low as pH4.5, e.g. Brae reservoir in the North Sea, (Hardy et al., 1992) to about pH8.5, depending on geochemistry (Slentz, 1981) and gas composition. Most fields have some CO_2 and this tends to make reservoirs acidic. Most field reservoirs fall within the pH range of ~5 to ~6.5. For this reason, pH5.5 is taken as an approximate average, and is the pH used for regular static IE tests (Yuan et al., 1998). Field reservoirs are often slightly acidic because of the effects of high pressure, particularly downhole. High pressure in the downhole environment keeps bicarbonate anions in the aqueous phase, thereby maintaining a pH of about 5.5. Many SI products tested in the laboratory are used in downhole "squeeze treatments" (Bunney et al., 1997; Jordan et al.,

1994, 1996; Montgomerie et al., 2009). The chemical reaction shown in Equation 7.1 is pushed to the right because of CO_2 in the gas phase and high pressure downhole – this is Le Chatilier's Principle. See Equation 7.2. Bicarbonate ions can also dissociate further, producing carbonic acid (Equation 7.3). Calcium cations in reservoirs react with the carbonate anions to produce calcium carbonate scale.

$$CO_2(g) + H_2O(l) \rightleftharpoons HCO_3^-(aq) + H^+(aq) \quad \text{(Eq. 7.1)}$$

$$CO_2(g) + H_2O(l) \overset{High\_P}{\rightleftharpoons} HCO_3^-(aq) + H^+(aq) \quad \text{(Eq. 7.2)}$$

$$HCO_3^-(aq) \rightleftharpoons CO_3^{2-}(aq) + H^+(aq) \quad \text{(Eq. 7.3)}$$

In the topside environment, reservoir pH could be slightly higher than pH5.5, possibly around pH6.5 because the pressure is lower in this location. pH varies depending on the specific location of the brine. Therefore, the present study investigating the effect of varying pH on barium sulphate IE is of relevance to oil and gas industry scale inhibitor applications as well as being of interest in establishing the mechanisms of inhibition of the various SI species studied.

In this Chapter, a series of results are presented, testing DETPMP, HMTPMP, EDTMPA and PPCA at pH 4.5, 5.5, 6.5 and 7.5. Equivalent IE results and MIC data, where the SIs have been tested at the (normal) pH level of 5.5 (by buffering) are included here, for comparison with the new IE results at pH levels 4.5, 6.5 and 7.5. Normally, a sodium acetate / acetic acid buffer is used to achieve pH 4.5 and pH 5.5; however, selected experiments at pH 4.5 and pH 5.5 were repeated by pH adjustment (i.e. buffer-free). All experiments carried out at pH 6.5 and pH 7.5 were done by pH adjustment (i.e. buffer-free) because these pH levels are outwith the pH range of the sodium acetate / acetic acid buffer system – see Table 3.16. For pH levels of 6.5 and 7.5, phosphate buffers are recommended; however, these buffers may have some influence on IE and are best avoided in this area of work. In the results and discussion section to follow, charts of IE vs. pH have been plotted for each SI tested at a fixed [SI]. In addition, graphs of MIC vs. pH for DETPMP and HMTPMP are also presented. The [SI]s selected for plotting the IE vs. pH charts were in the threshold, pre-2 hour or pre-22 hour MIC region, such that the effects of varying pH could be most clearly seen at 2 and/or 22 hours. NB − MICs were determined in standard IE tests at pH 5.5. The SIs were tested

varying pH, under "Base Case" and "Fixed Case" conditions, as explained in earlier Chapters.

In the "MIC versus NSSW/FW mixing ratio" IE tests presented in Chapters 5 and 6, "Base Case" NSSW/FW mixing ratio 80/20 was identified as being the mixing ratio which resulted in the highest 22 hour MICs for the majority of Type 2 phosphonate and polymer species, despite the highest barite SR mixing ratio being 60/40 NSSW/FW. This observation was due to the adverse effects of Mg^{2+} upon these Type 2 SIs at NSSW/FW mixing ratios >60% NSSW (Shaw et al., 2010a, 2010b). Phosphonate Type 2 SIs are much more sensitive to brine cations Ca^{2+} and Mg^{2+}, in particular, EDTMPA which was "ultra-sensitive", compared to Type 1 phosphonates. This results in unusually high MICs (i.e. higher MICs than would be predicted based upon the barite saturation ratio (SR) level only) for the Type 2 SIs for NSSW/FW mixing ratios >60% NSSW. It is for this reason, the Base Case mixing ratio 80/20 NSSW/FW was selected purposely for experiments varying pH. Of the 3 phosphonates tested in this work, EDTMPA and HMTPMP were Type 2, whereas DETPMP was Type 1 (Chapter 5). PPCA was a Type 2 and Type B polymer (Chapter 6). PPCA was Type B because its barite scale inhibition was severely suppressed in high [Ca^{2+}] brine, i.e. > ~1500ppm Ca^{2+}. All phosphonate SIs are Type A because they all function extremely well in high [Ca^{2+}] brine. Indeed, Ca^{2+} is known to enhance the IE of all phosphonate SIs whereas Mg^{2+} tends to "poison" them (Boak et al., 1999; Graham et al., 1997a, 2003; Sorbie et al., 2000).

Varying pH does not have a significant effect on barium sulphate SR. This was checked using MultiScale prediction software. SR was predicted for Base Case NSSW/FW mixing ratios 60/40 and 80/20 over the pH range of ~5 to ~9 at 95^{o}C. Charts of SR (barite) versus pH are shown in Figure 7.5 for 60/40 NSSW/FW; and Figure 7.6 for 80/20 NSSW/FW. In both cases, the variation in SR over the pH range of ~5 to ~9 is < 1 SR unit. The effect of varying pH on barite SR is therefore insignificant and for the purposes of the experimental results presented in this Chapter, the SR will be considered as being constant at each pH level examined.

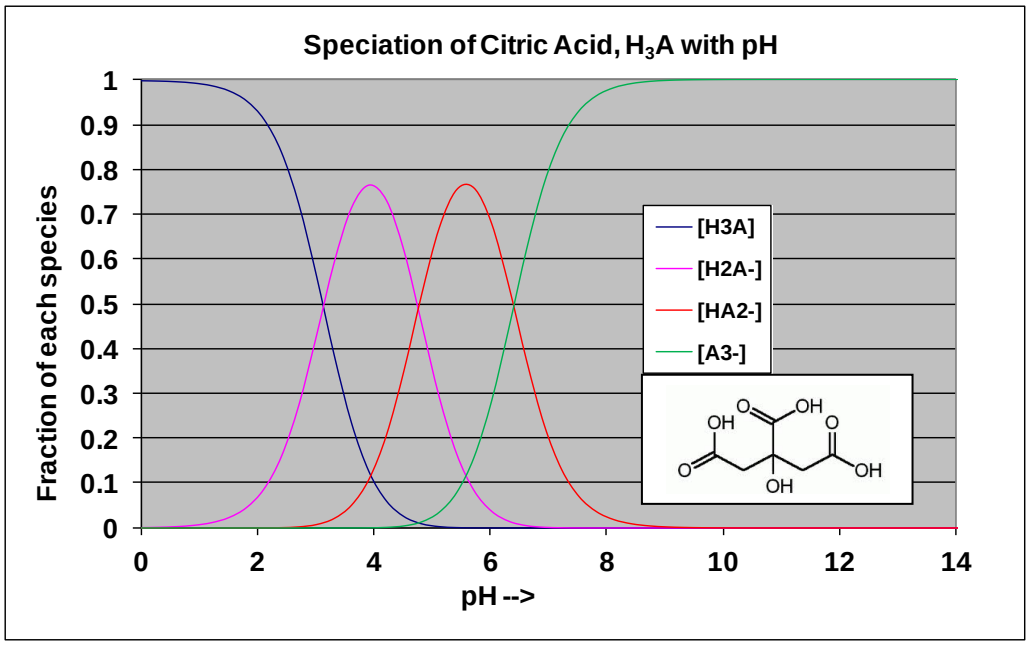

Figure 7.1 – Speciation of citric acid, H_3A with pH (citric acid structure is shown on chart).

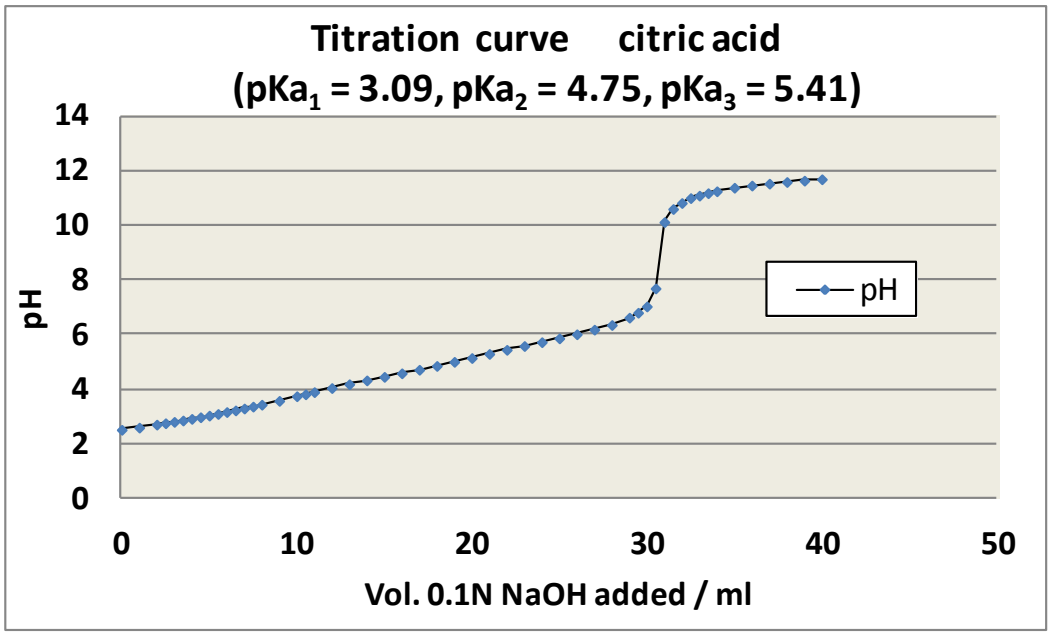

Figure 7.2 – Example of a pH curve obtained for the titration of citric acid with sodium hydroxide (Shaw and Sorbie, 2012).

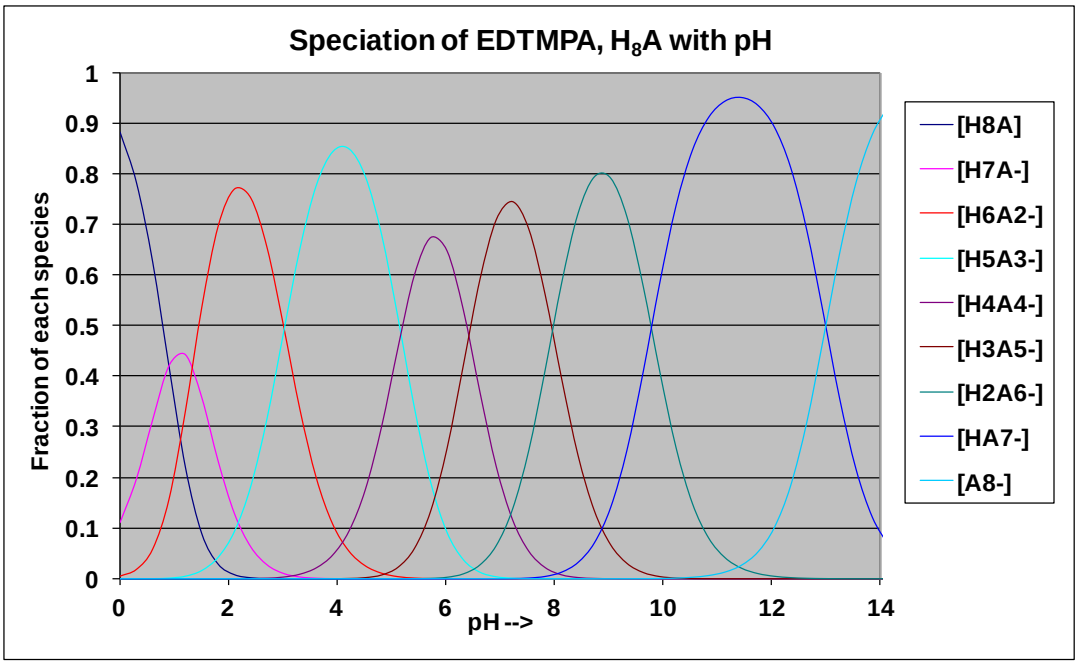

Figure 7.3 – Speciation of EDTMPA (H_8A) with pH (Bull. 53-39(E) ME-3, 1988).

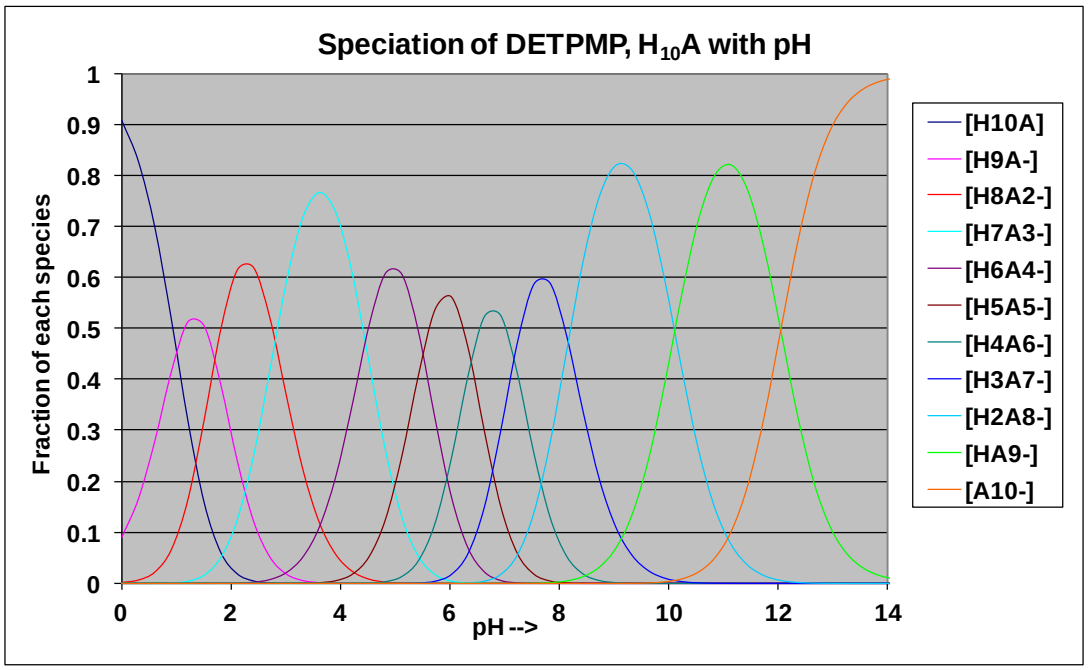

Figure 7.4 – Speciation of DETPMP ($H_{10}A$) with pH (Bull. 53-39(E) ME-3, 1988).

Scale Inhibitor Name	**Associated Phosphonic Acid / SI Formula**	**Number of Possible Dissociation Species**	**Possible Dissociation Species**
OMTHP (Hexa-Phosphonate)	$H_{12}A$	12	$H_{11}A^-$, $H_{10}A^{2-}$, H_9A^{3-} , H_8A^{4-}, H_7A^{5-}, H_6A^{6-}, H_5A^{7-}, H_4A^{8-}, H_3A^{9-}, H_2A^{10-}, HA^{11-} , A^{12-}
DETPMP (Penta-Phosphonate)	$H_{10}A$	10	H_9A^- , H_8A^{2-} , H_7A^{3-} , H_6A^{4-}, H_5A^{5-}, H_4A^{6-}, H_3A^{7-}, H_2A^{8-}, HA^{9-}, A^{10-}
HMTPMP (Penta-Phosphonate)	$H_{10}A$	10	H_9A^- , H_8A^{2-} , H_7A^{3-} , H_6A^{4-}, H_5A^{5-}, H_4A^{6-}, H_3A^{7-}, H_2A^{8-}, HA^{9-}, A^{10-}
HMDP (Tetra-Phosphonate)	H_8A	8	H_7A^- , H_6A^{2-} , H_5A^{3-} , H_4A^{4-}, H_3A^{5-}, H_2A^{6-}, HA^{7-}, A^{8-}
EDTMPA (Tetra-Phosphonate)	H_8A	8	H_7A^- , H_6A^{2-} , H_5A^{3-} , H_4A^{4-}, H_3A^{5-}, H_2A^{6-}, HA^{7-}, A^{8-}
NTP (Tri-Phosphonate)	H_6A	6	H_5A^- , H_4A^{2-} , H_3A^{3-} , H_2A^{4-}, HA^{5-}, A^{6-}
EABMPA (Di-Phosphonate)	H_4A	4	H_3A^- , H_2A^{2-} , HA^{3-} , A^{4-}
HEDP (Di-Phosphonate)	H_4A	4	H_3A^- , H_2A^{2-} , HA^{3-} , A^{4-}
HPAA (Mono-Phosphonate, Mono-Carboxylate)	H_3A	3	H_2A^-, HA^{2-}, A^{3-}

Table 7.1 − Phosphonate scale inhibitors tested in this work, their associated phosphonic acid (protonated) formulae and all possible dissociated anionic formulae.

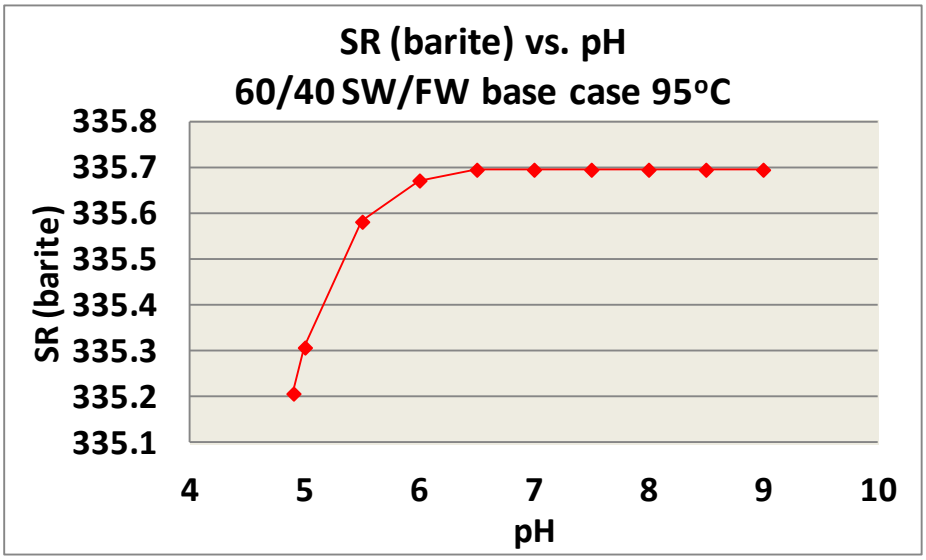

Figure 7.5 – SR (barite) vs. pH, 60/40 NSSW/FW Base Case, 95°C.

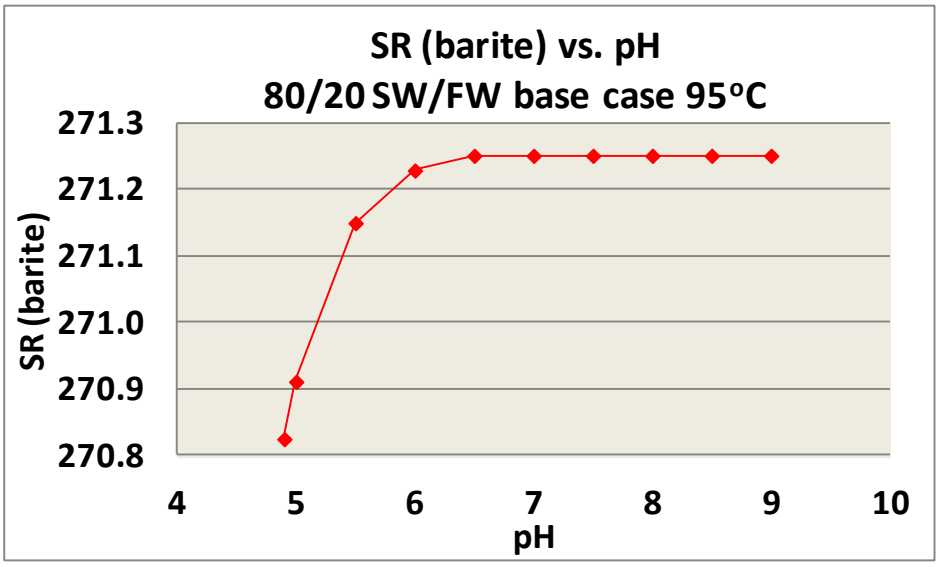

Figure 7.6 – SR (barite) vs. pH, 80/20 NSSW/FW Base Case, 95°C.

7.2 Experimental Methods

The four SIs were tested in two different brine systems. In one brine system, referred to as the "Base Case" conditions, the produced water [Ca^{2+}] = 742ppm and [Mg^{2+}] = 1242ppm, molar ratio Ca^{2+}/Mg^{2+} = 0.36. In the other brine system, referred to as "Fixed Case" conditions, the produced water [Ca^{2+}] = 2000ppm and [Mg^{2+}] = 739ppm, molar ratio Ca^{2+}/Mg^{2+} = 1.64. An 80/20 NSSW/FW mixing ratio was selected. The Fixed Case tests are

therefore examining the effect of pH on IE in a higher [Ca^{2+}], lower [Mg^{2+}] brine. Hence, in this Chapter, any differences in the pH effect on IE (for any selected SI) under Base Case and Fixed Case test conditions, is also investigated. It is known from previous inhibition efficiency (IE) work, that phosphonate SIs perform better in the Fixed Case brine (Chapter 5) whereas PPCA performs worse, due to precipitation of a Ca−PPCA compound (Chapter 6). In all cases, pre-MIC [SI]s were tested, such that the specific effect of varying pH was visible in the results. It should be noted the pre-MIC [SI]s were in relation to MICs determined at the standard test pH of 5.5 (by buffering), 95^{o}C, under either Base Case or Fixed Case test conditions, and mixing ratio 80/20 NSSW/FW (Chapters 5 and 6).

Four different pH levels were tested: pH 4.5, 5.5, 6.5 and 7.5. In order to achieve a produced water pH of 4.5 or 5.5, a sodium acetate / acetic acid buffer was originally used. 2ml of this buffer solution was added to the NSSW bottles prior to the mixing stage. All 2ml of the buffer solution was added to the NSSW bottles only, because the NSSW represents 80% of the total final volume (i.e. 200ml). The 40ml of FW (un-buffered) was added to 160ml of NSSW – this gives a mix pH of either 4.5 or 5.5, depending on the composition of the buffer solution – see Table 3.15. The pH 4.5 and pH 5.5 buffer solutions were checked prior to commencement of the IE experiments, to ensure pH 4.5 or pH 5.5 was achieved and maintained – this procedure is followed in all IE experiments involving buffer. This check was done by adding 2ml of buffer to 160ml NSSW, adding 40ml of FW (un-buffered), and measuring the mix pH, checking it is of appropriate value (either pH 4.5 or pH 5.5, as appropriate). As mentioned earlier, selected experiments were repeated at pH 4.5 and pH 5.5 by the pH adjustment method (i.e. buffer free). The sodium acetate / acetic acid buffer is unsuitable to achieve and maintain pH levels of 6.5 and 7.5 – therefore, for pH 6.5 and pH 7.5 tests, it was decided to pH adjust the NSSW and FW bottles to these pH levels, prior to the mixing stage, instead of using a buffer. The recommended pH buffering range for a sodium acetate / acetic acid buffering system is pH 3.7−5.6 (Table 3.16).

For the pH 6.5 and pH 7.5 tests, the bulk FW was pH adjusted to pH 6.5 or pH 7.5 prior to measuring into individual plastic test bottles. However, this could not be done for the NSSW because the addition of SI to the NSSW usually causes a decrease in pH (if the SI formulation is acidic). Therefore, in all cases, the NSSW test bottles were individually pH adjusted to pH 6.5 or pH 7.5 after the SI dilutions had been completed and NSSW solutions measured into

the test bottles. Tests carried out at pH 4.5 and pH 5.5 in the absence of buffer were carried out following the same procedure. As a further check, after completion of the static IE experiments (at all 4 pH levels), the final pH of each test bottle was measured using a pH meter – thus ensuring that a pH level of ~4.5, ~5.5, ~6.5 or ~7.5 had been maintained throughout the IE experiments, irrespective of whether buffer was present or not. Occasionally some drifting of the pH had occurred, but the results of the experiments as a whole, should still be qualitatively interpretable.

7.3 Results and Discussion

Note that in the captions below the results charts (Figure 7.7−Figure 7.45), the suffix "(a)" denotes that the pH was achieved by pH adjustment, whereas the suffix "(b)" denotes that the pH was achieved by using a sodium acetate / acetic acid buffer, where compositions are given in Table 3.15 for achieving pH 4.5 and pH 5.5.

7.3.1 DETPMP and HMTPMP

In the experiments varying pH, the 2 penta-phosphonates, DETPMP and HMTPMP were tested first, with the aim of determining their 2 and 22 hour MIC levels at the new pH levels of 4.5, 6.5 and 7.5. The 2 and 22 hour MICs could not be reached for either product at pH4.5 due to the IE being too suppressed at this low pH level. However, 2 and 22 hour MICs were determined for both products at the higher pH levels of 6.5 and 7.5 (MICs at pH5.5 were already known from Chapter 5). In the various IE tests carried out at pH 4.5, 6.5 and 7.5, the SIs were not always tested at the same [SI]s because clearly the MIC concentration (or MIC range) was different at each pH level. Where each SI was tested at the same [SI] at multiple pH levels (including pH5.5), charts of 2 and 22 hour IE versus pH were plotted. Furthermore, DETPMP and HMTPMP were re-tested under Base Case conditions, at all 4 pH levels, in a buffer-free environment (DETPMP at 10ppm; HMTPMP at 20 and 80ppm). These charts are presented in Figure 7.7−Figure 7.12 for DETPMP and HMTPMP under Base Case test conditions (i.e. $[Ca^{2+}]$ = 742ppm, $[Mg^{2+}]$ = 1242ppm, molar ratio Ca^{2+}/Mg^{2+} = 0.36) and Figure 7.16−Figure 7.21 under Fixed Case test conditions (i.e. $[Ca^{2+}]$ = 2000ppm, $[Mg^{2+}]$ = 739ppm, molar ratio Ca^{2+}/Mg^{2+} = 1.64). Base Case 2 and 22 hour MIC versus pH charts are presented for DETPMP and HMTPMP in Figure 7.13, Figure 7.14 and Figure 7.15 (22hr only). Fixed Case 2 and 22 hour MIC versus pH charts are presented for DETPMP and HMTPMP in Figure 7.22 and Figure 7.23.

7.3.1.1 DETPMP and HMTPMP − Base Case Conditions – 80/20 NSSW/FW, Ca^{2+}/Mg^{2+} = 0.36

By examining Figure 7.7−Figure 7.12, it is clear that the 2 and 22 hour Base Case IE of both penta-phosphonates is increasing with increasing pH. In both cases, the highest IE is achieved at pH 7.5. When DETPMP was tested by pH adjustment at all pH levels (Figure 7.8), the 2 and 22 hour IE vs. pH curves were much smoother compared to when buffer was present at pH 4.5 and pH 5.5 (Figure 7.7). This could be because the presence of buffer is falsely enhancing the IE at pH 5.5 (Figure 7.7). On the contrary, when HMTPMP was re-tested at 20ppm and 80ppm, by the pH adjustment method at all 4 pH levels (Figure 7.10 and Figure 7.12), the results were very similar compared to when buffer was present at pH 4.5 and pH 5.5 (Figure 7.9 and Figure 7.11). The IE of both products appears to be affected similarly by variations in pH, however, if one considers their MIC level at each pH level (see Figure 7.13, Figure 7.14 and Figure 7.15), clearly the HMTPMP 22 hour MIC is much more severely influenced by pH. Note that no MICs were reached at pH 4.5. Figure 7.14 shows the 22 hour Base Case HMTPMP MIC at pH 5.5 (in the presence of buffer) = 90ppm, this reduces to just 25ppm at pH 6.5. Figure 7.15 shows the 22 hour Base Case HMTPMP MIC at pH 5.5 (by pH adjustment) = 80ppm, this reduces to just 25ppm at pH 6.5. The 22 hour pH 5.5 MIC (by pH adjustment) could in fact be < 80ppm because the SI was only re-tested at two fixed [SI]s: 20ppm and 80ppm, not a full range of [SI]s. Note that in Figure 7.15, only the 22 hour MIC has been plotted vs. pH because the 2 hour MIC at pH 5.5 was not re-determined in the absence of buffer (HMTPMP was only tested at 20ppm which is below 2 hour MIC and at 80ppm which is above 2 hour MIC). Figure 7.13 shows the DETPMP 2 hour MIC is unaffected by variations in pH and the 22 hour MIC is barely affected. The effect of pH (i.e. $[H^+]$) on the MIC of these two SIs appears to be analogous to the effects of $[Ca^{2+}]$ and $[Mg^{2+}]$, in that the HMTPMP (type 2) MIC is much more sensitive to variations in pH compared to the DETPMP (type 1) MIC.

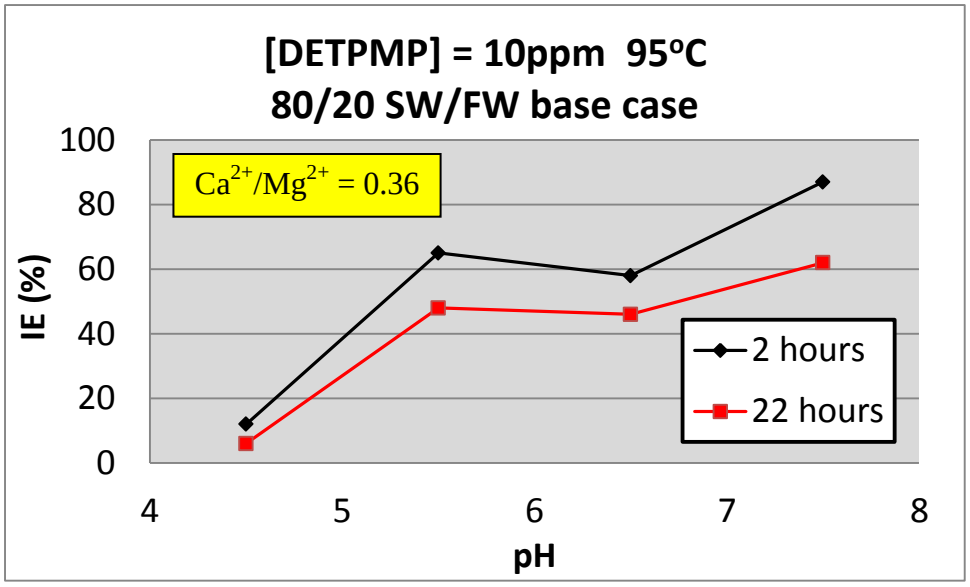

Figure 7.7 – Base Case 2 and 22 hour IE vs. pH. Conditions: 95°C, 80/20 NSSW/FW, [DETPMP] fixed = 10ppm. pH4.5 (b), pH5.5 (b), pH6.5 (a), pH7.5 (a).

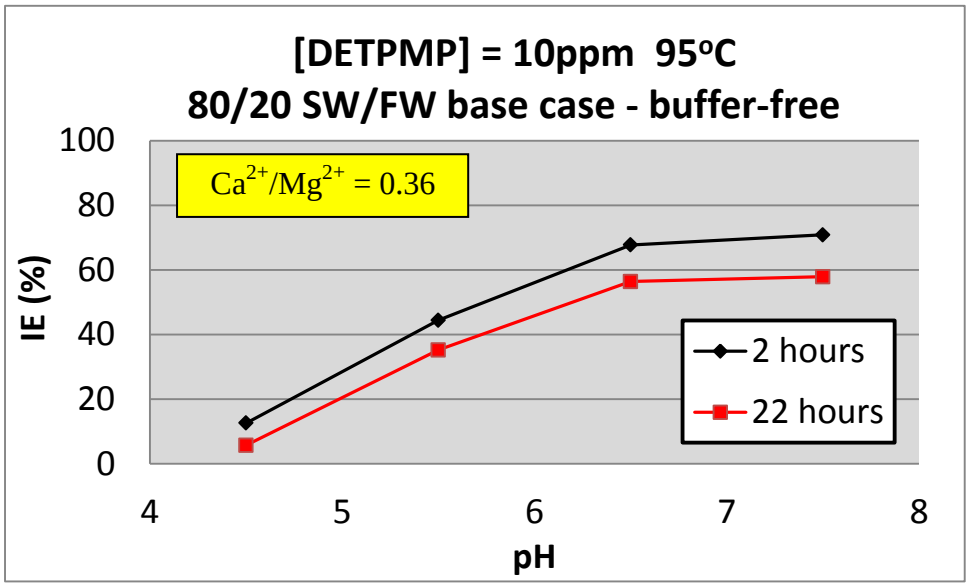

Figure 7.8 – Base Case 2 and 22 hour IE vs. pH. Conditions: 95°C, 80/20 NSSW/FW, [DETPMP] fixed = 10ppm. pH4.5 (a), pH5.5 (a), pH6.5 (a), pH7.5 (a).

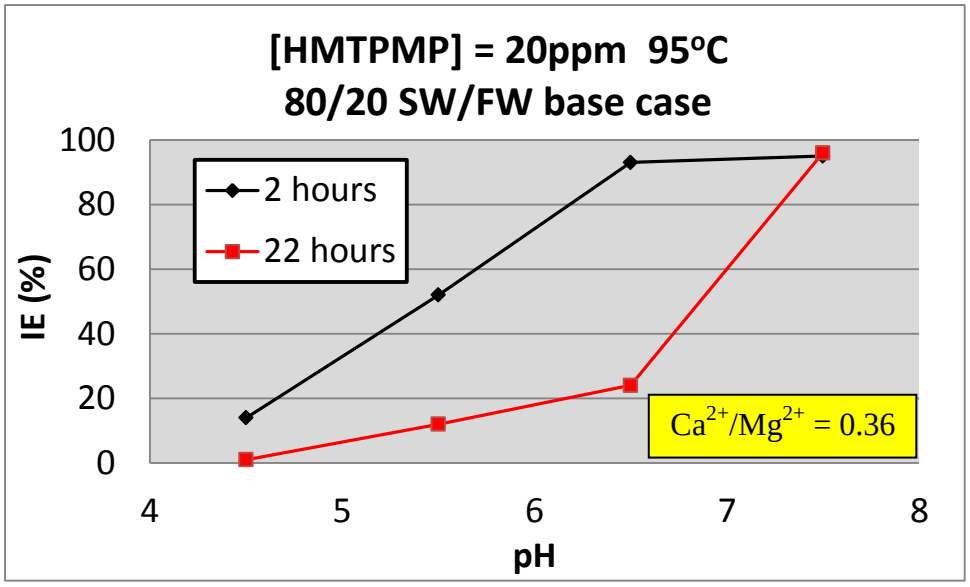

Figure 7.9 – Base Case 2 and 22 hour IE vs. pH. Conditions: 95°C, 80/20 NSSW/FW, [HMTPMP] fixed = 20ppm. pH4.5 (b), pH5.5 (b), pH6.5 (a), pH7.5 (a).

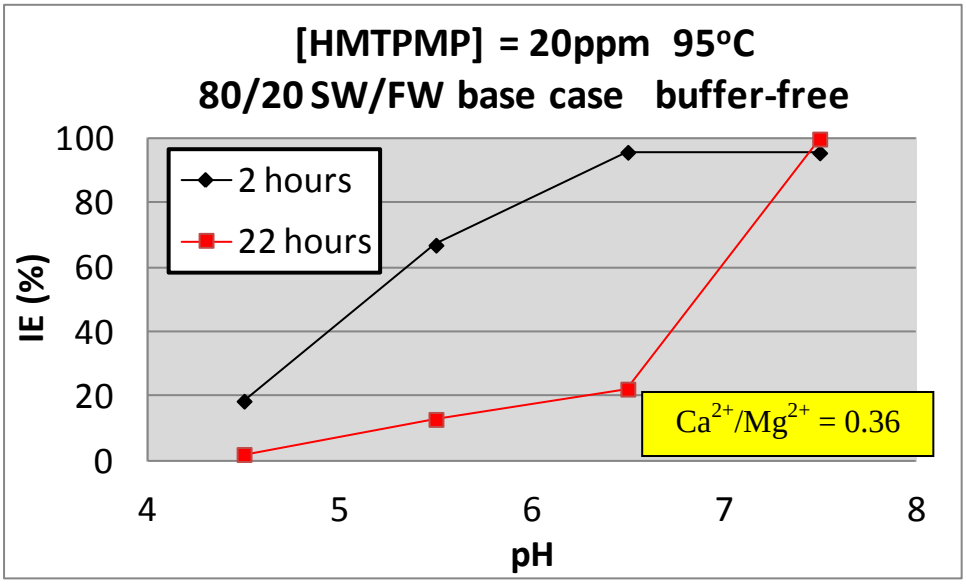

Figure 7.10 – Base Case 2 and 22 hour IE vs. pH. Conditions: 95°C, 80/20 NSSW/FW, [HMTPMP] fixed = 20ppm. pH4.5 (a), pH5.5 (a), pH6.5 (a), pH7.5 (a).

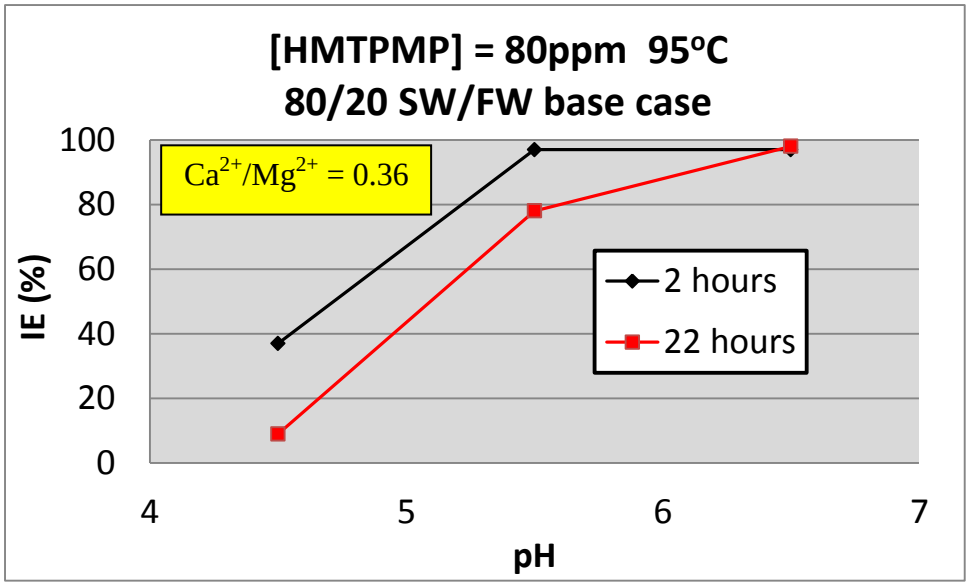

Figure 7.11 – Base Case 2 and 22 hour IE vs. pH. Conditions: 95°C, 80/20 NSSW/FW, [HMTPMP] fixed = 80ppm. pH4.5 (b), pH5.5 (b), pH6.5 (a).

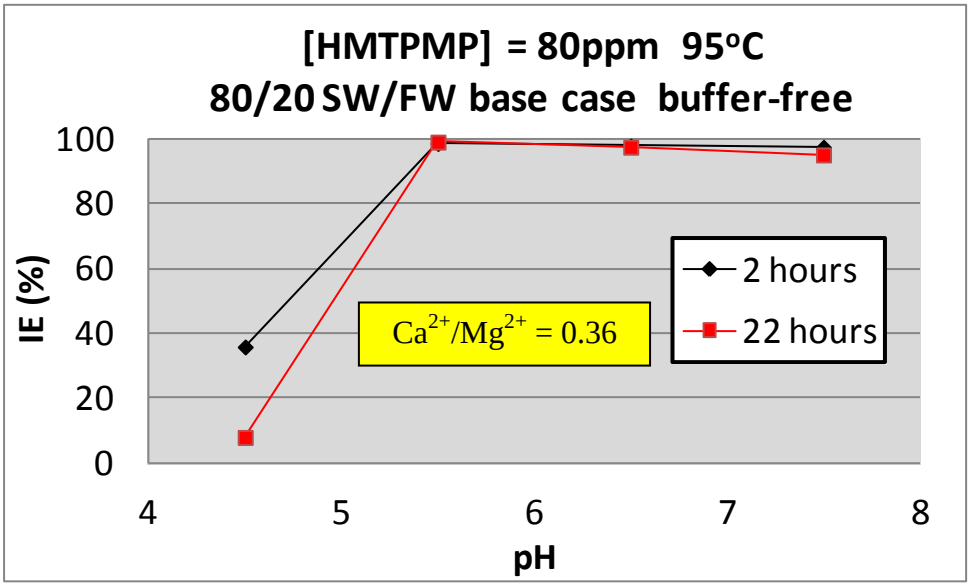

Figure 7.12 – Base Case 2 and 22 hour IE vs. pH. Conditions: 95°C, 80/20 NSSW/FW, [HMTPMP] fixed = 80ppm. pH4.5 (a), pH5.5 (a), pH6.5 (a), pH7.5 (a).

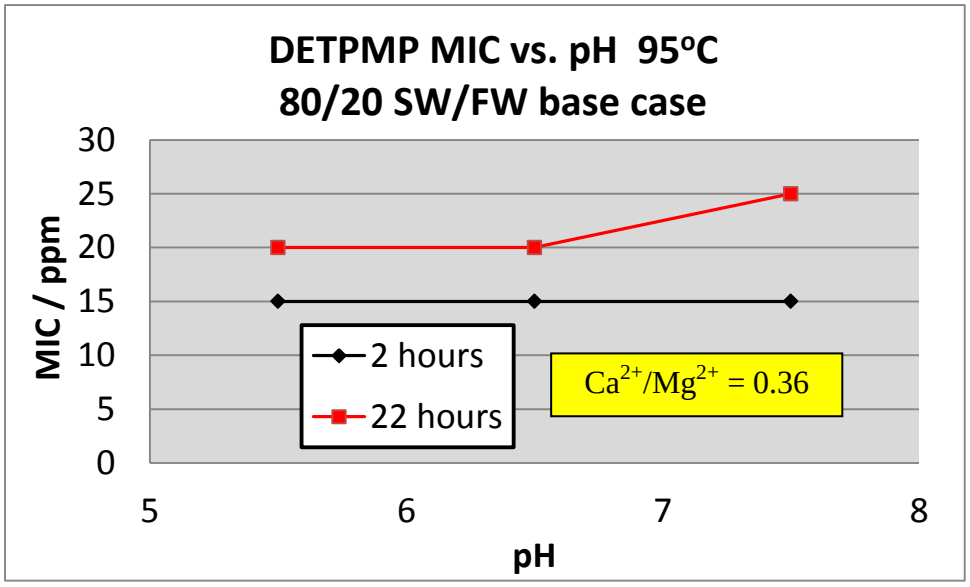

Figure 7.13 – DETPMP Base Case 2 and 22 hour MIC vs. pH. Conditions: 95°C, 80/20 NSSW/FW. pH5.5 (b), pH6.5 (a), pH7.5 (a).

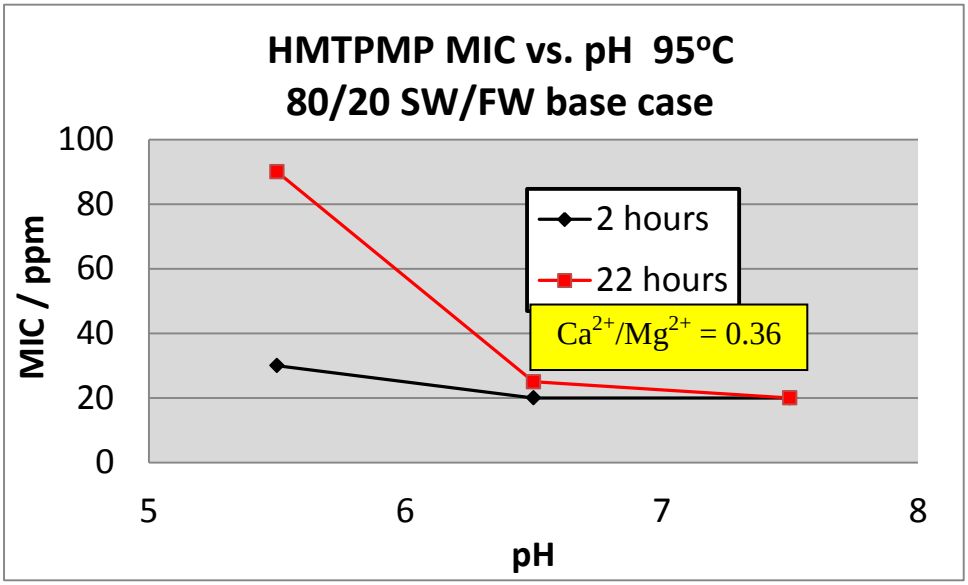

Figure 7.14 – HMTPMP Base Case 2 and 22 hour MIC vs. pH. Conditions: 95°C, 80/20 NSSW/FW. pH5.5 (b), pH6.5 (a), pH7.5 (a).

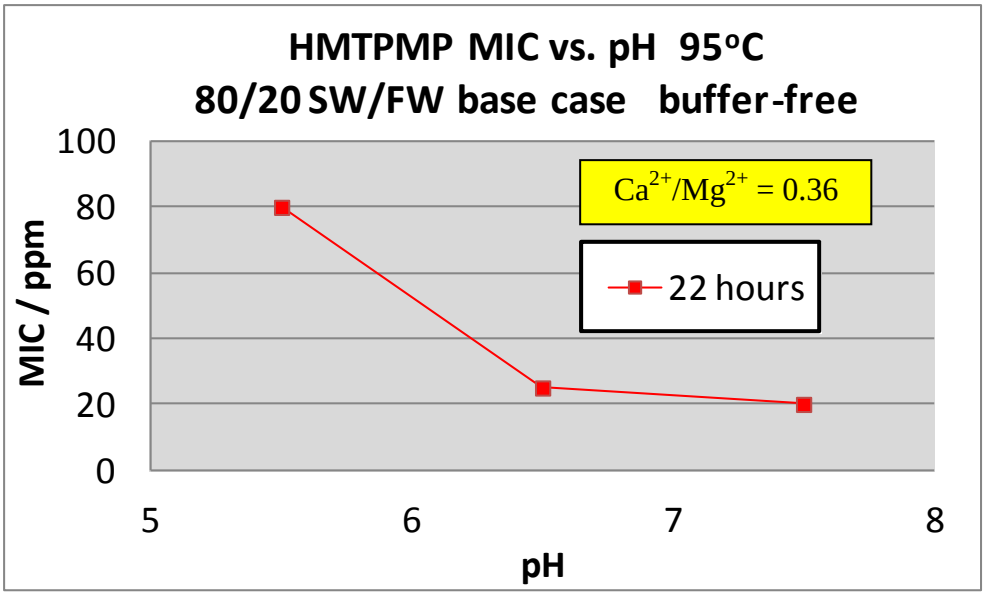

Figure 7.15 – HMTPMP Base Case 22 hour MIC vs. pH. Conditions: 95°C, 80/20 NSSW/FW. pH5.5 (a), pH6.5 (a), pH7.5 (a).

7.3.1.2 DETPMP and HMTPMP − Fixed Case Conditions – 80/20 NSSW/FW, Ca^{2+}/Mg^{2+} = 1.64

From the results presented in Figure 7.19−Figure 7.21, it is clear that the HMTPMP IE increases with increasing pH – the same trend observed under Base Case conditions. However, DETPMP behaves slightly differently under Fixed Case conditions (Figure 7.16−Figure 7.18), in that there now appears to be a maximum in IE at pH 6.5. For example, Figure 7.17 shows the 2 and 22 hour DETPMP IE lower at pH 7.5 compared to at pH 6.5, when tested at 3ppm. Similarly, Figure 7.18 shows a maximum in DETPMP 2 and 22 hour IE at pH 6.5, when tested at 4ppm. There appears to be an "optimum" operating pH of 6.5 for DETPMP under Fixed Case conditions, although the IE at pH 7.5 is only slightly lower than at pH 6.5 (Figure 7.17 and Figure 7.18).

Figure 7.22 and Figure 7.23 present the 2 and 22 hour Fixed Case DETPMP and HMTPMP MICs versus pH. Again, under Fixed Case conditions, no MICs are reached at pH 4.5. Figure 7.22 shows that the 2 hour Fixed Case DETPMP MIC is almost unaffected by pH whereas there is a minimum in the 22 hour MIC at pH 6.5. The 22 hour Fixed Case DETPMP MIC = 4ppm at pH 6.5, = 6ppm at pH 5.5, and = 7ppm at pH 7.5. This minimum

in 22 hour Fixed Case DETPMP MIC at pH 6.5 correlates with the observed maximum in IE at pH 6.5 (e.g. Figure 7.17 and Figure 7.18). Figure 7.23 shows that the 2 hour HMTPMP Fixed Case MIC is almost unaffected by pH, whereas the lowest 22 hour MICs are measured at pH levels of 6.5 and 7.5. The 22 hour Fixed Case HMTPMP MIC = 15ppm at pH 5.5 and this reduces to just 5ppm at pH 6.5 and pH 7.5.

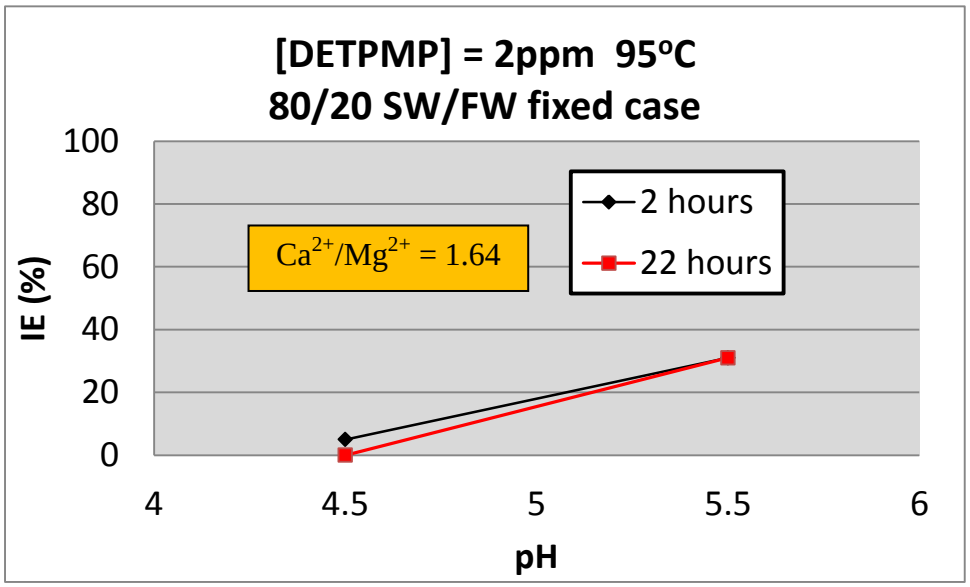

Figure 7.16 – Fixed Case 2 hour IE vs. pH. Conditions: 95°C, 80/20 NSSW/FW, [DETPMP] fixed = 2ppm. pH4.5 (b), pH5.5 (b).

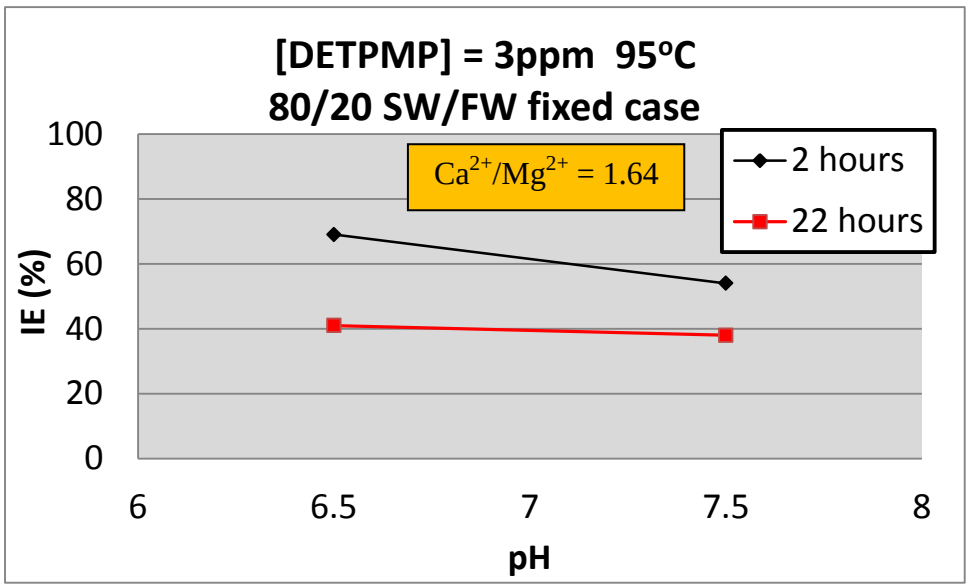

Figure 7.17 – Fixed Case 2 hour IE vs. pH. Conditions: 95°C, 80/20 NSSW/FW, [DETPMP] fixed = 3ppm. pH6.5 (a), pH7.5 (b).

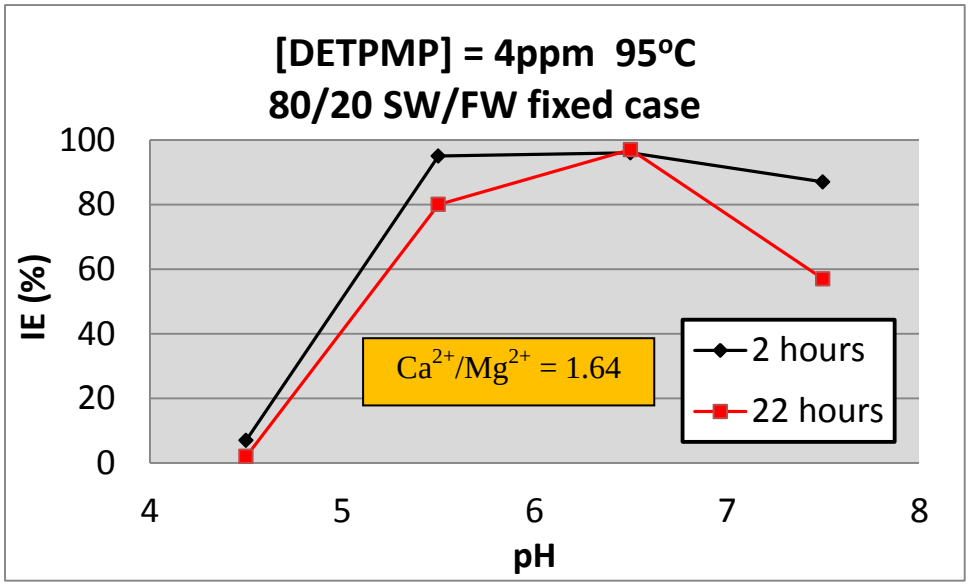

Figure 7.18 – Fixed Case 2 and 22 hour IE vs. pH. Conditions: 95°C, 80/20 NSSW/FW, [DETPMP] fixed = 4ppm. pH4.5 (b), pH5.5 (b), pH6.5 (a), pH7.5 (a).

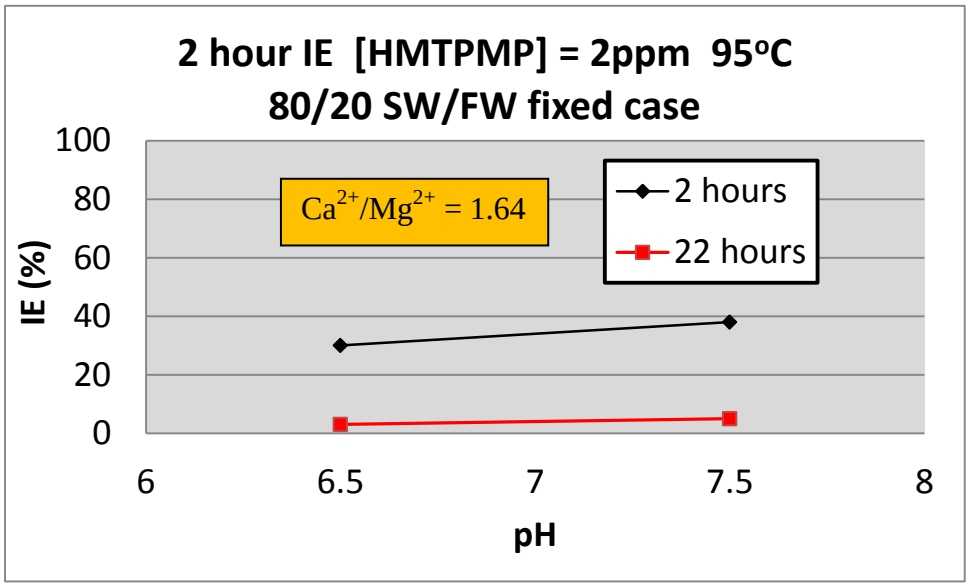

Figure 7.19 – Fixed Case 2 and 22 hour IE vs. pH. Conditions: 95°C, 80/20 NSSW/FW, [HMTPMP] fixed = 2ppm. pH6.5 (a), pH7.5 (a).

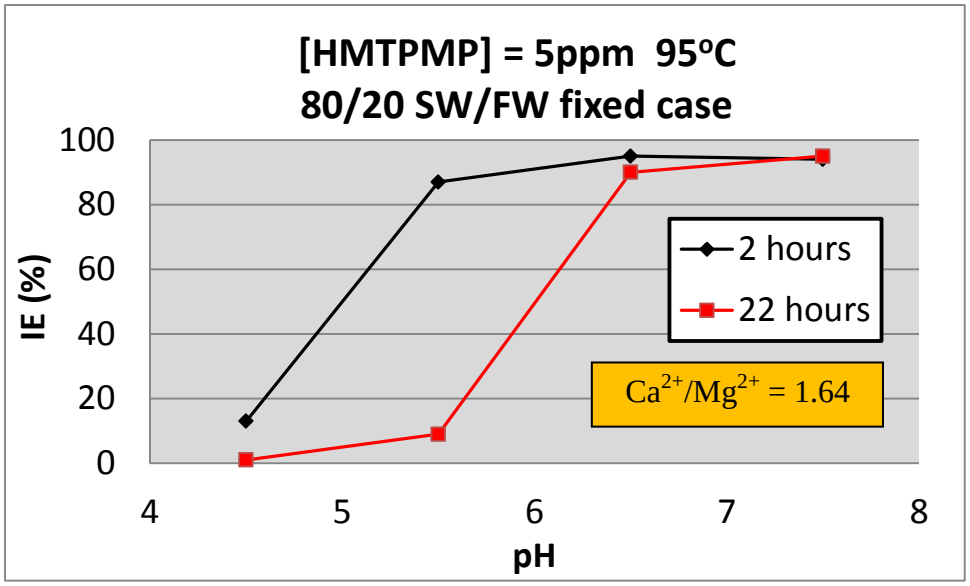

Figure 7.20 – Fixed Case 22 hour IE vs. pH. Conditions: 95°C, 80/20 NSSW/FW, [HMTPMP] fixed = 5ppm. pH4.5 (b), pH5.5 (b), pH6.5 (a), pH7.5 (a).

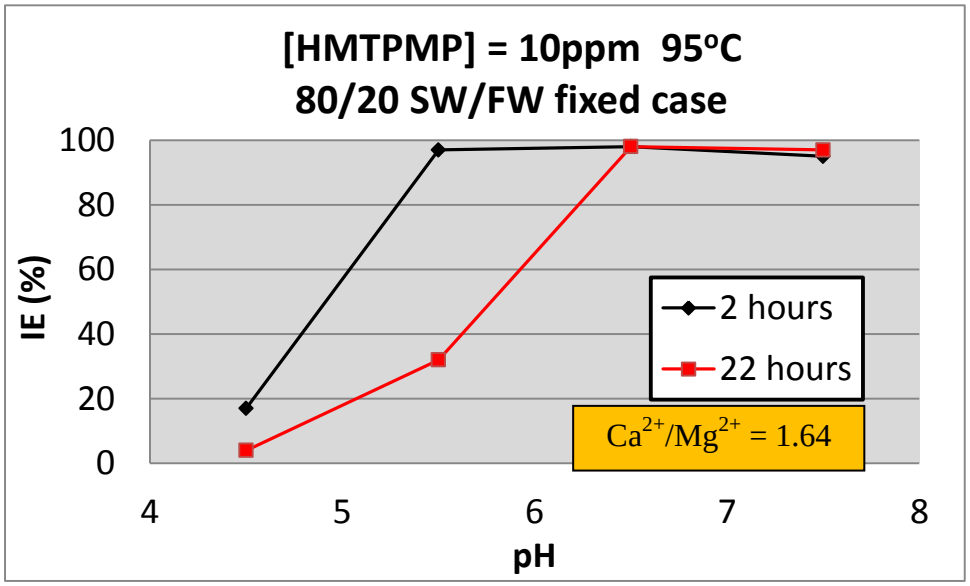

Figure 7.21 – Fixed Case 2 and 22 hour IE vs. pH. Conditions: 95°C, 80/20 NSSW/FW, [HMTPMP] fixed = 10ppm. pH4.5 (b), pH5.5 (b), pH6.5 (a), pH7.5 (a).

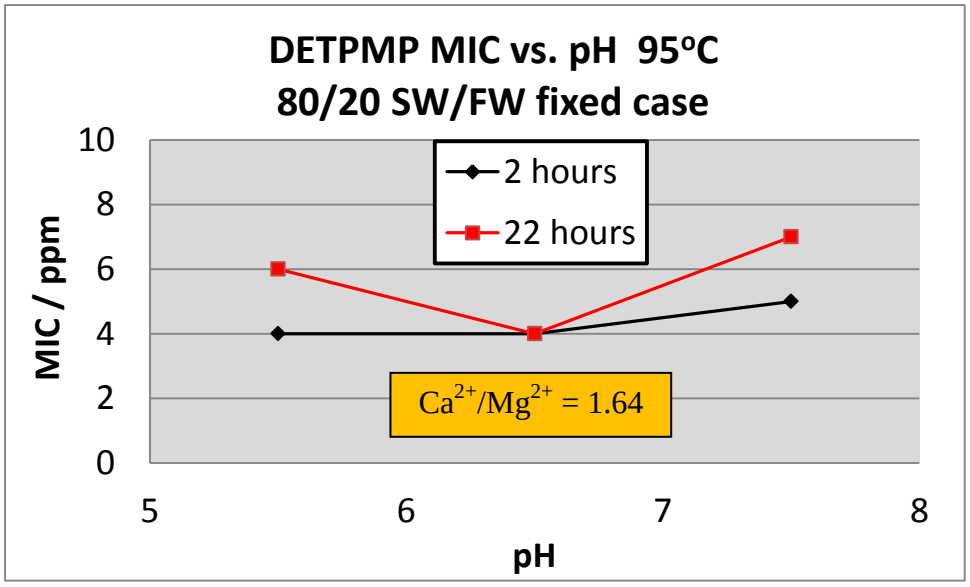

Figure 7.22 – DETPMP Fixed Case 2 and 22 hour MIC vs. pH. Conditions: 95°C, 80/20 NSSW/FW. pH5.5 (b), pH6.5 (a), pH7.5 (a).

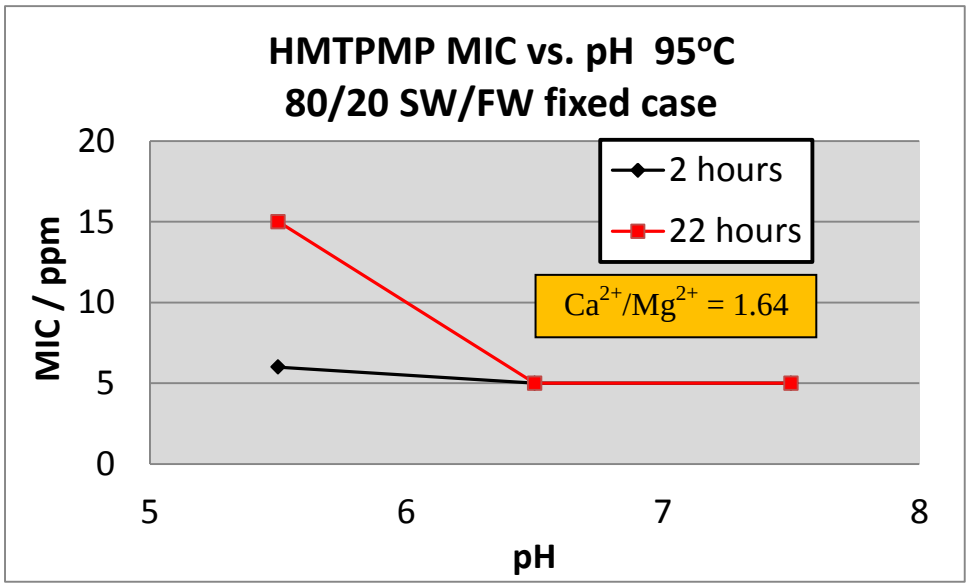

Figure 7.23 – HMTPMP Fixed Case 2 and 22 hour MIC vs. pH. Conditions: 95°C, 80/20 NSSW/FW. pH5.5 (b), pH6.5 (a), pH7.5 (a).

7.3.2 EDTMPA and PPCA

These 2 SIs were tested in the same way as the 2 penta-phosphonates, except the experiments were designed more systematically, in that the aim was to compare their IE at a selection of fixed [SI]s at each pH level, i.e. 4.5, 5.5, 6.5 and 7.5, rather than trying to determine their MICs at the 3 new pH levels (as done testing the 2 penta-phosphonates). By only comparing

selected [SI]s at each pH level for EDTMPA and PPCA, this reduced the workload significantly. MICs were not determined for EDTMPA and PPCA at the new pH levels of 4.5, 6.5 and 7.5. The 22 hour MICs of polymers, including PPCA are usually much higher than for phosphonates. Furthermore, the 22 hour MICs for EDTMPA were the highest of all 8 phosphonate SIs tested in MIC vs. %NSSW tests (Chapter 5), therefore experiments here would require a wide range of EDTMPA [SI]s to be tested. In this work, the EDTMPA and PPCA were tested at a selection of pre-MIC [SI]s (pre-2-hour pH5.5 MIC or pre-22-hour pH 5.5 MIC) such that variations in IE with pH would be apparent. The pH 5.5 (by buffering method) 80/20 NSSW/FW Base Case and Fixed Case 2 and 22 hour MICs are already known for these 2 SIs from Chapters 5 and 6.

Figure 7.24−Figure 7.37 present the Base Case 2 and 22 hour EDTMPA and PPCA IE versus pH. Figure 7.38−Figure 7.45 present the Fixed Case 2 and 22 hour EDTMPA and PPCA IE versus pH. EDTMPA was tested under Base Case conditions at 25ppm and 55ppm (both pre-2-hour Base Case 80/20 NSSW/FW pH5.5 MIC [SI]s) and 100 and 250ppm (both pre-22-hour Base Case 80/20 NSSW/FW pH 5.5 MIC [SI]s). EDTMPA was re-tested at 25ppm and 55ppm by the pH adjustment method at all 4 pH levels. PPCA was tested under Base Case conditions at 2ppm and 5ppm (both pre-2-hour Base Case 80/20 NSSW/FW pH 5.5 MIC [SI]s) and 10ppm and 20ppm (both pre-22-hour Base Case 80/20 NSSW/FW pH5.5 MIC [SI]s). PPCA was re-tested at all 4 [SI]s by the pH adjustment method at all 4 pH levels. In Fixed Case experiments, EDTMPA was tested at 1ppm and 2ppm (both pre-2-hour Fixed Case 80/20 NSSW/FW pH5.5 MIC [SI]s) and 2.5ppm and 3ppm (both pre-22-hour Fixed Case 80/20 NSSW/FW pH 5.5 MIC [SI]s). In Fixed Case tests, PPCA was tested at 2ppm, 5ppm and 10ppm (all pre-2-hour Fixed Case 80/20 NSSW/FW pH 5.5 MIC [SI]s) and 20ppm (a pre-22-hour Fixed Case 80/20 NSSW/FW pH 5.5 MIC [SI]).

7.3.2.1 EDTMPA and PPCA − Base Case Conditions – 80/20 NSSW/FW, Ca^{2+}/Mg^{2+} = 0.36

Figure 7.24−Figure 7.29 show that there is a maximum in the 2 and 22 hour Base Case IE of EDTMPA at pH 6.5, which is much more marked at 22 hours. Figure 7.24−Figure 7.28 show a slight maximum in the 2 hour Base Case IE at pH 6.5 when EDTMPA is tested at 25, 55 and 100ppm. All 6 Figure 7.24−Figure 7.29 show a clear maximum in EDTMPA IE at 22

hours, at pH 6.5. The IE results obtained by both test methods (i.e. buffering vs. pH adjustment for pH 4.5 and pH 5.5) are very similar – compare Figure 7.24 and Figure 7.25; and Figure 7.26 and Figure 7.27. The maximum in Base Case EDTMPA IE at pH 6.5 is similar to what was observed testing DETPMP under Fixed Case conditions (Figure 7.17 and Figure 7.18).

Figure 7.30−Figure 7.37 present the 2 and 22 hour PPCA Base Case IE, when tested at 2, 5, 10 and 20ppm. Four of these figures show the PPCA Base Case IE at pH 7.5 > IE at pH 6.5 (Figure 7.30, Figure 7.32, Figure 7.34 and Figure 7.36). Similarly, in all 8 Figures, the PPCA Base Case IE at pH 5.5 > IE at pH 4.5. Both these observations suggest a trend of increasing IE at higher pH. However, in 6 of the figures (Figure 7.32−Figure 7.37), the PPCA Base Case IE at pH 5.5 > IE at pH 6.5. It could be the case that there is an "optimum" operating pH level of 5.5 for PPCA under Base Case conditions. Tests carried out by the pH adjustment method for pH 4.5 and pH 5.5 (Figure 7.31, Figure 7.33, Figure 7.35 and Figure 7.37) gave similar results to when buffer was present (Figure 7.30, Figure 7.32, Figure 7.34 and Figure 7.36), except the 2 hours IE vs. pH curves were slightly smoother. The maximum in 22 hour IE at pH 5.5 is still apparent in these latter results.

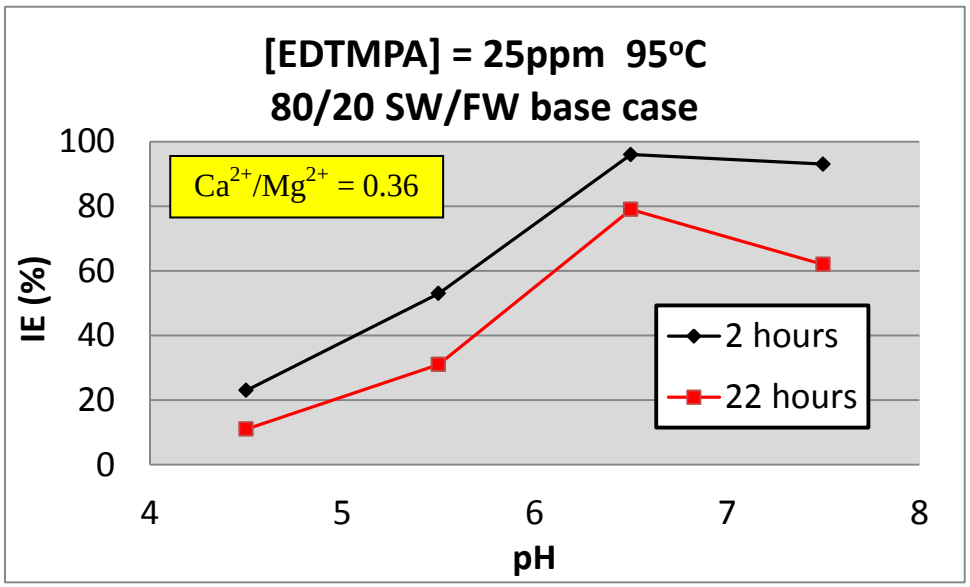

Figure 7.24 – Base Case 2 and 22 hour IE vs. pH. Conditions: 95°C, 80/20 NSSW/FW, [EDTMPA] fixed = 25ppm. pH4.5 (b), pH5.5 (b), pH6.5 (a), pH7.5 (a).

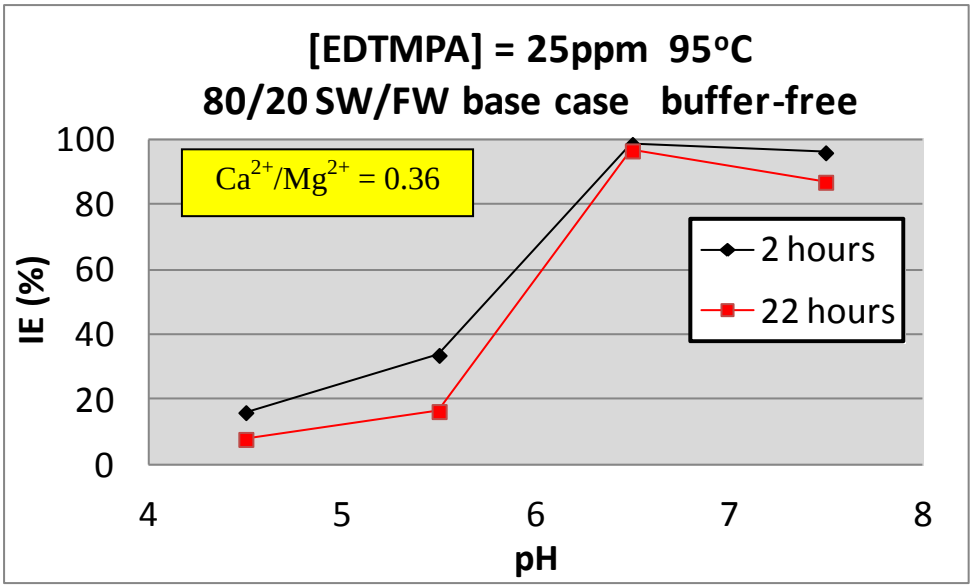

Figure 7.25 – Base Case 2 and 22 hour IE vs. pH. Conditions: 95°C, 80/20 NSSW/FW, [EDTMPA] fixed = 25ppm. pH4.5 (a), pH5.5 (a), pH6.5 (a), pH7.5 (a).

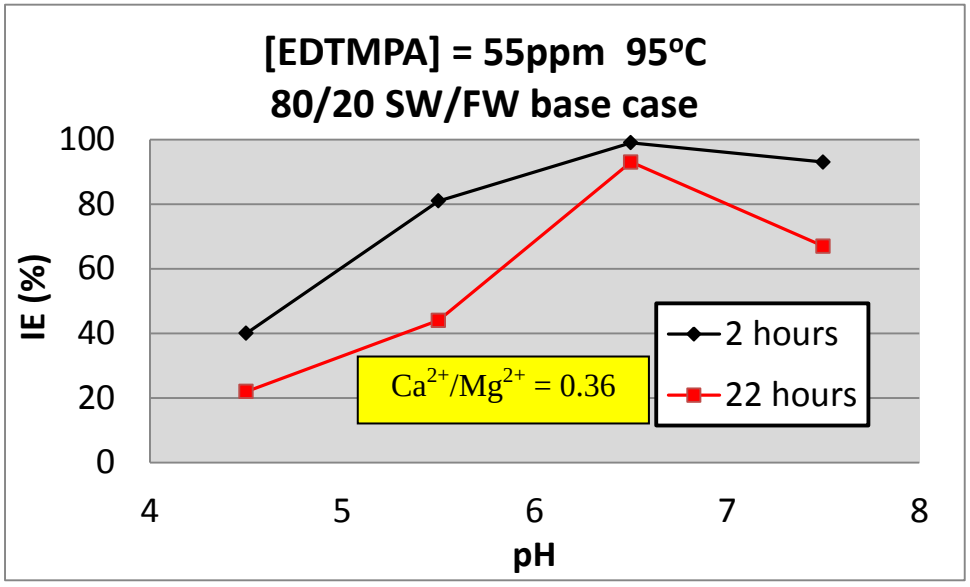

Figure 7.26 – Base Case 2 and 22 hour IE vs. pH. Conditions: 95°C, 80/20 NSSW/FW, [EDTMPA] fixed = 55ppm. pH4.5 (b), pH5.5 (b), pH6.5 (a), pH7.5 (a).

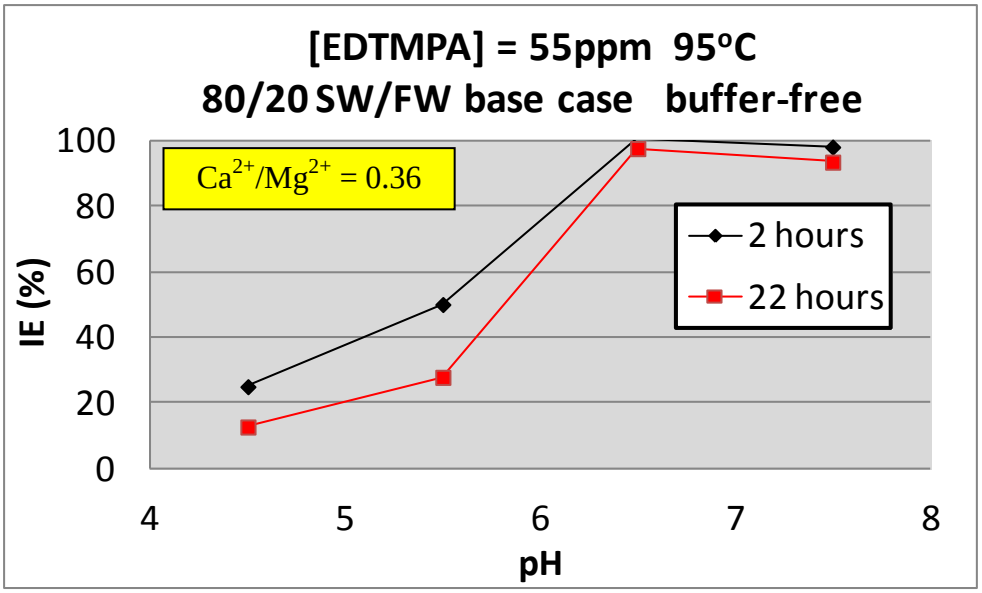

Figure 7.27 – Base Case 2 and 22 hour IE vs. pH. Conditions: 95°C, 80/20 NSSW/FW, [EDTMPA] fixed = 55ppm. pH4.5 (a), pH5.5 (a), pH6.5 (a), pH7.5 (a).

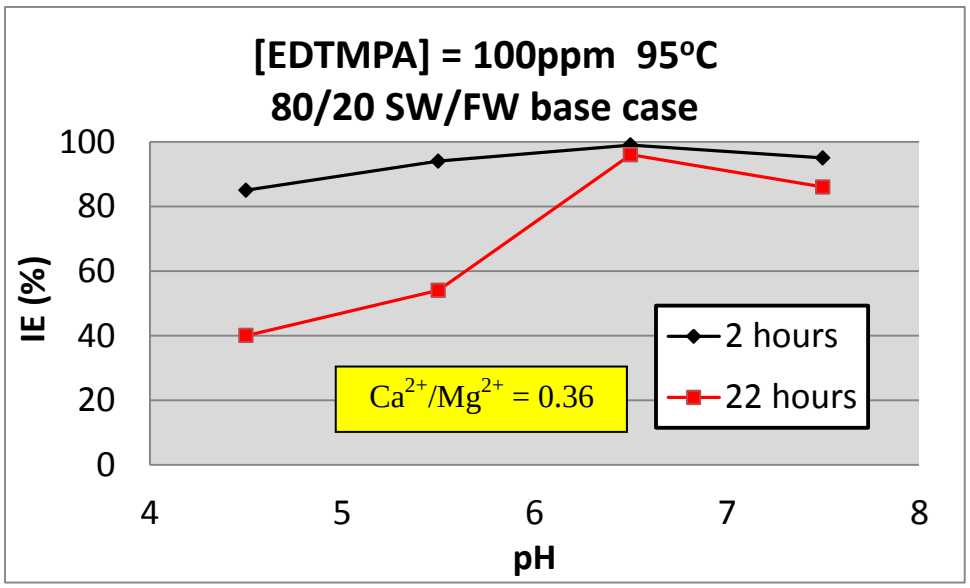

Figure 7.28 – Base Case 2 hour IE vs. pH. Conditions: 95°C, 80/20 NSSW/FW, [EDTMPA] fixed = 100ppm. pH4.5 (b), pH5.5 (b), pH6.5 (a), pH7.5 (a).

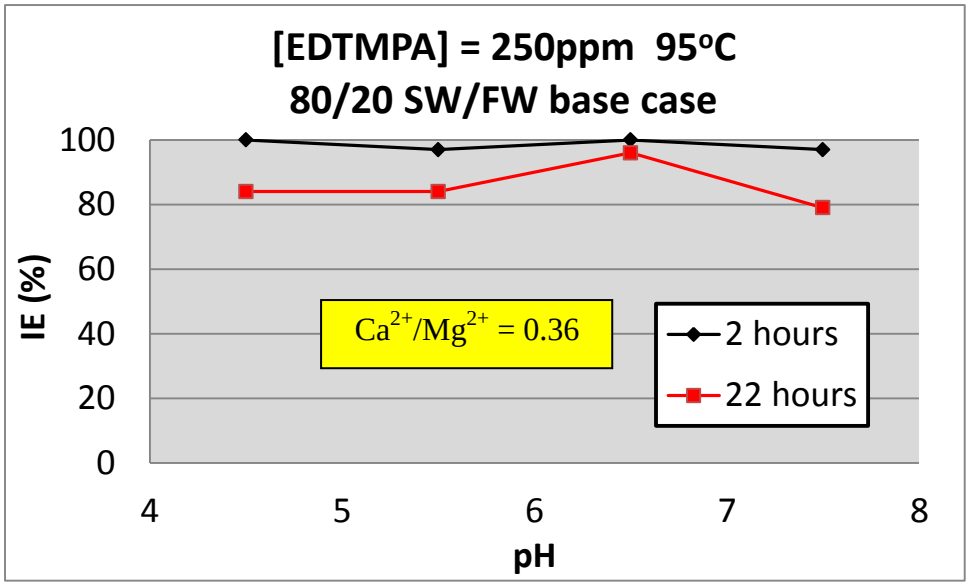

Figure 7.29 – Base Case 2 and 22 hour IE vs. pH. Conditions: 95°C, 80/20 NSSW/FW, [EDTMPA] fixed = 250ppm. pH4.5 (b), pH5.5 (b), pH6.5 (a), pH7.5 (a).

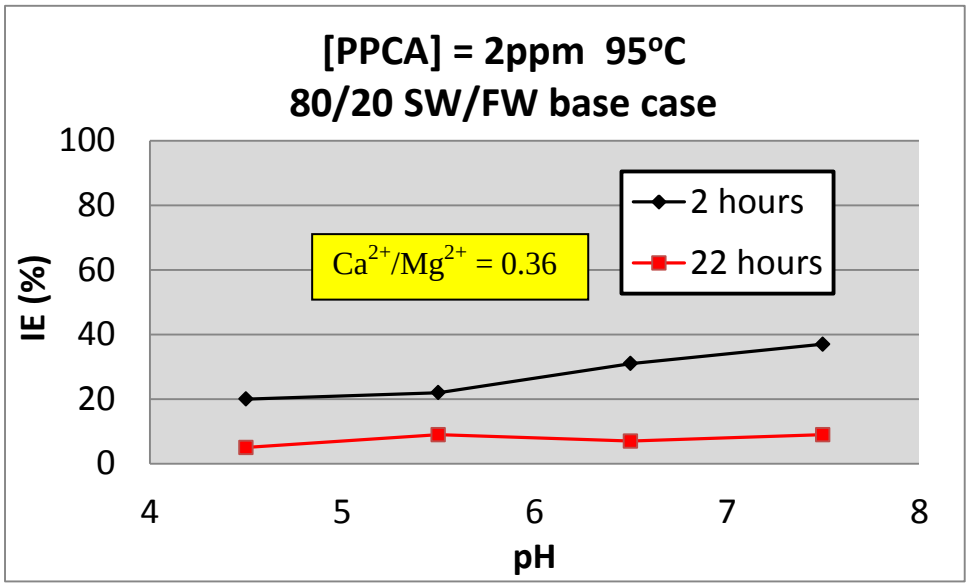

Figure 7.30 – Base Case 2 and 22 hour IE vs. pH. Conditions: 95°C, 80/20 NSSW/FW, [PPCA] fixed = 2ppm. pH4.5 (b), pH5.5 (b), pH6.5 (a), pH7.5 (a).

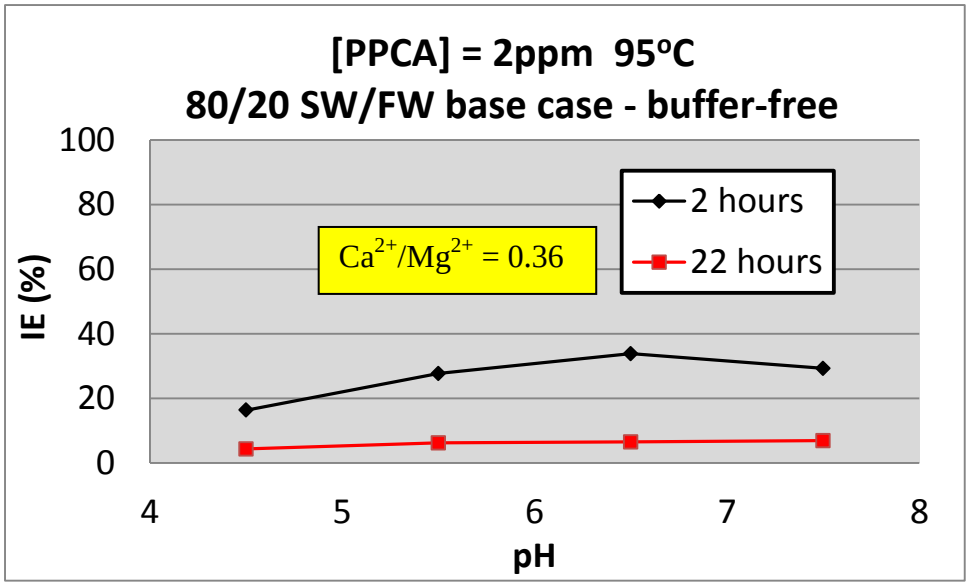

Figure 7.31 – Base Case 2 and 22 hour IE vs. pH. Conditions: 95°C, 80/20 NSSW/FW, [PPCA] fixed = 2ppm. pH4.5 (a), pH5.5 (a), pH6.5 (a), pH7.5 (a).

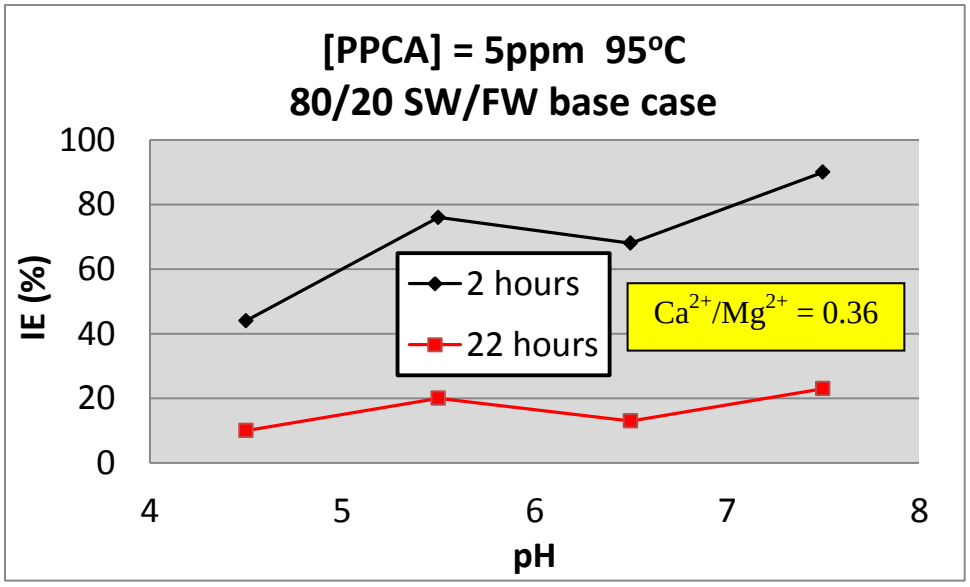

Figure 7.32 – Base Case 2 and 22 hour IE vs. pH. Conditions: 95°C, 80/20 NSSW/FW, [PPCA] fixed = 5ppm. pH4.5 (b), pH5.5 (b), pH6.5 (a), pH7.5 (a).

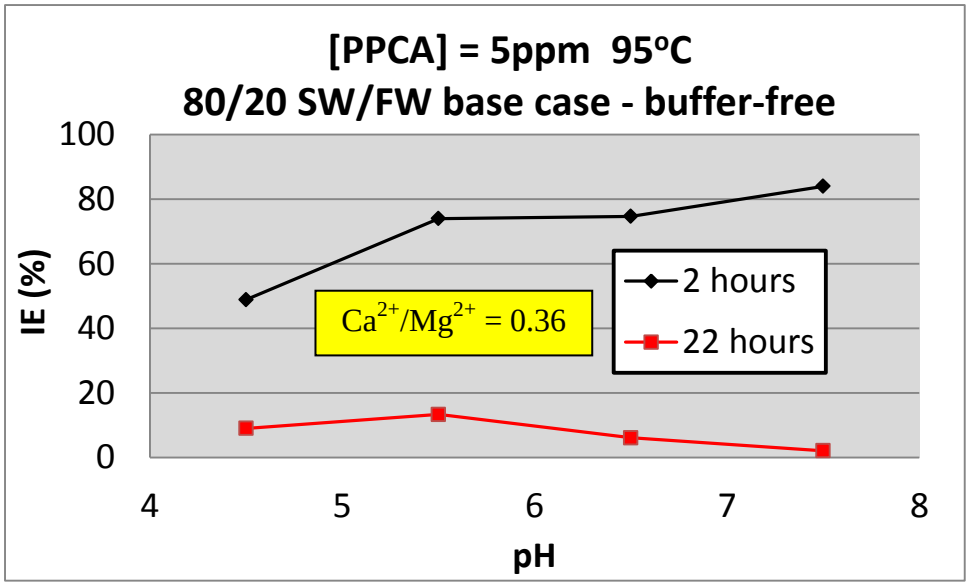

Figure 7.33 – Base Case 2 and 22 hour IE vs. pH. Conditions: 95°C, 80/20 NSSW/FW, [PPCA] fixed = 5ppm. pH4.5 (a), pH5.5 (a), pH6.5 (a), pH7.5 (a).

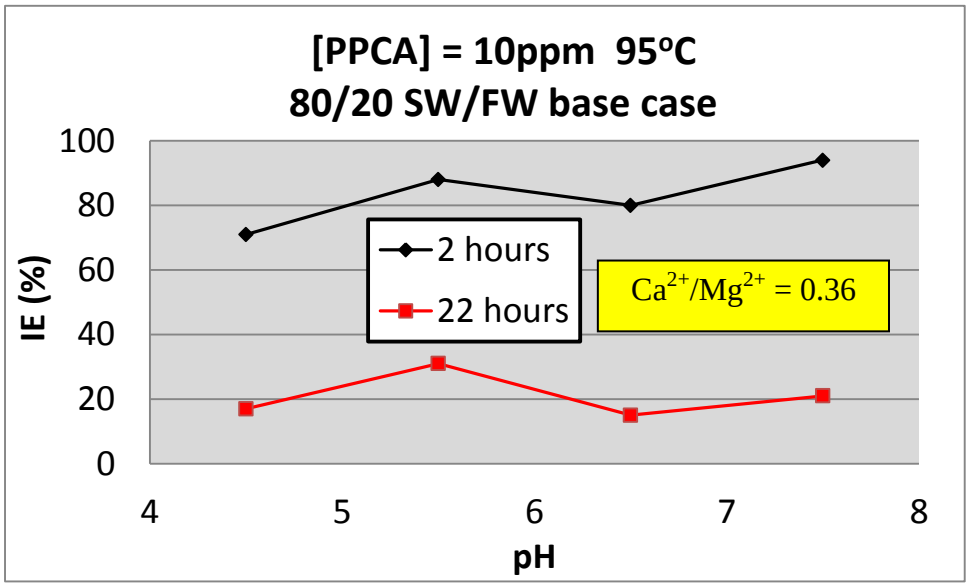

Figure 7.34 – Base Case 2 and 22 hour IE vs. pH. Conditions: 95°C, 80/20 NSSW/FW, [PPCA] fixed = 10ppm. pH4.5 (b), pH5.5 (b), pH6.5 (a), pH7.5 (a).

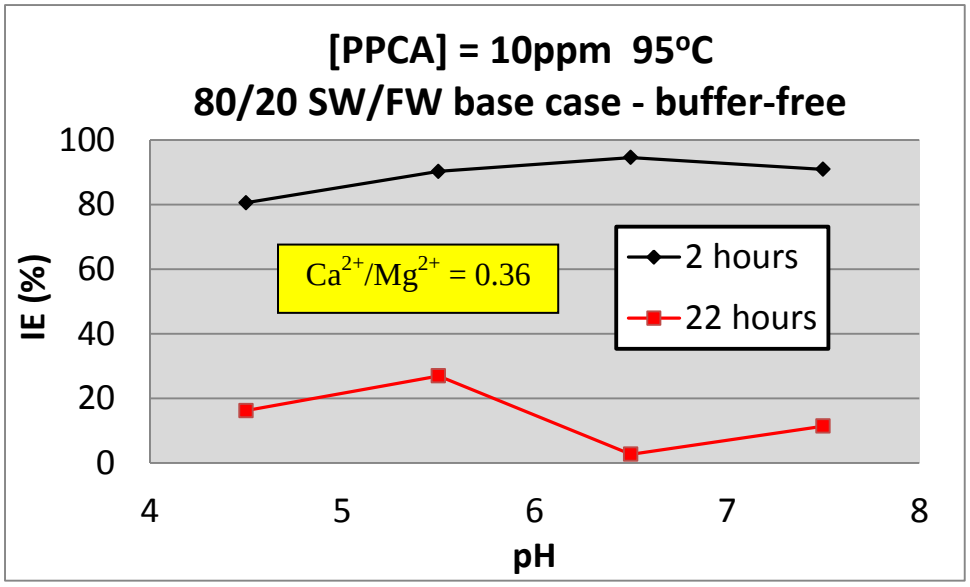

Figure 7.35 – Base Case 2 and 22 hour IE vs. pH. Conditions: 95°C, 80/20 NSSW/FW, [PPCA] fixed = 10ppm. pH4.5 (a), pH5.5 (a), pH6.5 (a), pH7.5 (a).

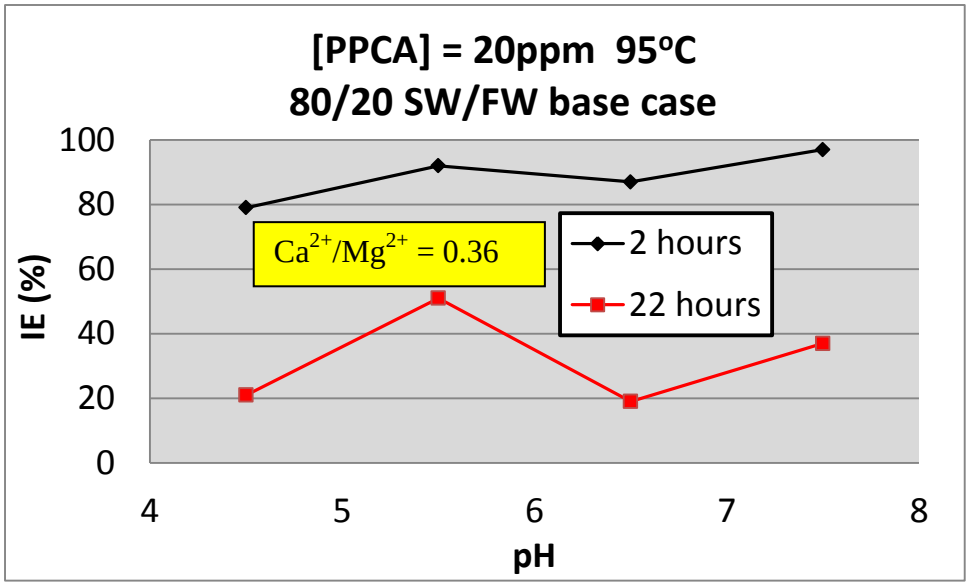

Figure 7.36 – Base Case 2 and 22 hour IE vs. pH. Conditions: 95°C, 80/20 NSSW/FW, [PPCA] fixed = 20ppm. pH4.5 (b), pH5.5 (b), pH6.5 (a), pH7.5 (a).

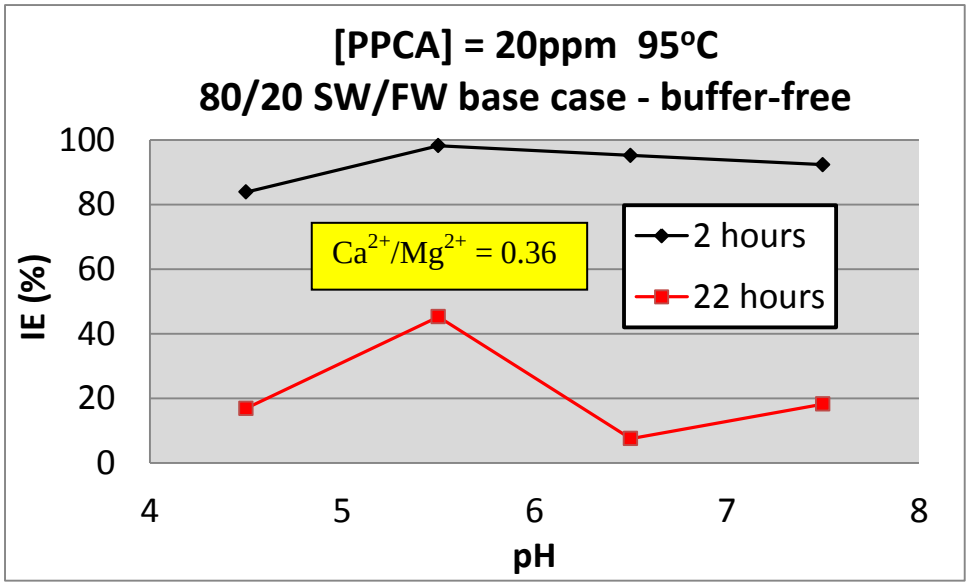

Figure 7.37 – Base Case 2 and 22 hour IE vs. pH. Conditions: 95°C, 80/20 NSSW/FW, [PPCA] fixed = 20ppm. pH4.5 (a), pH5.5 (a), pH6.5 (a), pH7.5 (a).

7.3.2.2 EDTMPA and PPCA − Fixed Case Conditions – 80/20 NSSW/FW, Ca^{2+}/Mg^{2+} = 1.64

Figure 7.38−Figure 7.41 present the Fixed Case EDTMPA IE versus pH when tested at 1, 2, 2.5 and 3ppm levels. Clearly there still appears to be a maximum in 2 and 22 hour IE at pH 6.5 (see Figure 7.38−Figure 7.41), although it is not as marked as under Base Case conditions (Figure 7.24−Figure 7.29). It must also be remembered that a direct comparison cannot be made between the Base Case and Fixed Case EDTMPA IE because different [SI]s were tested in each series of experiments. In some cases the 2 and 22 hour EDTMPA Fixed Case IE is at about the same level at pH 6.5 and pH 7.5, as shown in Figure 7.40 and Figure 7.41 when tested at 2.5 and 3ppm respectively – however this may be simply because the [SI] is sufficiently high enough to allow the IE at pH 7.5 to almost match the IE at pH 6.5, i.e. in other words masking the pH effect on IE, in a similar way to how the effect of Ca^{2+} and Mg^{2+} on IE is masked if too high a [SI] is selected for the test.

Figure 7.42−Figure 7.45 present the 2 and 22 hour PPCA Fixed Case IE when tested at 2, 5, 10 and 20ppm. Unlike in the Base Case tests, there is very little variation in 2 or 22 hour IE at all 4 [SI]s tested. Indeed, when tested at 5ppm, there is no variation in IE at all at 22 hours

– see Figure 7.43. The IE level is constant at all 4 pH levels tested (13%). Similarly, at 2 hours there is almost no variation in IE (~60% at all pH levels). It is known that there is a SI incompatibility issue with Ca^{2+} in high [Ca^{2+}] brine mixes such as in this Fixed Case produced water where [Ca^{2+}] = 2000ppm. This incompatibility issue has already been discussed in Chapter 6. It is highly probable that SI–Ca^{2+} precipitation in these Fixed Case IE tests varying pH, testing PPCA, is masking the effect of varying pH – resulting in the broadly constant IE results at each pH level, presented in Figure 7.42−Figure 7.45. It is very likely that the pH effect on the PPCA IE would be mild under Fixed Case conditions, similar to under Base Case conditions, if the SI/Ca^{2+} incompatibility issue was eliminated. Of the 4 products tested in this work, the PPCA is least affected by variations in pH, under both Base Case and Fixed Case test conditions.

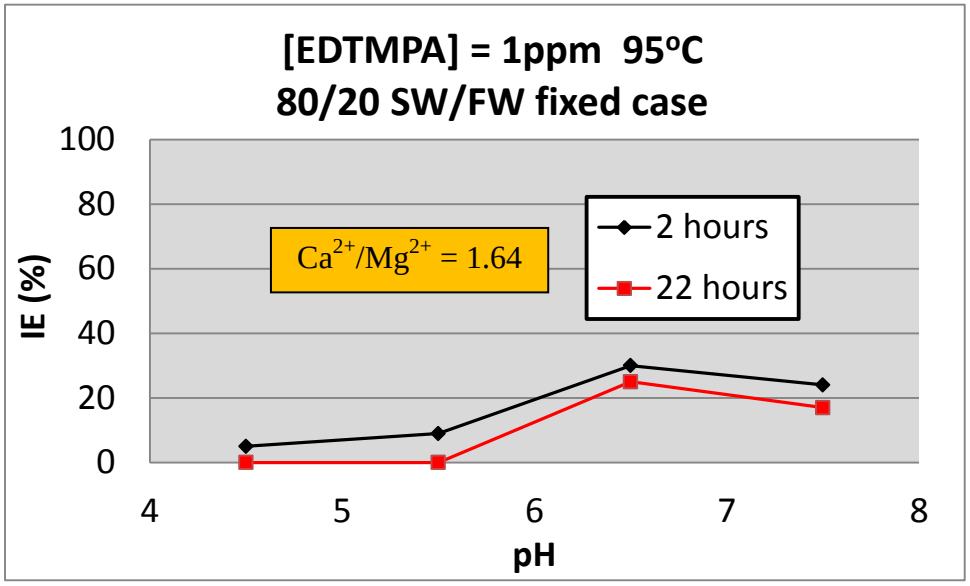

Figure 7.38 – Fixed Case 2 and 22 hour IE vs. pH. Conditions: 95°C, 80/20 NSSW/FW, [EDTMPA] fixed = 1ppm. pH4.5 (b), pH5.5 (b), pH6.5 (a), pH7.5 (a).

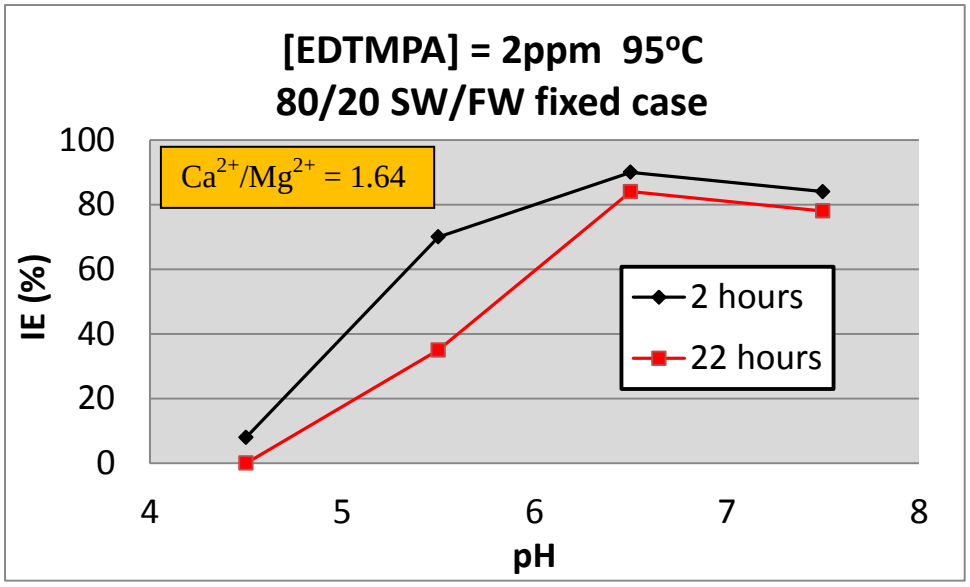

Figure 7.39 – Fixed Case 2 and 22 hour IE vs. pH. Conditions: 95°C, 80/20 NSSW/FW, [EDTMPA] fixed = 2ppm. pH4.5 (b), pH5.5 (b), pH6.5 (a), pH7.5 (a).

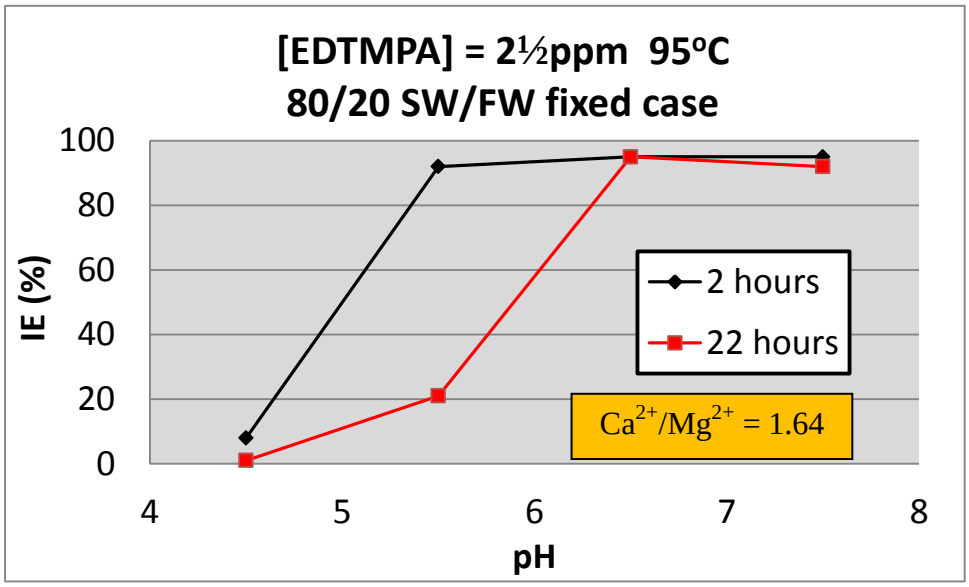

Figure 7.40 – Fixed Case 2 and 22 hour IE vs. pH. Conditions: 95°C, 80/20 NSSW/FW, [EDTMPA] fixed = 2½ppm. pH4.5 (b), pH5.5 (b), pH6.5 (a), pH7.5 (a).

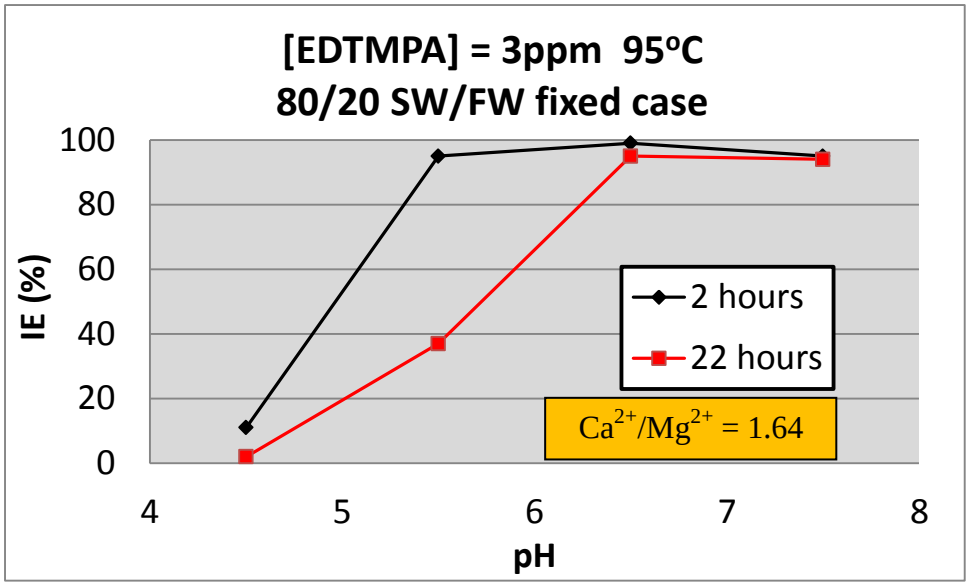

Figure 7.41 – Fixed Case 2 and 22 hour IE vs. pH. Conditions: 95°C, 80/20 NSSW/FW, [EDTMPA] fixed = 3ppm. pH4.5 (b), pH5.5 (b), pH6.5 (a), pH7.5 (a).

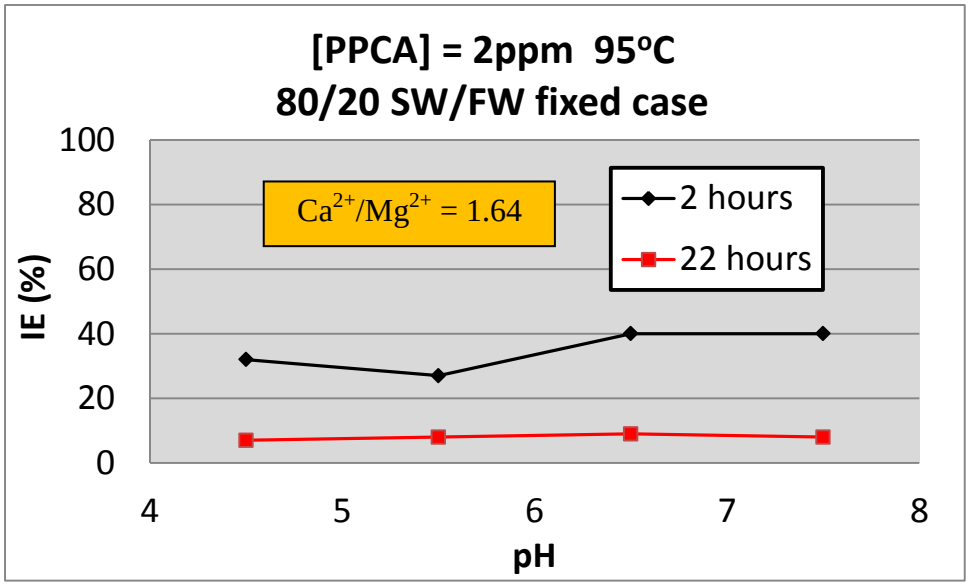

Figure 7.42 – Fixed Case 2 and 22 hour IE vs. pH. Conditions: 95°C, 80/20 NSSW/FW, [PPCA] fixed = 2ppm. pH4.5 (b), pH5.5 (b), pH6.5 (a), pH7.5 (a).

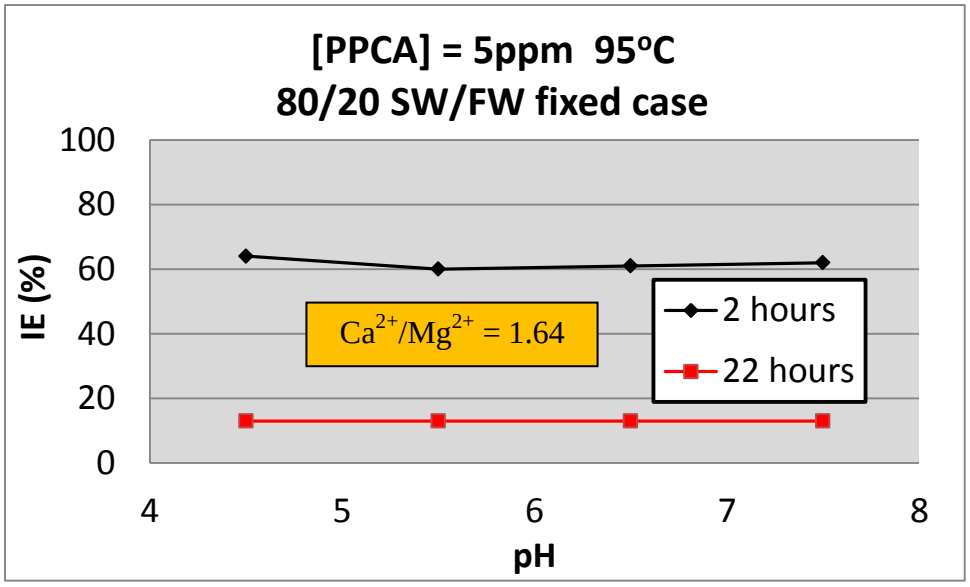

Figure 7.43 – Fixed Case 2 and 22 hour IE vs. pH. Conditions: 95°C, 80/20 NSSW/FW, [PPCA] fixed = 5ppm. pH4.5 (b), pH5.5 (b), pH6.5 (a), pH7.5 (a).

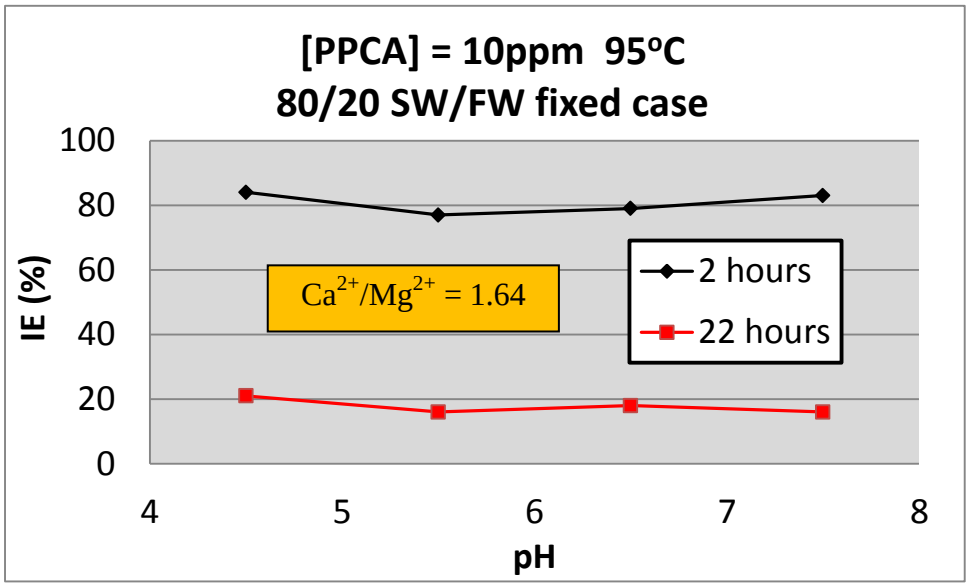

Figure 7.44 – Fixed Case 2 hour IE vs. pH. Conditions: 95°C, 80/20 NSSW/FW, [PPCA] fixed = 10ppm. pH4.5 (b), pH5.5 (b), pH6.5 (a), pH7.5 (a).

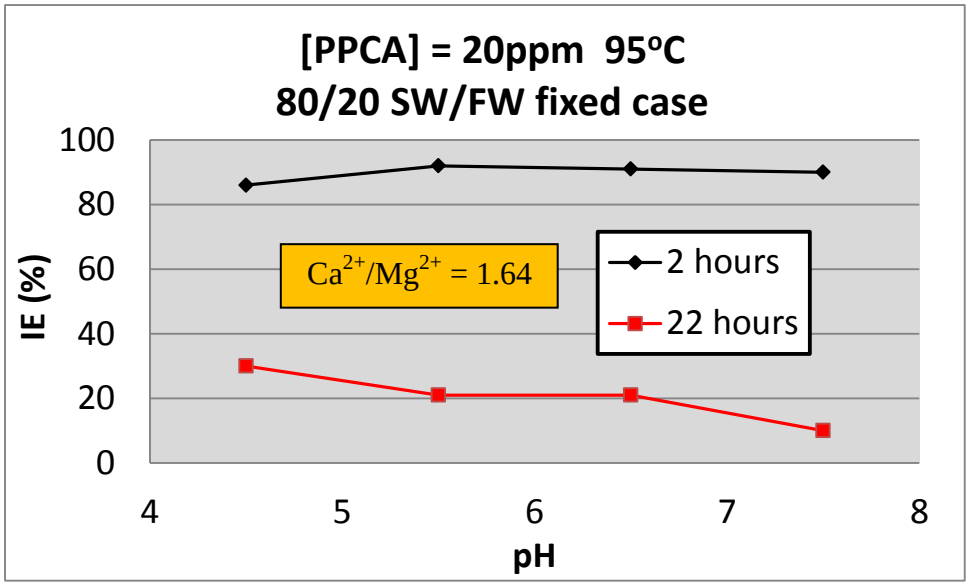

Figure 7.45 – Fixed Case 2 hour IE vs. pH. Conditions: 95°C, 80/20 NSSW/FW, [PPCA] fixed = 20ppm. pH4.5 (b), pH5.5 (b), pH6.5 (a), pH7.5 (a).

7.3.3 Final pH of Test Bottles

The final pH of test bottles was spot checked after static IE experiments had been completed with the intention of checking if the test pH had been maintained throughout the IE experiments. Often the final pH values were within ~± 0.2 of the initial pH. With regard to all Base Case IE experiments in which all 4 pH levels were achieved by pH adjustment (i.e. Figure 7.8, Figure 7.10, Figure 7.12, Figure 7.25, Figure 7.27, Figure 7.31, Figure 7.33, Figure 7.35 and Figure 7.37), the final pH of the test bottles was checked and recorded at the end of the experiment. Blank test bottles; 10ppm DETPMP; 20 and 80ppm HMTPMP; 25 and 55ppm EDTMPA; and 2, 5, 10 and 20ppm PPCA test bottles were spot checked for pH at the end of IE experiments, on cooling. The initial pH was plotted against the final pH. These charts are presented in Figure 7.46(a)–(j). In these 10 figures, the dashed black lines indicate the theoretical result (i.e. $x = y$) which would be obtained if each pH level was maintained throughout the IE experiment. It is clear to see any deviations from this theoretical result. The best agreement between initial pH and final pH is observed for test bottles containing SI EDTMPA (Figure 7.46(e) and (f)). Some drifting of pH has occurred in other test bottles – in particular at pH 7.5, especially in test bottles containing 2 and 5ppm PPCA (Figure 7.46(g) and (h)). The extent of pH drifting may depend upon the nature of the SI present in the test

bottle (if any), e.g. functional groups present etc., and the [SI]. For example, in the pH 7.5 test, there was a larger decrease in pH in test bottles containing 2 and 5ppm PPCA, compared to the 10 and 20ppm PPCA bottles. Unfortunately pH is a variable which can be difficult to control, particularly in the absence of buffer, as in these examples. However, the IE results obtained by doing these tests (buffer present and buffer-free tests) nevertheless give an invaluable qualitative insight into the effect of pH on the speciation and barium sulphate IE of the SIs tested.

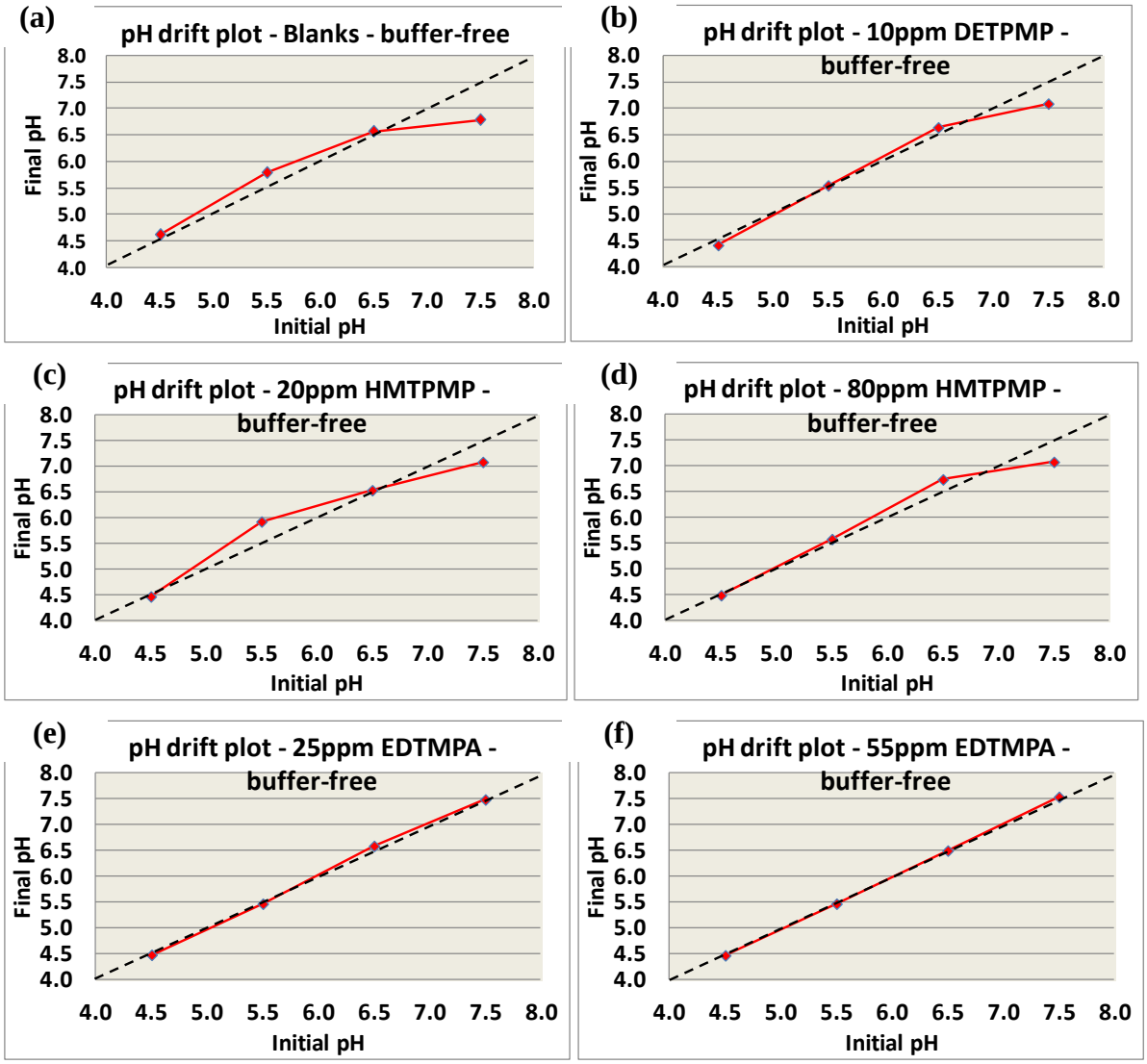

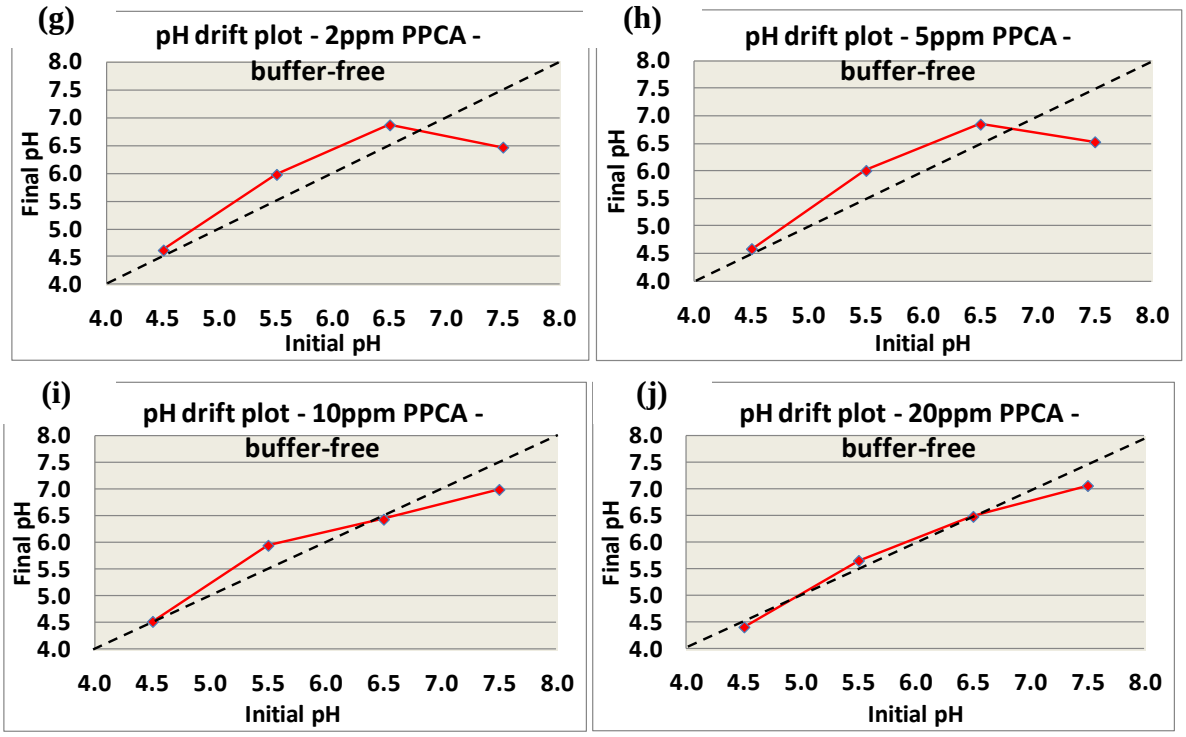

Figure 7.46(a)–(j) – Final pH versus initial pH of IE test bottles retained from experiments where all 4 pH levels were achieved by pH adjustment. (a) = blanks; (b) = 10ppm DETPMP; (c) = 20ppm HMTPMP, (d) = 80ppm HMTPMP, (e) = 25ppm EDTMPA, (f) = 55ppm EDTMPA, (g) = 2ppm PPCA; (h) = 5ppm PPCA; (i) = 10ppm PPCA; (j) = 20ppm PPCA.

7.4 Summary and Conclusions

Of the four products tested in this work, the IE of HMTPMP is the most straightforward to explain, in that its IE increases with increasing pH under both Base Case and Fixed Case conditions, which is interpretable in terms of SI speciation. At higher pH levels, SI molecules become more highly dissociated (i.e. more highly charged). Generally, the more dissociated SI molecules become as pH increases, the greater their barite scale inhibition potential should become. This is because it becomes progressively more favourable for SI anions to form stable chelates with Ca^{2+} cations. SI-metal chelates containing multiple chelate rings can form only at higher pH levels (Shaw et al., 2012). SI which is bound to Ca^{2+} can be incorporated into growing barite scale, and so inhibit further crystal growth (Boak et al., 1999; Graham et al., 1997a, 2003; Sorbie et al., 2000; Sorbie and Laing, 2004). When DETPMP was tested under Base Case conditions, the same trend in IE versus pH was

observed as for HMTPMP. The explanation for this behaviour is the same as that described for HMTPMP.

The IE versus pH behaviour of EDTMPA (Base Case and Fixed Case conditions) and DETPMP (Fixed Case conditions only) require a different explanation to that for HMTPMP. Again increasing IE with increasing pH was observed – but this time only up to pH 6.5. The IE at pH 7.5 was lower than at pH 6.5, albeit in some cases only marginally lower. Clearly, pH 6.5 is an "optimum" operating pH for EDTMPA (under Base Case and Fixed Case conditions) and DETPMP (under Fixed Case conditions only). The most likely explanation for this behaviour is in terms of SI speciation and SI binding to Ca^{2+} and Mg^{2+}. At pH 6.5, the speciation of these 2 SIs, under Base Case and Fixed Case conditions for EDTMPA and under Fixed Case conditions only for DETPMP, must be optimised to allow stable chelates to form with Ca^{2+}. The most stable chelates contain 5 or 6 atoms per chelate ring (Shaw et al., 2012). With regard to EDTMPA under both Base Case and Fixed Case conditions and DETPMP under Fixed Case conditions only, it is possible that at pH 7.5, the SI binding to Mg^{2+} becomes slightly stronger than to Ca^{2+}, i.e. $K_{Mg} > K_{Ca}$. K_{Ca} and K_{Mg} were defined by Equations 2.2, 2.3, 2.5 and 2.6 (see Chapter 2). Clearly this would result in the IE at pH 7.5 being lower than at pH 6.5. The specific experimental conditions affect the magnitude of the K_{Mg} and K_{Ca} values, including the brine composition – particularly $[Mg^{2+}]$ and $[Ca^{2+}]$; this is discussed in more detail in Chapter 12. This could explain differences between the DETPMP IE vs. pH under Base Case and Fixed Case test conditions. The factors affecting the relative magnitude of the SI–metal binding constants K_{Ca} and K_{Mg}, are as follows:

(i) Test pH

(ii) Test T

(iii) Brine mix $[Ca^{2+}]$ and $[Mg^{2+}]$

(iv) Ionic strength of the brine mix (i.e. concentration of all other ionic species, excluding Ca^{2+} or Mg^{2+}, e.g. Na^{+}, K^{+}, acetate (from buffer solution, if present), etc.

The effect of varying pH upon the IE of PPCA was much less compared to the 3 phosphonate SIs. This is plausible, since variations in pH would be expected to affect the speciation (and so IE) of PPCA much less than phosphonic acids. PPCA contains carboxylic acid functional groups (–COOH) which are affected by pH, and it is also a P-tagged polymer. Variations in

the PPCA IE with pH must be due to the dissociation of the –COOH functional groups. It is known that mechanistically, PPCA operates by both nucleation inhibition and crystal growth retardation by roughly equal amounts (Sorbie et al., 2000; Sorbie and Laing, 2004) – and so is probably mechanistically somewhere "in between" phosphonates and polyacrylate polymers. The dissociation of –COOH functional groups should enhance the crystal growth retardation mechanism. In the tests varying pH, under Base Case conditions, a maximum in PPCA IE at pH 5.5 was observed. This observation may be due to optimised dissociation of the carboxylic acid functional groups at pH 5.5, resulting in improved IE at this pH. If the polymer becomes too highly dissociated, at pH levels > 5.5, then this may hinder IE, based on Base Case results presented here. Indeed, similar findings have been found by Van der Leeden and Van der Rosmalen (1990), testing PAA/PMA-based polymers. Beyond ~pH7, there was no further increase in the IE of these polymers. Above a certain pH value, the dissociation (of –COOH groups) has already proceeded far enough to provide these polymers with sufficient anionic charge density for a strong electrostatic interaction with the barium sulphate crystal surface. It might be the case that under Base Case conditions, the PPCA $K_{Ca} > K_{Mg}$ at pH 5.5, but maybe at pH 4.5, pH 6.5 and pH 7.5, $K_{Ca} \approx K_{Mg}$. There will be an optimum operating pH for all polycarboxylate-type polymers (Van der Leeden and Van der Rosmalen, 1990).

Under Fixed Case conditions, there was virtually no variation in PPCA IE with pH. This is plausible, since polymers would be expected to be much less affected by variations in pH, compared to phosphonate SIs. It could be the case that PPCA incompatibility with Ca^{2+} in the Fixed Case tests is masking any small variation in IE with pH which would perhaps be visible otherwise (similar to the Base Case) however at this stage this is a conjecture. It is known that PPCA precipitates with Ca^{2+} in brine with $[Ca^{2+}]$ = 2000ppm (Shaw et al., 2010b), as in the Fixed Case IE tests described in Chapter 6.

The MIC level for HMTPMP was much more strongly affected by variations in pH compared to the DETPMP MIC, which was barely affected. Although MICs were not obtained for EDTMPA, its IE was strongly affected by varying pH. These observations are analogous to the effects of Ca^{2+} and Mg^{2+} upon these 3 phosphonate SIs (Chapter 5). DETPMP was classed as Type 1 because its MIC correlated primarily with the barite saturation ratio (SR) in "MIC versus NSSW/FW mixing ratio" IE tests and was mildly affected by Ca^{2+} and Mg^{2+}.

On the contrary, the HMTPMP and EDTMPA MICs were primarily affected by Ca^{2+} and Mg^{2+}, and less affected by SR. These 2 SIs (HMTPMP and EDTMPA) were classed as Type 2 because they were very sensitive to Ca^{2+} and Mg^{2+}. EDTMPA was the most sensitive Type 2 SI to Ca^{2+} and Mg^{2+}, hence its 80/20 NSSW/FW Base Case 22 hour MIC = ~400ppm at pH 5.5 and 95^{o}C (Chapter 5, Figure 5.12).

The IE results presented in this Chapter have demonstrated conclusively that DETPMP MIC is mildly affected by $[H^+]$ or pH, whereas the HMTPMP MIC is severely affected by $[H^+]$ or pH. This is analogous to the effects of $[Ca^{2+}]$ and $[Mg^{2+}]$ upon the IE of these 2 SIs. It may indeed be the case that the EDTMPA MIC is also severely affected by variations in $[H^+]$. To determine the pH effect upon the EDTMPA MIC would require an extensive series of further experiments, since the range of [SI]s tested would have to span the predicted 2 and 22 hour MIC concentration levels. Based on the effect of pH on the DETPMP and HMTPMP MICs and the known effects of Ca^{2+} and Mg^{2+} on the IE of DETPMP, HMTPMP and EDTMPA, it is possible that the EDTMPA MIC would be severely affected (more affected than HMTPMP) by $[H^+]$, mirroring the known effects of $[Ca^{2+}]$ and $[Mg^{2+}]$. For example, perhaps the EDTMPA 80/20 NSSW/FW Base Case MIC << 400ppm at pH 6.5. The EDTMPA IE versus pH results presented in this Chapter (where a maximum in IE was achieved at pH 6.5) suggest this might be the case.

There were sometimes differences in IE at a specific pH (i.e. either pH 4.5 or pH 5.5), depending upon whether buffer was present or absent. Why this is observed also requires further study although it does not affect the broad conclusions of this Chapter.

Chapter 8: Mild Scaling Inhibition Efficiency Experiments

Chapter 8 Summary: This Chapter describes a series of milder scaling static barium sulphate IE experiments in which the FW [Ba^{2+}] is lower than that used in previous studies. In these experiments, FW [Ba^{2+}] = 100ppm instead of the normal level of 269ppm. SIs DETPMP, HMTPMP and PPCA are tested in these experiments. Again, as in Chapters 5 and 6, MIC levels are measured for various brine mix compositions under both Base Case and Fixed Case conditions of Ca^{2+}/Mg^{2+} molar ratio.

8.1 Introduction

A series of *mild scaling* static barium sulphate inhibition efficiency (IE) experiments were carried out testing SIs: DETPMP (penta-phosphonate), HMTPMP (penta-phosphonate) and PPCA (polymeric). *Mild scaling* denotes the Forties FW contained a much reduced concentration of barium, i.e. 100ppm Ba^{2+} (cf. severe scaling FW [Ba^{2+}] = 269ppm). Mild scaling IE testing were performed testing mixing ratios NSSW/Forties FW: (i) 30/70, (ii) 60/40 and (iii) 80/20 (i.e. the same mixing ratios NSSW/FW focused on in the severe scaling IE tests presented in Chapters 5, 6 and 7). The aforementioned SIs were tested under both mild scaling Base Case (MSBC) and mild scaling Fixed Case (MSFC) experimental conditions at 95^{o}C and pH5.5. In the Base Case (MSBC) experiments, the [Ca^{2+}] and [Mg^{2+}] vary as normal in a NSSW/FW mix. However, in the Fixed Case (MSFC) experiments, the [Ca^{2+}] and [Mg^{2+}] are both kept constant in the produced water: [Ca^{2+}] = 2000ppm and [Mg^{2+}] = 739ppm; molar ratio Ca^{2+}/Mg^{2+} is constant, = 1.64, this is the same molar ratio Ca^{2+}/Mg^{2+} found in pure Forties FW. The NSSW and FW brine compositions used for the MSBC and MSFC experiments are given in Chapter 3, Tables 3.1 (MSBC NSSW), 3.3 (MSFC NSSW), 3.10 (MSBC FW), 3.11 (MSFC FW) and 3.12 (MSFC FW Ca^{2+}, Mg^{2+} and Cl^{-}). It follows that in the MSFC experiments, any variation in MICs (between NSSW/Forties FW mixing ratios) must be due to changes in the magnitude of the barite saturation ratio (see Figure 8.1), and not due to changes in [Ca^{2+}] or [Mg^{2+}] – since both [Ca^{2+}] and [Mg^{2+}] are fixed. Figure 8.1 also shows (if any), largely ignorable, marginal changes in the barium sulphate saturation ratio on changing from Base Case to Fixed Case mixing scenarios – for both severe and mild scaling conditions.

In these mild scaling experiments, the [Ba^{2+}] in the produced water = (100*X)ppm; X = (FW% / 100). For example, for NSSW/FW mixing ratio 60/40, [Ba^{2+}] in the produced water = (100*0.4)ppm = 40ppm (cf. severe scaling 60/40 NSSW/FW produced water [Ba^{2+}] = (269*0.4) = 107.6ppm) – hence the barium sulphate saturation ratio is much lower, see Figure 8.1 (barium sulphate SR) and Figure 8.2 (precipitated barium sulphate). Clearly, the SI MIC levels are expected to be significantly lower in the mild scaling tests (e.g. ~10ppm for a 22 hour mild scaling MIC), however the principal aim of these experiments is to see if the same trends are observed for each SI tested (as observed in the severe scaling tests – Chapters 5 and 6), with regard to Ca^{2+} and Mg^{2+} effects.

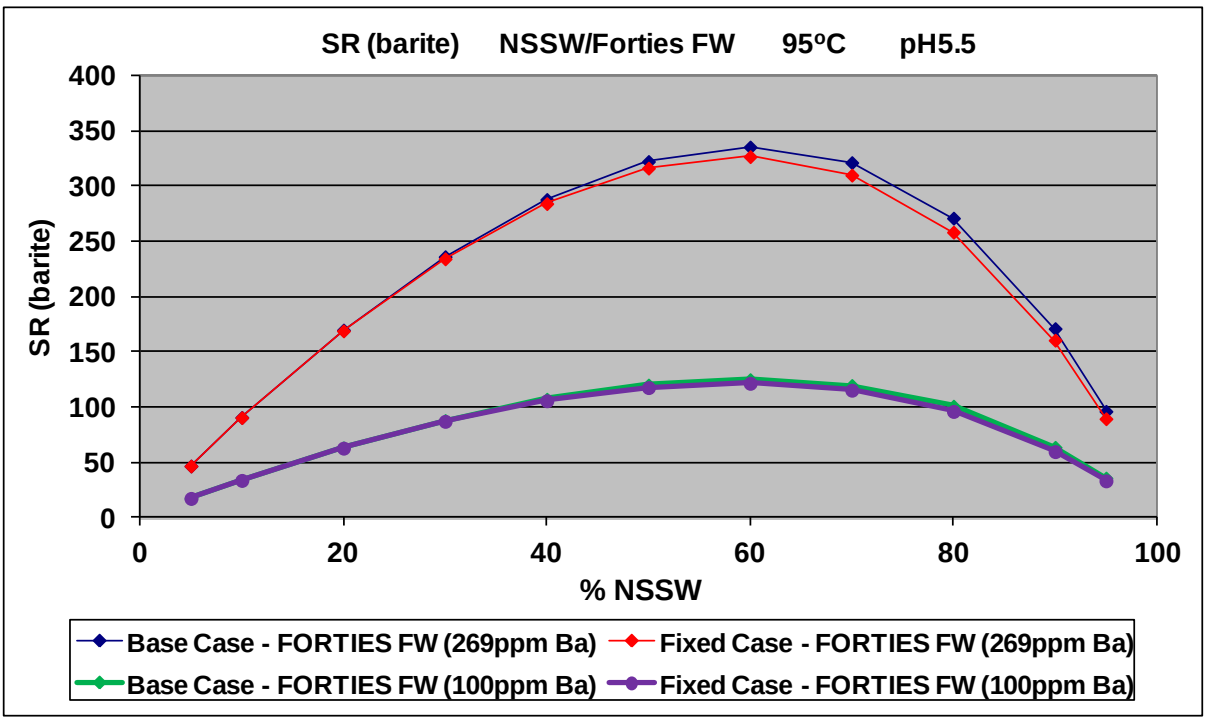

Figure 8.1 − Barium sulphate saturation ratio vs. mixing ratio NSSW/Forties FW – mild scaling (100ppm Ba^{2+} FW) and severe scaling (269ppm Ba^{2+} FW) systems. Fixed Case (i.e. fixed Ca^{2+} and Mg^{2+}) and Base Case (i.e. Ca^{2+} and Mg^{2+} varying) experimental conditions. T = 95ºC, pH = 5.5.

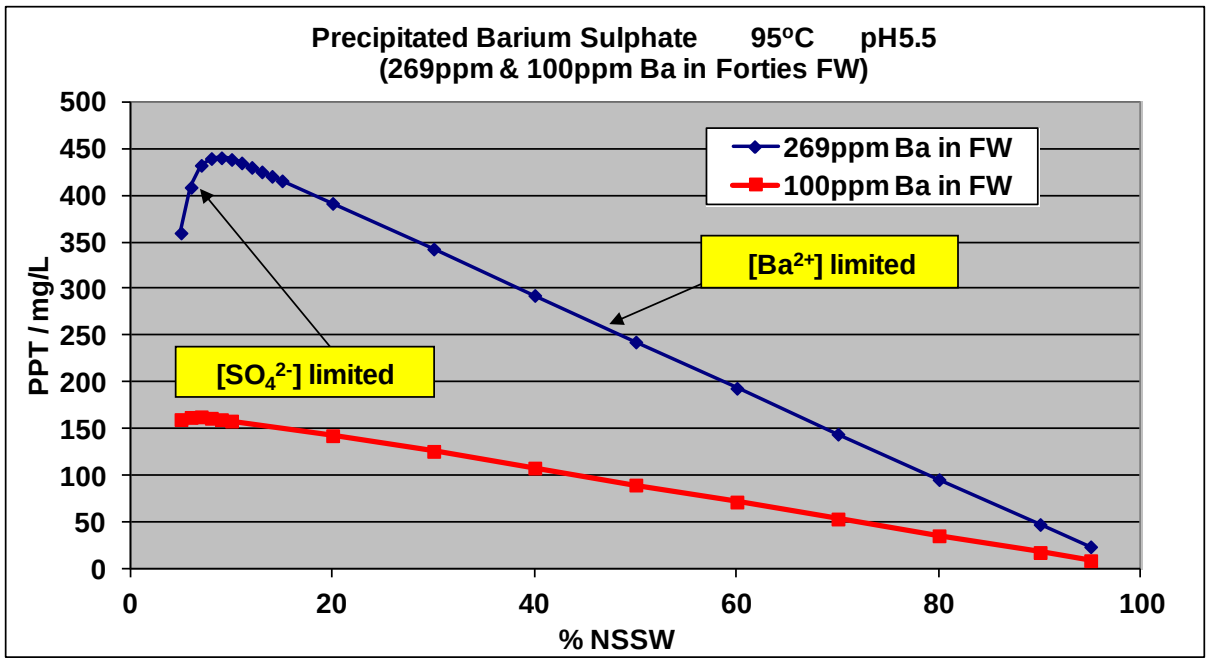

Figure 8.2 − Precipitated barium sulphate (mg/L) vs. mixing ratio NSSW/Forties FW – mild scaling (100ppm Ba^{2+} FW) and severe scaling (269ppm Ba^{2+} FW) conditions. T = 95°C, pH = 5.5.

8.2 DETPMP and HMTPMP (penta-phosphonates)

The mild scaling experimental MIC results, testing DETPMP, HMTPMP and PPCA have been presented in 2 different ways:

(i) MSBC and MSFC MIC are plotted together – separately for 2 and 22 hour sampling times; and

(ii) 2 hour MIC for DETPMP and HMTPMP are plotted together or for PPCA alone – separately for MSBC and MSFC test conditions. This procedure was repeated using the 22 hour MIC data.

All experimental results for DETPMP, HMTPMP and PPCA are first presented without comment in Figures 8.3 to 8.14. The results are fully discussed in Section 8.4.

8.2.1 MSBC MIC

Figures 8.3 and 8.4 present the 2 and 22 hour DETPMP and HMTPMP mild scaling brine mix MICs.

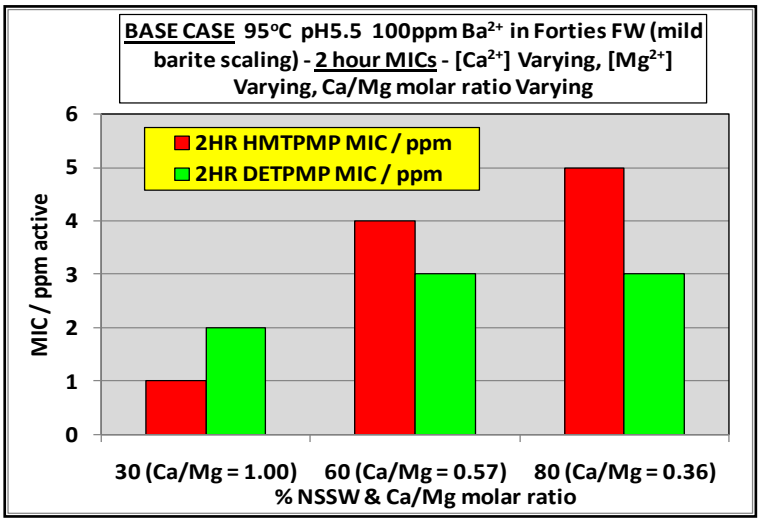

Figure 8.3 − 2 hour MSBC MICs for HMTPMP and DETPMP. 100ppm Ba^{2+} in FW, 95°C, pH5.5, NSSW/FW mixing ratios: 30/70, 60/40, and 80/20.

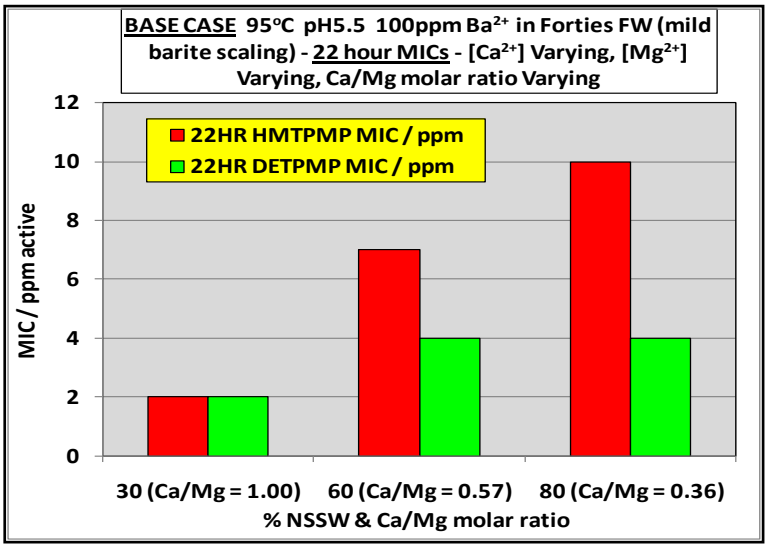

Figure 8.4 − 22 hour MSBC MICs for HMTPMP and DETPMP. 100ppm Ba^{2+} in FW, 95°C, pH5.5, NSSW/FW mixing ratios: 30/70, 60/40, and 80/20.

8.2.2 MSFC MIC

Figures 8.5 and 8.6 present the 2 and 22 hour DETPMP and HMTPMP MSFC MICs.

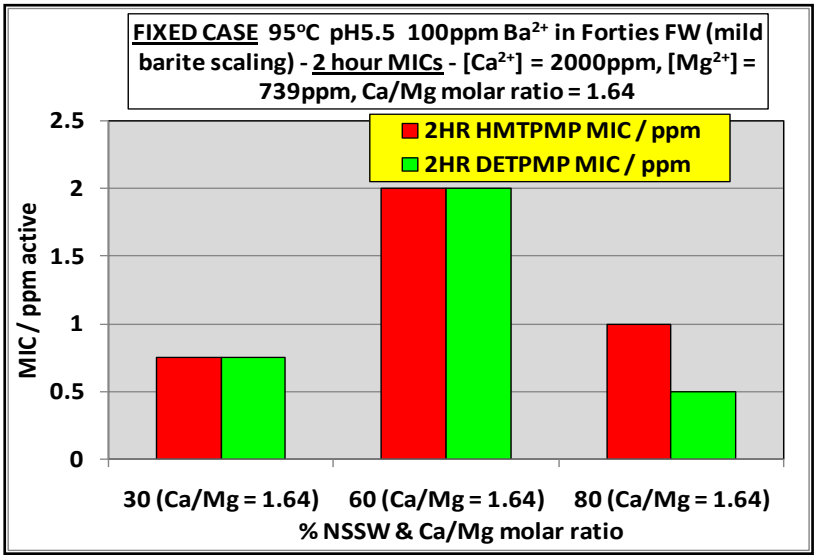

Figure 8.5 − 2 hour MSFC MICs for HMTPMP and DETPMP. 100ppm Ba^{2+} in FW, 95°C, pH5.5, NSSW/FW mixing ratios: 30/70, 60/40, and 80/20.

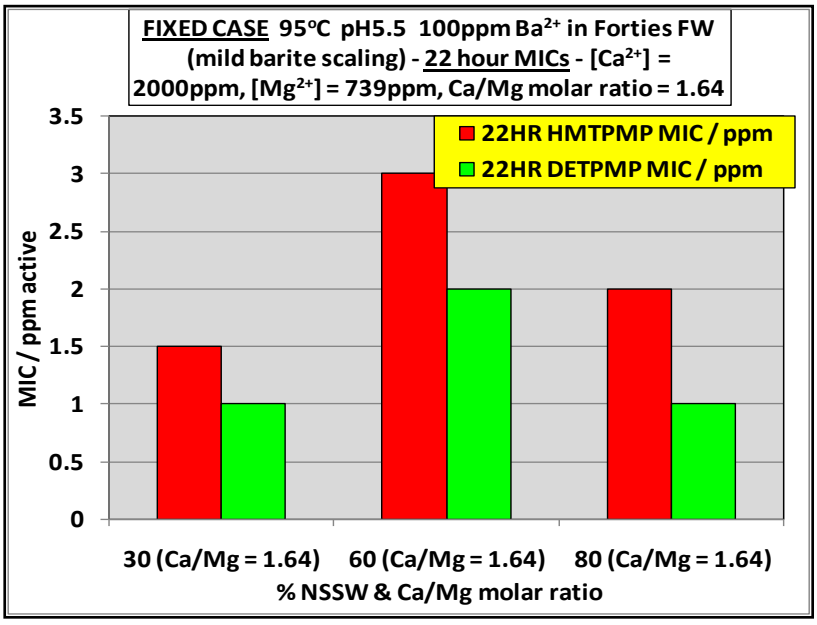

Figure 8.6 − 22 hour MSFC MICs for HMTPMP and DETPMP. 100ppm Ba^{2+} in FW, 95°C, pH5.5, NSSW/FW mixing ratios: 30/70, 60/40, and 80/20.

8.2.3 2 Hour MICs – MSBC and MSFC

Figures 8.7 and 8.8 present the 2 hour MSBC and MSFC DETPMP MICs plotted together for direct comparison.

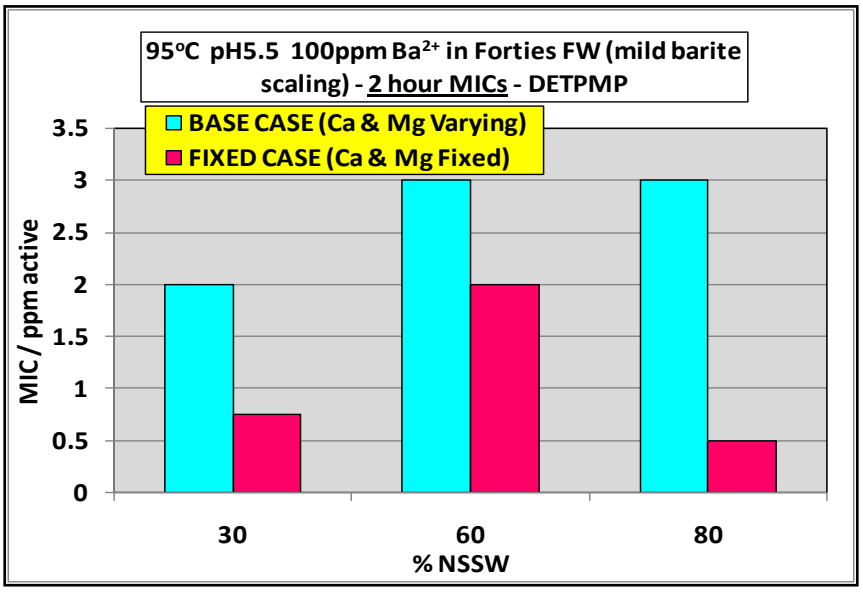

Figure 8.7 – 2 hour, MSBC and MSFC MICs (100ppm Ba^{2+} in the FW) for SI DETPMP. 95°C, pH5.5, NSSW/FW mixing ratios: 30/70, 60/40, and 80/20.

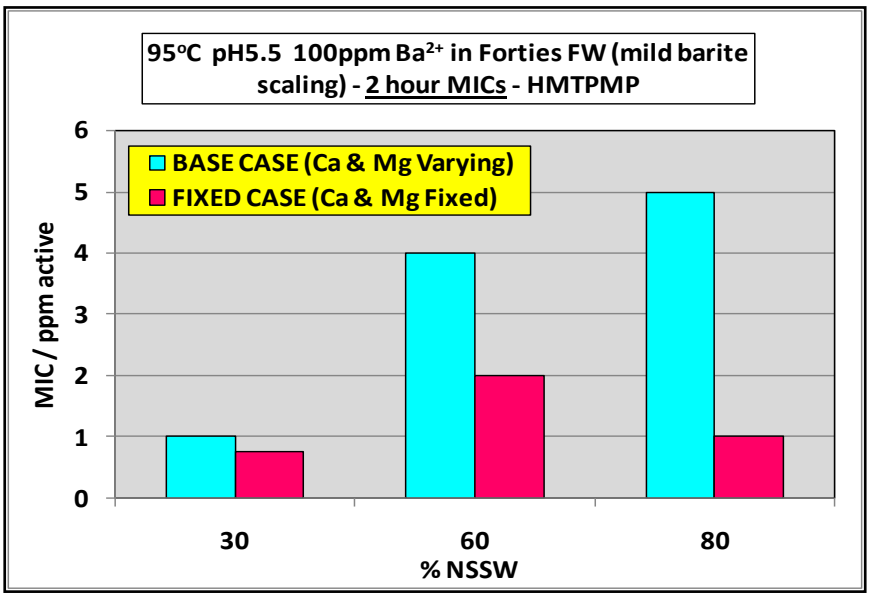

Figure 8.8 – 2 hour, MSBC and MSFC MICs (100ppm Ba^{2+} in the FW) for SI HMTPMP. 95°C, pH5.5, NSSW/FW mixing ratios: 30/70, 60/40, and 80/20.

8.2.4 22 Hour MICs – MSBC and MSFC

Figures 8.9 and 8.10 present the 22 hour MSBC and MSFC DETPMP and HMTPMP MICs plotted together for direct comparison.

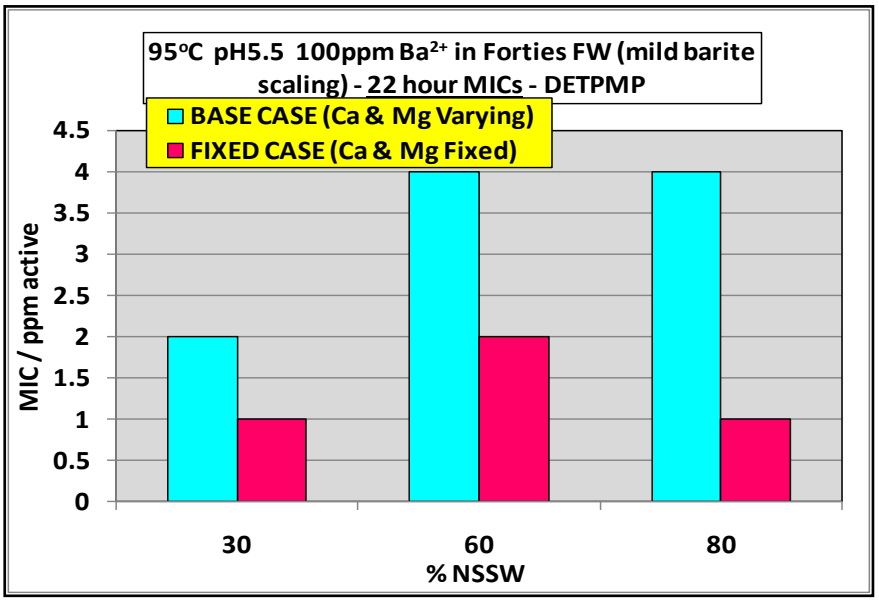

Figure 8.9 − 22 hour, MSBC and MSFC MICs (100ppm Ba^{2+} in the FW) for SI DETPMP. 95°C, pH5.5, NSSW/FW mixing ratios: 30/70, 60/40, and 80/20.

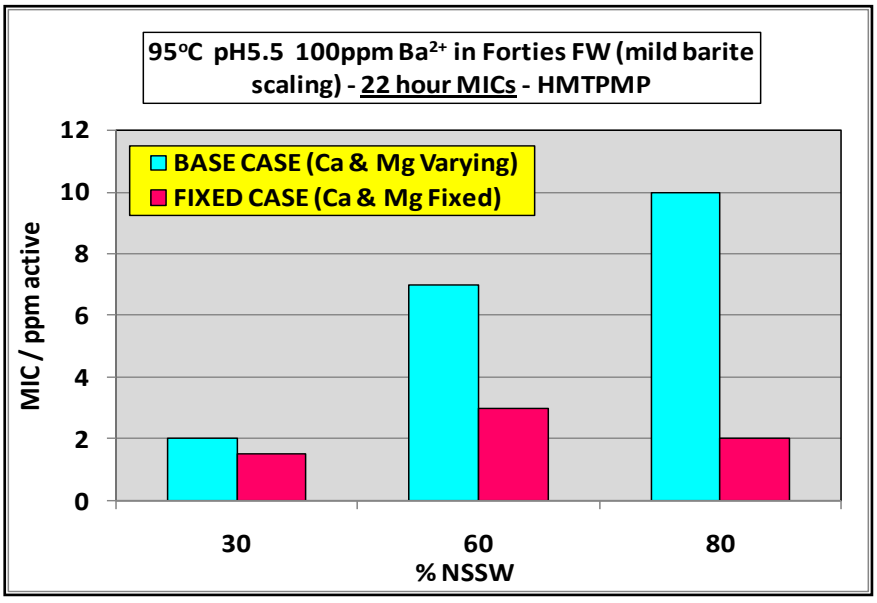

Figure 8.10 − 22 hour, MSBC and MSFC MICs (100ppm Ba^{2+} in the FW) for SI HMTPMP. 95°C, pH5.5, NSSW/FW mixing ratios: 30/70, 60/40, and 80/20.

8.3 PPCA (polymeric)

8.3.1 MSBC MIC

Figure 8.11 presents the 2 and 22 hour MSBC MICs for PPCA.

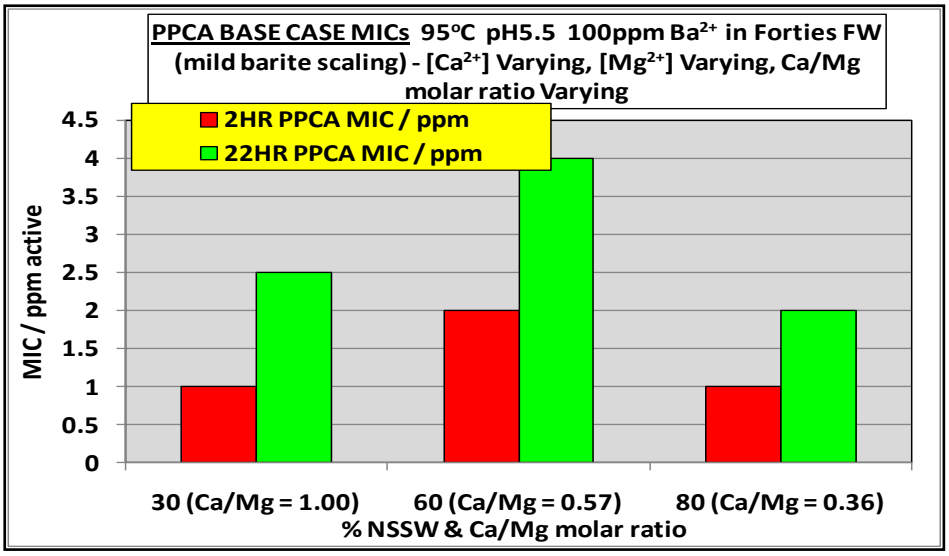

Figure 8.11 – 2 and 22 hour MSBC MICs for PPCA. 100ppm Ba^{2+} in FW, 95°C, pH5.5, NSSW/FW mixing ratios: 30/70, 60/40, and 80/20.

8.3.2 MSFC MIC

Figure 8.12 presents the 2 and 22 hour MSFC MICs for PPCA.

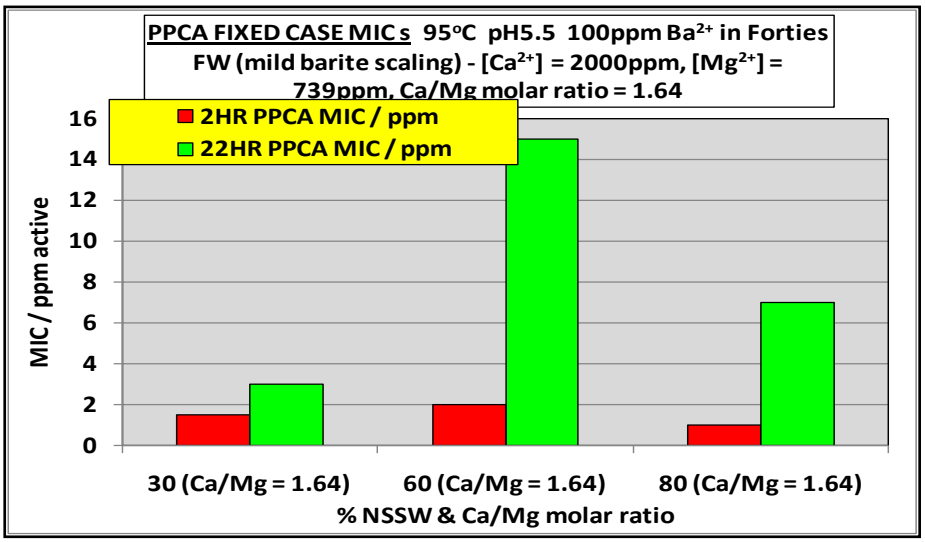

Figure 8.12 – 2 and 22 hour MSFC MICs for PPCA. 100ppm Ba^{2+} in FW, 95°C, pH5.5, NSSW/FW mixing ratios: 30/70, 60/40, and 80/20.

8.3.3 2 Hour MICs – MSBC and MSFC

Figures 8.13 presents the 2 hour MSBC and MSFC PPCA MICs plotted together for direct comparison.

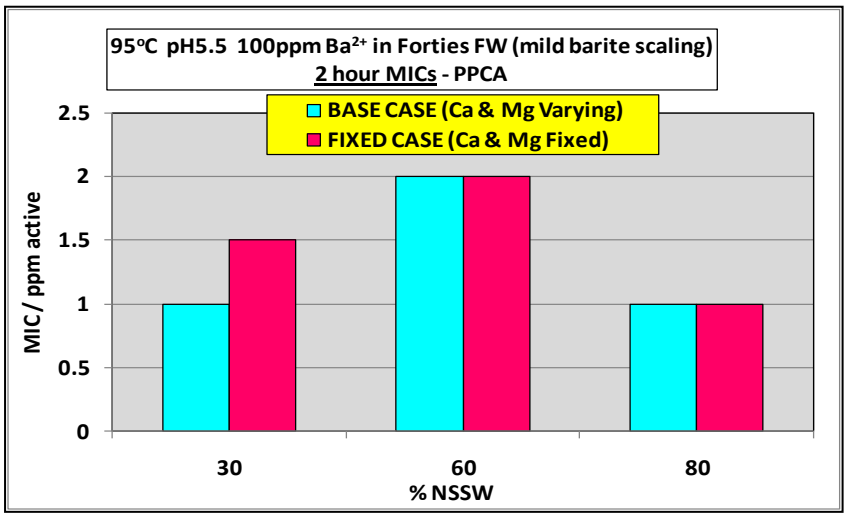

Figure 8.13 − 2 hour MSBC and MSFC MICs for PPCA. 100ppm Ba^{2+} in the FW, 95°C, pH5.5, NSSW/FW mixing ratios: 30/70, 60/40, and 80/20.

8.3.4 22 Hour MICs – MSBC and MSFC

Figures 8.14 presents the 22 hour MSBC and MSFC PPCA MICs plotted together for direct comparison.

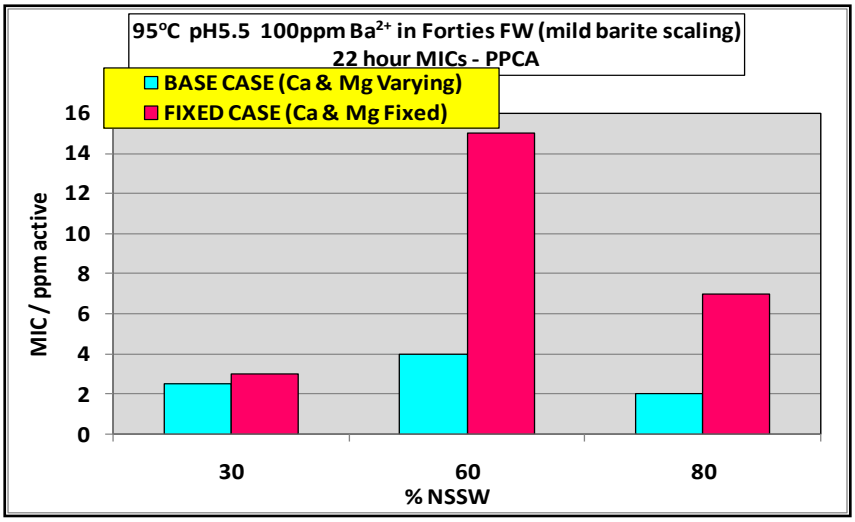

Figure 8.14 − 22 hour MSBC and MSFC MICs for PPCA. 100ppm Ba^{2+} in the FW, 95°C, pH5.5, NSSW/FW mixing ratios: 30/70, 60/40, and 80/20.

8.4 Summary and Conclusions

The series of experiments in this Chapter have illustrated that in a mild barium sulphate scaling system, SIs are affected by brine Ca^{2+} and Mg^{2+} in exactly the same way as observed in the more severe barium sulphate scaling system. The fundamental difference here is in the SI MIC levels – which are drastically reduced; for example, typically from ~50ppm (severe scaling system) to ~10ppm (mild scaling system) for a 60/40 NSSW/FW mix. In the severe scaling MIC vs. mixing ratio NSSW/FW experiments (i.e. Chapters 5 and 6), the barium content in the FW was 269ppm. In these mild scaling tests, this was reduced to 100ppm – the concentration of all other species in the system (i.e. NSSW/FW/produced water) being the same as in the severe scaling tests.

8.4.1 DETPMP and HMTPMP

When DETPMP and HMTPMP (both penta-phosphonates) were tested under mild scaling conditions, the highest 22 hour MIC for DETPMP was for the 60/40 and 80/20 NSSW/FW mixes (both = 4ppm, Figure 8.4 and/or Figure 8.9), whereas for HMTPMP, the highest 22 hour MIC was for the 80/20 NSSW/FW mix (=10ppm, Figure 8.4 and/or Figure 8.10). This is very similar to what was observed in severe scaling tests involving these species (Chapter 5). In the Base Case, severe scaling experiments, the highest HMTPMP 22 hour MIC was for the 80/20 NSSW/FW mix (=90ppm, see Chapter 5, Figure 5.3). The highest DETPMP 22 hour MIC was for the 60/40 NSSW/FW mix (=35ppm, see Chapter 5, Figure 5.3) – as would normally be expected, taking into consideration the barite saturation ratio levels (see Figure 8.1). Clearly, in both the mild scaling and severe scaling tests, the higher [Mg^{2+}] in the Base Case 80/20 NSSW/FW mix (=1242ppm) is causing the elevation of the HMTPMP 22 hour MIC. HMTPMP was previously identified as exhibiting "Type 2" IE behaviour – defined as being a high sensitivity to brine Ca^{2+} and Mg^{2+} (which has the primary influence on MIC) and poor long-term IE (at 22 hours). The DETPMP is also sensitive to Ca^{2+} and Mg^{2+}, but the effect is much less marked compared with HMTPMP. It is for this reason that the mild scaling 60/40 and 80/20 NSSW/FW DETPMP 22 hour MICs are equal and both much lower in value compared with HMTPMP. The barium sulphate saturation ratio (SR) for mixing ratio 80/20 NSSW/FW is lower than for 60/40 NSSW/FW (under mild scaling and severe scaling conditions, see Figure 8.1). Normally the 80/20 NSSW/FW MIC < 60/40 NSSW/FW MIC taking into account SR only, i.e. ignoring Ca^{2+}/Mg^{2+} effects.

In the Base Case mild scaling barium sulphate IE tests:

(i) 80/20 NSSW/FW 22hr DETPMP MIC = 60/40 NSSW/FW 22hr DETPMP MIC (see Figure 8.4 and/or Figure 8.9); and

(ii) 80/20 NSSW/FW 22hr HMTPMP MIC > 60/40 NSSW/FW 22hr HMTPMP MIC (see Figure 8.4 and/or Figure 8.10).

Both these observations are due to the detrimental effect of the higher [Mg^{2+}] in the 80/20 NSSW/FW mix, on the barium sulphate IE of DETPMP and HMTPMP – with HMTPMP being more sensitive to these divalent ions (type 2 behaviour).

When the IE tests were repeated (but with [Ca^{2+}] and [Mg^{2+}] fixed), i.e. MSFC tests, the 2 and 22 hour MICs for both DETPMP and HMTPMP then correlated very well with the saturation ratio (SR) level for the mixing ratio NSSW/FW tested – see Figure 8.5 (2 hour) and Figure 8.6 (22 hour). This is exactly the same trend observed in the Fixed Case, severe scaling IE tests, due to the effects of varying brine [Ca^{2+}] and [Mg^{2+}] being eliminated.

Thus, in the Fixed Case mild scaling barium sulphate IE tests:

(i) 80/20 NSSW/FW 22hr DETPMP MIC (=1ppm) < 60/40 NSSW/FW 22hr DETPMP MIC (=2ppm) (see Figure 8.6); and

(ii) 80/20 NSSW/FW 22hr HMTPMP MIC (=2ppm) < 60/40 NSSW/FW 22hr HMTPMP MIC (=3ppm) (see Figure 8.6).

The above observations would normally be expected, based on the mild scaling barium sulphate saturation ratio (SR) alone (see Figure 8.1).

In all mild scaling cases: 22hr DETPMP MIC < (or =) 22hr HMTPMP MIC (Figure 8.4 and Figure 8.6). This is because, overall, DETPMP is generally more efficient at preventing barium sulphate scale (in both mild and severe scaling brines). HMTPMP rarely performs better (i.e. has a lower MIC) than DETPMP. In fact, this has only ever occurred in high [Ca^{2+}] mixes, such as 20/80 and 30/70 Base Case – see Figure 5.3. In these rare cases where MIC HMTPMP < MIC DETPMP, the difference between the DETPMP and HMTPMP MICs is insignificant. The differences in the performance of DETPMP and HMTPMP may be partly due to molecular stereochemical reasons and differences in their binding constants (K_{Ca} and K_{Mg}); indeed, both of these factors are related. Structurally, it is only the number of methylene groups (–CH_2–) per molecule which differs between DETPMP and HMTPMP. A DETPMP molecule contains 4 methylene groups in the main carbon chain whereas HMTPMP contains 12. Their structures are presented in Chapter 3, Section 3.9.1.

8.4.2 PPCA

PPCA performed better in the MSBC IE experiments compared to the corresponding MSFC IE experiments (compare Figure 8.11 and Figure 8.12) – i.e. Base Case MIC < Fixed Case MIC. Once again, this is the same as observed in earlier severe scaling IE testing of PPCA (Chapter 6, Section 6.2.2; Shaw et al., 2010b). High brine [Ca^{2+}] of 2000ppm in the Fixed Case IE experiments (this applies to both mild and severe barite scaling tests) is detrimental to the IE of SI PPCA because it causes precipitation of a Ca–PPCA compound or complex (as discussed in Chapter 6, Section 6.2.1). The precipitated PPCA (as Ca–PPCA) is ineffective, resulting in a decline in the barium sulphate IE (%). PPCA is also affected by Ca^{2+} and Mg^{2+} in the same way as phosphonate SIs, i.e. a high [Mg^{2+}] is detrimental, and a severe level of Ca^{2+} (e.g. up to ~1000ppm) is beneficial., At calcium concentrations > ~1000ppm, precipitation of a Ca–PPCA compound begins to occur, resulting in poorer IE and thus, higher MICs. At lower to moderate [Ca^{2+}] levels – PPCA will perform well – because the [Ca^{2+}] is not yet high enough to result in incompatibility with PPCA (i.e. precipitation of Ca–PPCA).

Chapter 9: Phosphonate SI Consumption Experiments, ESEM & EDAX

Chapter 9 Summary: In this Chapter, [SI] is assayed in addition to [Ba^{2+}] in static barium sulphate IE experiments, thus obtaining two result profiles: IE vs. time and %SI remaining in solution vs. time. These latter experimental results are referred to as "SI consumption" profiles. The SI consumption behaviour of the Type 1 and Type 2 phosphonate SIs is determined. These experiments are carried out over much longer residence times, compared to in the standard IE experiments (Chapters 5 and 6), i.e. up to 96 hours rather than the usual 22 hours, and multiple sampling times are involved (up to ~10). ESEM images of some scale deposits formed during static IE tests are also obtained, together with EDAX analyses of these deposits. In this Chapter, the differences in the SI consumption behaviour of the Type 1 and Type 2 phosphonate species and the significance of the ESEM/EDAX data are discussed.

9.1 Introduction

It has been demonstrated previously in this thesis that there are differences in how the various phosphonate SIs perform in static barium sulphate IE experiments. This led us to introduce the Type 1 / Type 2 classification described in Chapter 5. In order to investigate this issue further, an extensive series of experiments monitoring the level of SI in solution at various times during a Base Case or Fixed Case IE experiment after the mixing of NSSW and Forties FW were performed. These experiments are referred to as "SI consumption" experiments. How SI consumption (i.e. depletion from solution) correlates with IE is investigated. In this work, all the phosphonate SIs mentioned in this thesis were tested (except EABMPA). The molar ratio Ca^{2+}/Mg^{2+} affects the level of SI consumption; this finding is illustrated in this Chapter. Several sampling times (~10) were involved in such experiments and the sampling occurred frequently over several days (sometimes up to 96 hours, i.e. 4 days after initial mixing NSSW/FW). The normal time when an IE test is stopped is 22 hours. The objective of this study was to investigate if there were any differences in the extent of SI consumption (i.e. depletion from solution, possibly incorporating the SI into the growing barite lattice) between the different SI types and to see if this gives us any clues as to the inhibition mechanism that these species operate through (Gill and Varsanik, 1986; Sorbie and Laing,

2004). The factor that led us to examine SI consumption was that the Type 1 species appear to show similar IE at 2 and 22 hours whereas the IE of Type 2 species usually declines markedly over time.

Many SI consumption type experiments have been performed (>100), under both Base Case (Ca^{2+}/Mg^{2+} molar ratio varying) and Fixed Case (Ca^{2+}/Mg^{2+} molar ratio fixed) experimental conditions, and a pattern has emerged. Assay for [SI] is easily carried out by ICP spectroscopy by detecting [P] (Boak and Sorbie, 2010). In addition, solid scale deposits formed during some of these SI consumption IE tests were analysed by ESEM/EDAX. Differences in the crystal structures and EDAX scale deposit compositions, between blank samples (no SI present), Type 1 SI-containing and Type 2 SI-containing deposits is examined and discussed.

9.2 Base Case, 50/50 NSSW/FW – OMTHP, DETPMP, HMTPMP, HMDP and NTP

- Sampling times = 0.5, 1, 2, 4, 6 and 22 hours after mixing NSSW/FW.
- T = 95^{o}C, pH 5.5.
- [OMTHP] = 4ppm, [DETPMP] = 10ppm, [HMTPMP] =16ppm. [HMDP] = 25ppm, [NTP] = 40ppm.
- Molar ratio Ca^{2+}/Mg^{2+} (mix) = 0.70.

Results for these experiments are shown in Figures 9.1–9.5, where graphs of IE(%) and %SI in solution at various residence times are presented, testing each SI at a given fixed initial concentration. The SI concentration levels in these experiments are set somewhat below the 2 hour MIC for the various species, since the correspondence between IE decline and the SI consumption is being investigated. The Ca^{2+}/Mg^{2+} molar ratio in the Base Case 50/50 brine mix = 0.70.

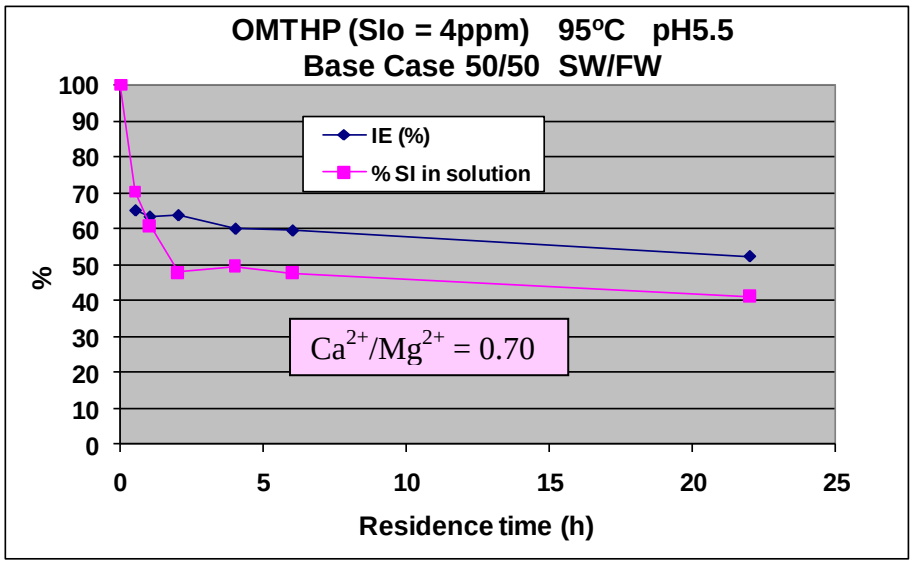

Figure 9.1 – Graph of IE (%) and %SI in solution vs. time, testing OMTHP at 4ppm, Base Case 50/50 NSSW/FW, 95°C, pH5.5.

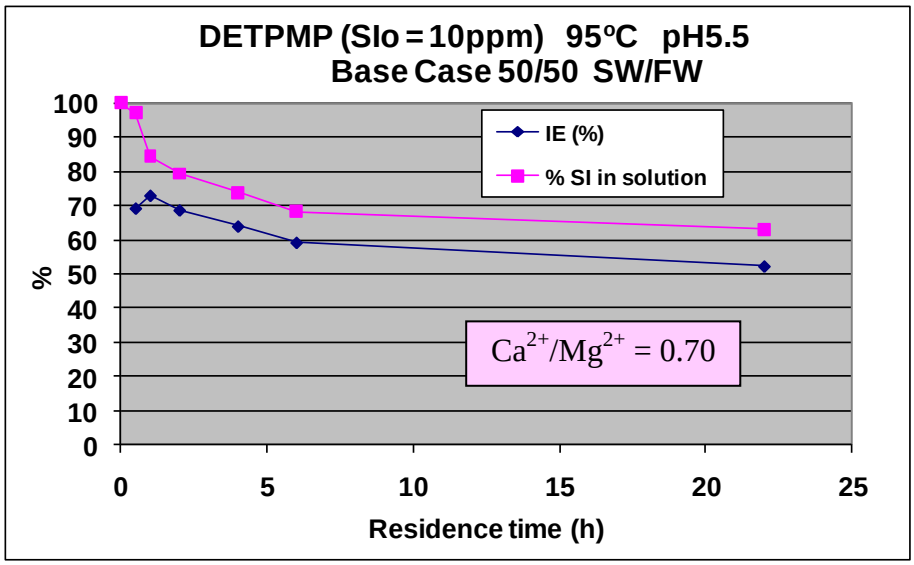

Figure 9.2 – Graph of IE (%) and %SI in solution vs. time, testing DETPMP at 10ppm, Base Case 50/50 NSSW/FW, 95°C, pH5.5.

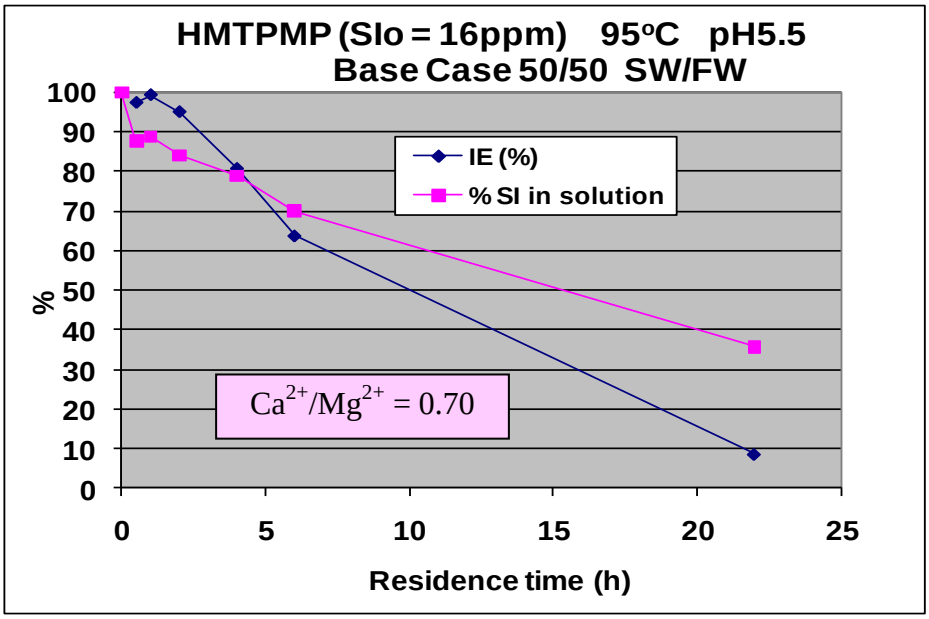

Figure 9.3 – Graph of IE (%) and %SI in solution vs. time, testing HMTPMP at 16ppm, Base Case 50/50 NSSW/FW, 95°C, pH5.5.

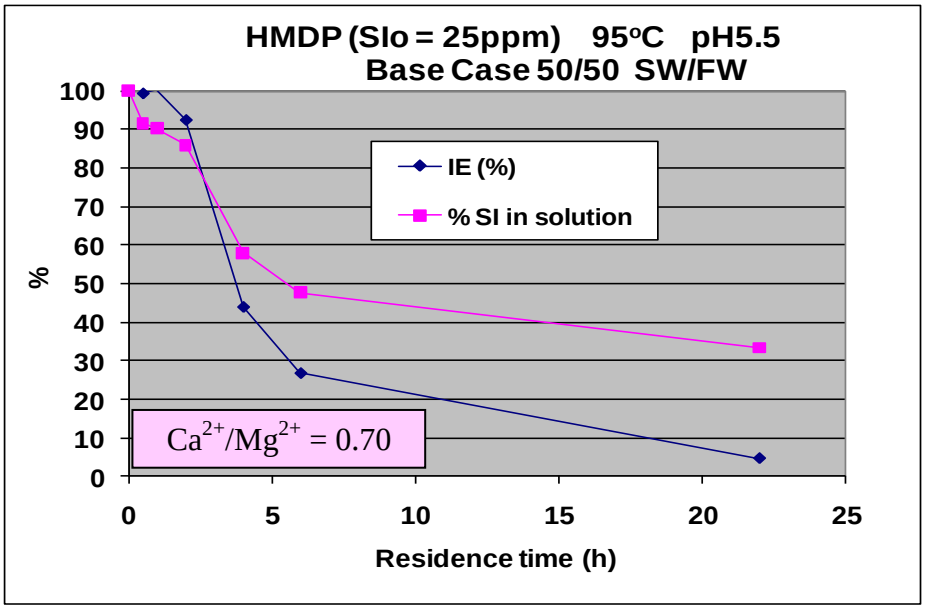

Figure 9.4 – Graph of IE (%) and %SI in solution vs. time, testing HMDP at 25ppm, Base Case 50/50 NSSW/FW, 95°C, pH5.5.

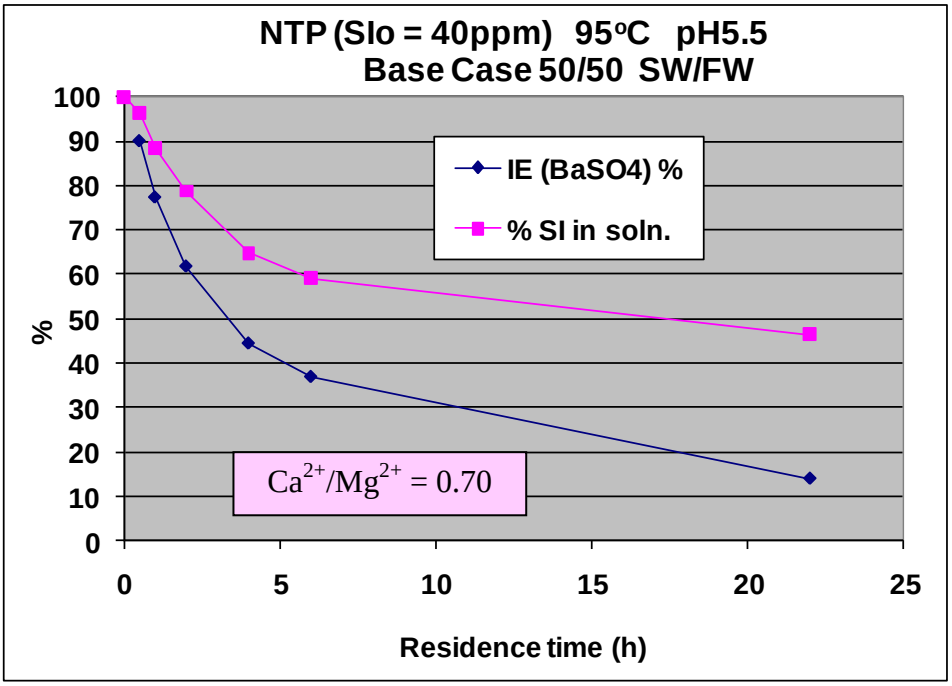

Figure 9.5 – Graph of IE (%) and %SI in solution vs. time, testing NTP at 40ppm, Base Case 50/50 NSSW/FW, 95°C, pH5.5.

9.3 DETPMP – 50/50 NSSW/FW, Molar Ratios Ca^{2+}/Mg^{2+} = 1, 2 and 4, Fixed [SI] = 5ppm

9.3.1 9.3.1 SI Consumption Experiment

- Sampling times = 0.5, 1, 2, 4, 6 and 22 hours after mixing NSSW/FW.
- T = 95°C, pH 5.5.
- In all cases, the total number of moles of divalent ions (Ca^{2+} + Mg^{2+}) in the produced water = 0.05 mol/L.
- Three brine mix compositions were tested: molar ratios Ca^{2+}/Mg^{2+} = 1, 2 and 4.
- The NSSW and FW brine compositions used for this experiment are given in Chapter 3, Tables 3.3, 3.4 and 3.6.
- Fixed [DETPMP] = 5ppm.

Figure 9.6 presents the [Ba^{2+}] in solution versus time for the 3 brine conditions: molar ratios Ca^{2+}/Mg^{2+} = 1, 2 and 4, in the blank (SI-free) *and* SI-containing test bottles. Note that duplicate blank samples are required for each brine composition – total number of "blank"

test bottles = 6. From the [Ba^{2+}] versus time data (for blank and SI-containing) samples, and control [Ba^{2+}]s, it is possible to calculate the IE versus time – this is presented in Figure 9.7 for the 3 brine conditions. Figure 9.8 presents the supernatant [DETPMP] at the various sampling times, for the 3 brine conditions.

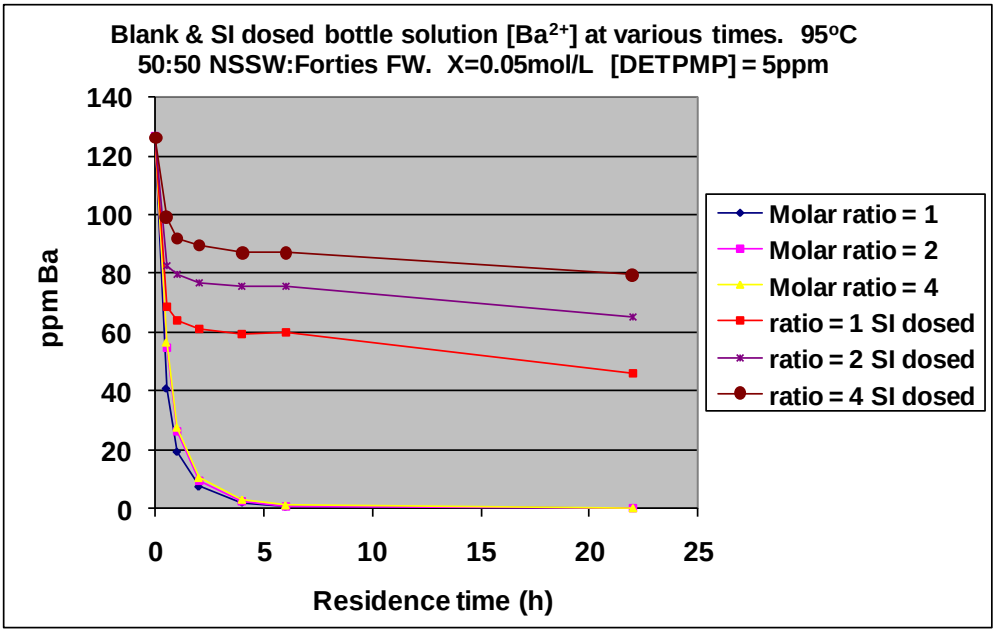

Figure 9.6 – [Ba^{2+}] in solution vs. time for blank and DETPMP-containing bottles where the produced water molar ratio Ca^{2+}/Mg^{2+} = 1, 2 and 4. In all cases the initial [DETPMP] = 5ppm active. 95°C, pH5.5.

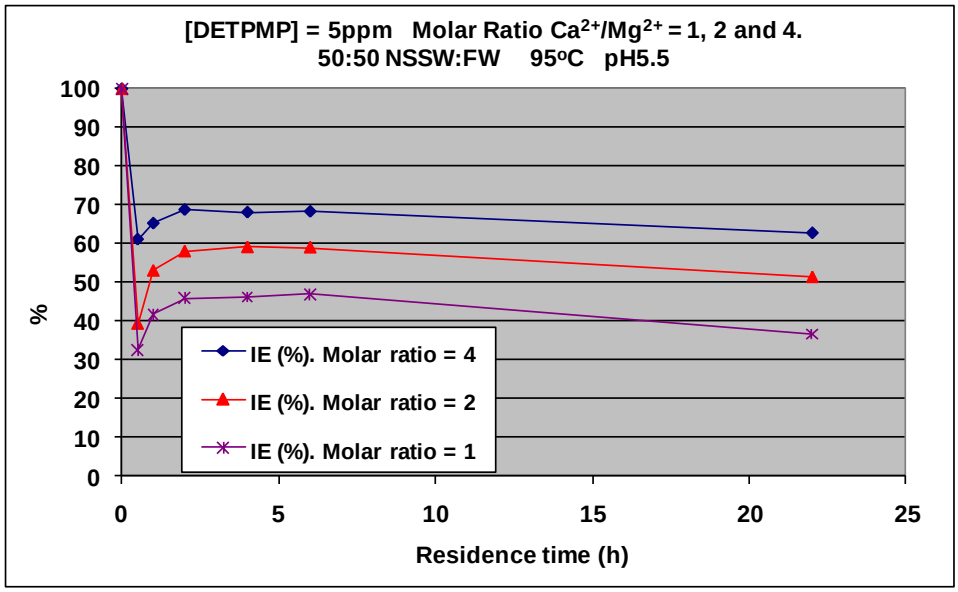

Figure 9.7 – IE(%) vs. time for DETPMP-containing bottles where the produced water molar ratio Ca^{2+}/Mg^{2+} = 1, 2 and 4. In all cases the initial [DETPMP] = 5ppm active. 95°C, pH5.5.

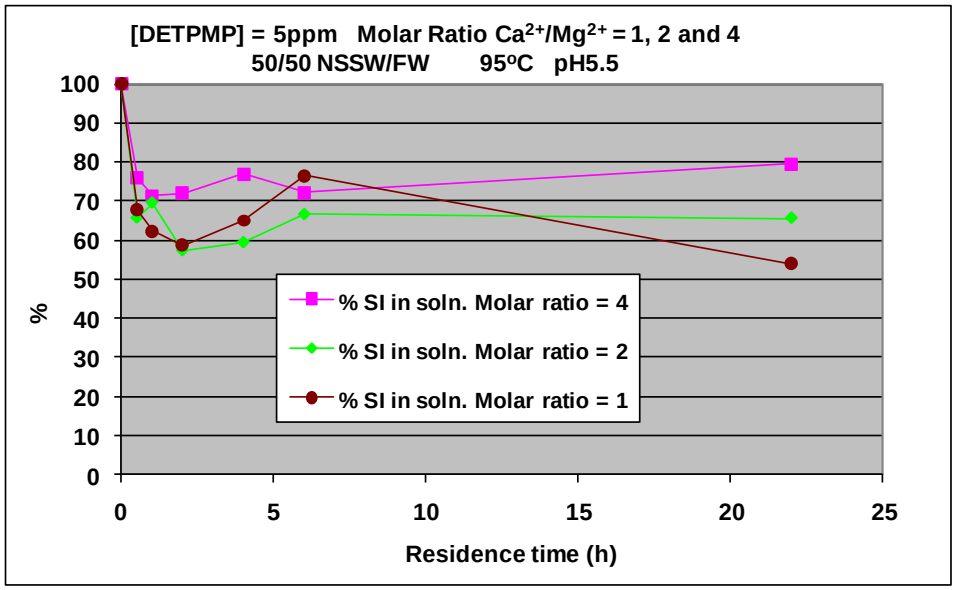

Figure 9.8 – %SI in solution vs. time for DETPMP-containing bottles where the produced water molar ratio Ca^{2+}/Mg^{2+} = 1, 2 and 4. In all cases the initial [DETPMP] = 5ppm active. 95°C, pH5.5.

9.3.2 ESEM Images of Scale Deposits and EDAX Analyses

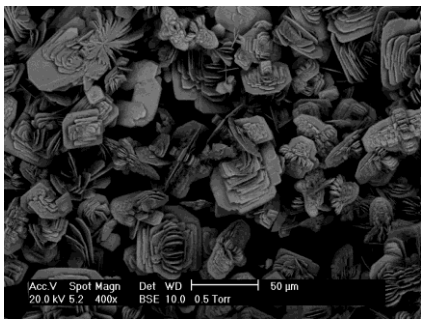

(a) = Blank (Ca/Mg = 1)

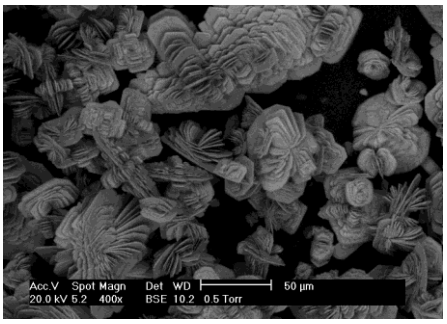

(b) = Blank (Ca/Mg = 2)

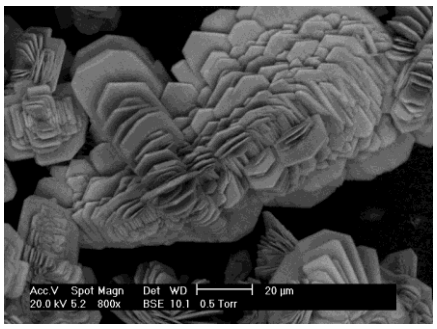

(c) = Blank (Ca/Mg = 2)

(d) = Blank (Ca/Mg = 4)

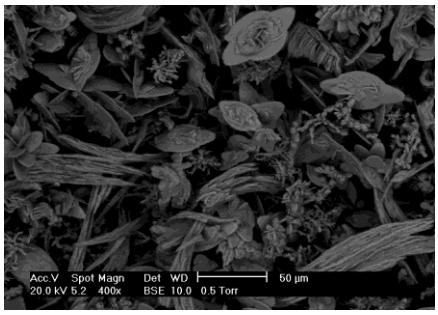

(e) = DETPMP-containing (Ca/Mg = 1)

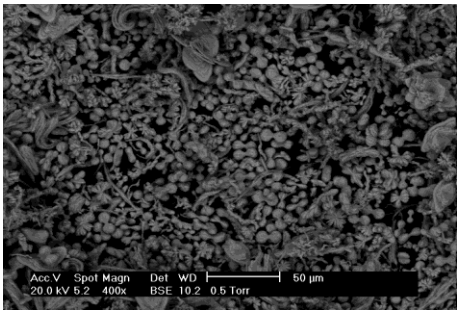

(f) = DETPMP-containing (Ca/Mg = 2)

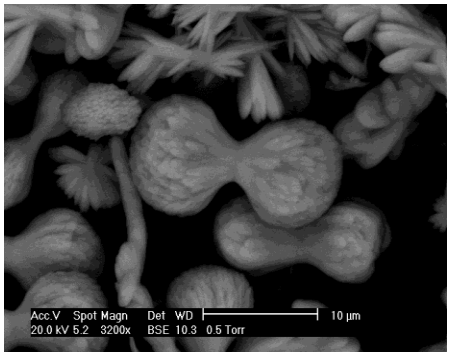

(g) = DETPMP-containing (Ca/Mg = 2)

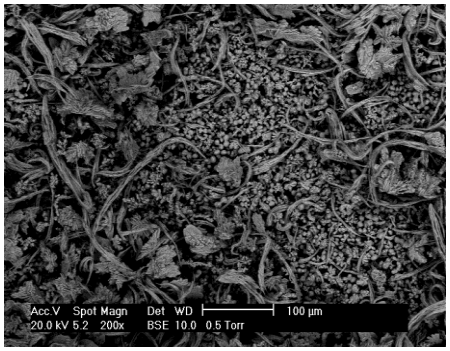

(h) = DETPMP-containing (Ca/Mg = 4)

Figure 9.9(a)−(h) – ESEM images of scale deposits (blanks and DETPMP-containing).

Element	Theoretical Atomic % 50/50 Ca/Mg=1 *	Theoretical Atomic % 50/50 Ca/Mg=2 *	Theoretical Atomic % 50/50 Ca/Mg=4 *	Experimental Atomic % (blank 50/50 Ca/Mg=1)	Experimental Atomic % (blank 50/50 Ca/Mg=2)	Experimental Atomic % (blank 50/50 Ca/Mg=4)	5ppm DETPMP 50/50 Ca/Mg=1	5ppm DETPMP 50/50 Ca/Mg=2	5ppm DETPMP 50/50 Ca/Mg=2 (2nd analysis)	5ppm DETPMP 50/50 Ca/Mg=4
Ba	3.61	3.62	3.62	5.45	5.19	3.42	9.75	15.72	11.29	11.29
Sr	13.05	13.05	13.05	15.19	15.25	13.76	7.52	5.72	6.77	6.31
Ca	0.00	0.00	0.00	1.72	1.95	1.44	1.93	1.94	1.82	2.35
S	16.67	16.67	16.67	19.45	17.79	17.57	16.87	18.95	17.04	16.22
O	66.67	66.67	66.67	58.19	59.83	63.81	63.93	56.14	63.08	63.83
P	0.00	0.00	0.00	0.00	0.00	0.00	0.00	1.53	0.00	0.00
SUM	100.00	100.01	100.01	100.00	100.01	100.00	100.00	100.00	100.00	100.00

* Data obtained from MultiScale software.

Table 9.1 – Theoretical atomic % Ba, Sr, Ca, S, O and P in scale deposits, obtained from MultiScale and the experimental values for comparison.

9.4 OMTHP, DETPMP, HMTPMP and HMDP – Varying [SI], 60/40 and 80/20 NSSW/FW, Base Case and Fixed Case

In these experiments, all 4 SIs - OMTHP, DETPMP, HMTPMP and HMDP - were tested at various threshold [SI], either pre-2 hour MIC or pre-22 hour MIC such that detectable declines in solution [SI] and [Ba^{2+}] could be observed over time. Furthermore, mixing ratios NSSW/FW 60/40 and 80/20 were chosen because mixing ratio 60/40 represents the highest SR level and 80/20 was the mixing ratio for which the highest Type 2 phosphonate SI MICs were measured (see Chapter 5). In addition, these consumption tests were carried out under Base Case and Fixed Case experimental conditions over 48 hours. Sampling times = ½, 1, 2, 4, 6, 22, 48 and sometimes also 72 hours after mixing NSSW/FW.

9.4.1 60/40 NSSW/FW, Base Case, Molar Ratio Ca^{2+}/Mg^{2+} = 0.57

Note: OMTHP was tested at 6ppm in this Base Case experiment, however, these results have been presented in Section 9.5.1 where all 4 SIs are tested at 6ppm.

Figures 9.10−9.12 present the IE and supernatant [SI] versus time profiles for DETPMP at 25ppm, HMTPMP at 35ppm and HMDP at 35ppm respectively (all pre-22 hour 60/40 Base Case MICs).

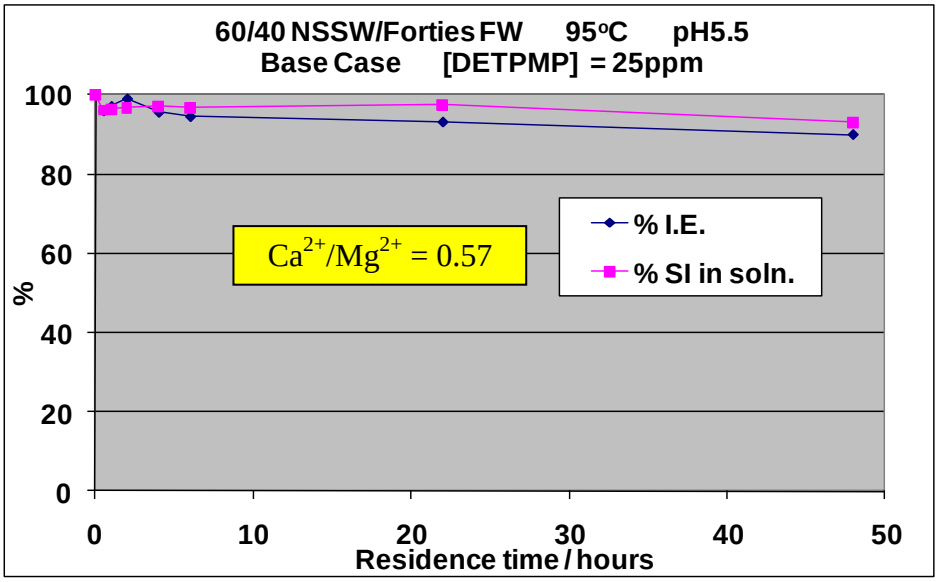

Figure 9.10 – Base Case IE and %SI vs. time, testing DETPMP at 25ppm. 60/40 NSSW/Forties FW, 95°C, pH5.5.

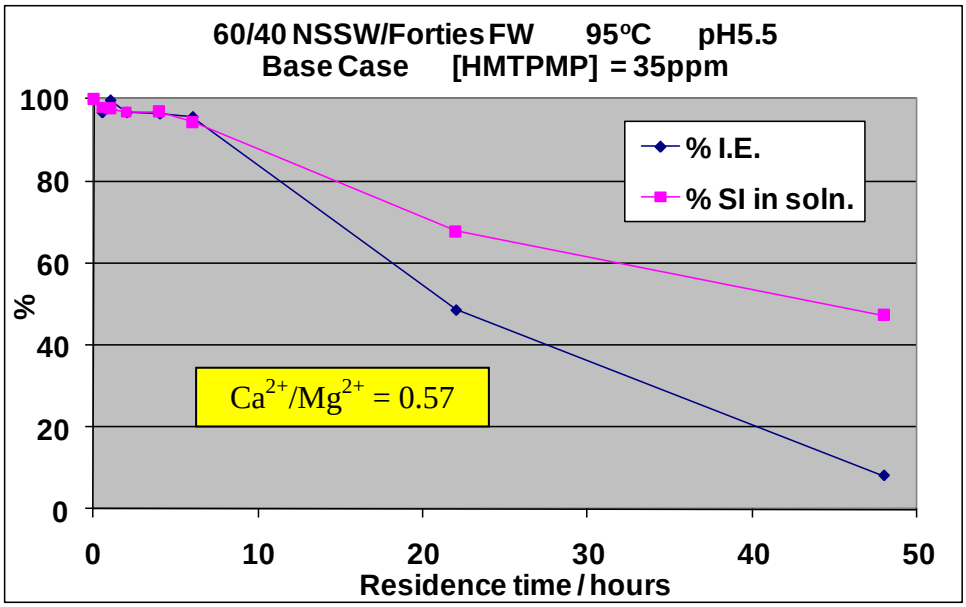

Figure 9.11 – Base Case IE and %SI vs. time, testing HMTPMP at 35ppm. 60/40 NSSW/Forties FW, 95°C, pH5.5.

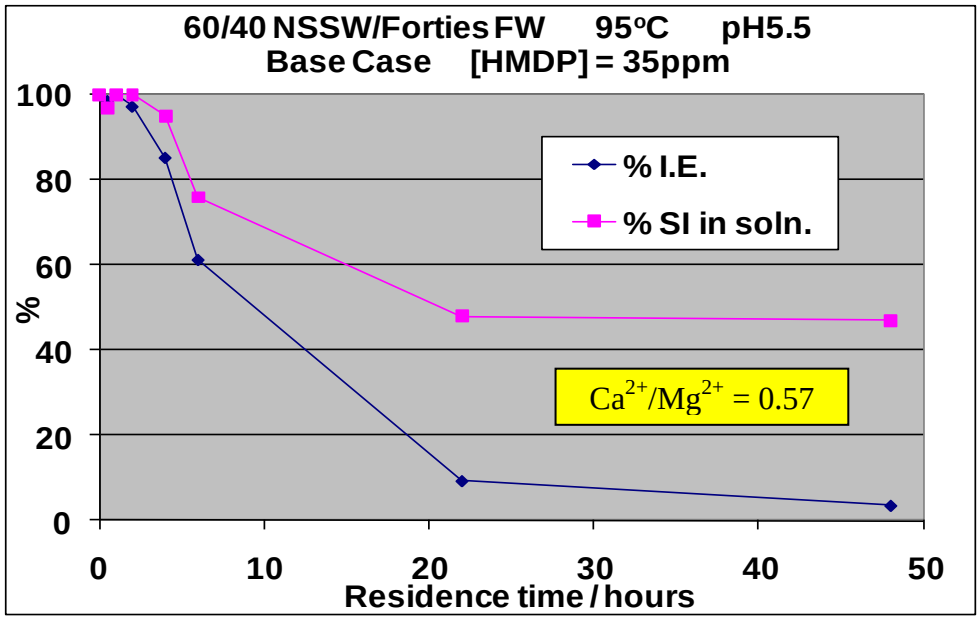

Figure 9.12 – Base Case IE and %SI vs. time, testing HMDP at 35ppm. 60/40 NSSW/Forties FW, 95°C, pH5.5.

9.4.2 60/40 NSSW/FW, Fixed Case, Molar Ratio Ca^{2+}/Mg^{2+} = 1.64

Figures 9.13−9.16 present the IE and supernatant [SI] versus time profiles for OMTHP at 3ppm, DETPMP at 8ppm, HMTPMP at 8ppm and HMDP at 12ppm respectively (all pre-2 hour 60/40 Fixed Case MICs).

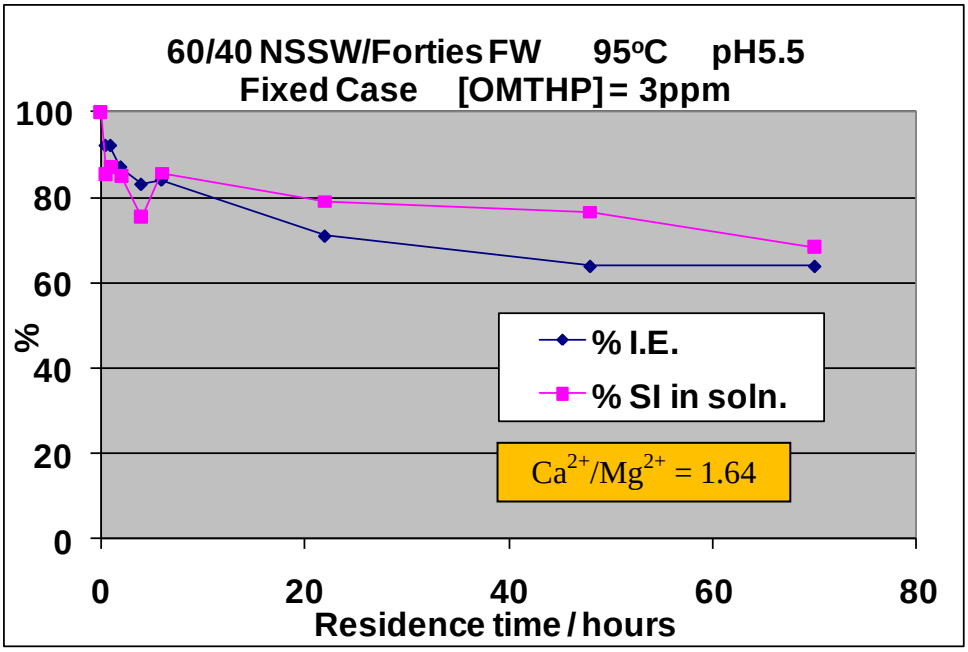

Figure 9.13 – Fixed Case IE and %SI vs. time, testing OMTHP at 3ppm. 60/40 NSSW/Forties FW, 95°C, pH5.5.

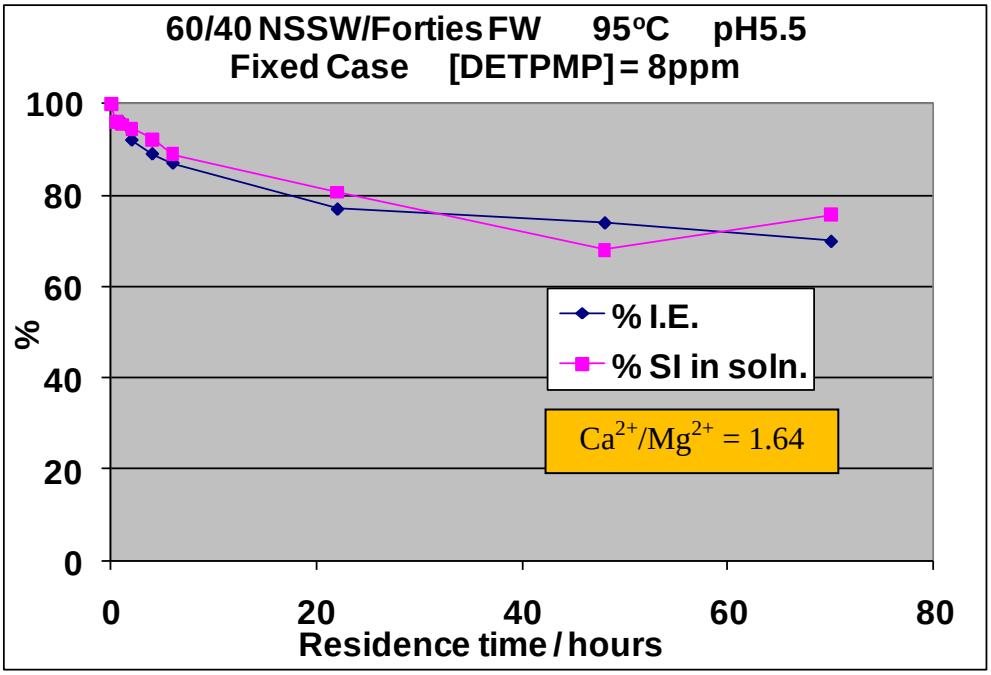

Figure 9.14 – Fixed Case IE and %SI vs. time, testing DETPMP at 8ppm. 60/40 NSSW/Forties FW, 95°C, pH5.5.

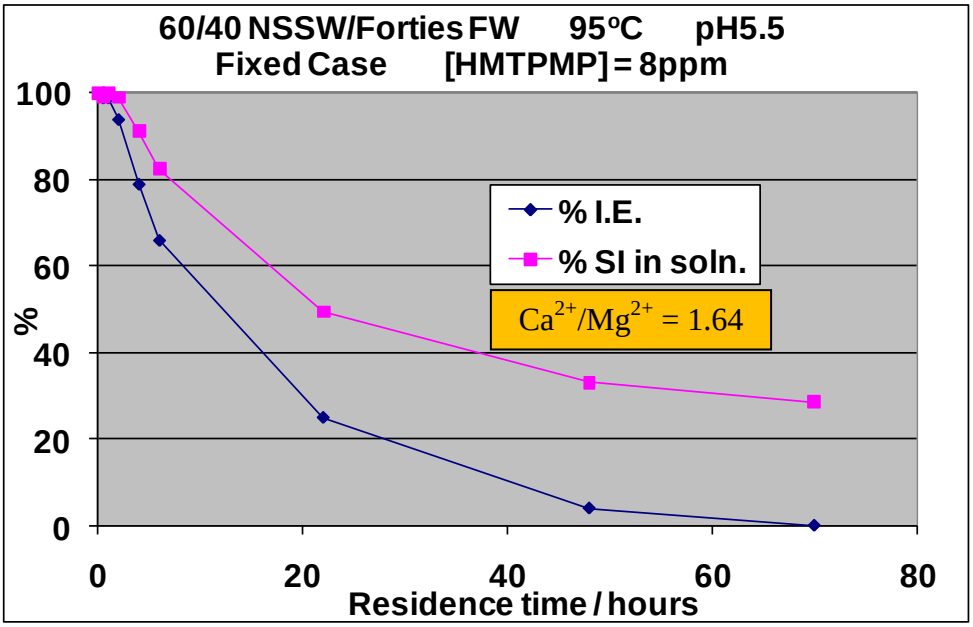

Figure 9.15 – Fixed Case IE and %SI vs. time, testing HMTPMP at 8ppm. 60/40 NSSW/Forties FW, 95°C, pH5.5.

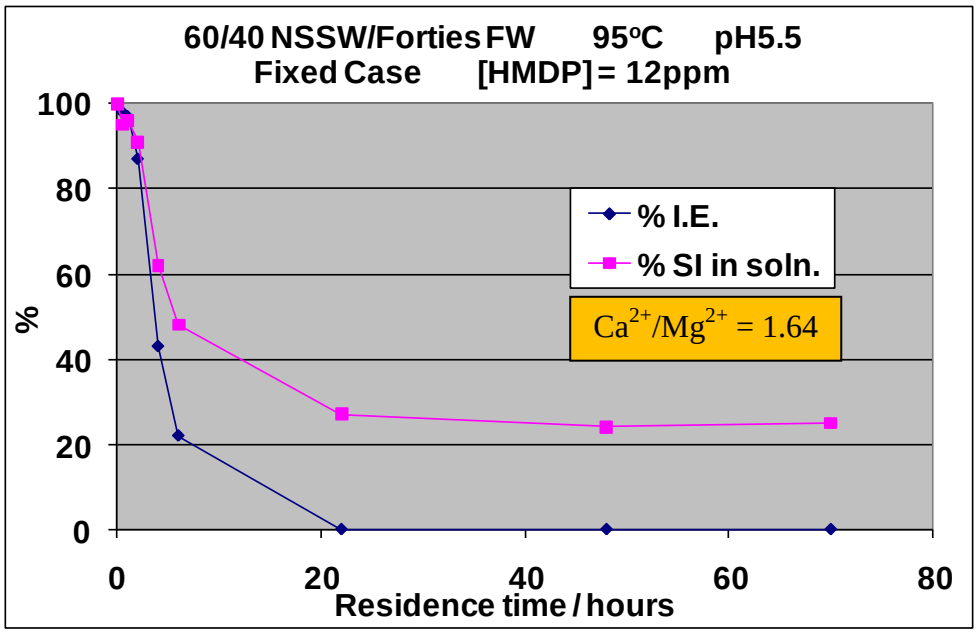

Figure 9.16 – Fixed Case IE and %SI vs. time, testing HMDP at 12ppm. 60/40 NSSW/Forties FW, 95°C, pH5.5.

9.4.3 80/20 NSSW/FW, Base Case, Molar Ratio Ca^{2+}/Mg^{2+} = 0.36

Figures 9.17−9.20 present the IE and supernatant [SI] versus time profiles for OMTHP at 4ppm, DETPMP at 15ppm, HMTPMP at 70ppm and HMDP at 60ppm respectively (all pre-22 hour 80/20 Base Case MICs).

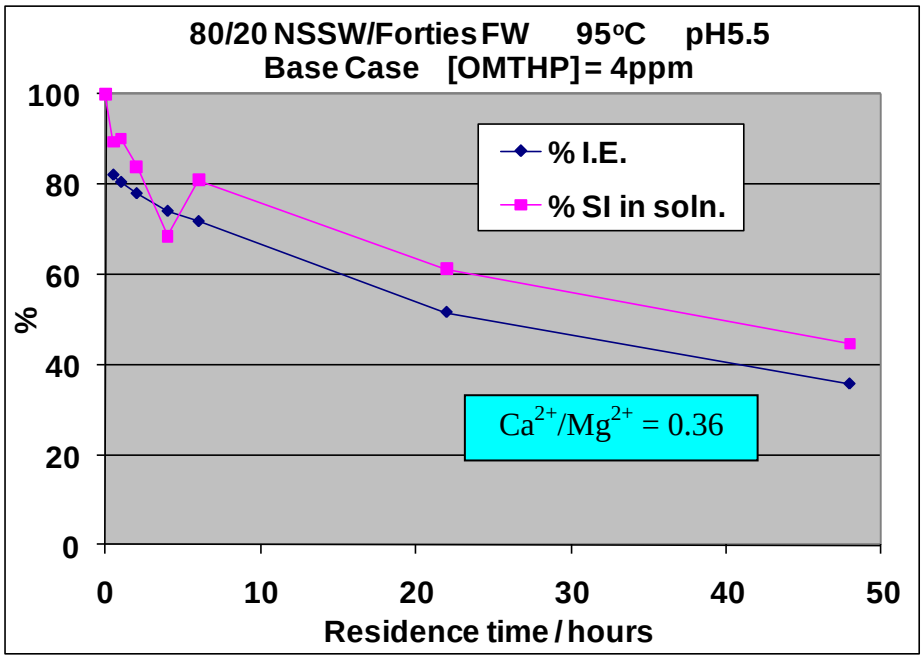

Figure 9.17 – Base Case IE and %SI vs. time, testing OMTHP at 4ppm. 80/20 NSSW/Forties FW, 95°C, pH5.5.

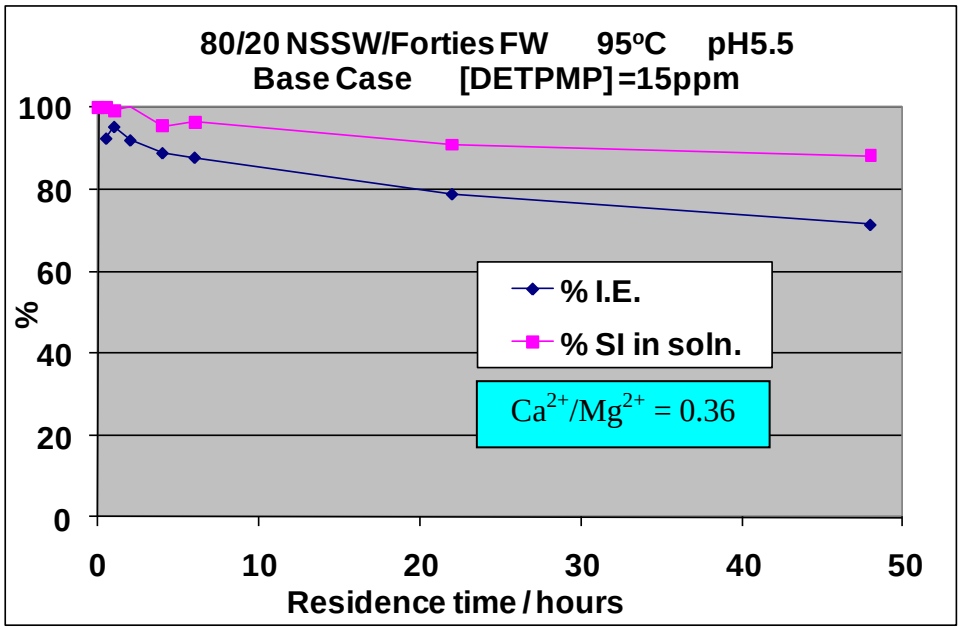

Figure 9.18 – Base Case IE and %SI vs. time, testing DETPMP at 15ppm. 80/20 NSSW/Forties FW, 95°C, pH5.5.

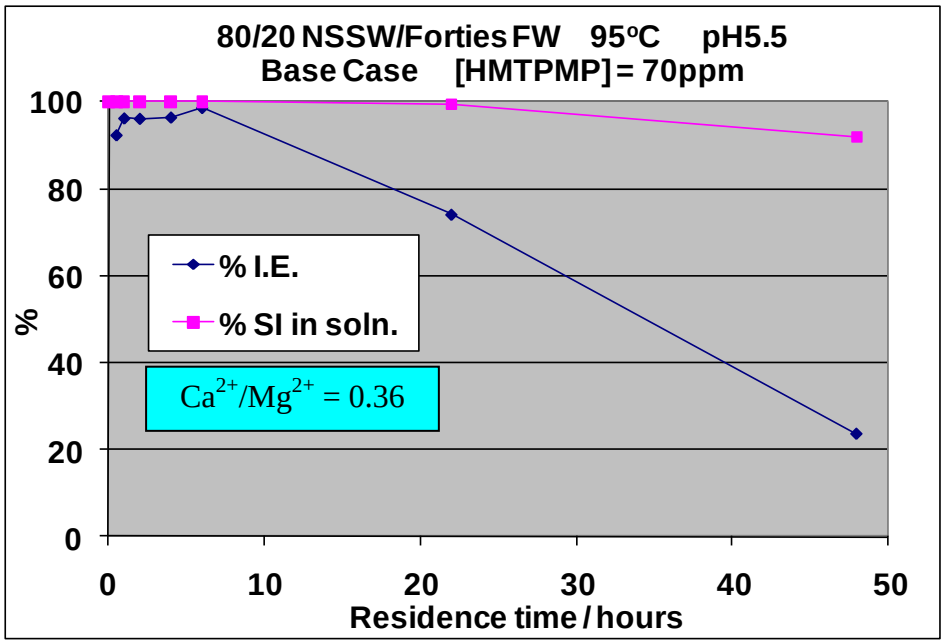

Figure 9.19 – Base Case IE and %SI vs. time, testing HMTPMP at 70ppm. 80/20 NSSW/Forties FW, 95°C, pH5.5.

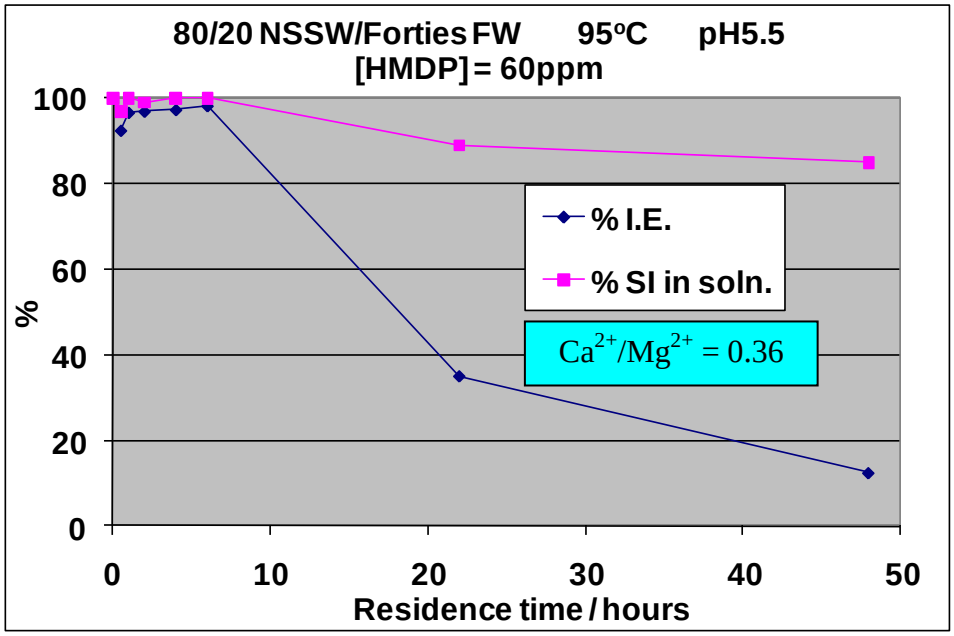

Figure 9.20 – Base Case IE and %SI vs. time, testing HMDP at 60ppm. 80/20 NSSW/Forties FW, 95°C, pH5.5.

9.4.4 80/20 NSSW/FW, Fixed Case, Molar Ratio Ca^{2+}/Mg^{2+} = 1.64

Figures 9.21−9.24 present the IE and supernatant [SI] versus time profiles for OMTHP at 3ppm, DETPMP at 8ppm, HMTPMP at 8ppm and HMDP at 12ppm respectively (all pre-2 hour 80/20 Fixed Case MICs).

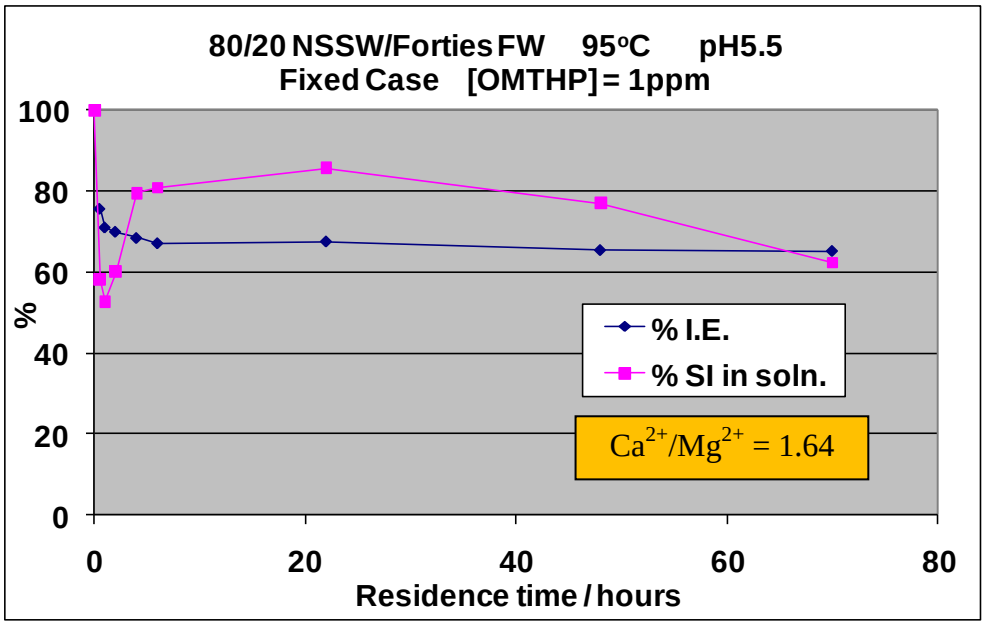

Figure 9.21 – Fixed Case IE and %SI vs. time, testing OMTHP at 1ppm. 80/20 NSSW/Forties FW, 95°C, pH5.5.

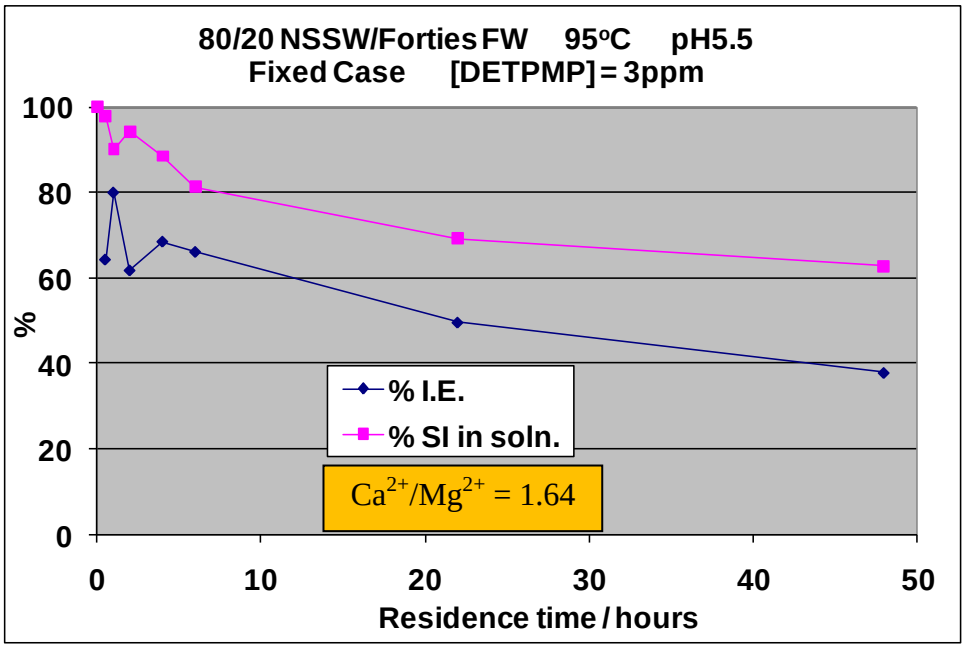

Figure 9.22 – Fixed Case IE and %SI vs. time, testing DETPMP at 3ppm. 80/20 NSSW/Forties FW, 95°C, pH5.5.

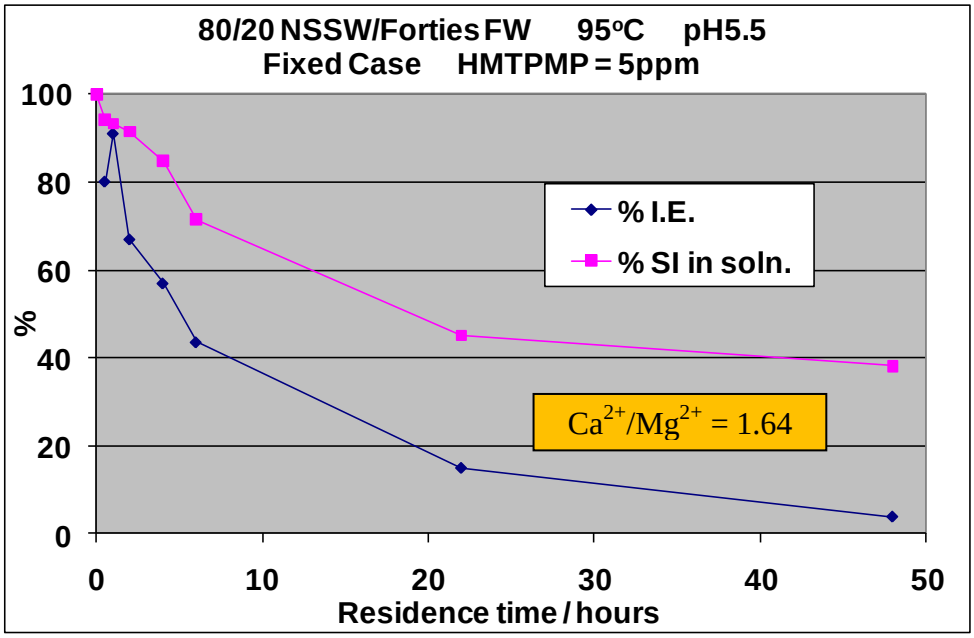

Figure 9.23 – Fixed Case IE and %SI vs. time, testing HMTPMP at 5ppm. 80/20 NSSW/Forties FW, 95°C, pH5.5.

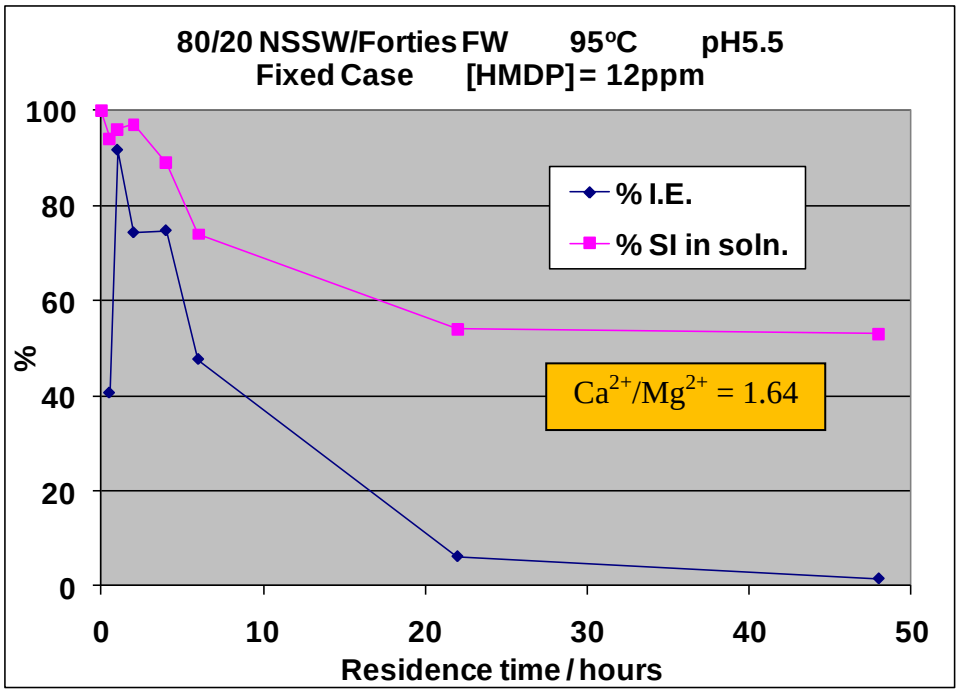

Figure 9.24 – Fixed Case IE and %SI vs. time, testing HMDP at 12ppm. 80/20 NSSW/Forties FW, 95°C, pH5.5.

9.5 OMTHP, DETPMP, HMTPMP and HMDP – Fixed [SI] = 6ppm, 60/40 and 80/20 NSSW/FW, Base Case and Fixed Case

In these experiments, all 4 SIs - OMTHP, DETPMP, HMTPMP and HMDP - were tested at the same [SI] such that differences in their SI consumption and IE could be compared with one another. Furthermore, mixing ratios NSSW/FW 60/40 and 80/20 were selected because mixing ratio 60/40 represents the highest SR level and 80/20 was the mixing ratio for which the highest Type 2 phosphonate SI MICs were measured (see Chapter 5). In addition, these consumption tests were carried out under Base Case and Fixed Case experimental conditions – such that differences in SI consumption (between Base Case and Fixed Case) induced by the changing mix molar ratio Ca^{2+}/Mg^{2+} (from 0.57 to 1.64) would become apparent.

9.5.1 60/40 NSSW/FW, Base Case, Molar Ratio Ca^{2+}/Mg^{2+} = 0.57

Figures 9.25−9.28 present the IE and supernatant [SI] versus time profiles for OMTHP, DETPMP, HMTPMP and HMDP respectively, all tested at 6ppm.

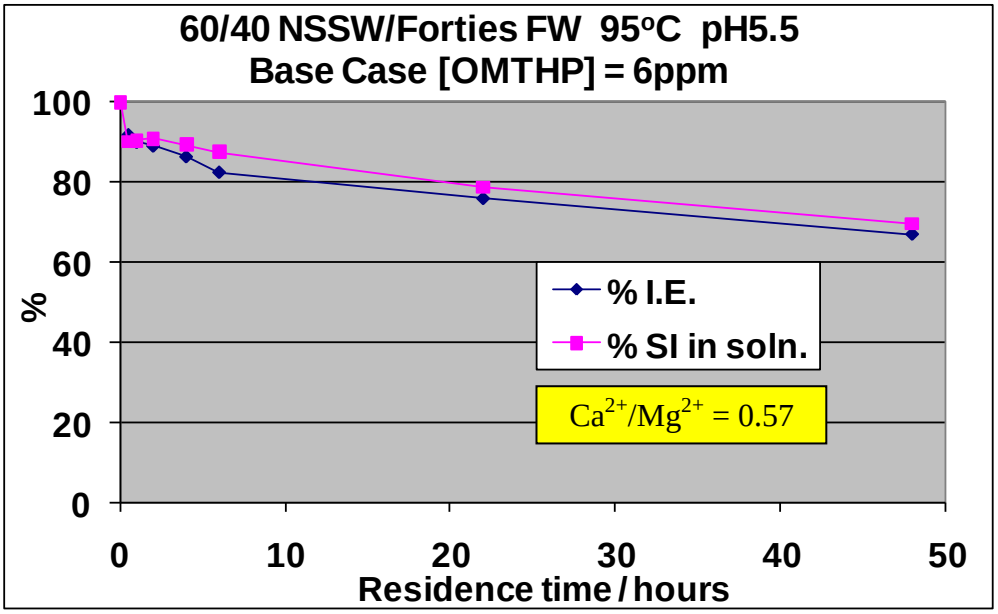

Figure 9.25 – Base Case IE and %SI vs. time, testing OMTHP at 6ppm. 60/40 NSSW/Forties FW, 95°C, pH5.5.

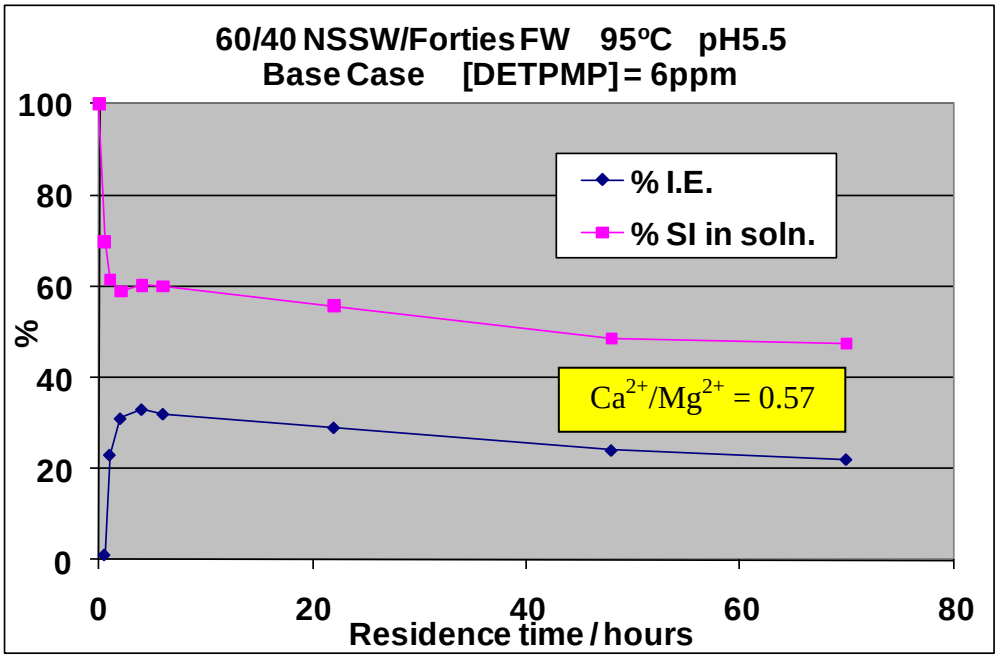

Figure 9.26 – Base Case IE and %SI vs. time, testing DETPMP at 6ppm. 60/40 NSSW/Forties FW, 95°C, pH5.5.

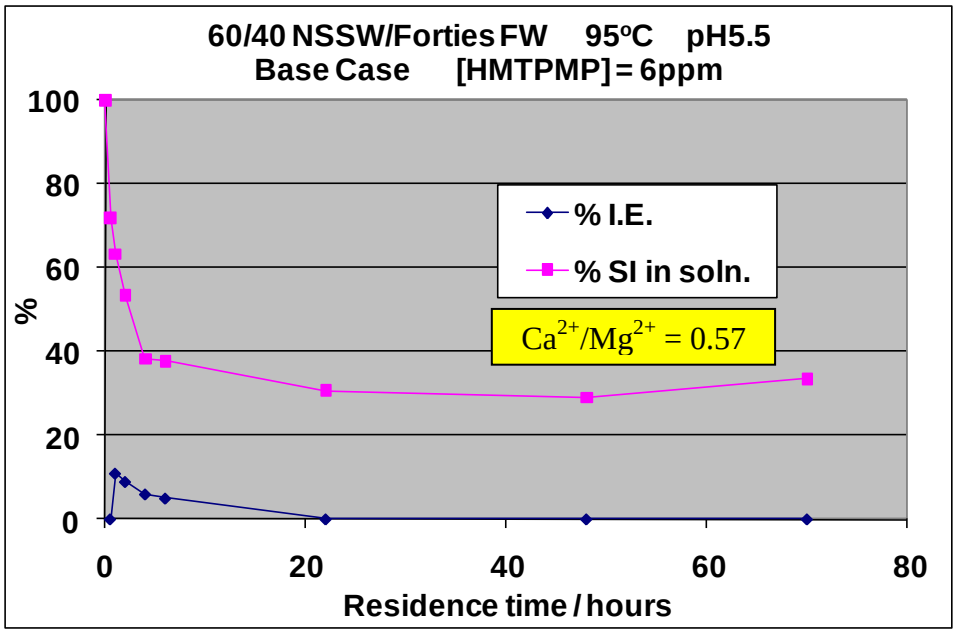

Figure 9.27 – Base Case IE and %SI vs. time, testing HMTPMP at 6ppm. 60/40 NSSW/Forties FW, 95°C, pH5.5.

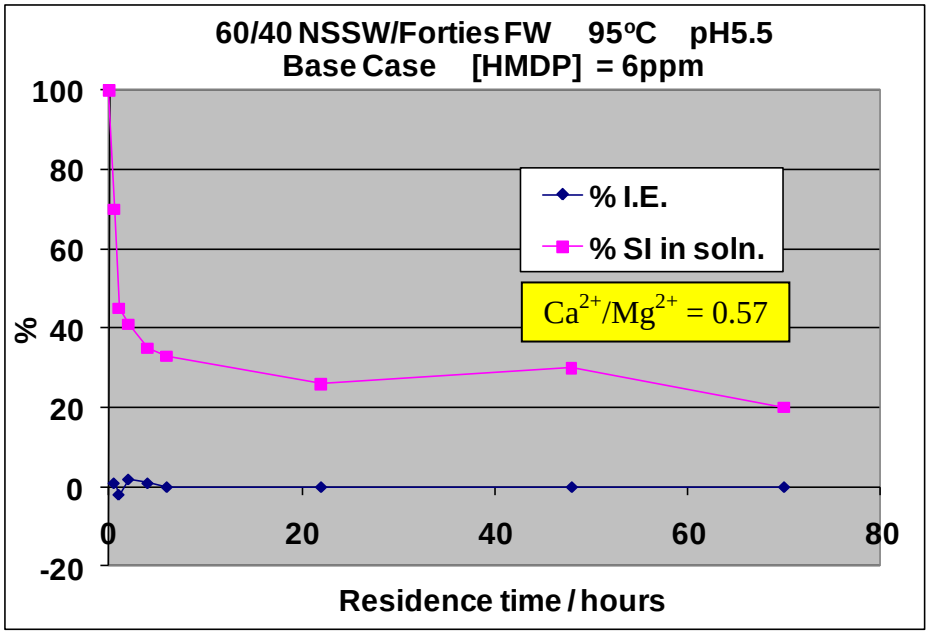

Figure 9.28 – Base Case IE and %SI vs. time, testing HMDP at 6ppm. 60/40 NSSW/Forties FW, 95°C, pH5.5.

9.5.2 60/40 NSSW/FW, Fixed Case, Molar Ratio Ca^{2+}/Mg^{2+} = 1.64

Figures 9.29−9.32 present the IE and supernatant [SI] versus time profiles for OMTHP, DETPMP, HMTPMP and HMDP respectively, all tested at 6ppm.

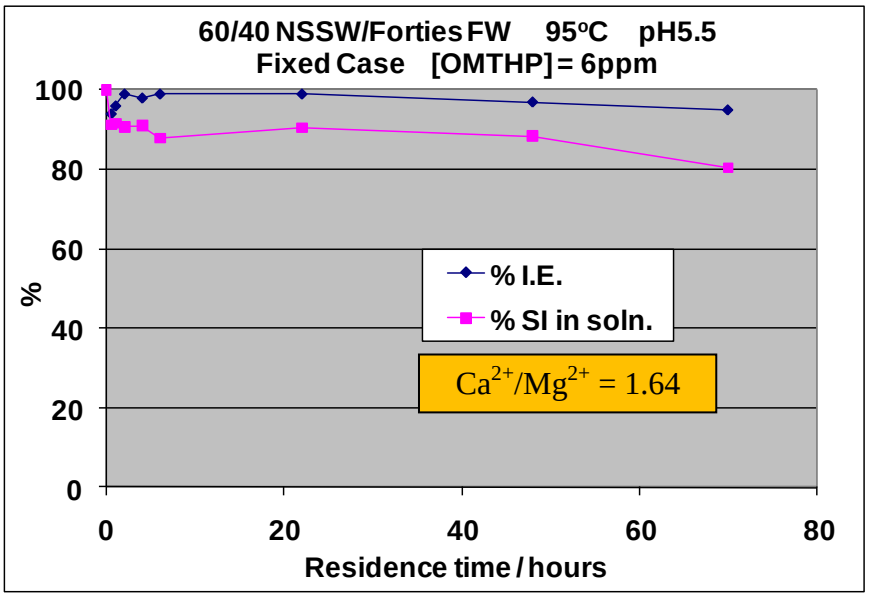

Figure 9.29 – Fixed Case IE and %SI vs. time, testing OMTHP at 6ppm. 60/40 NSSW/Forties FW, 95°C, pH5.5.

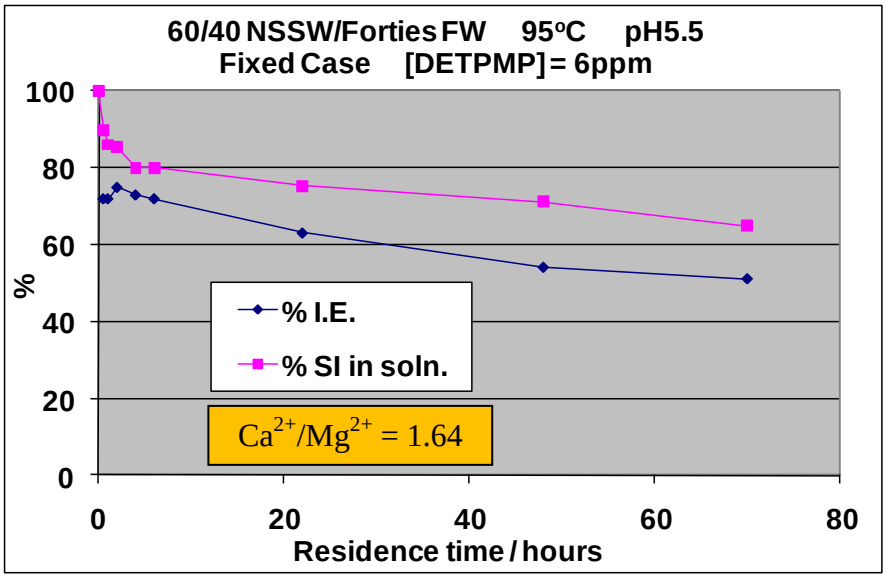

Figure 9.30 – Fixed Case IE and %SI vs. time, testing DETPMP at 6ppm. 60/40 NSSW/Forties FW, 95°C, pH5.5.

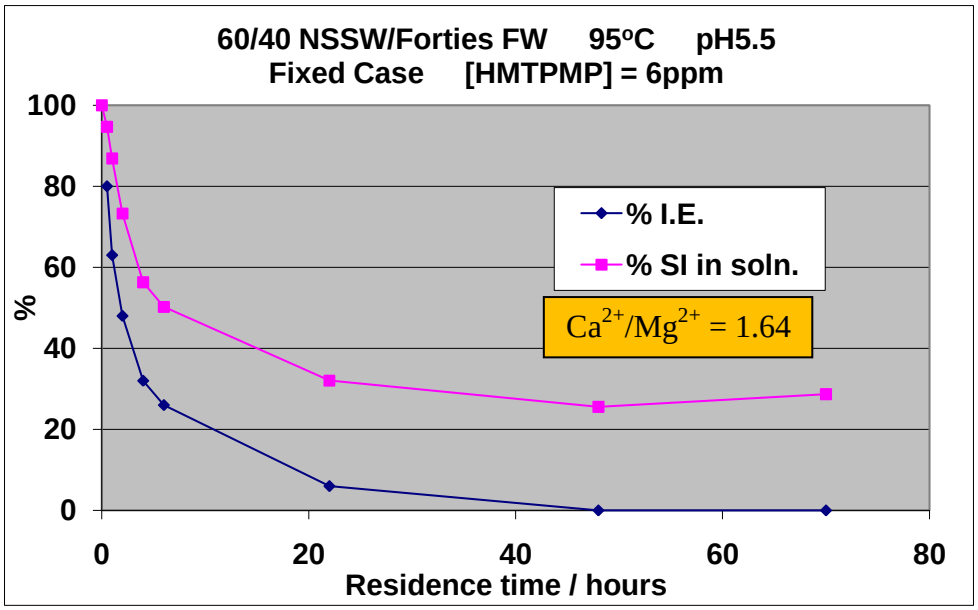

Figure 9.31 – Fixed Case IE and %SI vs. time, testing HMTPMP at 6ppm. 60/40 NSSW/Forties FW, 95°C, pH5.5.

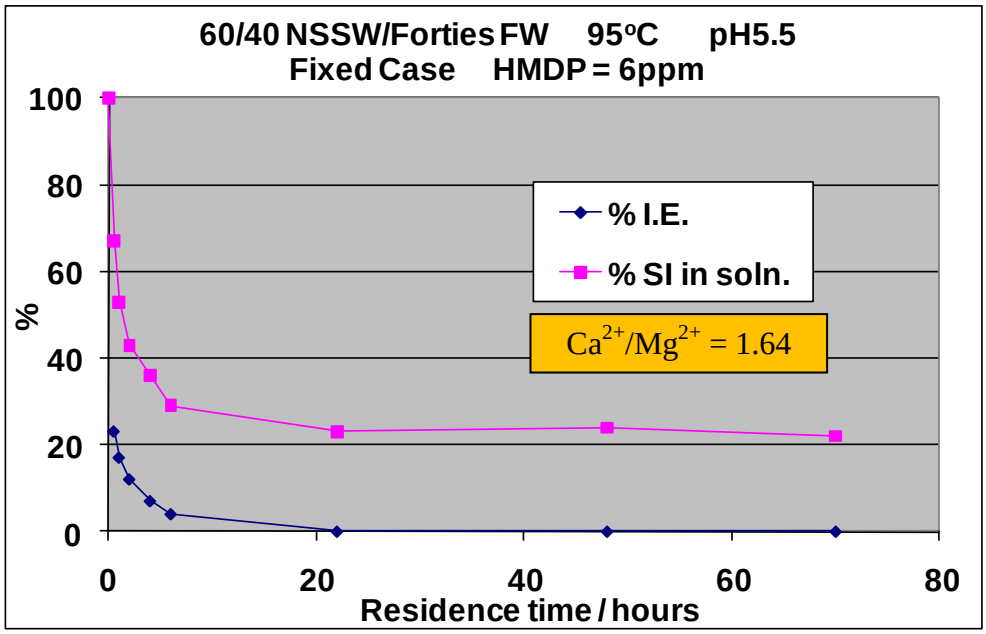

Figure 9.32 – Fixed Case IE and %SI vs. time, testing HMDP at 6ppm. 60/40 NSSW/Forties FW, 95°C, pH5.5.

9.5.3 80/20 NSSW/FW, Base Case, Molar Ratio Ca^{2+}/Mg^{2+} = 0.57

Figures 9.33−9.36 present the IE and supernatant [SI] versus time profiles for OMTHP, DETPMP, HMTPMP and HMDP respectively, all tested at 6ppm.

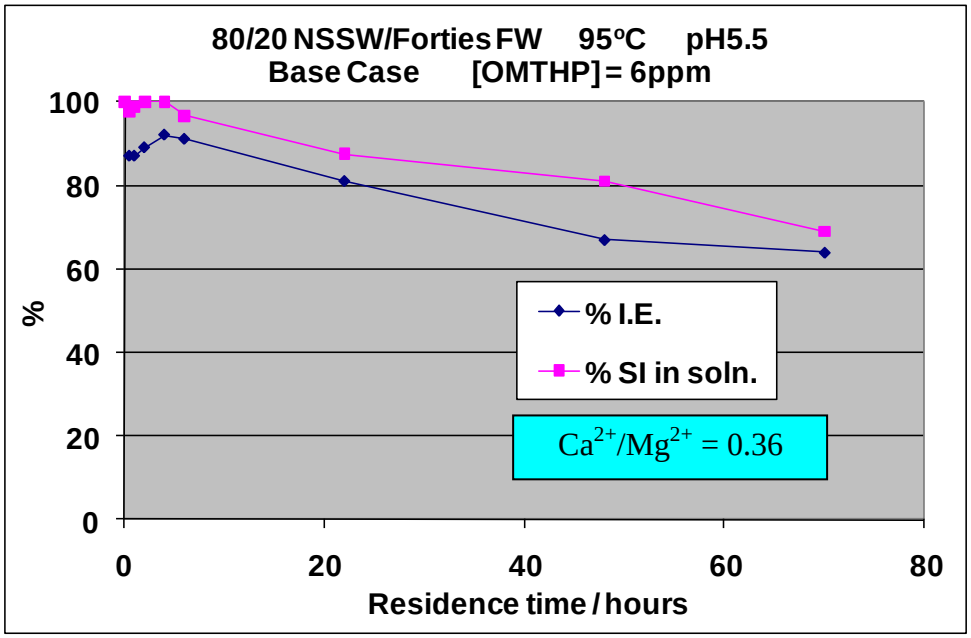

Figure 9.33 – Base Case IE and %SI vs. time, testing OMTHP at 6ppm. 80/20 NSSW/Forties FW, 95°C, pH5.5.

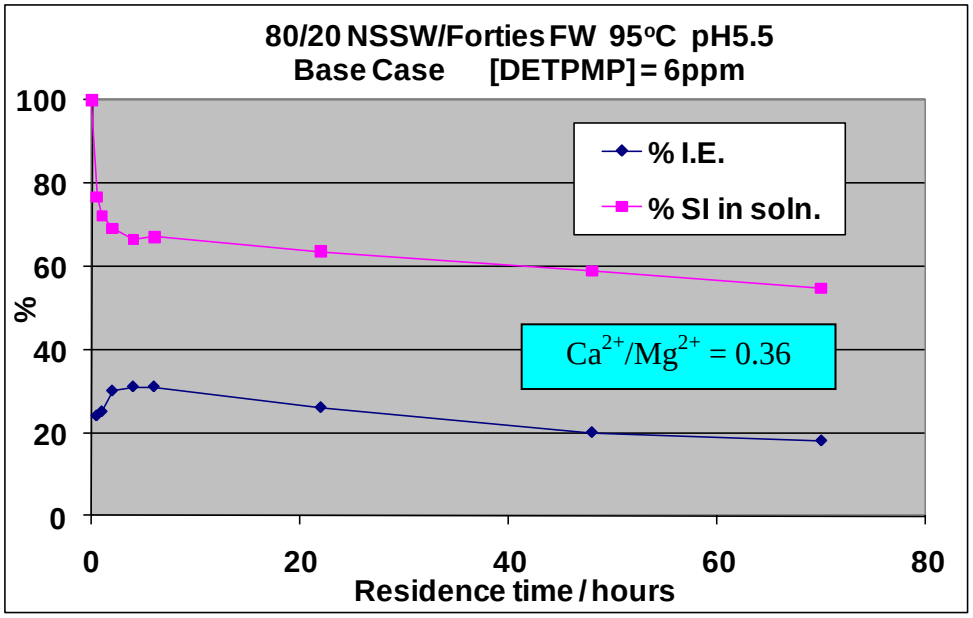

Figure 9.34 – Base Case IE and %SI vs. time, testing DETPMP at 6ppm. 80/20 NSSW/Forties FW, 95°C, pH5.5.

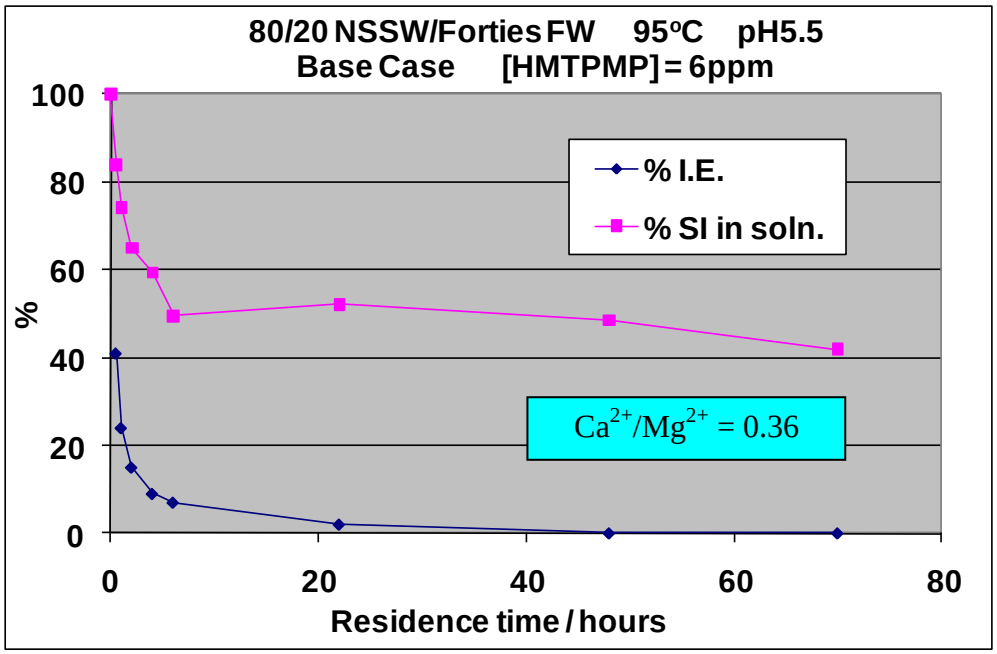

Figure 9.35 – Base Case IE and %SI vs. time, testing HMTPMP at 6ppm. 80/20 NSSW/Forties FW, 95°C, pH5.5.

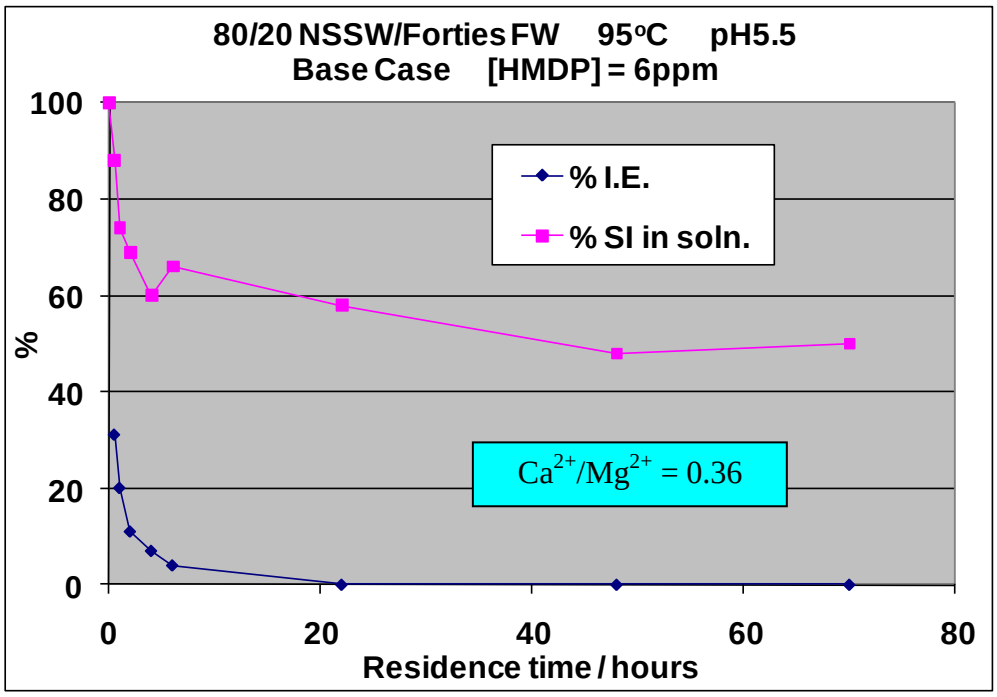

Figure 9.36 – Base Case IE and %SI vs. time, testing HMDP at 6ppm. 80/20 NSSW/Forties FW, 95°C, pH5.5.

9.5.4 80/20 NSSW/FW, Fixed Case, Molar Ratio Ca^{2+}/Mg^{2+} = 1.64

Figures 9.37−9.40 present the IE and supernatant [SI] versus time profiles for OMTHP, DETPMP, HMTPMP and HMDP respectively, all tested at 6ppm.

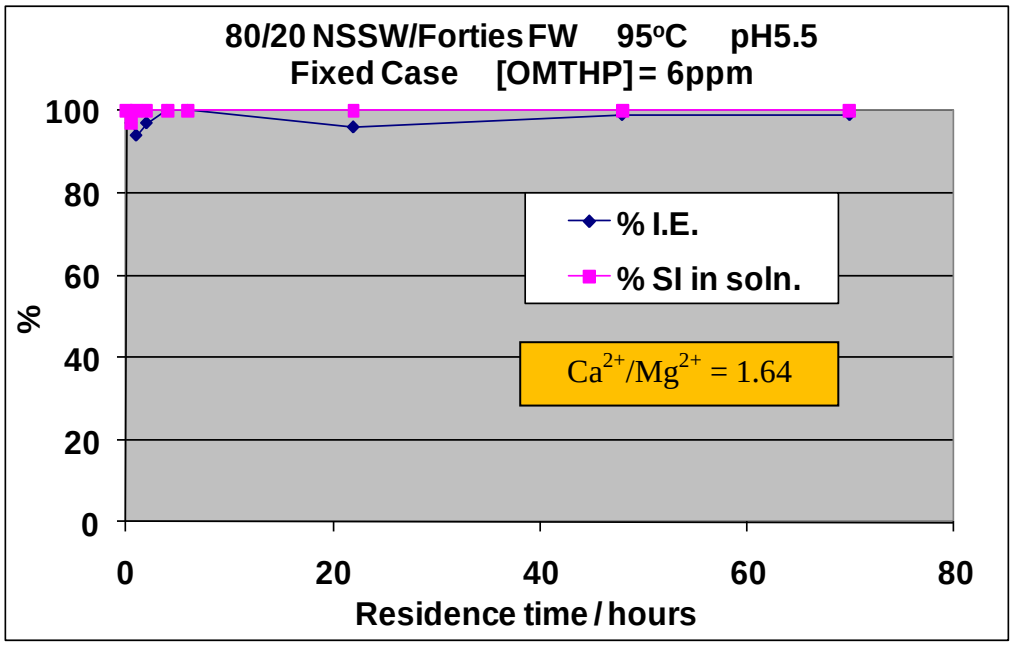

Figure 9.37 – Fixed Case IE and %SI vs. time, testing OMTHP at 6ppm. 80/20 NSSW/Forties FW, 95°C, pH5.5.

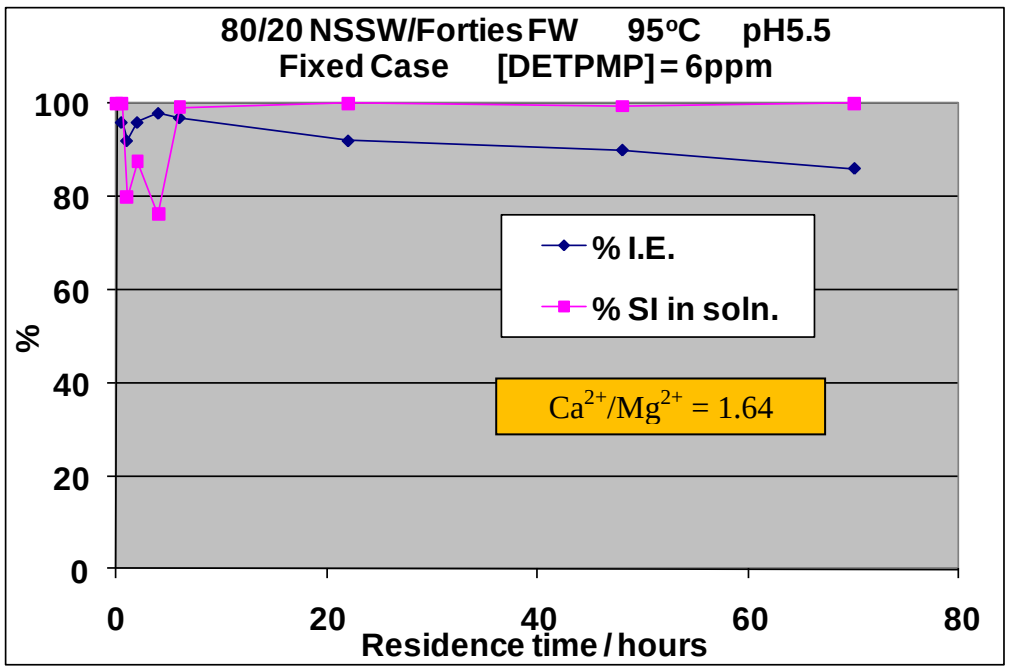

Figure 9.38 – Fixed Case IE and %SI vs. time, testing DETPMP at 6ppm. 80/20 NSSW/Forties FW, 95°C, pH5.5.

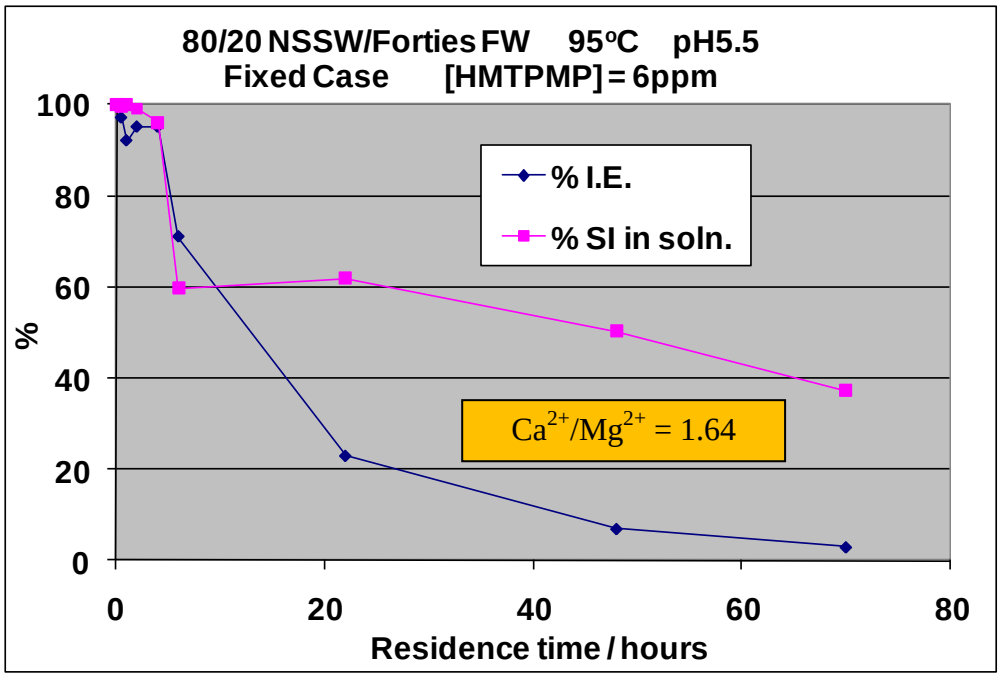

Figure 9.39 – Fixed Case IE and %SI vs. time, testing HMTPMP at 6ppm. 80/20 NSSW/Forties FW, 95°C, pH5.5.

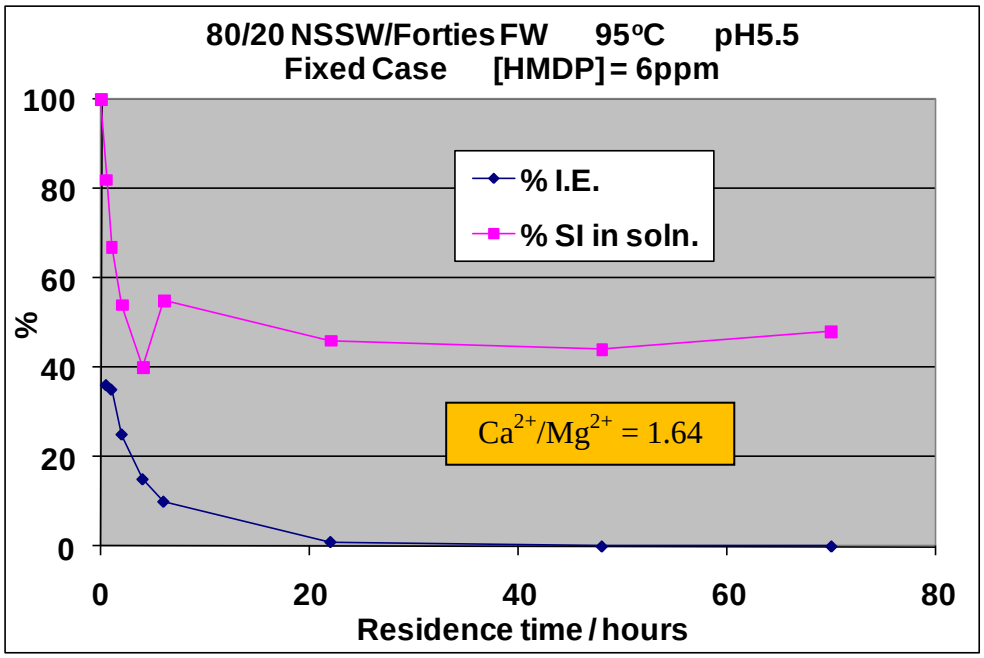

Figure 9.40 – Fixed Case IE and %SI vs. time, testing HMDP at 6ppm. 80/20 NSSW/Forties FW, 95°C, pH5.5.

9.6 ESEM Images and EDAX Analyses

An extensive collection of ESEM images were obtained of scale deposits formed in test bottles during the above series of SI consumption experiments (Sections 9.4 and 9.5). In this Section, a selection of ESEM images is presented.

Figures 9.41(a)−(z) present ESEM images of scale deposits formed in the absence of SI, and in the presence of OMTHP, DETPMP, HMTPMP and HMDP. Under each image, it is stated whether SI was present or absent, and if present, *which* SI and [SI]. The test molar ratio Ca^{2+}/Mg^{2+} is stated (i.e. whether the deposit originated from a Base Case or Fixed Case experiment), the mixing ratio NSSW/FW and the magnification of the images are also given.

(a) BLANK
Ca/Mg = 0.57
60/40 NSSW/FW
X800

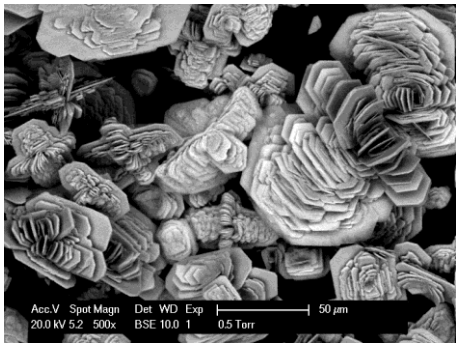

(b) BLANK
Ca/Mg = 0.57
60/40 NSSW/FW
X500

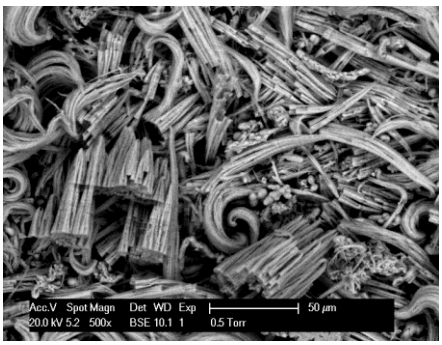

(c) 6ppm OMTHP
Ca/Mg = 0.57
80/20 NSSW/FW
X500

(d) 4ppm OMTHP
Ca/Mg = 0.36
80/20 NSSW/FW
X400

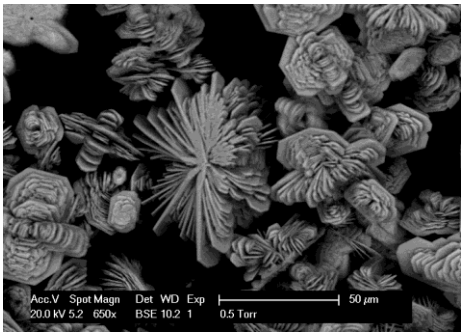

(e) BLANK
Ca/Mg = 1.64
60/40 NSSW/FW
X650

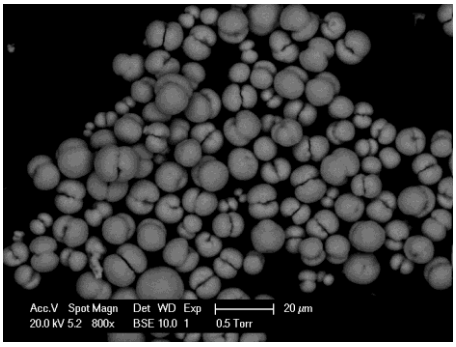

(f) 6ppm OMTHP
Ca/Mg = 1.64
80/20 NSSW/FW
X800

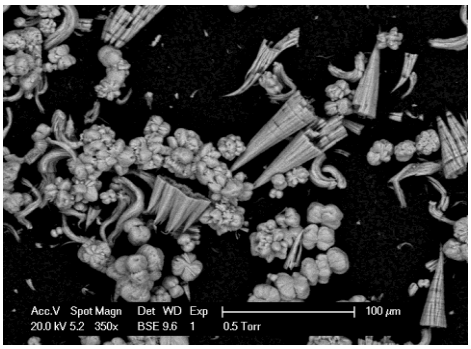

(g) 6ppm OMTHP
Ca/Mg = 1.64
60/40 NSSW/FW
X350

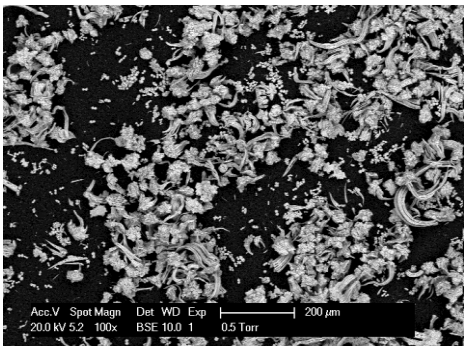

(h) 1ppm OMTHP
Ca/Mg = 1.64
80/20 NSSW/FW
X100

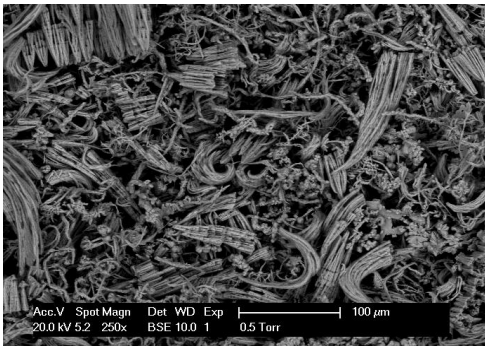

(i) 8ppm DETPMP
Ca/Mg = 1.64
60/40 NSSW/FW
X250

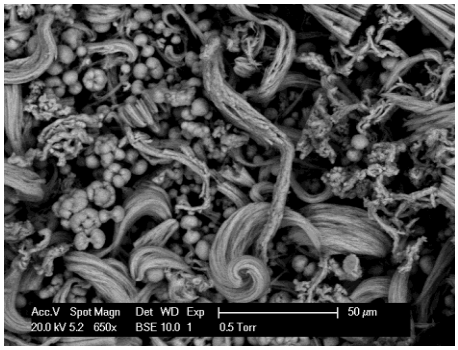

(j) 6ppm DETPMP
Ca/Mg = 1.64
80/20 NSSW/FW
X650

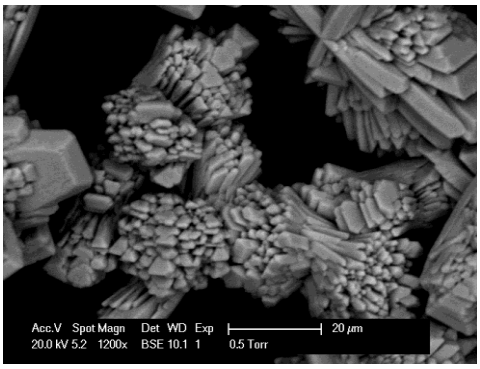

(k) 6ppm DETPMP
Ca/Mg = 0.57
60/40 NSSW/FW
X1200

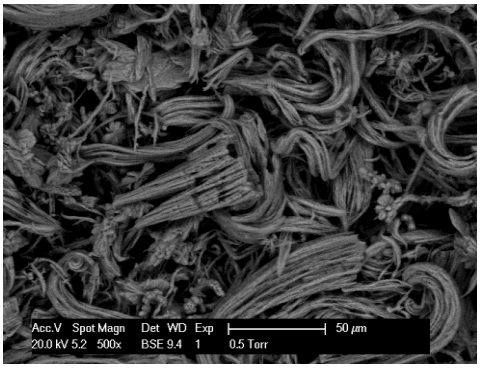

(l) 6ppm DETPMP
Ca/Mg = 1.64
60/40 NSSW/FW
X500

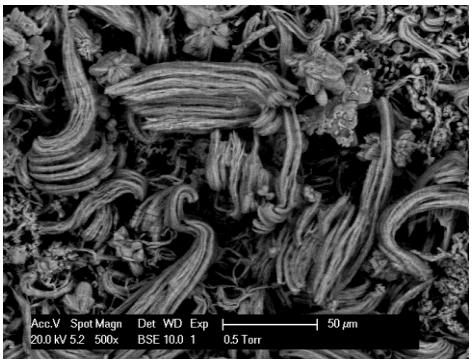

(m) 3ppm DETPMP
Ca/Mg = 1.64
80/20 NSSW/FW
X500

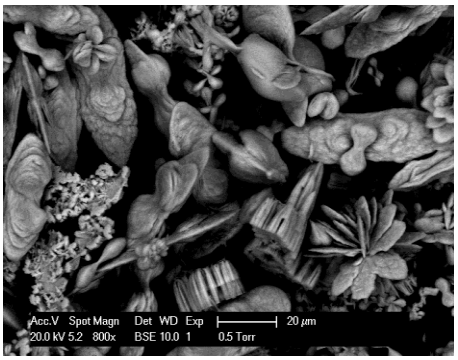

(n) 6ppm DETPMP
Ca/Mg = 0.36
80/20 NSSW/FW
X800

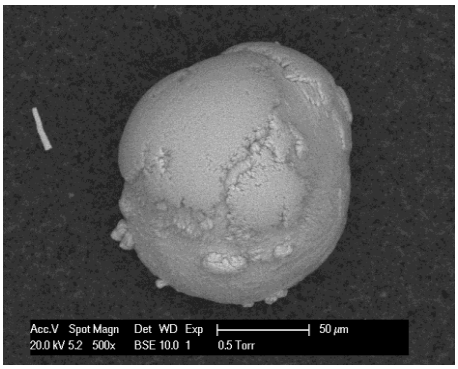

(o) 6ppm HMTPMP
Ca/Mg = 1.64
80/20 NSSW/FW
X500

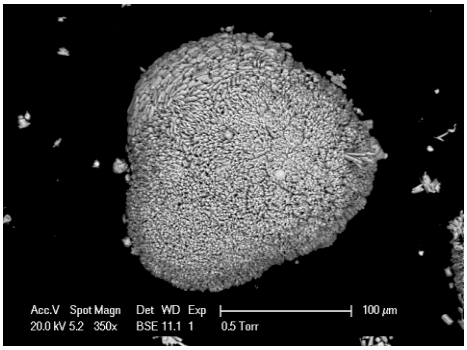

(p) 8ppm HMTPMP
Ca/Mg = 1.64
60/40 NSSW/FW
X350

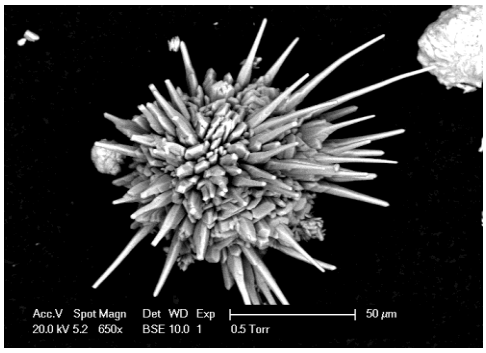

(q) 8ppm HMTPMP
Ca/Mg = 1.64
60/40 NSSW/FW
X650

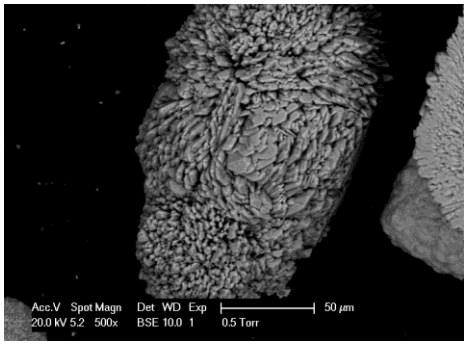

(r) 6ppm HMTPMP
Ca/Mg = 1.64
60/40 NSSW/FW
X500

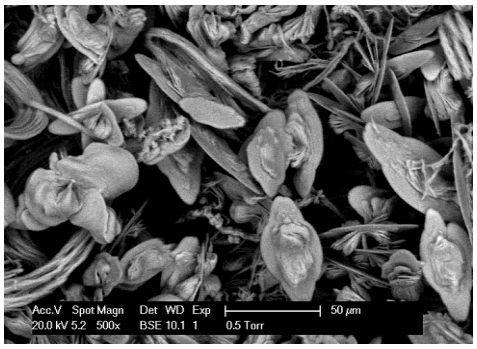

(s) 6ppm HMTPMP
Ca/Mg = 0.57
60/40 NSSW/FW
X500

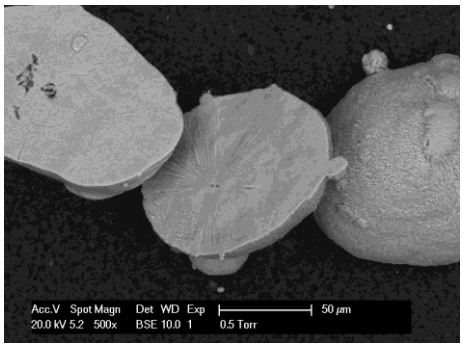

(t) 5ppm HMTPMP
Ca/Mg = 1.64
80/20 NSSW/FW
X500

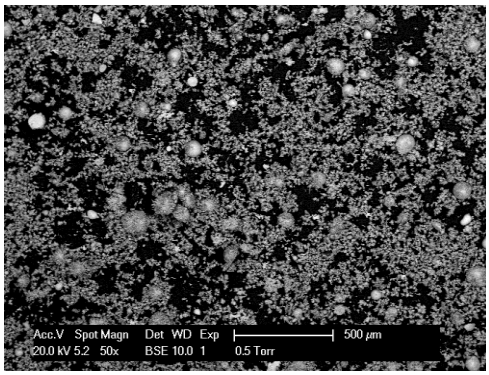

(u) 12ppm HMDP
Ca/Mg = 1.64
60/40 NSSW/FW
X50

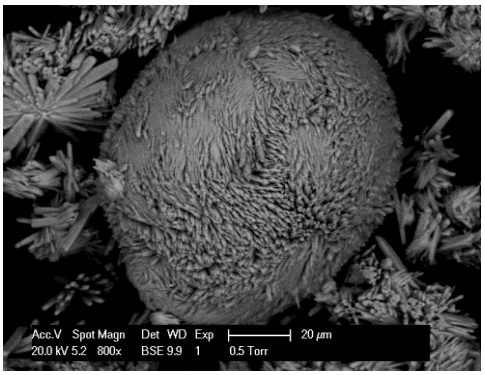

(v) 12ppm HMDP
Ca/Mg = 1.64
60/40 NSSW/FW
X800

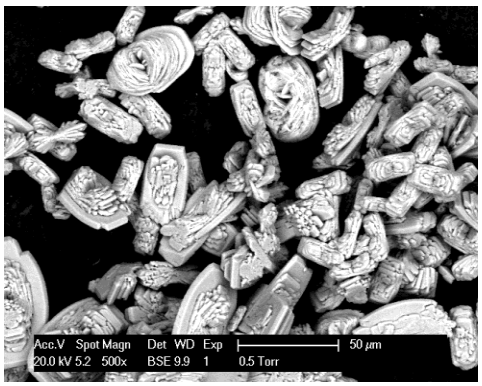

(w) 6ppm HMDP
Ca/Mg = 0.57
60/40 NSSW/FW
X500

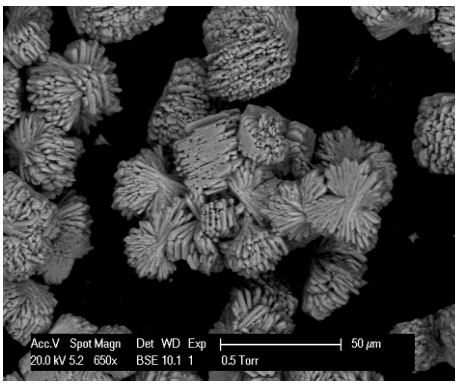

(x) 6ppm HMDP
Ca/Mg = 1.64
60/40 NSSW/FW
X650

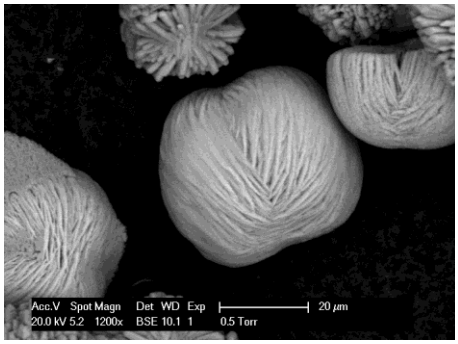

(y) 6ppm HMDP
Ca/Mg = 1.64
60/40 NSSW/FW
X1200

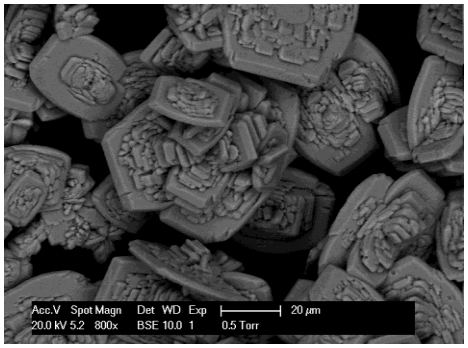

(z) 6ppm HMDP
Ca/Mg = 0.36
80/20 NSSW/FW
X800

Figure 9.41(a)–(z) – ESEM images of various scale deposits, obtained from static IE test bottles.

As mentioned earlier, a significant quantity of ESEM images were obtained of scale deposits and the same number of EDAX analyses were conducted on these scale deposits. In Figure 9.42, *all* EDAX analysis results are presented; conducted on an extensive range of scale deposits – all obtained from static IE experiments. Use the colour-code key given in Table 9.2 in relation to Figure 9.42. Table 9.2 gives specific test conditions, e.g. [SI], molar ratio Ca^{2+}/Mg^{2+}, etc.

Colour	Test Conditions
	60/40 NSSW/FW - Pre-22hr MICs Base Case Ca/Mg = 0.57 [OMTHP] = 6ppm, [HMTPMP] = 35ppm, [DETPMP] = 25ppm, [HMDP] = 35ppm.
	80/20 NSSW/FW - Pre-22hr MICs Base Case Ca/Mg = 0.36 [OMTHP] = 4ppm, [HMTPMP] = 70ppm, [DETPMP] = 15ppm, [HMDP] = 60ppm.
	60/40 NSSW/FW - Pre-2hr MICs Fixed Case Ca/Mg = 1.64 [OMTHP] = 3ppm, [HMTPMP] = 8ppm, [DETPMP] = 8ppm, [HMDP] = 12ppm.
	80/20 NSSW/FW - Pre-2hr MICs Fixed Case Ca/Mg = 1.64 [OMTHP] = 1ppm, [HMTPMP] = 5ppm, [DETPMP] = 3ppm, [HMDP] = 12ppm.
	60/40 NSSW/FW - All SIs tested at 6ppm. Base Case Ca/Mg = 0.57 [OMTHP] = 6ppm, [HMTPMP] = 6ppm, [DETPMP] = 6ppm, [HMDP] = 6ppm.
	80/20 NSSW/FW - All SIs tested at 6ppm. Base Case Ca/Mg = 0.36 [OMTHP] = 6ppm, [HMTPMP] = 6ppm, [DETPMP] = 6ppm, [HMDP] = 6ppm.
	60/40 NSSW/FW - All SIs tested at 6ppm. Fixed Case Ca/Mg = 1.64 [OMTHP] = 6ppm, [HMTPMP] = 6ppm, [DETPMP] = 6ppm, [HMDP] = 6ppm.
	80/20 NSSW/FW - All SIs tested at 6ppm. Fixed Case Ca/Mg = 1.64 [OMTHP] = 6ppm, [HMTPMP] = 6ppm, [DETPMP] = 6ppm, [HMDP] = 6ppm.

Table 9.2 – Colour key for Figure 9.42.

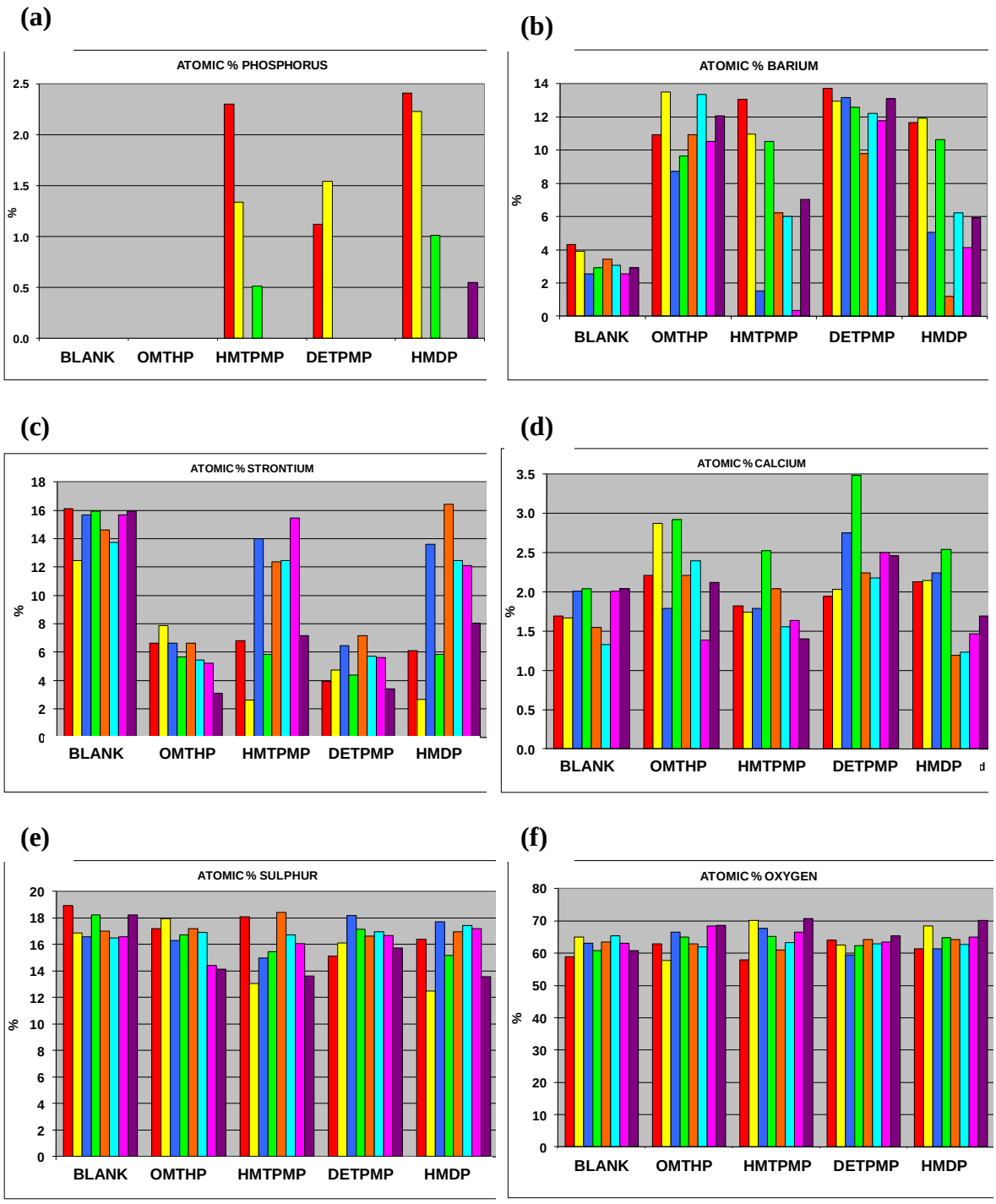

Figure 9.42(a)–(f) – EDAX analysis results. Analysis of scale deposits formed during static IE experiments. Data given: % P (a), % Ba (b), % Sr (c), % Ca (d), % S (e) and % O (f). Each chart states on the x-axis whether SI was present or not in the static IE test (either: Blank, OMTHP, DETPMP, HMTPMP or HMDP). Use colour key given in Table 9.2.

9.7 EDTMPA, HEDP and HPAA – Base Case 60/40 NSSW/FW

The 3 phosphonate SIs - EDTMPA, HEDP and HPAA - were tested in a SI consumption experiment similar to those carried out testing OMTHP, DETPMP, HMTPMP, HMDP and NTP. For this experiment, testing phosphonate SIs EDTMPA, HEDP and HPAA, mixing ratio 60/40 (highest SR) was chosen and Base Case test conditions, 95°C, pH5.5. This time, multiple samplings up to 96 hours (4 days) after mixing NSSW/FW were carried out. Note: these 3 products were received by FAST during the latter part of this PhD, hence the reason why these products were not included in previous experimental sections in this Chapter. As with the other phosphonate SIs, EDTMPA, HEDP and HPAA were assayed by ICP by means of [P]. These 3 products were tested at the following concentrations:

EDTMPA at 20ppm (pre-2hr MIC);
HEDP at 20ppm and 35ppm (both pre-2hr MIC);
HPAA at 30ppm, 50ppm (both pre-2hr MIC) and 85ppm (pre-22hr MIC).

Figures 9.43−9.48 present the IE and supernatant [SI] versus time profiles for EDTMPA at 20ppm, HEDP at 20ppm and 35ppm and HPAA at 30ppm, 50ppm and 85ppm.

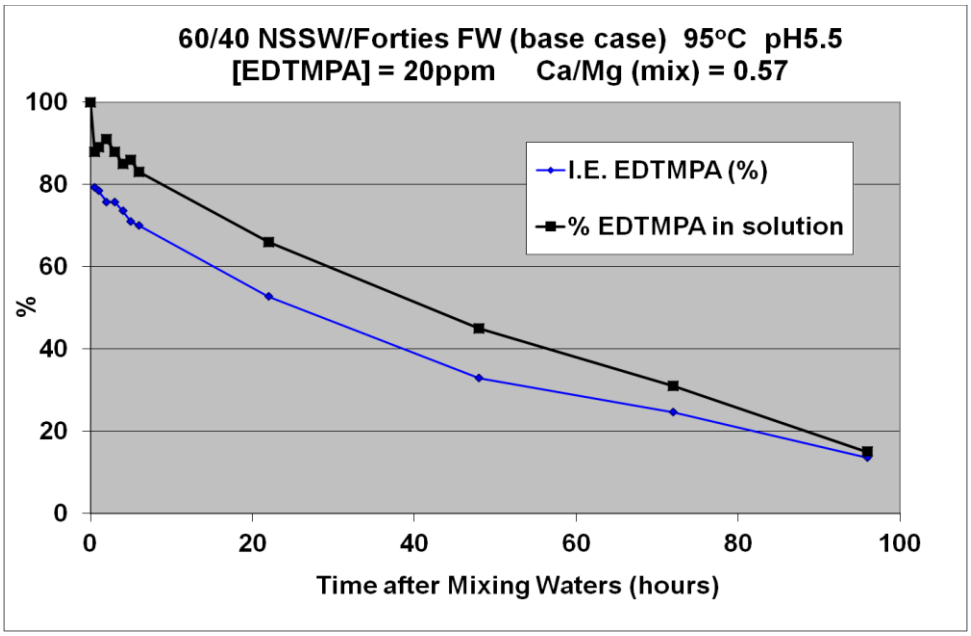

Figure 9.43 – IE and %SI in solution vs. time – up to 96 hours. [EDTMPA] = 20ppm; Base Case 60/40 NSSW/Forties FW; 95°C; pH5.5.

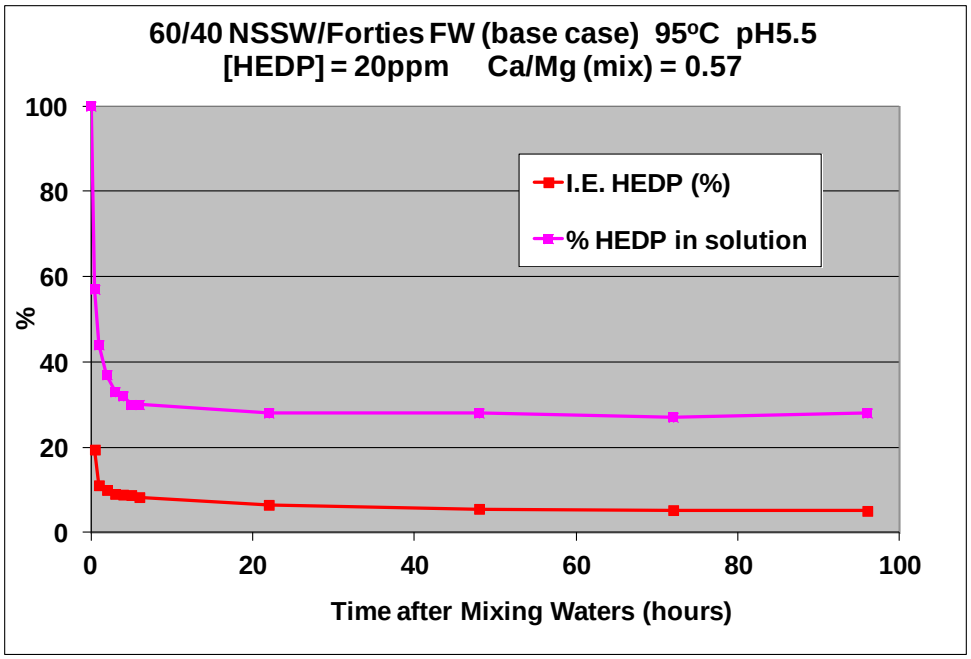

Figure 9.44 – IE and %SI in solution vs. time – up to 96 hours. [HEDP] = 20ppm; Base Case 60/40 NSSW/Forties FW; 95°C; pH5.5.

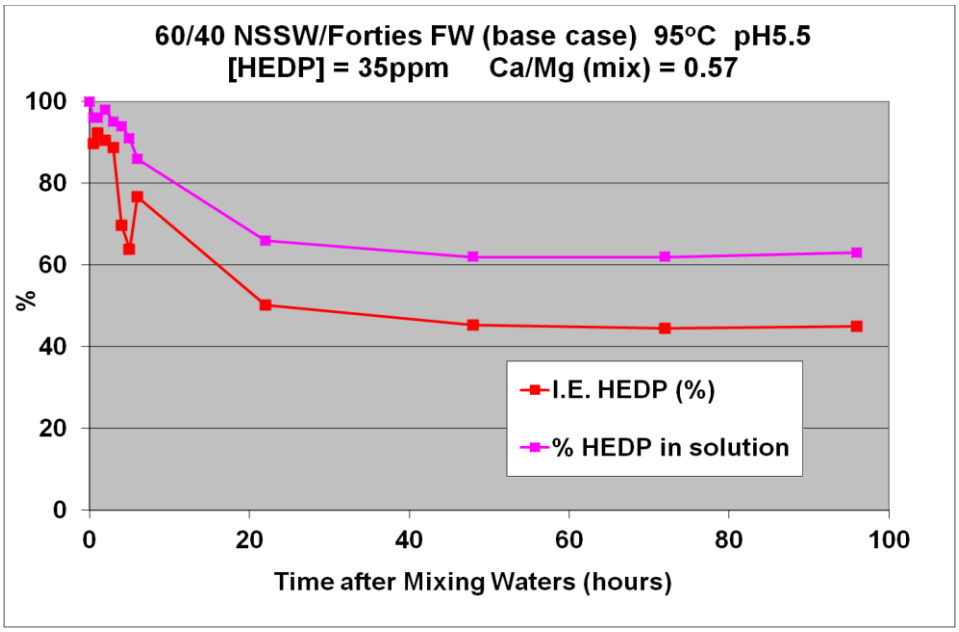

Figure 9.45 – IE and %SI in solution vs. time – up to 96 hours. [HEDP] = 35ppm; Base Case 60/40 NSSW/Forties FW; 95°C; pH5.5.

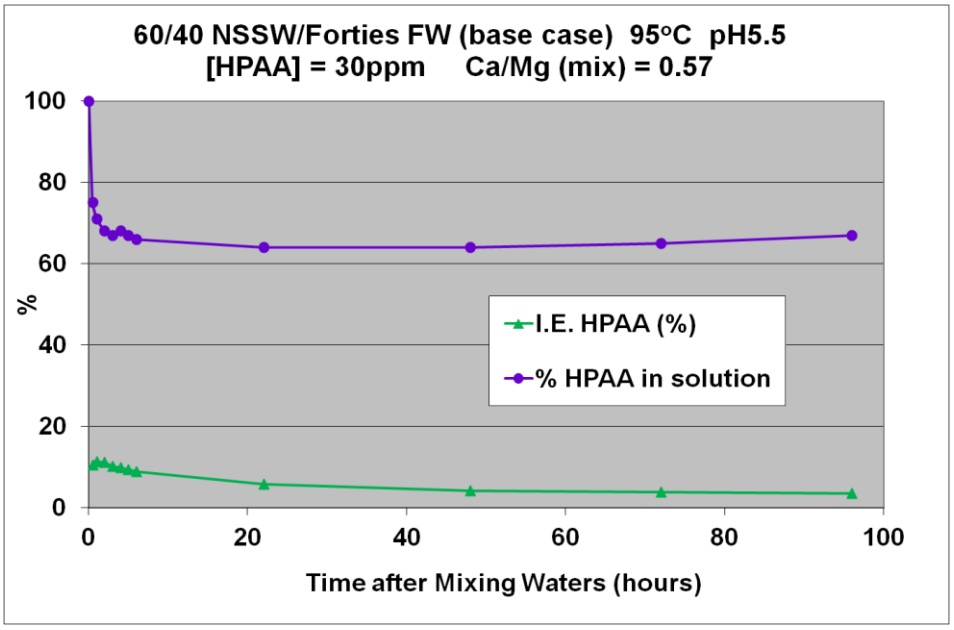

Figure 9.46 – IE and %SI in solution vs. time – up to 96 hours. [HPAA] = 30ppm; Base Case 60/40 NSSW/Forties FW; 95°C; pH5.5.

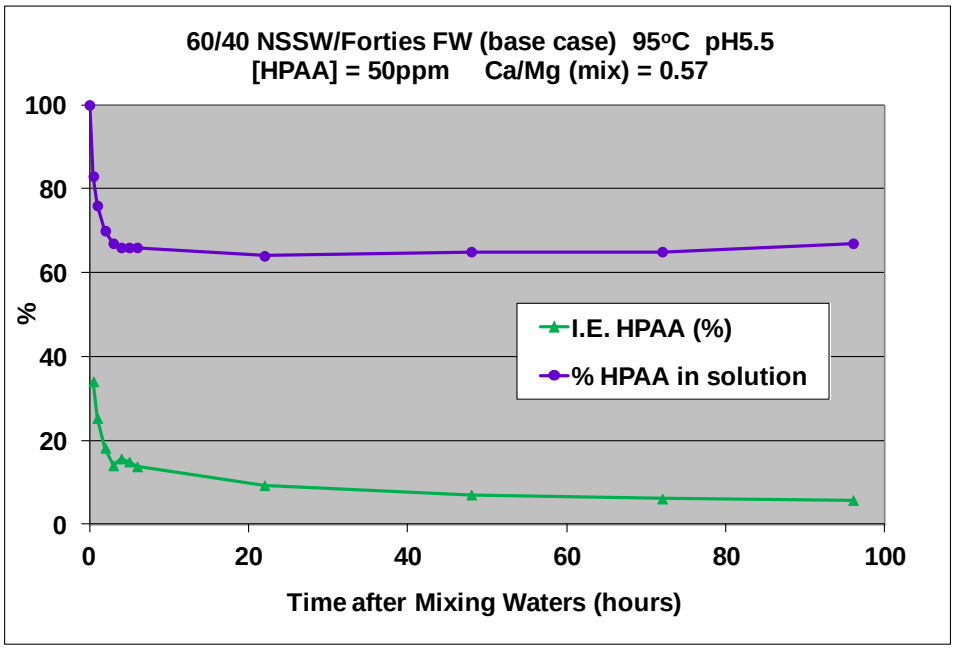

Figure 9.47 – IE and %SI in solution vs. time – up to 96 hours. [HPAA] = 50ppm; Base Case 60/40 NSSW/Forties FW; 95°C; pH5.5.

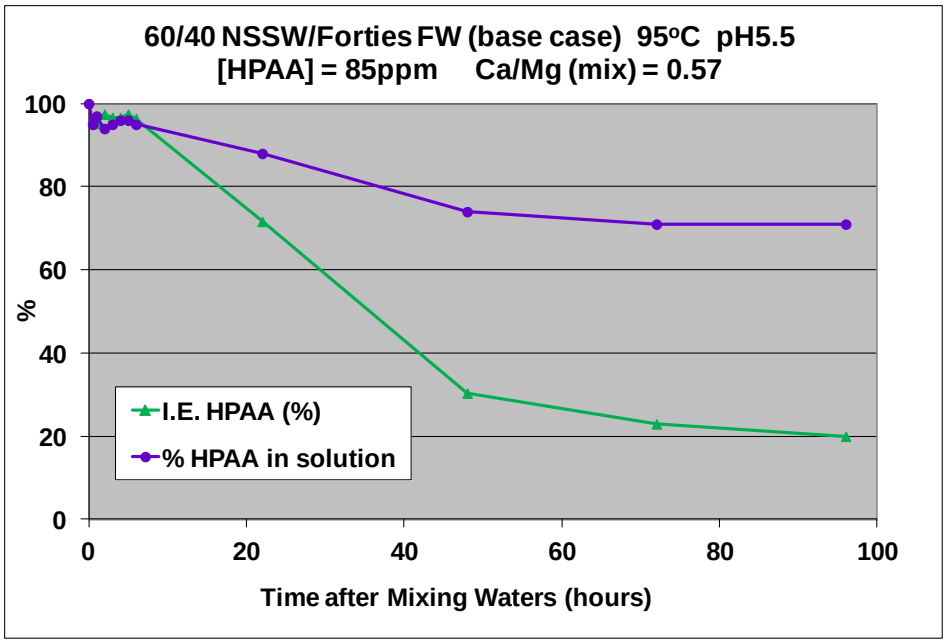

Figure 9.48 – IE and %SI in solution vs. time – up to 96 hours. [HPAA] = 85ppm; Base Case 60/40 NSSW/Forties FW; 95°C; pH5.5.

9.8 Summary and Conclusions

9.8.1 SI Consumption Experiments

The 50/50 NSSW/FW Base Case SI consumption experiments presented in Section 9.2 illustrate that the Type 1 phosphonates OMTHP and DETPMP (Figure 9.1 and Figure 9.2) are not consumed into the growing scale deposit to the same extent as the Type 2 species (Figure 9.3 – Figure 9.5) when all are tested at pre-22 hour Base Case 50/50 MIC [SI]s. Indeed, the Type 1 products maintain a good level of IE and [SI] in solution over long periods, up to 22 hours. At 22 hours, both OMTHP and DETPMP have IE > 50%. In contrast, both the IE and %SI in solution for the Type 2 species (HMTPMP, HMDP and NTP) declined rapidly to levels below 50% at 22 hours.

The experiment testing DETPMP (Type 1) at fixed [SI] = 5ppm, varying the molar ratio Ca^{2+}/Mg^{2+} (Section 9.3) illustrates conclusively the effect of Ca^{2+}/Mg^{2+} molar ratio on IE and SI consumption. With reference to Figure 9.7, the highest IE is achieved when the molar ratio Ca^{2+}/Mg^{2+} = 4, whereas the lowest IE is achieved with Ca^{2+}/Mg^{2+} = 1. In terms of SI consumption, there is generally less SI consumption when molar ratio Ca^{2+}/Mg^{2+} = 4 (Figure

9.8). Perhaps the best set of data to draw conclusions from in Figure 9.8 is the long-term 22 hour data, which shows least SI consumption with Ca^{2+}/Mg^{2+} = 4 (~80% SI in solution), followed by Ca^{2+}/Mg^{2+} = 2 (~65% SI in solution), followed by Ca^{2+}/Mg^{2+} = 1 (~55% SI in solution). This SI consumption pattern correlates very well with the DETPMP IE (Figure 9.7) and the known effects of Ca^{2+}/Mg^{2+} on phosphonate SIs (Chapter 5), i.e. Ca^{2+} beneficial, Mg^{2+} detrimental, because more active SI is remaining in solution when the Ca^{2+}/Mg^{2+} molar ratio is higher.

The experimental results presented in Section 9.4 demonstrate that the Type 2 species HMTPMP and HMDP are consumed more rapidly over time than the Type 1 species OMTHP and DETPMP when tested at threshold pre-MIC [SI]s. It is frequently the case that IE has declined to near-zero or zero, but some SI is remains in solution at the same residence time. For example, Figure 9.11 shows ~10% IE for HMTPMP and ~50% SI in solution at 48 hours. Similarly, Figure 9.12 shows ~5% IE for HMDP and ~50% SI in solution at 48 hours. SI remaining in solution (once IE has declined) is *inactive* and very likely bound to Mg^{2+} (as SI−Mg). The quantity of SI consumed depends to some degree on the [SI] being tested. If higher [SI]s were tested, it is much more likely a larger %SI will remain in solution, for example, as in Figure 9.19. This figure shows ~25% IE at 48 hours for HMTPMP and ~90% SI still in solution. Under these test conditions, i.e. Ca^{2+}/Mg^{2+} = 0.36, 80/20 NSSW/FW, Base Case, a significant quantity of the active HMTPMP SI must have been "poisoned" by Mg^{2+} at 48 hours, giving rise to extremely poor IE and almost all SI in solution ineffective (or inactive). This SI consumption result correlates with MIC versus %NSSW experimental results (Chapter 5), where the highest MIC for HMTPMP, 80/20, Base Case, was = 90ppm. Similar SI consumption results were obtained for HMDP (Figure 9.20). Figures such as 9.19 and 9.20 show quantifiably how much SI poisoning occurs with Mg^{2+}. It is also worth noting that the analytical method for assaying SI, i.e. ICP spectroscopy, detects all SI present in test samples, regardless of whether it is "free" unbound SI or SI in solution complexed with Mg^{2+}, Ca^{2+}, etc.

Under Fixed Case experimental conditions, Type 2 phosphonates HMTPMP and HMDP were consumed more than their Type 1 analogues OMTHP and DETPMP – compare Figure 9.14 and Figure 9.15 where DETPMP and HMTPMP were both tested at 8ppm under the same test conditions. Clearly, the Type 2 species (HMTPMP) is consumed rapidly whereas the Type 1

species (DETPMP) is not. At 70 hours, ~75% of the DETPMP is in solution compared to ~30% of the HMTPMP. In both figures, IE correlates with the SI consumption profile. When OMTHP, DETPMP, HMTPMP and HMDP were all tested at 6ppm (Section 9.5), clearly the Type 1 species (OMTHP and DETPMP) always outperform the Type 2 species (HMTPMP and HMDP) under any set of test conditions, e.g. compare Figure 9.25 and Figure 9.26 (Type 1 SIs) with Figure 9.27 and Figure 9.28 (Type 2 SIs). Secondly, the IE is improved for any selected SI, under Fixed Case conditions, and SI consumption suppressed (with only few exceptions to this). For example, compare the following pairs of figures:

(i) For 60/40 NSSW/FW:

OMTHP: Figure 9.25 (Base Case) and Figure 9.29 (Fixed Case);
DETPMP: Figure 9.26 (Base Case) and Figure 9.30 (Fixed Case);
HMTPMP: Figure 9.27 (Base Case) and Figure 9.31 (Fixed Case);
HMDP: Figure 9.28 (Base Case) and Figure 9.32 (Fixed Case).

(ii) For 80/20 NSSW/FW:

OMTHP: Figure 9.33 (Base Case) and Figure 9.37 (Fixed Case);
DETPMP: Figure 9.34 (Base Case) and Figure 9.38 (Fixed Case);
HMTPMP: Figure 9.35 (Base Case) and Figure 9.39 (Fixed Case);
HMDP: Figure 9.36 (Base Case) and Figure 9.40 (Fixed Case).

The SI consumption result presented in Section 9.7 for EDTMPA (a Type 2 phosphonate) is consistent with results obtained for the other Type 2 species HMTPMP, HMDP and NTP, in that both % SI in solution and IE are declining rapidly up to 96 hours (Figure 9.43). The SI consumption results for HEDP and HPAA are somewhat unusual in that the % SI profiles are more typical of a Type 1 species (see Figure 9.44 – Figure 9.48). Two possible explanations for this behaviour can be given. It could be because HEDP and HPAA are somewhat "borderline" between Type 1 and Type 2, giving rise to these anomalies *or* it could also be because these two species are very soluble – both molecules contain hydroxide functional

groups and, more importantly, both molecules can form very stable 6-membered chelate rings with M^{2+} cations, as illustrated in Chapter 12 (Figure 12.2(a) and (b)). Furthermore, the HPAA is a mono-phosphonated carboxylic acid. It may be the case that a large proportion of these molecules are "poisoned" by Mg^{2+} cations – thus remaining in solution but ineffective. Perhaps Mg^{2+}-complexed 6-membered HEDP and HPAA chelates are particularly stable. This is highly likely, since the size of the Mg^{2+} cation is very similar to the size of the other 5 atoms present in the chelate ring (1 x C, 2 x P and 2 x O in both cases), whereas other cations such as Ca^{2+}, Ba^{2+} and Sr^{2+} are markedly larger.

The phosphonate SI consumption results presented in this chapter have illustrated that Type 2 phosphonates (excluding HEDP and HPAA) are consumed rapidly from solution when tested at *pre-MIC* threshold [SI]s, whereas Type 1 phosphonates remain in solution over extended periods of time (up to 70 hours) and also maintain good IE. Testing all phosphonates (i.e. both types), the level of IE *always* correlates with the SI consumption profile.

SI consumption is suppressed in brine mixes containing a higher molar ratio of Ca^{2+}/Mg^{2+} (i.e. higher $[Ca^{2+}]$, lower $[Mg^{2+}]$). Thus, when SIs are tested at a fixed [SI] under Base Case and Fixed Case test conditions, there is almost always less SI consumption in the Fixed Case. Testing DETPMP at 5ppm (Section 9.3.1), the highest IE was achieved with $Ca^{2+}/Mg^{2+} = 4$, followed by $Ca^{2+}/Mg^{2+} = 2$, followed by $Ca^{2+}/Mg^{2+} = 1$. At 22 hours, this correlated with least SI consumption with $Ca^{2+}/Mg^{2+} = 4$, followed by $Ca^{2+}/Mg^{2+} = 2$, followed by $Ca^{2+}/Mg^{2+} = 1$. Similar observations were found in results for OMTHP, DETPMP, HMTPMP and HMDP, when tested at fixed [SI] under Base Case and Fixed Case conditions (Section 9.5).

9.8.2 ESEM Images – Crystal Morphologies

By examining the ESEM images of scale deposits in Sections 9.3.2 and 9.6, it is clear that the Type 1 SIs (OMTHP and DETPMP) change the crystal morphology in a different way than the Type 2 SIs (HMTPMP and HMDP). The presence of Type 1 SI tends to cause the break-up, disintegration, or dispersion of the barite / celestite crystal structure – normal crystal growth is largely inhibited. For example, see Figure 9.41(d)–(n). When Type 2 SIs are present, normal crystal growth is again inhibited, but there is a tendency for larger, globular, spherical scale / SI particles to form, such as in Figure 9.41(o)–(z). In uninhibited test bottles

(i.e. containing no SI), normal scale crystals grow – "desert rose" crystal forms are clearly visible, such as in Figure 9.41(a)–(c). See Table 9.3 – Crystal morphologies of various types of scale deposit. It should be remembered that scale deposits are *not* pure barium sulphate, but a *mixture* of barium, strontium and calcium sulphates. In blank (uninhibited) test bottles, there will be a large proportion of strontium in the scale deposit, however, in SI-containing test bottles, the proportion of strontium in the deposit will be reduced dramatically – this is due to the fact that strontium sulphate scale is easily inhibited by SIs (SR strontium sulphate is several orders of magnitude smaller than SR barium sulphate). Only a small proportion of calcium is integrated into the growing scale, typically up to ~6% of Ba^{2+} can be replaced by Ca^{2+} (Sorbie and Laing, 2004), clearly there is likely to be greater Ca^{2+} integration into the scale deposit in Fixed Case tests where the brine [Ca^{2+}] is higher. These factors will be reflected in the EDAX analyses results (see Section 9.8.3).

Precipitate Sample	Crystal Morphology
Blank	Uninhibited crystal growth – "desert roses" present.
Type 1 SI present	Inhibited crystal growth. Dispersion and disintegration of crystals. Small particles of scale / SI.
Type 2 SI present	Inhibited crystal growth. Large, spherical globules visible.

Table 9.3 – Crystal morphologies of various types of scale deposit.

9.8.3 EDAX Analyses

9.8.3.1 Phosphorus

It appears the detection of phosphorus in the precipitate samples depends largely on the [SI] selected for the IE tests. Thus, the largest atomic % phosphorus is detected in the precipitate samples obtained from experiments where pre-22hr MIC [SI]s were tested – see Figure 9.42(a). More phosphorus was detected in the HMTPMP and HMDP precipitate samples compared to in the DETPMP samples. In the 60/40 Base Case consumption experiment, [SI]s varied as follows: [HMTPMP] = 35ppm, [HMDP] = 35ppm and [DETPMP] = 25ppm.

In the 80/20 Base Case experiment, [SI]s varied as follows: [HMTPMP] = 70ppm, [HMDP] = 60ppm and [DETPMP] = 15ppm. The atomic % phosphorus detected by EDAX is therefore broadly a function of the [SI] used in the original static efficiency experiment. This explains why no phosphorus was detected in the OMTHP precipitate samples – since OMTHP is the best performing SI and as such, the [OMTHP]s selected for the IE tests were the lowest of all the SIs tested – therefore no phosphorus was detected by EDAX. The main reason why no phosphorus was detected in the majority of the precipitate sample analysed in this series of experiments is because the concentration of phosphorus is so low in comparison to the other main elements present (i.e. Ba, Sr, S, O). [P] is undetectable unless the [SI] is high enough for detection to be possible by EDAX, e.g. 70ppm HMTPMP and 60ppm HMDP – samples obtained from these test bottles had the highest phosphorus detected – see Figure 9.42(a).

9.8.3.2 Barium

The atomic % barium in the blank samples is much less than in the SI dosed samples – see Figure 9.42(b). This is because strontium sulphate scale is not inhibited in the blank test bottles which results in there being a larger proportion of strontium in the precipitate formed in the blank test bottles and thus, a lower proportion of barium. The presence of SI largely inhibits strontium sulphate scale. It appears that generally there is a larger atomic % of barium in the Type 1 SI dosed precipitate samples compared to the Type 2 SI dosed samples. This suggests that the Type 1 SIs are better barite scale inhibitors – since clearly the Type 2 SIs have allowed more strontium sulphate to precipitate. The % barium in the Type 2 SI dosed precipitate samples is generally in between that in the blank and Type 1 SI precipitate deposits.

9.8.3.3 Strontium

With reference to Figure 9.42(c), the largest atomic % strontium is detected in the blank precipitate deposits, followed by the Type 2 SI dosed precipitate deposits, followed by the Type 1 SI dosed precipitate deposits. The reasons behind this were explained in Section 9.8.3.2 above. The higher the atomic ratio of Ba/Sr in the precipitate deposits, the better the SI (if SI present) since this means more strontium sulphate precipitate has been prevented.

No strontium sulphate scale inhibition occurs in the blank sample, and the EDAX results reflect this. See Table 9.4.

Type of PPT deposit	Atomic Ratio Ba/Sr in deposit (as fraction) *	Atomic Ratio Ba/Sr in deposit (as number) *	Comments
Blank	~3/16	~0.19	Totally uninhibited system
Type 1 SI dosed	~11/5	~2.2	$SrSO_4$ scale largely inhibited
Type 2 SI dosed	~8/9	~0.88	Ratio Ba/Sr nearer to that detected in blank PPT deposits => poorer scale inhibitors than Type 1 phosphonates.

* ~average atomic % values used for calculation, based on all EDAX results presented in Figure 9.42.

Table 9.4 – Atomic ratio Ba/Sr detected in PPT deposit samples obtained from static barium sulphate inhibition efficiency experiments.

9.8.3.4 Calcium

It appears that there is some degree of calcium inclusion into the scale lattice in all precipitate deposits, i.e. from blank and SI dosed test bottles. Some of the highest atomic % calcium values were detected in Type 1 SI dosed precipitate samples – in one instance = 3.5%, testing DETPMP at 3ppm, 80/20 NSSW/FW, Fixed Case – see Figure 9.42(d). In this static IE test, brine [Ca^{2+}] was = 2000ppm which may have aided the high Ca^{2+} inclusion. The results show in most cases there is more calcium inclusion into the scale deposits obtained from the Fixed Case experiments compared to the Base Case experiments – due to the higher brine [Ca^{2+}] in the Fixed Case tests. These findings agree entirely with previous findings by other workers, where Ca^{2+} inclusion into the barite scale lattice was shown to (i) increase in the presence of SI (compared to blanks), up to ~12% of Ba^{2+} replaced by Ca^{2+}; and (ii) increase as the brine mix [Ca^{2+}] increases (Sorbie and Laing, 2004). In a blank test (no SI present), it is known ~6% of Ba^{2+} can be replaced by Ca^{2+} (Sorbie and Laing, 2004).

The results presented in this Chapter suggest that there may be slightly more calcium inclusion into the scale when Type 1 SIs are being tested compared to Type 2. From this, it follows that the Type 1 SIs must be better crystal growth blockers, compared to the Type 2 SIs – since the SI is integrated into the scale in conjunction with calcium (i.e. SI bonded to calcium) (Sorbie and Laing, 2004). This would support earlier findings where Type 1 SIs were more efficient at 22 hours, compared to Type 2 SIs (Chapter 5). The atomic % calcium in the Type 2 precipitate deposits is about the same level as for the blank samples – indicating that the presence of Type 2 SI is not greatly influencing the integration of calcium into the scale deposit, and presumably they are not as good as Type 1 species at crystal growth inhibition – hence the rapid decline in IE over time in the static IE experiments. There are some instances where the atomic % calcium detected in the Type 2 SI dosed precipitate samples is actually less than in the blank precipitate samples – experiments at fixed [SI] = 6ppm, Fixed Cases – testing both HMTPMP and HMDP. This means the presence of these SIs is actually causing less calcium to be integrated into the scale lattice compared to when no SI is present at all. Overall (i.e. for blanks and SI dosed precipitate samples), calcium inclusion into the scale is in the region 1–3.5% (atomic %). See Table 9.5.

Type of SI present	**Approximate Ca lattice inclusion (atomic %)**	**SI Mechanism**
No SI (blanks)	~1.5–2%.	No crystal growth inhibition.
Type 1	Higher than for uninhibited (blank) sample, up to 3.5%.	Mainly crystal growth inhibition – Ca and SI integration into the scale lattice.
Type 2	About same as for uninhibited (blank) sample. In some cases lower – 1.25–1.5%	More limited crystal growth inhibition. Exhibit some nucleation inhibition qualities.

Table 9.5 Approximate atomic % calcium in various types of scale deposits and possible scale inhibition mechanisms.

9.8.3.5 Sulphur and Oxygen

Broadly the atomic % sulphur and oxygen in all the precipitate samples is about the same – ~16% sulphur and ~60% oxygen – see Figure 9.42(e) and (f). This is because it does not matter whether sulphate (SO_4^{2-}) is bonded to Ba^{2+}, Sr^{2+} or Ca^{2+} – the atomic % sulphur and oxygen remains constant – since the molar ratio of sulphate to Ba, Sr and Ca remains constant, i.e. 1:1. Likewise, it does not matter what the actual mass of precipitate is since this does not alter atomic ratios. All the precipitate samples are compositionally mixed sulphate scale, i.e. a mix of Ca/Sr/Ba sulphate. It is only the atomic % of Ca, Sr and Ba that varies and this depends only on the specific experimental conditions, viz. the type of SI present in the system (if any), and also the brine composition – particularly [Ca^{2+}].

9.8.4 Overall Conclusions

The experimental results presented in this Chapter have illustrated clearly that there are clear differences in the SI consumption of Type 1 and Type 2 phosphonate SIs, whereby the Type 2 species are consumed much more rapidly and to a greater degree than the Type 1 products. Often Type 1 SI remains in solution over extended periods of time, even when IE has declined. The only two exceptions to this general observation are HEDP and HPAA, which were both identified as being Type 2 products in the MIC vs. %NSSW tests presented in Chapter 5, but produced SI consumption profiles similar to OMTHP and DETPMP. Because of these two anomalies, the "Type 1" and "Type 2" classification of phosphonate SIs must be fundamentally based on their performance in the MIC vs. %NSSW tests, in other words, their sensitivity to Ca^{2+}/Mg^{2+}. SI consumption experiments could be considered a "secondary" test for SI Type, but less reliable. SI consumption profiles are also dependant on the [SI] being tested – therefore it is paramount that a pre-MIC [SI] is always tested. The experiments presented in this Chapter have also uncovered another finding. There are clear differences in SI consumption, depending upon the brine composition – in particular [Ca^{2+}] and [Mg^{2+}]. In IE tests presented in this thesis, Ca^{2+} suppresses SI consumption whereas Mg^{2+} enhances SI consumption. These findings correlate with the effects of Ca^{2+} and Mg^{2+} upon phosphonate IE, i.e. Ca^{2+} enhances IE, Mg^{2+} suppresses IE. The EDAX analysis of scale deposits has indicated that there is a greater % of Ca inclusion into the forming scale when Type 1 SIs are present (vs. blanks and Type 2 SI-containing deposits). This suggests the Type 1 products are better crystal growth blockers. The good performance of the Type 1 SIs in IE

experiments at 22 hours and beyond also supports this finding. Products which inhibit well at 22 hours and beyond are the best crystal growth blockers. OMTHP, DETPMP and PMPA fall into this category (all Type 1 products). PMPA SI consumption tests will be presented in Chapter 10.

Chapter 10: Penta-phosphonates and Polymers – SI Consumption Experiments

Chapter 10 Summary: This Chapter presents two series of SI consumption experiments testing penta-phosphonates DETPMP and HMTPMP alongside a small range of phosphorus-containing polymers. Two brine systems are tested – one with Ca^{2+}/Mg^{2+} = 0.19, the other with Ca^{2+}/Mg^{2+} = 1.64. The total number of moles of divalent ions in the mix (Ca^{2+} + Mg^{2+}) and all other test conditions are kept constant in both experiments, in order to make direct comparisons between the two experiments.

10.1 Introduction

In the experiments described in this Chapter, a range of 4 phosphorus containing polymeric SIs: PPCA, SPPCA, PFC and PMPA were tested in static IE tests involving multiple sampling times, as early as half an hour (30 minutes), up to 96 hours (i.e. 4 days) after mixing NSSW with FW. In addition to analysing for [Ba^{2+}] at each sampling time, SI was assayed by ICP spectroscopy, by means of [P], in the same way as phosphonate SIs (Chapter 9). Analysis data in Chapter 4 indicated that PMPA contains > 20% phosphorus, whereas the other polymers tested in this Chapter each contain ~5% phosphorus. Thus, all these P-containing polymers clearly contain enough phosphorus to enable us to analyse for them successfully by ICP spectroscopy. DETPMP (Type 1 penta-phosphonate) and HMTPMP (Type 2 penta-phosphonate) are tested alongside these polymers, in order for generic comparisons between results to be made (polymer vs. phosphonate). The SIs are tested in two different brine systems – one a high [Mg^{2+}] mix, molar ratio Ca^{2+}/Mg^{2+} = 0.19 and one a high [Ca^{2+}] mix, molar ratio Ca^{2+}/Mg^{2+} = 1.64. In order for a direct comparison to be made between the two test results – in both experiments, the total number of moles of (Ca^{2+} + Mg^{2+}), X_m in the brine mix is fixed = 72.3 millimoles/L and mixing ratio NSSW/FW = 60/40. Furthermore, *all* the polymers (except PMPA) are tested at 20ppm in *both* SI consumption experiments (i.e. Ca^{2+}/Mg^{2+} = 0.19 and 1.64). 20ppm is the pre-2 hour 60/40 MIC level for all the polymers (except PMPA) – although clearly MIC depends upon the brine molar ratio Ca^{2+}/Mg^{2+}. In the Ca^{2+}/Mg^{2+} = 0.19 experiment, both penta-phosphonates *and* PMPA are tested at 20ppm (pre-2 hour 60/40 MIC with Ca^{2+}/Mg^{2+} = 0.19) whereas in the Ca^{2+}/Mg^{2+} =

1.64 experiment, all 3 are tested at 6ppm (pre-2 hour 60/40 MIC with Ca^{2+}/Mg^{2+} = 1.64) – since it is well known from Chapters 5 and 6 that the MIC of these 3 products decreases with increasing molar ratio Ca^{2+}/Mg^{2+}. 0.19 is the molar ratio Ca^{2+}/Mg^{2+} found naturally in NSSW whereas 1.64 is the molar ratio found in Forties formation water. However, since X_m = 72.3 mol/L in the brine mix, the initial $[Ca^{2+}]$ and $[Mg^{2+}]$ in the formation water used for the Ca^{2+}/Mg^{2+} = 1.64 test ≠ $[Ca^{2+}]$ = 2000ppm and $[Mg^{2+}]$ = 739ppm (as in Forties FW) – instead the $[Ca^{2+}]$ and $[Mg^{2+}]$ FW concentrations are marginally lower than these values, giving a lower value of X_m =72.3 mol/L in the brine mix once mixed with "blank" NSSW containing 0ppm Ca^{2+} and 0ppm Mg^{2+}. See Chapter 3, Tables 3.3, 3.4 and 3.9 for NSSW and FW brine compositions.

10.2 DETPMP, HMTPMP, PPCA, SPPCA, PTC, PMPA – Ca^{2+}/Mg^{2+} = 0.19

Figures 10.1 to 10.6 present the entire set of IE and [SI] remaining in solution vs. residence time for all the experiments carried out at Ca^{2+}/Mg^{2+} = 0.19. This will be followed by a detailed discussion of these results and the main conclusions from this series of experiments.

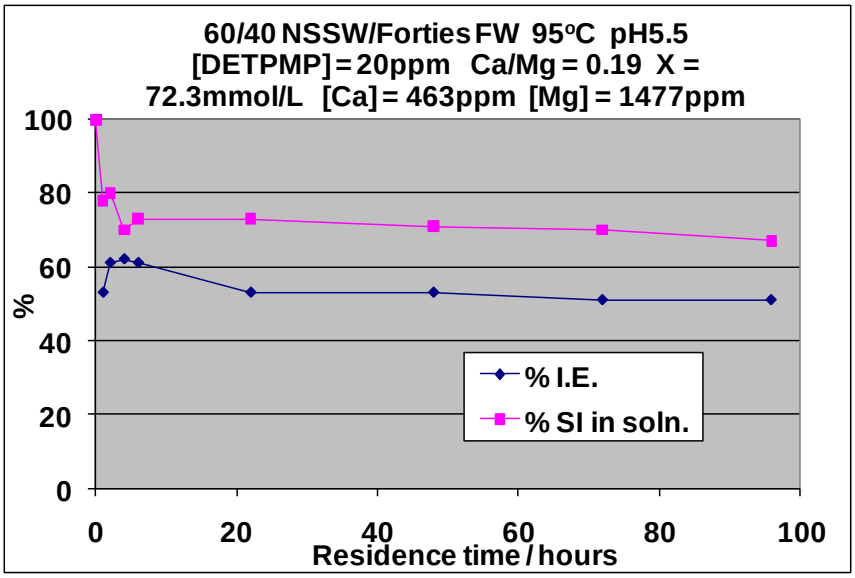

Figure 10.1 – IE and %SI in solution vs. time: [DETPMP] = 20ppm; Molar Ratio Ca^{2+}/Mg^{2+} = 0.19; X = moles (Ca^{2+}+Mg^{2+}) = 72.3millimoles/L, 95°C, pH5.5.

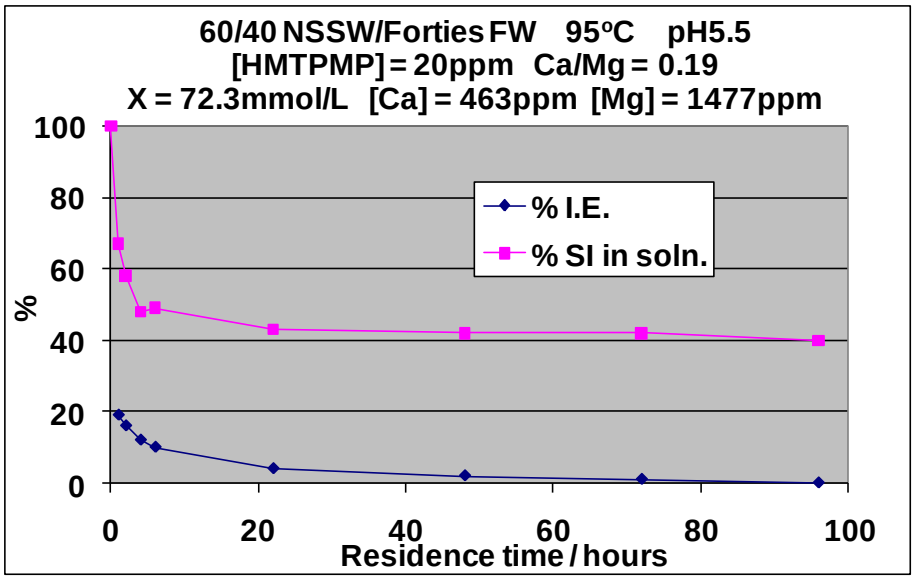

Figure 10.2 – IE and %SI in solution vs. time: [HMTPMP] = 20ppm; Molar Ratio Ca^{2+}/Mg^{2+} = 0.19; X = moles (Ca^{2+}+Mg^{2+}) = 72.3millimoles/L, 95°C, pH5.5.

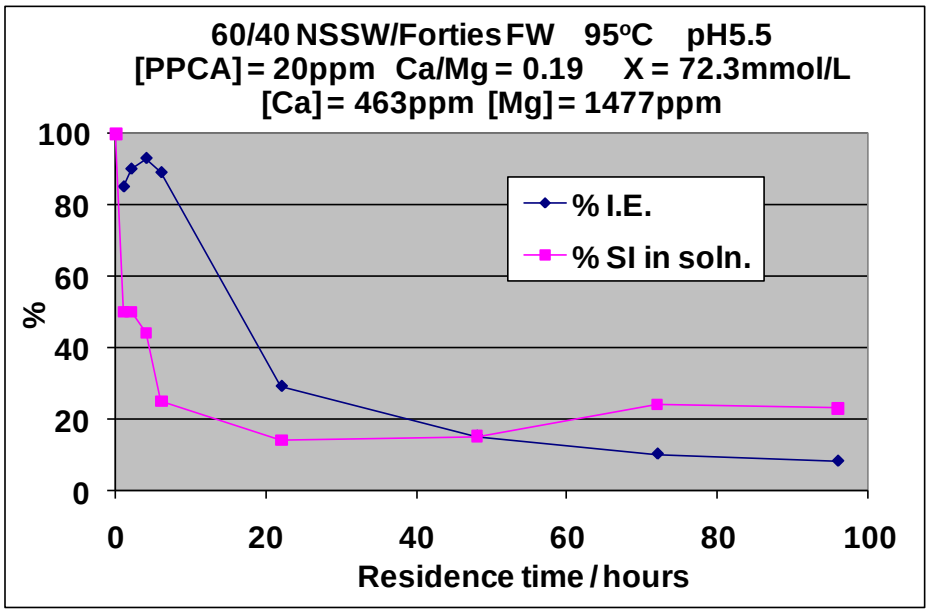

Figure 10.3 – IE and %SI in solution vs. time: [PPCA] = 20ppm; Molar Ratio Ca^{2+}/Mg^{2+} = 0.19; X = moles (Ca^{2+}+Mg^{2+}) = 72.3millimoles/L, 95°C, pH5.5.

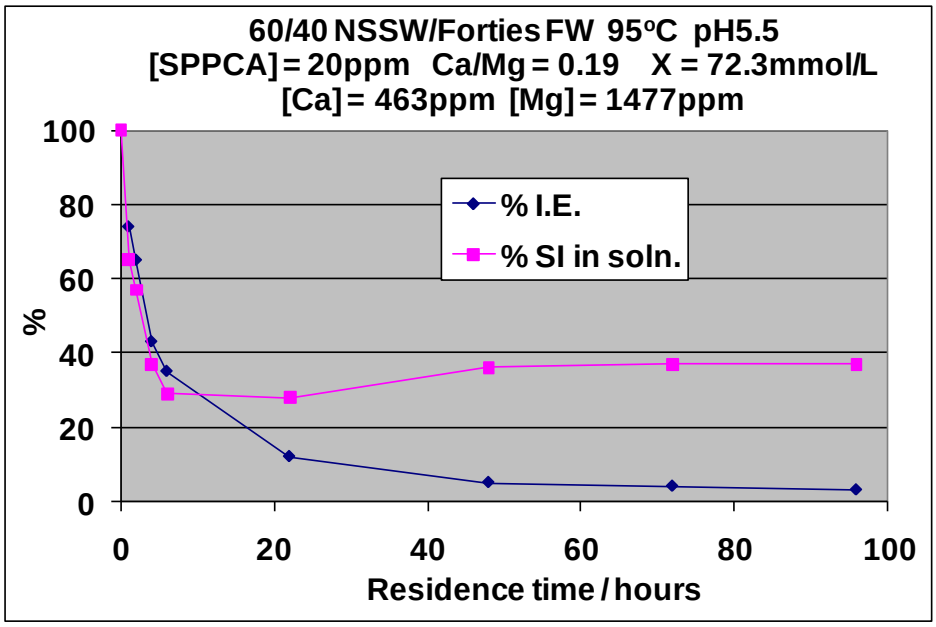

Figure 10.4 – IE and %SI in solution vs. time: [SPPCA] = 20ppm; Molar Ratio Ca^{2+}/Mg^{2+} = 0.19; X = moles (Ca^{2+}+Mg^{2+}) = 72.3millimoles/L, 95°C, pH5.5.

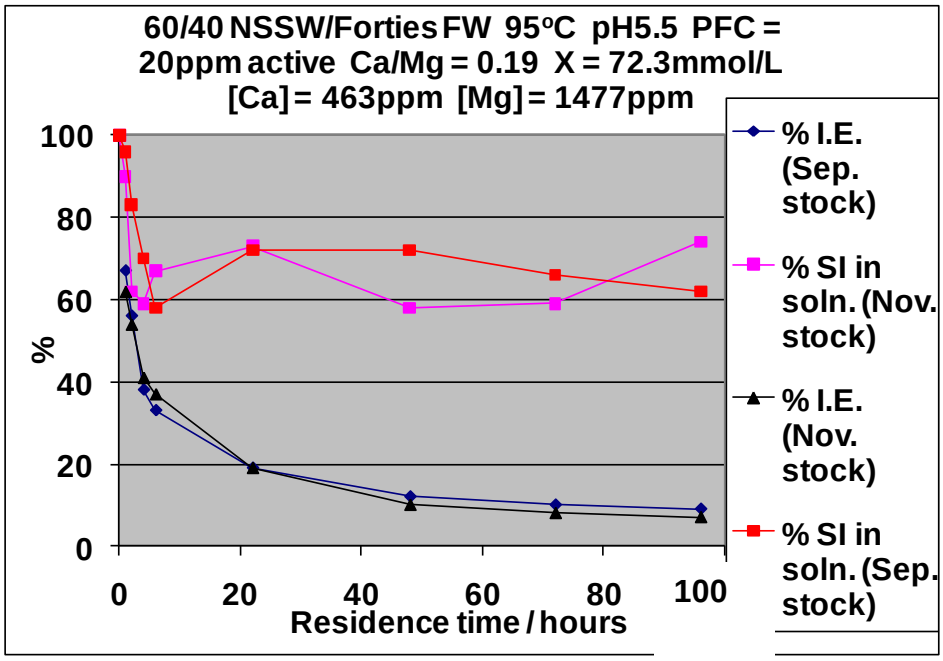

Figure 10.5 – IE and %SI in solution vs. time: [PFC] = 20ppm; Molar Ratio Ca^{2+}/Mg^{2+} = 0.19; X = moles (Ca^{2+}+Mg^{2+}) = 72.3millimoles/L, 95°C, pH5.5.

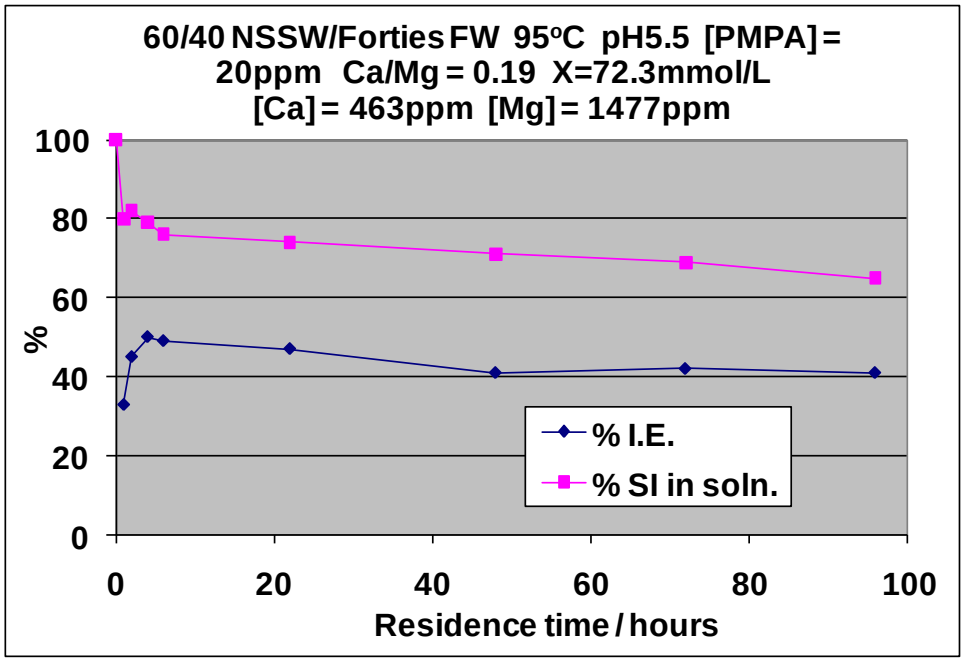

Figure 10.6 – IE and %SI in solution vs. time: [PMPA] = 20ppm; Molar Ratio Ca^{2+}/Mg^{2+} = 0.19; X = moles (Ca^{2+}+Mg^{2+}) = 72.3millimoles/L, 95°C, pH5.5.

10.3 DETPMP, HMTPMP, PPCA, SPPCA, PTC, PMPA – Ca^{2+}/Mg^{2+} = 1.64

Figures 10.7 to 10.12 present the entire set of IE and [SI] remaining in solution vs. residence time for all the experiments carried out at Ca^{2+}/Mg^{2+} = 1.64. This will be followed by a detailed discussion of these results and the main conclusions from this series of experiments.

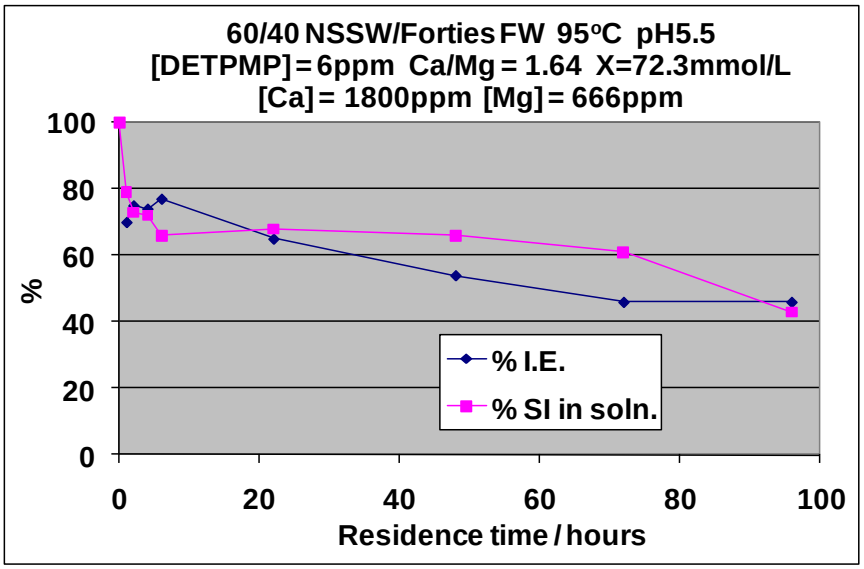

Figure 10.7 – IE and %SI in solution vs. time: [DETPMP] = 6ppm; Molar Ratio Ca^{2+}/Mg^{2+} = 1.64; X = moles (Ca^{2+}+Mg^{2+}) = 72.3millimoles/L, 95°C, pH5.5.

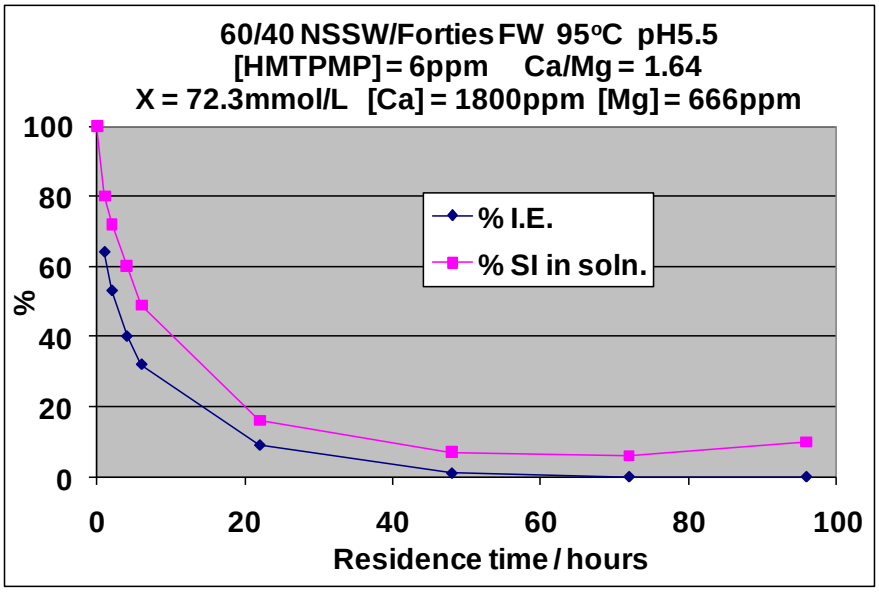

Figure 10.8 – IE and %SI in solution vs. time: [HMTPMP] = 6ppm; Molar Ratio Ca^{2+}/Mg^{2+} = 1.64; X = moles (Ca^{2+}+Mg^{2+}) = 72.3millimoles/L, 95°C, pH5.5.

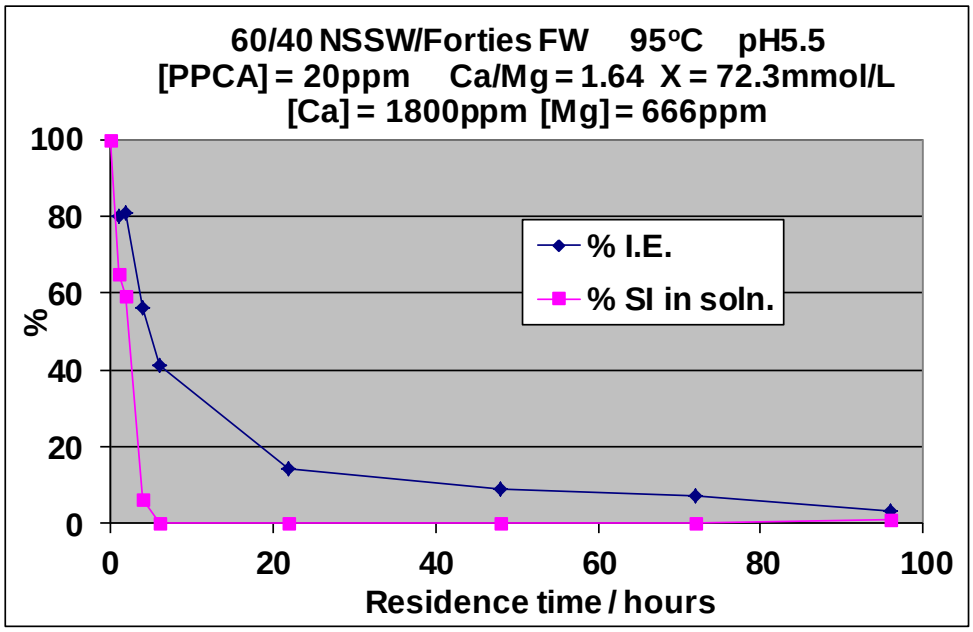

Figure 10.9 – IE and %SI in solution vs. time: [PPCA] = 20ppm; Molar Ratio Ca^{2+}/Mg^{2+} = 1.64; X = moles (Ca^{2+}+Mg^{2+}) = 72.3millimoles/L, 95°C, pH5.5.

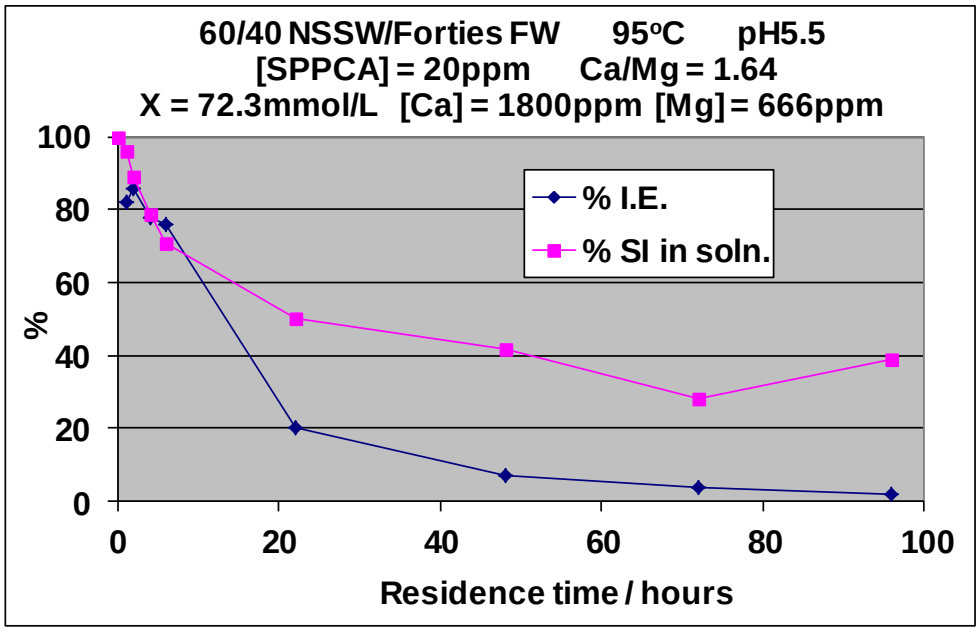

Figure 10.10 – IE and %SI in solution vs. time: [SPPCA] = 20ppm; Molar Ratio Ca^{2+}/Mg^{2+} = 1.64; X = moles (Ca^{2+}+Mg^{2+}) = 72.3millimoles/L, 95°C, pH5.5.

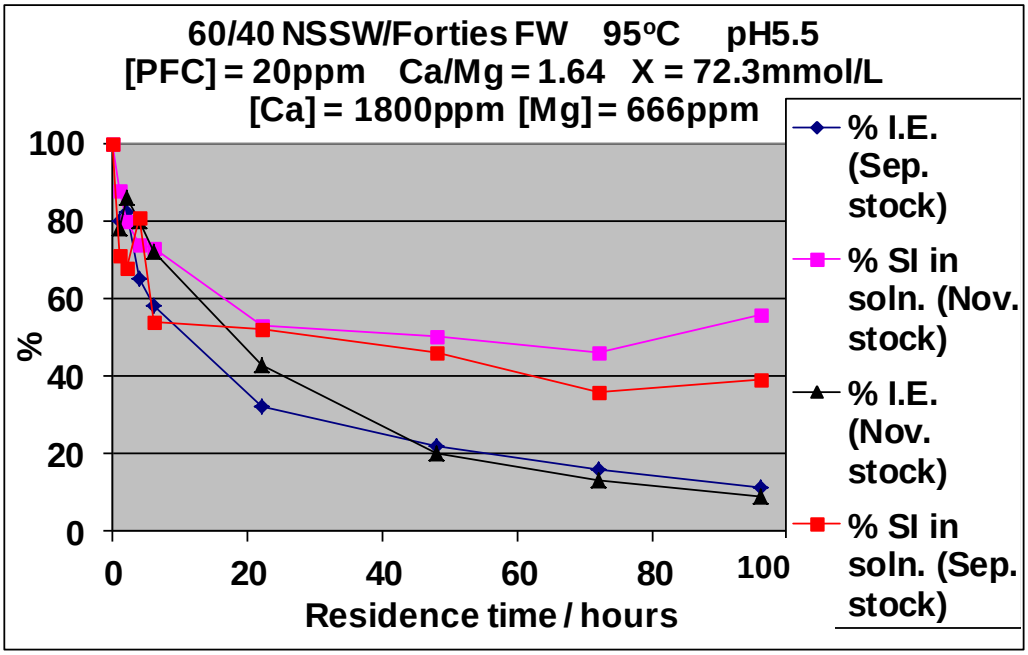

Figure 10.11 – IE and %SI in solution vs. time: [PFC] = 20ppm; Molar Ratio Ca^{2+}/Mg^{2+} = 1.64; X = moles (Ca^{2+}+Mg^{2+}) = 72.3millimoles/L, 95°C, pH5.5.

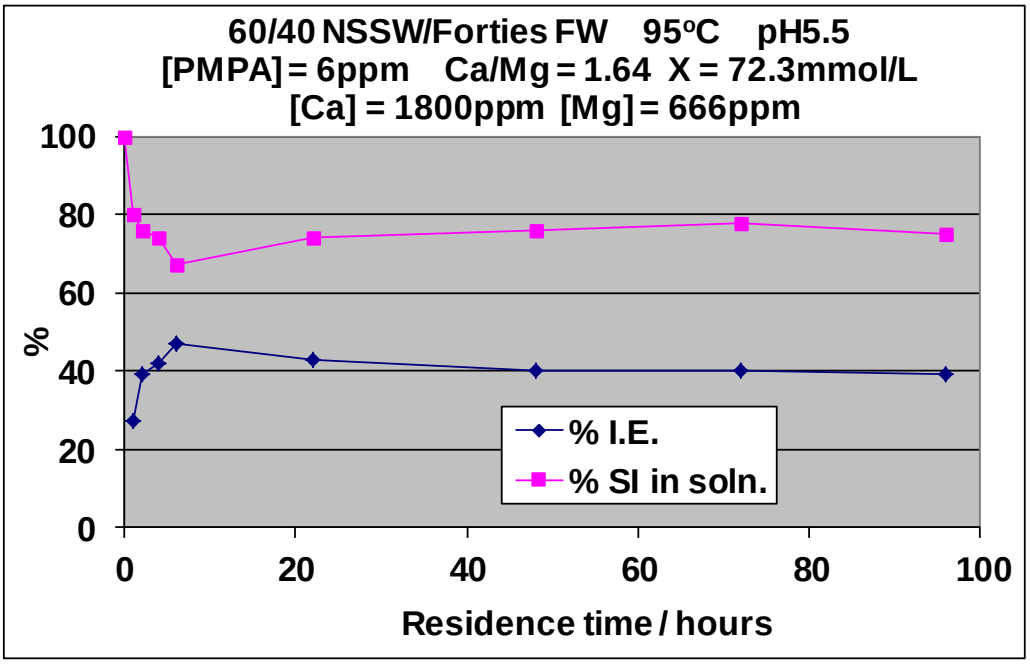

Figure 10.12 – IE and %SI in solution vs. time: [PMPA] = 6ppm; Molar Ratio Ca^{2+}/Mg^{2+} = 1.64; X = moles (Ca^{2+}+Mg^{2+}) = 72.3millimoles/L, 95°C, pH5.5.

10.4 Summary and Conclusions

10.4.1 Ca^{2+}/Mg^{2+} = 0.19

From Figures 10.1 and 10.6, is clear from the IE and %SI in solution versus time results, that the PMPA behaves almost identically to the DETPMP when both SIs are tested at 20ppm with Ca^{2+}/Mg^{2+} = 0.19. In both cases, the %SI in solution is ~70%, whereas the DETPMP IE is ~10% higher compared to PMPA at most sampling times. This similarity between DETPMP and PMPA in SI consumption experiments correlates very well with the categorisation of SIs in Chapter 6, where PMPA was classed as Type 1. Clearly PMPA behaves more like a phosphonate SI than like a polymeric SI. Indeed, there has been some suggestion recently that PMPA is *not* in fact polymeric at all and this would be very consistent with observations here. This knowledge was gained through communication with the PMPA manufacturer.

The SI consumption result for HMTPMP (Figure 10.2) is rather unusual, in that the %SI in solution is maintained at ~40%, even when the IE is near-zero. This kind of SI consumption result resembles similar results obtained testing phosphonate SIs HEDP and HPAA in Chapter 9 – see Figures 9.44 (HEDP) and Figures 9.46–9.48 (HPAA). In all these cases, a large quantity of SI remains in solution when the IE is near-zero. The %SI in solution profiles in all these cases are more typical of Type 1 species and these observations re-iterate the requirement to base the Type 1 / Type 2 classification of SIs fundamentally on MIC versus mixing ratio test results (Chapters 5 and 6).

SI consumption results obtained testing PPCA and SPPCA with Ca^{2+}/Mg^{2+} = 0.19 (Figure 10.3 and Figure 10.4) *are* typical of Type 2 species, i.e. rapid SI consumption and declining IE with time. In the case of SPPCA, there is less SI consumption (Figure 10.4), almost 40% of SI remains in solution at 48, 72 and 96 hours. This could be due to the presence of sulphonate functional groups which do not bind strongly to Ca^{2+} and Mg^{2+}. If the sulphonate functional groups do not bind to Ca^{2+}, this could be inhibiting the SI consumption, implying that the SPPCA is consumed less than the non-sulphonated analogue, PPCA. On the contrary, carboxylate functional groups *do* bind quite strongly to Ca^{2+}.

Testing PFC (Figure 10.5), the %SI in solution has not declined rapidly over time whereas the IE has. Analytical data (Chapter 4) indicated the PFC may contain 10-15% sulphur – see Figure 4.6. This is a much higher sulphur content compared to SPPCA. It could be the case that the sulphonate functional groups are limiting the degree of SI consumption. PTC was identified as Type 2 in Chapter 6; the IE profile in Figure 10.5 is definitely Type 2.

10.4.2 Ca^{2+}/Mg^{2+} = 1.64

Once again, the SI consumption and IE profiles for DETPMP and PMPA are remarkably similar (see Figure 10.7 and Figure 10.12), i.e. %SI in solution and IE are both maintained over long periods of time. Testing the HMTPMP with Ca^{2+}/Mg^{2+} = 1.64, both IE and %SI decline rapidly over time and this result is a classic Type 2 profile (Figure 10.8). Perhaps the higher [Ca^{2+}] in the Ca^{2+}/Mg^{2+} = 1.64 case is enabling a larger % of SI to be consumed into the forming scale. As already established in Chapter 5, phosphonate SIs perform better in high [Ca^{2+}] mixes – however note that HMTPMP was tested at 6ppm in Figure 10.8 (Ca^{2+}/Mg^{2+} = 1.64) and at 20ppm in Figure 10.2 (Ca^{2+}/Mg^{2+} = 0.19), i.e. HMTPMP was not tested at the same [SI] in both tests.

Testing PPCA with Ca^{2+}/Mg^{2+} = 1.64, the decline in IE and %SI in solution is much more marked compared to the Ca^{2+}/Mg^{2+} = 0.19 case (compare Figure 10.9 and Figure 10.3). This is very plausible, since in Chapter 6 PPCA performed best in low to moderate [Ca^{2+}] mixes and there is a SI incompatibility issue with Ca^{2+} at [Ca^{2+}] = ~1000ppm+, whereby the SI precipitates with Ca^{2+}. The precipitated SI is ineffective in terms of IE. In this case, the depletion of SI from solution could be as a result of a combination of two effects: (i) SI consumption into the growing scale; and (ii) precipitation of SI with calcium. There is less SI consumption of SPPCA compared to PPCA with Ca^{2+}/Mg^{2+} = 1.64 (compare Figure 10.9 and Figure 10.10). This is the same trend as observed in the Ca^{2+}/Mg^{2+} = 0.19 case. This could now be a result of two factors: (i) PPCA is incompatible with 1800ppm Ca^{2+} whereas SPPCA is compatible; and (ii) sulphonate functional groups in SPPCA may be limiting the depletion of SI from solution. If PPCA is precipitating with Ca^{2+}, this will reduce [PPCA] in solution rapidly.

Testing PFC with Ca^{2+}/Mg^{2+} = 1.64, there is more SI depletion compared to the Ca^{2+}/Mg^{2+} = 0.19 case (compare Figure 10.11 with Figure 10.5). A similar explanation can be given for this as for PPCA. With reference to the IE vs. mixing ratio tests in Chapter 6, PPCA and PFC both function worse (i.e. lower IE, higher MICs) in the Fixed Case tests compared to the Base Case tests. If limited precipitation of PFC with Ca^{2+} *is* occurring where [Ca^{2+}] = 1800ppm, which is entirely possible, clearly this will result in a decline in solution [PFC] and could result in a %SI profile such as in Figure 10.11. In the case of PFC, there could be two conflicting factors. The presence of sulphonate functional groups on the PFC molecules may help limit SI consumption whereas possible incompatibility with Ca^{2+} would aid SI consumption. Both these factors could result in an "intermediate" %SI profile such as in Figure 10.11 where there is neither rapid SI depletion nor a high % of SI in solution maintained over time.

There was less SI consumption testing DETPMP, HMTPMP and PMPA in the Ca^{2+}/Mg^{2+} = 1.64 test conditions, compared to the Ca^{2+}/Mg^{2+} = 0.19 test conditions. This is as expected, since these 3 products perform better in higher molar ratio Ca^{2+}/Mg^{2+} mixes (Chapters 5 and 6). Differences in IE between Ca^{2+}/Mg^{2+} = 0.19 and 1.64 cannot be compared directly as these 3 products were tested at different [SI]s in each test. SPPCA performed similarly in the Ca^{2+}/Mg^{2+} = 0.19 and 1.64 tests (compare Figure 10.4 with Figure 10.10). There was less PPCA and PFC depletion from solution with Ca^{2+}/Mg^{2+} = 0.19 compared with Ca^{2+}/Mg^{2+} = 1.64, due to the detrimental effects of *calcium* in the Ca^{2+}/Mg^{2+} = 1.64 tests.

10.4.3 Interpretation of SI Consumption Results – All SIs

With regard to the SI consumption of phosphonate *and* polymeric SIs, the classification Type 1 or Type 2 must be *primarily* based upon their performance in MIC vs. mixing ratio experiments (Chapters 5 and 6). The SI consumption experiments (Chapters 9 and 10) are a "*secondary*" test. If long-term IE / SI consumption test results are to be used for Type 1 / Type 2 categorisation purposes, particular emphasis should be focussed on the long-term IE profiles (e.g. up to 96 hours), rather than the %SI vs. time profile. Three main points should be considered when interpreting an SI consumption test result:

1. If the *IE* and %SI in solution are both *maintained* and correlate with one another (e.g. Figure 10.6 testing PMPA), the product may be *Type 1*.
2. If the *IE* profile declines rapidly over time *and* a large quantity of SI remains in solution (e.g. Figure 10.5 testing PFC), the product may be *Type 2*.
3. If *both IE and %SI* profiles decline rapidly (e.g. Figure 10.8 testing HMTPMP), the product is very likely *Type 2*.

The two ambiguous phosphonate SIs HEDP and HPAA tested in Chapter 9 would clearly fall into category 2 above. Both were identified as Type 2 in Chapter 5.

Chapter 11: Non-ICP Analytical Methods for SI Assay

Chapter 11 Summary: In this Chapter, SI consumption experiment results are presented where the %SI in solution has been assayed by a non-ICP analytical technique – either by the C18 Hyamine or Pinacyanol wet chemical methods. In some cases, the %SI results determined by non-ICP methodology are compared with ICP assayed %SI results. In this Chapter, polymeric SIs PPCA, PFC, PVS and VS-Co are tested. The relevance, accuracy and advantages of non-ICP analytical methods over ICP spectroscopy for SI assay in this context, is discussed.

11.1 Introduction

SI consumption type experiments presented in Chapters 9 and 10 assayed for SI and Ba^{2+} at various stages of a static IE test using ICP spectroscopy (for P and Ba, respectively). However, in some cases, it is not possible to apply ICP spectroscopy for SI assay since the SI molecule contains no detectable atom e.g. it may only contain C, H and O. This is the case for many "green" SIs, for example, Maleic Acid Ter-polymer (MAT) which does not contain any ICP-detectable phosphorus or sulphur atoms in the chemical structure, making these molecules non-ICP detectable. Similarly, sulphonated species such as PVS and VS-Co which are *non-P-tagged* also cannot be assayed by ICP spectroscopy by means of [S] because of the presence of sulphate anions in the brine mix. If these products were assayed in a sulphate-containing matrix, the ICP spectrometer would detect all sulphur present in the test samples, i.e. sulphur which is part of the SI structure plus sulphur which is part of sulphate anions in the brine. These SIs could be detected by ICP spectroscopy by means of [S] if they were in a distilled water (DW) matrix, i.e. only SI. Indeed, this is how the % sulphur in these products was determined by ICP analysis in Chapter 4. A further complication is that the quenching solution routinely used in the static IE tests contains 1,000ppm "as supplied" PVS (see Chapter 3, Section 3.5.1). Sulphur present in the quenching solution PVS molecules would also be detected by ICP spectroscopy. In order for green SIs and non-P-tagged sulphonated species to be tested in SI consumption experiments (like those in Chapters 9 and 10), alternative wet chemical analytical methods for assaying [SI] must be employed, or solid phase extraction, HPLC, etc. (Graham et al., 2010).

The C18 / Hyamine / spectrophotometric (CHS) analytical method is suitable for assaying for *non-sulphonated* polymers such as MAT, PPCA, etc. Most green SIs and non-sulphonated SIs can be assayed by this method. The technique involves firstly passing the test samples through a C18 cartridge (after pH adjustment to ~pH4). The SI product *adsorbs* onto the cartridge. The adsorbed SI is subsequently desorbed from the cartridge using a *desorbing agent.* This process is essentially a separation technique – it separates the *analyte*, i.e. SI, from other components within the sample, such as brine cations and anions and quenching solution. Note – the PVS from the quenching solution *does not* adsorb onto the C18 cartridges (because it is sulphonated), and is thus separated from the SI which is being assayed. After the analyte has been separated from other sample components (i.e. the C18 procedure has been completed), a quantity of the reagent, Hyamine is added to each test sample (one at a time). The Hyamine reagent reacts with the non-sulphonated polymers to form a turbid solution. After a designated time interval, the sample is assayed by UV/visible spectrophotometry at 500nm. The absorbance is proportional to the concentration of SI in the test sample. Clearly SI calibration standards must be prepared for this analytical technique. Full details of the CHS technique are given in Chapter 3, Section 3.6. The CHS analytical technique was used to assay for SIs MAT and PPCA during SI consumption experiments. Clearly, the PPCA had already been tested in SI consumption experiments in Chapter 10, however the aim of assaying by CHS was to compare the % SI in solution results with those obtained by ICP spectroscopy and see if any differences are apparent. In addition to assaying for MAT and PPCA by CHS, Ba^{2+} was assayed by ICP spectroscopy, as normal, in order to determine the IE. In this Chapter, SI consumption results for MAT and PPCA, determined by the CHS technique, are presented.

As discussed above, the CHS analytical technique is not suitable for sulphonated species, therefore an alternative analytical technique must be applied for the assay of *non-P-tagged, sulphonated SIs* in SI consumption experiments. In order to assay for SIs PVS and VS-Co in SI consumption experiments, the Pinacyanol / spectrophotometric (PS) analytical technique was used. This method is very similar to CHS, except a C18 cartridge separation procedure is not required. A specified volume of test-sample (containing the PVS or VS-Co) is added to a specific volume of *Pinacyanol reagent*, then after a specified time interval has elapsed, the sample is assayed by UV/visible spectrophotometry at 485nm. Again, like CHS, the absorbance is proportional to the concentration of PVS or VS-Co present in the sample. PVS

or VS-Co calibration standards must also be prepared for the PS analytical technique. The clear purple Pinacyanol reagent reacts with sulphonated polymers to produce a cloudy light blue solution which absorbs light at 485nm. Full details of the PS analytical technique are given in Chapter 3, Section 3.7. In order to apply the PS analytical technique for the assay of PVS and VS-Co in SI consumption experiments, the static IE sampling procedure had to be modified. The PVS in the quenching solution had to be replaced with DETPMP (see Chapter 3, Section 3.5.2). Clearly if a PVS-containing quenching solution was used, this PVS would also be detected by the PS analysis – giving false, enhanced results for [SI]. The PS technique was used to assay for PFC in a SI consumption experiment, but in the same experiment, PFC was also assayed by ICP spectroscopy. The aim was to compare the results for [PFC] obtained by PS with the ICP [PFC] results as was done for PPCA, ICP [PPCA] vs. CHS [PPCA]. Hence, in this Chapter, results are presented for PVS, VS-Co and PFC tested in SI consumption experiments, over 96 hours, where all 3 products were assayed by the PS technique.

11.2 PPCA – ICP Spectroscopy versus C18 / Hyamine / Spectrophotometry (CHS)

PPCA was tested at 40ppm – this is pre-2 hour MIC [SI].
60/40 NSSW/FW, Base Case, 95^{o}C, pH5.5, Ca^{2+}/Mg^{2+} = 0.57.
Sampling times (9) = ½, 1, 2, 4, 6, 22, 48, 72 and 96 hours.

Figures 11.1, 11.3 and 11.4 present the SI consumption results (by both analytical methods) for PPCA. The CHS calibration graph for PPCA is presented in Figure 11.2. This will be followed by a detailed discussion of these results and the main conclusions from this experiment.

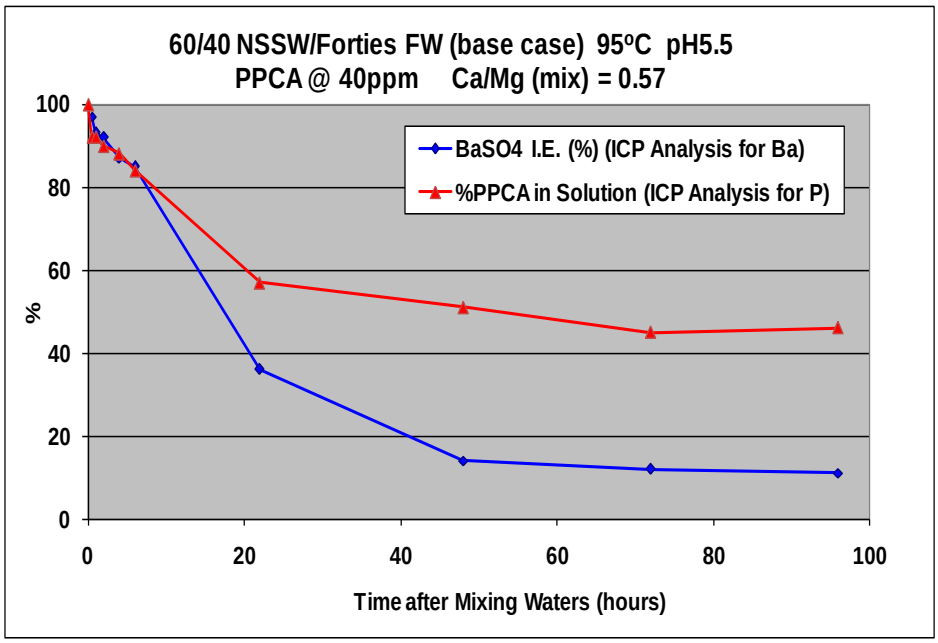

Figure 11.1 − $BaSO_4$ IE (%) and % PPCA in solution vs. time, up to 96 hours after mixing NSSW and Forties FW. PPCA was assayed by ICP spectroscopy by means of [P]. 95ºC; pH5.5; 60/40 NSSW/FW. [PPCA] = 40ppm.

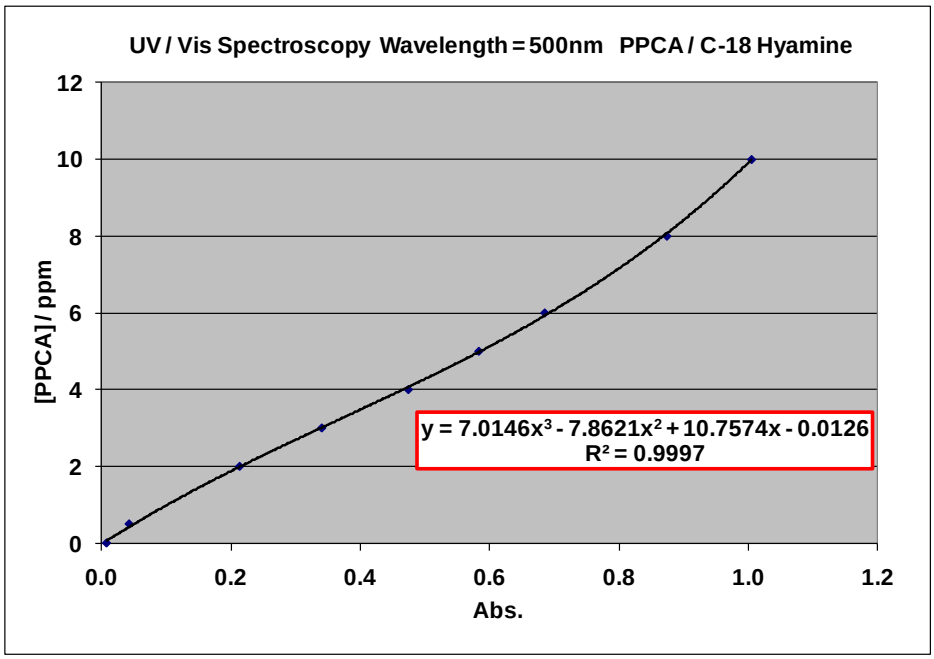

Figure 11.2 − CHS calibration graph used for the PPCA analysis.

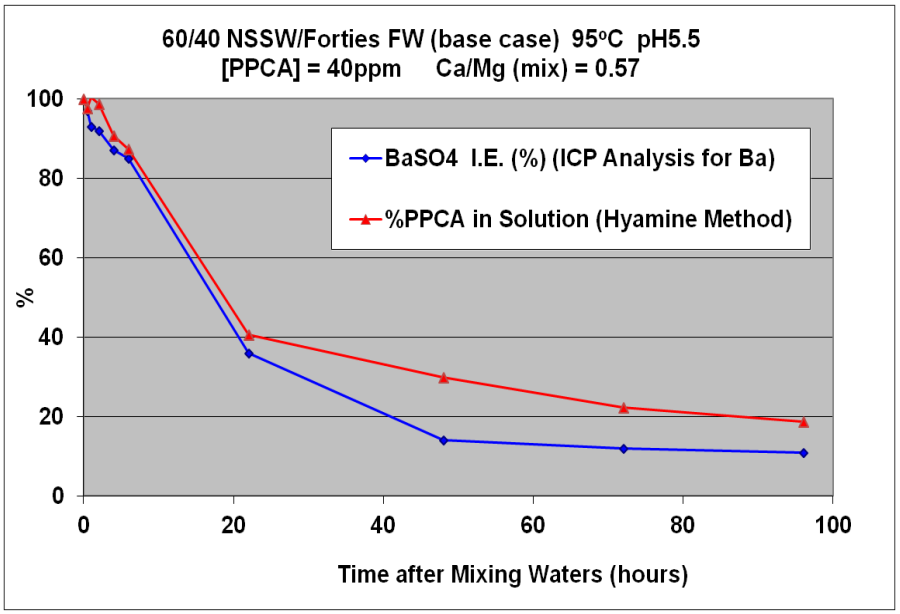

Figure 11.3 − $BaSO_4$ IE (%) and % PPCA in solution vs. time, up to 96 hours after mixing NSSW and Forties FW. PPCA was assayed by the CHS method. 95°C; pH5.5; 60/40 NSSW/FW. [PPCA] = 40ppm.

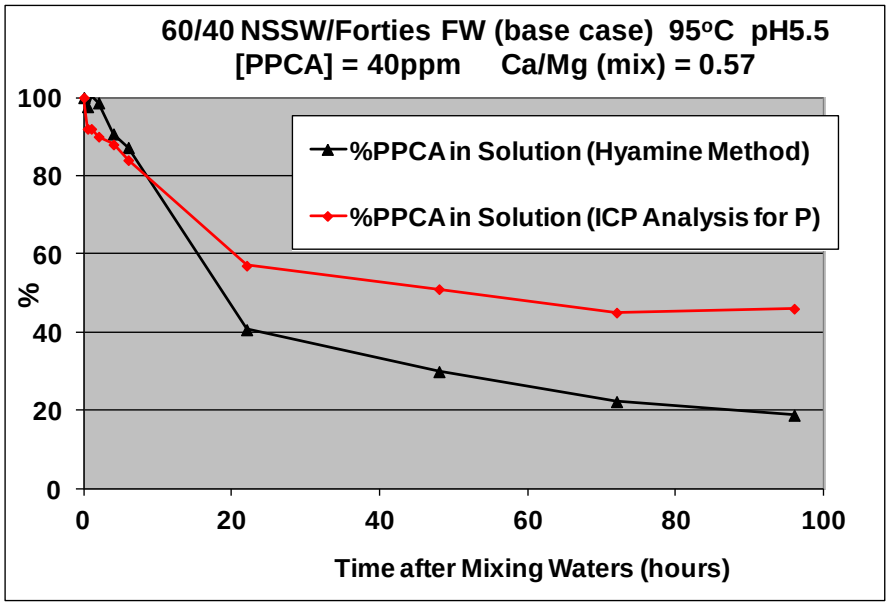

Figure 11.4 − % PPCA in solution vs. time – measured by ICP spectroscopy and CHS method – plotted together for comparison. 95°C; pH5.5; 60/40 NSSW/FW. [PPCA] = 40ppm.

11.3 MAT – by C18 / Hyamine / Spectrophotometric (CHS) Technique

MAT was tested at 15ppm – this is pre-2 hour MIC [SI].

60/40 NSSW/FW, Base Case, 95°C, pH5.5, Ca^{2+}/Mg^{2+} = 0.57.

Sampling times (9) = ½, 1, 2, 4, 6, 22, 48, 72 and 96 hours.

Figure 11.6 presents the SI consumption result for MAT by the CHS method. The CHS calibration graph for MAT is presented in Figure 11.5. This will be followed by a detailed discussion of these results and the main conclusions from this experiment.

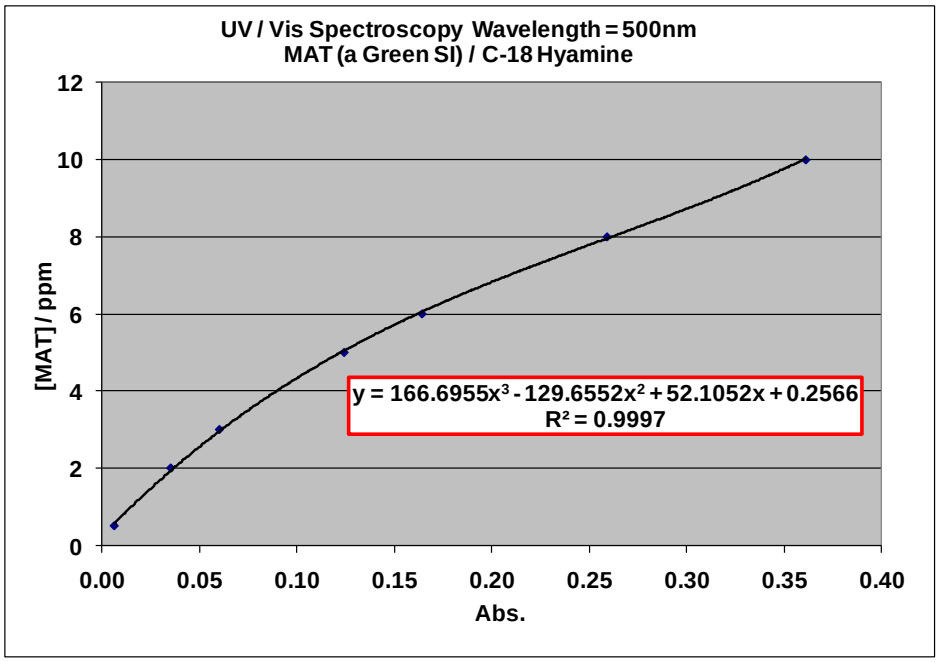

Figure 11.5 − CHS calibration graph used for the MAT analysis.

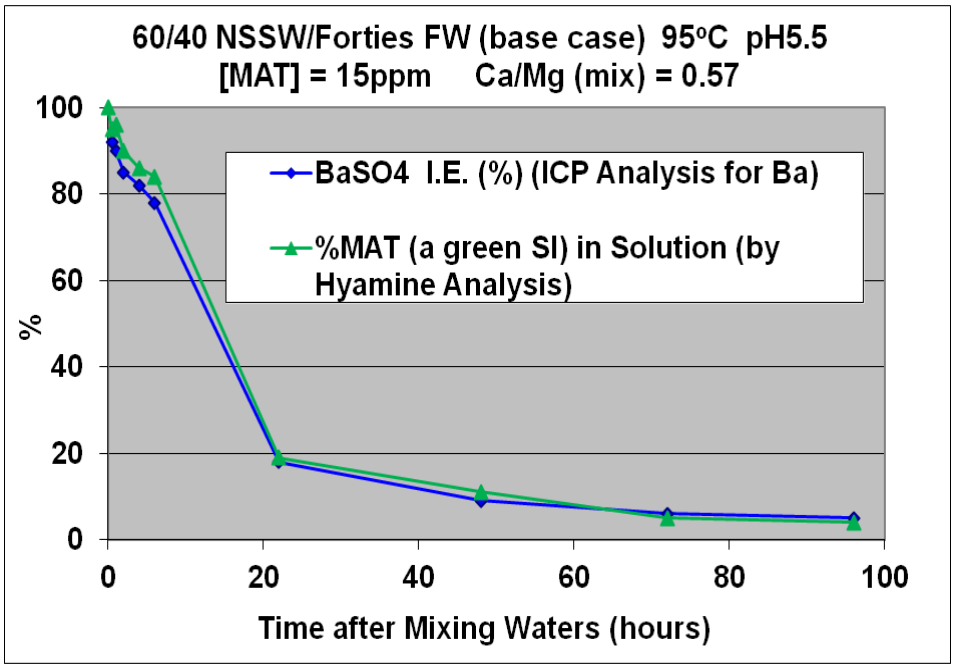

Figure 11.6 − $BaSO_4$ IE (%) and % MAT in solution vs. time, up to 96 hours after mixing NSSW and Forties FW. MAT was assayed by the CHS method. 95°C; pH5.5; 60/40 NSSW/FW. [MAT] = 15ppm.

11.4 PFC – ICP Spectroscopy versus Pinacyanol / Spectrophotometric (PS) Technique

PFC was tested at 15ppm – this is pre-2 hour MIC [SI].

60/40 NSSW/FW, Base Case, 95°C, pH5.5, Ca^{2+}/Mg^{2+} = 0.57.

Sampling times (11) = ½, 1, 2, 3, 4, 5, 6, 22, 48, 72 and 96 hours.

Figures 11.7 and 11.9 present the SI consumption results (by both analytical methods) for PFC. The PS calibration graph for PFC is presented in Figure 11.8. This will be followed by a detailed discussion of these results and the main conclusions from this experiment.

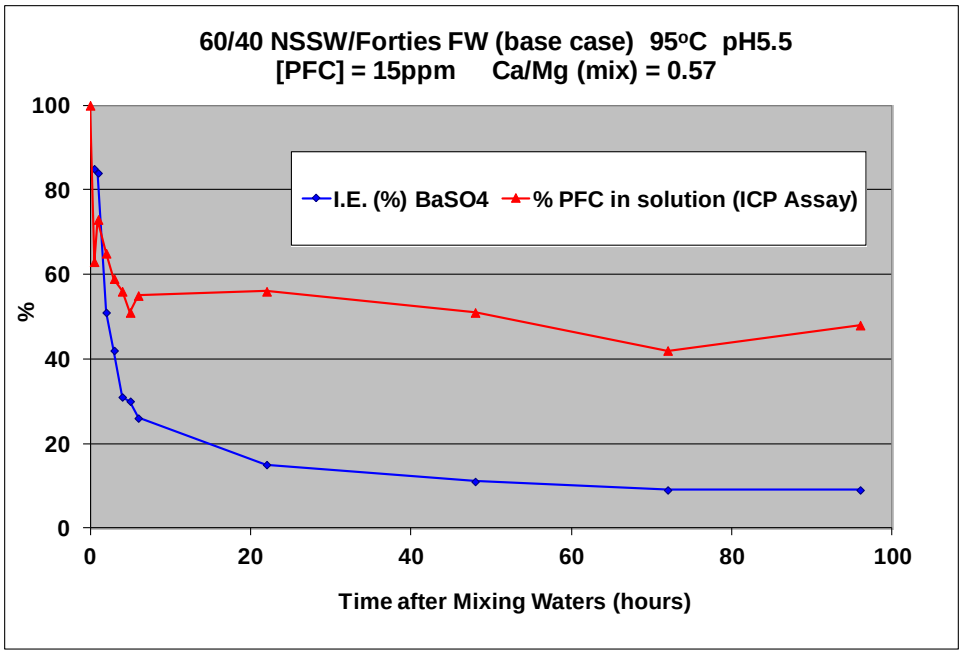

Figure 11.7 – $BaSO_4$ IE (%) and % PFC in solution vs. time, up to 96 hours after mixing NSSW and Forties FW. PFC was assayed by the ICP spectroscopic method by means of [P]. 95°C; pH5.5; 60/40 NSSW/FW. [PFC] = 15ppm.

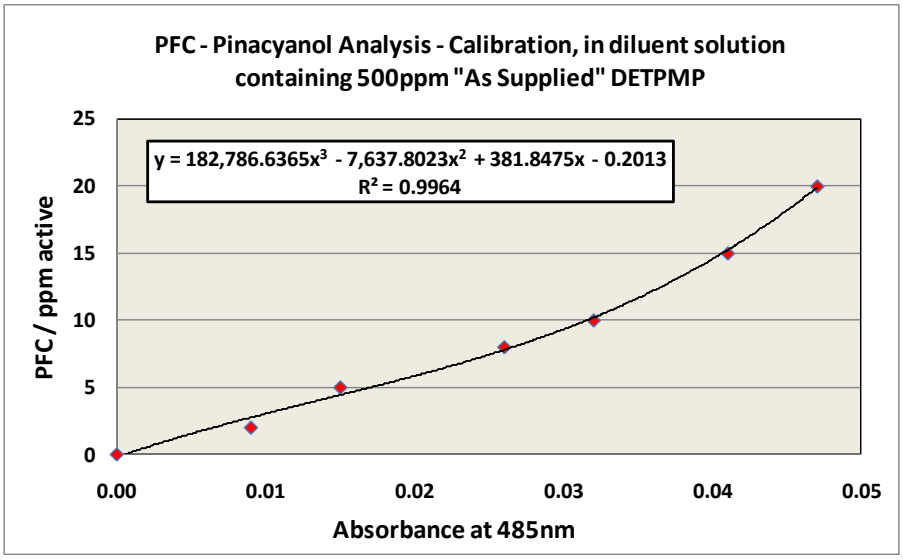

Figure 11.8 – 3rd order calibration graph obtained for the PS PFC assay (at 485nm) in a sample matrix containing 50% 1,000ppm "as supplied" DETPMP quenching solution; 30% NSSW (sulphate-free); and 20% Forties FW.

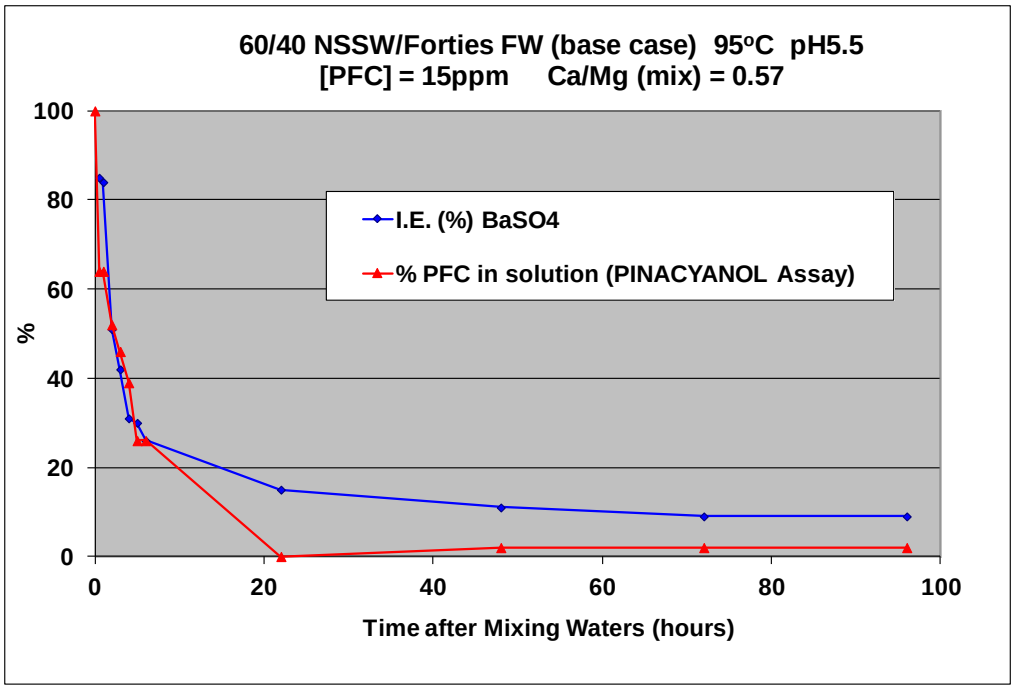

Figure 11.9 − $BaSO_4$ IE (%) and % PFC in solution vs. time, up to 96 hours after mixing NSSW and Forties FW. PFC was assayed by the PS method. 95°C; pH5.5; 60/40 NSSW/FW. [PFC] = 15ppm.

11.5 PVS – by Pinacyanol / Spectrophotometric (PS) Technique

PVS was tested at 20ppm – this is pre-2 hour MIC [SI].

60/40 NSSW/FW, Base Case, 95°C, pH5.5, Ca^{2+}/Mg^{2+} = 0.57.

Sampling times (11) = ½, 1, 2, 3, 4, 5, 6, 22, 48, 72 and 96 hours.

Figure 11.11 presents the SI consumption result for PVS by the PS method. The PS calibration graph for PVS is presented in Figure 11.10. This will be followed by a detailed discussion of these results and the main conclusions from this experiment.

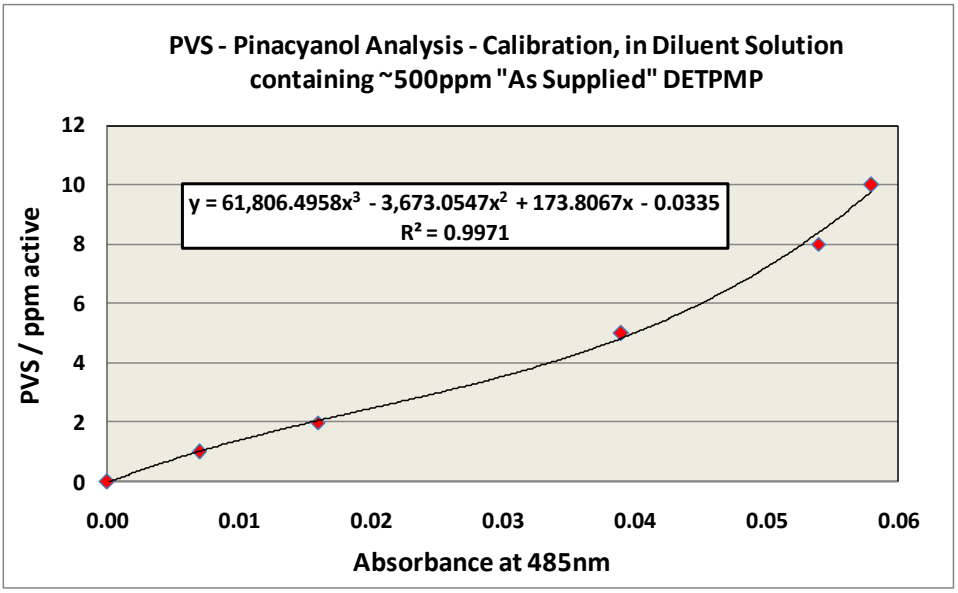

Figure 11.10 – 3rd order calibration graph obtained for the PS PVS assay (at 485nm) in a sample matrix containing 50% 1,000ppm "as supplied" DETPMP quenching solution; 30% NSSW (sulphate-free); and 20% Forties FW.

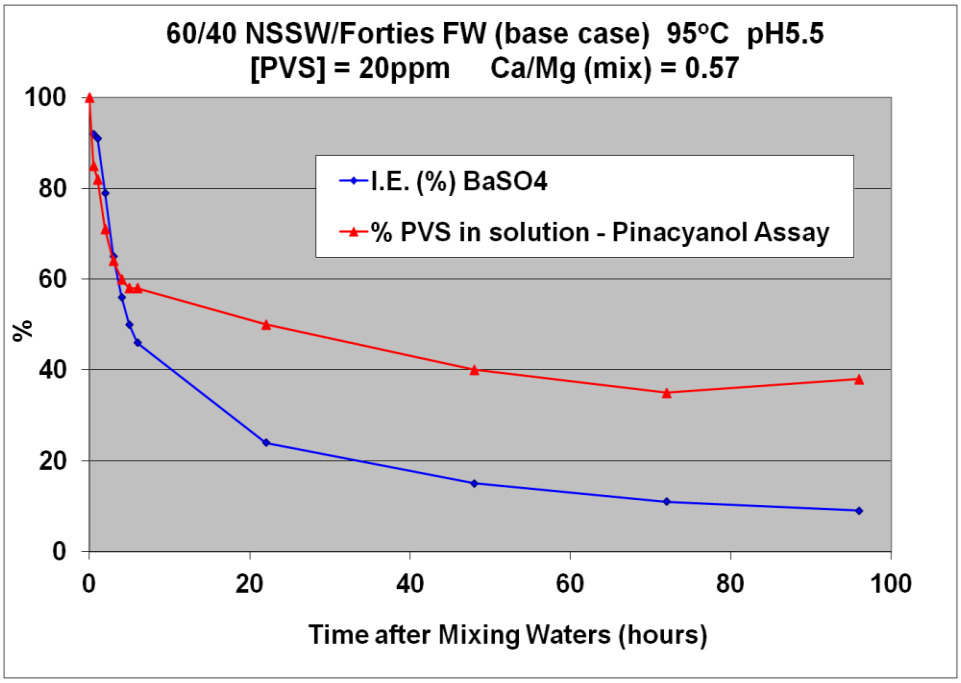

Figure 11.11 – IE (%) and %PVS in solution vs. time. PS analysis for SI. 95°C; pH5.5; 60/40 NSSW/FW. [PVS] = 20ppm.

11.6 VS-Co – by Pinacyanol / Spectrophotometric (PS) Technique

VS-Co was tested at 15ppm – this is pre-2 hour MIC [SI].

60/40 NSSW/FW, Base Case, 95°C, pH5.5, Ca^{2+}/Mg^{2+} = 0.57.

Sampling times (11) = ½, 1, 2, 3, 4, 5, 6, 22, 48, 72 and 96 hours.

Figure 11.13 presents the SI consumption result for VS-Co by the PS method. The PS calibration graph for VS-Co is presented in Figure 11.12. This will be followed by a detailed discussion of these results and the main conclusions from this experiment.

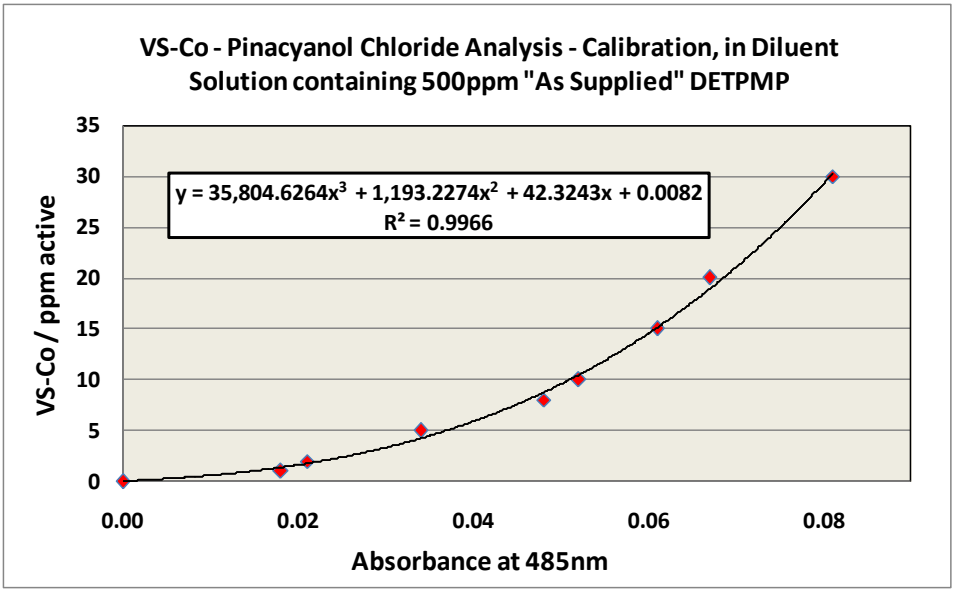

Figure 11.12 – 3rd order calibration graph obtained for the PS analysis of VS-Co (at 485nm) in a sample matrix containing 50% 1,000ppm "as supplied" DETPMP quenching solution; 30% NSSW (sulphate-free); and 20% Forties FW.

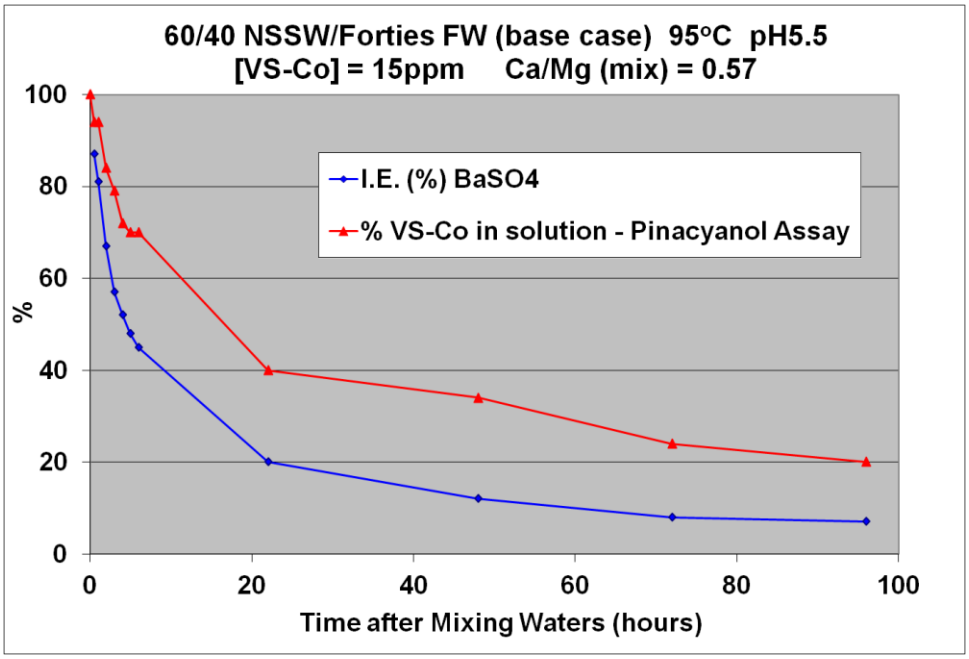

Figure 11.13 − IE (%) and %VS-Co in solution vs. time. PS analysis for SI. 95°C; pH5.5; 60/40 NSSW/FW. [VS-Co] = 15ppm.

11.7 Summary and Conclusions

11.7.1 PPCA – ICP vs. CHS and PFC – ICP vs. PS

In both cases (PPCA and PFC), the non-ICP analytical method provides the "best" assay for [SI]. When PPCA is assayed by CHS (Figure 11.3), clearly the %SI in solution profile follows the IE much more closely – this result is regarded as being the "true" result for %SI in solution. The quantity of SI (PPCA) detected in test samples by ICP spectroscopy (Figure 11.1) is enhanced, and thus a false result. This is due to the fact that there is "P" containing species in PPCA which contribute little to barite inhibition; e.g. this may simply be lower molecular weight PPCA which does not inhibit or other P-containing by-product species from the synthesis. Similarly, in testing the IE of PFC, the ICP assay for [PFC] is also enhanced (Figure 11.7), whereas the PS assayed [PFC] profile follows the IE closely (Figure 11.9). These differences in %SI again occur because the ICP spectrometer detects *all* phosphorus present in test samples – regardless of whether the phosphorus is part of the SI structure or not. Thus, ICP spectroscopic analysis for PPCA or PFC will also detect phosphorus which is *not* part of the SI structure, but a constituent of other components present in the test samples, for example, un-reacted P-tagged monomers.

The CHS analytical technique involves a cartridge separation step and it is this step which separates the PPCA from other P-containing sample components. Only polymer molecules adsorb onto the C18 cartridges. The adsorbed, extracted PPCA is subsequently desorbed and then assayed. Furthermore, the Hyamine reagent only reacts with carboxylated, non-sulphonated polymers. Thus, the CHS analytical technique provides a much more accurate assay for SI over ICP because only SI is assayed – the [SI] is *not* enhanced by the presence of other P-containing components, as these components have already been separated from the active SI and are *not* assayed. The CHS analysis is a much better "active polymer" assay in terms of IE than ICP for these products. Similarly, the Pinacyanol reagent only reacts with sulphonated polymers to produce a turbid solution. Therefore, the presence of other P-containing compounds within a sample has no effect on the PFC Pinacyanol assay. On the contrary, all P-containing compounds within a sample (including PFC) are detectable by ICP spectroscopy, giving an enhanced assay for PFC.

Four final points to make are that if no other P-containing ingredients were present in SI formulations, i.e. if all P was part of SI structure, then ICP assayed [SI] would be expected to *match* the CHS or PS assayed [SI] profile very well. This would be very rare however, as most SI syntheses involve the production of P-containing by-products or the presence of some leftover non-reacted monomers within the sample. Secondly, Chapter 10 concluded (discussing Type 1 / Type 2 SI classifications) with the statement that in some cases, a SI may be classed as Type 2 if the IE declines rapidly *but* the level of SI in solution is maintained (i.e. if %SI profile is more typical of a Type 1 species) – point number 2 in Section 10.4.3. From the experimental results presented in this Chapter, in some cases, for example as observed testing PFC (Chapter 10) this kind of SI consumption experimental result can be obtained because of the presence of non-SI-P-containing components in test samples. A perfect example of this occurrence is shown in Chapter 10, Figure 10.5 (testing PFC). The IE profiles are correct (and Type 2), but the %SI profiles are *false*. If no non-SI-P-containing ingredients were detected by the ICP spectrometer, the %SI profile in Figure 10.5 would follow the IE much more closely (e.g. as in Figure 11.9). This is essentially why SIs producing the kind of SI consumption result shown in Figure 10.5 *must* be classed as Type 2, as stated in Section 10.4.3. Thirdly, the SI consumption results presented here for PPCA and PFC re-confirm these 2 SIs are Type 2 – in particular, the much more accurate CHS and PS determined SI consumption results (Figures 11.3 and 11.9). Fourthly, the

disadvantages of the CHS and PS techniques are that they are both very time consuming and extremely laborious whereas ICP analysis is much quicker and is automated. The Pinacyanol reagent also goes off (degrades) very quickly and must be used straight away for a complete analysis, i.e. calibration and test-samples. C18 separation cartridges (used for CHS analysis) can only be used *once* and are very expensive. One C18 cartridge is required for every calibration sample and every test sample – hence one analysis can require ~40 C18 cartridges.

11.7.2 MAT – Assay by CHS

Figure 11.6 shows that the CHS assay for MAT yields excellent SI consumption results – the IE and %SI profiles are almost superimposed. There is no doubt that these results assaying MAT by CHS are extremely accurate. The ICP assayed barium results (to calculate IE) correlate with the CHS assay for MAT. This result re-confirms conclusively that MAT is a Type 2 SI, as identified in Chapter 10 by MIC vs. mixing ratio experiments.

11.7.3 PVS and VS-Co – Assay by PS

Figure 11.11 (PVS) and Figure 11.13 (VS-Co) are both clearly Type 2 SI consumption profiles. Again, these findings agree with the classification of both these SIs as Type 2 in Chapter 10 (by MIC vs. mixing ratio experiments). The VS-Co %SI in solution and IE profiles follow each other quite closely, whereas when testing PVS, there is a larger %SI remaining in solution. The IE profiles PVS and VS-Co for both SIs are remarkably similar and this could be because the [SI] selected for each SI is in the same threshold pre-2 hour MIC region. The VS-Co was tested at 15ppm whereas the PVS was tested at 20ppm – giving similar IE at each residence time. The differences in the SI consumption profiles of PVS and VS-Co can be explained in the same way as for the differences between the %SI profiles of SPPCA and PPCA in Chapter 10. The presence of sulphonate functional groups may help limit SI consumption and prevent SI precipitation with Ca^{2+} (e.g. PPCA/SPPCA). Since the PVS is a homopolymer (containing only sulphonate functional groups), it would be expected to be consumed *less* than the VS-Co. It is easier for SI to be consumed into the growing barite lattice in combination with Ca^{2+} (i.e. bonded to or complexed with Ca^{2+}. As discussed in earlier Chapters, sulphonate functional groups do not bind to Ca^{2+} or Mg^{2+}, they are highly acidic – significantly more acidic than their carboxylate and phosphonate analogues (Sorbie

et al., 2004). Thus, PVS is consumed *less* than the VS-Co, but both are Type 2 SIs. The carboxylate functional groups present in the VS-Co mean that it can be consumed more readily than PVS – since the carboxylate groups can bond with Ca^{2+} and thereby aid the SI consumption process. This explains sufficiently the difference between Figures 11.11 and 11.13.

Chapter 12: Explaining Scale Inhibition: Chemical Structures and Mechanisms

Chapter 12 Summary: In this Chapter, the possible reasons behind Type 1 and Type 2 IE behaviour in phosphonate and polymeric SIs are discussed, in terms of SI molecular structure, pH, SI speciation, SI binding constants to Ca^{2+} and Mg^{2+} cations, and the possible mononuclear or polynuclear chelate structures with M^{2+} cations that can form under the test conditions. Possible SI–M^{2+} complex structures are proposed, and through molecular modelling, explanations are provided for why Type 1 and Type 2 behaviour is exhibited by phosphonate and polymeric SIs.

12.1 Introduction

This Chapter tries to establish the relationship between static barium sulphate IE and the structure of the possible metal-phosphonate and/or metal carboxylate complexes (or chelates) that can form under experimental conditions. The ideas conjectured in this Chapter apply to all SIs, i.e. phosphonates and polymers. Chapter 5 discussed a range of eight phosphonate SIs (OMTHP, DETPMP, HMTPMP, EDTMPA, HMDP, NTP, HEDP and HPAA) that are classified as being either Type 1 or Type 2, based on their static barium sulphate IE and sensitivity to divalent cations Ca^{2+} and Mg^{2+} in "MIC vs. % North Sea Sea Water (NSSW)" IE tests. A full set of "MIC vs. %NSSW" test results were obtained for eight products. EABMPA was classed as Type 2 based on IE only – no IE was achieved at 22 hours under Base Case or Fixed Case conditions, testing this SI. Type 1/Type 2 classifications were therefore assigned to all nine phosphonate products. In this Chapter, the molecular structures of all nine phosphonate SIs referred to above are considered, and the possible chelates that each SI can form with divalent cations, such as Ca^{2+} and Mg^{2+}. This is then related to the observed barium sulphate IE measured at pH 5.5 and 95°C (Chapter 5). Clearly, the effects of Ca^{2+} and Mg^{2+} on phosphonate SI IE, as described in earlier chapters, must depend to some extent on the chelates that can form and on the SI binding constants to Ca^{2+} and Mg^{2+} (K_{Ca} and K_{Mg}) at the specific test temperature and pH (usually, pH 5.5). It must be stressed that the binding constants K_{Ca} and K_{Mg} vary with pH and temperature. Changes in pH cause the SI speciation distribution to change; consequently, SI binding constants to divalent

cations and the possible chelate structures that can form also change. Because the pH and temperature are both fixed at pH 5.5 and 95°C, respectively, in regular static IE tests, one need only consider the speciation of each product at pH 5.5 and 95°C. This can be determined by knowing the acid dissociation constant values (K_a) or pK_a values for each SI. The speciation products (anions) of all nine phosphonate SIs described in this thesis were given in Table 7.1. Note that in Table 7.1, the hydroxide functional groups (not part of phosphonic acid functional groups) present in the SI molecules EABMPA, HEDP, and HPAA are not considered acidic.

The phosphonate SI products bind preferentially to M^{2+} cations, depending on the relative magnitude of the SI-metal binding constants (K_b) to the various M^{2+} species present in the system. The binding constant for SI to M^{2+} varies, depending on the dissociative state of the SI; for example, SI^- will have a different binding constant (K_{Mg}) to Mg^{2+} than SI^{2-}, and this is why pH is extremely important in scale-inhibition studies (Sorbie et al., 2000; Sorbie and Laing, 2004; Shaw et al., 2012). The same principle applies to other common chelating agents, such as EDTA (the carboxylated analogue of EDTMPA) and DTPA (the carboxylated analogue of DETPMP). Preferential M^{2+} binding must also be taken into consideration when interpreting SI IE, and this depends on the magnitude of SI–M^{2+} binding constants *and* the concentration of each M^{2+} species present in the system. In this Chapter, differences between the IE of all nine SIs are discussed, including, specifically, differences between the IE of the two penta-phosphonates (DETPMP and HMTPMP) and the two tetra-phosphonates (HMDP and EDTMPA). In this Chapter, only the relationship between SI structure and the IE of barium sulphate scale is considered. Other works have also studied the mechanisms of inhibition of barite and other problematic scales, such as calcite, gypsum, iron carbonate, and sulphides (Graham et al., 1997a, 2003; Greenberg and Tomson, 1991; He et al., 1994; Kan et al., 2004; Okocha et al., 2008; Sorbie et al., 2000; Sorbie and Laing, 2004; Tomson et al., 2002, 2004; Chen et al., 2005b, 2006).

12.2 Phosphonates − Structural Explanation

Table 12.1 presents the molecular structures of the nine phosphonate SIs studied in this thesis, their Type (1 or 2), the maximum number of chelate rings they can form with M^{2+} (per molecule) involving N–M bonding at approximately pH 5.5 (except HEDP and HPAA, which

are N-free species), the number of atoms per chelate ring, and the maximum possible molar ratio of M^{2+}/SI (per molecule). The SI species which can form complexes at ~pH5.5 are also given in column 7 of Table 12.1.

Scale Inhibitor	Molecular Structure	Type (1 or 2)	Maximum Number of Chelate Rings Involving N-M Bonding (per molecule)	Number of Atoms per Chelate Ring	Maximum Molar Ratio M^{2+}/SI (per molecule)	SI Species Involved in the Complex Formation
OMTHP (hexa-p)	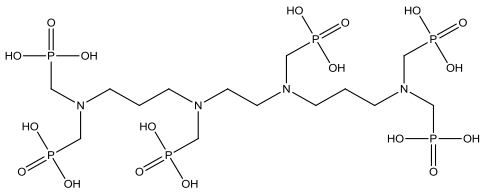	1	6	5	4	$H_{11}A^{-}$(1), $H_{10}A^{2-}$(2), H_9A^{3-}(3), H_8A^{4-}(4), H_7A^{5-}(5), H_6A^{6-}(6)
DETPMP (penta-p)	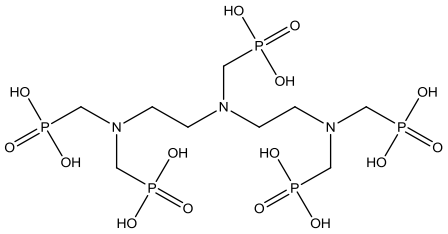	1	5	5	3	H_9A^{-}(1), H_8A^{2-}(2), H_7A^{3-}(3), H_6A^{4-}(4), H_5A^{5-}(5)
HMTPMP (penta-p)	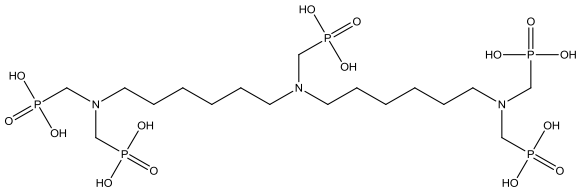	2	5	5	3	H_9A^{-}(1), H_8A^{2-}(2), H_7A^{3-}(3), H_6A^{4-}(4), H_5A^{5-}(5)
HMDP (tetra-p)	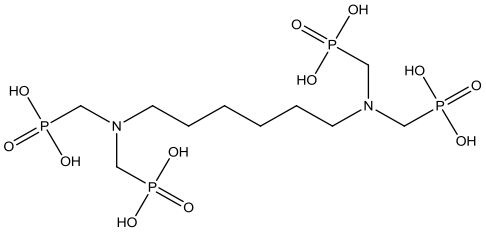	2	4	5	2	H_7A^{-}(1), H_6A^{2-}(2), H_5A^{3-}(3), H_4A^{4-}(4)
EDTMPA (tetra-p)	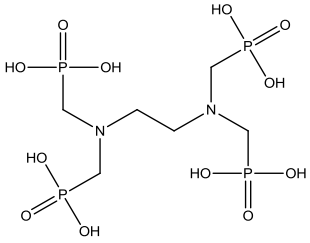	2	4	5	2	H_7A^{-}(1), H_6A^{2-}(2), H_5A^{3-}(3), H_4A^{4-}(4)

NTP (tri-p)	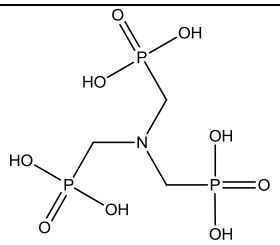	2	3	5	1	H_5A^-(1), H_4A^{2-}(2), H_3A^{3-}(3)
EABMPA (di-p)	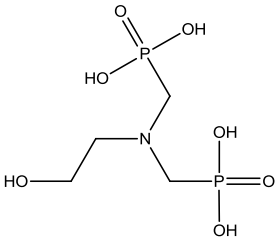	2	2	5	1	H_3A^-(1), H_2A^{2-}(2)
HEDP (di-p)	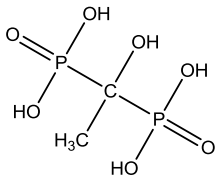	2	1	6	1	H_2A^{2-}(1)
HPAA (mono-p, mono-c)	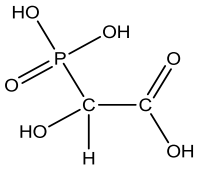	2	1	6	1	HA^{2-}(1)

Table 12.1 − Molecular structures of the nine phosphonate scale inhibitors tested in this work, their type (1 or 2), maximum number of chelate rings they can form with M^{2+} at ~pH5.5 (per molecule) involving N−M bonding[a], number of atoms per chelate ring, maximum molar ratio M^{2+}/SI (per molecule), and the SI species involved in the complex formation[b].

[a]Except HEDP and HPAA. These 2 molecules are N-free but can form N-free chelate rings by means of P-O-M-O-P (HEDP) or P-O-M-O-C (HPAA) bonding.

[b]Excluding HEDP and HPAA, the number of 5-membered chelate rings that can form equals the number of protons removed from the SI. The number in brackets after each species in column 7 equals the number of 5- or 6-membered chelate rings that the species can form.

For all the phosphonate species discussed in this thesis, the smallest possible chelate rings are formed by means of N–M bonding—only these chelates are considered in primary discussions; only the smallest possible chelate rings are considered in Table 12.1 (i.e., containing six or less atoms). Excluding HEDP and HPAA, the number of 5-membered chelate rings that can form per molecule equals the number of protons removed from the SI. In the seventh column of Table 12.1, the number in brackets after each SI species indicates the number of chelate rings the species can form. HEDP and HPAA can only form 6-membered chelate rings at pH 5.5—there are no other possibilities. In experiments described in this thesis, M^{2+} can be Mg^{2+}, Ca^{2+}, Sr^{2+} or Ba^{2+}, where the physical size of these cations increases in that order, from Mg^{2+} to Ba^{2+}. The ionic radii (expressed in picometres) of these four cations were presented in Table 2.1. The thermodynamic stability of metal chelates of a given SI will decrease in the same order of increasing ionic radius of the cation, M^{2+}. As the thermodynamic stability of the chelates decreases, the metal binding constants will also decrease because these physical properties are closely inter-related. It is for this reason that the DETPMP–Ba^{2+} metal binding constant (quoted earlier) is two orders of magnitude lower (10^8) than that for DETPMP–Mg^{2+} and DETPMP–Ca^{2+} (both 10^{10}) (Sorbie and Laing 2004). A number of scientific papers discuss the thermodynamic stability, structure, and chemistry of various ligand-metal complexes, including phosphonate complexes, the chelate effect, and the ligand-M^{2+} binding constants (Barnett and Uchtman 1979; Demadis and Katarachia 2003; Duan et al., 1999; Ockerbloom and Martell 1957; Poonia and Bajaj 1979; Popov et al., 2001; Sanchez-Moreno et al., 2004; Sawada et al., 1986, 1988, 1991, 1993a, 1993b, 2000; Tomson et al., 1994; Uchtman and Gloss 1972; Uchtman 1972; Uchtman and Oertel 1973; Uchtman and Jandacek 1979). The metal complexation chemistry of PPCA (a polymeric SI) is discussed by Xiao et al. (2001). For the purposes of this structural explanation, M^{2+} will be considered as being Mg^{2+} throughout, thus ignoring the effect of changes in the SI-metal-binding constant caused by changing M^{2+}.

From Table 12.1, clearly nitrogen atoms present in the backbone (or side chains) of SI molecules can bind to divalent cations such as Mg^{2+}, Ca^{2+}, Ba^{2+}, Sr^{2+}, Zn^{2+}, Cu^{2+}, Mn^{2+}, etc. by means of dative bonds involving the nitrogen atom sp^3 orbital lone pair of electrons – this applies to *both* N-containing conventional phosphonate and polymeric species, e.g. OMTHP, DETPMP, PMPA, SPPCA, etc. SPPCA contains amide functional groups on the AMPS side chains. SPPCA is synthesised from acrylic acid (source of carboxylate functional groups)

and AMPS (source of sulphonate and amide N-containing functional groups) monomer units (i.e. it is a P, S and N-containing co-polymer). It has been observed that by having more nitrogen atoms present in phosphonate or polymeric SI molecules improves IE (Boak et al., 1999; Graham et al., 2003; Sorbie et al., 2000). PMPA, for example, contains many nitrogen atoms in its structure (i.e. it is a poly-nitrogenated and poly-phosphonated species); the majority of conventional phosphonate SIs also contain nitrogen atoms in their main carbon chain, e.g. OMTHP contains 4; DETPMP and HMTPMP contain 3; and HMDP contains 2 (see Table 12.1). The abundance of nitrogen atoms in SI molecules could be another factor influencing Type 1 / Type 2 IE behaviour (as explained previously in Chapter 5). SIs containing nitrogen atoms (e.g. PMPA) may have a greater probability of exhibiting Type 1 IE characteristics due to the additional possibility of M^{2+}–N dative bonding rather than exclusively M^{2+}–O bonding by means of dissociated phosphonate or carboxylate functional group oxygen donor ions.

By examining Table 12.1, it is clear that a fundamental structural characteristic required for the formation of stable 5-membered chelate rings is the presence of nitrogen atoms within the main carbon chain that can form dative bonds to the metal cation (except HEDP and HPAA, which are N-free and form 6-membered chelate rings). Figure 12.1(a)−(g) illustrate some of the possible structures by which each of the phosphonate SIs discussed in this thesis (except HEDP and HPAA) can complex divalent cations, M^{2+}, with up to 33% (⅓) of the total number of protons dissociated, by forming 5-membered chelate rings, at ~pH 5.5. HEDP and HPAA form 6-membered chelate rings, with up to 66% of the total number of protons dissociated (Figure 12.2(a) and (b)). There are some examples of similar chelate structures in the literature, for example, as shown in Figure 12.3 (Stone et al., 2002). Figure 12.3 illustrates how the amino-acid, glycine, can complex Fe^{2+} ions, by forming a 5-membered chelate ring. This chelate ring is formed in exactly the same way as those shown in Figure 12.1(a)−(g) for the amino-phosphonates. Glycine (can be denoted HA) is the carboxylated (monoprotic) analogue of amino-methylphosphonic acid ($NH_2{-}CH_2{-}PO_3H_2$).

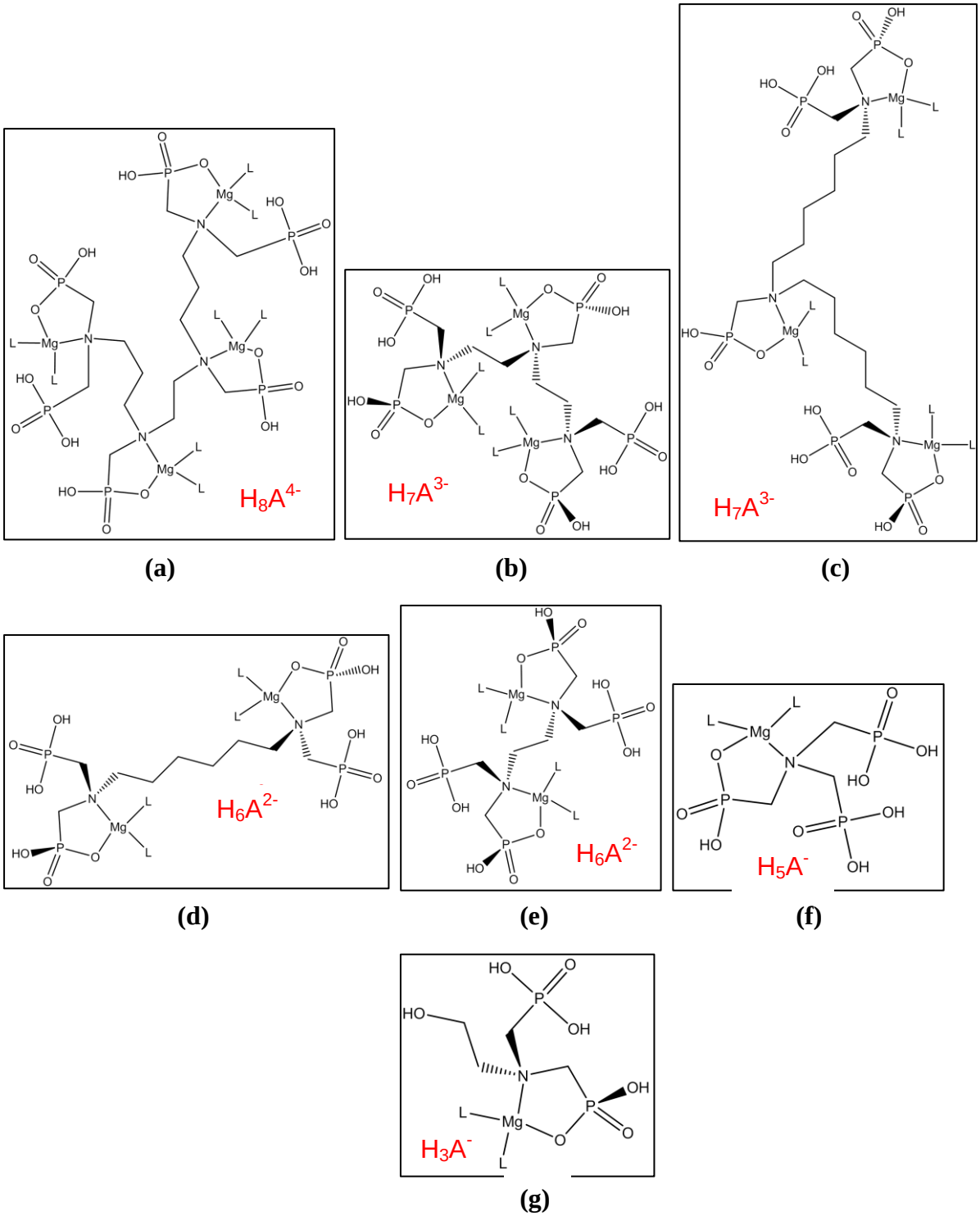

Figure 12.1(a)−(g) − 5-membered chelate rings formed by (a) OMTHP ($H_{12}A$), (b) DETPMP ($H_{10}A$), (c) HMTPMP ($H_{10}A$), (d) HMDP (H_8A), (e) EDTMPA (H_8A), (f) NTP (H_6A), and (g) EABMPA H_4A. In these figures, a maximum of 33% of the SI protons are dissociated (OMTHP, DETPMP, HMTPMP, and EABMPA are 33% dissociated; HMDP and EDTMPA are 25% dissociated; and NTP is 0.17% dissociated). The anionic SI species that forms the complex is stated in each case (Shaw et al., 2012).

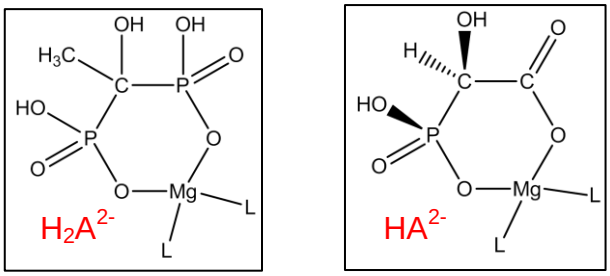

(a) **(b)**

Figure 12.2(a)−(b) − 6-membered chelate rings formed by (a) HEDP (H_4A) and (b) HPAA (H_3A). HEDP is 50% dissociated and HPAA is 66% dissociated. The anionic SI species that forms the complex is stated in each case (Shaw et al., 2012).

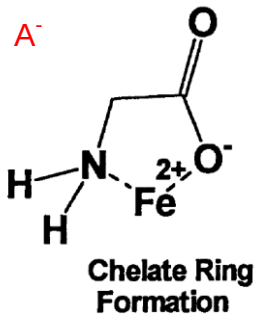

Figure 12.3 – A 5-membered chelate ring formed by Glycine (HA) and Fe^{2+} (Stone et al., 2002).

Figure 12.4(a)−(g) illustrate how each of the SIs (except HEDP and HPAA) can complex M^{2+} cations in a more highly dissociated state (i.e., with 50% (½) of the total number of protons removed).

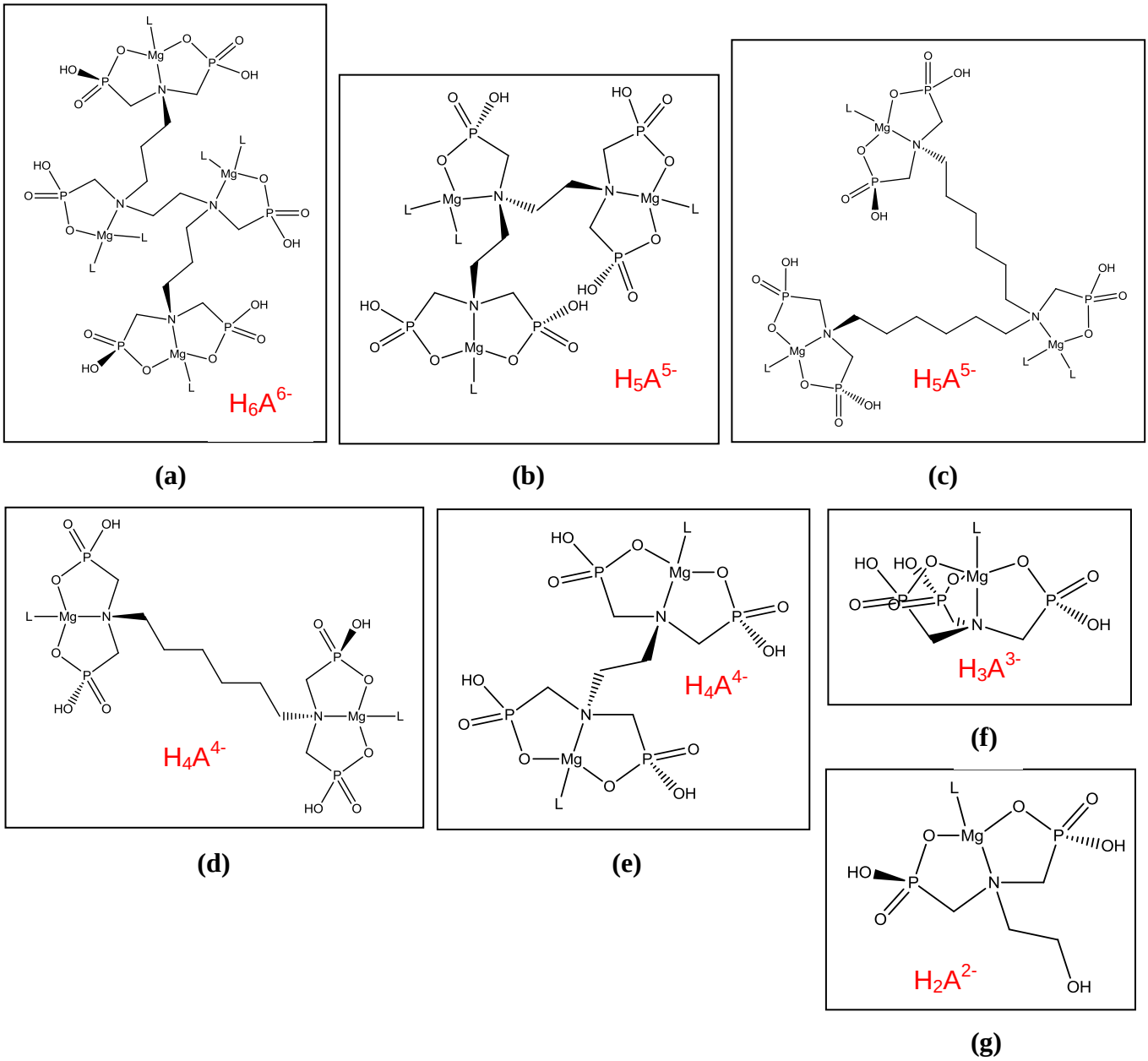

Figure 12.4(a)−(g) − 5-membered chelate rings formed by (a) OMTHP ($H_{12}A$), (b) DETPMP ($H_{10}A$), (c) HMTPMP ($H_{10}A$), (d) HMDP (H_8A), (e) EDTMPA (H_8A), (f) NTP (H_6A), and (g) EABMPA (H_4A). All SIs are 50% dissociated. The anionic SI species that forms the complex is stated in each case (Shaw et al., 2012).

A key structural feature of Figure 12.4(a)−(g) is that multiple chelate rings share a M−N bond, and these structures form when the SI is 50% dissociated (i.e., with half the protons removed; e.g., H_6A^{6-} (OMTHP), H_5A^{5-} (DETPMP), etc.). The structure proposed in Figure 12.4(f) for M^{2+}−NTP is also shown in Sawada et al., (1986, 1988). In Figure 12.1, Figure 12.2 and Figure 12.4, the SI species that forms each complex is stated (e.g., H_8A^{4-}). The concentration of each of these complexes in solution will depend on the SI speciation at the particular pH (e.g. see Figure 7.3 and Figure 7.4 for EDTMPA and DETPMP speciation respectively). In Figure 12.1 and Figure 12.4, the number of 5-membered chelate rings that can form *equals* the number of protons removed from the SI. Note that in all figures illustrating SI−M complex structures in this Chapter, for clarity, charges have been omitted and Mg^{2+} tetra-co-ordinated is shown (i.e., with 4 chemical bonds joined to it); however, Mg^{2+} could equally be hexa-co-ordinated. In all figures, the ligand, denoted "L", may be neighbouring SI species or aqua ligands (i.e., water molecules bonded datively to the Mg^{2+} by means of a lone-pair of electrons on the water-molecule oxygen atom).

Duan et al. (1999) and Sawada et al. (1986, 1988, 1991, 1993a, 1993b, 2000) have reported the formation of several metal-phosphonate and metal-carboxylate complexes containing M−N bonding. Although nitrogen atoms present in SI molecules (e.g., NTP) can be protonated under certain conditions, this proton can often be displaced by certain metal cations – particularly divalent transition metal ions. 5- and 6-membered chelate rings are known to be the most thermodynamically stable, much more so than 7- and 8-membered chelate rings. The chelate effect is reduced with 7- or 8-membered rings because the large rings are less rigid, and so less entropy is lost in forming them (Greenwood and Earnshaw, 1997). It has been widely reported that the inclusion of nitrogen atoms within SI structures improves their IE; this is in agreement with the data presented in Table 12.1 and the complex structures presented in Figure 12.1 and Figure 12.4. As the molar ratio of M^{2+}/SI decreases (per molecule), IE is likely to decrease (Table 12.1), but this is just a "rule-of-thumb". Clearly, EABMPA is the worst-performing SI against barite, and HEDP and HPAA performed better than NTP (Chapter 5).

It should be noted that all the SIs discussed in this thesis (except HEDP and HPAA) can also form larger, less-stable 8-membered chelate rings containing nitrogen, but *not* involving

N–M dative bonding, at around pH 5.5. This is achieved by dative bonding to M^{2+} by means of two adjacent dissociated (anionic) phosphonate functional group oxygen atoms − these complex structures are presented in Figure 12.5(a)−(g). Again, in each figure, the SI species which forms the complex is stated (e.g., H_8A^{4-}). In these figures, the SIs are up to 50% dissociated.

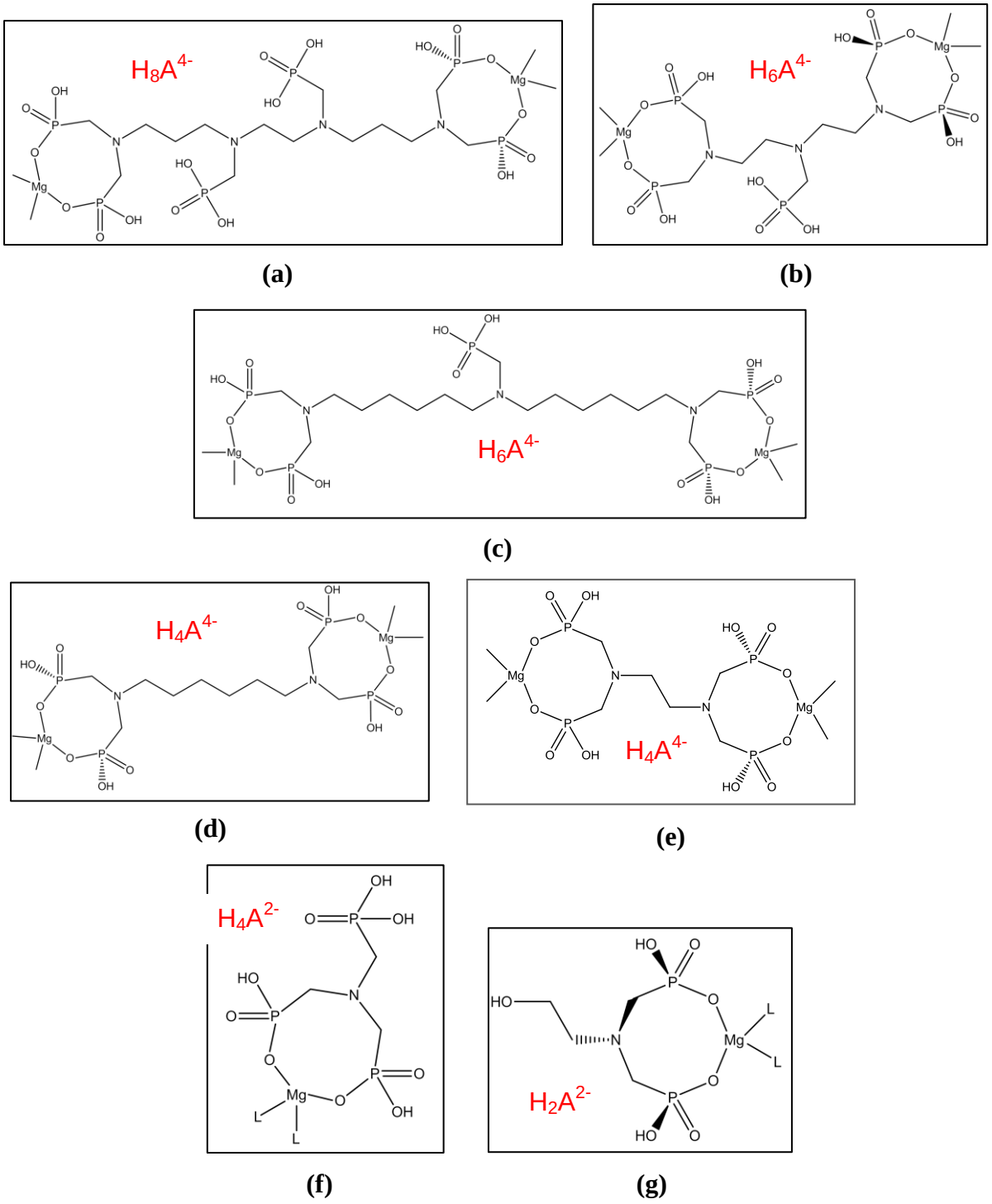

Figure 12.5(a)−(g) − 8-membered chelate rings formed by (a) OMTHP ($H_{12}A$), (b) DETPMP ($H_{10}A$), (c) HMTPMP ($H_{10}A$), (d) HMDP (H_8A), (e) EDTMPA (H_8A), (f) NTP (H_6A), and (g) EABMPA (H_4A). In these figures, a maximum of 50% of the SI protons are dissociated (OMTHP is 33% dissociated; DETPMP and HMTPMP are 40% dissociated; HMDP, EDTMPA, NTP, and EABMPA are 50% dissociated). The anionic SI species that forms the complex is stated in each case (Shaw et al., 2012).

A similar structure to Figure 12.5(f) for M^{2+}–NTP is shown in Sawada et al., (1986, 1988) containing three M–O dative bonds and two 8-membered chelate rings – the NTP species which have the ability to from this complex include: H_3A^{3-}, H_2A^{4-}, HA^{5-}, and A^{6-}. This structure is illustrated in Figure 12.6. In Figure 12.6, all three NTP phosphonate groups are bonded to M^{2+} by means of O^-. The NTP species shown in Figure 12.6 is HA^{5-}, because the nitrogen atom is shown to be protonated, and the 3 non-chelating phosphonate –OH functional groups are shown to be dissociated. However, as previously mentioned, the NTP species H_3A^{3-} could form this same complex, or any species more highly dissociated than H_3A^{3-}. It is also worth noting that the metal cation in Figure 12.6 is shown to be hexa-coordinated. In all the complex structures illustrated for phosphonates, Mg^{2+} is shown to be tetra-coordinated, however, the co-ordination number of Mg^{2+} is immaterial because it would not change the chelate structures proposed.

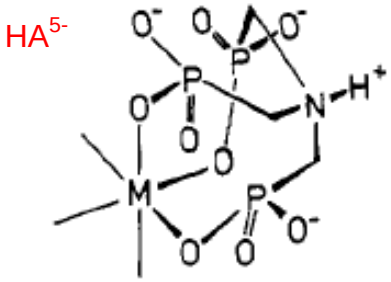

Figure 12.6 – NTP–metal complex formed by NTP species HA^{5-} (Sawada et al., 1986, 1988).

For any of the SIs (except HEDP and HPAA), 8- and 5-membered chelate rings could be formed simultaneously, as shown in Figure 12.7(a)–(g), making the complex polynuclear; however, this requires the SI to be up to 75% dissociated. This would only occur at higher pH levels, >> 5.5.

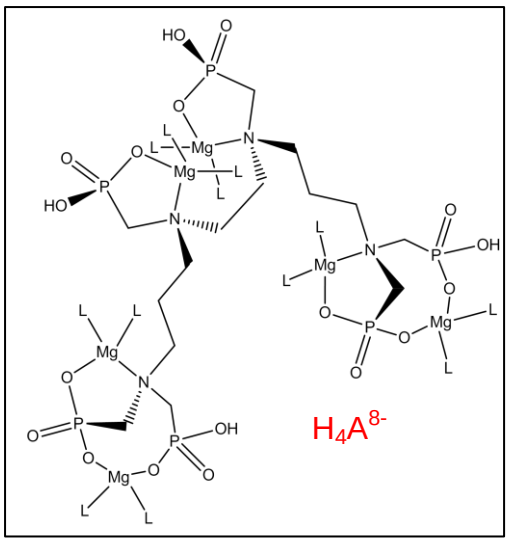

(a)

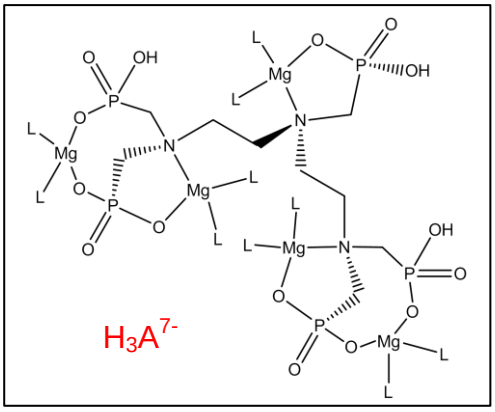

(b)

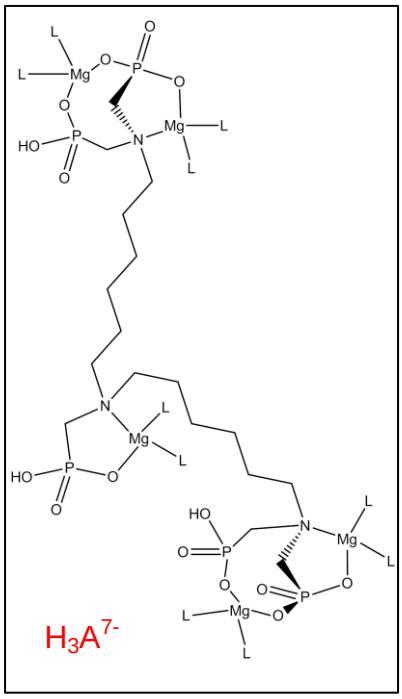

(c)

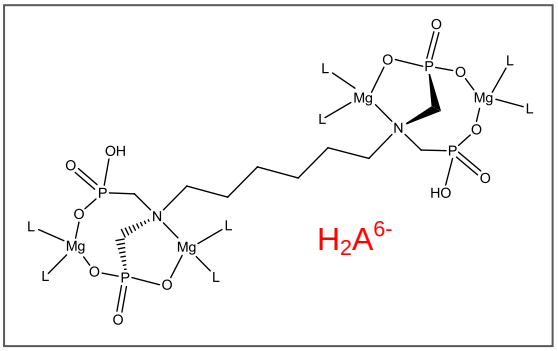

(d)

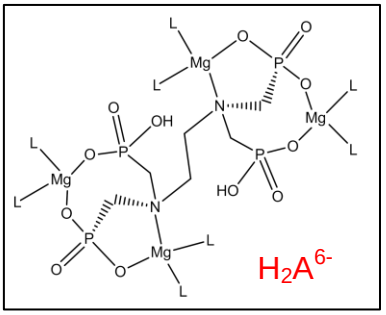

(e)

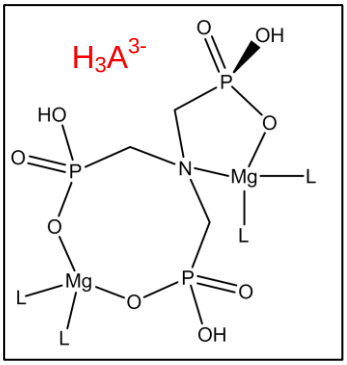

(f)

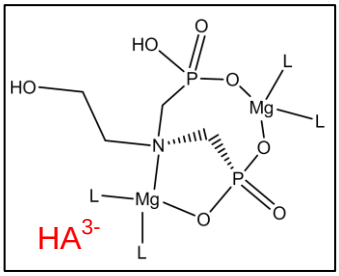

(g)

Figure 12.7(a)−(g) − SI-metal chelates that could form at higher pH levels: (a) OMTHP ($H_{12}A$); (b) DETPMP ($H_{10}A$); (c) HMTPMP ($H_{10}A$); (d) HMDP (H_8A); (e) EDTMPA (H_8A); (f) NTP (H_6A); and (g) EABMPA (H_4A). In these figures, a maximum of 75% of the SI protons are dissociated (OMTHP is 67% dissociated; DETPMP and HMTPMP are 70% dissociated; HMDP, EDTMPA, and EABMPA are 75% dissociated, and NTP is 50% dissociated). These chelates contain 5 and 8-membered chelate rings. The anionic SI species that forms the complex is stated in each case (Shaw et al., 2012).

The OMTHP complex (Figure 12.7 (a)) is hexa-nuclear; the DETPMP and HMTPMP complexes (Figure 12.7 (b) and (c)) are penta-nuclear; the HMDP and EDTMPA complexes (Figure 12.7 (d) and (e)) are tetra-nuclear; and the NTP and EABMPA complexes (Figure 12.7 (f) and (g)) are di-nuclear. The nature of the complexes formed depends on the system pH; for instance, the structure shown in Figure 12.7(f) would be formed by the NTP species H_3A^{3-}. There will in fact be a mixture of complexes of any given SI, depending on the test pH, and therefore SI speciation. The metals to which each species is bonded will depend on SI-metal-binding constants under such conditions and preferential M^{2+} binding, as discussed previously. SI-metal-binding constants quoted for any given SI, at a specific pH, are in fact "average" values because each of the speciation entities will have a different affinity for a particular metal cation. For example, for NTP, the species H_4A^{2-} will have a different binding constant to Mg^{2+} compared to H_3A^{3-}. Generally, the higher the charge on the SI anion, the greater the metal binding constant will be. So, applying this to the NTP example, $K_b\ H_3A^{3-} > K_b\ H_4A^{2-}$.

HEDP can also form two 6-membered chelate rings simultaneously (resulting in the formation of a further 8-membered chelate ring), as illustrated in Figure 12.8(a), but only when the SI is 100% dissociated, at, for example, pH 14. This complex could only be formed by the fully dissociated HEDP species A^{4-}; thus, it would never form at pH 5.5. Similarly, HPAA can form a complex containing a 6- and a 5-membered chelate ring at extremely high pH, but only if the hydroxide (–OH) functional group dissociates (Figure 12.8(b)).

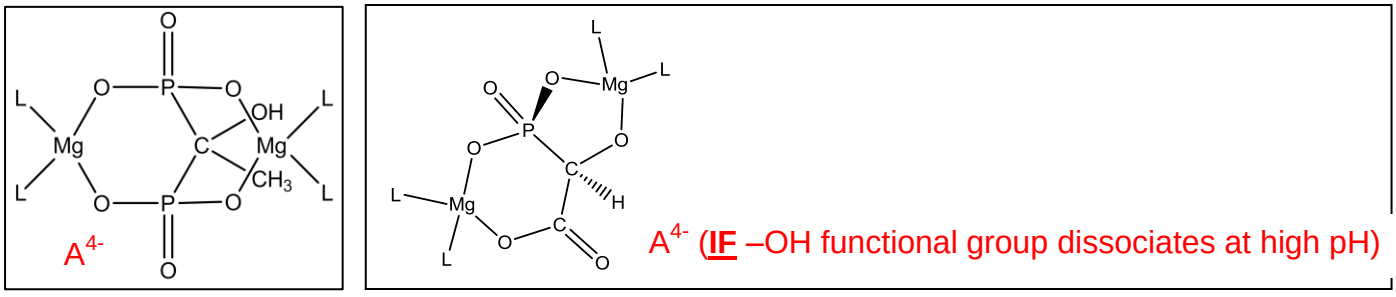

(a) **(b)**

Figure 12.8(a)–(b) – (a) HEDP (H_4A) and (b) HPAA (H_4A if –OH considered acidic) chelates that could form at extremely high pH (e.g., pH 14). Both SIs are 100% dissociated. The anionic SI species that forms the complex is stated in each case (Shaw et al., 2012).

To explain differences in static barium sulphate IE, one must begin by considering the four Type 2 phosphonate SIs: NTP, EABMPA, HEDP, and HPAA. In IE work, HEDP and HPAA had much lower MICs than NTP and EABMPA (Chapter 5). Indeed, 2- and 22-hr MICs could not be reached at all for EABMPA. By examining Figure 12.1(f) and (g), Figure 12.4(f) and (g), and Figure 12.5(f) and (g), clearly NTP and EABMPA can form 5- and 8-membered chelate rings, whereas HEDP and HPAA can form only 6-membered chelate rings at ~pH 5.5. At first glance, it might appear that the former two SIs would be better at barite inhibition. However, a large proportion of the NTP and EABMPA in solution (perhaps around half of the available SI) might form the less-stable 8-membered chelate rings; whereas, when HEDP and HPAA are deployed, *exclusively* 6-membered chelate rings will form at ~pH 5.5, which are clearly extremely stable entities. This is very likely why HEDP and HPAA outperform NTP and EABMPA in static barite IE tests. Furthermore, in the IE tests, HEDP performed slightly better than HPAA. This is probably because P–O–M bonding is stronger than C–O–M bonding, implying that HEDP chelates will be more stable than HPAA chelates at any particular pH. HEDP bonds to M^{2+} by means of two P–O–M dative bonds (Figure 12.2 (a)); whereas HPAA bonds to M^{2+} by means of one P–O–M dative bond and one C–O–M dative bond (Figure 12.2 (b)). Hence, HEDP–M^{2+} binding constants will be > HPAA–M^{2+} binding constants under any set of test conditions.

The more chelate rings that can form per SI molecule, the better the SI should be at barite inhibition. This is indeed what was observed in IE work. The best-performing SI was OMTHP (hexa-phosphonate). From Table 12.1, it can be seen that OMTHP is the only SI that can form a tetra-nuclear SI–M^{2+} complex at ~pH 5.5 (in the H_8A^{4-}, H_7A^{5-}, or H_6A^{6-} dissociated states) by forming only 5-membered chelate rings. This is illustrated structurally in Figure 12.1(a) and Figure 12.4(a). When OMTHP dissociates further to H_4A^{8-} (i.e., at higher pH), a hexa-nuclear SI–M^{2+} complex can form (Figure 12.7(a)). Clearly, the IE ability of phosphonate SIs does not only depend on the number of phosphonate functional groups per molecule, but much more importantly, on the number of stable chelate rings that can form at the test pH (i.e., 5- or 6-membered chelate rings, in particular). This important property, in turn, depends crucially on the inclusion of nitrogen atoms within the backbone of larger phosphonate SI molecules (e.g., OMTHP, DETPMP, and HMTPMP). When new phosphonate SI molecules are being synthesised, these factors should be taken into consideration. Table 12.2 lists all nine phosphonate SIs studied in this thesis, a selection of

the SI speciation products, the maximum possible molar ratio of M^{2+}/SI in the complexes that each of these species has the ability to form, and % protons dissociated. Generally, the more highly dissociated SI becomes, the more chelate rings can form, and the molar ratio M^{2+}/SI increases. Where a figure has been provided in this Chapter for the complex described, this information is listed in column 5 of Table 12.2.

Scale Inhibitor	Species	Maximum Possible Chelate Molar Ratio M^{2+}/SI	% Protons Dissociated[a]	Figures
OMTHP ($H_{12}A$)	$H_{11}A^-$	1	8	—
OMTHP ($H_{12}A$)	$H_{10}A^{2-}$	2	17	—
OMTHP ($H_{12}A$)	H_9A^{3-}	3	25	—
OMTHP ($H_{12}A$)	H_8A^{4-}	4 (= 4 in Fig. 12.1(a), = 2 in Fig 12.5(a))	33	12.1(a) and 12.5(a)
OMTHP ($H_{12}A$)	H_7A^{5-}	4	42	—
OMTHP ($H_{12}A$)	H_6A^{6-}	4	50	12.4(a)
OMTHP ($H_{12}A$)	H_5A^{7-}	5	58	—
OMTHP ($H_{12}A$)	H_4A^{8-}	6	67	12.7(a)
DETPMP and HMTPMP ($H_{10}A$)	H_9A^-	1	10	—
DETPMP and HMTPMP ($H_{10}A$)	H_8A^{2-}	2	20	—
DETPMP and HMTPMP ($H_{10}A$)	H_7A^{3-}	3	30	12.1(b) (DETPMP) and 12.1(c) (HMTPMP)
DETPMP and HMTPMP ($H_{10}A$)	H_6A^{4-}	3 (= 2 in Figs. 12.5(b) and 12.5(c), but structures shown in Figs. 12.1(b) and 12.1(c) can still form, with molar ratio M^{2+}/SI = 3)	40	12.5(b) (DETPMP) and 12.5(c) (HMTPMP)
DETPMP and HMTPMP ($H_{10}A$)	H_5A^{5-}	3	50	12.4(b) (DETPMP) and 12.4(c) (HMTPMP)
DETPMP and HMTPMP ($H_{10}A$)	H_4A^{6-}	4	60	—
DETPMP and HMTPMP ($H_{10}A$)	H_3A^{7-}	5	70	12.7(b) (DETPMP) and 12.7(c) (HMTPMP)
HMDP and EDTMPA (H_8A)	H_7A^-	1	13	—
HMDP and EDTMPA (H_8A)	H_6A^{2-}	2	25	12.1(d) (HMDP) and 12.1(e) (EDTMPA)
HMDP and EDTMPA (H_8A)	H_5A^{3-}	2	38	—
HMDP and EDTMPA (H_8A)	H_4A^{4-}	2	50	12.4(d) and 12.5(d) (HMDP) 12.4(e) and 12.5(e) (EDTMPA)
HMDP and EDTMPA (H_8A)	H_3A^{5-}	3	63	—
HMDP and EDTMPA (H_8A)	H_2A^{6-}	4	75	12.7(d) (HMDP) and 12.7(e) (EDTMPA)
NTP (H_6A)	H_5A^-	1	17	12.1(f)
NTP (H_6A)	H_4A^{2-}	1	33	12.5(f)
NTP (H_6A)	H_3A^{3-}	2 (= 1 in Fig. 12.4(f), = 2 in Fig. 12.7(f))	50	12.4(f) and 12.7(f)
EABMPA (H_4A)	H_3A^-	1	25	12.1(g)
EABMPA (H_4A)	H_2A^{2-}	1	50	12.4(g) and 12.5(g)
EABMPA (H_4A)	HA^{3-}	2	75	12.7(g)
HEDP (H_4A)	H_3A^-	0	25	—
HEDP (H_4A)	H_2A^{2-}	1	50	12.2(a)
HEDP (H_4A)	HA^{3-}	1	75	—
HEDP (H_4A)	A^{4-}	2	100	12.8(a)
HPAA (H_3A)	H_2A^-	0	33	—
HPAA (H_3A)	HA^{2-}	1	67	12.2(b)
HPAA (H_3A)	A^{3-}	1	100	—
HPAA (if –OH considered acidic, H_4A)	A^{4-}	2	100	12.8(b)

[a]Rounded off to nearest whole number.

Table 12.2 − List of SIs tested in this work, a selection of their speciation products, the maximum possible chelate molar ratio M^{2+}/SI for each species, % protons dissociated and figure numbers for complexes that have been presented.

It is well known that SI bonded to Mg^{2+} is rendered ineffective, whereas SI bonded to Ca^{2+} has the ability to incorporate into the growing barite scale and therefore inhibit further crystal growth (Boak et al., 1999; Graham et al., 2003; Shaw et al., 2010a, 2012; Sorbie et al., 2000; Sorbie and Laing, 2004). Ca^{2+} therefore enhances phosphonate SI IE. SI bonded to Mg^{2+} cannot be incorporated into the growing scale and remains in solution, but ineffective. It must be remembered that chelated SI can be bonded to a mixture of Mg^{2+}, Ca^{2+}, Sr^{2+}, or Ba^{2+} (if it is a polynuclear complex; e.g., OMTHP, Figure 12.1(a) and Figure 12.4(a)). The SI preferential binding will determine the proportion of each cation bonded to SI or the molar ratio of each M^{2+}/SI (per molecule).

Some preliminary experiments investigated the precipitation of OMTHP and DETPMP with Ca^{2+} at pH 5.5 (in distilled water) at various temperatures (i.e., in the absence of any other cations that could complex with the SI). The experimental procedure for these experiments is given in Chapter 3, Section 3.8. Supernatant [Ca^{2+}] and [SI] were both assayed after 24 hr. pH was fixed at 5.5 (by pH adjustment), [Ca^{2+}] was fixed at 2,000 ppm; [SI] = 500 ppm, 1,000 ppm, 2,000 ppm, and 3,000 ppm (all "active" concentrations). The number of moles of Ca, OMTHP and DETPMP present in each test is given in Table 12.3 (OMTHP) and Table 12.4 (DETPMP). Note that the initial level of calcium, $[Ca^{2+}]_o$, is expressed in mmol/L, whereas $[OMTHP]_o$ and $[DETPMP]_o$ are expressed in μM/L.

$[Ca]_o$/ppm	$[OMTHP]_o$/ppm	Initial Millimoles/L Ca	Initial Micromoles/L OMTHP
2,000	500	49.9	677
2,000	1,000	49.9	1,354
2,000	2,000	49.9	2,709
2,000	3,000	49.9	4,063

Table 12.3 − OMTHP–Ca precipitation experiment: [Ca] and [OMTHP]s.

$[Ca]_o$/ppm	$[DETPMP]_o$/ppm	Initial Millimoles/L Ca	Initial Micromoles/L DETPMP
2,000	500	49.9	872
2,000	1,000	49.9	1,745
2,000	2,000	49.9	3,489
2,000	3,000	49.9	5,234

Table 12.4 − DETPMP–Ca precipitation experiment: [Ca] and [DETPMP]s.

The findings in this study corroborate the SI–M^{2+} structures conjectured in Figure 12.1(a) (OMTHP, as H_8A^{4-}), Figure 12.1(b) (DETPMP, as H_7A^{3-}), Figure 12.4(a) (OMTHP, as H_6A^{6-}), and Figure 12.4(b) (DETPMP, as H_5A^{5-}), except, obviously, SI is bonded exclusively to Ca^{2+}, not Mg^{2+} (only Ca^{2+} was present in this experimental system). When OMTHP was tested at 20, 50, 75, and 95°C, at pH 5.5 (fixed), it was found that the molar ratio of Ca^{2+}/OMTHP precipitated = ~4. This is shown graphically in Figure 12.9(a)−(d), where ΔCa (moles/L) is plotted against ΔOMTHP (moles/L) at each temperature. ΔCa and ΔOMTHP are the moles/L Ca and moles/L OMTHP lost from solution (after 24 hr.), respectively.

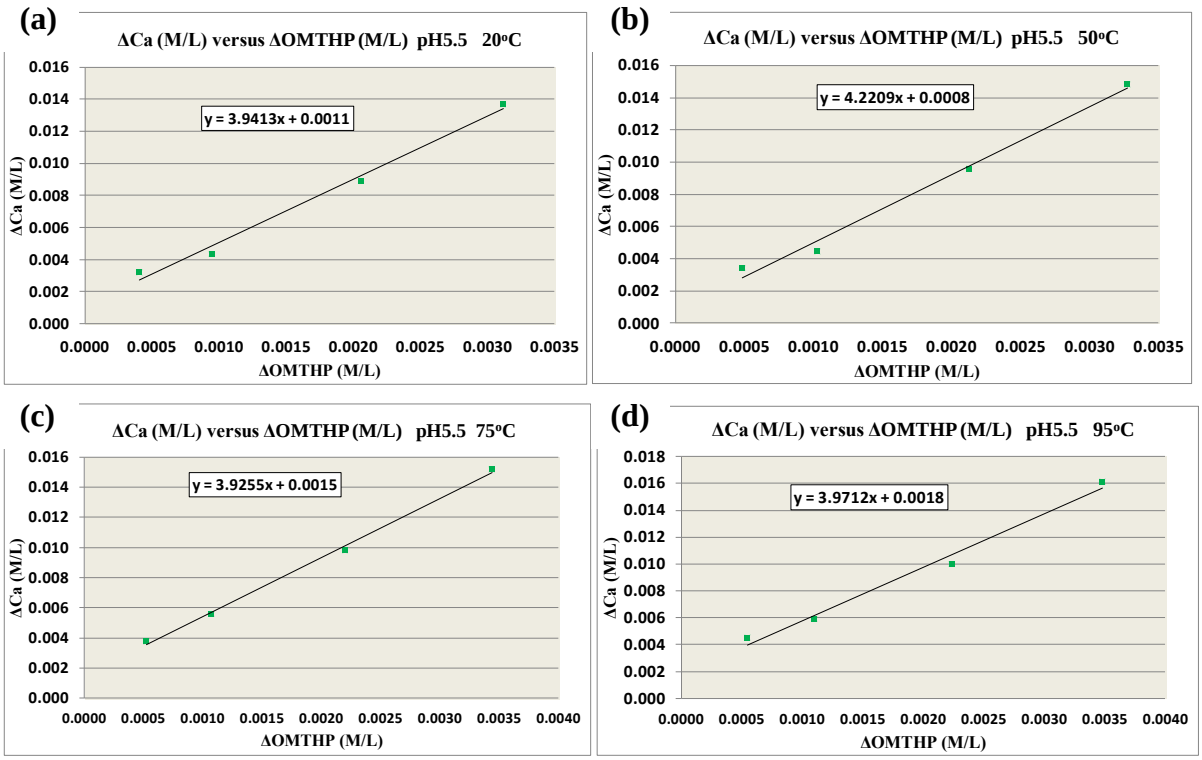

Figure 12.9(a)−(d) − Precipitation experiment results (SI and Ca^{2+}): ΔCa(M/L) vs. ΔOMTHP (M/L) at (a) 20°C; (b) 50°C; (c) 75°C, and (d) 95°C; pH 5.5 (Shaw et al., 2012).

Similarly, when DETPMP was tested, it was found that the molar ratio of Ca^{2+}/DETPMP precipitated = ~3.5 to 4 (Figure 12.10(a)−(d)).

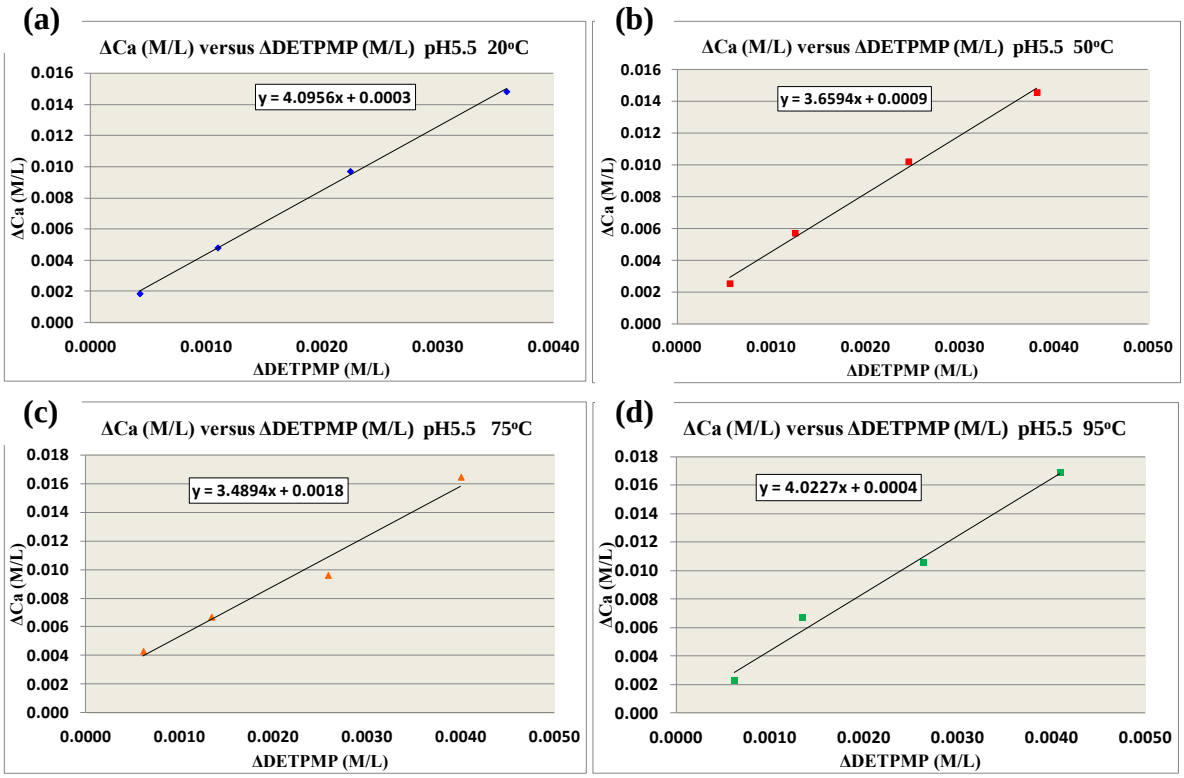

Figure 12.10(a)−(d) − Precipitation experiment results (SI and Ca^{2+}): ΔCa(M/L) vs. ΔDETPMP (M/L) at (a) 20°C; (b) 50°C; (c) 75°C, and (d) 95°C; pH 5.5 (Shaw et al., 2012).

Similar findings were reported by Oddo and Tomson (1990), who investigated the stoichiometry of DETPMP−Ca precipitation. Clearly, this molar ratio of Ca^{2+}/DETPMP is greater than that shown per DETPMP molecule in Figure 12.1(b) and Figure 12.4(b). Browning and Fogler (1995) discuss the effects of synthesis parameters, including pH and the molar ratio Ca^{2+}/HEDP on the chemical structure of calcium-phosphonate precipitates. The chemical structures Browning and Fogler present for Ca−HEDP compounds (shown in Figure 12.11(a) and (b)) are *exactly* the same as the complex structures presented in this Chapter for M^{2+}−HEDP (i.e., Figure 12.2(a) and Figure 12.8(a)). Browning and Fogler report that the Ca−HEDP complex shown in Figure 12.11(b) forms in high pH conditions when HEDP (H_4A) is *fully dissociated* (A^{4-}) whereas the Ca−HEDP complex shown in Figure 12.11(a) can form when the HEDP molecule is only half-dissociated, i.e. HA^{2-}, at lower pH. In Figure 12.11(a) and (b), the HEDP species which forms the complex is stated.

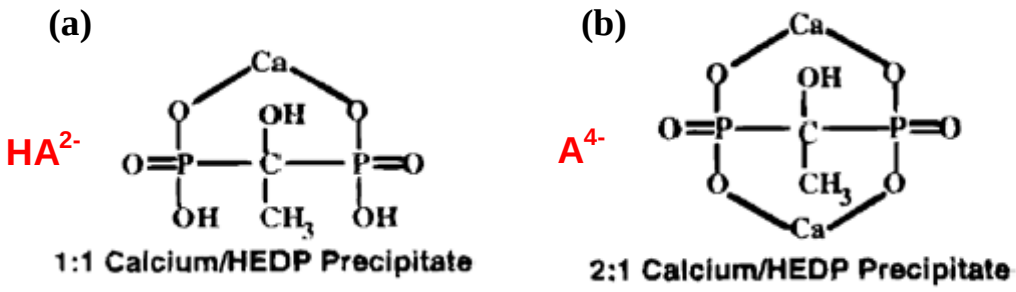

Figure 12.11(a)−(b) − Calcium−HEDP complexes formed at low pH (a) and high pH (b) (Browning and Fogler, 1995).

Individual SI molecules can form a mixture of 5- and 8-membered chelate rings simultaneously, but this occurs more frequently at higher pH levels, as shown in Figure 12.7(a) for OMTHP (as H_4A^{8-}) and Figure 12.7(b) for DETPMP (as H_3A^{7-}), when there are higher concentrations of more highly dissociated (charged) SI. The OMTHP complex shown in Figure 12.7(a) is hexa-nuclear, and the DETPMP complex shown in Figure 12.7(b) is penta-nuclear (Table 12.2). In these experiments, the pH was fixed at pH 5.5, and the pH of the test bottles were checked at the end of the experiment. All test bottles had final pH levels no greater than ~ ±0.3 of a pH unit. At pH 5.5, lower concentrations of the more highly dissociated DETPMP species, such as H_4A^{6-} will also exist (see Figure 7.4), which has the ability to bind four Ca^{2+} cations. Although, in Figure 12.7(b), DETPMP is in the state H_3A^{7-}, the four terminal chelate rings could still be formed by the less-charged species H_4A^{6-}, producing a tetra-nuclear chelate (Table 12.2). This could explain why the molar ratio of Ca^{2+}/DETPMP precipitated in this experiment was in the range of 3 to 4 (e.g., there might be a small proportion of "total" DETPMP that is bound to four Ca^{2+} cations, as shown in Figure 12.7(b)) with $M^{2+} = Mg^{2+}$ (except with the middle 5-membered chelate ring omitted).

The DETPMP speciation chart (Figure 7.4) gives an indication of the likely proportion of the various Ca–DETPMP complexes that can be formed at pH 5.5. Clearly, the majority of DETPMP molecules will form the complex structures shown in Figure 12.1(b) (DETPMP as H_7A^{3-}), Figure 12.4(b) (DETPMP as H_5A^{5-}), and Figure 12.5(b) (DETPMP as H_6A^{4-}) at pH 5.5. It is very important to note that SI molecules that are more highly dissociated than the minimum required to form a particular complex still retain the ability to form the complex. For example, the species H_6A^{4-} can still form the complex shown in Figure 12.1(b)

(DETPMP as H_7A^{3-}). Excess functional groups might be dissociated but not bound to M^{2+}, but rather charge-balanced by counter ions. All SI-complexes that have an overall positive charge will be charge-balanced by other ionic species present in the system (e.g., Cl^-). Overall charge is always = 0 in all experimental systems. For this reason, overall charges have been omitted in Figure 12.1−Figure 12.8. In the Ca/OMTHP and Ca/DETPMP precipitation experiments, Cl^- was also present (calcium chloride hexa-hydrate was used); the Cl^- charge-balances the positively charged SI–Ca complexes that form. It should be noted that the complexes given are illustrative of the processes involved. The ligands, "L", could be other inhibitor molecules, aqua ligands, or be with the same inhibitor molecule forming stabilised cage structures. The ring structures proposed are supported by numerous publications (Martell, 1971a, 1971b; Ockerbloom and Martell, 1957; Sawada et al., 1986, 1988) and are a convenient method of visualised inhibitors and their functionality. So, why OMTHP is the best-performing SI and the differences between NTP, EABMPA, HEDP, and HPAA have now been explained:

- As the maximum possible molar ratio of M^{2+}/SI (per molecule) decreases, IE is likely to decrease.
- The best SIs have the ability to form multiple 5- or 6-membered chelate rings (e.g., OMTHP, DETPMP, and HMTPMP).

Chelate rings containing 7 or more atoms are significantly less stable (e.g., 8-membered chelate rings formed by NTP and EABMPA, Figure 12.5(f) and Figure 12.5(g)). The order of decreasing molar ratio of bound M^{2+}/SI (per molecule) listed in Table 12.1 is similar but not identical to the order of decreasing IE ability. For any subset of molar ratios (e.g., molar ratio M^{2+}/SI = 1), other factors must be considered (i.e., chelate ring size, for example, as discussed for NTP, EABMPA, HEDP, HPAA, etc.). Differences between the two penta-phosphonates DETPMP (Type 1) and HMTPMP (Type 2) and between the two tetra-phosphonates EDTMPA (Type 2) and HMDP (Type 2) will now be explained.

Structurally, the only difference between the penta-phosphonates DETPMP and HMTPMP is that the DETPMP molecule contains eight fewer methylene groups (–CH_2–) (Table 12.1). HMTPMP contains 12 methylene groups, whereas DETPMP contains only 4. Similarly, the only structural difference between the tetra-phosphonates EDTMPA and HMDP is that EDTMPA contains 4 fewer methylene groups (Table 12.1). HMDP contains 6 methylene

groups, whereas EDTMPA contains only 2. All four of these SI molecular structures are chemically similar: HMTPMP is basically two HMDP molecules joined together by a central nitrogen atom, resulting in the molecule formed having an extra phosphonate functional group. Similarly, DETPMP is basically two EDTMPA molecules joined together by a central nitrogen atom, again resulting in the molecule formed having one additional phosphonate functional group.

Because both DETPMP and HMTPMP can form the same number of chelate rings per molecule (5- or 8-membered), differences in their IE must be a result of the chemical differences between their molecular structures, as outlined above. The molecular weight of HMTPMP = 685.49 g/mole, compared to 573.25 g/mole for DETPMP; this weight difference is exclusively caused by the difference in the number of methylene functional groups. The difference in their IE must be explained in terms of intermolecular packing within growing barite-scale deposits. The HMTPMP molecule is significantly more elongated than the DETPMP molecule (Table 12.1). This means it is likely to be more difficult for the HMTPMP to crystallise in a thermodynamically favorable conformation with neighbouring SI anions and Ca^{2+} cations. Note that in all SI-metal complex structures presented in this Chapter, bonds to "L" have been included, which denotes a neighbouring ligand (SI anion or aqua ligand), i.e., where a neighbouring SI anion or a lone-pair of electrons could bond to the metal cation. If M^{2+} is Mg^{2+}, clearly this would occur in the liquid phase. If M^{2+} = Ca^{2+}, Sr^{2+}, or Ba^{2+}, this could occur in the liquid or solid phase. The very small size of Mg^{2+} means it cannot be incorporated into the solid phase (Table 2.1).

It is much more difficult for HMTPMP to be incorporated into scale deposits (bound to Ca^{2+}) caused by conformational, stereochemical reasons; this implies that DETPMP will be a better crystal-growth blocker than HMTPMP. This is indeed what was observed in static IE tests involving these two products (Shaw et al., 2010a). DETPMP inhibited much better over long residence times (i.e., 22 hr.), when the crystal-growth-blocking mechanism of inhibition is required. Hence, when predicting the static IE capability of a phosphonate SI, one further factor must be considered: the thermodynamic favorability of intermolecular packing within solid barite-scale deposits, in terms of molecular stereochemistry. Polymers are known to be poor crystal-growth blockers (Sorbie et al., 2000; Sorbie and Laing 2004); this too could be caused by the fact that it is difficult for these large molecules to be incorporated into the

growing scale, inhibit further crystal growth, and pack together efficiently. Polyacrylate SIs have one structural similarity to the HMTPMP in that there are many methylene functional groups in these molecules. Van der Leeden and Van Rosmalen (1990) reported that the presence of hydrophobic functional groups within SI molecules, such as methylene, reduces the IE of PMA/PAA type inhibitors. This may apply to all inhibitors, including HMTPMP (which contains 12 methylene groups) and HMDP (which contains 6 methylene groups in a row).

The difference between the static IE of tetra-phosphonate SIs HMDP and EDTMPA is slightly more complex to explain. Firstly, the HMDP can be incorporated into barite scale deposits more easily than HMTPMP because the molecule is roughly half the length of HMTPMP (Table 12.1). In static IE tests, EDTMPA was ultrasensitive to the divalent cations Ca^{2+} and Mg^{2+} (see Figure 5.11 and Figure 5.12); however, it too would be expected to incorporate easily into barite, in conjunction with Ca^{2+}. The stability constants for EDTMPA–Mg^{2+} complexes may be so large that it resulted in 22-hr EDTMPA MICs >>> 22-hr MICs for HMDP, NTP, HEDP, and HPAA for "base-case" brine mix 80/20 NSSW/FW (Chapter 5). The 80/20 NSSW/FW base-case brine mix contained a high concentration of [Mg^{2+}] = 1,242 ppm, lower [Ca^{2+}] = 742 ppm, and the barite SR was also relatively high (Figure 5.1). The molar ratio Ca^{2+}/Mg^{2+} in the produced water = 0.36 (Figure 5.1). Despite HMDP and EDTMPA being able to form the same number of chelate rings per molecule at ~pH 5.5 (Table 12.1, Figure 12.1(d), Figure 12.1(e), Figure 12.4(d), Figure 12.4(e), Figure 12.5(d), and Figure 12.5(e)), large differences in their MICs are apparent. For example, HMDP 80/20 NSSW/FW base-case 22-hr MIC = 80 ppm, whereas EDTMPA 80/20 NSSW/FW base-case 22-hr MIC = ~400 ppm (both at 95^{o}C and pH 5.5; see Chapter 5). Under these test conditions, the EDTMPA 22-hr MIC was exactly 5 times larger than that for HMDP. This example highlights that there are several factors that affect phosphonate SI IE, not only the maximum possible molar ratio of M^{2+}/SI, as presented in Table 12.1. Clearly, the specific experimental conditions are also very important; in particular, the brine pH, [Ca^{2+}] and [Mg^{2+}]. The presence of 6 consecutive hydrophobic methylene functional groups in the HMDP may also hinder its IE (Van der Leeden and Van Rosmalen, 1990).

The same explanation proposed for DETPMP/HMTPMP IE does not apply to the HMDP/EDTMPA comparison, except the argument regarding the consecutive hydrophobic

methylene groups present in HMTPMP and HMDP molecules which may hinder IE (Van der Leeden and Van Rosmalen, 1990). Clearly, the EDTMPA molecule is much shorter than the HMDP molecule (Table 12.1), and so this would contradict the earlier explanation for DETPMP/HMTPMP. An EDTMPA molecule contains 4 atoms in the main backbone (2 carbon and 2 nitrogen), whereas HMDP contains double that amount (8 atoms; 6 carbon and 2 nitrogen). In the case of the HMDP and EDTMPA comparison, differences between their IE must be primarily a result of large differences in the magnitude of the SI–M^{2+} binding constants for each species at pH 5.5; particularly, the magnesium binding constants K_{Mg}. Obviously, the K_{Mg} EDTMPA >>> K_{Mg} HMDP at pH 5.5. This explanation is very plausible, given that EDTMPA is actually the phosphonate analogue of the widely used strong chelating agent EDTA. Thus, one further factor must be considered with regard to SI IE − the magnitude of the binding constants K_{Mg} and K_{Ca} at the test pH. Testing various SIs at different pH levels has shown that EDTMPA actually inhibits better at pH 6.5, and this appears to be an "optimum" operating pH (Chapter 7). The relative magnitude of the K_{Mg} and K_{Ca} values for EDTMPA and HMDP might not change significantly at pH 6.5 (i.e., the same differences between the IE of EDTMPA and HMDP could still be apparent at pH 6.5).

12.3 PMPA – Structural Explanation

The IE of PMPA was remarkably similar to that of phosphonates such as DETPMP (Chapters 5 and 6). This is because the chemical structure of PMPA is similar to aminomethylene phosphonates such as OMTHP, DETPMP, HMTPMP, etc. PMPA can form exactly the same chelate rings as shown in Figure 12.1 and Figure 12.4 when *moderately* dissociated. PMPA contains many nitrogen atoms. Every nitrogen atom in the PMPA structure has the ability to form a 5-membered chelate ring with M^{2+}. The methylene phosphonate functional group joined to each nitrogen atom forms part of the chelate ring, in exactly the same way as illustrated in Figure 12.1(a)−(g) for simple aminomethylene phosphonate molecules. The terminal phosphonate functional groups in the PMPA molecule can also form 8-membered chelate rings, in the same way as shown for simple aminomethylene phosphonates in Figure 12.5. When PMPA is more dissociated, two 5-membered chelate rings can form, involving the terminal phosphonate groups and terminal nitrogen atoms, as shown in Figure 12.4 for simple aminomethylene phosphonates. Like the aminomethylene phosphonates, at higher pH levels, PMPA can also form a mixture of 5- and 8-membered chelate rings at higher pH levels >> 5.5, involving the terminal phosphonate functional groups. Since the metal

chelation ability of PMPA mirrors that of the simple aminomethylene phosphonates, this explains why PMPA IE resembles that of SIs such as DETPMP and HMTPMP. Assuming "R" in Figure 3.29 = $-CH_2-$, "n" = 1, and "x" = 1, Figure 12.12 illustrates how PMPA can form multiple 5-membered chelate rings when moderately dissociated. This simplified PMPA structure alone contains eight 5-membered chelate rings and has the capability of chelating 6 moles of M^{2+} ions. Compare OMTHP, which can only chelate 6 moles of M^{2+} ions at high pH, as shown in Figure 12.7(a). In reality, the PMPA molecule will be much larger than shown in Figure 12.12, and so its metal chelation potential will be even greater. PMPA is in effect a "poly" chelating agent.

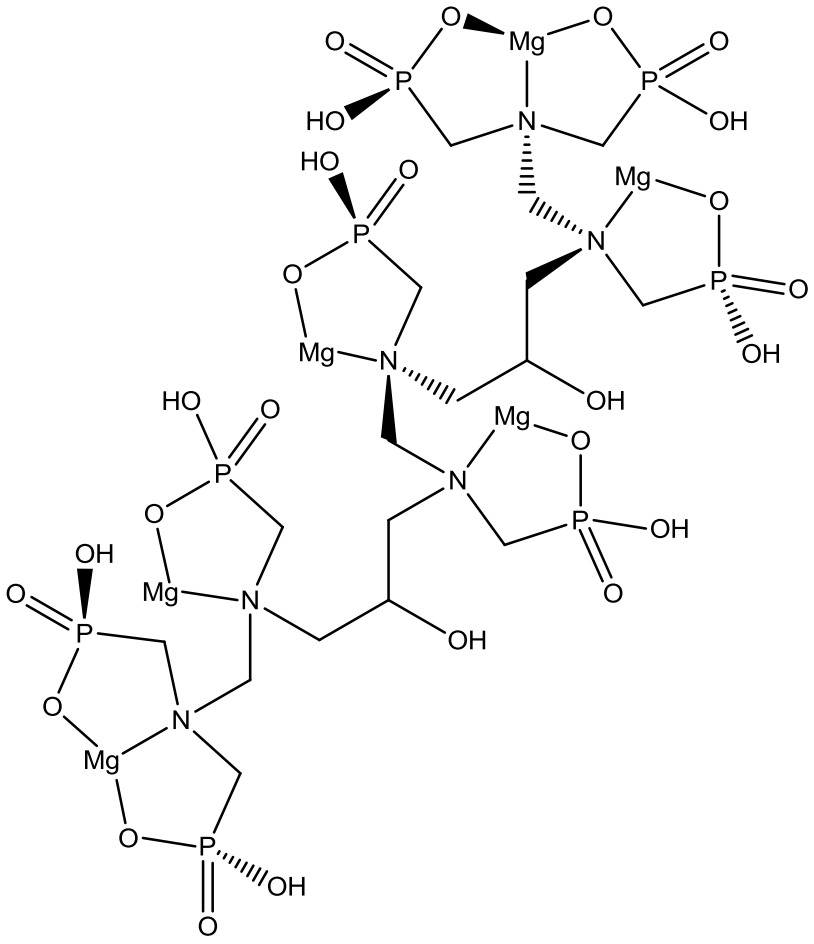

Figure 12.12 – Simplified structure of PMPA (R = $-CH_2-$, n = 1, and x = 1), illustrating how multiple 5-membered chelate rings can be formed simultaneously.

12.4 PPCA and other Polymers – Structural Explanation

PPCA and other polycarboxylated polymers do not have the same chelation potential as PMPA and phosphonate SIs. For example, PPCA cannot form 5-membered chelate rings, but *can* form 8-membered chelate rings by means of two adjacent dissociated carboxylic acid functional groups, as shown in Figure 12.13. Figure 12.13 is a "simplified" structure of PPCA, where, with reference to Figure 3.24, m = 3 and n = 3. As mentioned earlier in this Chapter, with regard to phosphonate SIs, 7- and 8-membered chelate rings are not as stable as 5- or 6-membered chelate rings. This applies to all chemicals, including polymers. Carboxylate functional groups also do not bind as strongly to M^{2+} cations, compared to phosphonate functional groups. These reasons explain why the polymers (excluding PMPA) perform less well by the crystal growth blocking mechanism. Good chelation ability is advantageous for long-term IE.

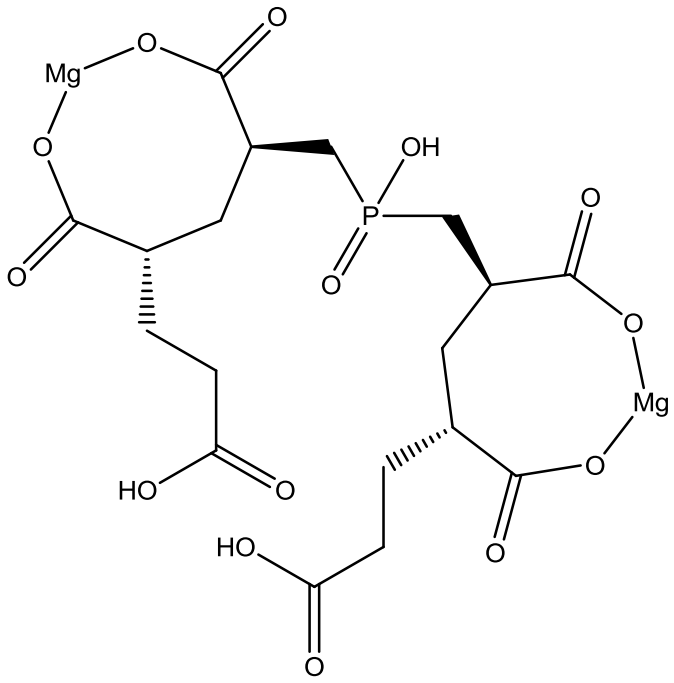

Figure 12.13 – Simplified structure of PPCA (m = 3, and n = 3), illustrating how multiple 8-membered chelate rings can be formed simultaneously.

Figure 12.14 illustrates how 3 MAT monomer units (see Figure 3.25) can polymerise together (in the order: maleic acid, vinyl acetate, ethyl acrylate), and more crucially, how M^{2+} ions could be chelated by this species. This structure consists of two 7-membered chelate rings and one 9-menbered chelate ring. These chelate rings would not be very stable, and secondly, two of the chelate rings proposed require dative bonding to M^{2+} by means of

carbonyl or ester functional group oxygen atom lone-pairs of electrons (these oxygen atoms are not negatively charged – this bonding is analogous to dative bonds formed to M^{2+} by means of a nitrogen atom lone-pair of electrons). Dative bonding to M^{2+} by means of uncharged oxygen atoms which are part of carbonyl or ester functional groups is much less likely to occur than bonding to M^{2+} by means of dissociated (negatively charged) carboxylic acid functional group oxygen anions. Therefore, in Figure 12.14, only one 7-membered chelate ring could form if oxygen atom dative bonding to M^{2+} is disregarded. Again, this means MAT lacks chelation ability, and would not be expected to perform well over longer residence times.

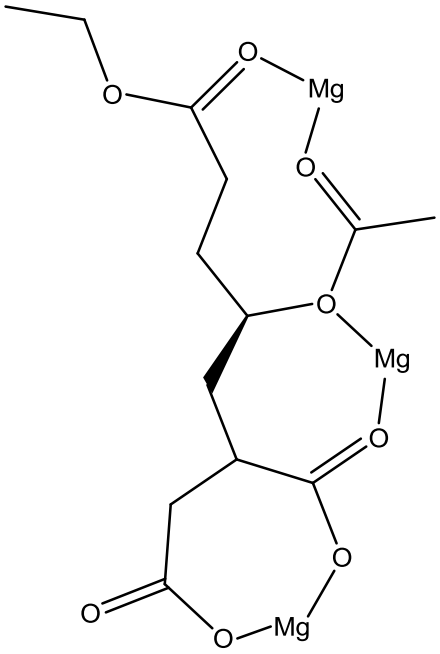

Figure 12.14 – Simplified structure consisting of 3 MAT monomer units joined together in the order: maleic acid, vinyl acetate, ethyl acrylate, illustrating how multiple 7- and 9-membered chelate rings can be formed simultaneously.

Figure 12.15 illustrates two SPPCA monomers joined together and how an 8-membered chelate ring could form. This structure involves bonding to M^{2+} by means of a dissociated carboxylic acid functional group and a dative bond involving the nitrogen atom in the AMPS monomer unit. In this structure, charges on the nitrogen atom and sulphonate functional group have been shown to emphasise that the sulphonate functional group would only be associated at very low pH.

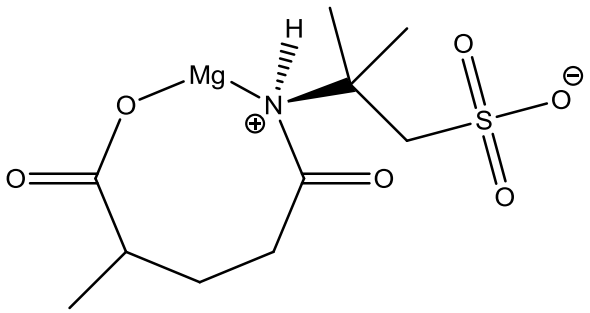

Figure 12.15 – Simplified structure consisting of 2 SPPCA monomer units joined together in the order: acrylic acid, AMPS, illustrating how multiple 8-membered chelate rings can be formed simultaneously.

No structures will be proposed here for PVS, as it has no chelation ability due to the highly dissociated, non-metal binding sulphonate functional groups at pH 5.5 (Sorbie and Laing, 2004). Vinyl sulphonate acrylic acid co-polymer (VS-Co) *does* have limited chelation ability due to the presence of acrylic acid repeating units (carboxylate functional groups), this permits the formation of 8-membered chelate rings in locations where two acrylic acid monomer units have been polymerised adjacently, as shown in Figure 12.16.

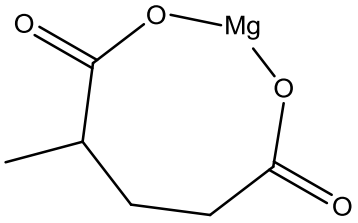

Figure 12.16 – Two acrylic acid monomers joined together illustrating how 8-membered chelate rings can be formed.

Although not tested in IE work, polymaleic acid, PMA (Figure 12.17) actually has greater chelation ability than polyacrylic acid, PAA (Figure 12.18) and VS-Co, because double the number of chelate rings can form per repeating unit, as illustrated in Figure 12.19. Hence, PMA is likely to outperform PAA in IE tests, particularly over longer residence times. In the PMA structure, a carboxylic acid functional group is attached to every carbon atom in the main chain, whereas in the PAA structure, a carboxylic acid group is attached to every second carbon atom – it is this structural difference which alters their chelation ability. 8-membered chelate rings can only form in the VS-Co polymer structure at locations where 2 acrylic acid units have been polymerised in a row, as shown in Figure 12.16.

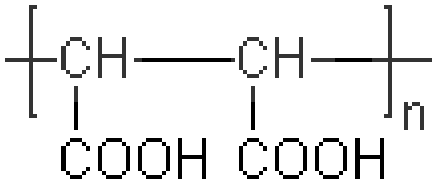

Figure 12.17 – Chemical molecular structure of PMA.

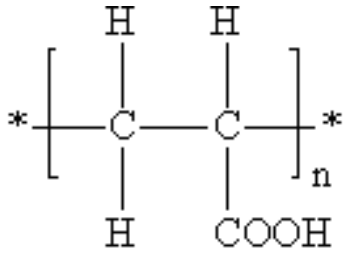

Figure 12.18 – Chemical molecular structure of PAA.

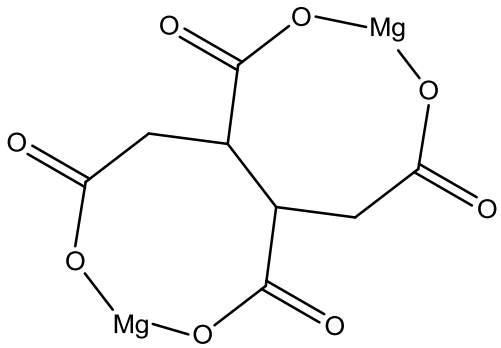

Figure 12.19 – Two maleic acid monomers joined together, illustrating how 8-membered chelate rings can be formed.

The cationic ter-polymers (CTP-A and CTP-B) also have some chelation ability because of the inclusion of maleic acid monomers (Figure 3.30). This permits the formation of 7-membered chelate rings, as illustrated in Figure 12.20. Without the maleic acid monomer being present, this polymer would not have any chelation ability. In Figure 12.20, on the cationic monomer, $R_1 = -H$, $R_2 = -CH_3$, $R_3 = C_2H_5$ and $R_4 = -CH_2-CH=CH_2$.

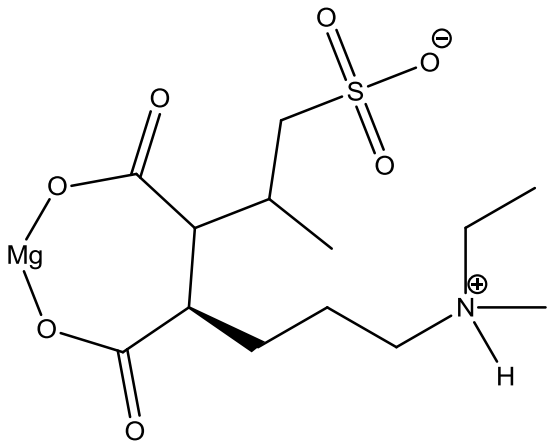

Figure 12.20 – Three cationic ter-polymer monomers joined together in the order: allyl sulphonate anion, maleic acid, allyl quaternary ammonium cation, illustrating how 7-membered chelate rings can be formed.

12.5 Polymers − Summary

Table 12.5 summarises the properties of the majority of the polymers tested in IE work (Chapter 6). PFC is excluded because the exact chemical structure is unknown. Clearly, the presence of aminomethylene phosphonate functional groups in SI molecules and nitrogen atoms within the main carbon chain are both required to facilitate the formation of stable 5-membered chelate rings (e.g. PMPA). The presence of maleic acid repeating units in polymers is advantageous as is allows the formation of 7-membered chelate rings, e.g. MAT, PMA, CTP-A and CTP-B. 7-membered chelate rings can be formed by these polymers because 2 carboxylic acid functional groups are attached to adjacent carbon atoms in the main carbon chain. On the other hand, PPCA, SPPCA, VS-Co and PAA can only form slightly larger, 8-membered chelate rings because the carboxylic acid functional groups are attached to every *second* carbon atom in the main carbon chain. The IE of the majority of polymers examined in Chapter 6 was worse than that of a regular phosphonate such as DETPMP, with the main exception being PMPA, which performed comparably similarly to DETPMP. This is most likely because PMPA is the *only* polymer which can form stable 5-membered chelate rings (Figure 12.12), like all other *aminomethylene phosphonates* tested in this work. 7- and 8-membered chelate rings are unstable (Greenwood and Earnshaw, 1997); this is most likely why the remaining polymers performed worse than phosphonates, particularly over longer residence times, i.e. 22 hours. PVS is unique in that it cannot form any chelate rings at pH5.5

because of the strongly acidic nature of sulphonate functional groups. PVS is a nucleation inhibitor (Sorbie and Laing, 2004) – this is why the 2 hour IE was often good, but a 22 hour MIC could not be achieved. Chelation theory discussed in this Chapter re-confirms this statement. With regard to polymers, hydrophobic functional groups such as methylene ($-CH_2-$) are known to be detrimental to performance, whereas the introduction of –OH, $-NH_2$ or $-SO_3H$ functionalities improves IE (Van der Leeden and Van Rosmalen, 1990). This is most likely because functional groups such as –OH and $-NH_2$ have the ability to form dative bonds with metal cations, whereas $-CH_2-$ functional groups do not have that ability because there are no non-bonding electrons on the carbon atom. This most likely applies to all molecules, including phosphonates.

Polymer(s)	**Number of Atoms (including M^{2+}) in Smallest Possible Chelate Ring at ~pH5.5**
PMPA	5
MAT, CTP-A, CTP-B, PMA	7
PPCA, SPPCA, VS-Co, PAA	8
PVS	None can be formed at pH5.5

Table 12.5 – A selection of polymeric SIs and the number of atoms (including M^{2+}) in chelate rings they can form at ~pH5.5.

12.6 Summary and Conclusions

This Chapter discussed the various factors that must be considered with regard to the barium sulphate IE capability of phosphonate and polymeric SIs:

1. The number of phosphonate groups per molecule is important. The more phosphonate groups there are per molecule, the better the IE should be;
2. The larger the value of the maximum possible molar ratio of M^{2+}/SI (per SI molecule), the more likely SI will inhibit barite. Clearly, this molar ratio depends on the number of possible chelate rings that can form at the test pH.
3. The number of chelate rings that can form per SI molecule (at the test pH), and how many atoms form part of the chelate rings is important. Chelate rings containing five or six atoms (including M^{2+}) are the most thermodynamically stable. SI molecules that can form multiple 5- or 6-membered chelate rings are likely to inhibit well.
4. Aminomethylene phosphonates (e.g. OMTHP, DETPMP, etc.) are likely to perform better than equivalent non-aminomethylene phosphonates because nitrogen atoms are key in the formation of stable 5-membered chelate rings with M^{2+}.
5. Polymers, like phosphonates, cannot form stable 5-membered chelate rings unless aminomethylene phosphonate functional groups are included in the chemical structure, e.g. PMPA. For this reason, nitrogen-free and phosphorus-free polymers, e.g. MAT, VS-Co, PVS, are more likely to perform worse than polyaminomethylene phosphonates and aminomethylene phosphonates, particularly at longer residence times.
6. In regards to SI molecular size/stereochemistry, the thermodynamic favourability of incorporation of SI into barite scale (in conjunction with Ca^{2+}) must be considered, in terms of intermolecular packing. Molecules that can pack together in a favourable conformation are likely to perform better by the crystal growth inhibition mechanism (e.g., DETPMP). Molecules that are more elongated (e.g., HMTPMP) are likely to have more limited crystal-growth-inhibition qualities but might resemble polyacrylate polymers somewhat, in that they might perform well by the nucleation inhibition mechanism (i.e., inhibit barite well at 2 hr.; for example, HMTPMP). In a few instances, in higher [Ca^{2+}] brine mixes (e.g., Base Case 10/90, 20/80, 40/60, and 50/50 NSSW/FW), the 2-hr HMTPMP MIC < 2-hr DETPMP MIC (Chapter 5).

7. Van der Leeden and Van Rosmalen (1990) report that hydrophobic functional groups present in polymeric SIs, such as methylene, are detrimental to IE. This finding may apply to all SIs. HMTPMP and HMDP both contain many hydrophobic methylene functional groups in their chemical structures (12 and 6 respectively − see Table 12.1) – this structural feature could be making their IE more comparable to polymers.
8. Magnitude of the SI binding constants to the divalent cations Ca^{2+} and Mg^{2+} at the test pH (K_{Ca} and K_{Mg} vary with pH). SIs that have unusually large binding constants to Mg^{2+} at pH 5.5 (as is very likely the case for EDTMPA) will have elevated MIC levels, particularly in brine mixes containing a high concentration of Mg^{2+}. On the contrary, SIs that have large K_{Ca} values at the test pH, and under the specific test conditions, are likely to inhibit well. The function of any SI essentially depends on the relative magnitude of the K_{Mg} and K_{Ca} values under the specific test conditions (i.e., pH, $[Ca^{2+}]$ and $[Mg^{2+}]$).
9. Specific test conditions (i.e., pH, $[Ba^{2+}]$, $[Sr^{2+}]$, $[Ca^{2+}]$, $[Mg^{2+}]$ and T). In "base-case" IE tests, the mixing ratio NSSW/FW selected determines $[Ba^{2+}]$, $[Sr^{2+}]$, $[Ca^{2+}]$ and $[Mg^{2+}]$.

It should be noted that these 9 factors are inter-related. Factors 1, 2, 3, 4 and 9 are applicable to all SIs. Factor 5 explains polymer IE, and why PMPA performed better than the others. Factor 6 explains differences between DETPMP and HMTPMP. Factor 7 applies to HMTPMP and HMDP, regarding the hydrophobic nature of the consecutive methylene groups in these molecules possibly being detrimental to IE. Factor 8 applies specifically to EDTMPA which may have a very large binding constant, K_b, to Mg^{2+} at pH 5.5. The order of decreasing IE potential of the SIs will change, depending on the specific experimental conditions: pH, $[Ba^{2+}]$, $[Sr^{2+}]$, $[Ca^{2+}]$, $[Mg^{2+}]$ and temperature. For example, the order of decreasing IE capability at Base Case 60/40 NSSW/FW (highest barite SR mixing ratio) might be completely different to the order at Base Case 80/20 NSSW/FW because the composition of the brine mix (produced water) has changed; in particular, $[Ba^{2+}]$, $[Sr^{2+}]$, $[Ca^{2+}]$ and $[Mg^{2+}]$. Therefore, factor 9 listed above would be altered. Differences in static barium sulphate IE at various brine mix compositions were the main focus of Chapters 5 and 6 in this thesis and Shaw et al., (2010a) (phosphonates) and Shaw et al., (2010b) (polymers). Changes in the test pH might also alter the sequence of decreasing or increasing IE of the

phosphonate and polymeric SIs because this changes the % SI dissociation, and so, the metal-chelation ability of the species. pH effects on static barite IE were examined in Chapter 7 and Shaw and Sorbie (2012).

All SI type categorisations were based on static IE tests carried out at pH 5.5 and 95°C. If tests had been carried out at a different pH and/or temperature, it is possible some SI categorisations (Type 1/Type 2) would change because SI dissociation and also the magnitude of the binding constants K_{Ca} and K_{Mg} would change. Changing these parameters would mean the possible chelate/complex structures that can form would also change. The Type 1 or Type 2 SI classification is clearly strongly influenced by the factors listed above – particularly factor 4, regarding the inclusion of nitrogen atoms within molecular structures. This is most likely the reason why, of all the polymers, PMPA was the only Type 1 product. Of the polymers, only PMPA contains nitrogen atoms in the main carbon chain. Polymers such as SPPCA and the cationic ter-polymers also contain nitrogen, but *not within the main carbon chain*; instead in side chain functional groups, e.g. AMPS side groups in SPPCA. SPPCA can form chelate rings involving the nitrogen atom in the AMPS side chains, however the chelate rings formed contain 8 atoms and are thus unstable (Figure 12.15).

The findings of this Chapter suggest the crucial structural feature which is likely to lead to a Type 1 SI categorisation is the presence of **amino methylene phosphonate** functional groups in SI molecules, *regardless* of whether the SI is polymeric or non-polymeric. SIs containing *multiple* amino methylene phosphonate functional groups (e.g. OMTHP, DETPMP and PMPA) have the greatest tendency to be Type 1. The inclusion of nitrogen atoms within the main carbon chain of SI molecules is also very important. Of all the products tested in this work, less than half of the species tested were amino methylene phosphonates (8 products): PMPA, OMTHP, DETPMP, HMTPMP, HMDP, EDTMPA, NTP and EABMPA. All other products tested were non-amino methylene phosphonated (PFC is a sulphonated P-tagged co-polymer, but there was no indication that this product contained nitrogen. For the purposes of this structural explanation, PFC will be considered nitrogen-free). It is highly likely the absence of amino methylene phosphonate functional groups will lead to a Type 2 categorisation. HEDP and HPAA are unique in that they are nitrogen-free phosphonate SIs which can form stable 6-membered chelate rings. As discussed previously, this is probably why these two products behaved like Type 1 products in SI consumption tests (Chapter 9).

However, both these products were shown to be Type 2 in MIC vs. %NSSW experiments (Chapter 5), which forms the basis of the Type 1 / Type 2 categorisation.

Chapter 13: Final Conclusions and Future Work

Chapter 13 Summary: In this final Chapter, the main findings of each of the *results* Chapters in this thesis are described and summarised. A number of areas for future work are also suggested.

13.1 Chapter 4 – Chemical Analysis of SI Products

In this Chapter, the chemical nature of the SI formulations and the %P and %S in SI molecules was determined. The majority of the phosphonate SI formulations used in this work exist as acid solutions – only two existed as salt solutions – OMTHP and HMDP. The OMTHP formulation exists as a sodium salt solution whereas the HMDP formulation exists as a potassium salt solution. Of the polymers, PFC, PVS and VS-Co were identified as possibly existing as salt solutions (CTP-A and CTP-B were excluded from this analysis). Of particular interest was the VS-Co formulation which was shown to contain significant amounts of sodium and potassium. As noted in the Chapter, the presence of sodium and/or potassium in the polymeric formulations could also be due to other chemicals being in the formulation, such as synthesis activators, etc.

P-tagged polymers such as PFC, SPPCA and PPCA contain < 5% phosphorus, this was determined experimentally. The phosphonates contain the highest % phosphorus, in the range 19-32% P. The phosphonates are frequently classed as "red" products whereas P-tagged polymers are considered "yellow". Phosphorus-free and sulphur-free products such as MAT are classed as "green" SIs. PVS contained the highest [S] since it is a sulphonated homopolymer (~35%), followed by VS-Co (~17%), followed by CTP-A, CTP-B and PFC (all 10-15%), followed by SPPCA (~5%). This analytical information regarding the SI formulations was useful for experiments described in subsequent chapters, involving SI analysis by ICP spectroscopy or alternative methods. This knowledge about the nature of the SI formulations is also useful in helping to explain differences in their IE performance, mechanisms, etc.

13.2 Chapter 5 – MIC vs. Mixing Ratio NSSW/FW Experiments – Phosphonate SIs

In this Chapter, Type 1 and Type 2 categorisations were introduced for phosphonate SIs in terms of their MIC vs. %NSSW, sensitivity to Ca^{2+}/Mg^{2+}, and long-term IE. Previously, this distinction had not been made and this thesis introduced this idea and widens it to all scale inhibitor types. The MIC of the Type 1 phosphonate SIs primarily correlates with barium sulphate SR whereas the MIC of the Type 2 phosphonates primarily correlates with the Ca^{2+}/Mg^{2+} molar ratio. Furthermore, at fixed SR and fixed Ca^{2+}/Mg^{2+} molar ratio, *most* phosphonate SIs performed better (i.e. higher IE, lower MIC) in high salinity brine, *regardless* of their Type. There is therefore *no relationship* between phosphonate *Type*, and their IE at fixed SR *and* fixed molar ratio Ca^{2+}/Mg^{2+}, when varying only ionic strength, *I*. Table 12.1 summarises findings for all of the phosphonate SIs studied in this thesis.

SI abbreviation and full name	**Chemical Structure**	**Base Case 22 Hour MIC vs. % NSSW chart (Base Case 50/50 NSSW/FW IE chart for EABMPA only)**	**Type 1 or Type 2**	**Comments**
OMTHP – OctaMethylene Tetraamine Hexa (methylenePhosphonic acid)	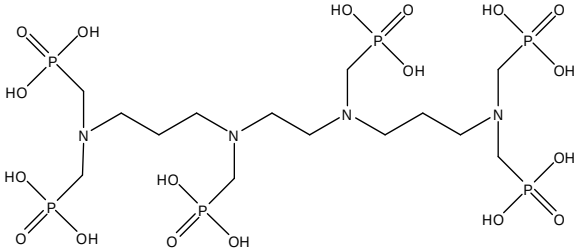	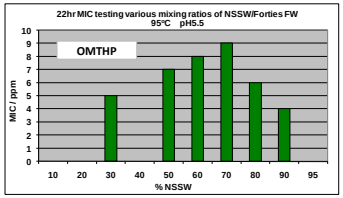	1	All Base Case 22hr MICs < 10ppm. MIC correlates with barite SR profile.
DETPMP – DiEthylene Triamine Penta (MethylenePhosphonic acid)	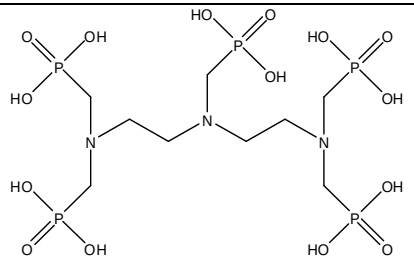	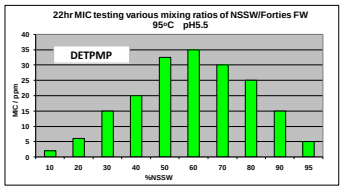	1	MIC correlates with barite SR profile.
HMTPMP – Bis(HexaMethylene) Triamine Pentabis(Methylene Phosphonic acid)	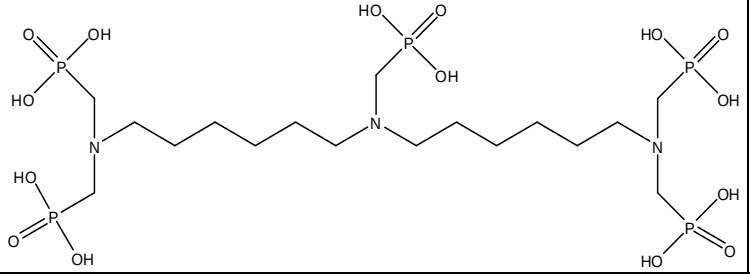	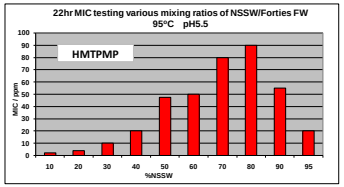	2	Sensitive to the brine mix molar ratio Ca^{2+}/Mg^{2+}. Highest 22hr Base Case MIC

				for brine mix 80:20 NSSW:FW. MIC does NOT correlate exclusively with barite SR.
HMDP – HexaMethylene Diamine tetra(methylene Phosphonic acid)	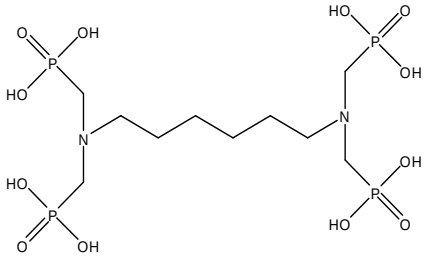	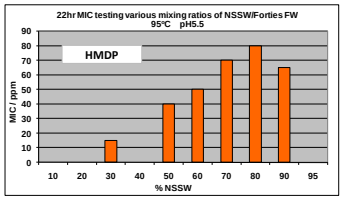	2	Sensitive to the brine mix molar ratio Ca^{2+}/Mg^{2+}. Highest 22hr Base Case MIC for brine mix 80:20 NSSW:FW. MIC does NOT correlate exclusively with barite SR.

EDTMPA – Ethylene Diamine Tetra(Methylene Phosphonic Acid)	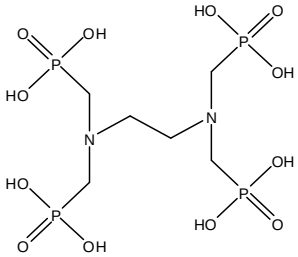	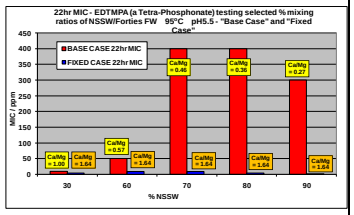	2	Most severe case of a Type 2 phosphonate SI – Base Case 70:30 and 80:20 NSSW:FW 22hr MICs ~400ppm.
NTP – NitriloTris (methylene Phosphonic acid)	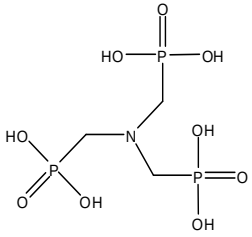	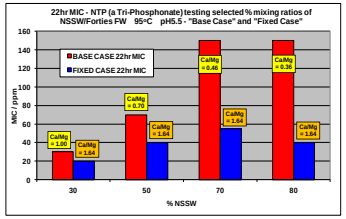	2	Sensitive to the brine mix molar ratio Ca^{2+}/Mg^{2+}. Highest 22hr Base Case MIC for brine mixes 70:30 and 80:20 NSSW:FW. MIC does NOT correlate exclusively with barite SR.

EABMPA – EthanolAmineBis (Methylene Phosphonic Acid)	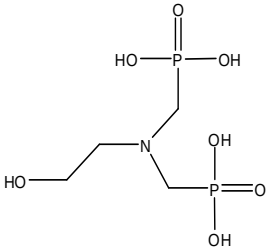	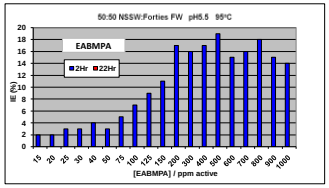	2	IE not good enough for MIC vs. % NSSW profile to be compiled. 2hr Base Case IE < 20%; no 22hr IE - 50:50 NSSW:FW, [SI]s up to 1000ppm active were tested. This SI is not recommended for barite prevention.
HEDP – 1-HydroxyEthylidene-1,1-Di-Phosphonic Acid	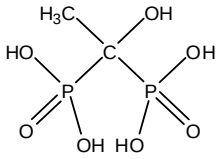	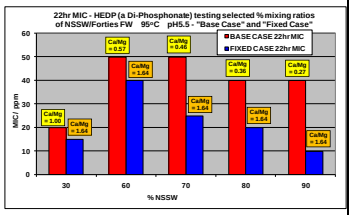	2	May be "borderline" Type 1 / Type 2 – but shown to be Type 2 in

				Chapter 5.
HPAA – 2-HydroxyPhosphonoAcetic Acid	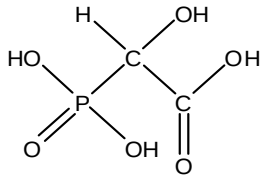	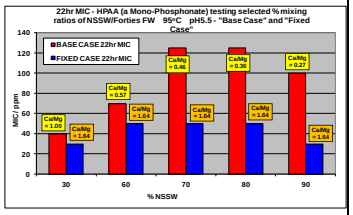	2	Sensitive to the brine mix molar ratio Ca^{2+}/Mg^{2+} in the same way as Type 2 SIs HMTPMP, HMDP and NTP. Highest 22hr Base Case MIC for brine mixes 70:30 and 80:20 NSSW:FW, both ~125ppm.

Table 13.1 – List of phosphonate SIs, their chemical structure, 22 hour Base Case MIC vs. %NSSW chart and classification Type 1 or Type 2.

13.3 Chapter 6 – MIC vs. Mixing Ratio NSSW/FW Experiments – Polymeric SIs

All of the polymers, except PMPA, were identified as Type 2, based on their performance in MIC versus mixing ratio experiments in the same manner as was done in Chapter 5 for the phosphonate SIs. The PMPA is most likely not actually polymeric, and may in fact have a network-like structure comprising of an array of phosphonate molecules joined together. This would explain the anomalous performance of PMPA which is very much phosphonate-like, and not like any other polymeric SI species studied here. Furthermore, in this Chapter, a sub-categorisation system for both phosphonate and polymeric SIs was introduced. In IE experiments testing the polymeric species, 3 of them: PPCA, MAT and PFC performed worse (i.e. higher MIC / lower IE) in the Fixed Case tests compared with the Base Case tests, whereas the converse was true of *all* the other polymers. It was the high [Ca^{2+}] in the Fixed Case experiments which was causing the functionality problems when PPCA, MAT and PFC were being tested. Specifically, in the case of PPCA, Chapter 6 illustrated conclusively this was due to SI precipitation with calcium, causing the decline in IE. Thus, PPCA, MAT, and PFC were sub-categorised *Type B* SIs, whereas all the other polymers and *all* the phosphonate SIs were sub-classified *Type A* SIs. Type A SIs performed better in the Fixed Case tests (2000ppm Ca^{2+}) compared to the Base Case tests whereas the converse was true of Type B SIs. Each SI was assigned a categorisation code, based on their Type (1 or 2 and A or B). For example, SPPCA was Type 2 and Type A, and thus would be categorised "2A". This procedure was applied to categorise *all* SIs tested in this work. Table 13.2 summarises findings for the 9 polymeric SIs and states their categorisation code. Note that *all* phosphonate SIs were Type A.

Polymeric Scale Inhibitor	**Main Functional Groups Present**	**P-Containing ? (Y or N)**	**Sulphonated ? (Y or N)**	**22 hour MIC vs. Mixing Ratio (except PVS, CTP-A and CTP-B). PVS – 2 hour data shown. CTP-A/B – 60/40 MICs shown (Base Case and Fixed Case)**	**Categorisation Code**
PMPA – PhosphinoMethylated PolyAmine	Phosphonate	Y	N	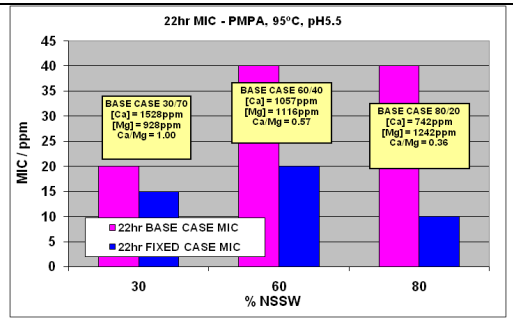	1A
PPCA – Phosphino PolyCarboxylic Acid	Carboxylate	Y	N	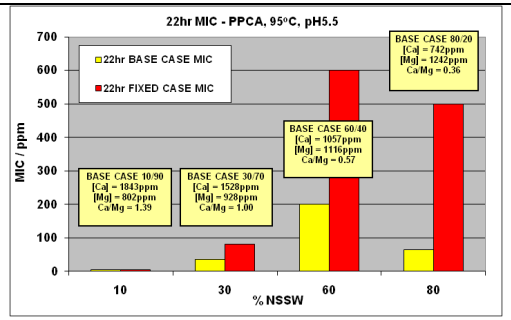	2B

MAT – Maleic Acid Ter-Polymer	Carboxylate, Acetate and Ethoxycarbonyl	N	N	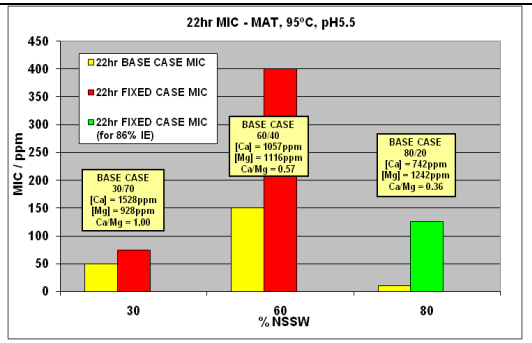	2B
SPPCA – Sulphonated Phosphino PolyCarboxylic Acid	Carboxylate, Sulphonate and Amide	Y	Y	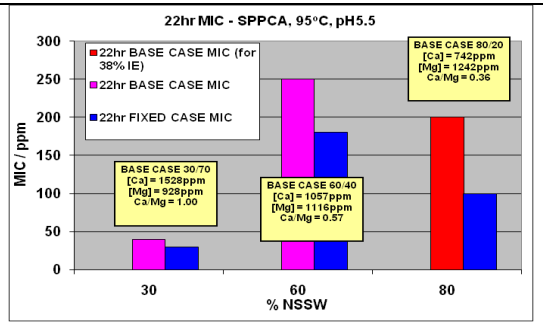	2A
PVS – PolyVinylSulphonate	Sulphonate	N	Y	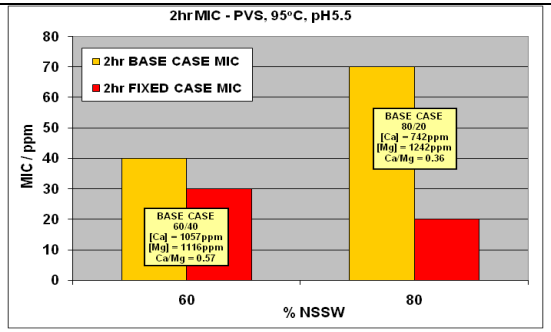	2A

VS-Co – VinylSulphonate Acrylic Acid Co-Polymer	Carboxylate and Sulphonate	N	Y	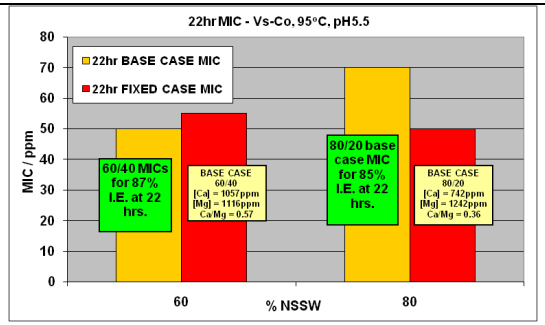	2A
PFC – P-Functionalised Co-Polymer	Carboxylate and Sulphonate	N	Y	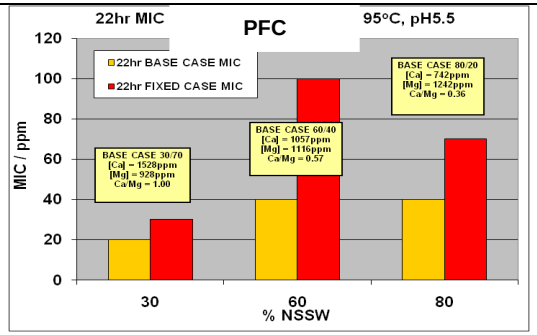	2B
Cationic Ter-Polymers A and B	Carboxylate, Sulphonate and Cationic Groups	N	Y	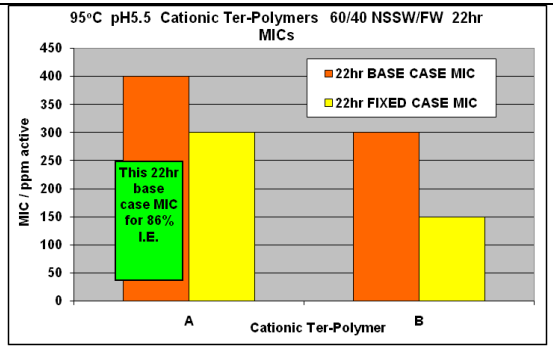	2A (both)

Table 13.2 – List of polymeric SIs, main functional groups present in the molecules, 22 hour Base Case MIC vs. %NSSW chart and categorisation codes.

13.4 Chapter 7 – Inhibition Efficiency (IE) Experiments Varying pH

In this Chapter, the effect of varying pH on the MIC of various SIs was established, which had already been well characterised in terms of their IE behaviour at the main test pH 5.5. Varying the pH changes the speciation of phosphonate SI molecules and thus, their ability to inhibit scale. For example, the 22 hour 80/20 Base Case MIC for HMTPMP is ~90ppm at pH5.5, ~25ppm at pH 6.5 and ~20ppm at pH7.5. In order to inhibit scale formation successfully, SIs must be in a dissociated state. Generally it was found that phosphonate SIs perform better at higher pH levels because under such conditions they are highly dissociated and in this charged state, have the greatest ability to complex scaling ions such as Ba^{2+} *or* form complexes with Ca^{2+}. If an SI forms complexes with Ca^{2+}, this makes it easier to inhibit barite crystal growth. It is easier for an SI to integrate into the growing scale in combination with calcium. At lower pH levels, IE is suppressed and SIs perform much worse, for example, at pH4.5. This is because at lower pH, phosphonate SI molecules become much more *associated*, thus losing their ability to complex strongly with metal ions such as Ba^{2+} and Ca^{2+}. The same general rule applies to polymeric SIs. Carboxylate functional groups are affected in much the same way as phosphonate functional groups by changing pH. Most certainly, PMPA will be affected in exactly the same way as phosphonate SIs by varying pH, since it is a "poly-phosphonate". Sulphonated polymers, e.g. PVS are least affected by changing pH because an extremely low pH is required to associate the highly acidic sulphonate functional groups, e.g. pH < 1.

13.5 Chapter 8 – Mild Scaling IE Experiments

It has been demonstrated quite conclusively that, under mild scaling conditions (100ppm Ba^{2+} in FW), the effects of Ca^{2+}/Mg^{2+} on MIC are exactly the same as observed in the standard severe scaling IE tests (269ppm Ba^{2+} in FW). For example, the highest 22 hour MSBC MIC (=10ppm) for HMTPMP was measured testing brine mix 80/20 NSSW/FW. All MICs in the mild scaling tests were clearly much lower than in the severe scaling tests (compare 10ppm (mild scaling) with 90ppm (severe scaling) for HMTPMP, 80/20, Base Case, 22 hour MIC). This is because it is much easier to inhibit barium sulphate when the SR is much lower in the mild scaling system, but the same clear effects of Ca^{2+}/Mg^{2+} were still visible. Testing DETPMP and HMTPMP in the mild scaling system, their MSFC MIC < MSBC MIC, whereas testing PPCA, MSBC MIC < MSFC MIC. These observations are the same as

observed testing these three SIs in the equivalent severe scaling experiments (Chapters 5 and 6).

13.6 Chapter 9 – Phosphonate SI Consumption Experiments, ESEM & EDAX

Type 1 and Type 2 SIs (categorised in Chapters 5) are consumed into the growing barium sulphate scale at different rates – broadly depending on their Type. Testing the Type 1 phosphonate SIs, e.g. OMTHP, at threshold [SI], e.g. pre-2 hour MIC, there was an initial drop in %SI in solution, and then the level of [SI] in solution was generally maintained over long periods of time, e.g. up to 72 hours after mixing NSSW/FW. The IE profile always correlates very well with the %SI in solution for these Type 1 species. On the contrary, testing Type 2 phosphonate SIs, e.g. HMTPMP at the same threshold [SI], rapid depletion of [SI] from solution occurred, which often declined to near-zero, or zero and the corresponding IE mirrored this profile. The only two exceptions to this general finding were HEDP and HPAA (both Type 2) which both produced SI consumption profiles more typical of a Type 1 species. This could be because these two species are somewhat "intermediate" between Type 1 and Type 2, or it could be related to the chemical nature of these SI molecules, causing them to be consumed less. Both molecules can form 6-membered chelate rings with M^{2+} cations (as shown in Chapter 12, Figure 12.2(a) and (b)) – which could be a very soluble species (−OH functional groups present in both molecules) – they will certainly be very thermodynamically stable entities. Because of these anomalies, do *not* categorise SIs (Type 1 or Type 2) based solely on SI consumption experimental results. The categorisation must be *primarily* based on SI performance in MIC vs. mixing ratio experiments (Chapters 5 and 6). SI consumption experiments are a *secondary* test which may possibly re-confirm Type 1 / Type 2 classifications.

The second general observation was that there is less SI consumption in higher molar ratio Ca^{2+}/Mg^{2+} mixes. Thus, there was almost always less SI consumption in the Fixed Case tests, compared to the Base Case tests when tested at the same [SI]. Testing DETPMP at 5ppm with molar ratio Ca^{2+}/Mg^{2+} = 1, 2, and 4, at 22 hours, the largest quantity of SI was consumed with Ca^{2+}/Mg^{2+} = 1, followed by Ca^{2+}/Mg^{2+} = 2, followed by Ca^{2+}/Mg^{2+} = 4. This correlated with IE, which was the highest with Ca^{2+}/Mg^{2+} = 4, followed by Ca^{2+}/Mg^{2+} = 2, followed by Ca^{2+}/Mg^{2+} = 1.

ESEM images illustrated that the presence of SI inhibits normal crystal growth and changes the crystal morphology. The presence of Type 1 SI caused the break up and disintegration of the scale into small particles, whereas the presence of Type 2 SI caused much larger globular, spherical particles to form. It may be possible to use images of scale deposits to identify which *Type* of SI was present in an IE test. The EDAX results indicated that phosphorus is only detected if the [SI] used in the IE test is sufficiently high, e.g. 70ppm. Phosphorus was only detected in a minority of the scale deposits – all of which originated from IE tests with the highest [SI]s. Generally, a small % of calcium (up to 3.5%) was present in the scale deposits (blanks and SI-containing). This is as expected, since ~6% of Ba^{2+} can be replaced by Ca^{2+} in barium sulphate (Sorbie et al., 2004). Furthermore, phosphonate SIs are incorporated into the growing scale in combination with SI. There was a *larger* atomic % of strontium and a *lower* atomic % barium in the blank deposits compared to the SI-containing deposits. This can be explained by the fact that strontium sulphate scale is easily inhibited by SI, because the SR strontium sulphate is very low (several orders of magnitude lower than for barite), therefore, compositionally, the precipitate which forms *in the presence* of SI contains a *larger* atomic % of barium and a *smaller* atomic % of strontium, compared to blank deposits.

13.7 Chapter 10 – Penta-phosphonates and Polymers – SI Consumption Experiments

From the results in this Chapter, three factors should be considered when trying to interpret SI consumption results for categorisation purposes (testing phosphonates and polymers):

1. If the *IE* and %SI in solution are both *maintained* and correlate with one another (e.g. Figure 10.6 testing PMPA), the product may be *Type 1*.
2. If the *IE* profile declines rapidly over time *and* a large quantity of SI remains in solution (e.g. Figure 10.5 testing PFC), the product may be *Type 2*.
3. If *both IE and %SI* profiles decline rapidly (e.g. Figure 10.8 testing HMTPMP), the product is very likely *Type 2*.

All polymers classified as Type 2 in Chapter 6 produced Type 2 consumption profiles (except CTP-A and CTP-B which were not tested in consumption experiments). PMPA produced a Type 1 profile resembling that obtained testing DETPMP – this result was entirely consistent with the Type 1 classification of PMPA in Chapter 6. However, it is highly likely PMPA is

structurally *not* a regular polymer and may have a network-like structure comprising of many phosphonate molecules joined together. This would explain this anomaly. Of the polymers, only PPCA and PFC were consumed *more* in the higher molar ratio Ca^{2+}/Mg^{2+} = 1.64 consumption experiment compared to Ca^{2+}/Mg^{2+} = 0.19. This observation is consistent with the categorisation of these 2 SIs as *Type B* in Chapter 6, whereby higher [Ca^{2+}] was detrimental to their IE. All other polymers, plus the two penta-phosphonates were classified as *Type A* in Chapter 6, and thus performed *better* (i.e. higher IE, less SI consumption) in the Ca^{2+}/Mg^{2+} = 1.64 consumption test. Finally, SI consumption tests are secondary with regard to SI categorisation. MIC vs. NSSW/FW mixing ratio tests (Chapters 5 and 6) are the primary experiments for SI categorisation purposes.

13.8 Chapter 11 – Non-ICP Analytical Methods for SI Assay

The experiments presented in this Chapter illustrated that ICP spectroscopy is not always the most accurate method of assaying for [SI] in SI consumption type experiments, or indeed for any analytical purpose. This is because there are often non-SI P-containing components present in SI formulations which are also detectable by ICP spectroscopy. The ICP spectrometer detects *all* phosphorus present in test-samples regardless of its origin. P-containing un-reacted monomers or by-products can be present in SI formulation samples. This could also have a small impact on chemical assay of SI products in Chapter 4 where the % phosphorus was determined in various SI products – although clearly results for the phosphonate SIs are very accurate – the experimental % P values agreed very well with calculated % P values from RMM – see Figure 4.1 in Chapter 4. This issue of non-SI P-containing components is most likely a much bigger issue with regard to *polymeric* SI formulations. Where PPCA and PFC were assayed by CHS and PS respectively, the results were much more accurate than the ICP results for [SI]. The CHS (C18 / Hyamine / Spectrophotometric) and PS (Pinacyanol / Spectrophotometric) assays for [SI] correlated very closely with the IE whereas the ICP [SI] values were artificially enhanced due to the detection of non-SI [P]. This is the reason why SI consumption results as described in point 2 in Section 13.7 are encountered. If the ICP spectrometer only detected SI [P], the %SI profile *would* follow the IE profile much more closely in these cases. It is most likely that smaller, non-SI P-containing, soluble molecules are remaining in solution, the ICP spectrometer

detects this, resulting in a false Type 1 classification of %SI in solution profile being produced in some cases where it is clearly a Type 2 species being tested, e.g. PFC.

In Chapter 11, non-ICP assayable products MAT, PVS and VS-Co were tested in SI consumption experiments. PVS and VS-Co are non ICP assayable due to the presence of other S-containing species within the sample matrix, e.g. sulphate anions. These consumption results re-confirmed that these three products are indeed Type 2, as concluded at the end of Chapter 6. The CHS and PS analytical techniques provided an accurate assay of these three products. Assaying for MAT by CHS, the IE and %SI profiles were virtually superimposable when plotted on the same chart. In all these consumption experiments, IE was determined by ICP spectroscopy as standard, by means of [Ba^{2+}].

13.9 Chapter 12 – Scale Inhibition Mechanisms: Chemical Structures and Mechanisms

In this penultimate chapter, the relationship between SI chemical structure and static barium sulphate IE was discussed. A number of factors were identified which influence strongly, a SIs IE ability. The most important factors were:

1. The number of phosphonate functional groups per molecule;
2. The presence of nitrogen atoms in the main carbon chain;
3. The presence of amino methylene phosphonate functional groups;
4. If "yes" to points 2 and 3, the number of amino methylene phosphonate functional groups per molecule;
5. The number of chelate rings which can form per SI molecule at the test pH;
6. The number of atoms per chelate ring;
7. The molar ratio of M^{2+}/SI (although this final factor can only be applied to phosphonates, not polymers. It would be too complex to apply this idea to polymers because the whole polymer structure would need to be drawn, etc.).

All SIs which were classified as Type 1 in Chapters 5 and 6 were amino methylene phosphonates: PMPA, OMTHP and DETPMP. In Chapter 12, it was identified that *amino methylene phosphonated* SIs are the most likely to exhibit Type 1 behaviour regardless of whether polymeric or non-polymeric, because these species have the ability to form multiple 5-membered chelate rings at about pH5.5. If a SI is *amino methylene phosphonated*, this does not guarantee a Type 1 classification, it just makes it much more likely.

It is also true to state that all non-amino methylene phosphonated SIs were classified as Type 2: HEDP, HPAA, PPCA, SPPCA, PFC, MAT, PVS, VS-Co, CTP-A and CTP-B.

The *amino methylene phosphonated* species which were not Type 1 include: HMTPMP, HMDP, EDTMPA, NTP and EABMPA. For these 5 products, other factors must be taken into consideration to explain their IE, as detailed in Chapter 12, including the number of methylene phosphonate functional groups per molecule, relative SI-binding constants to Ca^{2+} and Mg^{2+}, molecular stereochemistry and hydrophobicity:

1. EDTMPA may have a particular high affinity for Mg^{2+} (K_{Mg}), causing extensive SI "poisoning".
2. HMTPMP and HMDP both have elongated chemical structures comprising of many consecutive methylene functional groups (6 in HMDP, 12 in HMTPMP) which may cause these products to show similarities to polymeric SIs. Methylene functional groups are known to be hydrophobic and detrimental to the IE of polymers (Van der Leeden and Van der Rosmalen, 1990).
3. NTP and EABMPA only contain one nitrogen atom per molecule, which may not be sufficient for Type 1 behaviour. Although these 2 products can form 2 (EABMPA) or 3 (NTP) 5-membered chelate rings at ~pH5.5, the maximum molar ratio of M^{2+}/SI = 1 in both cases because there is only one nitrogen atom per molecule. Higher phosphonates such as HMDP and EDTMPA have an advantage over NTP and EABMPA in that they can chelate double the molar quantity of M^{2+} per molecule at ~pH5.5.

All of the factors summarised in this section can affect Type 1 and Type 2 classifications, but it seems the most crucial factor is the presence of nitrogen atoms within the main carbon chains of molecules (whether polymeric or non-polymeric) and in particular, the presence of *amino methylene phosphonate* functional groups, because these chemical properties clearly affect all the other sub-factors relating to static barium sulphate IE of SIs such as the 3 factors listed above. To conclude, the presence of nitrogen atoms in the main carbon chain, and the presence of *amino methylene phosphonate* functional groups makes a Type 1 classification much more likely.

13.10 Areas of Future Work

A number of novel findings have been reported in this thesis but there are still many issues that might be fruitfully studied in research that follows this work. The main topics which should be pursued are as follows:

1. Researchers should continue to test new phosphonate and polymeric SIs which appear in future in the ways used in this work, i.e. MIC vs. mixing ratio experiments, as described in Chapters 5 and 6, and in SI consumption experiments, as described in Chapters 9–11. This will enable these species to be classified as Type 1 or Type 2 and Type A or Type B.

2. Chosen *blends* of SI Type 1 / SI Type 2 should be tested in a similar manner to establish if these can give some mechanistic synergy in terms of their IE behaviour. Such blends could be used for topside applications. SIs HEDP and HPAA examined in this thesis are used in synergy in cooling systems to prevent calcium carbonate scale *and* corrosion (Marín-Cruz et al., 2006). The use of Type 1 / Type 2 and Type A / Type B properties of SI blends for barium sulphate prevention should be investigated. For example, a blend of a Type 1 SI with Type 2 SI could be tested, and/or phosphonate SI with polymeric SI.

3. Laboratory experiments should be planned to determine experimentally the SI-metal binding constants to M^{2+} cations – particularly Ca^{2+} and Mg^{2+}, and see how these SI−Ca^{2+} and SI−Mg^{2+} binding constants correlate with the experimental findings and *SI categorisations* presented in this thesis (particularly for phosphonates). The SI−M^{2+} binding constants are pH and temperature dependant. In the first instance, the SI−M^{2+} binding constants should be determined at the standard test conditions of pH = 5.5 and T = 95^{o}C.

4. The acid dissociation constants (K_a) values of various SIs (particularly phosphonates) should be determined experimentally by acid-base titration and how these K_a values correlate with the static IE of the various species, in particular, for DETPMP, HMTPMP, EDTMPA and PPCA, at pH levels = 4.5, 5.5, 6.5 and 7.5. The IE of DETPMP, HMTPMP, EDTMPA and PPCA has already been determined at these four pH levels in Chapter 7. How the experimentally determined K_a values for SIs compare with the literature values should be checked.

5. Further ESEM/EDAX analyses of scale deposits formed in the presence of phosphonate and polymeric SIs should be studied in detail, to see if any further crystallographic patterns are apparent, e.g. crystallographic characteristics which may indicate whether the SI present is Type 1 or Type 2 *and* Type A or Type B. More emphasis could be placed on deposits formed in the presence of *polymers – Type A* and *Type B* products. In the work described in this thesis, the main focus of the ESEM/EDAX work was on phosphonate SIs. Differences between scale deposits containing the Type 1 products DETPMP and OMTHP and the Type 2 products HMTPMP and HMDP have already been outlined in Chapter 9 but this work can be greatly extended to study many other SI species.

REFERENCES

S.A.Abu-Khamsin and S.J.Ahmad: "Laboratory Study on Precipitation of Calcium Sulphate in Berea Sandstone Cores", Paper SPE 106336, presented at the SPE Technical Symposium of Saudi Arabia Section, Dhahran, Saudi Arabia, 14−16 May 2005.

G.W.Akin and J.V.Lagerwerff: "Calcium Carbonate Equilibria in Solutions Open to the Air. II. Enhanced Solubility of $CaCO_3$ in the Presence of Mg^{2+} and SO_4^{2-}", Geochimica et Cosmochimica Acta, Vol.29, Issue 4, p.353−360, 1965.

M.Al-Riyami, E.Mackay, G.Deliu, M.Jordan and J.McElhiney: "When Will Low-Sulphate Seawater No Longer Be Required on the Tiffany Field?", Paper SPE 112537, presented at the SPE International Symposium and Exhibition on Formation Damage Control, Lafayette, Louisiana, USA, 13−15 February 2008.

B.L.Barnett and V.A.Uchtman: "Structural Investigations of Calcium Binding Molecules. IV. Calcium Binding to Aminocarboxylates. Crystal Structures of Ca(CaEDTA).$7H_2O$ and Na(CaNTA)", Inorganic Chemistry, Vol.18, No.10, p.2674–2678, 1979.

R.T.Barthorpe: "The Impairment of Scale Inhibitor Function by Commonly Used Organic Anions", Paper SPE 25158, presented at the SPE International Symposium on Oilfield Chemistry, New Orleans, Louisiana, USA, 2−5 March 1993.

B.Bazin, N.Kohler and A.Zaitoun: "Some Insights Into the Tube-Blocking-Test Method To Evaluate the Efficiency of Mineral Scale Inhibitors", Paper SPE 96560, presented at the SPE Annual Technical Conference and Exhibition, Dallas, Texas, USA, 9−12 October 2005.

P.G.Bedrikovetsky, R.P.Lopes, P.M. Gladstone, F.F.Rosario, M.C.Bezerra and E.A.Lima: "Barium Sulphate Oilfield Scaling: Mathematical and Laboratory Modelling", Paper SPE 87457, presented at the SPE International Symposium on Oilfield Scale, Aberdeen, UK, 26−27 May 2004.

M.C.Bezerra, F.F.Rosario, F.Prais and J.R.P.Rodrigues: "Process for the Controlled Precipitation of the Inhibitor Scale in a Subterranean Formation", Paper SPE 50774 presented at the 1999 SPE International Symposium on Oilfield Chemistry held in Houston, Texas, USA, 16−19 February 1999.

E.J.Billo: "Calculation of Binding Constants" in *Excel for Chemists: A Comprehensive Guide*, Chap. 22. New York: Wiley, 2001.

L.S.Boak, G.M.Graham and K.S.Sorbie: "The Influence of Divalent Cations on the Performance of $BaSO_4$ Scale Inhibitor Species", Paper SPE 50771 presented at the 1999 SPE International Symposium on Oilfield Chemistry held in Houston, Texas, USA, 16−19 February 1999.

L.S.Boak, H.Al-Mahrouqi, E.J.Mackay, C.E.Inches, K.S.Sorbie, M.C.M.Bezerra and R.O.Mota: "What Level of Sulphate Reduction is Required to Eliminate the Need for Scale Inhibitor Squeezing?", Paper SPE 95089, presented at the SPE International Symposium on Oilfield Scale, Aberdeen, UK, 11−12 May 2005.

L.S.Boak and K.S.Sorbie: "New Developments in the Analysis of Scale Inhibitors", Paper SPE 130401, SPE Production and Operations, Vol.25, No.4, p.533−544, November 2010.

P.J.Breen, B.N.Diel and H.H.Downs: "Correlation of Scale Inhibitor Structure With Adsorption Thermodynamics and Performance in Inhibition of Barium Sulfate in Low-pH Environments", Paper SPE 20688, presented at the 65th SPE Annual technical Conference and Exhibition held in New Orleans, Louisiana, September 23−26, 1990.

H.F.Browning and S.H.Fogler: "Effect of Synthesis Parameters on the Properties of Calcium Phosphonate Precipitates". Langmuir, American Chemical Society, Vol.11, No.10, p.4143−4152, 1985.

Bull. 53-39(E) ME-3. Deepquest 2040, 2050, and 2060 Series of Multifunctional Metal Ion Control Agents in Aqueous Solutions, 1986. Monsanto, Creve Coeur, Missouri (July 1988).

J.R.Bunney, M.M.Jordan and K.S.Sorbie: "The Prediction and Avoidance of Formation Damage Induced by Scale Inhibitor Squeeze Treatments", Paper SPE 38165, presented at the SPE European Formation Damage Conference, The Hague, Netherlands, 2−3 June 1997.

B.J.Burr, T.M.Howe and J.Goulding: "The Development and Application of a Detectable polymeric Scale Inhibitor to Control Sulfate Scales by Squeeze Applications", Paper SPE 16261, presented at the SPE International Symposium on Oilfield Chemistry, San Antonio, Texas, 4−6 February 1987.

A.Castanares, J.Sanders and R.Pongratz: "Ready For REACH? A Service Company Approach to REACH Sustainable Solutions", Paper SPE 111633, presented at the SPE International Conference on Health, Safety, and Environment in Oil and Gas Exploration and Production, Nice, France, 15−17 April 2008.

T.Chen, A.Neville and M.Yuan: "Calcium Carbonate Scale Formation – Assessing the Initial Stages of Precipitation and Deposition", Journal of Petroleum Science and Engineering 46, p.185−194, 2005. (2005a)

T.Chen, A.Neville and M.Yuan: "Assessing the Effect of Mg^{2+} on $CaCO_3$ Scale Formation – Bulk Precipitation and Surface Deposition", Journal of Crystal Growth 275, p.1341−1347, 2005. (2005b)

T.Chen, A.Neville and M.Yuan: "Influence of Mg^{2+} on $CaCO_3$ Formation – Bulk Precipitation and Surface Deposition", Chemical Engineering Science 61, p.5318−5327, 2006.

H.J.Chen, C.J.Hinrichsen, C.A.Burnside and M.Widener: "Assessment of Barite Scaling Potentials, Sulfate Removal Options, and Chemical Treating Strategies for the Tombua-Landana Development", Paper SPE 106480, presented at the International Symposium on Oilfield Chemistry, Houston, Texas, USA, 28 February−2 March 2007.

T.Chen, P.Chen, H.Montgomerie, T.Hagen and H.Ekpeni: "Development of Environmentally Friendly Calcium Carbonate Scale Inhibitor for HTHP Squeeze Application in the Oil and Gas Field Water Treatment", Paper NACE 11389, presented at CORROSION, Houston, Texas, USA, March 13−17, 2011.

W.C.Cheong, A.Neville, P.H.Gaskell and S.Abbott: "Using Nature to Provide Solutions to Calcareous Scale Deposition", Paper SPE 114082, presented at the SPE International Oilfield Scale Conference, Aberdeen, UK, 28−29 May 2008.

A.F.Clemmit, D.C.Balance and A.G.Hunton: "The Dissolution of Scales in Oilfield Systems", Paper SPE 14010, Offshore Europe, 10−13 September, 1985.

I.R.Collins, R.Stalker and G.M.Graham: "Sulphate Removal for Barium Sulphate Scale Mitigation a Deepwater Subsea Production System", Paper SPE 87465, presented at the SPE International Symposium on Oilfield Scale, Aberdeen, UK, 26−27 May 2004.

I.R.Collins: "Predicting the Location of Barium Sulfate Scale Formation in Production Systems", Paper SPE 94366, presented at the SPE International Symposium on Oilfield Scale, Aberdeen, UK, 11−12 May 2005.

M.C.Cushner, J.L.Przbylinski and J.W.Ruggeri: "How Temperature and pH Affect the Performance of Barium Sulfate Inhibitors", Paper NACE 428, presented at NACE Corrosion 88 held in St. Louis, MO, March 21−25, 1988.

R.A.Davis and J.E.McElhiney: "The Advancement of Sulfate Removal from Seawater in Offshore Waterflood Operations", Paper NACE 02314, presented at CORROSION, Denver, Colorado, USA, April 7−11, 2002.

K.P.Davis, S.D.Fidoe, G.P.Otter, R.E.Talbot and M.A.Veale: "Novel Scale Inhibitor Polymers with Enhanced Adsorption Properties", Paper SPE 80381, presented at the International Symposium on Oilfield Scale, Aberdeen, UK, 29−30 January 2003.

K.D.Demadis and S.D.Katarachia: "Metal-Phosphonate Chemistry: Synthesis, Crystal Structure of Calcium-Amino-Tris-(Methylene Phosphonate) and Inhibition of $CaCO_3$ Crystal Growth", Phosphorus, Sulfur, and Silicon 179, p.627–648, 2003.

W.Dickinson, R.Griffin, L.Sanders and C.Lowen: "Development and Performance of Biodegradable Antiscalants for Oilfield Applications", Paper OTC 21788, presented at the Offshore Technology Conference, Houston, Texas, USA, 2−5 May 2011.

E.L.Dromgoole and L.M.Walter: "Iron and Manganese Incorporation into Calcite: Effects of Growth Kinetics, Temperature and Solution Chemistry", Chemical Geology, Vol. 81, Issue 4, p.311−336, 1990.

W.Duan, H.Oota and K.Sawada: "Stability and Structure of Ethylenedinitrilopoly(methylphosphonate) Complexes of the Alkaline-Earth Metal Ions in Aqueous Solution", Journal of the Chemical Society 17, p.3075–3080, 1999.

S.J.Dyer, G.M.Graham and K.S.Sorbie: "Factors Affecting the Thermal Stability of Conventional Scale Inhibitors for Application in High Pressure/High Temperature Reservoirs", Paper SPE 50717, presented at the SPE International Symposium on Oilfield Chemistry, Houston, Texas, USA, 16−19 February 1999.

V.Eroini; N.Kapur; A.Neville and M.Euvrard: "Preventing Scale Formation Using Modified Surfaces", Paper NACE 11344, presented at CORROSION 2011, Houston, Texas, March 13−17, 2011.

C.Fan, A.T.Kan, P.Zhang and M.B.Tomson: "Barite Nucleation and Inhibition at 0 to 200°C With and Without Thermodynamic Hydrate Inhibitors", Paper SPE 121559, SPE Journal, Vol.16, No.2, p.440−450, 2011.

FAST database of field formation water compositions, IPE, HWU.

FAST Experimental Procedures Manual (EPM), IPE, HWU, 2006.

N.D.Feasey, M.M.Jordan, E.J.Mackay and I.R.Collins: "The Challenge that Completion Types Present to Scale Inhibitor Squeeze Chemical Placement: A Novel Solution Using a Self-Diverting Scale Inhibitor Squeeze Process", Paper SPE 86478, presented at the SPE International Symposium and Exhibition on Formation Damage Control, Lafayette, Louisiana, USA, 18−20 February 2004.

N.Fleming, G.Ross and C.Hobden: "Enhanced Scale Inhibitor Performance through Utilization of End Capped Technology", Paper NACE 04387, presented at CORROSION, New Orleans, Louisiana, March 28−April 1, 2004.

W.W.Frenier and M.Ziauddin: "A Multifaceted Approach for Controlling Complex Deposits in Oil and Gas Production", Paper SPE 132707, presented at the SPE Annual Technical Conference and Exhibition, Florence, Italy, 19−22 September 2010.

J.Galvan and C.Smith: "The Impact of REACH on the E&P Industry: a Service Company", Paper SPE 126995, presented at the SPE International Conference on Health, Safety and Environment in Oil and Gas Exploration and Production, Rio de Janeiro, Brazil, 12−14 April 2010.

J.S.Gill and R.G.Varsanik: "Computer Modelling of the Specific Matching Between Scale Inhibitors and Crystal Structure of Scale Forming Minerals", Journal of Crystal Growth, Vol.76, No.1, p. 57–62, 1986.

J.S.Gill: "Development of Scale Inhibitors", Paper NACE 96229, presented at CORROSION, Denver, Colorado, March 24–29, 1996.

G.M.Graham, L.S. Boak and K.S. Sorbie: "The Influence of Formation Calcium on the Effectiveness of Generically Different Barium Sulphate Oilfield Scale Inhibitors", SPE 37273, presented at the SPE International Symposium on Oilfield Chemistry, Houston, Texas, 18−21 February 1997. (1997a)

G.M.Graham, M.M.Jordan, G.C.Graham, W.Sablerolle, K.S.Sorbie, P.Hill and J.Bunney: "The Implication of HP/HT Reservoir Conditions on the Selection and Application of Conventional Scale Inhibitors: Thermal Stability Studies", Paper SPE 37274, presented at the SPE International Symposium on Oilfield Chemistry, Houston, Texas, 18−21 February 1997. (1997b)

G.M.Graham, D.M.Frigo, I.R.McCracken, G.C.Graham, W.J.Davidson, S.Kapusta and P.Shone: "The Influence of Corrosion Inhibitor / Scale Inhibitor Interference on the Selection of Chemical Treatments Under Harsh (HP/HT/HS) Reservoir Conditions", Paper SPE 68330, presented at the International Symposium on Oilfield Scale, Aberdeen, UK, 30−31 January 2001. (2001a)

G.M.Graham, L.S.Boak and C.M.Hobden: "Examination of the Effect of Generically Different Scale Inhibitor Species (PPCA and DETPMP) on the Adherence and Growth of Barium Sulphate Scale on Metal Surfaces", Paper SPE 68298, presented at the SPE International Symposium on Oilfield Scale, Aberdeen, UK, 30−31 January 2001. (2001b)

G.M.Graham, I.R.Collins, R.Stalker and I.J.Littlehales: "The Importance of Appropriate Laboratory Procedures for the Determination of Scale Inhibitor Performance", Paper SPE 74679, presented at the International Symposium on Oilfield Scale, Aberdeen, UK, 30−31 January 2002. (2002a)

G.M.Graham and C.P.McMahon: "The Effect of Scale Inhibitor Performance Against Bulk (Homogeneous) and Surface (Heterogeneous) Scale Nucleation and Growth by the Addition of Film Forming Corrosion Inhibitors", Paper NACE 02315, presented at CORROSION, Denver, Colorado, April 7−11, 2002.

G.M.Graham, E.J.Mackay, S.J.Dyer and H.M.Bourne: "The Challenges for Scale Control in Deepwater Production Systems: Chemical Inhibition and Placement", Paper NACE 02316, presented at CORROSION, Denver, Colorado, April 7−11, 2002. (2002b)

G.M.Graham, S.J.Dyer and P.Shone: "Potential Application Of Amine Methylene Phosphonate Based Inhibitor Species In HP/HT Environments For Improved Carbonate Scale Inhibitor Performance", Paper 60217, SPE Production and Facilities, Vol. 17, No. 4, p.212−220, November 2002. (2002c)

G.M.Graham, L.S.Boak and K.S.Sorbie: "The Influence of Formation Calcium and Magnesium on the Effectiveness of Generically Different $BaSO_4$ Oilfield Scale Inhibitors", SPE 81825, SPE Production and Facilities, p.28−44, February 2003.

A.L.Graham, E.Vieille, A.Neville, L.S.Boak and K.S.Sorbie: "Inhibition of $BaSO_4$ at a Hastelloy Metal Surface and in Solution: The Consequences of Falling Below the Minimum Inhibitor Concentration (MIC)", Paper SPE 87444, presented at the SPE International Symposium on Oilfield Scale, Aberdeen, UK, 26−27 May 2004.

G.M.Graham, I.Munro, N.Harvison, K.Marshall and M.Kyle: "Improved Scale Inhibitor Assay for Sulphonated Polymers in Oilfield Brines", Paper SPE 131100, presented at the SPE International Conference on Oilfield Scale, Aberdeen, UK, 26−27 May 2010.

J.Greenberg and M.Tomson: "Precipitation and Dissolution Kinetics and Equilibria of Aqueous Ferrous Carbonate versus Temperature", Applied Geochemistry, Vol.7, p.185−190, 1992.

N.N.Greenwood and A.Earnshaw: "Chemistry of the Elements", 2nd Ed, Oxford: Butterworth-Heinemann,p.910, 1997.

A.Gutjahr, H.Dabringhaus and R.Lacmann: "Studies of the growth and dissolution kinetics of the $CaCO_3$ polymorphs calcite and aragonite II. The influence of divalent cation additives on the growth and dissolution rates", Journal of Crystal Growth, Vol. 158, Issue 3, p.310−315, 1996.

J.A.Hardy, R.T.Barthorpe, M.A.Plummer and J.S.Rhudy: "Control of Scaling in the South Brae Field", Paper OTC 7058, presented at the Offshore Technology Conference, Houston, Texas, 4 May−7 May 1992.

D.Hasson, H.Shemer and A.Sher: "State of the Art of Friendly "Green" Scale Control Inhibitors: A Review Article", Ind. Eng. Chem. Res., Vol.50, No.12, p.7601–7607, 2011.

S.He, J.E.Oddo and M.B.Tomson: "The Inhibition of Gypsum and Barite Nucleation in NaCl Brines at Temperatures from 25 to 90°C", Applied Geochemistry, Vol. 9, p.561−567, 1994.

J.Hen, A.Brunger, B.K.Peterson, M.D.Yuan and J.P.Renwick: "A Novel Scale Inhibitor Chemistry for Downhole Squeeze Application in High Water Producing North Sea Wells", Paper SPE 30410, presented at the Offshore Europe, Aberdeen, UK, 5−8 September 1995.

P.D.Henson, M.D.Pritchard and R.Weare: "A Chemical Manufacturer", Paper SPE 141019, presented at the SPE European Health, Safety and Environmental Conference in Oil and Gas Exploration and Production, Vienna, Austria, 22−24 February 2011.

C.E.Inches, K.El Doueiri and K.S.Sorbie: "Green Inhibitors: Mechanisms in the Control of Barium Sulfate Scale", Paper NACE 06485, presented at the NACE Corrosion 2006, San Diego, CA, March 12−16, 2006.

G.E.Jackson, N.Poynton; K.McLaughlin, D.R.Clark: "Novel Polymeric Phosphonate Scale Inhibitors for Improved Squeeze Treatment Lifetimes", presented at the 7th International Symposium, Geilo, Norway, March 17−20, 1996.

D.Jacoby: "Global Trade Restrictions and Related Compliance Issues Pertaining to Oil and Gas Production Chemicals", Paper OTC 22005, presented at the Offshore Technology Conference, Houston, Texas, USA, 2−5 May 2011.

M.M.Jordan, K.S.Sorbie, P.Jiang, M.D.Yuan, A.C.Todd, K.Taylor, K.E.Hourston and K.Ramstad: "Mineralogical Controls on Inhibitor Adsorption/Desorption in Brent Group Sandstone and Their Importance in Predicting and Extending Field Squeeze Lifetimes", Paper SPE 27607, presented at the European Production Operations Conference and Exhibition, Aberdeen, UK, 15−17 March 1994.

M.M.Jordan, K.S.Sorbie, M.D.Yuan, K.Taylor, K.E.Hourston, K.Ramstad and P.Griffin: "Static and Dynamic Adsorption of Phosphonate and Polymeric Scale Inhibitors onto Reservoir Core from Laboratory Tests to Field Application", Paper SPE 29002, presented at the SPE International Symposium on Oilfield Chemistry, San Antonio, Texas, 14−17 February 1995.

M.M.Jordan, K.S.Sorbie, G.M.Graham, K.Taylor, K.E.Hourston: "The Correct Selection and Application Methods for Adsorption and Precipitation Scale Inhibitors for Squeeze Treatments in North Sea Oilfields", Paper SPE 31125, presented at the SPE Formation Damage Control Symposium, Lafayette, Louisiana, USA, 14−15 February 1996.

M.M.Jordan, I.R.Collins and E.J.Mackay: "Low Sulfate Seawater Injection for Barium Sulfate Scale Control: A Life-of-Field Solution to a Complex Challenge", Paper SPE 98096, SPE Productions and Operations Journal, p.192−209, 2008.

M.M.Jordan, E.Sorhaug, D.Marlow and G.M.Graham: ""Red" vs. "Green" Scale Inhibitors for Extending Squeeze Life – A Case Study from North Sea, Norwegian Sector", Paper NACE 10137, presented at the NACE International Corrosion Conference and Exposition, 2010.

M.M.Jordan, E.Sorhaug and D.Marlow: ""Red" vs. "Green" Scale Inhibitors for Extending Squeeze Life - A Case Study From North Sea, Norwegian Sector - Part II", Paper SPE 140752, presented at the SPE International Symposium on Oilfield Chemistry, The Woodlands, Texas, USA, 11−13 April 2011.

A.T.Kan, G.Fu and M.B.Tomson: "Adsorption and Precipitation of an Aminoalkylphosphonate onto Calcite", Journal of Colloid and Interface Science 281, p.275−284, 2005.

A.T.Kan, G.Fu, D.Shen, H.Al-Saiari and M.B.Tomson: "Enhanced Inhibitor Treatments with the Addition of Transition Metal Ions", SPE 114060, presented at the Oilfield Scale Conference, Aberdeen, 28−29 May 2008.

S.L.Kokal, K.U.Raju and H.Bayona: "Cost-Effective Design of Scale-Inhibitor Squeeze Treatments Using a Mathematical Model", Paper SPE 29819, SPE Production & Facilities, Vol. 11, No. 2, p.77−82, May 1996.

S.Labille, A.Neville, G.M.Graham and L.S. Boak: "An Assessment of Adhesion of Scale and Electrochemical Pre-treatment for the Prevention of Scale Deposition on Metal Surfaces", Paper SPE 74676, presented at the International Symposium on Oilfield Scale, Aberdeen, UK, 30−31 January 2002.

N.Laing, G.M.Graham and S.J.Dyer: "Barium Sulphate Inhibition in Subsea Systems – The Impact of Cold Seabed Temperatures on the Performance of Generically Different Scale Inhibitor Species", Paper SPE 80229, presented at the SPE International Symposium on Oilfield Chemistry held in Houston, Texas, USA, 5−7 February 2003.

D.Litchinsky, N.Purdie, M.B.Tomson and W.D.White: "A Rigorous Solution to the Problem of Interfering Dissociation Steps in the Titration of Polybasic Acids", Analytical Chemistry, Vol.41, No.13, 1969.

S.Liu and D.W.Griffiths: "Adsorption Of Aminomethylphosphonic Acids On The Calcium Sulfate Dihydrate Crystal Surface", Paper SPE 7863, presented at the SPE Oilfield and Geothermal Chemistry Symposium, Houston, Texas, USA, 22−24 January 1979.

J.Majzlan, A.Navrotsky and J.M.Neil: "Energetics of anhydrite, barite, celestine, and anglesite: A high-temperature and differential scanning calorimetry study", Geochimica et Cosmochimica Acta, Vol.66, No.10, p.1839−1850, 2002.

A.Malandrino, M.D.Yuan, K.S.Sorbie and M.M.Jordan: "Mechanistic Study and Modelling of Precipitation Scale Inhibitor Squeeze Processes", Paper SPE 29001, presented at the SPE International Symposium on Oilfield Chemistry, San Antonio, Texas, 14−17 February 1995.

J.Marín-Cruz, R.Cabrera-Sierra, M.A.Pech-Canul and I. González: "EIS study on corrosion and scale processes and their inhibition in cooling system media", Electrochimica Acta, Vol.51, Issue 8–9, p.1847–1854, 2006.

A.E.Martell: "Coordination Chemistry" Volume 1. New York City, New York: Van Nostrand Reinhold Co., 1971. (1971a)

A.E.Martell: "Coordination Chemistry" Volume 2. New York City, New York: Van Nostrand Reinhold Co., 1971. (1971b)

A.D.Martinod; A.Neville and M.Euvrard: "An In-Situ Flow Cell to Highlight Different Mechanisms of $CaCO_3$ Inhibition by Green and Non Green Polymers", Paper OTC 22309, presented at the OTC Brasil, Rio de Janeiro, Brazil, 4−6 October 2011.

E.Mavredaki, A.Neville and K.S.Sorbie: "Study of $BaSO_4$ Formation Kinetics and Inhibition Effect of Polyphosphino-Carboxylic Acid (PPCA) on Barite Formation with Synchrotron X-Ray Diffraction (SXRD)", Paper SPE 114039, presented at the SPE International Oilfield Scale Conference, Aberdeen, UK, 28−29 May 2008.

E.Mavredaki, A.Neville and K.S.Sorbie: "Initial Stages of Barium Sulfate Formation at Surfaces in the Presence of Inhibitors", published as part of a virtual special issue of selected papers presented at the 2010 Annual Conference of the British Association for Crystal Growth (BACG), Manchester, UK, 5−7 September, 2010.

E.Mavredaki, A.Neville and K.S.Sorbie: "Assessment of Barium Sulphate Formation and Inhibition at Surfaces with Synchrotron X-Ray Diffraction (SXRD)", Applied Surface Science 257, p.4264−4271, 2011.

J.E.McElhiney, M.B.Tomson and A.T.Kan: "Design of Low Sulphate Seawater Injection Based upon Kinetic Limits", Paper SPE 100480, presented at the SPE International Oilfield Scale Symposium, Aberdeen, UK, 31 May−1 June 2006.

M.D.K.McTeir, P.D.Ravenscroft and C.Rudkin: "Modified methods for the Determination of Polyacrylic/Phospinopolycarboxylic acid Polyvinylsulphonic acid Scale Inhibitors in Oilfield Brines", Paper SPE 25160, presented at the SPE International Symposium on Oilfield Chemistry, New Orleans, LA, 2−5 March 1993.

H.Montgomerie, P.Chen, T.Hagen, O.Vikane, R.Matheson, V.Leirvik, C.Frøytlog and J.O.Saeten: "Development of a New Polymer Inhibitor Chemistry for Downhole Squeeze Applications", Paper SPE 113926, SPE Production and Operations, Vol.24, No.3, p.459−564, August 2009.

A.P.Morizot and A.Neville: "Barium Sulfate Deposition and Precipitation Using a Combined Electrochemical Surface and Bulk Solution Approach", Paper NACE 60638, Corrosion Journal, Vol.56, No.6, June 2000.

C.L.Mowery: "Formulation of a Cost-Effective Chemical Treatment Program", Paper SPE 14406, presented at the SPE Annual Technical Conference and Exhibition, Las Vegas, Nevada, USA, 22−26 September 1985.

A.Mucci and J.W.Morse: "The Incorporation of Mg^{2+} and Sr^{2+} into Calcite Overgrowths: Influences of Growth Rate and Solution Composition", Geochimica et Cosmochimica Acta, Vol.47, Issue 2, p.217−233, 1983.

G.H.Nancollas and M.M.Reddy: "The Kinetics of Crystallization of Scale-Forming Minerals", SPE Journal, Vol.14, No.2, p.117−126, 1974.

G.H.Nancollas and S.T.Liu: "Crystal Growth and Dissolution of Barium Sulfate", SPE Journal, Vol.15, No.6, p.509−516, 1975.

G.H.Nancollas: "Oilfield Scale – Physical Chemical Studies of its Formation and Prevention", Chemicals in the Oil Industry, p.143−164, 1985.

G.H.Nancollas, D.Gerard and W.Zachowicz: "Calcium Carbonate Scaling. A Kinetics and Surface Energy Approach", Paper NACE 04072, presented at CORROSION, New Orleans, Louisiana, March 28−April 1, 2004.

H.Naono: "The Effect of Triphosphate on the Crystallization of Strontium Sulphate", Bull. Chem. Soc. Japan, Vol.40, No.5, p.1104−1110, 1967.

G.Nenniger, J.Nenniger and P.Bulkowski: “A Valuable Tool For Addressing Scale Problems”, Paper 90-54, Petroleum Society, Annual Technical Meeting, Calgary, Alberta, Jun 10−13, 1990.

A.Neville, A.P.Morizot and T. Hodgkiess: “Investigation of Barium Sulfate Deposition and Precipitation Using a Novel Approach”, Paper NACE 99113, presented at CORROSION 99, San Antonio, Texas, USA, April 25−30, 1999.

A.Neville, A.P.Morizot, S.Labille and G.M.Graham: “Optimizing Inhibitor Efficiency Using Electrochemical Methods”, Paper NACE 02318, presented at CORROSION, Denver, Colorado, USA, April 7−11, 2002.

N.Ockerbloom and A.E.Martell: “Chelating Tendencies of Aminomethylenephosphonic-N,N-diacetic Acid”, J. Am. Chem. Soc., Vol.80, No.10, p.2351–2354, 1957.

J.E.Oddo and M.B.Tomson: “The Solubility and Stoichiometry of Calcium-diethylenetriaminepenta(methylene phosphonate) at 70^{o}C in Brine Solutions at 4.7 and 5.0 pH”, Applied Geochemistry, Vol.5, p.527−532, 1990.

C.Okocha, K.S.Sorbie and L.S.Boak: “Novel Inhibition Mechanism for Sulphide Scales”, Paper SPE 112538 presented at the SPE International Symposium and Exhibition on Formation Damage Control held in Lafayette, Louisiana, U.S.A., 13–15 February 2008.

J.E.Pardue: “A New Inhibitor for Scale Squeeze Applications”, Paper SPE 21023, presented at the 1991 SPE International Symposium on Oilfield Chemistry held in Anaheim, California, USA, 20−22 February 1991.

N.S.Poonia and A.V.Bajaj: “Coordination Chemistry of Alkali and Alkaline Earth Cations”. Chemical Reviews, American Chemical Society, Vol.79, No.5, p.389–445, 1979.

K. Popov, H. Rönkkömäki, L.H.J. Lajunen, A. Popov and A. Vendilo: "Critical Evaluation of Stability Constants of Phosphonic Acids", poster presented at the IUPAC Congress / General Assembly, July 2001.

J.L.Przybylinski, R.H.Nguyen, and J.W.Ruggeri: "Field Test of a Unique Phosphonate Scale Inhibitor for Extended-Life Squeeze Treatment in Sandstone", Paper SPE 50703, presented at the SPE International Symposium on Oilfield Chemistry, Houston, Texas, USA, 16−19 February 1999.

A.Putnis, C.V.Putnis and J.M.Paul: "The Efficiency of a DTPA-Based Solvent in the Dissolution of Barium Sulfate Scale Deposits", Paper SPE 29094, presented at the SPE International Symposium on Oilfield Chemistry, San Antonio, Texas, USA, 14−17 February 1995.

M.H.V.Quiroga, J.C.N.Calmeto, S.L.Pinto, C.A.S.Assis, I. Santos: "Hard Scale Mechanical Removal: A Solution for Brazilian Offshore Operations", Paper SPE 89627, presented at the SPE/ICoTA Coiled Tubing Conference and Exhibition, Houston, Texas, USA, 23−24 March 2004.

M.R.Rabaioli and T.P.Lockhart: "Solubility and Phase Behaviour of Polyacrylate Scale Inhibitors and Their Implications for Precipitation Squeeze Treatment", Paper SPE 28998, presented at the 1995 SPE International Symposium on Oilfield Chemistry held in San Antonio, Texas, USA, 14−17 February 1995.

P.H.Ralston: "Scale Control with Aminomethylenephosphonates", Paper SPE 2294, Journal of Petroleum Technology, Vol.21, No.8, p.1029−1036, August 1969.

J.E.Ramsey and L.M.Cenegy: "A Laboratory Evaluation of Barium Sulfate Scale Inhibitors at Low pH for Use in Carbon Dioxide EOR Floods", Paper SPE 14407, presented at the SPE Annual Technical Conference and Exhibition, Las Vegas, Nevada, USA, 22−26 September 1985.

M.L.Re and J.S.Gill: "The Effect of Polyamino Polyether Methylene Phosphonate on the Crystallization Kinetics of Calcium Carbonate: A Constant Composition Study", Paper NACE 96157, presented at CORROSION, Denver, Colorado, March 24–29 1996.

P.A.Read and J.K.Ringen: "The Use of Laboratory Tests to Evaluate Scaling Problems During Water Injection", Paper SPE 10593, presented at the SPE Oilfield and Geothermal Chemistry Symposium, Dallas, Texas, USA, 25−27 January 1982.

M.M.Reddy and G.H.Nancollas: "The Crystallization of Calcium Carbonate: IV. The Effect of Magnesium, Strontium and Sulfate Ions", Journal of Crystal Growth, Vol.35, Issue 1, p.33−38, 1976.

M.J.Sánchez-Moreno, A.Fernández-Botello, R.B.Gómez-Coca, R.Griesser, J.Ochocki, A.Kotynski, J.Niclós-Gutiérrez, V.Moreno and H.Sigel: "Metal Ion-Binding Properties of (1H-Benzimidazol-2-yl-methyl)phosphonate (Bimp2-) in Aqueous Solution. Isomeric Equilibria, Extent of Chelation, and a New Quantification Method for the Chelate Effect", Inorganic Chemistry, Vol. 43, No.4, p.1311–1322, 2004.

K.Sawada, T.Araki, and T.Suzuki: "Complex Formation of Amino Polyphosphonates. 1. Potentiometric and Nuclear Magnetic Resonance Studies of Nitrilotris(methylenephosphonato) Complexes of the Alkaline Earth Metal Ions", Inorganic Chemistry, American Chemical Society, Vol. 26, No. 8, p.1199, 1986.

K.Sawada, T.Araki, T.Suzuki, and K.Doi: "Complex Formation of Amino Polyphosphonates. 2. Stability and Structure of Nitrilotris(methylenephosphonato) Complexes of Divalent Transition-Metal Ions", Inorganic Chemistry, American Chemical Society, Vol.28, p.2688−2691, 1988.

K.Sawada, M.Kuribayashi, T.Suzuki and H.Miyamoto: "Protonation equilibria of nitrilotris(methylenephosphonato)-and ethylenediamine-tetrakis(methylenephosphonato)-complexes of scandium, yttrium, and lanthanoids", Journal of Solution Chemistry, Vol.20, No.8, p. 829−839, 1991.

K.Sawada, T.Miyagawa, T.Sakaguchi and K.Doi: "Structure and Thermodynamic Properties of Aminopolyphosphonate Complexes of the Alkaline-Earth Metal Ions", J. Chem. Soc. Dalton Trans., J. Chem. Soc., Dalton Trans, p.3777−3784, 1993. (1993a)

K.Sawada, T.Kanda, Y.Naganuma and T.Suzuki: "Formation and Protonation of Aminopolyphosphonate Complexes of Alkaline-Earth and Divalent Transition-Metal Ions in Aqueous Solution", J. Chem. Soc. Dalton Trans, p.2557−2562, 1993. (1993b)

K.Sawada, W.Duan, M.Ono and K.Satoh: "Stability and structure of nitrilo(acetate–methylphosphonate) complexes of the alkaline-earth and divalent transition metal ions in aqueous solution", J. Chem. Soc. Dalton Trans, Issue 6, p. 919−924, 2000.

J.A.Scott: "Pilot Testing of Membrane Technology To Selectively Remove Sulfate Ion From Seawater in the Wilmington Field", Paper SPE 25152, presented at the SPE International Symposium on Oilfield Chemistry, New Orleans, Louisiana, USA, 2−5 March 1993.

C.M.Simpson, G.M.Graham, I.R.Collins, J. McElhiney and R.Davis "Sulphate Removal for Barium Sulphate Mitigation - Kinetic vs. Thermodynamic Controls in Mildly Oversaturated Conditions", Paper SPE 95082, presented at the SPE International Symposium on Oilfield Scale, Aberdeen, UK, 11−12 May 2005.

S.S.Shaw, K.S.Sorbie and L.S.Boak: "The Effects of Barium Sulphate Saturation Ratio, Calcium and Magnesium on the Inhibition Efficiency: I: Phosphonate Scale Inhibitors", Paper SPE 130373, presented at the SPE International Conference on Oilfield Scale, Aberdeen, UK, 26−27 May 2010. (2010a)

S.S.Shaw, K.S.Sorbie and L.S.Boak: "The Effects of Barium Sulphate Saturation Ratio, Calcium and Magnesium on the Inhibition Efficiency: II: Polymeric Scale Inhibitors", Paper SPE 130374, presented at the SPE International Conference on Oilfield Scale, Aberdeen, UK, 26−27 May 2010. (2010b)

S.S.Shaw and K.S.Sorbie: "The Effect of pH on Static Barium Sulphate Inhibition Efficiency and Minimum Inhibitor Concentration of Generic Scale Inhibitors", Paper SPE 155094, presented at the SPE International Conference on Oilfield Scale, Aberdeen, UK, 30−31 May 2012.

S.S.Shaw, T.D.Welton and K.S.Sorbie: "The Relation between Barite Inhibition by Phosphonate Scale Inhibitors and the Structures of Phosphonate-Metal Complexes", Paper SPE 155114, presented at the SPE International Conference on Oilfield Scale, Aberdeen, UK, 30−31 May 2012.

M.A.Singleton, J.A.Collins, N.Poynton and H.J.Formston: "Developments in PhosphonoMethylated PolyAmine (PMPA) Scale Inhibitor Chemistry for Severe $BaSO_4$ Scaling Conditions", Paper SPE 60216, presented at the 2000 Second International Symposium on Oilfield Scale held in Aberdeen, UK, 26–27 January 2000.

L.W.Slentz: "Geochemistry of Reservoir Fluids as a Unique Approach to Optimum Reservoir Management", Paper SPE 9582, presented at the Middle East Technical Conference and Exhibition, Bahrain, 9−12 March 1981.

J.K.Smith, J.Hammons, G.Boyd and Q.Fu: "Performance of Scale Inhibitors under Carbonate and Sulfide Scaling Conditions", Paper SPE 114075, presented at the SPE International Oilfield Scale Conference, Aberdeen, UK, 28−29 May 2008.

K.S.Sorbie, P.Jiang, M.D.Yuan, P.Chen, M.M.Jordan and A.C.Todd: "The Effect of pH, Calcium, and Temperature on the Adsorption of Phosphonate Inhibitor onto Consolidated and Crushed Sandstone", Paper SPE 26605, presented at the 68th SPE Annual Technical Conference and Exhibition held in Houston, Texas, 3−6 October, 1993.

K.S.Sorbie, G.M.Graham and M.M.Jordan: "How Scale Inhibitors Work and How this Affects Test Methodology", Paper OFC-1, presented at the 4th Chemistry in Industry Conference and Exhibition, 2000.

K.S.Sorbie and N.Laing: "How Scale Inhibitors Work: Mechanisms of Selected Barium Sulphate Scale Inhibitors Across a Wide Temperature Range", Paper SPE 87470, presented at the 2004 SPE International Symposium on Oilfield Chemistry held in Aberdeen, UK, 26−27 May 2004.

A.T.Stone, M.A.Knight and B.Nowack: "Speciation and Chemical Reactions of Phosphonate Chelating Agents in Aqueous Media", Chapter 4, American Chemical Society Symposium Series 806, Chemicals in the Environment: Fate, Impacts and Remediation, 2002.

L.Stoppelenburg and M.Yuan: "The Performance of Barium Sulfate Inhibitors in Iron Containing Waters in Both Aerated and Anaerobic Systems", Paper NACE 00114, presented at CORROSION, Orlando, Florida, USA, March 26−31, 2000.

F.M.Sweeney and S.D.Cooper: "The Development of a Novel Scale Inhibitor for Severe Water Chemistries", Paper SPE 25159, presented at the SPE International Symposium on Oilfield Chemistry held in New Orleans, LA, USA, 2−5 March 1993.

S.Taj, S.Papavinasam and R.W.Revie: "Development of Green Inhibitors for Oil and Gas Applications", Paper NACE 06656, presented at the 61st Annual NACE International Corrosion Conference and Exposition, 2006.

A.C.Todd and M.D.Yuan: "Barium and Strontium Solid-Solution Formation in Relation to North Sea Scaling Problems", SPE 18200, SPE Production Engineering, Vol.5, No.3, p.279−285, August 1990.

A.C.Todd and M.D.Yuan: "Barium and Strontium Sulfate Solid-Solution Scale Formation at Elevated Temperatures", SPE 19762, SPE Production Engineering, Vol.7, No.1, p.85−92, February 1992.

M.J.Todd, C.J.Strachan, G.Moir and J.Goulding: "Development of the Next Generation of Phosphorus Tagged Polymeric Scale Inhibitors", Paper SPE 130733 presented at the SPE International Conference on Oilfield Scale, Aberdeen, UK, 26−27 May 2010.

M.B.Tomson, A.T.Kan and J.E.Oddo: "Acid/Base and Metal Complex Solution Chemistry of the Polyphosphonate DTPMP versus Temperature and Ionic Strength". Langmuir, American Chemical Society, Vol.10, No.5, 1994.

M.B.Tomson, G.Fu, M.A.Watson and A.T.Kan: "Mechanisms of Mineral Scale Inhibition", Paper SPE 74656 presented at the SPE Oilfield Scale Symposium, Aberdeen, UK, 30–31 January, 2002.

M.B.Tomson, G.Fu, M.A.Watson and A.T.Kan: "Mechanisms of Mineral Scale Inhibition", Paper SPE 84958, SPE Production and Facilities, Vol.18, No.3, p.192−199, August 2003.

M.Tomson, A.Kan, G.Fu and M.Al-Thubaiti: "A Molecular Theory of Mineral Scale Inhibition", NACE Paper 04075, presented at CORROSION, New Orleans, Louisiana, USA, 28 March–1 April , 2004.

V.A.Uchtman and R.A.Gloss: "Structural Investigations of Calcium Binding Molecules. I. The Crystal and Molecular Structures of Ethane-1-hydroxy-1,1-diphosphonic acid Monohydrate, $C(CH_3)(OH)(PO_3H_2)_2.H_2O$", J. Phys. Chem., Vol.76, No.9, p.1298–1304, 1971.

V.A.Uchtman: "Structural Investigations of Calcium Binding Molecules. II. The Crystal and Molecular Structures of Calcium Dihydrogen Ethane-1-hydroxy-1,1-diphosphonate Dihydrate, $CaC(CH_3)(OH)(PO_3H)_2.2H_2O$; Implications for Polynuclear Complex Formation, . J. Phys. Chem., Vol.76, No.9, p.1304–1310, 1971.

V.A.Uchtman and R.P.Oertel: "Structural Investigations of Calcium Binding Molecules. III. The Calcium-Oxydiacetic Acid System. Crystal and Molecular Structures of Calcium Oxydiacetate Hexahydrate and Raman Spectroscopic Comparison with Species in Aqueous Solution", J. Am. Chem. Soc., Vol.95, No.6, p.1802–1811, 1972.

V.A.Uchtman and R.J.Jandacek: "Structural Investigations of Calcium Binding Molecules. V. Structure Analysis of a Calcium Salt of Benzenehexacarboxylic Acid (Mellitic Acid), $Ca_2C_{12}H_2O_{12}.9H_2O$", Inorganic Chemisty, Vol.19, No.2, p.350–355, 1979.

M.C.Van der Leeden and G.M.Van Rosmalen: “Inhibition of Barium Sulfate Deposition by Polycarboxylates of Various Molecular Structures”, Paper SPE 17914, SPE Production Engineering, Vol. 5, No. 1, p.70−76, February 1990.

V.K.Vu; C.Hurtevent and R.A.Davis: “Eliminating the Need for Scale Inhibition Treatments for Elf Exploration Angola's Girassol Field”, Paper SPE 60220, presented at the International Symposium on Oilfield Scale, Aberdeen, UK, 26−27 January 2000.

P.J.C.Webb, T.A.Nistad, B.Knapstad, P.D.Ravenscroft and I.R.Collins: “Economic and Technical Features of a Revolutionary Chemical Scale Inhibitor Delivery Method for Fractured and Gravel Packed Wells: Comparative Analysis of Onshore and Offshore Subsea Applications”, Paper SPE 39451, presented at the SPE Formation Damage Control Conference, Lafayette, Louisiana, USA, 18−19 February 1998.

D.J.Weintritt and J.C.Cowan: “Unique Characteristics of Barium Sulfate Scale Deposition”, Paper SPE 1523, Journal of Petroleum Technology, Vol.19, No.10, p.1381−1394, October 1967.

J.Weston: “Biochemistry of Magnesium”, Institute for Organic Chemistry and Macromolecular Chemistry, Friedrich-Schiller-Universität, Humboldtstraße 10, D-07743 Jena, Germany, 2009.

D.Wilson, K.Harris and M.Toole: “Towards a Better Environment: Improved Biodegradability from a Polymeric Scale Inhibitor”, Paper NACE 10047, presented at CORROSION, San Antonio, Texas, USA, March 14−18, 2010.

J.J.Wylde, G.C.Allen and I.R.Collins: “A Novel, Surface Sensitive Approach to Quantitatively Measure the Prediction and Inhibition of Scale Growth”, Paper SPE 68299, presented at the SPE International Symposium on Oilfield Scale, Aberdeen, UK, 30−31 January 2001.

J.J.Wylde, G.C.Allen and I.R.Collins: "A Surface Sensitive Study of the Influence of Corrosion Inhibitor on Chemical Scale Inhibition", Paper SPE 74677, presented at the International Symposium on Oilfield Scale, Aberdeen, UK, 30−31 January 2002.

J.A.Xiao, A.T.Kan and M.B.Tomson: "Acid-Base and Metal Complexation Chemistry of Phosphino-polycarboxylic Acid under High Ionic Strength and High Temperature", Langmuir, American Chemical Society, Vol.17, No.15, p.4661–4667, 2001.

M.D.Yuan and A.C.Todd: "Prediction of Sulfate Scaling Tendency in Oilfield Operations", Paper SPE 18484, SPE Production Engineering, Vol.6, No.1, p.63−72, February 1991.

M.D.Yuan, M.Anderson and E.Jamieson: "Investigation and Improvement of $BaSO_4$ Scale Inhibition Tests", Paper SPE 37304, presented at the International Symposium on Oilfield Chemistry, Houston, Texas, 18−21 February 1997. (1997a)

M.D.Yuan, P.Hammonds, B.Riley, M.Anderson and R.Tidswell: "Scale Inhibition in High Barium Waters and at High Temperatures", Paper SPE 38766, presented at the SPE Annual Technical Conference and Exhibition, San Antonio, Texas, 5−8 October 1997. (1997b)

M.D.Yuan, E.Jamieson and P.Hammonds: "Investigation of Scaling and Inhibition Mechanisms and the Influencing Factors in Static and Dynamic Inhibition Tests", Paper SPE 98067, presented at CORROSION, San Diego, California, USA, March 22–27 1998.

M.Yuan: "Barium Sulfate Scale Inhibition in the Deepwater Cold Temperature Environment", Paper SPE 68311, presented at the SPE International Symposium on Oilfield Scale, Aberdeen, UK, 30−31 January 2001.

M.Yuan: "Effect of Temperature on Barium Sulfate Scale Inhibition of Diethylene Triamine Penta (Methylene Phosphonic Acid)", Advances in Crystal Growth Inhibition Technologies, p.151−163, 2002.

Y.Zhanga, H.Shaw, R.Farquhar and R.Dawe: "The Kinetics of Carbonate Scaling − Application for the Prediction of Downhole Carbonate Scaling", Journal of Petroleum Science and Engineering, Vol.29, Issue 2, p.85−95, 2001.

Webpages:

[1] http://encyclopedia.thefreedictionary.com/metastable

[2] http://chemistry.about.com/od/solutionsmixtures/a/solubility-rules.htm

[3] http://www.rsc.org/chemsoc/visualelements/pages/data/intro_ groupii_data.html

[4] http://en.wikipedia.org/wiki/Standard_enthalpy_change_of_formation_(data_table)

[5] http://www.georgeglazer.com/decarts/instruments/barite.html

[6] http://sortingoutscience.net/2011/05/23/the-scientific-tourist-175-desert-rose-barite/

[7] http://www.the-vug.com/vug/minerala-c.html

[8] http://www.brightok.net/~rockman/Comanche/Comphoto.htm

[9] http://www.exceptionalminerals.com/tucson2010.htm

[10] http://en.wikipedia.org/wiki/Buffer_solution